

**DEVELOPMENT OF THE FIRST DUAL
INHIBITORS FOR STEROID SULFATASE (STS)
AND 17 β -HYDROXYSTEROID
DEHYDROGENASE TYPE 1 (17 β -HSD1): A
NOVEL TREATMENT APPROACH FOR
ENDOMETRIOSIS**

Dissertation

zur Erlangung des Grades

des Doktors der Naturwissenschaften

der Naturwissenschaftlich-Technischen Fakultät

der Universität des Saarlandes

von

M.Sc. Mohamed Salah Rezk Abdelrahim

Saarbrücken 2019

| | |
|-----------------------------|---|
| Tag des Kolloquiums: | 08.Juli.2019 |
| Dekan: | Prof. Dr. Guido Kickelbick |
| Berichterstatter: | Prof. Dr. R. W. Hartmann Priv.-Doz. Dr. M. Frotscher Prof. Dr. Anna K.H. Hirsch Prof. Dr. C. E. Müller |
| Akad. Mitarbeiter: | Dr. J. Hoppstädter |
| Vorsitz: | Prof. Dr. M. Schneider |

Die vorliegende Arbeit wurde von Oktober 2014 bis März 2019 unter Anleitung von Prof. Dr. Rolf W. Hartmann und PD Dr. Martin Frotscher in der Fachrichtung Pharmazie der Naturwissenschaftlich-Technischen Fakultät der Universität des Saarlandes im Fach Pharmazeutische und Medizinische Chemie angefertigt.

بسم الله الرحمن الرحيم

”وَفَوْقَ كُلِّ ذِي عِلْمٍ عَلِيمٌ“

جزء من الآية 76 من سورة يوسف - القرآن الكريم

"Und über jedem, der Wissen besitzt, steht einer, der (noch mehr) weiß. "

Sure 12:76- Der Heilige Quran

Acknowledgements

First and foremost, I would like to thank ALLAH (the Arabic word for God) for guiding me and charging me with persistence to complete this project.

I would like to express my sincere gratitude to my supervisor PD Dr. Martin Frotscher, for his continuous scientific guidance and support as well as his patience and motivation. I could not have wished for a better supervisor.

It was my great honor to be given the opportunity by Prof. Dr. Rolf W. Hartmann to prepare my thesis as a member of his research group.

I would like to thank my official referee Prof. Dr. Anna K.H. Hirsch for the revision of this dissertation.

I am deeply grateful for working with Dr. Ahmed Saad and Dr. Mostafa Hamed. They always showed great scientific support and encouragement during my working years.

I wish to thank Dr. Mathias Engel for his rich scientific discussions and valuable suggestions.

I am grateful to Dr. Mohammad Abdel-Halim for introducing me in the field of medicinal chemistry and his endless encouragement.

I would like to thank my HSD co-workers, especially Dr. Chris J. van Koppen, Prof. Dr. Matthias W. Laschke, Dr. Claudia Scheuer, Mariam G. Tahoun, Jannine Ludwig and Abdel-Rahman, for the fruitful collaboration.

I wish to thank all my undergraduate researchers, Caroline Hoffmann, Sebastian Neumann and Ramona Mostashiri for their help and contribution in the project.

I would like to thank Dr. Ahmed kamal, Dr. Antonio Martins and all the members of Prof. Dr. Hartmann group.

My gratitude to my wife Sarah El-Gamal, who stood by me and encouraged me to complete my goal, could not be described by words; it is beyond boundaries of language.

Very special thanks to my family, especially my beloved mother, father, father-in-law, mother-in-law and my siblings for unconditional support and encouragement to pursue my interests. Without you all I could not have achieved anything.

Papers included in the thesis

- I. **First Dual Inhibitors of Steroid Sulfatase (STS) and 17 β -Hydroxysteroid Dehydrogenase Type 1 (17 β -HSD1): Designed Multiple Ligands as Novel Potential Therapeutics for Estrogen-Dependent Diseases**
Mohamed Salah, Ahmed S. Abdelsamie, and Martin Frotscher
J. Med. Chem. 2017, 60 (9), 4086–4092. doi:10.1021/acs.jmedchem.7b00062
- II. **Monograph: Potent Dual Inhibitors of Steroid Sulfatase (STS) and 17 β -Hydroxysteroid Dehydrogenase Type 1 (17 β -HSD1) with a Suitable Pharmacokinetic Profile for in Vivo Proof-of-Principle Study in Endometriosis Mouse Model**
- III. **Treatment of estrogen-dependent diseases: Design, synthesis and profiling of a selective 17 β -HSD1 inhibitor with sub-nanomolar IC₅₀ for a proof-of-principle study**
Ahmed S. Abdelsamie, Chris J. van Koppen, Emmanuel Bey, Mohamed Salah, Carsten Borger, Lorenz Siebenbürger, Matthias W. Laschke, Michael D. Menger, Martin Frotscher
Eur. J. Med. Chem. 2017, 127, 944–957. doi: 10.1016/j.ejmech.2016.11.004
- IV. **Targeted Endocrine Therapy: Design, Synthesis, and Proof-of-Principle of 17 β -Hydroxysteroid Dehydrogenase Type 2 Inhibitors in Bone Fracture Healing**
Ahmed S. Abdelsamie, Steven Herath, Yannik Biskupek, Carsten Borger, Lorenz Siebenburger, Mohamed Salah, Claudia Scheuer, Sandrine Marchais-Oberwinkler, Martin Frotscher, Tim Pohlemann, Michael D. Menger, Rolf W. Hartmann, Matthias W. Laschke, and Chris J. van Koppen
J. Med. Chem. 2019, 62 (3), 1362–1372. doi: 10.1021/acs.jmedchem.8b01493
- V. **First Structure-Activity Relationship of 17 β -Hydroxysteroid Dehydrogenase Type 14 Nonsteroidal Inhibitors and Crystal Structures in Complex with the Enzyme**
Florian Braun, Nicole Bertoletti, Gabriele Möller, Jerzy Adamski, Torsten Steinmetzer, Mohamed Salah, Ahmed S. Abdelsamie, Chris J. van Koppen, Andreas Heine, Gerhard Klebe, and Sandrine Marchais-Oberwinkler
J. Med. Chem. 2016, 59 (23), 10719–10737. doi: 10.1021/acs.jmedchem.6b01436

VI. Inhibitors of 17 β -hydroxysteroid dehydrogenase type 1, 2 and 14: Structures, biological activities and future challenges

Mohamed Salah*, Ahmed S. Abdelsamie*, and Martin Frotscher

Mol. Cell. Endocrinol. 2018. doi: 10.1016/j.mce.2018.10.001

* These authors contributed equally

VII. Design and synthesis of conformationally constraint Dyrk1A inhibitors by creating an intramolecular H-bond involving a benzothiazole core

Mohamed Salah*, Mohammad Abdel-Halim* and Matthias Engel

Medchemcomm 2018, 9 (6), 1045–1053. doi: 10.1039/c8md00142a

* These authors contributed equally

VIII. Development of novel 2,4-bispyridyl thiophene-based compounds as highly potent and selective Dyrk1A inhibitors. Part I: Benzamide and benzylamide derivatives

Sarah S. Darwish, Mohammad Abdel-Halim, Mohamed Salah, Ashraf H. Abadi, Walter Becker, Matthias Engel

Eur. J. Med. Chem. 2018, 157, 1031–1050. doi: 10.1016/j.ejmech.2018.07.050

IX. Development of novel amide-derivatized 2,4-bispyridyl thiophenes as highly potent and selective Dyrk1A inhibitors. Part II: Identification of the cyclopropylamide moiety as a key modification

Sarah S. Darwish, Mohammad Abdel-Halim, Ahmed K. ElHady, Mohamed Salah, Ashraf H. Abadi, Walter Becker, Matthias Engel

Eur. J. Med. Chem. 2018, 158, 270–285. doi: 10.1016/j.ejmech.2018.08.097

Contribution Report

The author wishes to clarify his contributions to the papers **I-IX** in the thesis:

- I. The author contributed significantly to the rational design concept. He planned, synthesized and characterized all the compounds. He further performed the cell-free and cellular activity assays. Additionally, he established and performed the stimulated growth assays. He conceived and wrote the manuscript.
- II. The author performed the synthesis and characterization of the compounds, the in vitro cell-free and cellular inhibition assays, and the in vitro toxicity assays.
- III. The author contributed to the design, synthesis and characterization of the compounds. He further contributed in the biological assays and the interpretation of the results.
- IV. The author contributed significantly to the in vitro biological evaluation of the synthesized compounds. Furthermore, He contributed in the interpretation of the results and writing the manuscript.
- V. The author planned, performed and interpreted the radiolabeled biological assays. Additionally, he contributed in writing the manuscript.
- VI. The author collected the data for all 17 β -HSD1 inhibitors from literature, and significantly contributed in the selection of the represented candidates of each class. He wrote this part in the review and contributed in the other parts.
- VII. The author contributed significantly to the design concept. He planned, synthesized and characterized all the compounds. He further performed the biological activity assays. The author conceived and wrote the manuscript together with Mohammad Abdel-Halim, who contributed equally.
- VIII. The author performed the kinase inhibition assays as well as the cellular viability assays. He further carried out the in silico physiochemical characterization of the compounds. He contributed in the interpretation of the results.

- IX. The author significantly contributed in the kinase inhibition assays as well as the cellular viability assays. He further carried out the *in silico* physiochemical characterization of the compounds. He contributed in the interpretation of the results.

Further work of the author not included in the thesis

I. Design, Synthesis and Biological Characterization of Orally Active 17 β -Hydroxysteroid Dehydrogenase Type 2 Inhibitors for the Prevention of Osteoporosis.

Ahmed S. Abdelsamie, Mohamed Salah, Lorenz Siebenbürger, Ahmed Merabet, Claudia Scheuer, Martin Frotscher, Sebastian T. Müller, Oliver Zierau, Günter Vollmer, Michael D. Menger, Matthias W. Laschke, Chris J. van Koppen, Sandrine MarchaisOberwinkler, Rolf W. Hartmann

Submitted to *J. Med. Chem.* and currently under revision.

II. Monograph: Dual Targeting of STS and 17 β -HSD1 by Drug Prodrug Approach; a Novel Therapeutic option for the Treatment of Estrogen-Dependent Diseases.

Manuscript in preparation.

Abbreviations

| | |
|-------------------|--|
| 17 β -HSD | 17 β -hydroxysteroid dehydrogenase |
| 3 β -HSD2 | 3 β -hydroxysteroid dehydrogenase/ δ 5 \rightarrow 4-isomerase type 2 |
| A4 | Androstenedione |
| Adiol(-S) | Androstenediol(-Sulfate) |
| AhR | Aryl hydrocarbon receptor |
| AKR | Aldo-keto reductase |
| AUC | Area under the curve |
| BSH | Bicyclic substituted hydroxyphenylmethanone |
| Cl _{int} | Intrinsic clearance |
| COX-2 | Cyclooxygenase type 2 |
| CYP | Cytochrome P450 |
| CYP11A1 | Cholesterol desmolase |
| CYP17A1 | Bifunctional 17 α -hydroxylase/17,20 lyase |
| CYP19A1 | Aromatase enzyme |
| DASIs | Dual aromatase and STS inhibitors |
| DHEA(-S) | Dihydroepiandrosterone(-Sulfate) |
| DHT | Dihydrotestosterone |
| DMA | Dimethyl acetamide |
| DME | Dimethyl ether |
| DMF | Dimethyl formamide |
| DML | Designed multiple ligand |
| DSHIs | Dual STS and 17 β -HSD1 inhibitors |
| E1(-S) | Estrone(-Sulfate) |
| E2 | Estradiol |
| E2MATE | Estradiol-3-O-sulfamate |
| E3 | Estriol |
| EDDs | Estrogen dependent diseases |
| EMATE | Estrone-3-O-sulfamate |
| ER | Estrogen receptors |
| EREs | Estrogen-responsive elements |

| | |
|------------------|---|
| FSH | Follicle-stimulating hormone |
| GnRH | Gonadotropin-releasing hormone |
| LH | Luteinizing hormone |
| NAD ⁺ | Nicotinamide adenine dinucleotide |
| NADPH | Dihyronicotinamide adenine dinucleotide phosphate |
| NSAIDs | Non-steroidal anti-inflammatory drugs |
| OATPs | Organic anion transporting polypeptides |
| PGE ₂ | Prostaglandin type 2 |
| PK | Pharmacokinetic |
| SCC | Side-chain cleavage enzyme |
| SD | Standard deviation |
| SDR | Short chain dehydrogenase/reductase |
| SF | Selectivity factor |
| StAR | Steroid acute regulatory |
| STS | Steroid sulfatase |
| SULT(E1) | (Estrogen) Sulfotransferase |
| T | Testosterone |

Summary

Endometriosis is an estrogen dependent disease (EDD) that has no satisfying treatment option, as the existing ones mainly comprise endocrine treatments that lead to severe systemic hypo-estrogenic side effects. Steroid sulfatase (STS) and 17 β -hydroxysteroid dehydrogenase type 1 (17 β -HSD1) are attractive new targets for the treatment of EDDs. Their inhibition leads to blockage of the local biosynthesis of estrogen without significantly affecting the circulating estrogen. The simultaneous inhibition of both enzymes appears to be more promising than the blockage of only one protein.

The main aim of this study is the development of dual inhibitors of STS and 17 β -HSD1 (DSHIs) that offers a novel treatment option for endometriosis without severe side effects. Using a designed multiple ligand (DML) approach, the first DSHIs were identified. Upon structural optimizations, highly potent inhibitors in cell-free and cellular assays were achieved that are characterized by high selectivity over 17 β -HSD2 which plays a protective role in endometriosis. The DSHIs were able to efficiently reverse the E1-S and E1- induced T47D cell proliferation. The most interesting inhibitor described in this work is characterized by high metabolic stability in human and mouse hepatic S9 fraction, along with good physicochemical properties and high safety margins in cytotoxicity assays. Furthermore, this DSHI is considered a suitable candidate for in vivo proof-of-principle studies based on its pharmacokinetic profile.

Zusammenfassung

Endometriose ist eine Estrogen-abhängige Erkrankung für die bislang keine zufriedenstellende Therapieoption existiert. Zum Einsatz kommen hauptsächlich endokrine Behandlungen, die systemisch zu stark hypoestrogenen Zuständen und damit zusammenhängenden, ernsthaften Nebenwirkungen führen. Die Enzyme Steroid Sulfatase (STS) und 17 β -Hydroxysteroid Dehydrogenase Typ 1 (17 β -HSD1) sind attraktive, neuartige Targets zur Behandlung Estrogen-abhängiger Erkrankung. Ihre Inhibierung führt zur Hemmung lokaler Estrogen-Biosynthese, ohne starke Beeinflussung systemischer Estrogen-Konzentrationen. Die gleichzeitige Hemmung beider Enzyme erscheint vielversprechender als die Blockade eines einzelnen Proteins.

Ein Gegenstand der vorliegenden Arbeit ist die Entwicklung dualer Inhibitoren von STS und 17 β -HSD1 (DSHIs). Solche Wirkstoffe sind eine neuartige Therapieoption für Endometriose, die nicht zu den erwähnten Nebenwirkungen führt. Unter Anwendung eines Ansatzes zum gezielten Design von Liganden mehrerer biologischer Targets wurden die ersten DSHIs identifiziert. Anschließende Strukturoptimierungen führten zu Wirkstoffen, die in Zell-freien und zellbasierten Assays beide Targetenzyme hochpotent hemmten. Darüberhinaus waren die DSHIs in der Lage, die Estronsulfat- und Estron-induzierte Proliferation von T47D Zellen vollständig aufzuheben. Die vielversprechendste Verbindung zeigt hohe metabolische Stabilität in den S9-Lebermikrosomenfraktionen von Mensch und Maus, vorteilhafte physiko-chemische Eigenschaften und geringe Cytotoxizität. Darüberhinaus zeigte sie günstige pharmakokinetische Eigenschaften in der Maus, was sie zu einem geeigneten Kandidaten für eine proof-of-principle Studie macht.

Table of content

| | |
|---|------|
| Acknowledgements | V |
| Papers included in the thesis | VI |
| Contribution Report..... | VIII |
| Further work of the author not included in the thesis | X |
| Abbreviations | XI |
| Summary | XIII |
| Zusammenfassung..... | XIV |
| 1. Introduction..... | 1 |
| 1.1 Estrogen..... | 1 |
| 1.1.I Estrogen as a steroid hormone | 1 |
| 1.1.II Biosynthesis and regulation | 1 |
| 1.1.III Mechanism of action and physiological roles | 5 |
| 1.2 Endometriosis | 6 |
| 1.2.I General aspects | 6 |
| 1.2.II Etiology and pathogenesis..... | 6 |
| 1.2.III Current treatment interventions..... | 7 |
| 1.3 Local biosynthesis of estrogen in endometriosis | 9 |
| 1.3.I Sources of estrogen in endometriosis | 9 |
| 1.3.II Steroid sulfatases (STS) | 10 |
| 1.3.III 17 β -Hydroxysteroid dehydrogenase type 1 (17 β -HSD1)..... | 12 |
| 1.4 Novel treatment approaches for endometriosis | 16 |
| 1.4.I STS inhibitors | 16 |
| 1.4.II 17 β -HSD1 inhibitors | 17 |
| 1.4.III Designed multiple ligands | 19 |
| 2. Aim of the thesis | 21 |
| 3. Results..... | 24 |
| 3.1 Dual STS and 17 β -HSD1 inhibitors (DSHIs)..... | 24 |
| 3.1.I First Dual Inhibitors of Steroid Sulfatase (STS) and 17 β -Hydroxysteroid Dehydrogenase Type 1 (17 β -HSD1): Designed Multiple Ligands as Novel Potential Therapeutics for Estrogen-Dependent Diseases | 24 |
| 3.1.II Potent Dual Inhibitors of Steroid Sulfatase (STS) and 17 β -Hydroxysteroid Dehydrogenase Type 1 (17 β -HSD1) with a Suitable Pharmacokinetic Profile for an in Vivo Proof-of-Principle Study in an Endometriosis Mouse Model | 32 |

| | | |
|---------|--|-----|
| 3.2 | Selective inhibitors of 17 β -HSD1, 2 and 14..... | 53 |
| 3.2.I | Treatment of estrogen-dependent diseases: Design, synthesis and profiling of a selective 17 β -HSD1 inhibitor with sub-nanomolar IC ₅₀ for a proof-of-principle study..... | 53 |
| 3.2.II | Targeted Endocrine Therapy: Design, Synthesis, and Proof-of-Principle of 17 β -Hydroxysteroid Dehydrogenase Type 2 Inhibitors in Bone Fracture Healing | 68 |
| 3.2.III | First Structure Activity Relationship of 17 β -Hydroxysteroid Dehydrogenase Type 14 Nonsteroidal Inhibitors and Crystal Structures in Complex with the Enzyme..... | 80 |
| 3.2.IV | Inhibitors of 17 β -hydroxysteroid dehydrogenase type 1, 2 and 14: Structures, biological activities and future challenges | 100 |
| 4. | Final Discussion..... | 119 |
| 4.1 | Design rationale of DSHIs..... | 119 |
| 4.2 | Biological profiling of DSHIs | 120 |
| 4.3 | Effect of DSHIs on estrogen-stimulated growth | 122 |
| 4.4 | Further in vitro biological evaluation of DSHIs | 122 |
| 4.5 | In vivo evaluation of pharmacokinetic profile of DSHIs | 123 |
| 4.6 | Conclusion | 124 |
| 4.7 | Outlook | 125 |
| 5. | Supporting information..... | 126 |
| 5.1. | Supporting information for publication A | 126 |
| 5.1.I | Chemistry..... | 126 |
| 5.1.II | Biological methods..... | 158 |
| 5.1.III | Further results..... | 162 |
| 5.1.IV | References | 166 |
| 5.2 | Supporting information for Monograph B..... | 167 |
| 5.2.I | Chemistry..... | 167 |
| 5.2.II | Biological methods..... | 195 |
| 5.2.III | Oral bioavailability..... | 200 |
| 6. | References..... | 201 |
| 7. | Additional publications of the author | 213 |
| 7.1 | Design and synthesis of conformationally constraint Dyrk1A inhibitors by creating an intramolecular H-bond involving a benzothiazole core..... | 213 |
| 7.2 | Development of novel 2,4-bispyridyl thiophene-based compounds as highly potent and selective Dyrk1A inhibitors. Part I: Benzamide and benzylamide derivatives | 223 |
| 7.3 | Development of novel amide-derivatized 2,4-bispyridyl thiophenes as highly potent and selective Dyrk1A inhibitors. Part II: Identification of the cyclopropylamide moiety as a key modification..... | 244 |

| | | |
|-----|-------------------------------|-----|
| 8. | Appendix..... | 261 |
| 8.1 | Curriculum Vitae | 261 |
| 8.2 | Publications | 262 |
| 8.3 | Conference Contributions..... | 263 |

1. Introduction

1.1 Estrogen

1.1.I Estrogen as a steroid hormone

Steroid hormones are cholesterol-derived chemical messengers that exert transient physiological effects as well as permanent developmental actions on the body from fetal life to adulthood^{1,2}. They can be categorized into two groups according to the main sites of production in the body: corticosteroids which are mainly biosynthesized in the adrenal cortex and the sex steroids which are typically biosynthesized in the reproductive organs of males and females². The corticosteroids are further subdivided into mineralocorticoids which control the balance of water and minerals in the body, and glucocorticoids which control the glucose homeostasis and play a role in the feedback mechanism of the immune system. The sex steroids can be subcategorized into progestogens (C21 steroids), androgens (C19 steroids) and estrogens (C18 steroids). Progesterone is the most important progestogen in the human body which binds to the progesterone receptor and plays an important role in the female reproductive system during pregnancy and menstrual cycle. The main representatives of androgens are testosterone (T), dihydrotestosterone (DHT) which are the main sex steroid hormones in men. Dihydroepiandrosterone (DHEA) which is mainly secreted by the adrenal cortex and androstenedione (A4) are crucial androgens in the steroidogenesis pathway. Androstenediol (Adiol) is also a C21 steroid; however, it has an estrogenic effect³. Estrogens are the major sex steroid in females which arise from the aromatization of androgens steroidal A- ring. Estradiol (E2) is the most active form of the estrogen family, while estrone (E1) and estriol (E3) are less estrogenic.

1.1.II Biosynthesis and regulation

In women of reproductive age, circulating estrogens are biosynthesized mainly in the ovaries and released to the systemic circulation to act on target cells or tissues (endocrine mechanism)⁴. The biosynthesis (see figure 1) starts in the mitochondria in which the cholesterol side chain is cleaved by the action of CYP11A1 (side-chain cleavage enzyme SCC) to give pregnenolone. In the smooth endoplasmic reticulum, 3 β -hydroxysteroid dehydrogenase/ δ 5 \rightarrow 4-isomerase type 2 (3 β -HSD2) converts pregnenolone into progesterone by oxidizing the 3 β -hydroxy function and shifting the double bond position. The bifunctional 17 α -hydroxylase/17,20 lyase (CYP17A1) transforms the produced progestogens by oxidation at the 17 α position followed by lysis reaction at position 20 to give the corresponding

androgens DHEA and A4⁵. In principle, there are 2 pathways for estrogen formation. The first is through the irreversible aromatization of the steroidal A-ring of A4 by the action of the microsomal aromatase enzyme (CYP19A1), followed by the reversible reduction of the C-17 keto group by the action of 17 β -hydroxysteroid dehydrogenase (17 β -HSD) enzymes (will be discussed in details in section 1.3.3). Alternatively, the reduction step can be initially performed to give testosterone from DHEA via Adiol, followed by subsequent aromatization to give E2. In the ovaries the main pathway for estrogen biosynthesis consists of the conversion of DHEA to A4 by the action of 3 β -HSD2, followed by aromatization with CYP19A1 to give E1. The latter is subsequently reduced to E2 mainly by the action of 17 β -HSD 7 and 12^{6,7}.

Estrogen production from the ovaries is regulated through an endocrine mechanism that involves hypothalamus-pituitary-gonadal glands⁸. Gonadotropin-releasing hormone (GnRH) is secreted by the hypothalamus to stimulate the anterior pituitary gland to produce follicle-stimulating hormone (FSH) and luteinizing hormone (LH). FSH triggers the follicle maturation, while LH stimulates the ovulation process and the corpus luteum formation. In the thecal cells of the mature follicle, LH stimulates the formation of androgens which will be converted into estrogens in the granulosa cells under the stimulation of FSH through the abovementioned biosynthetic pathway⁸⁻¹⁰. The levels of circulating E2 in premenopausal women are subjected to fluctuations during the menstrual cycle. In the follicular phase (the first half of the cycle), the E2 in the plasma comes mainly from the mature follicle cells, E2 increases gradually, reaching its highest level at ovulation time. After ovulation, the E2 level decreases temporarily until the corpus luteum is formed (luteal phase) which elevates the estrogen levels as well as the progesterone. At the end of the cycle basal levels are reached again which lead to the menses bleeding.

Estrogens are also produced by other peripheral tissues but to lower extent e.g. placenta, endometrium, liver, adipose tissue, brain and skin^{4,11,12}. These tissues use the inactive circulating sulfated forms of E1 (E1-S) and androgens which are secreted by the adrenal cortex (DHEA-S and Adiol-S), and convert them into their free parents by the action of the steroid sulfatase enzyme (STS) (will be discussed in further details in section 1.3.2). The formed E1 will then be converted into E2 by the reductive 17 β -HSD1 enzyme in a pathway known as the “sulfatase pathway”¹³. The androgens are transformed into testosterone which will be subsequently aromatized by CYP19A1 to give E2 “aromatase pathway”¹⁴. These tissues mainly utilize the E2 produced intracellularly via the intracrine mechanism, in which

the active steroids are directly biosynthesized in the target cells without release into the extracellular matrix ¹⁵.

In postmenopausal women, ovarian estrogen production is stopped and the plasma E2 levels drop significantly to one tenth of the premenopausal levels. The peripheral estrogens become the dominating one in the plasma without observed fluctuation ^{4,16}. Additionally, all the peripheral tissues become dependent on the intracellularly biosynthesized steroids which are utilized by intracrine fashion ¹⁷.

Estrogens are metabolized mainly in the liver; this involves the conversion of E2 into less active E1 by the action of 17 β -HSD2. E1 can be further sulfated by estrogen sulfotransferase enzyme (SULTE1) to give E1-S (inactive) ^{4,18}.

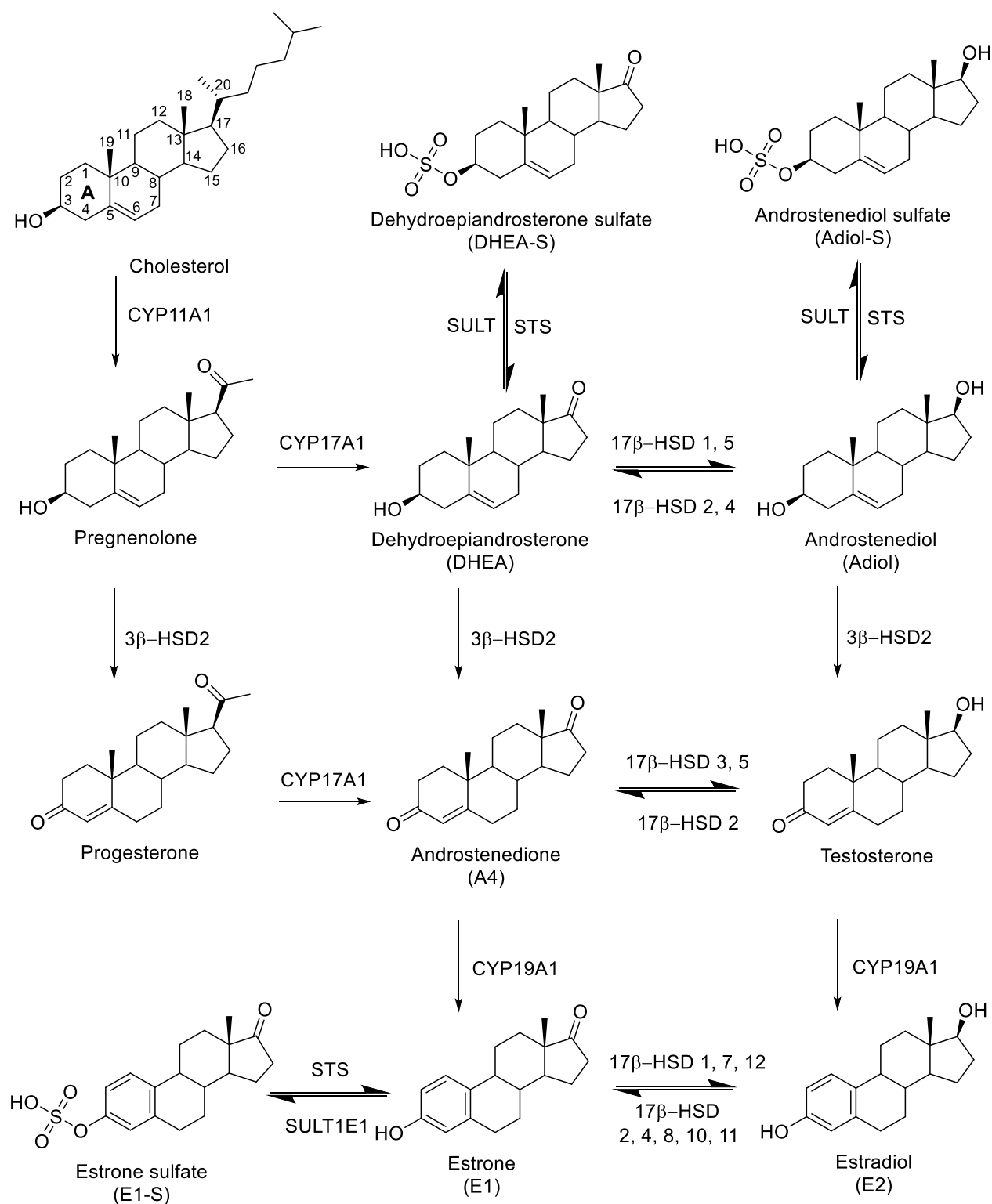


Figure 1 Estrogen biosynthesis from cholesterol E1-S, DHEA-S and Adiol-S.

17 β -HSD, 17 β -hydroxysteroid dehydrogenase; 3 β -HSD2, 3 β -hydroxysteroid dehydrogenase/ $\delta 5 \rightarrow 4$ -isomerase type 2; CYP19A1, aromatase; CYP11A1, Cholesterol desmolase; SULT, sulfotransferase; SULT1E1, estrogen sulfotransferase; STS, steroid sulfatase.

1.1.III Mechanism of action and physiological roles

Estrogens exert their effects mainly by binding to the widely spread estrogen receptors (ER)^{19,20}. Currently, two subtypes of the ER are known: ER α and ER β , having different isoforms with distinct tissue expression²¹. ERs located in the cytoplasm are activated upon binding to E2, and then this complex is translocated into the nucleus after dimerization. In the nucleus, these activated ER dimers activate or repress target genes either directly or via binding to estrogen-responsive elements (EREs) and other DNA-bound transcription factors²⁰. This pathway is known as the genomic signaling pathway of ERs (see figure 2).

The physiological actions that result from ER activation are dependent on the organ where the ERs are located. Classical roles of estrogens in females are the development of secondary sex characters and reproduction. In the female reproductive system, E2 helps in stimulating the proliferation of the granulosa cells and the development of the follicles in the ovaries^{8,22}. The endometrial growth is stimulated by estrogen²³, where the menstrual cycle is closely controlled by E2 and progesterone²⁴. Additionally, E2 and progesterone are essential for the maintenance of the pregnancy and the fetal development²⁵. In the breast, the E2 stimulates the proliferation of the normal breast epithelium^{26,27}. In addition to its classical roles, E2 has a wide range of physiological roles in extra-gonadal systems²⁰. In the skeletal system, E2 regulates the bone turnover by keeping balance between osteoblasts and the osteoclasts thus maintaining the bone density and preventing osteoporosis^{28,29}. Estrogens are also linked to the cardiovascular system, in which they have a cardio-protective effect through preventing the dysfunction of the myocytes in cases of ischemia and hypertension^{20,30}. Moreover, they exert a neuroprotective effect in the central nervous system by decreasing the inflammation in cases of stress and enhancing the memory^{31,32}.

These diverse crucial physiological roles of estrogens in the female body, especially the proliferative anti-apoptotic effects are closely linked to the initiation and the progression of many diseases whenever a misbalance in the estrogen levels occurs³³. These diseases are known as estrogen dependent diseases (EDDs), that include various kinds of female cancers³⁴: breast^{35,36}, ovarian^{37,38} and endometrial cancers^{39,40}. Endometriosis^{41,42} and osteoporosis⁴³⁻⁴⁵ are frequent disorders that are strongly linked to estrogens in females.

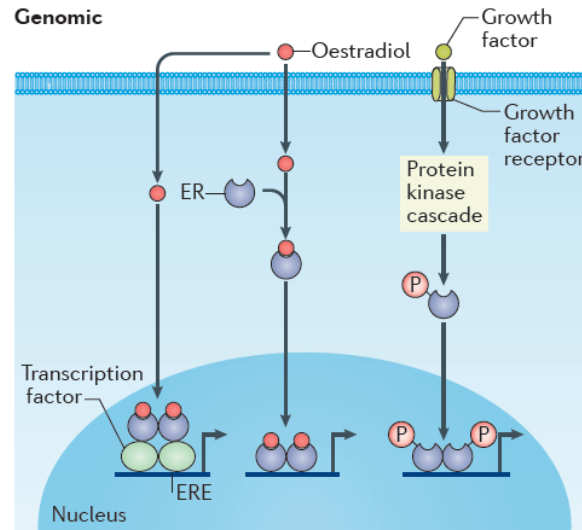


Figure 2 Genomic signaling pathway of estrogen receptor. ER, estrogen receptor; ERE, estrogen-responsive elements. Taken from Morselli *et al.*²⁰.

1.2 Endometriosis

1.2.I General aspects

Endometriosis is a chronic, inflammatory, estrogen dependent disease. This gynecological disorder is characterized by the presence of endometrial glands and stroma in ectopic locations outside the uterine cavity, typically in the ovaries (ovarian endometriosis), the pelvic peritoneum (peritoneal endometriosis), the rectovaginal septum (deep endometriotic nodules of the rectovaginal septum) and other pelvic sites (fallopian tubes, vagina, cervix and uterosacral ligaments)^{46,47}.

Symptoms of endometriosis include chronic pelvic pain, dysmenorrhea, dyspareunia, irregular uterine bleeding, and in many cases infertility^{48,49}. Thus, endometriosis significantly impair the quality of life^{49,50}. Endometriosis is estimated to be affecting 10% of women in reproductive age, while the frequency rises to 50–60% within women suffering from pain⁵¹.

1.2.II Etiology and pathogenesis

Although endometriosis is histologically a benign disorder, it has a malignant-like character as it can grow and develop in the surrounding tissues⁴¹. Despite years of research, the etiology of this disease is not fully understood. However, there are two main theories that explain the pathogenesis of endometriosis. The first theory postulates that the endometriotic lesions originate from the uterine endometrium cells which reach the pelvic sites through retrograde menstruation through the fallopian tubes (retrograde theory)^{52,53}. The second

theory hypothesizes that the implants arise from non-endometrium origin, via transformation of the pelvic cells into endometriosis (metaplasia theory) ⁵⁴. After the estrogen-sensitive endometriotic lesion is implanted on the surface of the peritoneum or ovaries, an inflammatory response is initiated which is accompanied by angiogenesis, adhesion to tissues, fibrosis, neuronal infiltration, and anatomical distortion resulting in pain and infertility ^{48,51}.

At the molecular level, there is a positive-feedback mechanism between E2 and prostaglandin type 2 (PGE₂) productions in endometriotic tissues which induce both pain and further tissue growth (see figure 3) ⁵⁵. The high levels of E2 in the endometriotic lesion on the one hand enhance the cellular proliferation and invasion of the endometriotic tissue (growth), and on the other induce cyclooxygenase type 2 (COX-2) ⁵⁶. The induction of COX-2 results in increased biosynthesis of PGE₂ which is the primary cause of inflammation and pain ⁵⁶. PGE₂ stimulates the de novo androgen synthesis from cholesterol via enhancing the expression of the steroid acute regulatory (StAR) proteins which transfer the cholesterol from the cytoplasm to the mitochondria. Moreover, the expressions of CYP11A1, CYP17A1 and 3β-HSD2 are enhanced by PGE₂ ^{57,58}. In the stromal cells of the endometriotic lesions, CYP19A1 -which is also induced by the PGE₂- will aromatize A4 (from intracellular and extracellular origins) into E1. The latter is reduced by 17β-HSD1 which is overexpressed in the lesions to give E2 ⁵⁹. This establishes a strong positive-feedback cycle that guarantees continuous biosynthesis of E2 and PGE₂ in the endometriosis that results in continuous pain and tissue progression ⁵⁵.

1.2.III Current treatment interventions

Current treatment interventions include surgical removal of the endometriotic lesions and/or medical therapy ^{51,60,61}. The surgical procedure, if possible at all, is only a temporary solution, since the endometriosis usually forms again after a while, even with subsequent drug therapy ⁶².

As shown in the previous section, E2 has a vital role in progression of the disease. Therefore, all current hormonal treatment options aim at decreasing the circulating estrogens ⁶¹. This makes the drug treatment challenging due to the need of tolerable chronic regimen, since it aims at reduction of pain symptoms and progression without definitely curing the disease which may persist and even progress after the termination of the therapy ^{63,64}.

The first line therapy includes NSAIDs co-administered with either combined oral contraceptives or progestins which decrease the GnRH release from the hypothalamus. The second line therapy includes GnRH (ant)agonists or aromatase inhibitors ^{51,61,63,64}.

Generally, all the systemic endocrine therapies result in the suppression of the ovulation and

radical non-selective reduction of circulating estrogen levels leading to severe postmenopausal-like side effects (e.g. loss of bone mineral density) that restrict its use to 6-9 months^{51,60}.

Danazol, an anterior pituitary suppressant that inhibits the production of gonadotropins, is applied when all other options are ineffective as it has severe hyper androgenic side effects that limit its use⁵¹.

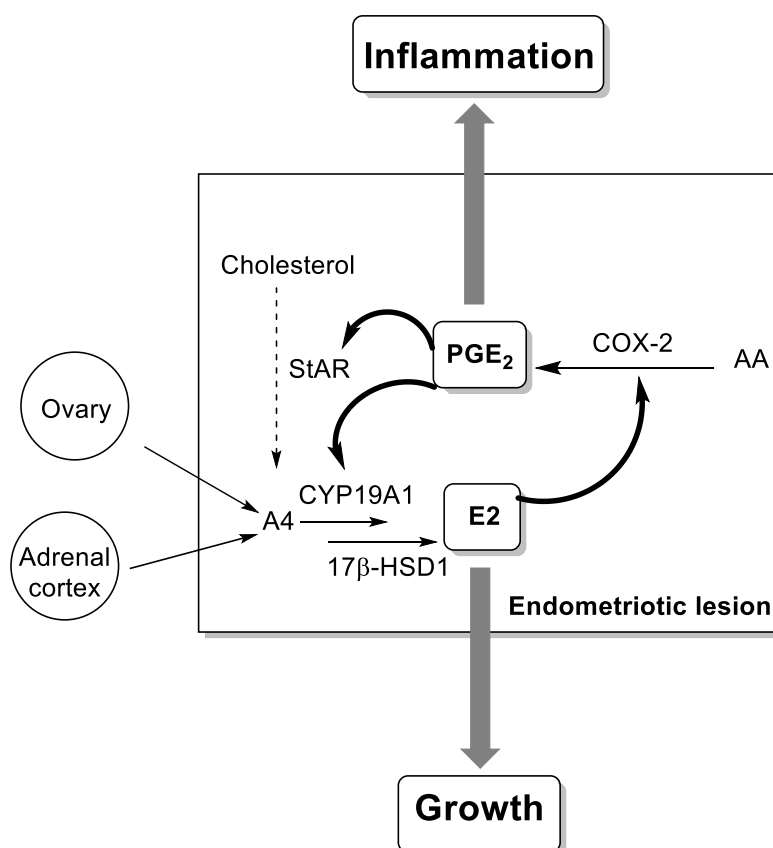


Figure 3 Schematic representation of the positive-feedback cycle for E2 and PGE₂ in endometriotic lesions. Revised from Bulun *et al.*⁵⁵.

AA: arachidonic acid; A4, androsterone; COX-2, cyclooxygenase-2; CYP19A1, aromatase; E2, estradiol; PGE₂: prostaglandin E₂; StAR, steroidogenic acute regulatory protein.

In summary, the existing medical treatments for endometriosis are not satisfying as they suffer from severe side effects which are linked to the suppression of the systemic estrogen levels. Thus, there is a medical need for a novel treatment approach for endometriosis that could efficiently regress it, without affecting the circulating E2 levels possibly offering a better safety profile and longer treatment window.

Intriguingly, the intra-endometriotic tissue levels of E2 and E1 were found to be 8-10 folds higher than the corresponding serum estrogens⁶⁵. Moreover, the enzymes involved in the de novo estrogen biosynthesis were found to be overexpressed inside the lesions^{66,67}. These findings suggest that E2 inside the endometriotic tissue is actively controlled by the local

biosynthesis of estrogen⁶⁸. In the following section, the local biosynthesis of estrogen in endometriosis and the main enzymes involved will be discussed in detail.

1.3 Local biosynthesis of estrogen in endometriosis

1.3.I Sources of estrogen in endometriosis

Endometriotic lesions are among the tissues that (over)express all the essential enzymes that enable the synthesis of estrogen via (see figure 4)⁶⁹:

- The classical de novo steroidogenesis from cholesterol
- The aromatase pathway from the circulating sulfated androgens
- The sulfatase pathway from circulating E1-S

For the de novo steroidogenesis, the StAR protein was found to be overexpressed in all types of endometriosis⁵⁷. Moreover, the mRNAs of CYP11A1, CYP17A1 and 3 β -HSD2 were found to be overexpressed^{58,70}. This enhances the conversion of cholesterol into androgens (DHEA and A4). The endometriotic lesion has the ability to locally produce DHEA from its circulating sulfate conjugate as the STS enzyme was found to be overexpressed^{59,71}, and the relatively high STS activity was found to be correlated with the disease severity⁷². CYP19A1 upregulation accelerates the conversion of the androgens into E1 (aromatase pathway)^{73–76}. E1 can also be synthesized by desulfatation of the circulating E1-S with STS enzyme (sulfatase pathway)⁷¹. The final crucial step in E2 synthesis involves the reduction of E1 produced from sulfatase pathway and aromatase pathway via the action of 17 β -HSD1 enzyme which is also overexpressed in endometriosis^{59,66,70}. E2 deactivation into E1 in the endometriotic lesions is impaired as a consequence of reduced expression of 17 β -HSD2^{66,77,78}.

Obviously, STS and 17 β -HSD1 play crucial roles in the elevation of E2 levels inside the endometriotic lesions. Consequently the inhibition of both enzymes can be considered a novel softer treatment approach for endometriosis. This approach on one hand does not completely cut the systemic biosynthesis of estrogen and on the other one it decreases significantly the peripheral biosynthesis of E2 in the endometriotic lesions as further demonstrated in the following chapters.

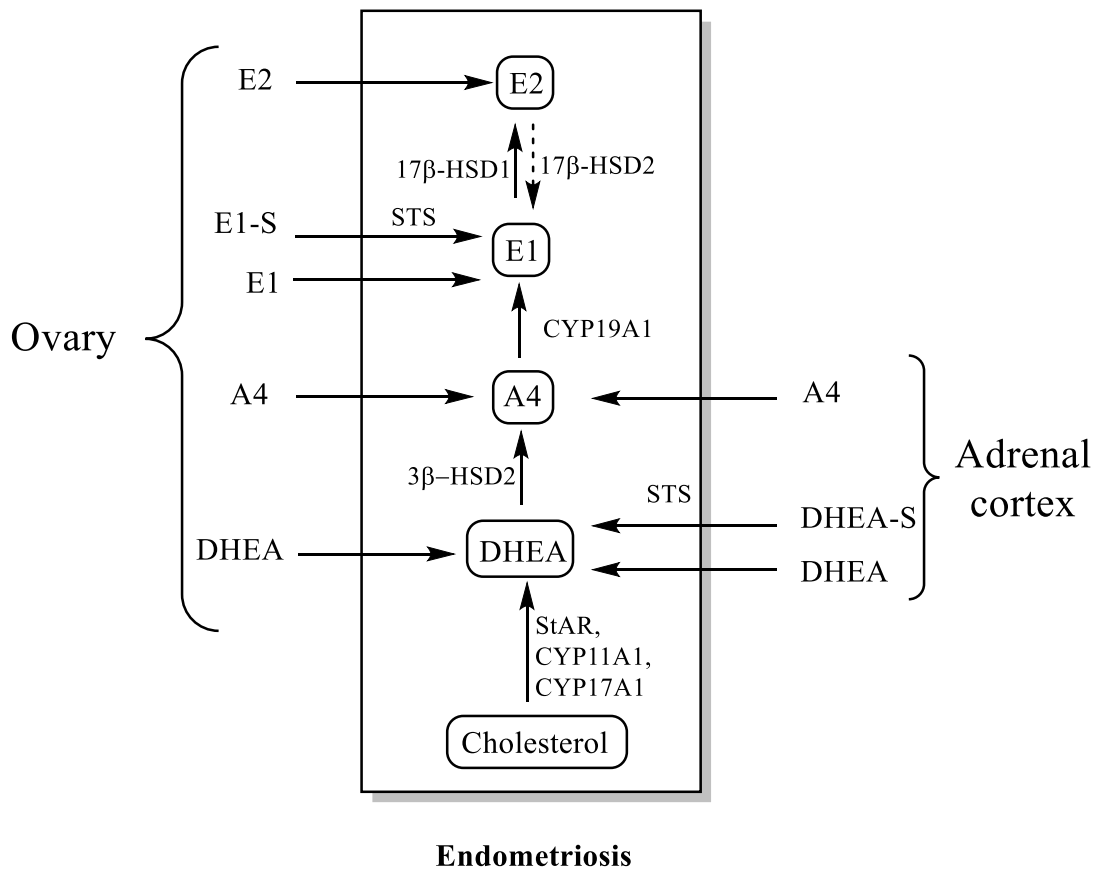


Figure 4 Sources of estradiol in endometriosis. Revised from Huhtinen *et al.* ⁶⁹.

DHEA(-S), Dehydroepiandrosterone (sulfate); A4, androsterone; E1(-S), estrone (sulfate); E2, estradiol; StAR, steroidogenic acute regulatory protein 17 β -HSD, 17 β -hydroxysteroid dehydrogenase; 3 β -HSD2, 3 β -hydroxysteroid dehydrogenase/ δ 5 \rightarrow 4-isomerase type 2; CYP19A1, aromatase; CYP11A1, Cholesterol desmolase; STS, steroid sulfatase.

1.3.II Steroid sulfatases (STS)

1.3.II.1 Sulfation and desulfation of steroids

The steroid sulfation and desulfation are fundamental biological processes that regulate steroidogenesis in the human body ⁷⁹. Two families of enzymes control them, the sulfotransferases (SULTs) and the sulfatases. The sulfation process involves the esterification of sulfate groups with alkyl (e.g. androgens and progestins) and aromatic rings (estrogens) ⁸⁰. The sulfatase action involves the hydrolysis of the above mentioned sulfate group to regenerate the corresponding steroid ⁸¹. The sulfated steroids are highly water soluble and more abundant in the circulation compared to their precursors (see Table 1 taken from ⁷⁹). They represent inactive forms of steroids that are considered as circulating reservoirs for the peripheral formation of bioactive steroids that can be used in an intracrine fashion ^{79,81,82}.

Table 1. Approximate estimates of plasma concentrations of steroids and their sulfated conjugates in females taken from Mueller et al.⁷⁹

| Steroid | Premenopausal females | Postmenopausal females |
|---------|-----------------------|------------------------|
| DHEA | 5-30 nmol/L | 2-20 nmol/L |
| DHEA-S | 1-8 μ mol/L | 1-6 μ mol/L |
| A4 | 2-4 nmol/L | not available |
| A4-S | 0.5-1 μ mol/L | not available |
| E1 | 15-500 pmol/L | 10-120 pmol/L |
| E1-S | 2-5 nmol/L | 0.5-2 nmol/L |
| E2 | 5-1000 pmol/L | 5-80 pmol/L |

1.3.II.2 *Biological characteristics of steroid sulfatase (STS)*

The sulfatase family of enzymes contains 3 main subtypes: aryl sulfatase A, B and C, in which subtype C is also known as steroid sulfatase (STS). The STS enzyme - not aryl sulfatases A or B- has been proven to be the primary enzyme to catalyze the hydrolysis of the sulfate ester bond from the steroid sulfates e.g. E1-S and DHEA-S (see figure 1)⁸⁰. Cells actively take up the hydrophilic circulating steroids (E1-S and DHEA-S) via organic anion transporting polypeptides (OATPs). Intracellularly, desulfatation is performed by STS, offering a crucial pathway in regenerating the active steroids (E1 and DHEA) from the predominant, circulating, inactive sulfated conjugates at steroidogenic and nonsteroidogenic tissues⁸¹.

STS (EC 3.1.6.2) is a membrane-bound protein with a molecular weight of 63 KDa, primarily localized to the endoplasmic reticulum^{81,83}. The native crystal structure of STS was published in 2003⁸⁴. The STS enzyme has a wide tissue distribution which includes placenta (the richest source of STS), endometrium, ovary, liver, testis, skin, bone, brain, kidney, prostate, aorta and fetal lung⁸¹.

1.3.II.3 *STS is a potential drug target*

The dysregulation of estrogen sulfation and desulfatation is associated with various EDDs^{79,85,86}. The local E1 production in hormone-dependent breast cancers is strongly linked to the

STS enzyme which shows higher activity and expression in the tumors⁸⁷⁻⁹⁰. In endometriosis, the STS activity is elevated and so is its expression, to which the level of disease severity was correlated^{66,72,91}. The STS up regulation is also associated with other EDDs for e.g. endometrial carcinoma^{92,93}. Obviously, the ability to inhibit STS will serve as a highly desirable pharmacological approach for the treatment of many EDDs.

1.3.III 17 β -Hydroxysteroid dehydrogenase type 1 (17 β -HSD1)

1.3.III.1 17 β -HSDs

Hydroxysteroid dehydrogenases (HSDs) are a family of NADPH/NAD⁺-dependent oxidoreductase, which catalyze regio- and stereo-selective interconversion of ketones and their corresponding secondary alcohol⁹⁴. HSDs play crucial role in the endocrine as well as the intracrine mechanism of steroid hormone actions by transforming inactive hormones to their active analogues and vice versa⁹⁵, which enable a pre-receptor modulation of the hormonal activity^{96,97}.

17 β -HSDs are a group of enzymes that catalyze the oxido/reduction reactions of the 17 β -hydroxy/keto group of androgens and estrogens backbone⁹⁸, however, 17 β -HSDs can also metabolize non-steroidal substrates^{99,100}. 15 mammalian 17 β -HSDs have been discovered so far, 12 of them from the human tissues¹⁰¹. They all belong to the short chain dehydrogenase/reductase (SDR) family with the exception of 17 β -HSD5 which belongs to the aldo-keto reductase (AKR) family¹⁰². Their nomenclature follows their chronological order of discovery, but later the international SDR-initiative proposed a new gene-based nomenclature^{103,104}. These enzymes have diverse tissue distributions, subcellular localizations, substrate affinities and catalytic preferences (oxidation or reduction).

The reducing 17 β -HSDs are mainly distributed among the steroidogenic tissues as shown in Table 2. Their primary physiological role is the synthesis of high levels of sex steroid hormones in the target tissues. Only 3 subtypes are involved in the biosynthesis of E2 from E1, 17 β -HSD1 besides 17 β -HSD12 and 7 which are the main enzymes expressed in the ovaries⁶.

On the other hand, the oxidizing 17 β -HSDs are widely spread in the whole body tissues and not confined to the gonadal tissues (Table 3). In principle, they play protective roles by the inactivation of the active steroids, leading to the decrease in levels of the active steroids in the target tissues. 17 β -HSD2 is the most important steroid deactivator enzyme, which is down regulated or deficient in many pathophysiological disorders^{105,106}.

1.3.III.2 Biological characteristics of 17 β -HSD1

17 β -HSD1 (EC1.1.1.62) was originally described by Langer and Engel in 1958¹⁰⁷. It exists in a soluble homodimer form in the cytosol, having a molecular weight of 34.9 KDa for both dimers representing 327 amino acids¹⁰⁸. The crystal structure of 17 β -HSD1 is known either in native form¹⁰⁹ or in complex with estrogenic ligands¹¹⁰ and steroidal based inhibitors¹¹¹. It catalyzes the final step of the E2 biosynthesis, via reducing the weakly active E1 into the most potent estrogen E2 in the presence of NADPH as a cofactor (see Figure 1). In vivo, the enzyme is only a unidirectional reductive enzyme, however, the purified enzyme or cell homogenates can be forced to catalyze the opposite reaction if the oxidative cofactor (NAD⁺) is abundant¹¹². 17 β -HSD1 can also reduce some forms of androgens e.g. DHEA, but only to a minor extent with 100 fold lower K_m relative to E1, this androgen discrimination was attributed to the steric hindrance of the 19 β -methyl group with the Leu149 amino acid of the enzyme¹¹³.

1.3.III.3 17 β -HSD1 is a potential drug target

In EDDs, increased levels of expression for 17 β -HSD1 are always observed on the mRNA and protein levels, accompanied by down regulation of 17 β -HSD2 which ultimately leads to an increase in the E2/E1 ratio¹¹⁴. In ER⁺ breast cancer patients, the 17 β -HSD1/17 β -HSD2 ratio is increased^{115–117}. In endometriotic patients, the lesions are characterized by up regulation of 17 β -HSD1 and decrease in the 17 β -HSD2 expression when compared to normal endometrium tissue^{55,59,66,71}. In other EDDs, 17 β -HSD1 is highly expressed, e.g. in ovarian cancer¹¹⁸ and endometrial hyperplasia¹¹⁹. Therapeutic approaches aiming to selectively inhibiting 17 β -HSD1 enzyme without affecting the activity of 17 β -HSD2, consequently, is considered an innovative treatment option for many EDDs¹¹⁴.

Table 2. Characteristics of the human reductive 17 β -HSDs

| Enzyme | SDR (AKR) nomenclature | Localization | Substrate | Physiological role | Disease- association | Ref. |
|-------------------|------------------------------|--|---|--|---|-------------|
| 17 β -HSD1 | SDR28C1 | (Cytosol) Breast, endometrium, Ovary, placenta | Estrogens, (androgens) | High concentration of active steroids (E2 and T) in target tissues | Endometriosis, breast and prostate cancer | 105,106,130 |
| 17 β -HSD3 | SDR12C2 | (Microsomes) Testis | Androgens | T synthesis | Pseudohermaphro- ditism in man | 131 |
| 17 β -HSD5 | AKR1C3 | (Cytosol) Breast, liver, prostate | Androgens and estrogens | T and E2 synthesis | Breast and prostate cancer | 132–134 |
| 17 β -HSD7 | SDR37C1 | (Membrane) Ovary, breast, placenta, liver | Estrogens, (cholester- one) | E2 synthesis, cholesterol synthesis | Breast cancer, malformation as CHILD syndrome | 6,135–137 |
| 17 β -HSD12 | SDR12C1 | (Microsomes) Ovary, breast, kidney, liver, placenta | Estrogens, (long chain fatty acids) | E2 synthesis, regulation of lipid biosynthesis | - | 6,138,139 |
| 17 β -HSD15 | - | Prostate | Androgens | - | Prostate cancer | 140 |

Table 3. Characteristics of the human oxidative 17 β -HSDs

| Enzyme | SDR nomenclature | Localization | Substrate | Physiological role | Disease- association | Ref. |
|-------------------|---------------------|--|---|---|---|-------------|
| 17 β -HSD2 | SDR9C2 | (Microsomes) Breast, endometrium, ovary, placenta | Estrogens, androgens | Steroid inactivation | Endometriosis, breast and prostate cancer | 105,106,141 |
| 17 β -HSD4 | SDR8C1 | (Peroxisomes) Breast, liver, lung, placenta | Estrogens, androgens, bile acids, fatty acids | Steroid inactivation, bile acid metabolism, β -oxidation of fatty acids | Prostate cancer | 142 |
| 17 β -HSD8 | SDR30C1 | (Microsomes) Liver, ovary | Estrogens, androgens | Steroid inactivation, fatty acid elongation | - | 98,143 |
| 17 β -HSD10 | SDR5C1 | (Mitochondria) Central nervous system | Estrogens, androgens, bile acids, fatty acids | Steroid inactivation, bile acid and fatty acids metabolism | Alzheimer's disease | 144,145 |
| 17 β -HSD11 | SDR6C2 | (Microsomes) Kidney, liver, lung | Estrogens, androgens | Steroid inactivation, fatty acid metabolism | - | 146,147 |
| 17 β -HSD14 | SDR47C1 | (Cytosol) Liver, placenta, kidney, breast cancer tissue | Estrogens, androgens | - | Breast cancer (prognostic marker) | 148–150 |

1.4 Novel treatment approaches for endometriosis

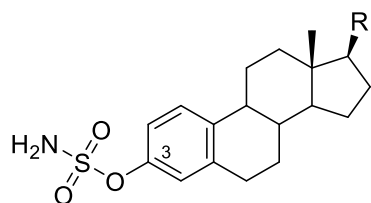
1.4.I STS inhibitors

The development of STS inhibitors as novel endocrine therapeutics for the treatment of EDDs has been initiated since the early 90s¹²⁰. The vast majority of these inhibitors are based on the aryl-O-sulfamate pharmacophore, and considered to be active-site directed, time and concentration dependent, irreversible inhibitors^{86,121}. It is assumed that the sulfamate group is covalently transferred to the post-translationally modified formyl-glycine moiety in the catalytic center of STS enzyme, irreversibly blocking its activity¹²².

Estrone-3-O-sulfamate (EMATE) and estradiol-3-O-sulfamate (E2MATE) were among the early highly potent (both in vitro and in vivo) STS inhibitors that were discovered (see figure 5)^{123,124}. The steroidal backbone of EMATE and E2MATE, however, resulted in considerable estrogenic effect, which contradict with its principal therapeutic goal¹²⁵. Research has focused on the development of non-estrogenic and non-steroidal STS inhibitors, leading to the discovery of a new class of STS inhibitors based on the coumarin-sulfamate scaffold (Coumate, see figure 5)¹²⁶. STX64 (also known as 667 Coumate or Irosustat) was the most important candidate in the Coumate class with one digit nM IC₅₀ values in both cell free and cellular assays¹²⁷. STX64 was orally very active (95% orally bioavailable) as it can evade the liver first-pass metabolism via binding reversibly to carbonic anhydrase II enzyme in red blood cells^{128,129}.

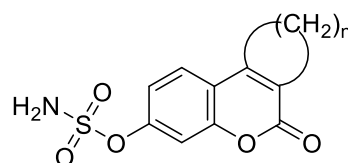
In vivo proof-of-principle studies of STS inhibitors in endometriosis have resulted in very promising outcomes. Collete *et al* have demonstrated that STS inhibition in a mouse endometriosis model led to significant regression in the development of the endometriotic lesion manifested by reduction in the size and weight of the lesion, without affecting the circulating estradiol levels¹⁵¹. Similarly, in a phase I proof-of-principle clinical trial Pohl *et al.* found that irreversible STS inhibition in healthy premenopausal women has no significant effect on E2 plasma levels and was generally well-tolerated by the patients¹⁵². Currently, phase II clinical trials are in progress to evaluate the efficacy, safety, pharmacokinetics and pharmacodynamics of STS inhibitors in endometriotic patients^{85,153}.

In other clinical trials STS inhibitors have been evaluated as therapeutics for various EDDs for e.g. breast cancer^{154–157} and endometrial cancer¹⁵⁸. Generally, the drugs significantly decreased the STS activity in the tumor tissue while being well-tolerated by the patients.



R= =O, Estrone 3-O sulfamate, EMATE

R= -OH, Estradiol 3-O sulfamate, E2MATE



General structure of Coumate-based STS inhibitors

n= 5, STX64 (667 Coumate or Irosustat)

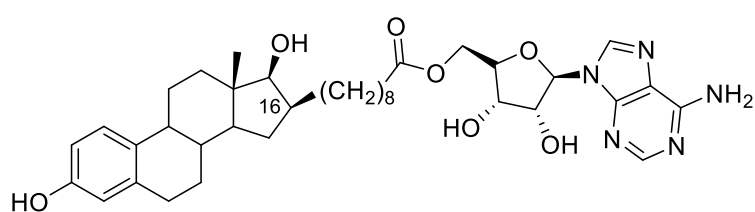
Figure 5 Structures of selected STS inhibitors

1.4.II 17 β -HSD1 inhibitors

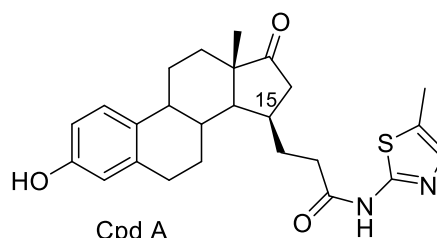
Salah *et al.* recently reviewed the efforts that have been dedicated over the last 35 years to develop 17 β -HSD1 inhibitors that have acceptable selectivity over the counterpart enzyme 17 β -HSD2¹⁵⁹. Various steroidal and non-steroidal inhibitors were shown to be effective in vitro and in vivo.

Steroidal inhibitors are usually derivatives of E1 or E2 that are substituted at one or more of the following positions: C2, C6, C15 and C16. EM-1745 (C16 derivative of E2, see figure 6) is one of the most potent steroidal 17 β -HSD1 inhibitors that is considered a bifunctional hybrid inhibitor binding to both the substrate and the cofactor binding sites¹⁶⁰. An example for C15-substituted derivatives of E1 is compound A (see figure 6), which displayed strong and selective inhibition of 17 β -HSD1 in cell-free and in cellular assays^{161,162}. Moreover, compound A showed strong reduction of E2 levels inside human endometriotic lesions in an ex vivo proof-of-principle study¹⁶³. FOR-6219 (exact structure not published) is a close structural analog of compound A, is currently in phase I clinical trials. In preclinical studies using non-human primates, it displayed the ability to act locally in the target tissues, without impacting systemic hormone levels^{164–166}.

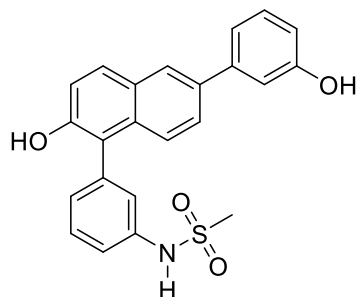
Non-steroidal inhibitors were generally showing several advantages when compared to the steroidal ones, such as low ER-affinity, good synthetic accessibility and drug-likeness. Our research group developed the best non-steroidal 17 β -HSD1 inhibitors known in literature. In general, they belong to 3 chemical classes developed by pharmacophore models (see figure 6): hydroxyphenyl naphthols (e.g. compound B)¹⁶⁷, bis(hydroxyphenyl) substituted arenes (e.g. compound C)¹⁶⁸ and the bicyclic substituted hydroxyphenyl methanones (e.g. compound D)¹⁶⁹ which is the most active class of non-steroidal 17 β -HSD1 inhibitors. Thiophenepyrimidinone derivatives (e.g. compound E, see figure 6) were reported by other group to be potent 17 β -HSD1 inhibitors¹⁷⁰.



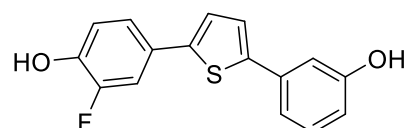
EM-1745
17β-HSD1 cell-free IC₅₀ = 52 nM



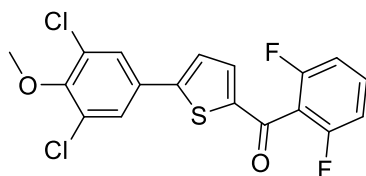
Cpd A
17β-HSD1 cell-free IC₅₀ = 4 nM



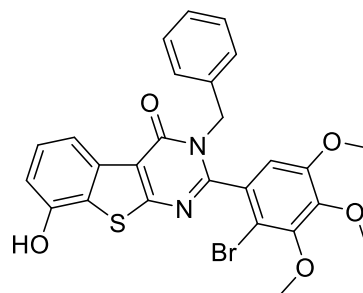
Cpd B
17β-HSD1 cell-free IC₅₀ = 15 nM
Selectivity factor 17β-HSD2/17β-HSD1 = 27



Cpd C
17β-HSD1 cell-free IC₅₀ = 8 nM
Selectivity factor 17β-HSD2/17β-HSD1 = 118



Cpd D
17β-HSD1 cell-free IC₅₀ = 0.5 nM
Selectivity factor 17β-HSD2/17β-HSD1 = 82



Cpd E
17β-HSD1 cell-free IC₅₀ = 5 nM

Figure 6 Structures and biological data of selected 17β-HSD1 inhibitors

1.4.III Designed multiple ligands

As previously mentioned, STS and 17 β -HSD1 activities are upregulated in endometriosis, playing crucial roles in controlling the intracellular E2 concentration inside the lesions⁶⁹. Moreover, it was shown that the administration of aromatase inhibitors in breast cancer patients led to increase in the levels of STS and 17 β -HSD1, which re-elevated the local E2 levels in these patients (estradiol escape)¹⁷¹. This estradiol escape may also play a role in endometriosis if only one of the 2 enzymes (STS or 17 β -HSD1) is blocked (e.g. increased STS expression to counteract the 17 β -HSD1 inhibition and vice versa). As a result, the idea of inhibiting both STS and 17 β -HSD1 is a promising novel approach to decrease the local estrogen biosynthesis in endometriotic lesions. The inhibition of additional pathways of E2 production should ultimately lead to stronger reduction of lesion proliferation and pain, improving the patient's quality of life. Moreover, this dual inhibition may block the estradiol escape that could happen in single therapeutic options avoiding potential relapse of the disease.

This dual inhibition approach could be achieved either by a multi-targeting fashion by co-administration of selective STS inhibitor alongside with selective 17 β -HSD1 inhibitor or via a designed multiple ligand (DML). In the latter approach, a single rationally designed molecule has a multi-target mode of action. There are strong scientific arguments in favor of a DML approach¹⁷², as it has several advantages when compared to the multi-component therapy. In DML, complex pharmacokinetic/pharmacodynamics relationships that could occur in multi-component therapy are avoided, more patient compliance, easier and less expensive clinical development, no drug-drug interaction, and possible decrease in the overall dose when compared to co-administration of 2 selective inhibitors¹⁷². A drawback in DML approach is the possible difficulty to adjust the ratio of activity at both targeted enzymes; however, this complicated design optimization is thought to be minimal in case of STS and 17 β -HSD1 inhibition as a result of the high structural similarity between the substrates of both targeted enzymes (E1-S and E1).

In this context, STS inhibition has been successfully coupled to aromatase inhibition in a DML fashion by using a merged pharmacophore strategy, in which potent aromatase inhibitor was used to build in the aryl sulfamate pharmacophore (essential for STS activity) giving potent dual aromatase and STS inhibitors (DASIs) see figure 7¹⁷³. In preclinical studies, STX681 was able to inhibit in vivo the growth of human breast cancer induced in a xenograft nude mouse model¹⁷⁴, however, it was shown that dual inhibition of STS and aromatase leads

to significant drop in the circulating estrogens which is accompanied by severe hypo-estrogenic side effects ¹⁵⁷.

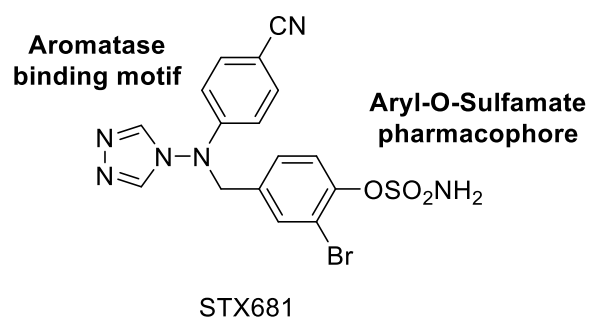


Figure 7 Structure of selected DASI

2. Aim of the thesis

In endometriotic patients, the inhibition of the local biosynthesis of estrogen is currently considered as a superior therapeutic option compared to the conventional endocrine therapy. The latter treatment option aims at stopping the ovulation leading to severe drop in the circulating estrogens accompanied by intolerable hypo-estrogenic side effects that limits the duration of the treatment to 6-9 months. On the other hand, targeting the peripheral E2 synthesis is believed to decrease the progression of endometriosis without significantly affecting E2 plasma levels.

STS and 17 β -HSD1 are pivotal enzymes in the local biosynthesis of E2 in the endometriotic lesions, as they were found to be overexpressed in all types of endometriosis where the levels of STS expression were correlated to the severity of the disease. The most abundant form of estrogen in the circulation (E1-S) is transformed by STS in the lesion to E1 which is further activated by 17 β -HSD1 into E2. This biosynthesis sequence is known as sulfatase pathway. E2 is the most potent activator of ER α/β that induces cell proliferation and pain inside the lesion. 17 β -HSD2 activity inside the lesion is down regulated, weakening its beneficial action in deactivating E2 into E1.

Recently, several proof-of-principle studies have shown the efficacy of STS or 17 β -HSD1 inhibition in endometriotic models. In endometriotic mouse model, STS inhibition led to significant decrease in the lesion size. Moreover, in a phase I clinical trial effective STS inhibition was found to have no significant effect on E2 levels in premenopausal women. On the other hand, 17 β -HSD1 inhibition in an ex vivo proof-of-principle study normalized the increase in E2 synthesis in endometriotic tissue of patients. Additionally, no effect was detected on the systemic E2 level in preclinical studies using non-human primates treated with potent 17 β -HSD1 inhibitor. Since the inhibition of STS or 17 β -HSD1 was shown to be effective in endometriosis, it was thought that their dual inhibition would even be more effective. This dual inhibition could be achieved by multi-component therapy or designed multiple ligands (DML). The DML approach has several advantages, e.g. less complicated pharmacokinetic and pharmacodynamics relationship, easier clinical development, avoiding drug-drug interaction and good patient compliance.

Accordingly, the aim of the thesis was to develop potent dual STS and 17 β -HSD1 inhibitors (DSHIs) that are suitable for in vivo application. These inhibitors could be used as scientific tools in proof-of-principle studies to elucidate the effect of the dual inhibition on the

local biosynthesis of E2 regulation in endometriotic models, and also serve as lead compounds for a novel therapeutic option for the treatment of endometriosis.

To achieve this purpose, the first DSHIs class shall be rationally designed via a combined pharmacophore strategy (see figure 8), in which the aryl sulfamate moiety has to be introduced to potent drug-like 17 β -HSD1 inhibitors. This should be followed by optimizing the position of the sulfamate group on the aryl system and evaluating the influence of adding different substituents on the biological activities of the synthesized compounds. The biological evaluation of the compounds should not be confined to their ability to inhibit STS and 17 β -HSD1 in cell-free assays, but also their selectivity towards 17 β -HSD2 should be evaluated. Furthermore, T47D cells (ER⁺ breast cancer cell line) which express both enzymes can be used to evaluate the intracellular potency of the promising DSHIs to have insights regarding their cellular permeability. Generally, sulfamate group containing STS inhibitors are irreversible active-site directed inhibitors, so the mode of STS inhibition by the most promising DSHIs has to be examined using intracellular assay. Evaluation of the effect of estrogen stimulation on the growth of T47D cells using E1-S or E1 or E2 should be done in order to show that the cells can convert E1-S and E1 into E2 leading to stimulation in the proliferation. Then the effect of the DSHIs on E1-S and E1 stimulated growth shall be investigated to appraise the outcome of dual inhibition of STS and 17 β -HSD1 on proliferation and hence the local estrogen biosynthesis. In this context, possible estrogenic activity, ER antagonism and cytotoxicity should also be evaluated for the most promising DSHIs. These results of investigations are presented in paper A chapter **3.1.I**.

In order to develop drug-like DSHIs that could be used as probes for in vivo proof-of-principle studies, a new class of DSHIs has to be developed after the former class showed poor metabolic stability (see figure 8). The same design approach shall be followed but using a new 17 β -HSD1 inhibitor class with a promising metabolic stability profile. Initially, structural modifications have to be performed to optimize the sulfamate group position and the influence of added substituents on the biological activity of the compounds in cellular assays using T47D cells. The metabolic stabilities of the most interesting compounds have to be evaluated using human and mouse hepatic S9 fraction. Cytotoxicity of the metabolically stable compounds shall be evaluated using HEK293 and HepG2 cells. The latter is a hepatocellular carcinoma cell line that assesses the cytotoxicity of the compounds as well as their metabolites. The compounds with promising results in the aforementioned experiments will enter candidate selection phase, in which their pharmacokinetic (PK) profiles are examined in mice using subcutaneous route of application. Further PK

assessments have to be performed to the candidate with the best plasma levels profile to optimize the route of administration (per oral or subcutaneous), frequency of dosing (daily or every second day) as well as evaluating its effect on the CYP metabolizing enzymes (either by induction or inhibition) after multiple dosing regimens. This work is introduced in paper B chapter **3.1.II**.

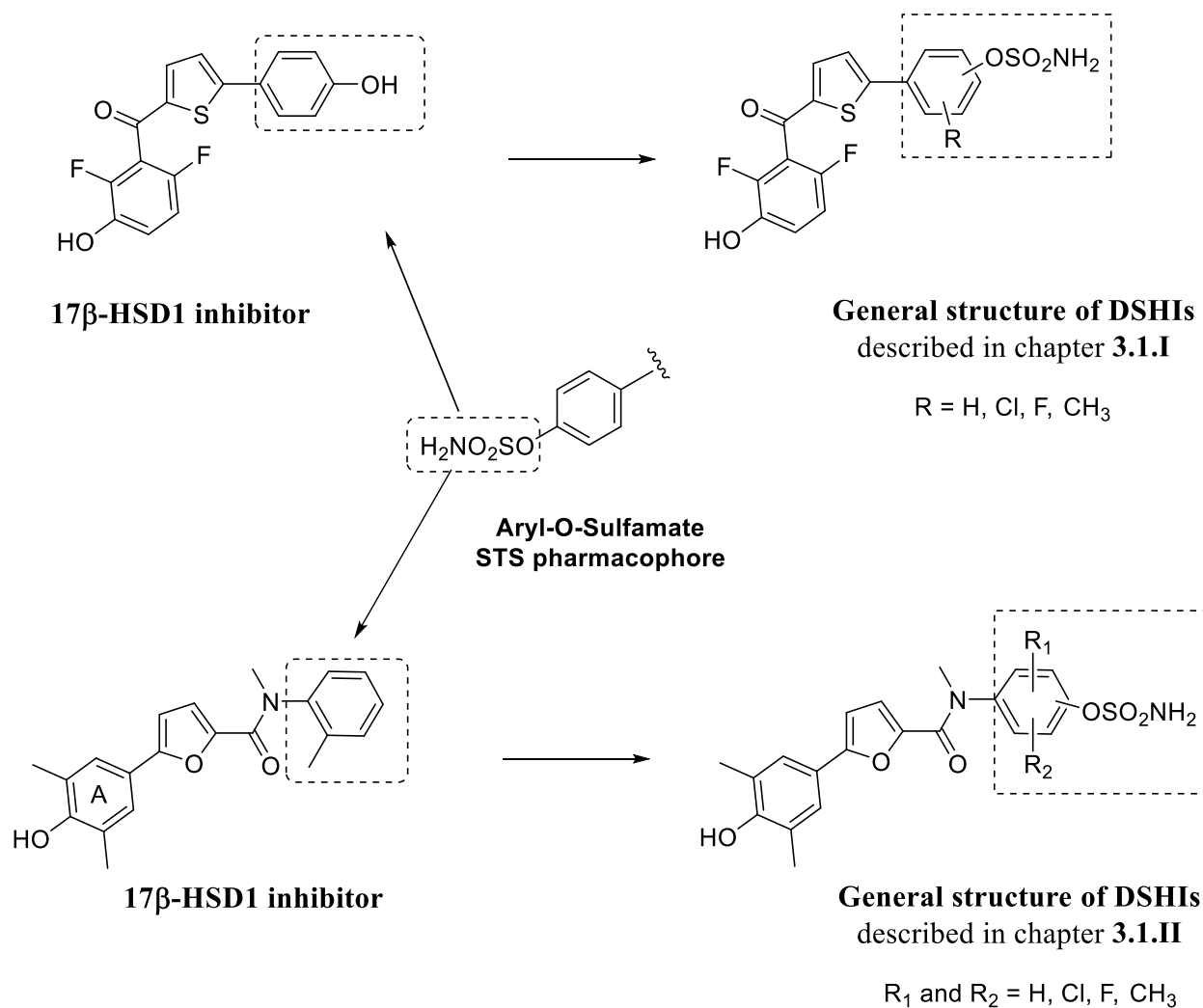


Figure 8 Proposed design and overview of the molecules described in this thesis

3. Results

3.1 Dual STS and 17 β -HSD1 inhibitors (DSHIs)

3.1.I First Dual Inhibitors of Steroid Sulfatase (STS) and 17 β -Hydroxysteroid Dehydrogenase Type 1 (17 β -HSD1): Designed Multiple Ligands as Novel Potential Therapeutics for Estrogen-Dependent Diseases

Mohamed Salah, Ahmed S. Abdelsamie, and Martin Frotscher

Reprinted with permission *J. Med. Chem.* 2017, 60 (9), 4086–4092.

DOI: 10.1021/acs.jmedchem.7b00062

Copyright (2017) American Chemical Society

Publication A

Contribution Report

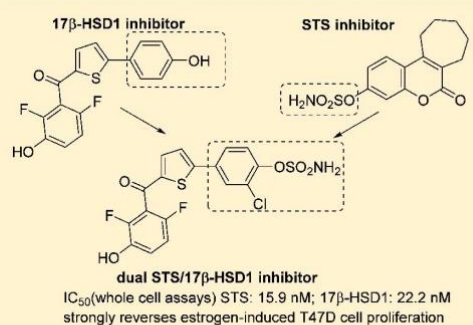
The author contributed significantly to the rational design concept. He planned, synthesized and characterized all the compounds. He further performed the cell-free and cellular activity assays. Additionally, he established and performed the stimulated growth assays. He conceived and wrote the manuscript.

First Dual Inhibitors of Steroid Sulfatase (STS) and 17 β -Hydroxysteroid Dehydrogenase Type 1 (17 β -HSD1): Designed Multiple Ligands as Novel Potential Therapeutics for Estrogen-Dependent Diseases

Mohamed Salah,[†] Ahmed S. Abdelsamie,^{†,‡} and Martin Frotscher^{*,†}[†]Pharmaceutical and Medicinal Chemistry, Saarland University, Campus C23, D-66123 Saarbrücken, Germany[‡]Chemistry of Natural and Microbial Products Department, National Research Centre, Dokki, 12622 Cairo, Egypt

S Supporting Information

ABSTRACT: STS and 17 β -HSD1 are attractive targets for the treatment of estrogen-dependent diseases like endometriosis and breast cancer. The simultaneous inhibition of both enzymes appears more promising than blockage of either protein alone. We describe a designed multiple ligand approach resulting in highly potent dual inhibitors. The most interesting compound **9** showed nanomolar IC₅₀ values for both proteins, membrane permeability, and no interference with estrogen receptors. It efficiently reversed E1S- and E1-induced T47D cell proliferation.



INTRODUCTION

Estrogens exert proliferative and antiapoptotic effects and are involved in the etiology of estrogen-dependent diseases (EDD) such as endometriosis and a high percentage of breast cancers. Therapeutic interventions comprise endocrine treatment with GnRH analogs, selective estrogen receptor modulators (SERMs), or aromatase inhibitors. These options, however, do not prevent relapses and often lead to severe side effects. Thus, there is considerable unmet medical need for novel treatments, and the exploration of novel biological targets is required.

Intriguingly, the progression of EDD is in many cases strongly coupled to the local estrogen biosynthesis, i.e., the formation of active estrogen within the diseased tissue itself. Normally, the activities of enzymes involved in local estrogen activation (steroid sulfatase (STS), aromatase, 17 β -HSD1) and deactivation (17 β -HSD2, sulfotransferase) are well balanced. In the case of EDD, a mismatch between activation and deactivation results in elevated local estrogen levels, leading to increased cell proliferation and reduced apoptosis. This mismatch is caused by aberrant expression of the involved enzymes *in situ*.^{1,2}

Therefore, the selective inhibition of local estrogen biosynthesis is a promising therapeutic approach, with the prospect of fewer side effects compared to existing therapies. In this context, STS and 17 β -HSD1 play major roles as they catalyze the final steps in estrogen biosynthesis within the target cell (intracrinology): STS converts the inactive estrone 3-sulfate

(E1S), the main transport and storage form of estrogens, to the weakly estrogenic estrone (E1). The latter is reduced to 17 β -estradiol (E2), the most potent estrogen in humans, predominantly by the action of 17 β -HSD1 (Figure 1).³ This route of estrogen biosynthesis has been termed "sulfatase pathway".⁴ It also includes the STS catalyzed transformation of androstenediol sulfate to the estrogenic androstenediol, whose proliferative effect on estrogen-sensitive cells is known.⁵ 17 β -HSD2 catalyzes the reverse reaction, i.e., the inactivation of E2 by oxidation to E1, and is the physiological adversary of the type 1 enzyme. Both STS and 17 β -HSD1 are overexpressed in endometriotic lesions,^{6,7} and there is strong evidence that elevated local E2 levels are mainly due to estrogen activation via the sulfatase pathway, whereas local E2 formation from androgen precursors ("aromatase pathway") is of considerably less relevance.⁸ The sulfatase pathway also plays a crucial role in estrogen-dependent breast cancer, and STS expression is an important prognostic factor in this disease.^{9,10} Strikingly, the tumor tissue of breast cancer patients who were treated with aromatase inhibitors showed increased expression of STS and 17 β -HSD1.¹¹ Thus, STS and 17 β -HSD1 are key enzymes for local estrogen activation in EDD. In conclusion, their inhibition is a promising approach for therapeutic intervention. The validity of this concept is supported by the observation that a 17 β -HSD1 inhibitor led to a decrease of E2 levels in

Received: January 13, 2017

Published: April 13, 2017

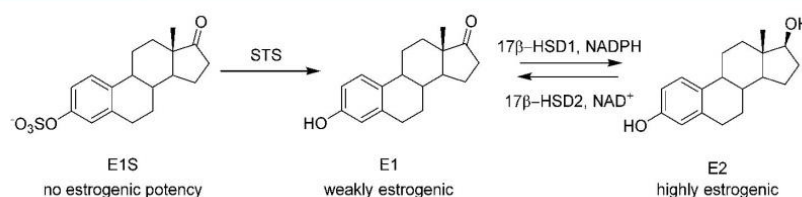


Figure 1. Sulfatase pathway of local estrogen biosynthesis.

endometriotic specimens.¹² In transgenic mice, 17 β -HSD1 inhibitors reversed estrogen-induced endometrial hyperplasia.¹³ 17 β -HSD1 inhibitors were shown to reduce the E1-stimulated tumor cell growth in vitro and in vivo, suggesting the suitability of this target for the treatment of breast cancer.^{14,15} In a mouse model, STS inhibition significantly reduced the growth of endometriotic lesions, while plasma E2 levels remained unchanged.¹⁶

Selective inhibition of either enzyme, however, bears intrinsic drawbacks: Selective 17 β -HSD1 inhibition does not prevent the formation of the estrogenic agents E1 and androstenediol. Selective STS inhibition, on the other hand, does not block E2 formation from E1, which is produced from testosterone via the aromatase pathway. The latter should not be very distinct but could be of relevance for the progression of EDD.

Consequently, the idea of simultaneous inhibition of STS and 17 β -HSD1 arises as a novel and attractive treatment approach. This aim could be achieved by administration of two single inhibitors, each selective for one of the two targets (multicomponent therapy). Different patient-specific rates of biotransformation, however, may result in complex PK/PD correlations, leading to difficult predictability of pharmacological effects. Another drawback is the risk of drug–drug-interactions.

An intriguing concept is the inhibition of both targets with a single drug whose structure is rationally derived for this dual mode of action (designed multiple ligand, DML).¹⁷ Preferably, 17 β -HSD2 should not be inhibited.

For 17 β -HSD1 and STS, a number of steroidal and nonsteroidal inhibitors have been described.^{18–22} Examples are compounds **13** (17 β -HSD1 inhibitor)²³ and **14** (STX-64) which was the first STS inhibitor to enter clinical trials (Figure 2).²⁴ Interestingly, DML approaches have successfully been applied for STS inhibitors, leading to the discovery of compounds combining STS inhibition with estrogen receptor

modulation or inhibition of aromatase (dual aromatase sulfatase inhibitors, DASIs).²⁰ First described by Woo et al.,²⁵ the DASI concept has been thoroughly investigated and led to the discovery of many dual inhibitors from different compound classes, described in a series of publications and summarized in a recent review article.²⁰ Selected DASIs showed favorable properties in vitro and in vivo.^{20,26} However, significant reduction of plasma E2 levels was reported indicating a not exclusively local mode of action.²⁵

In this report we describe for the first time the rational design, synthesis, and in vitro profiling of nonsteroidal dual STS/17 β -HSD1 inhibitors (DSHIs) as potential drugs for the treatment of EDD, with the prospect of local action.

RESULTS AND DISCUSSION

While STS inhibitors differ considerably regarding molecular structure, most of them bear an unsubstituted aryl sulfamate group (exemplified by **14**, Figure 2) as a common feature which serves as the main pharmacophore for target inhibition. This structural motif was adopted for the design of dual inhibitors and transferred to an appropriate position of a highly potent inhibitor of 17 β -HSD1.

We reported on the discovery of bicyclic substituted hydroxyphenylmethanones (BSHs) such as **13** (Figure 2) as highly active 17 β -HSD1 inhibitors.²³ Their scaffold consists of a phenyl moiety and a benzoyl moiety which are linked by a thiophene ring. Extensive SAR revealed that their 17 β -HSD1 inhibitory activity is maintained even if bulky substituents are attached to the phenyl moiety (Figure 2, **13**, dotted box). This characteristic triggered the implementation of the envisaged design strategy by attaching a sulfamate group essential for STS inhibition to the phenyl group of the BSHs. A general structure of the potential DSHIs based on the above-mentioned strategy is shown in Figure 2. The potential dual inhibitors **1–12** were synthesized using standard methods according to Scheme 1.

Inhibition of Human STS, 17 β -HSD1, and 17 β -HSD2 in Cell-Free Assays. STS inhibition was determined by incubation of human placental STS with E1S and inhibitor. E1 formation was quantified by ELISA (see Supporting Information). Inhibition of 17 β -HSD1 and 17 β -HSD2 was evaluated using the respective radiolabeled steroid (E1 or E2) and human placental 17 β -HSD1 (cytosolic fraction) or 17 β -HSD2 (microsomal fraction). The radiolabeled estrogens were separated and quantified using HPLC with scintillation detection (see Supporting Information). Inhibitory activities are expressed as IC₅₀ values (Table 1). **13** and **14** were used as reference compounds.

Compounds **1–3** were highly active toward 17 β -HSD1 but did not show inhibition of STS. Introduction of a fluorine atom to **3** led to the dual inhibitor **4**, whose inhibition of STS, however, was clearly less pronounced than that of 17 β -HSD1. Shifting the sulfamate group from position 3 to position 4 resulted in the highly active **5** which equipotently inhibited STS

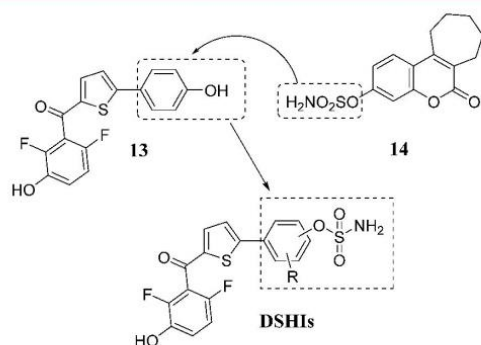
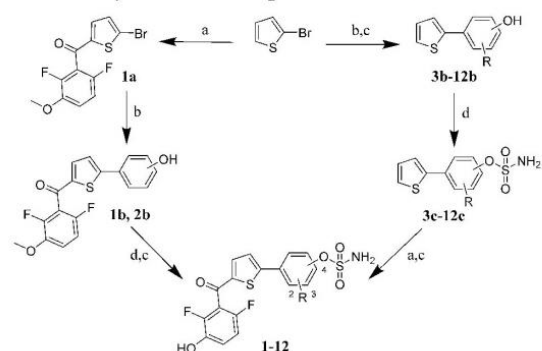


Figure 2. Structures of **13** and **14** and general structure of dual STS/17 β -HSD1 inhibitors (DSHIs). R = Cl, F, CH₃.

Scheme 1. Synthesis of Compounds 1–12^a

| Cpd | R | Position -OSO ₂ NH ₂ | Cpd | R | Position -OSO ₂ NH ₂ |
|-----|------|---|-----|----------|---|
| 1 | H | 4 | 7 | 2-Me | 4 |
| 2 | H | 2 | 8 | 3-F | 4 |
| 3 | H | 3 | 9 | 3-Cl | 4 |
| 4 | 2-F | 3 | 10 | 3-Me | 4 |
| 5 | 2-F | 4 | 11 | 2,3-diF | 4 |
| 6 | 2-Cl | 4 | 12 | 2-F,3-Cl | 4 |

^aReagents and conditions: (a) 2,6-difluoro-3-methoxybenzoyl chloride, anhydrous AlCl₃, anhydrous CH₂Cl₂, 0 °C, 0.5 h, and then room temperature, 3 h; (b) corresponding phenylboronic acid, Cs₂CO₃, Pd(PPh₃)₄, DME/water (1:1), 110 °C, 4 h; (c) BBr₃, CH₂Cl₂, −78 °C to room temperature, overnight; (d) DMA, sulfamoyl chloride, 0 °C, and then room temperature, overnight.

and 17β-HSD1. The STS inhibitory potency of **5** matched that of the reference **14**, one of the most potent STS inhibitors. The fluorine atom of **5** could be replaced with chlorine, leading to **6** with practically identical inhibitory properties, whereas a methyl group slightly decreased potency (**7**). Compounds **5** and **6** only showed marginal selectivity over 17β-HSD2. Relocation of the substituents F, Cl, and methyl from position 2 to position 3 (**8–10**) on the one hand led to a decrease of STS inhibition. On the other hand, in the case of the halogenated inhibitors **8** and **9** this modification further increased activity toward 17β-HSD1 and selectivity over 17β-HSD2. This finding prompted us to synthesize **11** and **12**, bearing halogen atoms in positions 2 and 3, thus possibly combining strong STS inhibition (halogen in position 3) with strong 17β-HSD1 inhibition and selectivity over 17β-HSD2 (halogen in position 2).

In fact, a strong 17β-HSD1 inhibition was achieved, comparable to that of **8** and **9**. In addition, **11** and **12** showed selectivity over 17β-HSD2. There was, however, no improvement concerning STS inhibition. Investigation of compound stability in buffer (20 mM Tris-HCl, pH = 7.2, 37 °C) revealed fast cleavage of the sulfamate moiety in the cases of **11** and **12**, under formation of the phenolic OH group (28% and 22% of parent compound remaining after 30 min, respectively), whereas the other compounds proved to be stable under these conditions. The different stabilities can be correlated to the pK_a values of the formed phenolic OH groups which are significantly lower in the cases of **11** and **12** compared to the other compounds (see Supporting Information, Table S2), making their phenolates better leaving groups in substitution reactions. The loss of the sulfamate “warhead” is in agreement with the comparably low STS inhibition by **11** and **12**. The fact

Table 1. Inhibitory Activities of Compounds 1–14 toward hSTS, h17β-HSD1, and h17β-HSD2 in Cell-Free Assays

| compd | R ₁ | R ₂ | IC ₅₀ [nM] ^a | | | SF ^c |
|-------|----------------|----------------|------------------------------------|------------------------|------------------------|-----------------|
| | | | hSTS ^b | h17β-HSD1 ^c | h17β-HSD2 ^d | |
| 1 | H | H | ni | 3.4 | 28.0 | 8.2 |
| 2 | H | H | ni | 22.5 | 4.1 | 0.2 |
| 3 | H | H | ni | 2.2 | 31.3 | 14.2 |
| 4 | F | H | 123.4 | 7.1 | 17.4 | 2.5 |
| 5 | H | F | 19.5 | 12.2 | 22.2 | 1.8 |
| 6 | H | Cl | 19.4 | 10.2 | 19.1 | 1.9 |
| 7 | H | Me | 35.0 | 43.5 | 40.0 | 0.9 |
| 8 | F | H | 81.8 | 2.5 | 13.7 | 5.5 |
| 9 | Cl | H | 143.1 | 1.1 | 36.1 | 33.0 |
| 10 | Me | H | 220.8 | 32.4 | 31.2 | 1.0 |
| 11 | F | F | 105.5 | 2.7 | 23.2 | 8.6 |
| 12 | Cl | F | 244.5 | 1.4 | 18.4 | 13.2 |
| 13 | ni | ni | 15.1 | 3.1 | 71.3 | 23.1 |
| 14 | ni | ni | 15.1 | ni | ni | NA |

^aMean value of at least two independent experiments each conducted in duplicate, with standard deviation less than 15%. ni: no inhibition (<10% inhibition at 1 μM). NA: not applicable. ^bHuman placenta, microsomal fraction, substrate E1S [300 nM]. ^cHuman placenta, cytosolic fraction, substrate [³H]-E1 + E1 [500 nM], cofactor NADH [0.5 mM]. ^dHuman placenta, microsomal fraction, substrate [³H]-E2 + E2 [500 nM], cofactor NAD⁺ [1.5 mM]. ^eSF (selectivity factor): IC₅₀(17β-HSD2)/IC₅₀(17β-HSD1).

that both compounds showed strong inhibition of 17β -HSD1 is not in conflict with their instability because the sulfamate group is not relevant for 17β -HSD1 inhibition.

Intracellular Inhibition of Human STS and 17β -HSD1. Irreversible Inhibition of Human STS. The estrogen-dependent human breast cancer cell line T47D expresses STS and 17β -HSD1.²⁷ Intact cells were incubated with **5**, **6**, **8**, and **9**, respectively, and the corresponding radiolabeled substrate E1S or E1. After incubation, the steroids were separated and quantified using HPLC with radio-detection. Table 2 shows the IC_{50} values of the cellular inhibition assays.

Table 2. Inhibitory Activities of Compounds **5, **6**, **8**, **9**, **13**, and **14** toward hSTS and $h17\beta$ -HSD1 in Cellular Assays**

| compd | R_1 | R_2 | IC_{50} [nM] ^a | | |
|-----------|-------|-------|-----------------------------|-------------------------------|--------------------------------|
| | | | hSTS ^b | $h17\beta$ -HSD1 ^c | hSTS ^b irreversible |
| 5 | H | F | 2.1 | 42.1 | 3.1 |
| 6 | H | Cl | 3.4 | 60.9 | 3.9 |
| 8 | F | H | 5.1 | 20.0 | 5.7 |
| 9 | Cl | H | 15.6 | 22.2 | 16.4 |
| 13 | | ni | | 7.9 | ni |
| 14 | | 1.9 | ni | | 2.1 |

^aMean value of at least two independent experiments each conducted in triplicate using intact T47D cells, with standard deviation less than 15%. ni: no inhibition (<5% inhibition at 1 μ M). ^bSubstrate [3 H]-E1S + E1S [5 nM]. ^cSubstrate [3 H]-E1 + E1 [50 nM].

All compounds displayed strong inhibition of the target enzymes with IC_{50} values in the nanomolar range, indicating good cell penetration. The fact that the compounds were able to strongly inhibit STS in spite of the long incubation time of 24 h suggested an irreversible mode of STS inhibition, as described for other sulfamate-containing STS inhibitors, e.g., for **14**.²⁰

For further support of this irreversible mode of action, T47D cells were pretreated with **5**, **6**, **8**, **9**, and the reference **14**, respectively. After removal of the compounds by extensive washing, STS activity was evaluated by incubation with E1S. In all cases, conversion to E1 was strongly inhibited with IC_{50} values very similar to those obtained in the "regular" assay for cellular STS inhibition (Table 2). In contrast, 17β -HSD1 activity was fully restored after incubation with **9** (Table S3), suggesting that the persisting STS inhibition is a result of irreversible inhibition rather than of compound retention.

Estrogen Stimulation of T47D Cell Proliferation. The proliferation of T47D cells in response to estrogen treatment was evaluated by adding E1S, E1, or E2 to the culture medium at concentrations ranging from 0.1 to 500 nM and evaluating cell viability after 7 days of incubation (Figure 3). Stimulation of proliferation was similar for E1S, E1, and E2. It was initially observed at an estrogen concentration of 10 nM and reached a maximum at 250 nM. In the following experiments, 100 nM estrogen (50 nM E1S and 50 nM E1, reflecting that both may be present in vivo, or 100 nM E2) was used.

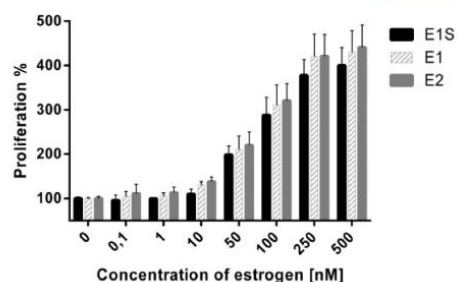


Figure 3. Concentration dependent stimulation of T47D cell proliferation: black bars, E1S-stimulation; striped, E1 stimulation; gray: E2 stimulation. The control (no estrogen stimulation) was arbitrarily set to 100%. Cells were incubated with the respective additives for 7 days without passage. Medium was changed every 2–3 days.

Effect of DSHIs on Estrogen Stimulated Cell Proliferation. Compound **9** was applied to E1S/E1-stimulated T47D cells at 100, 200, and 400 nM, approximately corresponding to 5, 10, and 20 times its IC_{50} of cellular 17β -HSD1 inhibition. The reference compounds **13** and **14** were applied in concentrations of 50, 100, and 200 nM, approximately corresponding to the same multiples of their IC_{50} values, in the case of **14** that of the cell-free assay. The dual inhibitor **9** was able to decrease the proliferative effect of E1S/E1 stimulation dose-dependently, reaching control levels when applied in a concentration of 400 nM (Figure 4). Similar results were obtained for **5**, **6**, and **8**

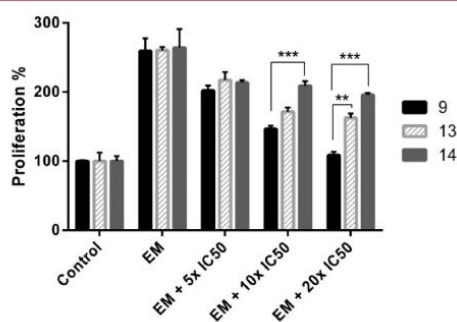


Figure 4. Concentration dependent inhibition of E1S- and E1-stimulated cell growth for **9**, **13**, and **14** on T47D cells. Cells were grown in phenol red-free RPMI 1640 medium supplemented with 5% stripped FCS. Control represents vehicle treated cells. EM (estrogenic medium) represents E1S [50 nM] and E1 [50 nM] treated cells. **9** was tested at 100, 200, and 400 nM, respectively. **13** and **14** were tested at 50, 100, and 200 nM, respectively. Cells were incubated with the respective additives for 7 days without passage. Medium was changed every 2–3 days. Vehicle: ethanol. (**) $p < 0.01$. (***) $p < 0.001$.

(Figure S1). In contrast, the selective references **13** and **14** did not decrease the stimulatory estrogen effect below 150% and 200% of the control, respectively.

The stronger antiproliferative effects of the dual inhibitors in comparison to the selective ones were assumed to be attributed to the differences in E2 and E1 levels in the medium after feeding the cells with E1S and E1, depending on the presence of the different types of inhibitors. This point was investigated by incubating the cells with radiolabeled E1S and E1 in the presence or absence of inhibitors, and quantification of estrogen levels after 48 h using HPLC with radio-detection

(Table 3). In the absence of inhibitor, almost complete conversion of E1S and E1 to E2 was observed, whereas in the

Table 3. Percentages of Estrogens upon Incubating T47D Cells with E1S and E1 (50 nM Each) for 48 h in the Presence of Vehicle, 9, 13, and 14

| compd | % ^a | | |
|----------------------|----------------|------|------|
| | E1S | E1 | E2 |
| vehicle ^b | 3.9 | 0.9 | 95.2 |
| 9 ^c | 50 | 48.9 | 1.1 |
| 13 ^d | 3.5 | 88.4 | 7.9 |
| 14 ^e | 50 | 0.8 | 49.2 |

^aMean value of at least two independent experiments each conducted in triplicate, with standard deviation less than 10%. ^bVehicle: ethanol. ^cCompound 9 [400 nM]. ^dCompound 13 [200 nM]. ^eCompound 14 [200 nM].

presence of the dual inhibitor 9 no significant conversion of E1S or E1 occurred. In the presence of 14 no conversion of E1S occurred but all the E1 was transformed into E2. In case of 13, E1S was almost completely consumed and 88.4% E1 was found besides a minor amount of E2 (7.9%). These results are in agreement with the residual proliferation induction found in the case of the selective inhibitors. In addition, they explain the more pronounced residual cell proliferation after application of 14 compared to 13 (200% vs 150%), as in the first case the amount of the strongly estrogenic E2 was high (49.2%) whereas in the latter case the less estrogenic E1 was the predominant estrogen.

As depicted in Figure 5, 9 has no effect on nonstimulated cells at 400 nM, which was the highest concentration in which

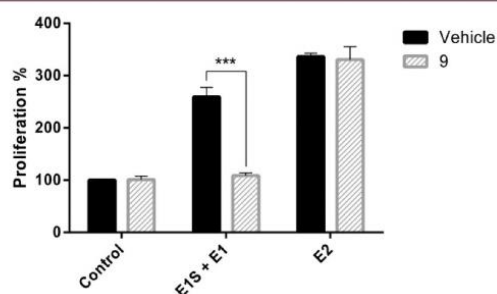


Figure 5. Effect of 9 on estrogen-stimulated cell proliferation of T47D. Cells were grown in phenol red-free RPMI 1640 medium supplemented with 5% stripped FCS. Proliferation was stimulated with E1S and E1 at 50 nM each or E2 (100 nM). 9 (400 nM) was added in the presence or absence of estrogens. Cells were incubated with the respective additives for 7 days without passage. Medium was changed every 2–3 days. Vehicle: ethanol. (***) $p < 0.001$.

9 was applied in the antiproliferation assay. Thus, the dual inhibitor 9 did not exert estrogenic or cytotoxic effects at this concentration. The lack of unspecific cytotoxicity was also confirmed using estrogen-independent cells: compound 9 did not affect the viability of HEK293 cells, even in the highest applied concentration of 1 μ M (see Supporting Information). Moreover, no influence of 9 on the proliferation of E2-stimulated cells could be detected, indicating that the compound did not deploy its antiproliferative effect by estrogen receptor antagonism. These data clearly demonstrate that the effect of 9 on E1S/E1-stimulated cells is caused by inhibition of

STS and 17 β -HSD1, which results in the blockage of E2 formation.

CONCLUSIONS

A designed multiple ligand approach was successfully applied, leading to the discovery of potent dual inhibitors of STS and 17 β -HSD1. Inhibitor design was facilitated by combining structural elements necessary for strong 17 β -HSD1 blockage, identified using in-house SAR information, with a sulfamate function which is the major pharmacophore for STS inhibition. Twelve potential dual inhibitors were synthesized, all of which proved to be highly active against 17 β -HSD1. Activity toward STS required an additional substituent at the aromatic moiety bearing the sulfamate group. An electron-withdrawing substituent is preferred; strong electron-withdrawing effects, however, impaired STS inhibition by reducing the chemical stability of the sulfamate function. Compound 9 turned out to be the most interesting dual inhibitor. In cellular assays it showed well-balanced activity against both target proteins, with IC₅₀ values of about 20 nM and an irreversible mode of action toward STS. Moreover, it displayed the highest selectivity over 17 β -HSD2. At 400 nM it efficiently reversed the E1S and E1 stimulated proliferation of T47D cells, showing neither cytotoxicity nor estrogen receptor interference.

In summary, 9 is the first rationally derived dual inhibitor of STS and 17 β -HSD1. It may serve as a lead for the development of novel therapeutics for EDD.

EXPERIMENTAL SECTION

The purity of all tested compounds was $\geq 95\%$, as evaluated by LC/MS. Purchased chemicals were reagent grade and used without purification (Supporting Information).

Compound 9a was prepared according to method B by the reaction of 2-bromothiophene (0.82 g, 5 mmol, 1 equiv) and (3-chloro-4-methoxyphenyl)boronic acid (1.11 g, 6.00 mmol, 1.2 equiv) in the presence of cesium carbonate (6.50 g, 20.00 mmol, 4 equiv) and tetrakis(triphenylphosphine)palladium (0.29 g, 0.25 mmol, 0.05 equiv) in DME/water 1:1 (50 mL). The product was purified by column chromatography (cyclohexane/dichloromethane 7:1) to give 1.01 g (4.50 mmol/90%) of the analytically pure compound. C₁₁H₉ClOS; MW 224; ¹H NMR (300 MHz, (CD₃)₂SO) δ 7.72 (d, J = 2.3 Hz, 1H), 7.57 (dd, J = 8.6, 2.3 Hz, 1H), 7.50 (dd, J = 5.1, 1.2 Hz, 1H), 7.47 (dd, J = 3.6, 1.2 Hz, 1H), 7.18 (d, J = 8.6 Hz, 1H), 7.11 (dd, J = 5.1, 3.6 Hz, 1H), 3.88 (s, 3H). MS (ESI): 225.07 (M + H)⁺.

Compound 9b was prepared according to method C by the reaction of 9a (0.90 g, 4.00 mmol, 1 equiv) and boron tribromide (1 M) in dichloromethane (12.00 mL, 12.00 mmol, 3 equiv) in anhydrous dichloromethane (20 mL). The product was purified by column chromatography (cyclohexane/dichloromethane 4:1) to give 0.65 g (3.08 mmol/77%) of the analytically pure compound. C₁₀H₇ClOS; MW 210; ¹H NMR (300 MHz, (CD₃)₂SO) δ 10.36 (s, 1H), 7.62 (d, J = 2.3 Hz, 1H), 7.46 (dd, J = 5.1, 1.2 Hz, 1H), 7.44–7.35 (m, 2H), 7.09 (dd, J = 5.1, 3.6 Hz, 1H), 7.00 (d, J = 8.4 Hz, 1H). MS (ESI): 211.03 (M + H)⁺.

Compound 9c was prepared according to method D by the reaction of 9b (0.63 g, 3.00 mmol, 1 equiv) and sulfamoyl chloride (1.73 g, 15.00 mmol, 5 equiv) in DMA (20 mL). The product was purified by column chromatography (cyclohexane/ethyl acetate 2:1) to give 0.45 g (1.56 mmol/52%) of the analytically pure compound. C₁₀H₈ClNO₃S₂; MW 289; ¹H NMR (300 MHz, (CD₃)₂SO) δ 8.29 (s, 2H), 7.88 (d, J = 2.2 Hz, 1H), 7.69 (dd, J = 8.6, 2.3 Hz, 1H), 7.64–7.59 (m, 2H), 7.52 (d, J = 8.6 Hz, 1H), 7.16 (dd, J = 4.9, 3.9 Hz, 1H). MS (ESI): 290.01 (M + H)⁺.

Compound 9d was prepared according to method A by the reaction of 2,6-difluoro-3-methoxybenzoyl chloride (0.41 g, 2.00 mmol, 1 equiv) and 9c (0.87 g, 3.00 mmol, 1.5 equiv) in the presence of

anhydrous aluminum chloride (0.53 g, 4.00 mmol, 2 equiv) in anhydrous dichloromethane (10 mL). The product was purified by column chromatography (cyclohexane/ethyl acetate 1:1) to give 0.59 g (1.30 mmol/65%) of the analytically pure compound. $C_{18}H_{12}ClF_2NO_3S_2$; MW 459; 1H NMR (300 MHz, $(CD_3)_2SO$) δ 8.37 (s, 2H), 8.11 (d, $J = 2.3$ Hz, 1H), 7.88 (dd, $J = 8.6, 2.3$ Hz, 1H), 7.79 (d, $J = 4.1$ Hz, 1H), 7.70 (d, $J = 4.1$ Hz, 1H), 7.59 (d, $J = 8.6$ Hz, 1H), 7.48–7.37 (m, 1H), 7.32–7.20 (m, 1H), 3.90 (s, 3H). MS (ESI): 459.99 ($M + H$) $^+$.

Compound **9** was prepared according to method C by the reaction of **9d** (0.23 g, 0.50 mmol, 1 equiv) and boron tribromide (1 M) in dichloromethane (1.50 mL, 1.50 mmol, 3 equiv) in anhydrous dichloromethane (10 mL). The product was purified by column chromatography (dichloromethane/methanol 98.5:1.5) to give 60.00 mg (0.13 mmol/27%) of the analytically pure compound. $C_{17}H_{10}ClF_2NO_3S_2$; MW 445; mp 172–173 $^{\circ}C$; 1H NMR (500 MHz, $(CD_3)_2CO$) δ 9.00 (s, 1H), 7.97 (d, $J = 2.3$ Hz, 1H), 7.80 (dd, $J = 8.6, 2.3$ Hz, 1H), 7.67 (d, $J = 4.1$ Hz, 1H), 7.64–7.62 (m, 1H), 7.62 (d, $J = 8.5$ Hz, 1H), 7.47 (s, 2H), 7.21–7.14 (m, 1H), 7.03–6.96 (m, 1H); ^{13}C NMR (126 MHz, $(CD_3)_2CO$) δ 180.76, 152.52 (dd, $J = 240.6, 5.9$ Hz), 152.31, 148.41 (dd, $J = 246.0, 7.6$ Hz), 148.06, 144.15, 142.67 (dd, $J = 12.8, 3.2$ Hz), 138.18, 133.45, 129.05, 129.03, 127.25, 127.04, 125.62, 120.44 (dd, $J = 9.1, 3.9$ Hz), 117.89 (dd, $J = 23.9, 19.6$ Hz), 112.45 (dd, $J = 22.8, 3.9$ Hz). MS (ESI): 446.12 ($M + H$) $^+$.

■ ASSOCIATED CONTENT

Supporting Information

The Supporting Information is available free of charge on the ACS Publications website at DOI: 10.1021/acs.jmedchem.7b00062.

Additional information on chemical methods and general synthetic methods A–E; detailed synthesis procedures and compound characterization; detailed biological assays; statistical method (PDF)

Molecular formula strings and some data (CSV)

■ AUTHOR INFORMATION

Corresponding Author

*E-mail: m.frotscher@mx.uni-saarland.de. Phone: +49-681 302 70330.

ORCID

Martin Frotscher: 0000-0003-1777-8890

Notes

The authors declare no competing financial interest.

■ ACKNOWLEDGMENTS

Thanks are due to C. Hoffmann and J. Ludwig for support in synthesis and biological evaluation. We are grateful to the Deutsche Forschungsgemeinschaft for financial support (Grant FR 3002/1-1) of this work.

■ DEDICATION

This work is dedicated to Professor Rolf W. Hartmann on the occasion of his 65th birthday.

■ ABBREVIATIONS USED

BSH, bicyclic substituted hydroxyphenylmethanone; DSHI, dual STS/17 β -HSD1 inhibitor; E2, 17 β -estradiol; EDD, estrogen-dependent diseases; E1, estrone; E1S, estrone 3-sulfate; 17 β -HSD1 or -2, 17 β -hydroxysteroid dehydrogenase type1 or 2; STS, steroid sulfatase

■ REFERENCES

- (1) Huhtinen, K.; Ståhle, M.; Perheentupa, A.; Poutanen, M. Estrogen Biosynthesis and Signaling in Endometriosis. *Mol. Cell. Endocrinol.* **2012**, 358 (2), 146–154.
- (2) Sasano, H.; Miki, Y.; Nagasaki, S.; Suzuki, T. In Situ Estrogen Production and Its Regulation in Human Breast Carcinoma: From Endocrinology to Intracrinology. *Pathol. Int.* **2009**, 59 (11), 777–789.
- (3) Laplante, Y.; Rancourt, C.; Poirier, D. Relative Involvement of Three 17 β -Hydroxysteroid Dehydrogenases (Types 1, 7 and 12) in the Formation of Estradiol in Various Breast Cancer Cell Lines Using Selective Inhibitors. *Mol. Cell. Endocrinol.* **2009**, 301 (1–2), 146–153.
- (4) Secky, L.; Svoboda, M.; Klameth, L.; Bajna, E.; Hamilton, G.; Zeillinger, R.; Jäger, W.; Thalhammer, T. The Sulfatase Pathway for Estrogen Formation: Targets for the Treatment and Diagnosis of Hormone-Associated Tumors. *J. Drug Delivery* **2013**, 2013, 957605.
- (5) Billich, A.; Nussbaumer, P.; Lehr, P. Stimulation of MCF-7 Breast Cancer Cell Proliferation by Estrone Sulfate and Dehydroepiandrosterone Sulfate: Inhibition by Novel Non-Steroidal Steroid Sulfatase Inhibitors. *J. Steroid Biochem. Mol. Biol.* **2000**, 73 (5), 225–235.
- (6) Reed, M. J.; Purohit, A.; Woo, L. W. L.; Newman, S. P.; Potter, B. V. L. Steroid Sulfatase: Molecular Biology, Regulation, and Inhibition. *Endocr. Rev.* **2005**, 26 (2), 171–202.
- (7) Šmuc, T.; Hevir, N.; Ribič-Pucelj, M.; Husen, B.; Thole, H.; Rižner, T. L. Disturbed Estrogen and Progesterone Action in Ovarian Endometriosis. *Mol. Cell. Endocrinol.* **2009**, 301 (1–2), 59–64.
- (8) Purohit, A.; Fusi, L.; Brosens, J.; Woo, L. W. L.; Potter, B. V. L.; Reed, M. J. Inhibition of Steroid Sulphatase Activity in Endometriotic Implants by 667 COUMATE: A Potential New Therapy. *Hum. Reprod.* **2008**, 23 (2), 290–297.
- (9) Suzuki, T.; Nakata, T.; Miki, Y.; Kaneko, C.; Moriya, T.; Ishida, T.; Akinaga, S.; Hirakawa, H.; Kimura, M.; Sasano, H. Estrogen Sulfotransferase and Steroid Sulfatase in Human Breast Carcinoma. *Cancer Res.* **2003**, 63 (11), 2762–2770.
- (10) Santner, S. J.; Feil, P. D.; Santen, R. J. In Situ Estrogen Production via the Estrone Sulfatase Pathway in Breast Tumors: Relative Importance versus the Aromatase Pathway. *J. Clin. Endocrinol. Metab.* **1984**, 59 (1), 29–33.
- (11) Chanplakorn, N.; Chanplakorn, P.; Suzuki, T.; Ono, K.; Chan, M. S. M.; Miki, Y.; Saji, S.; Ueno, T.; Toi, M.; Sasano, H. Increased Estrogen Sulfatase (STS) and 17 β -hydroxysteroid Dehydrogenase Type 1 (17 β -HSD1) Following Neoadjuvant Aromatase Inhibitor Therapy in Breast Cancer Patients. *Breast Cancer Res. Treat.* **2010**, 120 (3), 639–648.
- (12) Delvoux, B.; D'Hooghe, T.; Kyama, C.; Koskimies, P.; Hermans, R. J. J.; Dunselman, G. A.; Romano, A. Inhibition of Type 1 17 β -Hydroxysteroid Dehydrogenase Impairs the Synthesis of 17 β -Estradiol in Endometriosis Lesions. *J. Clin. Endocrinol. Metab.* **2014**, 99 (1), 276–284.
- (13) Saloniemi, T.; Järvensivu, P.; Koskimies, P.; Jokela, H.; Lamminen, T.; Ghaem-Maghamsi, S.; Dina, R.; Damdimopoulou, P.; Mäkelä, S.; Perheentupa, A.; Kujari, H.; Brosens, J.; Poutanen, M. Novel Hydroxysteroid (17 β) Dehydrogenase 1 Inhibitors Reverse Estrogen-Induced Endometrial Hyperplasia in Transgenic Mice. *Am. J. Pathol.* **2010**, 176 (3), 1443–1451.
- (14) Husen, B.; Huhtinen, K.; Poutanen, M.; Kangas, L.; Messinger, J.; Thole, H. Evaluation of Inhibitors for 17 β -Hydroxysteroid Dehydrogenase Type 1 in Vivo in Immunodeficient Mice Inoculated with MCF-7 Cells Stably Expressing the Recombinant Human Enzyme. *Mol. Cell. Endocrinol.* **2006**, 248 (1–2), 109–113.
- (15) Kruchten, P.; Werth, R.; Bey, E.; Oster, A.; Marchais-Oberwinkler, S.; Frotscher, M.; Hartmann, R. W. Selective Inhibition of 17 β -Hydroxysteroid Dehydrogenase Type 1 (17 β -HSD1) Reduces Estrogen Responsive Cell Growth of T47-D Breast Cancer Cells. *J. Steroid Biochem. Mol. Biol.* **2009**, 114 (3–5), 200–206.
- (16) Colette, S.; Defrère, S.; Lousse, J. C.; Van Langendonck, A.; Gotteland, J. P.; Loumaye, E.; Donnez, J. Inhibition of Steroid Sulfatase Decreases Endometriosis in an in Vivo Murine Model. *Hum. Reprod.* **2011**, 26 (6), 1362–1370.

- (17) Morphy, R.; Rankovic, Z. Designed Multiple Ligands. An Emerging Drug Discovery Paradigm. *J. Med. Chem.* **2005**, *48* (21), 6523–6543.
- (18) Maltais, R.; Poirier, D. Steroid Sulfatase Inhibitors: A Review Covering the Promising 2000–2010 Decade. *Steroids* **2011**, *76* (10–11), 929–948.
- (19) Purohit, A.; Foster, P. A. Steroid Sulfatase Inhibitors for Estrogen- and Androgen-Dependent Cancers. *J. Endocrinol.* **2012**, *212* (2), 99–110.
- (20) Thomas, M. P.; Potter, B. V. L. Discovery and Development of the Aryl O -Sulfamate Pharmacophore for Oncology and Women's Health. *J. Med. Chem.* **2015**, *58* (19), 7634–7658.
- (21) Brožič, P.; Lanišnik Rižner, T.; Gobec, S. Inhibitors of 17 β -Hydroxysteroid Dehydrogenase Type 1. *Curr. Med. Chem.* **2008**, *15* (2), 137–150.
- (22) Marchais-Oberwinkler, S.; Wetzel, M.; Ziegler, E.; Kruchten, P.; Werth, R.; Henn, C.; Hartmann, R. W.; Frotscher, M. New Drug-like Hydroxyphenylnaphthol Steroidomimetics as Potent and Selective 17 β -Hydroxysteroid Dehydrogenase Type 1 Inhibitors for the Treatment of Estrogen-Dependent Diseases. *J. Med. Chem.* **2011**, *54* (2), 534–547.
- (23) Abdelsamie, A. S.; van Koppen, C. J.; Bey, E.; Salah, M.; Börger, C.; Siebenbürger, L.; Laschke, M. W.; Menger, M. D.; Frotscher, M. Treatment of Estrogen-Dependent Diseases: Design, Synthesis and Profiling of a Selective 17 β -HSD1 Inhibitor with Sub-Nanomolar IC₅₀ for a Proof-of-Principle Study. *Eur. J. Med. Chem.* **2017**, *127*, 944–957.
- (24) Stanway, S. J.; Purohit, A.; Woo, L. W. L.; Sufi, S.; Vigushin, D.; Ward, R.; Wilson, R. H.; Stanczyk, F. Z.; Dobbs, N.; Kulinskaya, E.; Elliott, M.; Potter, B. V. L.; Reed, M. J.; Coombes, R. C. Phase I Study of STX 64 (667 Coumate) in Breast Cancer Patients: The First Study of a Steroid Sulfatase Inhibitor. *Clin. Cancer Res.* **2006**, *12* (5), 1585–1592.
- (25) Woo, L. W. L.; Sutcliffe, O. B.; Bubert, C.; Grasso, A.; Chander, S. K.; Purohit, A.; Reed, M. J.; Potter, B. V. L. First Dual Aromatase-Steroid Sulfatase Inhibitors. *J. Med. Chem.* **2003**, *46* (15), 3193–3196.
- (26) Wood, P. M.; Woo, L. W. L.; Humphreys, A.; Chander, S. K.; Purohit, A.; Reed, M. J.; Potter, B. V. L. A Letrozole-Based Dual Aromatase-sulphatase Inhibitor with in Vivo Activity. *J. Steroid Biochem. Mol. Biol.* **2005**, *94* (1–3), 123–130.
- (27) Chetrite, G. S.; Ebert, C.; Wright, F.; Philippe, A. C.; Pasqualini, J. R. Control of Sulfatase and Sulfotransferase Activities by Medrogestone in the Hormone-Dependent MCF-7 and T-47D Human Breast Cancer Cell Lines. *J. Steroid Biochem. Mol. Biol.* **1999**, *70* (1–3), 39–45.

3.1.II Potent Dual Inhibitors of Steroid Sulfatase (STS) and 17 β -Hydroxysteroid Dehydrogenase Type 1 (17 β -HSD1) with a Suitable Pharmacokinetic Profile for an in Vivo Proof-of-Principle Study in an Endometriosis Mouse Model

The following people contributed experimentally to this chapter:

Mohamed Salah: performed the synthesis and characterization of the compounds, the in vitro cell-free and cellular inhibition assays, and the in vitro toxicity assays.

Prof. Dr. Matthias W. Laschke and Dr. Claudia Scheuer: performed the in vivo pharmacokinetic studies in mice.

Mariam Tahoun: performed the metabolic stability studies, and the quantification of the compounds in the plasma samples of the pharmacokinetic studies.

Monograph B

Introduction

Steroids play fundamental physiological roles as hormones. Generally, their action is mediated by intracellular nuclear receptors. Estrogens are among the major steroid hormones in humans, where 17 β -estradiol (E2) is the most potent one. They exert proliferative and antiapoptotic effects that are beneficial to many organs¹. However, they are also involved in the onset and progression of many estrogen-dependent diseases (EDDs) such as endometriosis^{2,3} and a high percentage of breast cancers⁴.

Endometriosis is a chronic gynecological disorder characterized by the presence of endometrial glands and stroma outside the uterine cavity, typically in the ovaries (ovarian endometriosis), the pelvic peritoneum (peritoneal endometriosis), the rectovaginal septum (deep endometriotic nodules of the rectovaginal septum) and other pelvic sites (fallopian tubes, vagina, cervix and uterosacral ligaments)^{5,6}. Symptoms of endometriosis include chronic pelvic pain, dysmenorrhea, dyspareunia, irregular uterine bleeding, and/or infertility^{7,8} which significantly impair the quality of life of these women^{8,9}. Endometriosis is estimated to be affecting 10% of women in reproductive age, while the incidence rises to 50–60% within women suffering from pain¹⁰. Current treatment interventions include surgical removal of the endometriotic lesions and/or medical therapy^{10,11}. The surgical procedure, if possible at all, is only a temporary solution, since the endometriosis usually forms again after a while, even with subsequent drug therapy. Drug treatment aims at reduction of symptoms (NSAIDs, combined oral contraceptives, progestins) or consists of systemic endocrine therapy with GnRH receptor desensitizers or aromatase inhibitors. Generally, all the systemic endocrine therapies result in a radical non-selective reduction of circulating estrogen levels leading to severe postmenopausal-like side effects (e.g. loss of bone mineral density) that restrict its use to 6-9 months^{10,11}. Danazol, an anterior pituitary suppressant that inhibits the production of gonadotropins, is applied when all other options are ineffective as it has severe hyperandrogenic side effects that limit its use¹⁰. In summary, the existing medical treatments for endometriosis are not satisfying as they suffer from severe side effects which are linked to the suppression of the systemic estrogen levels. Thus, there is a medical need for a novel treatment approach for endometriosis, without strongly affecting the circulating E2 levels that could offer better safety profile and longer treatment window.

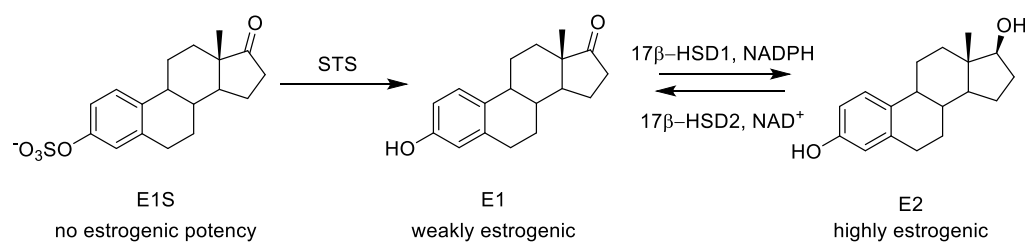
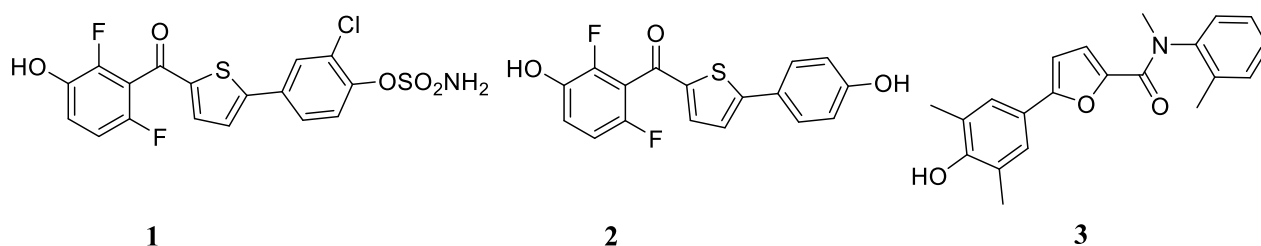


Figure 1: The sulfatase pathway of local estrogen biosynthesis

Interestingly, the progression of endometriosis is closely linked to the local biosynthesis of E2, i.e. the formation of active estrogen in the endometriotic tissue itself¹²; especially via the sulfatase pathway (see figure 1) in which steroid sulfatase (STS) and 17β-hydroxysteroid dehydrogenase type 1 (17β-HSD1) play major roles and are found to be over-expressed in the endometriotic tissue, and the amount of STS over-expression correlates with the severity of the disease^{13,14}. In addition, the activity of 17β-hydroxysteroid dehydrogenase type 2 (17β-HSD2) which has a protective role by converting E2 to the less active form E1 is down-regulated¹⁴.

Thus, STS and 17β-HSD1 are crucial enzymes for the local estrogen biosynthesis in endometriosis, so their inhibition offers a promising approach for the treatment of the disease. This concept is supported by various findings in the literature. In an ex vivo study, it was observed that a 17β-HSD1 inhibitor normalized the increased E2 synthesis in endometriotic tissue of endometriosis patients¹⁵. 17β-HSD1 inhibition was found to reverse the estrogen-induced endometrial hyperplasia in transgenic mice¹⁶. On the other hand, the growth of endometriotic lesions was significantly reduced after the inhibition of STS in a mouse endometriosis model¹⁷. In a randomized phase I proof-of-principle clinical study it was found that the STS inhibition has no effect on the levels of systemic E2¹⁸.

In a recent work, our group introduced the idea of simultaneous inhibition of both STS and 17β-HSD1 by a dual inhibitor (designed multiple ligand) as a novel approach for the treatment of EDDs e.g. endometriosis¹⁹. Compound **1** (Table 1) had a promising profile, as it showed well-balanced intracellular activity against both target proteins, with IC₅₀ values of about 20 nM and an irreversible mode of action towards STS. Moreover, it displayed good selectivity over 17β-HSD2 (SF=33). At 400 nM it efficiently reversed the E1-S and E1 stimulated proliferation of T47D cells, showing neither cytotoxicity nor estrogen receptor interference.

Table 1: Inhibitory activities towards *h*STS and *h*17 β -HSD1 in cellular assays and metabolic stability human and mouse hepatic S9 fraction

| Cpd | IC ₅₀ [nM] ^a | | SF ^d | <i>t</i> _{1/2} [min] ^{e,f} | |
|--------------|------------------------------------|--|-----------------|--|--------------------|
| | <i>h</i> STS ^b | <i>h</i> 17 β -HSD1 ^c | | Human ^g | Mouse ^h |
| 1 | 15.4 | 22.2 | 33 | <5 | <5 |
| 2 | n.i | 7.9 | 24 | <5 | n.d |
| 3 | n.i | 2.9 | 563 | 38.1 | 19.1 |
| STX64 | 2.1 | n.i | n.a | n.d | n.d |

^a Mean value of at least two independent experiments each conducted in triplicates using intact T47D cells, standard deviation less than 15%; ^b Substrate [³H]-E1-S + E1-S [5 nM]; ^c Substrate [³H]-E1 + E1 [50 nM]; ^d SF (selectivity factor): IC₅₀(17 β -HSD2) / IC₅₀(17 β -HSD1); ^e Mean value of three independent experiments, standard deviation less than 15%; ^f *t*_{1/2}: half-life; ^g Human liver S9 fraction; ^h Mouse liver S9 fraction; ni: no inhibition (< 10% inhibition at 1 μ M); n.d: not determined; n.a: not applicable.

Unfortunately, compound **1** turned out to be metabolically unstable when tested using human liver S9 fraction (see table 1). Further metabolic stability investigations showed that the core structure (without the sulfamate moiety) e.g. compound **2** (see table 1) is also metabolically unstable. However, compound **1** showed relative metabolic stability when evaluated against phase I only. This concludes that the metabolic instability of **1** is linked to phase II metabolism. This can be strongly attributed to the free hydroxyl function on the benzoyl moiety. This group additionally plays an essential role in the inhibition and selectivity profiles towards 17 β -HSD1 enzyme^{20,21}. Consequently, any further structural optimization on **1** like the omission or protection of the hydroxy group to enhance the metabolic stability will negatively affect the activity and selectivity.

Fortunately, another class of 17 β -HSD1 inhibitors has been recently discovered by our group seems to be more promising from the metabolic stability point of view. This class is based on a hydroxy phenyl furan carboxamide scaffold. The most potent member in this class compound **3** (see Table 1) has exceptionally high selectivity over 17 β -HSD2, and a very promising metabolic stability data.

In this report we will describe the design, synthesis and biological evaluation (in vitro and in vivo) of a new class of dual STS and 17 β -HSD1 inhibitors based on the newly discovered

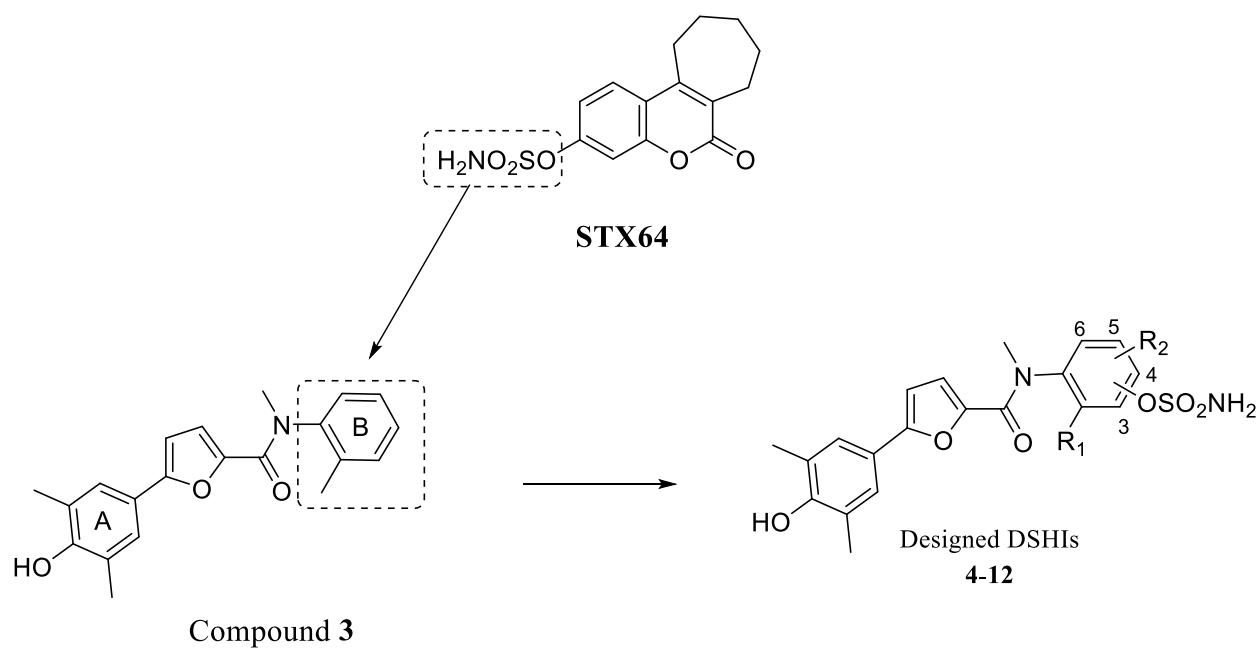
17 β -HSD1 class (see figure 2), which would probably bear a higher degree of metabolic stability and enhanced selectivity over the 17 β -HSD2 enzyme compared to the thiophene based class (e.g. compound **1**). This class could be potentially used for an in vivo proof a principle study in a mouse endometriosis model.

Design

The new class of dual STS and 17 β -HSD1 inhibitors (DSHIs) was rationally designed based on the successful approach which has been previously implemented by our group and led to the development of the first DSHI class (e.g. **1**)¹⁹. The structure activity relationship of the recently discovered furan carboxamide 17 β -HSD1 inhibitors (e.g. compound **3**) deploys that the substituents of ring A (Figure 2) are the main driving factors for the enhanced 17 β -HSD1 inhibitory activity, metabolic stability and selectivity over 17 β -HSD2. On the other hand, the SAR of ring B reveals that it could bear structural modifications without losing the 17 β -HSD1 inhibitory activity. Therefore, the essential feature of STS inhibition (sulfamate group) was combined to ring B of compound **3**, resulting in a hybrid structure that appropriately include the essential features for the simultaneous inhibition of both STS and 17 β -HSD1. Additional substituents were inserted to enhance the inhibitory profile of the DSHIs. The general structure of the potential DSHIs (compounds **4-12**) are shown in Figure 2.

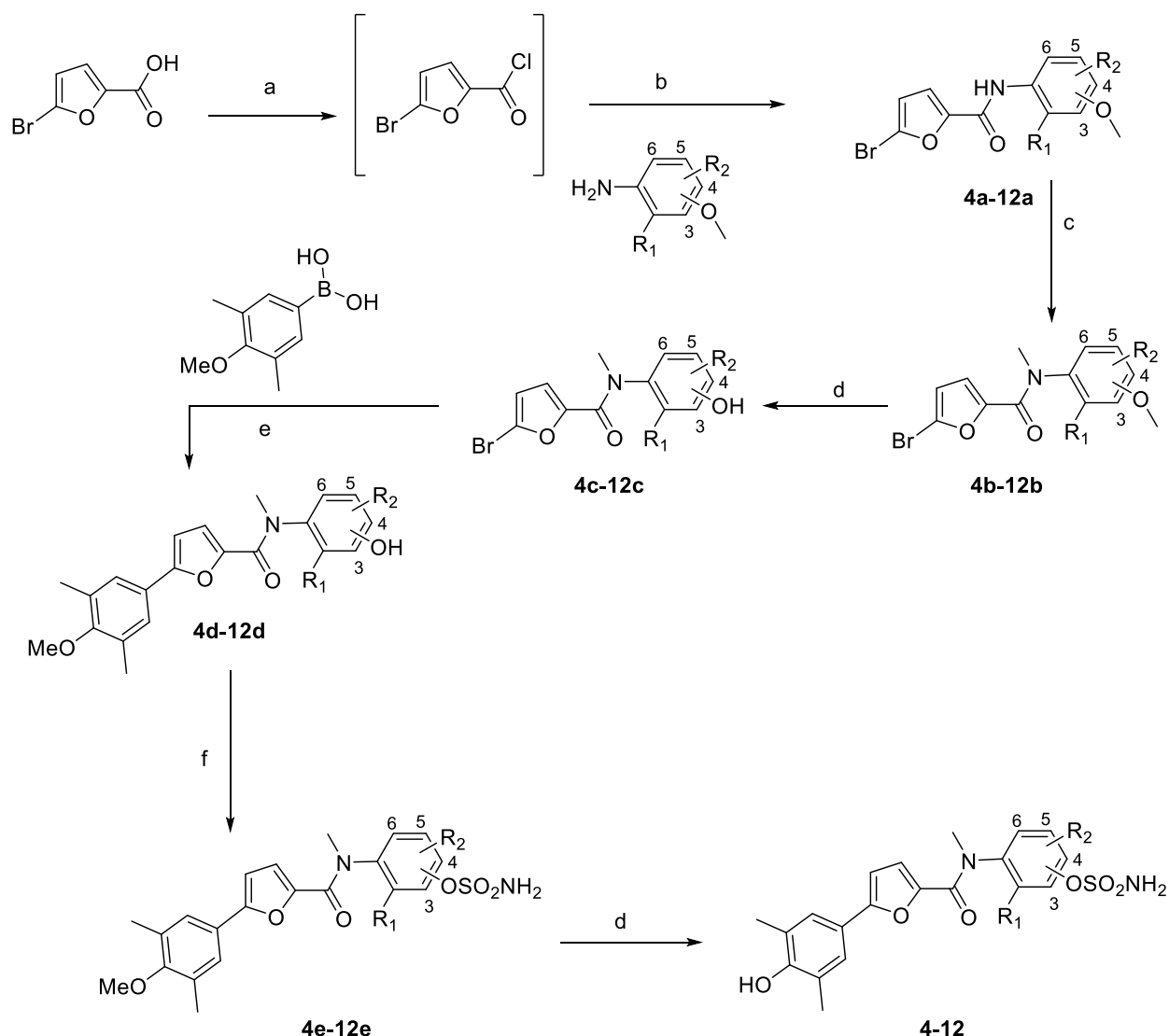
Chemistry

The synthesis of compounds **4-12** was achieved in seven steps for each compound (scheme 1). 5-Bromofuran-2-carbonic acid chloride was obtained from the corresponding carboxylic acid by reaction with SOCl₂ according to method A. It was subsequently reacted with the corresponding aniline according to method B yielding intermediates **4a-12a**. N-methylation was attained by the reaction with methyl iodide according to method C affording intermediates **4b-12b**. The latter was subjected to ether cleavage (method D) with BF₃.S(CH₃)₂ to achieve the phenols **4c-12c**. Subsequently, Suzuki coupling reaction (method E) with (4-methoxy-3,5-dimethylphenyl)boronic acid gave intermediates **4d-12d**. Sulfamoylation (method F) was achieved by the reaction with freshly prepared sulfamoyl chloride (method G) in DMA to obtain intermediates **4e-12e**. Ether cleavage (method D) with BF₃.S(CH₃)₂ in dichloromethane gave the final compounds **4-12**.



| Cpd | R ₁ | R ₂ | Position -OSO ₂ NH ₂ | Cpd | R ₁ | R ₂ | Position -OSO ₂ NH ₂ |
|-----|----------------|----------------|---|-----|----------------|----------------|---|
| 4 | Me | H | 3 | 9 | H | H | 5 |
| 5 | Me | H | 4 | 10 | H | 5-F | 4 |
| 6 | Me | H | 5 | 11 | H | 5-Cl | 4 |
| 7 | Me | H | 6 | 12 | Me | 5-Cl | 4 |
| 8 | H | H | 4 | | | | |

Figure 2. Structure of compounds **STX64**, **3-12** and the general structure of designed dual STS and 17 β -HSD1 inhibitors (DSHIs).



Scheme 1: a) method A, SOCl_2 , DMF cat., toluene, reflux 4h. b) method B, Et_3N , CH_2Cl_2 , room temperature, overnight. c) method C, NaH, DMF, MeI, 0°C to rt, 0.5h. d) method D, $\text{BF}_3 \cdot \text{S}(\text{CH}_3)_2$, CH_2Cl_2 , -20°C to rt, overnight. e) method E, Cs_2CO_3 , $\text{Pd}(\text{PPh}_3)_4$, DME/water (1:1), reflux, 4h. f) method F, DMA, sulfamoyl chloride, rt, overnight.

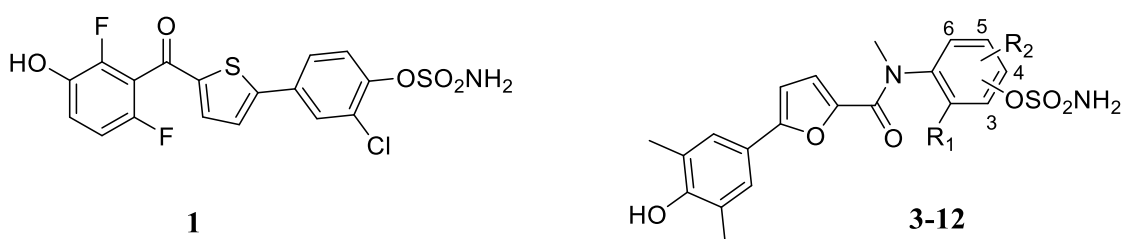
In vitro biological results and discussion

Intracellular inhibition of human STS and 17 β -HSD1

Cellular inhibitory potencies of all final compounds were evaluated using intact human breast cancer cells (T47D) expressing both STS and 17 β -HSD1. **4-12** were pre-incubated with the cells for 1 hour. Subsequently, the corresponding radiolabeled substrate (E1-S or E1) of STS or 17 β -HSD1 was added¹⁹. After incubation (24 h in case of STS and 40 minutes in case of 17 β -HSD1), the radiolabeled estrogens were separated and quantified using HPLC coupled to a radio detector. Inhibitory activities are expressed as IC_{50} values (Table 2).

In our initial attempts to develop a new DSHI class based on compound **3**, we synthesized compounds **4-7** to optimize the position of the sulfamate moiety on the phenyl ring of the lead compound **3** (ring B in figure 2). All the 4 compounds showed high intracellular 17 β -HSD1 inhibitory activity, where compounds **5** and **6** showed the most potent IC₅₀ values of this new class (10.7 nM and 3.2 nM, respectively) compared to the lead compound **3** (2.9 nM). Moreover, compounds **5** and **6** also showed intracellular inhibition of STS with IC₅₀ values in the range of 400 nM.

Table 2: Inhibitory activities of compounds **1, 2-12** towards *h*STS and *h*17 β -HSD1 in cellular assays



| Cpd | Position OSO ₂ NH ₂ | R ₁ | R ₂ | IC ₅₀ [nM] ^a | |
|-----------|--|----------------|----------------|------------------------------------|--|
| | | | | <i>h</i> STS ^b | <i>h</i> 17 β -HSD1 ^c |
| 1 | - | - | - | 15.4 | 22.2 |
| 3 | - | Me | H | ni | 2.9 |
| 4 | 3 | Me | H | ni | 58.2 |
| 5 | 4 | Me | H | 400.3 | 10.7 |
| 6 | 5 | Me | H | 448.1 | 3.2 |
| 7 | 6 | Me | H | ni | 137.3 |
| 8 | 4 | H | H | 148.5 | 106.5 |
| 9 | 5 | H | H | 92.5 | 78.5 |
| 10 | 4 | H | 5-F | 83.2 | 138.5 |
| 11 | 4 | H | 5-Cl | 38.3 | 87.5 |
| 12 | 4 | Me | 5-Cl | 76.1 | 53.3 |

^a Mean value of at least two independent experiments each conducted in triplicates using intact T47D cells, standard deviation less than 15%; ^b Substrate [³H]-E1-S + E1-S [5 nM]; ^c Substrate [³H]-E1 + E1 [50 nM]; ni: no inhibition (< 10% inhibition at 1 μ M).

The STS inhibitory activity of compounds **5** and **6** was aimed to be enhanced. For this purpose the removal of the methyl group on ring B was thought to be beneficial as it was previously found in other compound classes that alkyl substituents on the sulfamate ring lead to a decrease of STS inhibition²²⁻²⁴. In agreement with this, compounds **8** and **9** showed higher potency against

STS compared to their methylated analogues (Table 2). On the other hand, the removal of the methyl function dramatically decreased the 17 β -HSD1 inhibitory activities by a factor of 10 to 25.

The presence of an electron withdrawing group e.g. (F or Cl) was found in several occasions to enhance the STS inhibition which can be attributed to the enhanced sulfamoyl transfer potential resulting from the increased leaving group ability of the corresponding phenol precursors of sulfamates^{19,24,25}. Therefore, compounds **10** and **11** were synthesized which are the fluorinated and the chlorinated form of compound **8**, respectively. Compound **10** indeed showed better STS inhibition compared to **8**, however this was accompanied by a slight decrease in the 17 β -HSD1 inhibition. Compound **11** turned out to be the most potent STS inhibitor of this class with an IC₅₀ value of 38.3 nM, showing similarly potent 17 β -HSD1 inhibition compared to compound **8**.

At that point it was clear that the presence of the methyl group at position R₁ (Table 2) revealed the highest 17 β -HSD1 activity (compounds **5** and **6**) and the presence of the 5-chloro (compound **11**) resulted in the most potent STS inhibitor of this chemical class. Compound **12** was then rationally designed to combine both features aiming to achieve good STS and 17 β -HSD1 inhibitory activity. Indeed, compound **12** showed strongly enhanced STS inhibitory activity compared to its non-chlorinated analog **5** (IC₅₀ 76.1 nM vs 400.3 nM) and also a stronger inhibition of 17 β -HSD1 compared to its demethylated form **11** (IC₅₀ 53.3 vs 87.5).

From the aforementioned results, the promising compounds that show dual inhibitory activity against both target enzymes (promising DSHIs) could be categorized into 2 groups:

- The first group shows balanced intracellular activities between the 2 target enzymes (compounds **8-12**)
- The second group consists of highly potent 17 β -HSD1 inhibitors with moderate STS inhibitory activity (compounds **5** and **6**).

Selectivity for 17 β -HSD1 over 17 β -HSD2

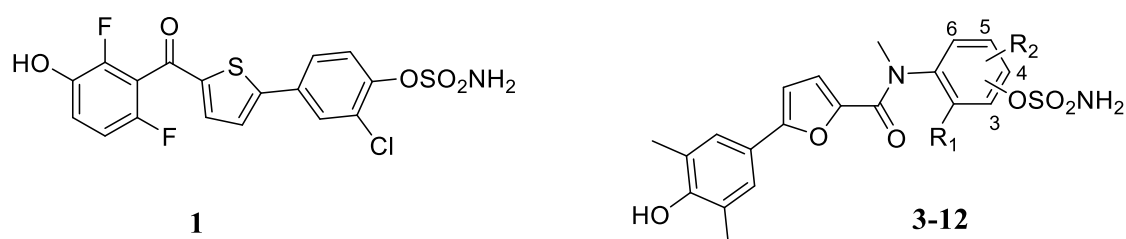
The beneficial role of 17 β -HSD2 in lowering the intracellular levels of E2 makes its inhibition unfavorable. However, this is a challenging characteristic in 17 β -HSD1 inhibitors as the two

enzymes have relatively similar substrates (E1 and E2). Thus, all the promising DSHIs were evaluated for their selectivity for 17 β -HSD1 over its counter partner enzyme 17 β -HSD2 (results are shown in Table 3). Inhibition of 17 β -HSD1 and 17 β -HSD2 was evaluated using the respective radiolabeled steroid (E1 or E2) and human placental 17 β -HSD1 (cytosolic fraction) or 17 β -HSD2 (microsomal fraction).

Compound **12** was the only compound from the first group of the promising DSHIs to show significantly better selectivity for 17 β -HSD1 over 17 β -HSD2 compared to our former lead DSHI compound **1** (SF= 110 vs 33). Other candidates from this group, either showed weaker selectivity e.g. **8**, **10** and **11**, or they showed no advantage over compound **1** (compound **9**).

The second group of the promising DSHIs displayed the highest selectivity for 17 β -HSD1 over 17 β -HSD2 of any other DSHI reported so far. Compounds **5** and **6** showed selectivity factors of 145 and 280, respectively.

Table 3: Inhibitory activities of compounds **1**, **3**, **5**, **6** and **8-12** towards *h*17 β -HSD1 and 2 in cell-free assays and the corresponding selectivity factors



| Cpd | Position OSO ₂ NH ₂ | R ₁ | R ₂ | IC ₅₀ [nM] ^a | | SF ^d |
|-----------|--|----------------|----------------|--|--|-----------------|
| | | | | <i>h</i> 17 β -HSD1 ^b | <i>h</i> 17 β -HSD2 ^c | |
| 1 | - | - | - | 1.1 | 36.1 | 33 |
| 3 | - | Me | H | 5.6 | 3155.2 | 563 |
| 5 | 4 | Me | H | 42.7 | 6158.2 | 145 |
| 6 | 5 | Me | H | 15.5 | 4347 | 280 |
| 8 | 4 | H | H | 425.2 | 7644.6 | 18 |
| 9 | 5 | H | H | 175.2 | 6352.8 | 36 |
| 10 | 4 | H | 5-F | 496.7 | 3196.6 | 6 |
| 11 | 4 | H | 5-Cl | 405.7 | 2396.4 | 6 |
| 12 | 4 | Me | 5-Cl | 67.6 | 7420.2 | 110 |

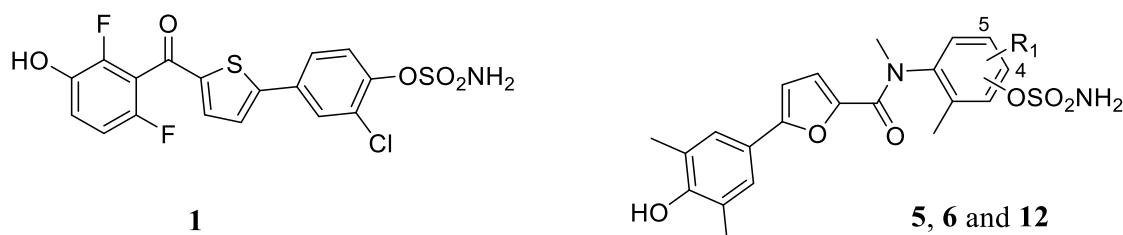
^a Mean value of at least two independent experiments each conducted in duplicates, standard deviation less than 15%; ^b Human placenta, cytosolic fraction, substrate [³H]-E1 + E1 [500 nM], cofactor NADH [0.5 mM]; ^c Human placenta, microsomal fraction, substrate [³H]-E2 + E2 [500 nM], cofactor NAD⁺ [1.5 mM]; ^d SF (selectivity factor): IC₅₀(17 β -HSD2) / IC₅₀(17 β -HSD1).

The selectivity towards 17 β -HSD1 (over 17 β -HSD2) clearly narrowed down the candidate selection for in vivo evaluation to compounds **5**, **6** and **12**. On one hand, compounds **5** and **6** are highly potent 17 β -HSD1 inhibitors with moderate inhibitory activity towards STS, but taken that they might be irreversible STS inhibitors (which seems to be a common characteristic of sulfamate containing STS inhibitors^{24,26} e.g. compound **1** and **STX64**) this could compensate the unbalanced dual inhibition. On the other one, compound **12** is considered an ideal classic dual inhibitor as it displayed balanced action towards both targets. Therefore, all further biological evaluations will be performed on these compounds (**5**, **6** and **12**).

Irreversible inhibition of human STS

The irreversible mode of inhibition was examined for compounds **5**, **6** and **12** as previously reported¹⁹. T47D cells were pre-incubated with the compounds as described for cellular assays. After the removal of the compounds by extensive washing with PBS, E1-S was incubated with the cells for 24 h and then the STS activity was evaluated. In all cases, the IC₅₀ values of this assay were similar to those acquired from the normal assay for intracellular STS inhibition, demonstrating irreversible inhibition of the STS enzyme by compounds **5**, **6** and **12** (Table 4).

Table 4: Irreversible inhibitory activities of compounds **1**, **5**, **6** and **12** towards *h*STS in cellular assays



| Cmpd | Position OSO ₂ NH ₂ | R ₁ | IC ₅₀ [nM] ^a | |
|-----------|--|----------------|------------------------------------|---|
| | | | <i>h</i> STS ^b | <i>h</i> STS ^b irreversible |
| 1 | - | - | 15.4 | 16.4 |
| 5 | 4 | H | 400.3 | 421.8 |
| 6 | 5 | H | 448.1 | 454.4 |
| 12 | 4 | 5-Cl | 76.1 | 78.8 |

^a Mean value of at least two independent experiments each conducted in triplicates using intact T47D cells, standard deviation less than 15%; ^b Substrate [³H]-E1-S + E1-S [5 nM].

In vitro metabolic stability studies

The metabolic stability is an important parameter to achieve low in vivo clearance of the drugs, which helps in reaching sufficient plasma concentrations for an adequate time interval after the in vivo application of the compounds. Thus, the in vitro metabolic half-lives of compounds **5**, **6** and **12** were determined using human and mouse hepatic S9 fractions. The half-lives and the intrinsic body clearances are shown in Table 5. It is noted that compound **5** showed the highest metabolic stabilities in both human and mouse liver S9 fraction detected so far for any DSHI or 17 β -HSD1 inhibitor developed by our group. In human hepatic S9 fraction, $t_{1/2}$ = 85.2 min and intrinsic clearance of 8.2 μ L/min/mg protein, while in mouse hepatic S9 fraction it had a $t_{1/2}$ of 52.1 min. Compound **12** showed a similar metabolic stability profile compared to lead compound **3**. Compound **6** was the least metabolically stable candidate in human hepatic S9 fraction, but it had a better stability than compound **12** in mouse hepatic S9 fraction. Obviously, the new compounds pose better metabolic stability than the previously discovered DSHI (exemplified by compound **1**).

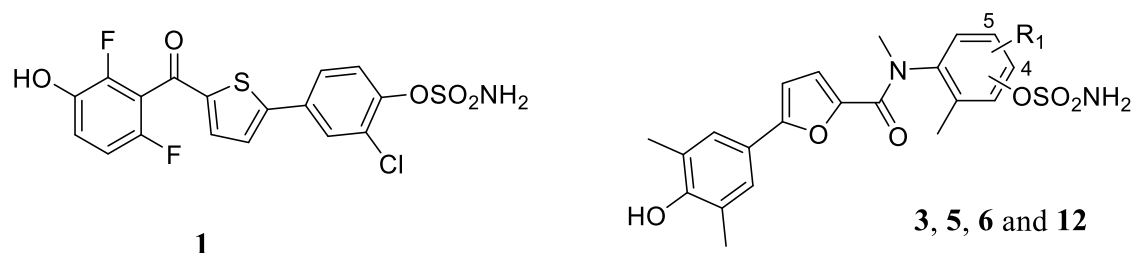
In vitro toxicity evaluation

Cytotoxicity

Compounds **5**, **6** and **12** were evaluated in cellular MTT cytotoxicity assay using HEK293 cells over 72 h. No effect on cell viability (LC_{20} values) was observed up to 31 μ M, 38 μ M and 27 μ M for compounds **5**, **6** and **12**, respectively. As the Derek-Nexus software (an expert knowledge-based software which gives predictions for a variety of toxicological endpoints) provided a plausible hepatotoxicity alert for compounds **5**, **6** and **12**, the toxicity of the compounds and their metabolites were also evaluated using the hepatocellular carcinoma HepG2 cell line in cellular MTT cytotoxicity assay over 48 h. The LC_{20} values were 23 μ M, 28 μ M and 31 μ M for compounds **5**, **6** and **12**, respectively. These values show acceptable safety profiles for these compounds.

Aryl hydrocarbon receptor activation

The aryl hydrocarbon receptor (AhR) assay evaluates the activation of the AhR which can lead to carcinogenicity. AhR activation is an initial event that triggers several toxic biochemical responses, including the induction of CYP1A1 and CYP1A2. These enzymes are responsible for the metabolic activation of many promutagens for e.g. polynuclear aromatic hydrocarbons to carcinogenic arene oxides²⁷. At a concentration of 3.16 μ M, compounds **5**, **6** and **12** did not show any activation of the AhR in HepG2 cells.

Table 5: Metabolic stability of compounds **3**, **5**, **6** and **12** using human and mouse hepatic S9 fraction

| Cmpd | Position OSO ₂ NH ₂ | R ₁ | <i>t</i> _{1/2} [min] ^{a,b} | | Cl _{int} [μL/min/mg protein] ^{a,c} |
|--------------------------------------|--|----------------|--|--------------------|---|
| | | | human ^c | mouse ^d | |
| 1 | - | - | <5 | <5 | n.a |
| 3 | - | H | 38.1 | 19.1 | 18.2 |
| 5 | 4 | H | 85.2 | 56.1 | 8.2 |
| 6 | 5 | H | 19.3 | 28.5 | 35.9 |
| 12 | 4 | 5-Cl | 35.6 | 22.5 | 19.4 |
| 7-Hydroxycoumarin^c | - | - | 5.2 | 7.4 | 138.6 |
| Testosterone^c | - | - | 9.3 | 24.4 | 74.5 |

^a Mean value of three independent experiments, standard deviation less than 15%; ^b *t*_{1/2}: half-life; ^c Human liver S9 fraction; ^d Mouse liver S9 fraction; ^e Reference compounds for the metabolic stability assays.

In vivo evaluation of plasma concentration

Single dose pharmacokinetic studies in mice

On the basis of the *in vitro* results, compounds **5**, **6** and **12** are considered to be possible candidates for a proof-of-principle study in a xenograft mouse model for endometriosis. Thus, their PK profiles after administration to female C57BI/6 mice were investigated. The plasma concentrations of the compounds were evaluated after subcutaneous administration of a single dose (50 mg/kg body weight, n=3) as a suspension in 0.5% gelatin|5% mannitol in water. Plasma samples were collected and concentrations of the compounds were analyzed using LC MS/MS.

As shown in figure 3a, the plasma concentration of compound **5** was always above the *in vitro* cellular IC₈₀ values for both target enzymes (STS and 17β-HSD1) even after 24 h, with a total area under the curve (AUC) of 11619 ng.h/mL. Compound **6** showed plasma concentrations exceeding the cellular IC₈₀ of 17β-HSD1 all over the duration of the experiment (figure 3b). However, these plasma concentrations were not sufficient to reach the cellular STS IC₈₀ of the compound. The compound showed an AUC of 1923 ng.h/mL which is much lower than that of compound **5**. Similarly, compound **12** showed a low AUC value (1883 ng.h/mL) with

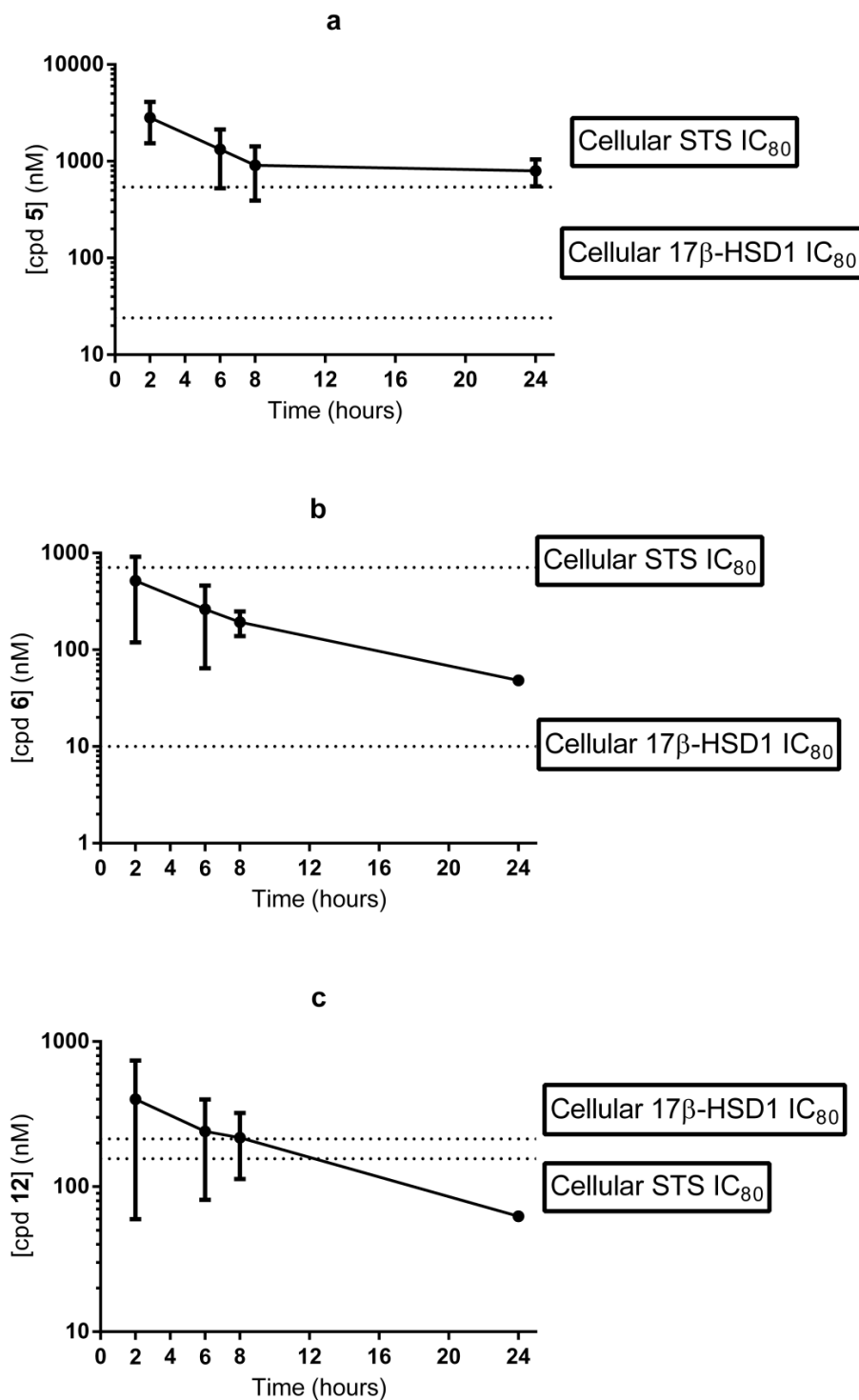


Figure 3. Mean profile (\pm SD) of plasma concentration [nM] in C57B1/6 mice vs time after subcutaneous (50 mg/kg) application of compounds **5** (a), **6** (b) and **12** (c) in single dosing experiments ($n=3$). Dotted lines represent the cellular IC₈₀ values of STS and 17β-HSD1 values for the corresponding compound.

plasma levels above the cellular IC₈₀ of both target enzymes (STS and 17 β -HSD1) up to 7 h as shown in figure 3c. The fact that compound **5** demonstrated higher plasma concentrations than **6** and **12** could be a result of various parameters, among them its higher metabolic stability (shown in table 5), and its physiochemical properties in which the calculated log D (pH=7.4) and the aqueous solubility of compound **5** is better than compounds **6** and **12** (values shown in table 6). Based on these promising data for compound **5**, an additional pharmacokinetic study was performed with per oral application of a single dose using the same dose and vehicle.

Table 6: Cellular IC₈₀ values of compounds **5**, **6** and **12** and their LogD and aqueous solubility

| Cmpd | IC ₈₀ [nM] ^a | | LogD ^d | Aqueous Solubility ^e |
|------|------------------------------------|--|-------------------|---------------------------------|
| | <i>h</i> STS ^b | <i>h</i> 17 β -HSD1 ^c | | |
| 5 | 542 | 24 | 2.20 | 40-60 μ M |
| 6 | 711 | 10 | 2.68 | 20-40 μ M |
| 12 | 156 | 213 | 2.75 | 20-40 μ M |

^a Mean value of at least two independent experiments each conducted in triplicates using intact T47D cells, standard deviation less than 15%; ^b Substrate [³H]-E1-S + E1-S [5 nM]; ^c Substrate [³H]-E1 + E1 [50 nM]; ^d Log D of the cpd, determined by ACD/Labs software; ^e Aqueous solubility of the compounds determined in PBS (Phosphate-buffered saline) with 1% DMSO.

As shown in figure 4, in the first eight hours after application there is no significant difference between the plasma concentrations of compound **5** after either subcutaneous or per oral administration. The main difference is observed after eight hours in which the plasma level in case of the oral route declined continuously reaching very low levels that were not sufficient for the inhibition of any of the target enzymes at 24 h. On the other hand, the subcutaneous route offered steady plasma levels with sufficient concentrations for fulfilling the IC₈₀ of both target enzymes up to 24 h. This can be a result of the extended release of the drug from the suspension formulation. Moreover, compound **5** showed poor oral bioavailability of about 1.5% (see Supporting information). Therefore, the subcutaneous route was selected for multiple dose pharmacokinetic studies.

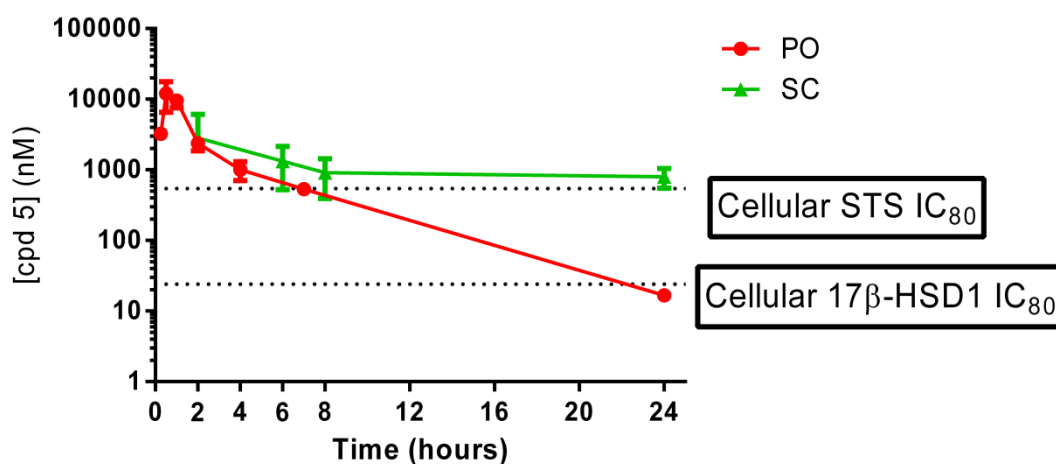


Figure 4. Mean profile (\pm SD) of plasma concentration [nM] in C57B1/6 mice vs time after oral (50 mg/kg) and subcutaneous (50 mg/kg) application of compounds **5** in single dosing experiments ($n=3$). Dotted lines represent the cellular IC_{80} values of STS and 17β -HSD1 values for compound **5**.

Multiple dose pharmacokinetic studies in mice

In order to develop a dosage regimen that could be used for compound **5** in a proof of principle study, the frequency of the subcutaneous drug administration was aimed to be optimized. Compound **5** was administered either every day or every second day subcutaneously (50 mg/Kg) for 5 days as a suspension in 0.5% gelatin|5% mannitol in water. Plasma samples were collected at 2 h and 24 h post-dosing (in addition after 48 h in case of every second day regimen). As shown in figure 5, the plasma concentrations of **5** in the daily dose regimen were -as expected- always above the cellular IC_{80} values of both target enzymes. Interestingly, the compound has a steady state behavior from the third dose in which the plasma concentration fluctuate between constant C_{max} which is measured 2 h post dosing (2350-2450 nM) and C_{min} measured 24 h post dosing (800-900 nM). This shows that the pharmacokinetic profile of compound **5** is not altered after taking multiple doses. This comes in accordance to the principle of superposition, which assumes that early doses do not affect the pharmacokinetics of subsequent doses²⁸. The constancy of the pharmacokinetics suggests that compound **5** does not alter the metabolizing enzymes, neither by inhibition nor induction. In the every second day dose regimen, the plasma levels at 48 h post dosing were sufficient for the 17β -HSD1 inhibition but below the levels needed for the STS inhibition, however, if we take into consideration the irreversible mode of inhibition of the STS enzyme, these amounts might be sufficient. Obviously, the subcutaneous single daily dose regimen (50mg/kg) of compound **5** could be used in an in vivo xenograft model for endometriosis offering an easy dosing frequency with a steady state plasma levels.

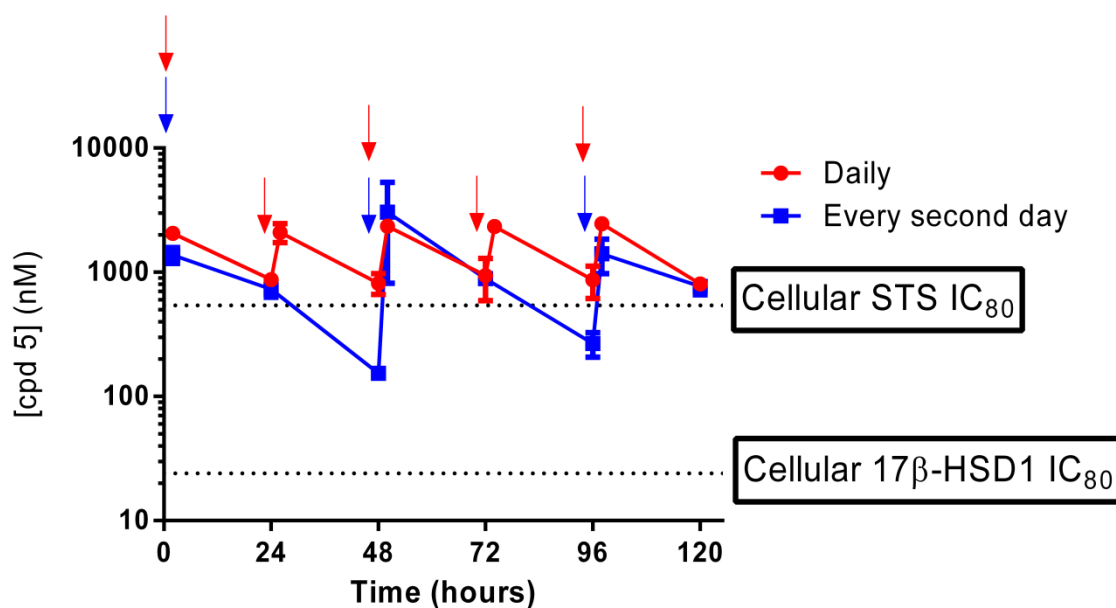


Figure 5. Mean profile (\pm SD) of plasma concentration [nM] in C57B1/6 mice vs time after subcutaneous (50 mg/kg) application of compounds **5** in multiple dosing experiments ($n=3$). Arrows represent the administration of compound **5**. Dotted lines represent the cellular IC_{80} values of STS and 17β -HSD1 values for compound **5**.

Conclusion

Dual inhibition of STS and 17β -HSD1 is considered a novel promising therapeutic approach for EDDs especially endometriosis. The recently developed dual inhibitor **1** has a very promising well-balanced inhibitory profile for both target enzymes. However, it is not considered a suitable candidate to be evaluated in a proof-of-principle endometriosis model as it was found to be metabolically unstable. The aim of the current work was to develop potent dual inhibitors of STS and 17β -HSD1 with increased metabolic stability that can be used for in vivo proof-of-principle studies. A designed multiple ligand approach using the merged pharmacophore strategy -that was previously reported¹⁹- was successfully applied. A newly developed metabolically stable 17β -HSD1 inhibitor class (e.g. compound **3**) was used to build the aryl sulfamate pharmacophore which is essential for STS inhibition. In a first step, the position of the sulfamate moiety on the benzoyl ring (ring B, see figure 2) was aimed to be optimized, resulting in compounds **5** and **6** which were the first dual inhibitors of this class. In cellular assays, they showed weaker inhibition of STS compared to compound **1**, but stronger 17β -HSD1 inhibition, higher selectivity over 17β -HSD2 and enhanced metabolic stability using human and mouse S9 fractions. The decreased inhibitory potency towards STS led to the synthesis of compounds **8-12** which aimed at the removal of the methyl group and/or the addition of electron withdrawing groups while maintaining the optimum position of the

sulfamate moiety. In deed these modifications enhanced the STS inhibitory activity but on the cost of 17 β -HSD1 inhibitory activity and selectivity over 17 β -HSD2 compared to compounds **5** and **6**. Compound **12** showed exceptionally high selectivity over 17 β -HSD2. Moreover, the compound has displayed good metabolic stability in human and mouse S9 fractions. Compounds **5**, **6** and **12** showed irreversible STS inhibition like other sulfamate-containing STS inhibitors. They also displayed acceptable safety profiles in cytotoxicity assays using HEK293 and HepG2 cell lines. The PK profiles of these compounds were evaluated in mice after single subcutaneous application. Compound **5** showed a 6-7 fold higher AUC values compared to **6** and **12**, maintaining the plasma levels above the cellular IC₈₀ of both target enzymes up to 24 h post dosing. The oral application of compound **5** resulted in plasma concentrations sufficient for strong inhibition of both target enzymes up to 8 h post dosing. In a multiple dose PK study, the plasma levels of compound **5** were sufficiently high for strong inhibition of 17 β -HSD1 even after 48 h post dosing. However, these plasma levels were not sufficient for STS inhibition after 24 h post dosing. In this PK study, compound **5** plasma levels showed steady state behavior up to 6 days after first dose, showing no signs of alteration of the CYP metabolizing enzymes neither by inhibition nor by induction.

In summary, compound **5** was found to be a potent dual inhibitor of STS and 17 β -HSD1 with a suitable pharmacokinetic profile for an in vivo proof-of-principle study in a xenograft mouse endometriosis model.

References:

- (1) Morselli, E.; Santos, R. S.; Criollo, A.; Nelson, M. D.; Palmer, B. F.; Clegg, D. J. The Effects of Oestrogens and Their Receptors on Cardiometabolic Health. *Nat. Rev. Endocrinol.* 2017, 13 (6), 352–364.
- (2) Kitawaki, J.; Kado, N.; Ishihara, H.; Koshiba, H.; Kitaoka, Y.; Honjo, H. Endometriosis: The Pathophysiology as an Estrogen-Dependent Disease. *J. Steroid Biochem. Mol. Biol.* 2002, 83 (1–5), 149–155.
- (3) Dizerega, G. S.; Barber, D. L.; Hodgen, G. D. Endometriosis: Role of Ovarian Steroids in Initiation, Maintenance, and Suppression. *Fertil. Steril.* 1980, 33 (6), 649–653.
- (4) Russo, J.; Fernandez, S. V.; Russo, P. A.; Fernbaugh, R.; Sheriff, F. S.; Lareef, H. M.; Garber, J.; Russo, I. H. 17-Beta-Estradiol Induces Transformation and Tumorigenesis in Human Breast Epithelial Cells. *FASEB J.* 2006, 20 (10), 1622–1634.
- (5) Giudice, L. C.; Kao, L. C. Endometriosis. *Lancet* 2004, 364 (9447), 1789–1799.
- (6) Nap, A. W.; Groothuis, P. G.; Demir, A. Y.; Evers, J. L. H.; Dunselman, G. A. J. Pathogenesis of Endometriosis. *Best Practice and Research: Clinical Obstetrics and Gynaecology.* 2004, pp 233–244.
- (7) Berkley, K. J.; Berkley, K. J.; Rapkin, A. J.; Rapkin, A. J.; Papka, R. E.; Papka, R. E. The Pains of Endometriosis. *Science* 2005, 308 (5728), 1587–1589.
- (8) Nnoaham, K. E.; Hummelshoj, L.; Webster, P.; D’Hooghe, T.; De Cicco Nardone, F.; De Cicco Nardone, C.; Jenkinson, C.; Kennedy, S. H.; Zondervan, K. T. Impact of Endometriosis on Quality of Life and Work Productivity: A Multicenter Study across Ten Countries. *Fertil. Steril.* 2011, 96 (2), 366–373.e8.
- (9) Ferreira, A. L. L.; Bessa, M. M. M.; Drezett, J.; De Abreu, L. C. Quality of Life of the Woman Carrier of Endometriosis: Systematized Review. *Reprod. e Clim.* 2016, 31 (1), 48–54.
- (10) Giudice, L. C. Endometriosis. *N. Engl. J. Med.* 2010, 362 (25), 2389–2398.
- (11) Dunselman, G. A. J.; Vermeulen, N.; Becker, C.; Calhaz-Jorge, C.; D’Hooghe, T.; De Bie, B.; Heikinheimo, O.; Horne, A. W.; Kiesel, L.; Nap, A.; Prentice, A.; Saridogan, E.; Soriano, D.; Nelen, W. ESHRE Guideline: Management of Women with Endometriosis. *Hum. Reprod.* 2014, 29 (3), 400–412.
- (12) Huhtinen, K.; Desai, R.; Ståhle, M.; Salminen, A.; Handelsman, D. J.; Perheentupa, A.; Poutanen, M. Endometrial and Endometriotic Concentrations of Estrone and Estradiol Are Determined by Local Metabolism Rather than Circulating Levels. *J. Clin. Endocrinol. Metab.* 2012, 97 (11), 4228–4235.
- (13) Purohit, A.; Fusi, L.; Brosens, J.; Woo, L. W. L.; Potter, B. V. L.; Reed, M. J. Inhibition of Steroid Sulphatase Activity in Endometriotic Implants by 667 COUMATE: A Potential New Therapy. *Hum. Reprod.* 2008, 23 (2), 290–297.
- (14) Šmuc, T.; Pucelj, M. R.; Šinkovec, J.; Husen, B.; Thole, H.; Lanišnik Rižner, T. Expression Analysis of the Genes Involved in Estradiol and Progesterone Action in Human Ovarian Endometriosis. *Gynecol. Endocrinol.* 2007, 23 (2), 105–111.

- (15) Delvoux, B.; D'Hooghe, T.; Kyama, C.; Koskimies, P.; Hermans, R. J. J.; Dunselman, G. A.; Romano, A. Inhibition of Type 1 17 β -Hydroxysteroid Dehydrogenase Impairs the Synthesis of 17 β -Estradiol in Endometriosis Lesions. *J. Clin. Endocrinol. Metab.* 2014, 99 (1), 276–284.
- (16) Saloniemi, T.; Järvensivu, P.; Koskimies, P.; Jokela, H.; Lamminen, T.; Ghaem-Maghamsi, S.; Dina, R.; Damdimopoulou, P.; Mäkelä, S.; Perheentupa, A.; Kujari, H.; Brosens, J.; Poutanen, M. Novel Hydroxysteroid (17 β) Dehydrogenase 1 Inhibitors Reverse Estrogen-Induced Endometrial Hyperplasia in Transgenic Mice. *Am. J. Pathol.* 2010, 176 (3), 1443–1451.
- (17) Colette, S.; Defrère, S.; Lousse, J. C.; Van Langendonckt, A.; Gotteland, J. P.; Loumaye, E.; Donnez, J. Inhibition of Steroid Sulfatase Decreases Endometriosis in an in Vivo Murine Model. *Hum. Reprod.* 2011, 26 (6), 1362–1370.
- (18) Pohl, O.; Bestel, E.; Gotteland, J. P. Synergistic Effects of E2MATE and Norethindrone Acetate on Steroid Sulfatase Inhibition: A Randomized Phase I Proof-of-Principle Clinical Study in Women of Reproductive Age. *Reprod. Sci.* 2014, 21 (10), 1256–1265.
- (19) Salah, M.; Abdelsamie, A. S.; Frotscher, M. First Dual Inhibitors of Steroid Sulfatase (STS) and 17 β -Hydroxysteroid Dehydrogenase Type 1 (17 β -HSD1): Designed Multiple Ligands as Novel Potential Therapeutics for Estrogen-Dependent Diseases. *J. Med. Chem.* 2017, 60 (9), 4086–4092.
- (20) Abdelsamie, A. S.; van Koppen, C. J.; Bey, E.; Salah, M.; Börger, C.; Siebenbürger, L.; Laschke, M. W.; Menger, M. D.; Frotscher, M. Treatment of Estrogen-Dependent Diseases: Design, Synthesis and Profiling of a Selective 17 β -HSD1 Inhibitor with Sub-Nanomolar IC₅₀ for a Proof-of-Principle Study. *Eur. J. Med. Chem.* 2017, 127, 944–957.
- (21) Mohamed Salah; Ahmed S Abdelsamie; Martin Frotscher. Inhibitors of 17 β -Hydroxysteroid Dehydrogenase Type 1, 2 and 14 as Novel Therapeutics for Estrogen-Dependent Diseases: Development, Current Knowledge and Future Challenges. 2018.
- (22) Reed, J. E.; Woo, L. W. L.; Robinson, J. J.; Leblond, B.; Leese, M. P.; Purohit, A.; Reed, M. J.; Potter, B. V. L. 2-Difluoromethyloestrone 3-O-Sulphamate, a Highly Potent Steroid Sulphatase Inhibitor. *Biochem. Biophys. Res. Commun.* 2004, 317 (1), 169–175.
- (23) Purohit, A.; Vernon, K. A.; Wagenaar Hummelinck, A. E.; Woo, L. W. L.; Hejaz, H. A. M.; Potter, B. V. L.; Reed, M. J. The Development of A-Ring Modified Analogues of Oestrone-3-O-Sulphamate as Potent Steroid Sulphatase Inhibitors with Reduced Oestrogenicity. *J. Steroid Biochem. Mol. Biol.* 1998, 64 (5–6), 269–275.
- (24) Thomas, M. P.; Potter, B. V. L. Discovery and Development of the Aryl O -Sulfamate Pharmacophore for Oncology and Women's Health. *J. Med. Chem.* 2015, 58 (19), 7634–7658.
- (25) Woo, L. W. L.; Bubert, C.; Sutcliffe, O. B.; Smith, A.; Chander, S. K.; Mahon, M. F.; Purohit, A.; Reed, M. J.; Potter, B. V. L. Dual Aromatase-Steroid Sulfatase Inhibitors. *J. Med. Chem.* 2007, 50 (15), 3540–3560.
- (26) Potter, B. V. L. SULFATION PATHWAYS: Steroid Sulphatase Inhibition via Aryl

- Sulphamates: Clinical Progress, Mechanism and Future Prospects. *J. Mol. Endocrinol.* 2018, 61 (2), T233–T252.
- (27) Machala, M.; Vondráček, J.; Bláha, L.; Ciganek, M.; Neča, J. Aryl Hydrocarbon Receptor-Mediated Activity of Mutagenic Polycyclic Aromatic Hydrocarbons Determined Using in Vitro Reporter Gene Assay. *Mutat. Res. Toxicol. Environ. Mutagen.* 2001, 497 (1–2), 49–62.
- (28) Siwale, R. C.; Sani, S. Multiple-Dosage Regimens. In *Applied Biopharmaceutics and Pharmacokinetics*; Shargel, Leon; Yu, A., Ed.; McGraw-Hill Education, 2016; pp 205–228.

3.2 Selective inhibitors of 17 β -HSD1, 2 and 14

3.2.I Treatment of estrogen-dependent diseases: Design, synthesis and profiling of a selective 17 β -HSD1 inhibitor with sub-nanomolar IC₅₀ for a proof-of-principle study

Ahmed S. Abdelsamie, Chris J. van Koppen, Emmanuel Bey, Mohamed Salah, Carsten Borger, Lorenz Siebenbürger, Matthias W. Laschke, Michael D. Menger, Martin Frotscher

Reprinted with permission *Eur. J. Med. Chem.* 2017, 127, 944–957.

DOI: 10.1016/j.ejmech.2016.11.004

Copyright (2017) ELSEVIER

Publication C

Contribution Report

The author contributed to the design, synthesis and characterization of the compounds. He further contributed in the biological assays and the interpretation of the results.



Contents lists available at ScienceDirect

European Journal of Medicinal Chemistry

journal homepage: <http://www.elsevier.com/locate/ejmech>

Research paper

Treatment of estrogen-dependent diseases: Design, synthesis and profiling of a selective 17 β -HSD1 inhibitor with sub-nanomolar IC₅₀ for a proof-of-principle study

Ahmed S. Abdelsamie^{a, b}, Chris J. van Koppen^c, Emmanuel Bey^c, Mohamed Salah^a, Carsten Börger^d, Lorenz Siebenbürger^d, Matthias W. Laschke^e, Michael D. Menger^e, Martin Frotscher^{a, *}

^a Pharmaceutical and Medicinal Chemistry, Saarland University, Campus C23, D-66123 Saarbrücken, Germany^b Chemistry of Natural and Microbial Products Department, National Research Centre, Dokki, 12622 Cairo, Egypt^c ElexoPharm GmbH, Campus A12, D-66123 Saarbrücken, Germany^d PharmBioTec GmbH, Science Park 1, D-66123 Saarbrücken, Germany^e Institute for Clinical and Experimental Surgery, Saarland University, D-66421, Homburg/Saar, Germany

ARTICLE INFO

Article history:

Received 22 September 2016

Received in revised form

2 November 2016

Accepted 3 November 2016

Available online 4 November 2016

Keywords:

17 β -Hydroxysteroid dehydrogenase type 1

Enzyme inhibitor

Steroidogenic enzymes

Estrogen-dependent disease

Intracrinology

ABSTRACT

Current endocrine therapeutics for the estrogen-dependent disease endometriosis often lead to considerable side-effects as they act by reducing estrogen action systemically. A more recent approach takes advantage of the fact that the weak estrogen estrone (E1) which is abundant in the plasma, is activated in the target cell to the highly estrogenic estradiol (E2) by 17 β -hydroxysteroid dehydrogenase type 1 (17 β -HSD1). 17 β -HSD1 is overexpressed in endometriosis and thus a promising target for the treatment of this disease, with the prospect of less target-associated side-effects. Potent inhibitors from the class of bicyclic substituted hydroxyphenylmethanones with sulfonamide moiety recently described by us suffered from high molecular weight and low selectivity over 17 β -HSD2, the physiological adversary of 17 β -HSD1. We describe the structural optimizations leading to the discovery of (5-(3,5-dichloro-4-methoxyphenyl)thiophen-2-yl)(2,6-difluoro-3-hydroxyphenyl)methanone **20**, which displayed a sub-nanomolar IC₅₀ towards 17 β -HSD1 as well as high selectivity over the type 2 enzyme, the estrogen receptors α and β and a range of hepatic CYP enzymes. The compound did neither show cellular toxicity, nor PXR activation nor mutagenicity in the AMES II assay. Additional favourable pharmacokinetic properties (rat) make **20** a suitable candidate for proof-of-principle studies using xenotransplanted immunodeficient rats.

© 2016 Elsevier Masson SAS. All rights reserved.

Abbreviations: (h)17 β -HSD1, (human) 17 β -hydroxysteroid dehydrogenase type 1; (h)17 β -HSD2, (human) 17 β -hydroxysteroid dehydrogenase type 2; ADME, absorption, distribution, metabolism, and excretion; BSHs, bicyclic substituted hydroxyphenylmethanones; CC, column chromatography; DBPO, dibenzoyl peroxide; DCM, dichloromethane; DME, dimethoxyethane; E1, estrone; E2, 17 β -estradiol; EDD, estrogen-dependent disease; ER, estrogen receptor; GnRH, gonadotropin-releasing hormone; HPLC, high performance liquid chromatography; MIT, 3-(4,5-dimethylthiazol-2-yl)-2,5-diphenyltetrazolium bromide; NAD(H), nicotinamide adenine dinucleotide; NADP(H), nicotinamide adenine dinucleotide phosphate; NBS, N-bromosuccinimide; PXR, pregnane X receptor; RBA, relative binding affinity; SEM, standard error of the mean; SERM, selective estrogen receptor modulator; SF, selectivity factor over 17 β -HSD2; TLC, thin layer chromatography.

* Corresponding author.

E-mail address: m.frotscher@mx.uni-saarland.de (M. Frotscher).

1. Introduction

17 β -Hydroxysteroid-dehydrogenase type 1 (17 β -HSD1) is a member of the NADPH/NAD⁺-dependent oxidoreductases. It catalyses the activation of estrone (E1) to the most potent estrogen estradiol (E2; Fig. 1) within the target cell. Besides its beneficial physiological effects, E2 is also known to play crucial roles in the development of estrogen-dependent diseases (EDD). Thus, endometriosis [1], breast cancer [2,3], ovarian tumor [4] and other EDD are typically attended by locally increased E2/E1-ratios and high levels of 17 β -HSD1 mRNA in the diseased tissue. Therefore, inhibition of 17 β -HSD1 is considered to be a valuable treatment option for EDD: The tissue-selective expression of 17 β -HSD1 and its intracrine mode of action [5] offer the prospect of a therapy which

<http://dx.doi.org/10.1016/j.ejmech.2016.11.004>

0223-5234/© 2016 Elsevier Masson SAS. All rights reserved.

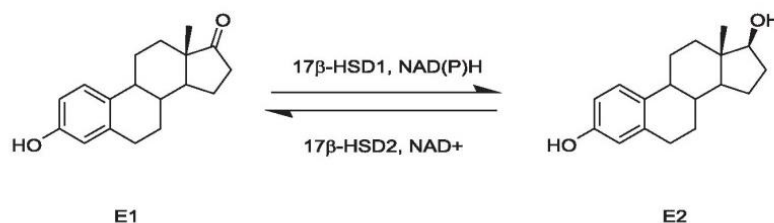


Fig. 1. Interconversion of E1 and E2.

is associated with less side-effects compared to established (but unsatisfactory) treatments with GnRH-analogues, [6,7], aromatase-inhibitors [8–13], anti-estrogens [14] and selective estrogen-receptor modulators (SERMs) [14]. The validity of this concept is supported by the observation that a 17 β -HSD1 inhibitor led to a decrease of E2-levels in endometriotic specimens [15]. In addition, 17 β -HSD1 inhibitors were shown to reduce the E1-stimulated tumor cell growth *in vitro* and in animal models, suggesting the suitability of this target for the treatment of breast cancer [16–18]. 17 β -HSD1 inhibitors should be selective over 17 β -HSD2, the physiological adversary of 17 β -HSD1 which inactivates E2 by oxidation to E1 (Fig. 1). Moreover, they should not bind to estrogen receptors in order to keep systemic interference with estrogenic pathways to a minimum.

A number of 17 β -HSD1 inhibitors are described in the literature, many of them with a steroidal scaffold [19–25]. Our group reported on several classes of non-steroidal 17 β -HSD1 inhibitors, [26–30], among them the bicyclic substituted hydroxyphenylmethanones (BSHs) which displayed very strong inhibition of the target protein [26,29]. Previous studies in this compound class revealed that inhibition of the target enzyme strongly depends on the substitution pattern of the benzoyl ring (Fig. 2, ring A) [26,29]. Here, already minor structural modifications were found to induce dramatic changes in activity. Thus, bulky substituents led to a loss of activity whereas the introduction of fluorine atoms resulted in considerably more active compounds [26,29]. In contrast, it was rather selectivity (towards 17 β -HSD2) than inhibitory potency which was influenced by substituents at the phenyl ring (ring C) [26].

The majority of these SAR data was derived from inhibitors bearing a bulky aromatic sulfonamide moiety. There was evidence, however, that - in terms of biological activities towards human 17 β -HSD1 and 2 - the sulfonamides do not have substantial advantages compared to compounds devoid of the sulfonamide group (Fig. 2) [29]. Consequently, the design and synthesis of novel potential inhibitors lacking this group was aimed at, thus lowering molecular weight while preserving or increasing inhibitory potency and

selectivity.

2. Design

As a starting point, structural modifications of lead compound **A** (Chart 1) were carried out focussing on the substitution patterns of rings A and C (compounds **1–25**, Chart 1), taking into account the following previous SAR data:

- The possibilities for variations of ring A-substitution are very restricted: An OH-group in position 3 of ring A is important for inhibitory activity towards 17 β -HSD1 and should be retained. In addition, the target enzyme only tolerates small additional substituents on ring A.
- Much more flexibility exists concerning the substitution pattern of ring C: here, even bulky substituents should be tolerated, and the OH-group can be omitted – albeit its presence can be expected to lead to increased selectivity over 17 β -HSD2.

First, based upon a simplified analogue of lead **A** (compound **1**, Chart 1), the synthesis of a couple of compounds bearing small substituents, especially fluorine, on ring A was envisaged in order to identify a beneficial substitution pattern (compounds **2–5**) which should be maintained in the further design process. Subsequent structural modifications aimed at the optimization of ring C and its substitution pattern. To this purpose, electron-donating and -withdrawing groups of different sizes were introduced. In addition, the effect of a replacement of benzene with pyridine was evaluated (compounds **6–25**).

Moreover, compounds **26** and **27** as non-fluorinated analogues of **20** and **21** were synthesized to re-evaluate the effect of the fluorine atoms on ring A on activity and selectivity. Finally, the phenyl ring C of the most interesting compounds **20** and **21** was decorated with heterocyclic moieties in order to increase solubility (compounds **28–32**, Chart 2).

| compound | R | IC ₅₀ (nM) | | M (g/mol) |
|----------|----|-----------------------|------------------|-----------|
| | | 17 β -HSD1 | 17 β -HSD2 | |
| A | | 8 | 199 | 598 |
| B | OH | 22 | 109 | 296 |

Fig. 2. Comparison of compound **A** with sulfonamide moiety and compound **B**, lacking this group.

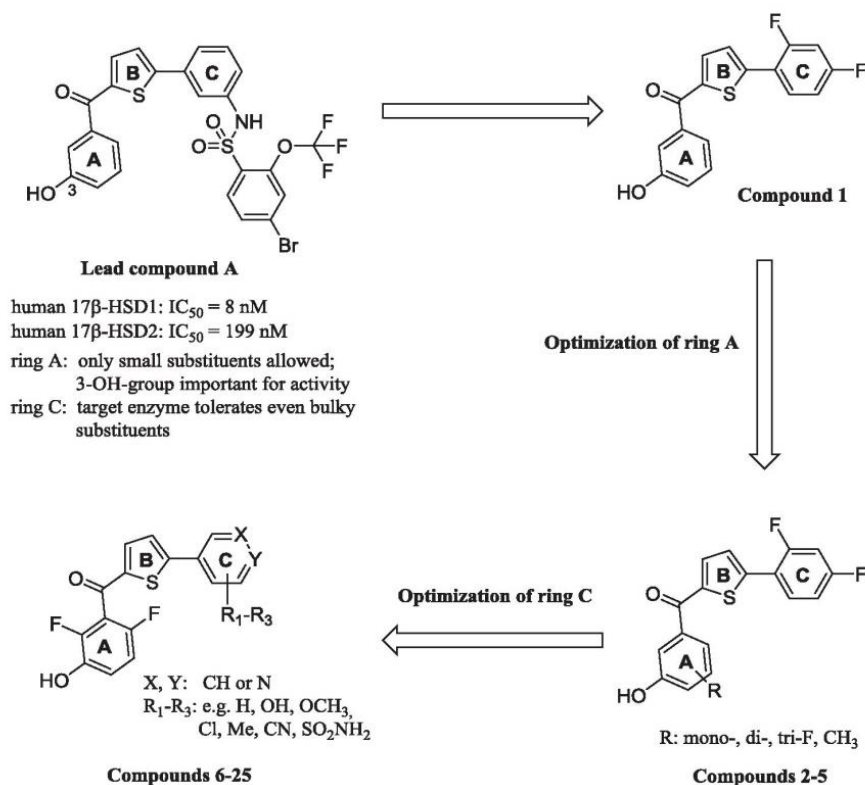


Chart 1. Design of synthesized compounds 1–25.

3. Chemistry

The key intermediates I–V were synthesized in good yield from the appropriate benzoyl chlorides and 2-bromothiophene using

Friedel-Crafts conditions (method A). Subsequent ether cleavage of intermediates I and IV (method B) yielded VI and VII, respectively, in a quantitative yield (Scheme 1).

For the preparation of compounds 1–7 the key intermediates

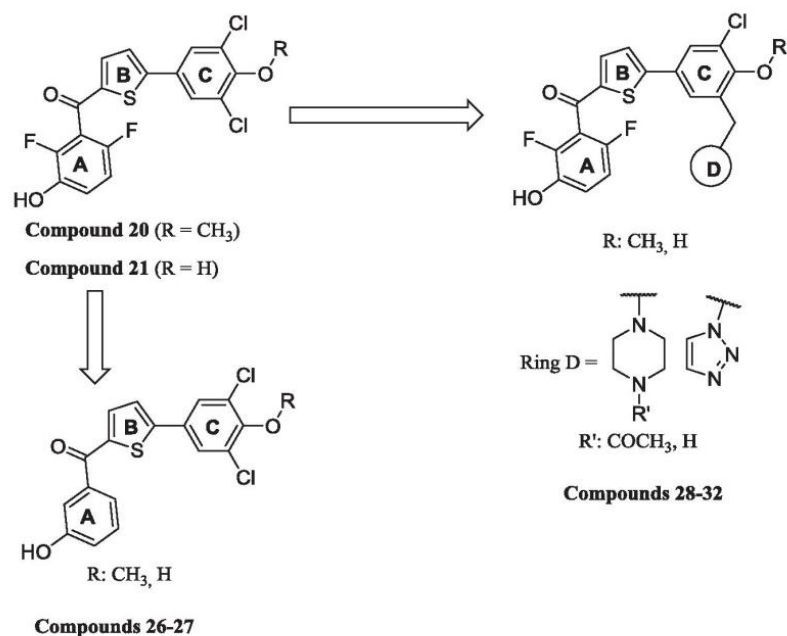
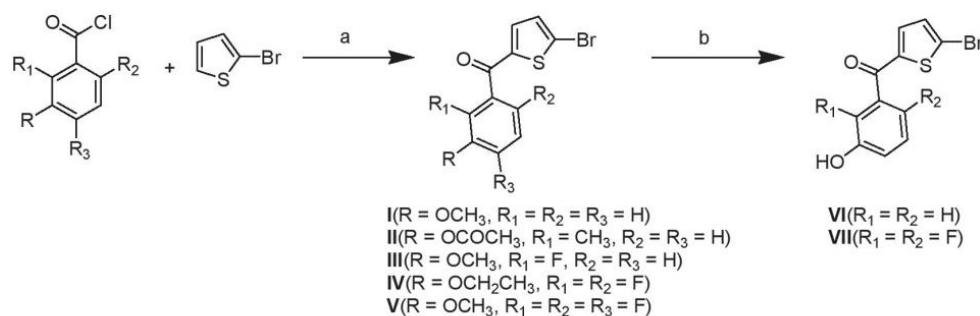


Chart 2. Design of synthesized compounds 26–32.



Scheme 1. Synthesis of intermediates I–VII. a) method A, AlCl_3 , anhydrous CH_2Cl_2 , 0 °C, 0.5 h and then rt, 3 h. b) method B, BBr_3 , CH_2Cl_2 , -78 °C to rt, overnight.

I–V were submitted to a Suzuki reaction (method C1 or C2) with the appropriate boronic acid to give **1a–7a**. The latter were submitted to ether cleavage with BBr_3 in dichloromethane to afford the final compounds (**1**, **3–7**) or hydrolysis using 10% NaOH in ethanol to give compound **2**, respectively (Schemes 2 and 3).

The compounds **8–21** and **24–27** were obtained from the intermediates **VI** or **VII** by standard methods (either Suzuki reaction (method C1) alone or followed by ether cleavage (method B)) (Scheme 4).

The synthesis of compound **23** was accomplished as shown in Scheme 5: Bromination of 2-chloro-6-methylphenol with NBS in acetic acid selectively gave the ring-brominated compound **22c**, which underwent methylation upon treatment with methyl iodide. The resulting compound **22b** was transformed to the boronic acid ester **22a**. Finally, Suzuki cross coupling reaction of the latter with **VII** yielded compound **22**, which was submitted to ether cleavage with BBr_3 , resulting in **23**.

The boronic acid ester **22a** was also used as starting material for the syntheses leading to compounds **28–30** (Scheme 5). By using NBS and DBPO in CCl_4 , **22a** was converted to the brominated intermediate **28b**. Nucleophilic substitution of the bromine atom with 1-piperazine-1-ylethanone yielded **28a**. The latter was reacted with **VII** in a Suzuki reaction (method C1) to afford compound **28**, which gave access to **29** (via ether cleavage) and **30** (via amide hydrolysis under acidic conditions).

The azide intermediate **31c** was prepared by reaction of **28b** with NaN_3 in DMF (Scheme 6). The subsequent Suzuki cross-coupling reaction with **VII** yielded **31b**, which was submitted to a cycloaddition reaction with acetic acid vinyl ester [31] to give the 1,2,3-triazole substituted compound. Interestingly, the latter was exclusively isolated as acetic acid ester **31a**. Saponification with 2M-NaOH gave the phenol **31**, which was transformed to the diol **32** by reaction with BBr_3 (method B).

4. Biological results and discussion

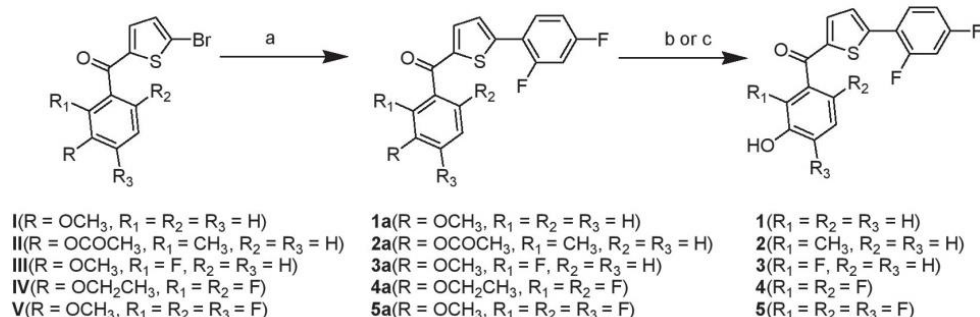
4.1. Inhibition of human 17β -HSD1 and selectivity towards 17β -HSD2, $\text{ER}\alpha$, and $\text{ER}\beta$

Human placental enzymes were used for both 17β -HSD assays and were obtained according to described methods [32–34]. In the 17β -HSD1 assay, incubations were run with cytosolic fractions, tritiated E1, cofactor and inhibitor. The separation of substrate and product was accomplished by HPLC. The 17β -HSD2 assay was performed similarly using tritiated E2 as substrate and the microsomal fraction. Activities are given as IC_{50} -values (Tables 1–4).

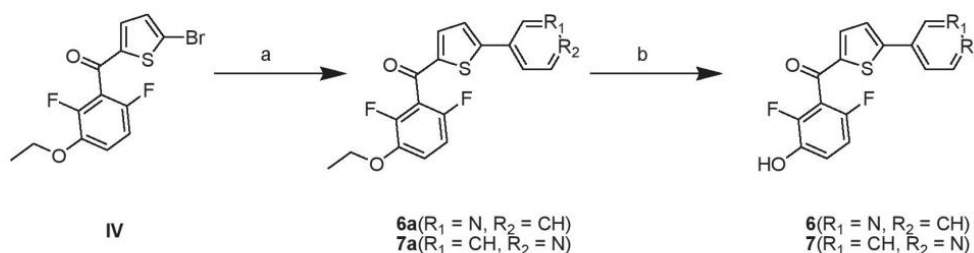
As expected, 17β -HSD1 inhibition of the synthesized compounds was strongly dependent on the substitution pattern of the benzoyl moiety (ring A, see Chart 1): Whereas compound **1** showed moderate activity ($\text{IC}_{50} = 105 \text{ nM}$, Table 1), the presence of a methyl group was detrimental for inhibitory potency (compound **2**). A very strong inhibition of the target enzyme, however, could be achieved by the introduction of one or more fluorine atoms (compounds **3–5**). The most interesting properties in terms of activity towards 17β -HSD1 and selectivity over 17β -HSD2 was detected for the 2,6-difluorinated compound **4**. Therefore, this substitution pattern of the benzoyl moiety was maintained in the subsequent optimization of ring C.

The replacement of the phenyl ring C with pyridine (compounds **6** and **7**) or omission of the fluorine substituents (**8**) led to a more or less pronounced drop in activity, compared to compound **4** (Table 2). For the sulfonamides **9–11** this effect was also observed. The introduction of a nitrile group proved to be beneficial for activity (compounds **12** and **13**), but led to low selectivity over 17β -HSD2.

Starting from **13**, the nitrile group was omitted or replaced by chlorine while maintaining an oxygen-function of ring C, in order to



Scheme 2. Synthesis of compounds 1–5. a) method C1, 2,4-difluorophenylboronic acid, Cs_2CO_3 , $\text{Pd}(\text{PPh}_3)_4$, DME/water (1:1), reflux, 4 h. b) method B, BBr_3 , CH_2Cl_2 , -78 °C to rt, overnight. c) 10% NaOH, ethanol, reflux, 2 h.



Scheme 3. Synthesis of compounds **6** and **7**. a) method C2, 3- pyridinylboronic acid pinacol ester or 4-pyridinylboronic acid for **6a** and **7a**, respectively, Na_2CO_3 , $\text{Pd}(\text{PPh}_3)_4$, toluene/ethanol (1:1), reflux, overnight. b) method B, BBr_3 , CH_2Cl_2 , -78°C to rt, overnight.

enhance selectivity (compounds **14**, **15**, **17–19**). Compound **16** lacks this oxygen function and was synthesized for comparison reasons. An OH-group in 4-position of ring C proved to be beneficial (see e.g. compound **15**: $\text{IC}_{50} = 3 \text{ nM}$, $\text{SF} = 24$ and compound **18**: $\text{IC}_{50} = 0.5 \text{ nM}$, $\text{SF} = 40$) whereas the removal of the OH-group (compound **16**) or shifting its position from *para* to *ortho* (compound **19**), led to a decrease or a complete loss of selectivity, respectively (Table 2). From this optimization step, compound **18** emerged as the most active and selective inhibitor.

It was striking that compounds bearing an additional substituent on ring C in *ortho*-position to the oxygen-functionality (hydroxy or methoxy) stand out in terms activity and selectivity (compounds **13**, **17** and **18**, Table 2). This prompted us to investigate compounds with two *ortho*-substituents (compounds **20–25**, Table 3). In fact, this structural modification resulted in highly active compounds, generally displaying sub-nanomolar IC_{50} -values for h17 β -HSD1 inhibition. Interestingly, compounds bearing chloro- and methyl-substituents showed similarly strong inhibition of the target enzyme. In terms of selectivity towards the type 2 enzyme it is noteworthy that generally the phenols were superior compared to their methoxy-analogs. An exception was compound **20** which was not only one of the most active but also the most selective compound of its class ($\text{IC}_{50}(\text{h17}\beta\text{-HSD1}) = 0.5 \text{ nM}$; $\text{SF} = 82$). To get an evidence for the importance of fluorine atoms on the benzoyl part on the inhibitory activity issue of this compound class, compounds **26** and **27** were synthesized. Comparison with the inhibition data of compound **20** and its analog non-fluorinated compound **26** highlights again the beneficial impact of the fluorine atoms at the benzoyl moiety. The same dependence of activity on benzoyl fluorination can be seen when comparing compounds **21** and **27** (Table 3).

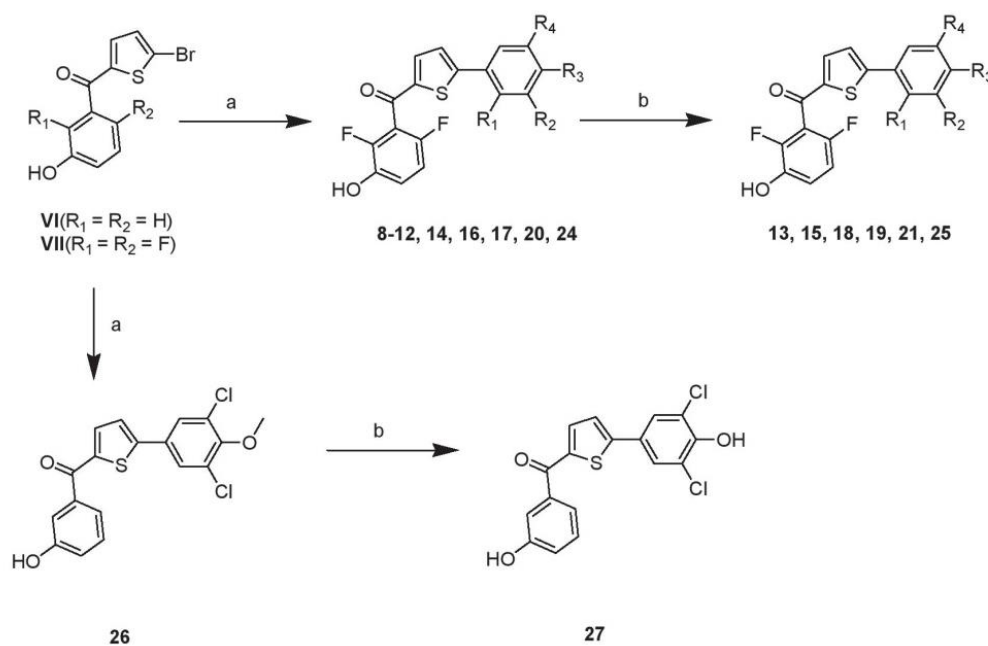
The dichlorinated inhibitor **20** showed favourable properties concerning activity and selectivity, but exhibited high lipophilicity (clogD ($\text{pH} = 7.4$): 4.9, as determined using the ACD-Labs *Percepta* software). In order to render the compound more hydrophilic, one of the chlorine atoms was replaced by heterocyclic substituents (compounds **28–32**, Table 4). The synthesized compounds showed greatly reduced lipophilicities (clogD range ($\text{pH} = 7.4$): 1.7 (**30**) – 3.3 (**31**)) and were highly active towards the target enzyme: apart from the dihydroxy compound **32**, all compounds displayed IC_{50} -values in the one-digit nanomolar range (Table 4). Selectivity over the type 2 enzyme, however, was in most cases less favourable than for compounds **20–25**.

The affinities of selected compounds to the recombinant human estrogen receptors α and β were determined by incubation of tritiated E2 with the respective receptor and compound in 1000-fold excess, based on E2 concentration. Receptor affinities are expressed as the percentage of E2 replaced by a compound. ER-binding of 50% is equal to a relative binding affinity (RBA) of 0.1% of that of E2 [35].

The determined estrogen receptor affinities are given in Table 5. The data suggest that fluorination of the benzoyl moiety increases ER-affinity (cf. compound **20** vs. **26**). Increasing the number or size of substituents adjacent to the oxygen-function of the phenyl ring (ring C) decreases ER-affinity (cf. compound **18** vs. **11**, **13**, **20**, **21**, **24**, and **25**).

Compounds **20** and **25**, which were highly active towards the target enzyme and selective over 17 β -HSD2, displayed very low affinities towards ER α and β , in particular in view of their sub-nanomolar activity towards 17 β -HSD1.

We next profiled the most interesting compound **20** in several relevant toxicity assays. First, compound **20** did not affect cell viability up to a concentration of $5.6 \mu\text{M}$, as measured in the MTT cytotoxicity assay in HEK293 cells after an incubation period of 66 h, yielding a safety margin of 11,160-fold (i.e., IC_{20} in the MTT assay divided by the IC_{50} value in the human 17 β -HSD1 assay). Secondly, for determination of the mutagenic potential of compound **20**, an Ames II test was performed using TA98 (frameshift mutation) or TAMix (base-pair substitution, TA7001-TA7006) strains of *Salmonella typhimurium* in the presence or absence of rat liver S9 fraction. Compound **20** did not show mutagenic potential up to the highest tested concentration of $100 \mu\text{M}$ in the absence or presence of rat liver S9 fraction. We next investigated whether compound **20** has the potential of CYP3A4 induction. For this, compound **20** was tested for activation of the pregnane X receptor (PXR), which is responsible for the induction of CYP3A4, and other members of the CYP3 subfamily of hepatic CYP450 enzymes, respectively. Compound **20** tested at a concentration of $3.16 \mu\text{M}$ did not stimulate the PXR receptor (effect < 5% activation, data not shown). Compound **20** was also profiled for inhibition of several hepatic CYP450 enzymes at a compound concentration of $1 \mu\text{M}$, which is 2000-fold higher than the IC_{50} value for 17 β -HSD1 inhibition. Compound **20** only moderately inhibited CYP1A2, 2B6, 2C9, 2C19, 2D6, and 3A4 by 11%, 4%, 0%, 27%, 0% and 36%, respectively. We next investigated whether our best current compound **20** can be administered to rodents to allow *proof-of-principle* testing of a potent 17 β -HSD1 inhibitor in a rodent model of endometriosis. For this, we subcutaneously administered compound **20** at a dose of $150 \mu\text{mol/kg}$ body weight once-a-day for four consecutive days, during which we determined plasma levels of **20**, and measured also the plasma level of compound **20** four days after the last dosing. As shown in Fig. 3, compound **20** subcutaneously administered as suspension in 0.5% gelatin/5% mannitol in water led to a gradual increase in the plasma concentration from 24 nM measured at day 2, 42 nM at day 4, and to 72 nM at day 8, 4 days after the last dosing at day 4. These *in vivo* plasma concentrations are 10-fold higher than the concentrations required *in vitro* in the 17 β -HSD1 assay to block 17 β -HSD1 by 80–100% (data not shown).



| Compd | R ₁ | R ₂ | R ₃ | R ₄ | Comd | R ₁ | R ₂ | R ₃ | R ₄ |
|-------|----------------|---------------------------------|---------------------------------|----------------|------|----------------|-----------------|------------------|-----------------|
| 8 | H | H | H | H | 16 | H | Cl | H | H |
| 9 | H | SO ₂ NH ₂ | H | H | 17 | H | Cl | OCH ₃ | H |
| 10 | H | H | SO ₂ NH ₂ | H | 18 | H | Cl | OH | H |
| 11 | H | | OCH ₃ | H | 19 | OH | Cl | H | H |
| 12 | H | CN | | H | 20 | H | Cl | OCH ₃ | Cl |
| 13 | H | CN | OH | H | 21 | H | Cl | OH | Cl |
| 14 | H | H | OCH ₃ | H | 24 | H | CH ₃ | OCH ₃ | CH ₃ |
| 15 | H | H | OH | H | 25 | H | CH ₃ | OH | CH ₃ |

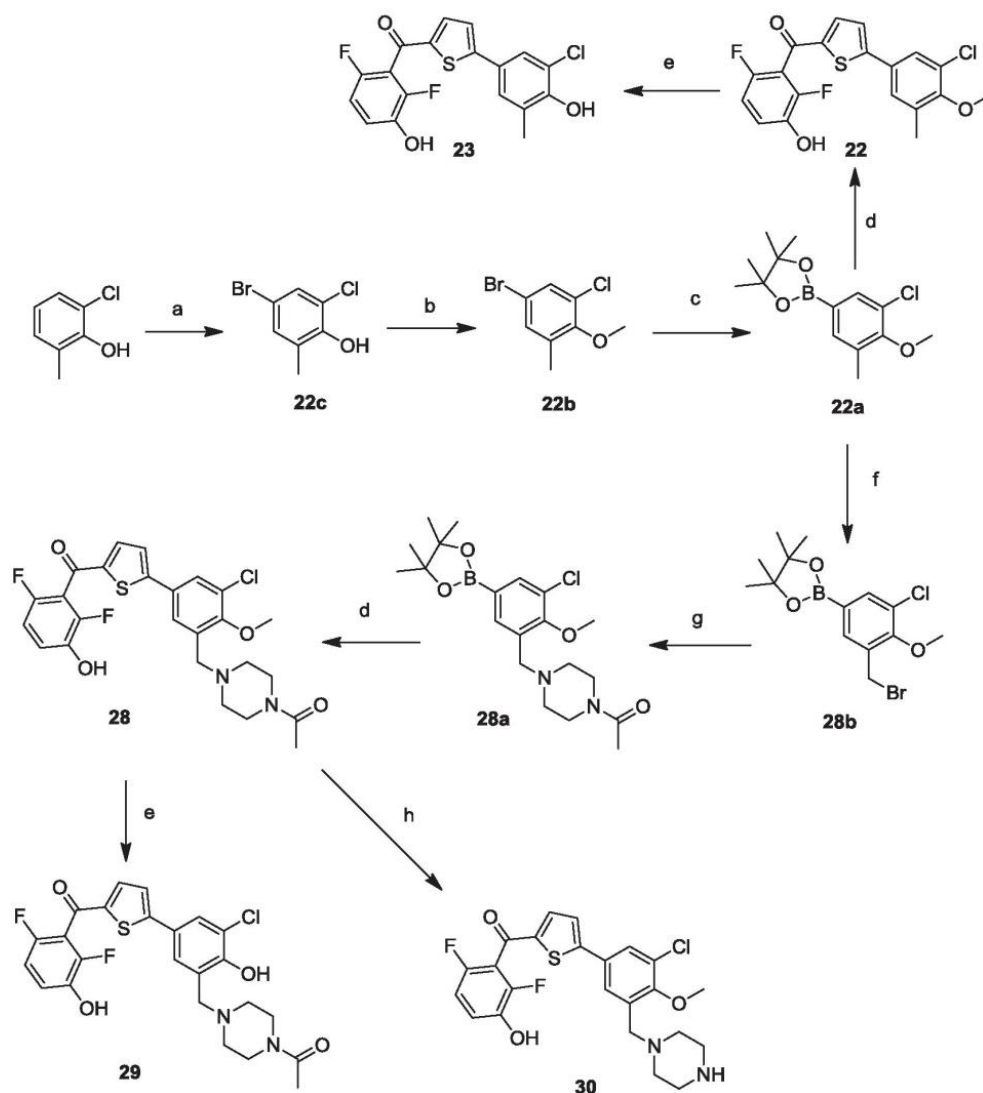
Scheme 4. Synthesis of compounds **8–21** and **24–27**. a) method C1, corresponding boronic acid, Cs₂CO₃, Pd(PPh₃)₄, DME/water (1:1), reflux, 4 h. b) method B, BBr₃, CH₂Cl₂, -78 °C to rt, overnight.

5. Conclusions

The aim of the present study was the design of potent and selective, low molecular weight inhibitors of human 17 β -HSD1, which can be used to conduct a proof of principle study in an animal disease model for EDD. Starting point were sulfonamide-substituted bicyclic substituted hydroxyphenylmethanones previously described by us. Structural modifications focused on the substitution patterns of the benzoyl- and the phenyl-moieties.

To our knowledge, the 17 β -HSD1 inhibitors identified in this study are the most active ones ever described for this enzyme. The most interesting compounds were **20**, **21**, and **25** as their high potency towards the target protein was accompanied by good selectivities over the human type 2 enzyme and the estrogen receptors α and β .

We profiled compound **20** in several ADME and toxicity assays. Compound **20** did not activate PXR at the tested concentration of 3.16 μ M and did not show mutagenicity in the AMES II assay up to



Scheme 5. Synthesis of compounds **22–23**, and **28–30**. a) NBS, AcOH, rt, overnight. b) CH_3I , K_2CO_3 , DMF, rt, overnight. c) bispinacolato diborane, $\text{Pd}(\text{dppf})\text{Cl}_2$, KOAc/DMSO, 2 h. d) method C1, **VII**, Cs_2CO_3 , $\text{Pd}(\text{PPh}_3)_4$, DME/water (1:1), reflux, overnight. e) method B, BBr_3 , CH_2Cl_2 , -78°C to rt, overnight. f) NBS, DBPO, CCl_4 , reflux, 2 h. g) NEt_3 , 1-piperazin-1-yl-ethanone. h) HCl 3 M, reflux, 3 h.

the highest tested concentration of 100 μM . Compound **20** also did not show cellular toxicity up to a concentration of 5.6 μM , as measured after 66 h of incubation in the MTT cell viability assay. Given the very potency of compound **20** towards 17 β -HSD1 (IC_{50} of 0.5 nM), it is therefore to be expected that no cytotoxic effects will be observed in therapeutic doses. In addition, compound **20** showed only moderate CYP450 enzyme inhibition at the relatively high concentration of 1 μM . Immunocompromised rodents such as athymic nude and severe-compromised immunodeficient (SCID) mice and rats are frequently utilized to determine *in vivo* efficacy of preclinical drug candidates towards implanted human cells, including breast cancer cells and human endometriotic tissue samples. The very promising pharmacokinetic profile of compound **20** in rat after repetitive subcutaneous administration will allow for the first time *proof-of-principle* studies in rodent models of breast cancer and endometriosis, in which inhibition of 17 β -HSD1 is considered to be therapeutically highly beneficial.

6. Experimental section

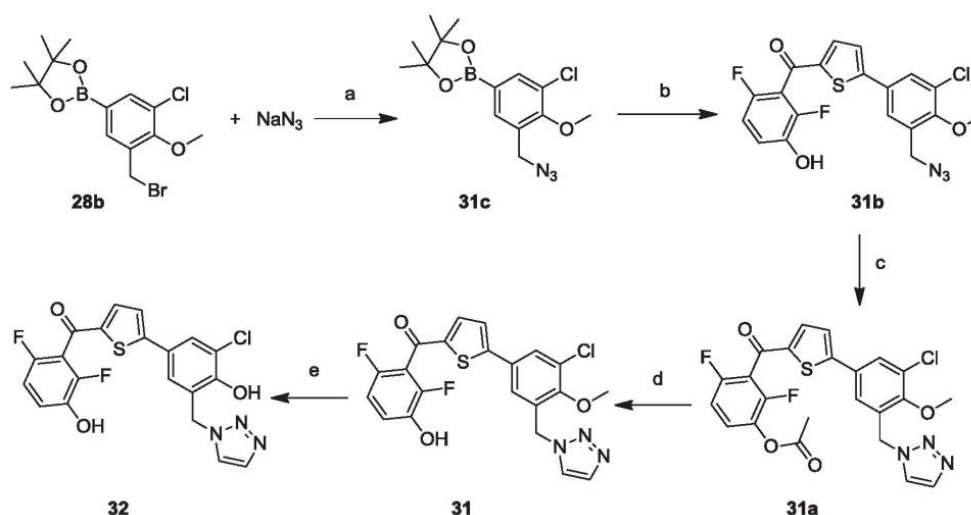
6.1. Chemical methods

Chemical names follow IUPAC nomenclature. Starting materials were purchased from Aldrich, Acros, Lancaster, Maybridge, Combi Blocks, Merck, or Fluka and were used without purification.

Column chromatography (CC) was performed on silica gel (70–200 μm), reaction progress was monitored by thin layer chromatography (TLC) on Alugram SIL G UV₂₅₄ (Macherey-Nagel).

All microwave irradiation experiments were carried out in a CEM-Discover monomode microwave apparatus.

^1H NMR and ^{13}C NMR spectra were measured on a Bruker AM500 spectrometer (500 MHz) at 300 K. Chemical shifts are reported in δ (parts per million: ppm), by reference to the hydrogenated residues of deuterated solvent as internal standard (CDCl_3 : $\delta = 7.24$ ppm (^1H NMR) and $\delta = 77$ ppm (^{13}C NMR), CD_3OD :



Scheme 6. Synthesis of compounds **31** and **32**. a) DMF, rt, overnight. b) method C1, **VII**, Cs_2CO_3 , $\text{Pd}(\text{PPh}_3)_4$, DME/water (1:1), reflux, overnight. c) $\text{CH}_3\text{COOCH}=\text{CH}_2$, microwave, 120°C , 10 h. d) 2 M NaOH, THF, rt, 2 h. e) method B, BBr_3 , CH_2Cl_2 , -78°C to rt, overnight.

Table 1

Optimization of A-ring-substitution: Activities of compounds **1–5** towards $h17\beta\text{-HSD1}$ and **2**.

1–5

| Cmpd | Ring A | IC_{50} [nM] ^a | | SF^{d} | Cmpd | Ring A | IC_{50} [nM] ^a | | SF^{d} |
|----------|--------|------------------------------------|----------------|------------------------|----------|--------|------------------------------------|----------------|------------------------|
| | | $h17\beta\text{-HSD Type}$ | | | | | $h17\beta\text{-HSD Type}$ | | |
| | | 1 ^b | 2 ^c | | | | 1 ^b | 2 ^c | |
| 1 | | 110 | 140 | 1.3 | 2 | | 3400 | 300 | 0.1 |
| 3 | | 47 | 55 | 1.1 | 4 | | 3.5 | 9.0 | 2.5 |
| 5 | | 7.2 | 1.4 | 0.2 | | | | | |

^a Mean value of three determinations, standard deviation less than 15%.

^b Human placenta, cytosolic fraction, substrate [^3H]-E1, 500 nM, cofactor NADH, 500 μM .

^c Human placenta, microsomal fraction, substrate [^3H]-E2, 500 nM, cofactor NAD^+ , 1500 μM .

^d SF (selectivity factor): $\text{IC}_{50}(17\beta\text{-HSD2})/\text{IC}_{50}(17\beta\text{-HSD1})$.

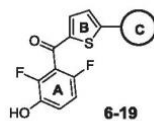
$\delta = 3.35$ ppm (^1H NMR) and $\delta = 49.3$ ppm (^{13}C NMR), CD_3COCD_3 : $\delta = 2.05$ ppm (^1H NMR) and $\delta = 29.9$ ppm (^{13}C NMR), CD_3SOCD_3 : $\delta = 2.50$ ppm (^1H NMR) and $\delta = 39.5$ ppm (^{13}C NMR). Signals are described as s, d, t, dd, ddd, m, dt, q, sep, br. for singlet, doublet, triplet, doublet of doublets, doublet of doublets of doublets, multiplet, doublet of triplets, quadruplet, septet, and broad, respectively. All coupling constants (J) are given in hertz (Hz).

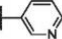
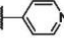
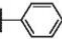
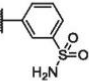
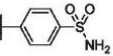
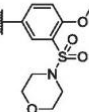
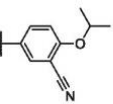
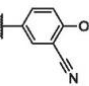


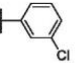
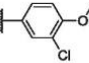
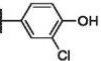
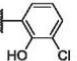
Mass spectra (ESI) were recorded on a TSQ Quantum (Thermo Finnigan) instrument.

Tested compounds are >95% chemical purity as measured by HPLC. The methods for HPLC analysis and a table of data for all tested compounds are provided in the supporting information.

The following compounds were prepared according to previously described procedures: (5-bromo-thiophen-2-yl)(3-methoxyphenyl)methanone (**I**), [26], (5-bromo-thiophen-2-yl)(3-hydroxy-phenyl)methanone (**IV**), [29], (5-bromo-thiophen-2-yl)(3-hydroxy-phenyl)methanone (**VI**), [26], (5-Bromo-thiophen-2-yl)-(2,6-difluoro-3-hydroxy-phenyl)-methanone (**VII**), [29], 4-bromo-2-chloro-6-methyl-phenol (**22c**), [36], 5-bromo-1-chloro-2-methoxy-3-methyl-benzene (**22b**) [37].

The Supplementary Data section reports the synthesis of compounds **II**, **V**, **1a–5a**, **7a**, **3–7**, **9–29**, **31b** and **32**. For each general synthetic procedure, one representative example is given below.

Table 2Optimization of C-ring-substitution: Activities of compounds **6–19** towards h17 β -HSD1 and 2.

| Cmpd | Ring C | IC ₅₀ [nM] ^a | | SF ^d | Cmpd | Ring C | IC ₅₀ [nM] ^a | | SF ^d |
|------|---|------------------------------------|----------------|-----------------|------|---|------------------------------------|----------------|-----------------|
| | | h17β-HSD Type | | | | | h17β-HSD Type | | |
| | | 1 ^b | 2 ^c | | | | 1 ^b | 2 ^c | |
| 6 |  | 27 | 47 | 1.7 | 7 |  | 150 | 39 | 0.7 |
| 8 |  | 11 | 35 | 3.2 | 9 |  | 55 | 86 | 1.6 |
| 10 |  | 150 | 85 | 0.6 | 11 |  | 130 | 180 | 1.4 |
| 12 |  | 8.0 | 19 | 2.4 | 13 |  | 3.3 | 29 | 8.8 |
| 14 |  | 18 | 38 | 2.1 | 15 |  | 3 | 71 | 24 |
| 16 |  | 1.2 | 10 | 8.3 | 17 |  | 1.3 | 11 | 8.5 |
| 18 |  | 0.5 | 20 | 40 | 19 |  | 27 | 29 | 1 |

^{a–d} See Table 1.**6.1.1. General procedure for Friedel-Crafts acylation. Method A. (I–V)**

An ice-cooled mixture of monosubstituted thiophene derivative (1.5 equiv), arylcarbonyl chloride (1 equiv), and aluminumtrichloride (1 equiv) in anhydrous dichloromethane was warmed to room temperature and stirred for 2–4 h. 1 M HCl was used to quench the reaction. The aqueous layer was extracted with ethyl acetate. The combined organic layers were washed with brine, dried over magnesium sulfate, filtered, and concentrated to dryness. The product was purified by CC.

6.1.2. General procedure for ether cleavage. Method B. (VI, VII, 13–7, 13, 15, 18, 19, 21, 23, 25, 27, 29, and 32)

To a solution of methoxybenzene derivative (1 equiv) in anhydrous dichloromethane at –78 °C (dry ice/acetone bath), boron tribromide in dichloromethane (1 M, 5 equiv per methoxy function) was added dropwise. The reaction mixture was stirred overnight at room temperature under nitrogen atmosphere. Water was added to quench the reaction, and the aqueous layer was extracted with ethyl acetate. The combined organic layers were washed with brine, dried over magnesium sulfate, filtered, and concentrated to dryness. The product was purified by CC.

6.1.3. General procedure for Suzuki coupling

6.1.3.1. Method C1. (1a–5a, 8–12, 14, 16, 17, 20, 22, 24, 26, 28, and 31b). A mixture of arylbromide (1 equiv), boronic acid derivative

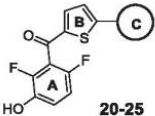
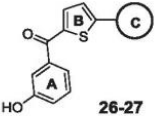
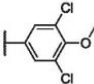
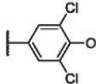
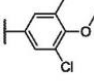
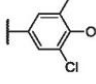
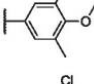
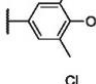
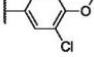
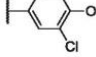
(1.2 equiv), cesium carbonate (4 equiv) and tetrakis(triphenylphosphine) palladium (0.05 equiv) was suspended in an oxygen-free DME/water (1:1) solution and refluxed under nitrogen atmosphere. The reaction mixture was cooled to room temperature. The aqueous layer was extracted with ethyl acetate. The combined organic layers were washed with brine, dried over magnesium sulfate, filtered and concentrated to dryness. The product was purified by CC.

6.1.3.2. Method C2. (6a and 7a). A mixture of arylbromide (1 equiv), boronic acid derivative (1.2 equiv), Na₂CO₃ (2 equiv) and tetrakis(triphenylphosphine) palladium (0.05 equiv) was suspended in an oxygen-free toluene/ethanol (1:1) solution and refluxed overnight under nitrogen atmosphere. The aqueous layer was extracted with ethyl acetate. The combined organic layers were washed with brine, dried over magnesium sulfate, filtered and concentrated to dryness. The product was purified by CC.

6.1.4. (5-Bromo-thiophen-2-yl)-(2-fluoro-3-methoxy-phenyl)-methanone (III)

The title compound was prepared by reaction of 2-bromothiophene (1297 mg, 7.95 mmol), 2-fluoro-4-methoxybenzoyl chloride (1000 mg, 5.30 mmol) and aluminum chloride (707 mg, 5.30 mmol) according to method A. The product was purified by CC (hexane/ethyl acetate 96:4); yield: 57% (1000 mg). ¹H NMR (500 MHz, acetone-*d*₆) δ 7.32 (d, *J* = 7.4 Hz, 1H),

Table 3Optimization of C-ring-substitution: Activities of compounds **20–27** towards *h*17 β -HSD1 and 2.

|  20-25 | | | | |  26-27 | | | | |
|--|---|------------------------------------|----------------|-----------------|---|---|------------------------------------|----------------|-----------------|
| Cmpd | Ring C | IC ₅₀ [nM] ^a | | SF ^d | Cmpd | Ring C | IC ₅₀ [nM] ^a | | SF ^d |
| | | <i>h</i> 17β-HSD Type | | | | | <i>h</i> 17β-HSD Type | | |
| | | 1 ^b | 2 ^c | | | | 1 ^b | 2 ^c | |
| 20 |  | 0.5 | 41 | 82 | 21 |  | 2.4 | 39 | 16 |
| 22 |  | 0.3 | 7.2 | 21 | 23 |  | 0.2 | 6.5 | 30 |
| 24 |  | 0.9 | 18 | 20 | 25 |  | 0.4 | 7.0 | 18 |
| 26 |  | 6.0 | 250 | 42 | 27 |  | 73 | 540 | 7.4 |

^{a-d} See Table 1.**Table 4**Introduction of hydrophilic moieties: Activities of compounds **28–32** towards *h*17 β -HSD1 and 2.

| | | | | | | | | | |
|-------------------|--|--|--|--|---------------|--|--|--|--|
| | | | | | | | | | |
| 28, 30, 31 | | | | | 29, 32 | | | | |

| Cmpd | Ring D | IC ₅₀ [nM] ^a | | SF ^d | Cmpd | Ring D | IC ₅₀ [nM] ^a | | SF ^d |
|-----------|--------|------------------------------------|----------------|-----------------|-----------|--------|------------------------------------|----------------|-----------------|
| | | <i>h</i> 17β-HSD Type | | | | | <i>h</i> 17β-HSD Type | | |
| | | 1 ^b | 2 ^c | | | | 1 ^b | 2 ^c | |
| 28 | | 1.4 | 21 | 15 | 29 | | 2.1 | 11 | 5 |
| 30 | | 4.7 | 26 | 6 | 31 | | 2.1 | 9 | 4 |
| 32 | | 18 | 26 | 1 | | | | | |

^{a-d} See Table 1.

7.33 (ddd, $J = 7.3, 4.9, 1.4$ Hz, 1H), 7.12 (d, $J = 7.4$ Hz, 1H), 7.09 (t, $J = 7.4$ Hz, 1H), 6.92–6.87 (m, 1H), 3.82 (s, 3H); ¹³C NMR (125 MHz, acetone-*d*₆) δ 184.05, 151.12 (d, $J = 246.0$ Hz), 149.54, 143.29, 136.87, 128.24 (dd, $J = 9.9, 4.4$ Hz), 126.67 (d, $J = 13.0$ Hz), 122.18 (d, $J = 4.3$ Hz), 117.46 (d, $J = 3.0$ Hz), 116.52 (d, $J = 1.3$ Hz), 115.94 (dd, $J = 12.8, 4.1$ Hz), 54.21; MS (ESI): 316.41 (M+H)⁺.

6.1.5. (5-(2,4-Difluoro-phenyl)-thiophen-2-yl)-(3-hydroxy-phenyl)-methanone (**1**)

The title compound was prepared by reaction of (5-(2,4-difluoro-phenyl)-thiophen-2-yl)-(3-methoxy-phenyl)-methanone (**1a**) (417 mg, 1.26 mmol) and boron tribromide (3.8 mmol) according to method B. The product was purified by CC

Table 5Binding affinities of selected compounds for the estrogen receptors α and β .

| Cmpd. | % Binding ^a | | Cmpd. | % Binding ^a | |
|-----------|--------------------------|-------------------------|-----------|--------------------------|-------------------------|
| | ER α ^b | ER β ^c | | ER α ^b | ER β ^c |
| 11 | 0 | 4 | 21 | 37 | 11 |
| 13 | 44 | 6 | 24 | 51 | 69 |
| 18 | 73 | 55 | 25 | 17 | 22 |
| 20 | 27 | 8 | 26 | 8 | 0 |

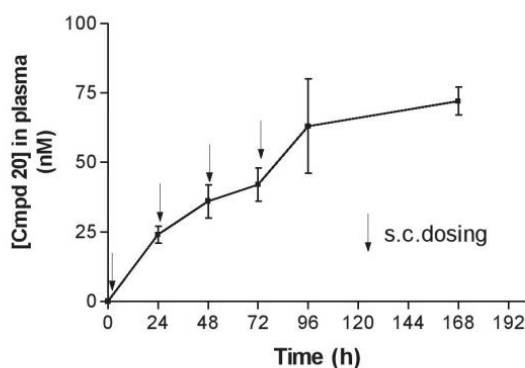
^a Mean value of three determinations, standard deviation less than 15%.^b c(ER α) = 1 nM, c(E2) = 3 nM, c(test compound) = 3 μ M.^c c(ER β) = 4 nM, c(E2) = 10 nM, c(test compound) = 10 μ M.

Fig. 3. Pharmacokinetic profile of compound **20** in Sprague-Dawley rats following repetitive subcutaneous administration. Compound **20** was subcutaneously administered once-a-day at a dose of 150 μ mol/kg body weight in 0.5% gelatin/5% mannitol in water to three female Sprague-Dawley rats. Plasma samples were taken at 24 h, 48 h, 72 h and 168 h. Arrows indicate the administration of compound **20** during the first four days, immediately after plasma sampling. Data shown are the mean \pm SEM of three animals.

(dichloromethane/methanol 99.75:0.25); yield: 41% (330 mg). ¹H NMR (500 MHz, acetone-*d*₆) δ 8.77 (s, 1H), 7.94 (td, *J* = 8.8, 6.3 Hz, 1H), 7.75 (dd, *J* = 4.0, 1.1 Hz, 1H), 7.63 (dd, *J* = 4.0, 1.0 Hz, 1H), 7.43–7.40 (m, 1H), 7.39–7.37 (m, 1H), 7.35 (ddd, *J* = 2.5, 1.5, 0.5 Hz, 1H), 7.27–7.21 (m, 1H), 7.20–7.15 (m, 1H), 7.14 (ddd, *J* = 7.7, 2.6, 1.5 Hz, 1H); ¹³C NMR (125 MHz, acetone-*d*₆) δ 187.84, 163.90 (dd, *J* = 250.2, 12.1 Hz), 160.35 (dd, *J* = 254.0, 13.3 Hz), 158.45, 144.41 (dd, *J* = 91.1, 3.7 Hz), 140.16, 136.06, 131.44 (dd, *J* = 9.9, 4.4 Hz), 130.63, 128.25–127.77 (m), 121.15, 120.39, 118.70 (dd, *J* = 12.9, 4.1 Hz), 116.32, 113.36 (dd, *J* = 21.8, 3.6 Hz), 105.70 (t, *J* = 26.4 Hz); MS (ESI): 317.63 (M+H)⁺.

6.1.6. (5-(2,4-Difluoro-phenyl)-thiophen-2-yl)-(3-hydroxy-2-methyl-phenyl)-methanone (**2**)

Compound **2a** (430 mg, 1.16 mmol) in ethanol (5 ml) was refluxed in 10% NaOH (15 mL) for 2 h on a water bath. The reaction mixture was cooled, diluted with water and neutralized with acetic acid. The product was purified by CC (dichloromethane/methanol 99.5:0.5); yield: 58% (220 mg). ¹H NMR (500 MHz, acetone-*d*₆) δ 9.51 (s, 1H, OH), 8.83 (dd, *J* = 15.1, 8.5 Hz, 1H), 8.49 (d, *J* = 3.4 Hz, 1H), 8.37 (d, *J* = 3.4 Hz, 1H), 8.24–8.02 (m, 3H), 7.95 (d, *J* = 7.9 Hz, 1H), 7.89 (d, *J* = 7.3 Hz, 1H), 3.11 (s, 3H); ¹³C NMR (125 MHz, acetone-*d*₆) δ 189.56, 163.02 (dd, *J* = 251.3, 12.8 Hz), 159.45 (dd, *J* = 253.4, 12.4 Hz), 155.85, 144.44 (dd, *J* = 10.1, 4.1 Hz), 140.21, 135.70, 130.55 (dd, *J* = 9.9, 4.4 Hz), 127.34, 127.28, 126.11, 122.33, 118.97, 117.80 (dd, *J* = 12.8, 4.0 Hz), 116.62, 112.45 (dd, *J* = 21.8, 3.6 Hz), 104.79 (t, *J* = 26.4 Hz), 11.99; MS (ESI): 331.04 (M+H)⁺.

6.1.7. (3-Ethoxy-2,6-difluoro-phenyl)-(5-pyridin-4-yl-thiophen-2-yl)-methanone (**6a**)

The title compound was prepared by reaction of (5-bromo-thiophen-2-yl)-(3-ethoxy-2,6-difluoro-phenyl)-methanone (**III**) (300 mg, 0.86 mmol), pyridine-3-boronic acid pinacol ester (355 mg, 1.73 mmol), sodium carbonate (2.5 mL, 2 M) and tetrakis(triphenylphosphine) palladium (5 μ mol) according to method C2. The product was purified by CC (dichloromethane/methanol 99.5:0.5); yield: 91% (450 mg). The product was used in the next step without any characterization.

6.1.8. (5-(3-Chloro-phenyl)-thiophen-2-yl)-(2,6-difluoro-3-hydroxy-phenyl)-methanone (**8**)

The title compound was prepared by reaction of (5-bromo-thiophen-2-yl)-(2,6-difluoro-3-hydroxy-phenyl)-methanone (**VII**) (430 mg, 1.35 mmol), 3-chlorophenylboronic acid (253 mg, 1.62 mmol), cesium carbonate (1756 mg, 5.39 mmol) and tetrakis(triphenylphosphine) palladium (5 μ mol) according to method C1. The product was purified by CC (hexane/ethyl acetate 90:10); yield: 74% (350 mg). ¹H NMR (500 MHz, acetone-*d*₆) δ 9.02 (s, 1H, OH), 7.84 (tt, *J* = 2.4, 1.2 Hz, 1H), 7.78–7.76 (m, 1H), 7.69 (d, *J* = 4.1 Hz, 1H), 7.66 (dt, *J* = 4.1, 0.9 Hz, 1H), 7.52 (td, *J* = 7.9, 0.5 Hz, 1H), 7.47 (ddd, *J* = 8.0, 2.0, 1.1 Hz, 1H), 7.23–7.21 (m, 1H), 7.06–7.04 (m, 1H); ¹³C NMR (125 MHz, acetone-*d*₆) δ 180.77, 153.31, 152.56 (dd, *J* = 240.6, 5.8 Hz), 148.44 (dd, *J* = 245.9, 7.7 Hz), 143.92, 142.68 (dd, *J* = 12.9, 3.2 Hz), 138.12, 135.80, 135.69, 131.92, 130.20, 126.96, 126.90, 125.81, 120.42 (dd, *J* = 9.1, 3.9 Hz), 117.97 (dd, *J* = 23.9, 19.7 Hz), 112.47 (d, *J* = 22.8 Hz); MS (ESI): 351.63 (M+H)⁺.

6.1.9. 2-(3-Chloro-4-methoxy-5-methyl-phenyl)-4,4,5,5-tetramethyl-(1,3,2)dioxaborolane (**22a**)

5-Bromo-1-chloro-2-methoxy-3-methylbenzene (**22b**) (5.00 g, 20.2 mmol, 1.00 equiv), bis(pinacolato)diboron (8.09 g, 31.8 mmol, 1.50 equiv), potassium acetate (5.95 g, 60.6 mmol, 3.00 equiv) and 1,1'-Bis(diphenylphosphino)ferrocene-palladium(II)dichloride (739 mg, 1.01 mmol, 0.05 equiv) were dissolved under N₂ in 40 mL dry DMSO and the mixture was stirred at 80 °C for 2 h. The reaction was quenched with water, diluted with diethyl ether and filtered over celite. The phases were separated and the aqueous layer was extracted two times with diethyl ether. The combined organic layers were washed three times with water; one time with brine, dried over MgSO₄, filtered and concentrated under reduced pressure. The crude product was purified by CC (hexane/ethyl acetate 85:15); yield: 88% (4.71 g). ¹H NMR (500 MHz, acetone-*d*₆) δ 7.54–7.56 (m, 1H), 7.48–7.50 (m, 1H), 3.82 (s, 3H), 2.31 (t, *J* = 0.6 Hz, 3H), 1.33 (s, 12H).

6.1.10. 2-(3-Bromomethyl-5-chloro-4-methoxy-phenyl)-4,4,5,5-tetramethyl-(1,3,2)dioxaborolane (**28b**)

2-(3-Chloro-4-methoxy-5-methylphenyl)-4,4,5,5-tetramethyl-1,3,2-dioxaborolane (**22a**) (200 mg, 0.71 mmol, 1.00 equiv) and *N*-bromosuccinimide (113 mg, 0.63 mmol, 0.90 equiv) were dissolved under N₂ in 17 mL CCl₄, followed by a catalytic amount of dibenzoyl peroxide. The mixture was stirred under reflux for 1 h. The reaction was quenched with water and extracted three times with dichloromethane. The combined organic layers were washed two times with water, one time with brine, dried over Na₂SO₄, filtered and concentrated under reduced pressure. The crude product was purified by CC (hexane/ethyl acetate 85:15); yield: 70% (180 mg). ¹H NMR (500 MHz, acetone-*d*₆) δ 7.75 (d, *J* = 1.5 Hz, 1H), 7.68 (d, *J* = 1.5 Hz, 1H), 4.71 (s, 2H), 4.00 (s, 3H), 1.33–1.35 (m, 12H).

6.1.11. 1-(4-(3-Chloro-2-methoxy-5-(4,4,5,5-tetramethyl-(1,3,2)dioxaborolan-2-yl)-benzyl)-piperazin-1-yl)-ethanone (**28a**)

2-(3-(Bromomethyl)-5-chloro-4-methoxyphenyl)-4,4,5,5-

tetramethyl-1,3,2-dioxaborolane (**28b**) (180 mg, 0.50 mmol, 1.00 equiv) was dissolved under N₂ in 1 ml dry THF and 1-acetylpiperazine was added. The mixture was stirred for 1 h under reflux. The reaction was quenched with water and extracted three times with ethyl acetate. The combined organic layers were washed two times with water, one time with brine, dried over MgSO₄, filtered and concentrated under reduced pressure. The crude product was purified by CC (ethyl acetate/ethanol 8:2), to give the desired product as yellow solid; yield: 70% (198 mg). ¹H NMR (500 MHz, acetone-*d*₆) δ 7.69 (d, *J* = 1.5 Hz, 1H), 7.65 (d, *J* = 1.5 Hz, 1H), 3.90 (s, 3H), 3.57 (s, 3H), 2.77 (t, *J* = 5.2 Hz, 2H), 2.70 (t, *J* = 5.2 Hz, 2H), 2.47 (t, *J* = 5.2 Hz, 2H), 2.42 (t, *J* = 5.2 Hz, 2H), 2.00 (s, 3H), 1.34 (s, 12H).

6.1.12. (5-(3-Chloro-4-methoxy-5-piperazin-1-ylmethyl-phenyl)-thiophen-2-yl)-(2,6-difluoro-3-hydroxy-phenyl)-methanone (30**)**

1-(4-(3-Chloro-5-(5-(2,6-difluoro-3-hydroxybenzoyl)-thiophen-2-yl)-2-methoxybenzyl)piperazin-1-yl)ethanone (**28**) (150 mg, 0.29 mmol, 1.00 equiv) was dissolved in 20 ml 3 M aqueous HCl and heated to 80 °C for 3 h. The reaction was washed two times with ethyl acetate, the aqueous layer was basified to pH 10 with 2 M NaOH and washed two times with ethyl acetate. The aqueous layer was neutralized with 2 M HCl and extracted three times with ethyl acetate. The combined organic layers were washed one time with water, one time with brine, dried over MgSO₄, filtered and concentrated under reduced pressure to give the desired pure product in 40% yield as pale yellow solid. ¹H NMR (500 MHz, acetone-*d*₆) δ 7.83–7.79 (m, 2H), 7.67–7.60 (m, 2H), 7.19 (m, 1H), 7.00 (td, *J* = 9.0, 1.9 Hz, 1H), 3.92 (s, 3H), 3.59 (s, 2H), 2.89–2.81 (m, 4H), 2.53–2.45 (m, 4H); ¹³C NMR (125 MHz, acetone-*d*₆) δ 180.8, 156.8, 153.3, 151.5, 149.4, 147.5, 143.6, 142.9, 142.7, 138.2, 135.4, 130.7, 129.6, 128.4, 127.9, 126.7, 120.5, 118.1, 112.3, 112.2, 62.0, 56.9, 50.4, 44.3; MS (ESI): 479.22 (M+H)⁺.

6.1.13. 2-(3-Azidomethyl-5-chloro-4-methoxy-phenyl)-4,4,5,5-tetramethyl-(1,3,2)dioxaborolane (31c**)**

2-(3-(Bromomethyl)-5-chloro-4-methoxyphenyl)-4,4,5,5-tetramethyl-1,3,2-dioxaborolane (**28b**) (800 mg, 2.19 mmol, 1.00 equiv) was dissolved under N₂ in 8 ml dry DMF and sodium azide (143 mg, 2.19 mmol, 1.00 equiv) was added. The mixture was stirred at room temperature overnight. The mixture was quenched with water and extracted three times with ethyl acetate. The combined organic layers were washed two times with water, one time with brine, dried over MgSO₄, filtered and concentrated under reduced pressure. The crude product was purified by CC (hexane/ethyl acetate 8:2); yield: 71% (503 mg). ¹H NMR (500 MHz, acetone-*d*₆) δ 7.72 (d, *J* = 1.6 Hz, 1H), 7.69 (d, *J* = 1.6 Hz, 1H), 4.55 (s, 2H), 3.93 (s, 3H), 1.34 (s, 12H).

6.1.14. Acetic acid 3-(5-(3-chloro-4-methoxy-5-(1,2,3)triazol-1-ylmethyl-phenyl)-thiophene-2-carbonyl)-2,4-difluoro-phenylester (31a**)**

(5-(3-(Azidomethyl)-5-chloro-4-methoxyphenyl)-thiophen-2-yl)(2,6-difluoro-3-hydroxyphenyl)methanone (**31b**) (50 mg, 0.11 mmol, 1.00 equiv), was dissolved in 106 μl vinyl acetate and the reaction was heated at 120 °C under microwave for 10 h. The reaction was concentrated under reduced pressure and purified by CC using ethyl acetate as eluent; yield: 27% (15 mg). ¹H NMR (500 MHz, DMSO-*d*₆) δ 8.11 (d, *J* = 0.9 Hz, 1H), 7.92 (d, *J* = 2.5 Hz, 1H), 7.70 (d, *J* = 0.9 Hz, 1H), 7.68–7.66 (m, 1H), 7.64–7.61 (m, 2H), 7.53 (td, *J* = 8.9, 5.5 Hz, 1H), 7.26 (td, *J* = 8.8, 1.9 Hz, 1H), 5.78 (s, 2H), 3.89 (s, 3H), 2.34 (s, 3H); MS (ESI): 504.12 (M+H)⁺.

6.1.15. (5-(3-Chloro-4-methoxy-5-(1,2,3)triazol-1-ylmethyl-phenyl)-thiophen-2-yl)-(2,6-difluoro-3-hydroxy-phenyl)-methanone (31**)**

Acetic acid 3-(5-(3-chloro-4-methoxy-5-(1,2,3)triazol-1-ylmethyl-phenyl)-thiophene-2-carbonyl)-2,4-difluoro-phenylester (**31a**) (110 mg, 0.24 mmol, 1.00 equiv) was dissolved under N₂ in a degassed mixture of 5 ml THF and 600 μl of 2 M NaOH. The mixture was stirred for 2 h at room temperature. The reaction was acidified to pH 6 with 1 M HCl and extracted three times with ethyl acetate. The combined organic layers were washed two times with water, one time with brine, dried over MgSO₄, filtered and concentrated under reduced pressure to give the desired product; yield: 95% (90 mg). ¹H NMR (500 MHz, acetone-*d*₆) δ 9.05 (br. s, 1H), 8.11 (d, *J* = 0.9 Hz, 1H), 7.91 (d, *J* = 2.2 Hz, 1H), 7.70 (d, *J* = 0.9 Hz, 1H), 7.67 (d, *J* = 2.2 Hz, 1H), 7.65–7.62 (m, 1H), 7.61–7.58 (m, 1H), 7.21 (td, *J* = 8.9, 5.5 Hz, 1H), 7.03 (td, *J* = 8.8, 1.9 Hz, 1H), 5.78 (s, 2H), 3.89 (s, 3H); MS (ESI): 462.15 (M+H)⁺.

6.2. Biological methods

[2,4,6,7-³H]-E1 and [2,4,6,7-³H]-E2 were bought from Perkin-Elmer, Boston. Quicksint Flow 302 scintillator fluid was bought from Zinsser Analytic, Frankfurt.

6.2.1. Preparation of human 17β-HSD1 and 17β-HSD2

Human 17β-HSD1 and 17β-HSD2 were obtained from human placenta according to previously described procedures [32]. Fresh human placenta was homogenized, and cytosolic fraction and microsomes were separated by fractional centrifugation. For the partial purification of 17β-HSD1, the cytosolic fraction was precipitated with ammonium sulfate. 17β-HSD2 was obtained from the microsomal fraction.

6.2.2. Inhibition of human 17β-HSD1

Inhibitory activities were evaluated by an established method with minor modifications [32]. Briefly, the enzyme preparation was incubated with NADPH (500 μM) in the presence of potential inhibitors at 37 °C in a phosphate buffer (50 mM) supplemented with 20% of glycerol and EDTA (1 mM). Inhibitor stock solutions were prepared in DMSO. The final concentration of DMSO was adjusted to 1% in all samples. The enzymatic reaction was started by addition of a mixture of unlabeled- and [2, 4, 6, 7-³H]-E1 (final concentration: 500 nM, 0.15 μCi). After 10 min, the incubation was stopped with HgCl₂ and the mixture was extracted with diethylether. After evaporation, the steroids were dissolved in acetonitrile. E1 and E2 were separated using acetonitrile/water (45:55) as mobile phase in a C18 reverse phase chromatography column (Nucleodur C18 125/3100-5, Macherey-Nagel) connected to a HPLC-system (Agilent 1200 Series, Agilent Technologies). Detection and quantification of the steroids were performed using a radioflow detector (Ramona, raytest). The conversion rate was calculated after analysis of the resulting chromatograms according to the following equation:

$$\% \text{conversion} = [\% \text{E2} / (\% \text{E2} + \% \text{E1})] \times 100$$

Each value was calculated from at least three independent experiments.

6.2.3. Inhibition of human 17β-HSD2

The h17β-HSD2 inhibition assay was performed similarly to the h17β-HSD1 procedure. The microsomal fraction was incubated with NAD⁺ [1500 μM], test compound and a mixture of unlabeled- and [2,4,6,7-³H]-E2 (final concentration: 500 nM, 0.11 μCi) for 20 min at 37 °C. Further treatment of the samples and HPLC separation was carried out as mentioned above.

The conversion rate was calculated after analysis of the resulting chromatograms according to the following equation:

$$\% \text{conversion} = [\%E1 / (\%E1 + \%E2)] \times 100$$

6.2.4. ER affinity

The binding affinity of selected compounds to ER α and ER β was determined according to the recommendations of the US Environmental Protection Agency (EPA) by their Endocrine Disruptor Screening Program (EDSP) using recombinant human proteins. Briefly, 1 nM of ER α and 4 nM of ER β , respectively, were incubated with [3 H]-E2 (3 nM for ER α and 10 nM for ER β) and test compound for 16–20 h at 4 °C.

The inhibitors were dissolved in DMSO (5% final concentration). Evaluation of non-specific [3 H]-E2 binding was performed with unlabeled E2 at concentrations 100-fold of [3 H]-E2 (300 nM for ER α and 1000 nM for ER β). After incubation, ligand-receptor complexes were selectively bound to hydroxyapatite (83.5 g/l in TE-buffer). The bound complex was washed three times and resuspended in ethanol. For radiodetection, scintillator cocktail (Quickszint 212, Zinsser Analytic, Frankfurt) was added and samples were measured in a liquid scintillation counter (1450 LSC & Luminescence Counter, Perkin Elmer).

From these results the percentage of [3 H]-E2 displacement by the compounds and unlabeled E2 was calculated. The plot of % displacement versus unlabeled E2 concentration resulted in sigmoidal binding curves. The E2 concentrations to displace 50% of the receptor bound [3 H]-E2 were determined in each experiment and E2 IC₅₀ values were used as reference. The E2 IC₅₀ values accepted were 3 \pm 20% nM for ER α and 10 \pm 20% nM for ER β .

Compounds were tested at concentrations of 1000 \cdot IC₅₀ (E2). Compounds with less than 50% displacement of [3 H]-E2 at a concentration of 1000 \cdot IC₅₀ (E2) were classified as RBA <0.1%.

6.2.5. MTT cell viability assay

Evidence of cell viability by the MTT assay is based on the reduction of the yellow, water-soluble dye 3-(4,5-dimethyl-2-yl)-2,5-diphenyltetrazolium bromide (MTT) to a blue-violet, water insoluble formazan. HEK293 cells (2 \times 10⁵ cells per well) were seeded in 24-well flat-bottom plates. Culturing of cells, incubations and absorbance measurements were performed as described previously [38] with minor modifications. 3 h after seeding the cells in Dulbecco's minimal essential medium with 5% fetal calf serum and penicillin G (100 units/ml)/streptomycin (100 μ g/ml), the incubation was started by the addition of compound **20** at 10, 5, 2.5, 1.25 and 0.625 μ M in a total volume of 1 ml with a final DMSO concentration of 1%. After 66 h, 50 μ l of a 5 mg/ml MTT in phosphate-buffered saline, pH 7.4 (PBS) was added to the medium, and incubated in a CO₂ incubator at 37 °C. After 30 min, medium was removed and 250 μ l of DMSO containing 10% SDS and 0.5% acetic acid were added to dissolve the cells and MTT crystals. Absorbance of formazane was measured at 570 nm in an Omega plate reader spectrometer. The decrease in fluorescence at 570 nm after incubation in the presence of compound **20** compared with the fluorescence measured in the presence of the vehicle control alone (1% DMSO) was determined, followed by the calculation of the IC₂₀ value using GraphpadPrism 3. Arbitrarily, below IC₂₀ cell viability is not considered to be affected.

6.2.6. Mutagenicity testing

Mutagenic potential of compound **20** was evaluated at 100, 33, 11, 3.7, 1.2 and 0.4 μ M using Xenometrix AMES II mutagenicity assay kit with TA98 and TA7001-TA7006 strains of *Salmonella*

typhimurium in the presence or absence of rat liver S9 fraction according to the manufacturer's instructions.

6.2.7. Hepatic CYP450 inhibition and PXR assays

The inhibition of hepatic CYP enzymes CYP1A2, CYP2B6, CYP2C9, CYP2C19, CYP2D6 and CYP3A4 by 1 μ M of compound **20** was determined in microsomes of baculovirus-infected insect cells expressing the recombinant human enzyme according to the manufacturer's instruction (BD Gentest/Corning). Agonist activity of compound **20** on the pregnane X receptor (PXR) was performed at CEREP (now Eurofins) in a cofactor recruitment cell-free assay.

6.2.8. Rat pharmacokinetics

All animal procedures were performed in accordance with the Guide for the Care and Use of Laboratory Animals. Experiments were conducted on female Sprague-Dawley rats (body weight 255–274 g) purchased from Charles River Laboratory (Sulzfeld, Germany). After an acclimatization period of 1 week, compound **20** was subcutaneously administered at a dose of 150 μ mol/kg (66 mg/kg) body weight (n = 3) per animal. Suspensions of compound **20** in 0.5% porcine gelatine/5% mannitol (w/w) in demineralized water were prepared every day following 10 min in an ultrasonic bath, 30 min before administration. Before application of suspension (4 mL/kg body weight) at 0 h, 24 h, 48 h and 72 h, rats were anesthetized with 2% isoflurane. At 24 h, 48 h, 72 h, 96 h and 168 h, blood samples of 50 μ l were taken from the tail vein (always before renewed subcutaneous administration of compound **20**) and collected in 0.2 ml Eppendorf tubes containing 5 μ l of 106 mM sodium citrate buffer. After centrifugation at 5000 rpm at 4 °C, the plasma samples were first frozen at –20 °C and within 24 h, stored at –80 °C. For bioanalysis, plasma samples were thawed and 10 μ L of plasma were added to 50 μ L acetonitrile containing diphenhydramine (750 nM) as internal standard. Samples and calibration standards (in rat plasma) were centrifuged at 15,000 rpm for 5 min at 4 °C. The solutions were transferred to fresh vials for HPLC-MS/MS analysis (Accucore RP-MS, TSQ Quantum triple quadrupole mass spectrometer, APCI interface). After injection of 10 μ L (performed in duplicate), data were analyzed based on the ratio of the peak areas of compound **20** and internal standard. Detection limit of compound **20** in plasma was 10 nM.

Author contributions

A.S.A., E.B., M.S. and M.F. are responsible for design, synthesis and chemical characterization of the compounds. C.J.v.K., M.S., C.B., L.S., M.F., M.W.L. and M.D.M. are responsible for the biological assays. A.S.A., C.J.v.K. and M.F. wrote the manuscript.

Notes

The authors declare no competing financial interest.

Acknowledgments

We are grateful to the Egyptian Ministry of Higher Education and Scientific Research (MoHESR) and the Deutscher Akademischer Austauschdienst (DAAD) for financial support of this work (A/09/92319). Thanks are due to Professor Rolf W. Hartmann for valuable discussions. We thank Dr. Claudia Scheuer and Julia Parakenings for their technical assistance in performing the pharmacokinetic profile experiments.

Appendix A. Supplementary data

Supplementary data related to this article can be found at <http://>

dx.doi.org/10.1016/j.ejmech.2016.11.004.

References

- [1] T. Šmuc, M.R. Pucelj, J. Sinkovec, B. Husen, H. Thole, T. Lanišnik Rižner, Expression analysis of the genes involved in estradiol and progesterone action in human ovarian endometriosis, *Gynecol. Endocrinol.* 23 (2007) 105–111.
- [2] Y. Miyoshi, A. Ando, E. Shiba, T. Taguchi, Y. Tamaki, S. Noguchi, Involvement of up-regulation of 17 β -hydroxysteroid dehydrogenase type 1 in maintenance of intratumoral high estradiol levels in postmenopausal breast cancers, *Int. J. Cancer* 94 (2001) 685–689.
- [3] A. Jansson, 17 β -hydroxysteroid dehydrogenase enzymes and breast cancer, *J. Steroid Biochem. Mol. Biol.* 114 (2009) 64–67.
- [4] C.H. Blomquist, M. Bonenfant, D.M. McGinley, Z. Posalaky, D.J. Lakatua, S. Tuli-Puri, D.G. Bealka, Y. Tremblay, Androgenic and estrogenic 17 β -hydroxysteroid dehydrogenase/17-ketosteroid reductase in human ovarian epithelial tumors: evidence for the type 1, 2 and 5 isoforms, *J. Steroid Biochem. Mol. Biol.* 81 (2002) 343–351.
- [5] T.M. Penning, Molecular endocrinology of hydroxysteroid dehydrogenases, *Endocr. Rev.* 18 (1997) 281–305.
- [6] W.R. Miller, J.M. Bartlett, P. Canney, M. Verrill, Hormonal therapy for postmenopausal breast cancer: the science of sequencing, *Breast Cancer Res. Treat.* 103 (2007) 149–160.
- [7] N.J. Bush, Advances in hormonal therapy for breast cancer, *Semin. Oncol. Nurs.* 23 (2007) 46–54.
- [8] A. Cavalli, A. Bisi, C. Bertucci, C. Rosini, A. Paluszczak, S. Gobbi, E. Giorgio, A. Rampa, F. Belluti, L. Piazzi, P. Valenti, R.W. Hartmann, M. Recanatini, Enantioselective nonsteroidal aromatase inhibitors identified through a multidisciplinary medicinal chemistry approach, *J. Med. Chem.* 48 (2005) 7282–7289.
- [9] M. Le Borgne, P. Marchand, M. Duflos, B. Delevoeye-Seiller, S. Piessard-Robert, G. Le Baut, R.W. Hartmann, M. Palzer, Synthesis and in vitro evaluation of 3-(1-azolylmethyl)-1H-indoles and 3-(1-azolyl-1-phenylmethyl)-1H-indoles as inhibitors of P450 arom, *Arch. Pharm. Wein.* 330 (1997) 141–145.
- [10] C. Jacobs, M. Frotscher, G. Dannhardt, R.W. Hartmann, 1-imidazolyl(alkyl)-substituted di- and tetrahydroquinolines and analogues: syntheses and evaluation of dual inhibitors of thromboxane A(2) synthase and aromatase, *J. Med. Chem.* 43 (2000) 1841–1851.
- [11] M. Le Borgne, P. Marchand, B. Delevoeye-Seiller, J.M. Robert, G. Le Baut, R.W. Hartmann, M. Palzer, New selective nonsteroidal aromatase inhibitors: synthesis and inhibitory activity of 2,3 or 5-(α -azolylbenzyl)-1H-indoles, *Bioorg Med. Chem. Lett.* 9 (1999) 333–336.
- [12] M.P. Lézé, M. Le Borgne, P. Pinson, A. Paluszczak, M. Duflos, G. Le Baut, R.W. Hartmann, Synthesis and biological evaluation of 5-[(aryl)(1H-imidazol-1-yl)methyl]-1H-indoles: potent and selective aromatase inhibitors, *Bioorg Med. Chem. Lett.* 16 (2006) 1134–1137.
- [13] R. Maltais, A. Trottier, A. Delhomme, X. Barbeau, P. Lagüe, D. Poirier, Identification of fused 16 β ,17 β -oxazinone-estradiol derivatives as a new family of non-estrogenic 17 β -hydroxysteroid dehydrogenase type 1 inhibitors, *Eur. J. Med. Chem.* 93 (2015) 470–480.
- [14] V. Adamo, M. Iorfida, E. Montalto, V. Festa, C. Garipoli, A. Scimone, M. Zanghi, N. Caristi, Overview and new strategies in metastatic breast cancer (MBC) for treatment of tamoxifen-resistant patients, *Ann. Oncol.* 18 (Suppl 6) (2007) vi53–57.
- [15] B. Delvoux, T. D'Hooghe, C. Kyama, P. Koskimies, R.J. Hermans, G.A. Dunselman, A. Romano, Inhibition of type 1 17 β -hydroxysteroid dehydrogenase impairs the synthesis of 17 β -estradiol in endometriosis lesions, *J. Clin. Endocrinol. Metab.* 99 (2014) 276–284.
- [16] B. Husen, K. Huhtinen, M. Poutanen, L. Kangas, J. Messinger, H. Thole, Evaluation of inhibitors for 17 β -hydroxysteroid dehydrogenase type 1 in vivo in immunodeficient mice inoculated with MCF-7 cells stably expressing the recombinant human enzyme, *Mol. Cell Endocrinol.* 248 (2006) 109–113.
- [17] B. Husen, K. Huhtinen, T. Saloniemi, J. Messinger, H.H. Thole, M. Poutanen, Human hydroxysteroid (17- β) dehydrogenase 1 expression enhances estrogen sensitivity of MCF-7 breast cancer cell xenografts, *Endocrinology* 147 (2006) 5333–5339.
- [18] J.M. Day, P.A. Foster, H.J. Tutill, M.F. Parsons, S.P. Newman, S.K. Chander, G.M. Allan, H.R. Lawrence, N. Vicker, B.V. Potter, M.J. Reed, A. Purohit, 17 β -hydroxysteroid dehydrogenase Type 1, and not Type 12, is a target for endocrine therapy of hormone-dependent breast cancer, *Int. J. Cancer* 122 (2008) 1931–1940.
- [19] D. Poirier, Advances in development of inhibitors of 17 β hydroxysteroid dehydrogenases, *Anticancer Agents Med. Chem.* 9 (2009) 642–660.
- [20] S. Starčević, P. Brozić, S. Turk, J. Cesar, T.L. Rižner, S. Gobec, Synthesis and biological evaluation of (6- and 7-phenyl) coumarin derivatives as selective nonsteroidal inhibitors of 17 β -hydroxysteroid dehydrogenase type 1, *J. Med. Chem.* 54 (2011) 248–261.
- [21] D. Poirier, Inhibitors of 17 β -hydroxysteroid dehydrogenases, *Curr. Med. Chem.* 10 (2003) 453–477.
- [22] D. Poirier, 17 β -Hydroxysteroid dehydrogenase inhibitors: a patent review, *Expert Opin. Ther. Pat.* 20 (2010) 1123–1145.
- [23] J.M. Day, H.J. Tutill, A. Purohit, M.J. Reed, Design and validation of specific inhibitors of 17 β -hydroxysteroid dehydrogenases for therapeutic application in breast and prostate cancer, and in endometriosis, *Endocr. Relat. Cancer* 15 (2008) 665–692.
- [24] J.M. Day, H.J. Tutill, A. Purohit, 17 β -hydroxysteroid dehydrogenase inhibitors, *Minerva Endocrinol.* 35 (2010) 87–108.
- [25] P. Brozić, T. Lanišnik Rižner, S. Gobec, Inhibitors of 17 β -hydroxysteroid dehydrogenase type 1, *Curr. Med. Chem.* 15 (2008) 137–150.
- [26] A. Oster, S. Hinsberger, R. Werth, S. Marchais-Oberwinkler, M. Frotscher, R.W. Hartmann, Bicyclic substituted hydroxyphenylmethanones as novel inhibitors of 17 β -hydroxysteroid dehydrogenase type 1 (17 β -HSD1) for the treatment of estrogen-dependent diseases, *J. Med. Chem.* 53 (2010) 8176–8186.
- [27] A. Spadaro, M. Frotscher, R.W. Hartmann, Optimization of hydroxybenzothiazoles as novel potent and selective inhibitors of 17 β -HSD1, *J. Med. Chem.* 55 (2012) 2469–2473.
- [28] A.S. Abdelsamie, E. Bey, N. Hanke, M. Empting, R.W. Hartmann, M. Frotscher, Inhibition of 17 β -HSD1: SAR of bicyclic substituted hydroxyphenylmethanones and discovery of new potent inhibitors with thioether linker, *Eur. J. Med. Chem.* 82 (2014) 394–406.
- [29] A.S. Abdelsamie, E. Bey, E.M. Gargano, C.J. van Koppen, M. Empting, M. Frotscher, Towards the evaluation in an animal disease model: fluorinated 17 β -HSD1 inhibitors showing strong activity towards both the human and the rat enzyme, *Eur. J. Med. Chem.* 103 (2015) 56–68.
- [30] S. Marchais-Oberwinkler, C. Henn, G. Möller, T. Klein, M. Negri, A. Oster, A. Spadaro, R. Werth, M. Wetzel, K. Xu, M. Frotscher, R.W. Hartmann, J. Adamski, 17 β -Hydroxysteroid dehydrogenases (17 β -HSDs) as therapeutic targets: protein structures, functions, and recent progress in inhibitor development, *J. Steroid Biochem. Mol. Biol.* 125 (2011) 66–82.
- [31] S.G. Hansen, H.H. Jensen, Microwave irradiation as an effective means of synthesizing unsubstituted N-linked 1,2,3-triazoles from vinyl acetate and azides, *Synlett* 20 (2009) 3275–3276.
- [32] P. Kruchten, R. Werth, S. Marchais-Oberwinkler, M. Frotscher, R.W. Hartmann, Development of a biological screening system for the evaluation of highly active and selective 17 β -HSD1-inhibitors as potential therapeutic agents, *Mol. Cell Endocrinol.* 301 (2009) 154–157.
- [33] W. Qiu, R.L. Campbell, A. Gangloff, P. Dupuis, R.P. Boivin, M.R. Tremblay, D. Poirier, S.X. Lin, A concerted, rational design of type 1 17 β -hydroxysteroid dehydrogenase inhibitors: estradiol-adenosine hybrids with high affinity, *FASEB J.* 16 (2002) 1829–1831.
- [34] K.M. Sam, S. Auger, V. Luu-The, D. Poirier, Steroidal spiro-gamma-lactones that inhibit 17 β -hydroxysteroid dehydrogenase activity in human placental microsomes, *J. Med. Chem.* 38 (1995) 4518–4528.
- [35] J. Moreno-Farre, P. Workman, F.J. Raynaud, Analysis of potential drug-drug interactions for anticancer agents in human liver microsomes by high throughput liquid chromatography/mass spectrometry assay, *Recent Adv. Res. Updat.* 7 (2006) 207–224.
- [36] D.J. Kertesz, C. Brotherton-Pleiss, M. Yang, Z. Wang, X. Lin, Z. Qiu, D.R. Hirschfeld, S. Gleason, T. Mirzadegan, P.W. Dunten, S.F. Harris, A.G. Villasenor, J.Q. Hang, G.M. Heilek, K. Klumpp, Discovery of piperidin-4-yl-aminopyrimidines as HIV-1 reverse transcriptase inhibitors. N-benzyl derivatives with broad potency against resistant mutant viruses, *Bioorg Med. Chem. Lett.* 20 (2010) 4215–4218.
- [37] M. Iwao, H. Takehara, S. Furukawa, M. Watanabe, A regiospecific synthesis of carbazoles via consecutive palladium-catalyzed cross-coupling and aryne-mediated cyclization, *Heterocycles* 36 (1993) 1483–1488.
- [38] J. Haupenthal, C. Baehr, S. Zeuzem, A. Piiper, RNase A-like enzymes in serum inhibit the anti-neoplastic activity of siRNA targeting polo-like kinase 1, *Int. J. Cancer* 121 (2007) 206–210.

3.2.II Targeted Endocrine Therapy: Design, Synthesis, and Proof-of-Principle of 17 β -Hydroxysteroid Dehydrogenase Type 2 Inhibitors in Bone Fracture Healing

Ahmed S. Abdelsamie, Steven Herath, Yannik Biskupek, Carsten Borger, Lorenz Siebenburger, **Mohamed Salah**, Claudia Scheuer, Sandrine Marchais-Oberwinkler, Martin Frotscher, Tim Pohlemann, Michael D. Menger, Rolf W. Hartmann, Matthias W. Laschke, and Chris J. van Koppen

Reprinted with permission *J. Med. Chem.* 2019, 62 (3), 1362–1372.

DOI: 10.1021/acs.jmedchem.8b01493

Copyright (2019) American Chemical Society

Publication D

Contribution Report

The author contributed significantly to the in vitro biological evaluation of the synthesized compounds. Furthermore, He contributed in the interpretation of the results and writing the manuscript.

Targeted Endocrine Therapy: Design, Synthesis, and *Proof-of-Principle* of 17β -Hydroxysteroid Dehydrogenase Type 2 Inhibitors in Bone Fracture Healing

Ahmed S. Abdelsamie,^{†,‡,§,||} Steven Herath,^{§,||} Yannik Biskupek,[§] Carsten Börger,^{||} Lorenz Siebenbürger,^{||} Mohamed Salah,^{‡,§} Claudia Scheuer,[#] Sandrine Marchais-Oberwinkler,[¶] Martin Frotscher,^{‡,§} Tim Pohlemann,[§] Michael D. Menger,[#] Rolf W. Hartmann,^{‡,¶,§} Matthias W. Laschke,[#] and Chris J. van Koppen^{*,†,‡,§}

[†]EllexoPharm GmbH, Im Stadtwald, Building A1.2, 66123 Saarbrücken, Germany

[‡]Chemistry of Natural and Microbial Products Department, National Research Centre, Dokki, 12622 Cairo, Egypt

[§]Department of Trauma, Hand and Reconstructive Surgery, and [#]Institute of Clinical & Experimental Surgery, Saarland University, 66421 Homburg/Saar, Germany

^{||}PharmBioTec GmbH, 66123 Saarbrücken, Germany

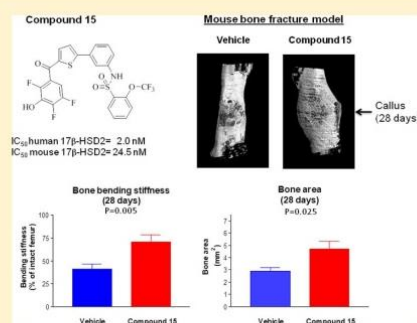
[‡]Department of Pharmaceutical and Medicinal Chemistry, Saarland University, 66123 Saarbrücken, Germany

[¶]Institute of Pharmaceutical Chemistry, Philipps-University, 35032 Marburg, Germany

[¶]Department of Drug Design and Optimization, Helmholtz Institute for Pharmaceutical Research Saarland (HIPS), 66123 Saarbrücken, Germany

S Supporting Information

ABSTRACT: Current therapies of steroid hormone-dependent diseases predominantly alter steroid hormone concentrations (or their actions) in plasma, in target and nontarget tissues alike, rather than in target organs only. Targeted therapy through the inhibition of steroidogenic enzymes may pose an attractive alternative with much less side effects. Here, we describe the design of a nanomolar potent 17β -hydroxysteroid dehydrogenase type 2 (17β -HSD2) inhibitor (compound 15) and successful targeted intracrine therapy in a mouse bone fracture model. Blockade of 17β -HSD2 in bone is thought to increase intracellular estradiol (E2) and testosterone (T), which thereby inhibits bone resorption by osteoclasts and stimulates bone formation by osteoblasts, respectively. Administration of compound 15 in the mouse fracture model strongly increases the mechanical stability of the healing fractured bone because of a larger periosteal callus with newly formed bone without changing the plasma E2 and T concentrations. Steroidogenic 17β -HSD2 inhibition thus enables targeted intracrine therapy.



INTRODUCTION

Current therapies of steroid hormone-dependent diseases, like osteoporosis and endometriosis, involve primarily treatment with drugs that alter the steroid hormone concentrations (or their actions) in plasma, in target and nontarget tissues alike, rather than in the target organs only. As a consequence, these treatments most often are accompanied with highly undesirable side effects.¹ Local intracrine inhibition of steroidogenic enzymes, affecting the intracellular concentrations in the target organs only, represents an attractive, alternative therapeutic paradigm with much less side effects and disturbances of the hypothalamus–pituitary organ axes. Unfortunately, successful *proof-of-principle* studies with steroidogenic enzyme inhibitors, which do not change systemic hormone concentrations, have been rather infrequent. These include 5α -reductase inhibitors

to treat patients with benign prostatic hyperplasia,² 11β -HSD1 inhibitors,³ and 17β -HSD1 inhibitors in an endometrial hyperplasia animal model.⁴ In the present study, we have developed novel nanomolar potent 17β -HSD2 inhibitors and successfully performed a *proof-of-principle* study in a mouse bone fracture healing model. Approximately 10% of the patients with bone fractures suffer from serious nonunion or delayed/impaired bone fracture healing.⁵ Inadequate bone healing is not only difficult to treat, with the therapeutic options being very limited,^{6–8} but the demand for novel drugs with fewer side effects is also increasing rapidly because of the relatively high prevalence of bone fractures, the anticipated

Received: September 25, 2018

Published: January 15, 2019

worldwide increase in postmenopausal osteoporosis-related bone fractures, and the growing elderly population. 17β -HSD2 in bone tissue converts the biologically active steroid hormones, estradiol (E2) and T, into the much less active estrone and androstenedione. The blockade of 17β -HSD2 in bone thus increases intracellular E2 and T, and, through estrogen and androgen receptor stimulation, inhibits bone resorption by osteoclasts and stimulates bone formation by osteoblasts,^{9–11} respectively. The expression and activity of 17β -HSD2 in human bone tissue are superior over that of 17β -HSD1, 17β -HSD3, and 17β -HSD4,^{12–14} the enzymes that catalyze the synthesis and degradation of E2 and T. A previous study in ovariectomized cynomolgus monkeys showed that a 17β -HSD2 inhibitor increases the so-called ultimate bone strength, that is, the maximum stress that an intact bone specimen can sustain.¹⁵ Here, we developed a nanomolar potent, metabolically sufficiently stable, nontoxic 17β -HSD2 inhibitor and tested this compound for activity in an established mouse bone fracture healing model¹⁶ during a *proof-of-principle* study of 28 days. Mouse bone cells express active 17β -HSD2 as demonstrated by 17β -HSD2 immunohistochemistry, using a validated antimouse 17β -HSD2 antibody (Figure S1, Supporting Information), and shown by enzymatic determination,¹⁷ together with androgen and estrogen receptors (ERs).^{12–14}

RESULTS AND DISCUSSION

As bicyclic substituted hydroxyphenylmethanones (BSHs) bearing a sulfonamide moiety were originally designed as inhibitors of human 17β -HSD1, most members show selectivity toward 17β -HSD1 over 17β -HSD2.¹⁸ In addition, BSHs display low metabolic stability, precluding their use in an *in vivo* *proof-of-principle* study. Thus, a rational two-stage drug design strategy focusing on rings A and D (Charts 1 and 2, see

human and murine 17β -HSD2 (*h* + *m* 17β -HSD2), resulting in a small library of 16 compounds. As a starting point, the nonsubstituted scaffold structure (compound A) was chosen.

Previous investigations revealed that the low metabolic stability of the BSHs was primarily due to phase II biotransformation of the phenolic OH group, which is essential for activity.¹⁹ Therefore, stage 1 of the design strategy, aiming at the improvement of metabolic stability, consisted in the introduction of small substituents on the hydroxyphenyl moiety (ring A) of compound A. These groups could protect the OH functionality from biotransformation by the electron withdrawal effect and/or steric hindrance (Chart 1, compounds 1–8).

Compound 8 showed an enhanced metabolic stability and was chosen as a starting point for the optimization of the substitution pattern of the D-ring (stage 2 of the design strategy). Only such groups were selected to be introduced that were likely to maintain potency toward both human and mouse 17β -HSD2.¹⁸ We aimed for a slight (three- to —fourfold) selectivity over the *h* 17β -HSD1 enzyme (Chart 2, 9–16). On the one hand, a highly selective 17β -HSD2 inhibitor would induce an undesirable increase in intracellular E2 in tissues that express similar levels of 17β -HSD2 and 17β -HSD1 and prone to E2-dependent proliferation (i.e., breast^{20,21} and endometrium²²), whereas on the other hand, a nonselective 17β -HSD2/1 inhibitor would likely affect the role of 17β -HSD1 in regulating the endometrium cyclicity in women of childbearing age.²²

The starting point for the syntheses of compounds 1–16 was a Friedel–Crafts reaction of 2-bromothiophene with the appropriate benzoyl chloride, which in case of the chlorinated 3b and 4b had to be prepared from the corresponding benzoic acids. The obtained intermediates 1b–8b were subjected to Suzuki cross-coupling reactions with 3-aminophenylboronic acid to afford anilines 1a–8a. The latter were reacted with the sulfonamides using the appropriately substituted sulfonic acid chloride, giving direct access to compound 1. Ether cleavage using BBr_3 in dichloromethane yielded the final compounds 2–16 (Scheme 1).

The introduction of an electron-donating methyl group on ring A (Table 1, 1) led to a twofold decrease in inhibitory potency toward *h* 17β -HSD2 compared to lead A. In contrast, the presence of an electron-withdrawing fluorine or chlorine atom in the same position strongly increased the activity; see 1 versus 2 and 3.

The beneficial effect of electron-withdrawing substituents on the inhibitory activity was also apparent for 4–8, in agreement with the observations made recently for the BSHs lacking the sulfonamide moiety.²² Metabolic stability was determined for 3, 7, and 8 as these compounds displayed selectivity over 17β -HSD1 and nanomolar potency toward *m* 17β -HSD2. The trifluoro substitution pattern of 8 resulted in an improved metabolic stability and was therefore maintained in the subsequent optimization of ring D. All eight compounds of this second series (9–16) showed a strong inhibition of human and mouse 17β -HSD2 as well as a low activity toward *m* 17β -HSD1. Compounds 14 and 15 were especially interesting as they displayed moderate *h* 17β -HSD2 selectivity, which was aimed at, as well as improved metabolic stability.

Because of their favorable potency, selectivity, and metabolic stability properties, 14 and 15 were selected for testing for potential cytotoxicity. Both 14 and 15 were not toxic in the MTT assay with HEK293 cells (i.e., <20% reduction in cell

Chart 1. Lead Compound A and Designed Compounds 1–8

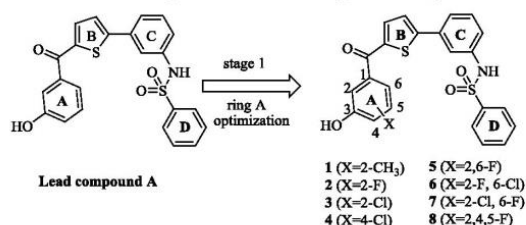
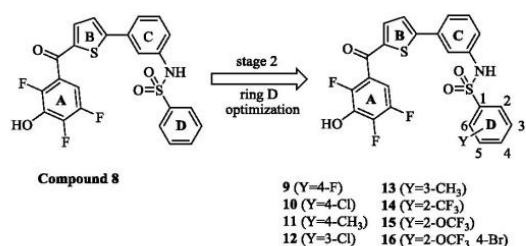


Chart 2. Lead Compound 8 and Designed Compounds 9–16



also Supporting Information for details) was applied that, on the one hand, aimed at improving the metabolic stability and, on the other, at enhancing the potency and selectivity for

[illegible]

We thus selected **15** for further profiling and investigated *in vitro* whether **15** does not induce the expression of hepatic CYP450 enzymes, which otherwise may reduce the plasma concentrations of **15** during repetitive dosing in the bone fracture healing study. At 3.16 μM , **15** did neither activate the aryl hydrocarbon receptor, constitutive androstane receptor, nor the pregnane X receptor (<5% activation). These nuclear

Next, to analyze bone fracture repair, C57BL/6 male mice received 15 subcutaneously once daily (50 mg/kg) or vehicle (0.5% gelatine/5% mannitol in water) for 14 or 28 days, starting immediately following fracturing of the femur under anesthesia. Bending stiffness of fractured bones, relative to the contralateral unfractured bones in the same animal, is the upmost important functional recovery parameter at the site of the fracture in bone fracture healing.^{16,24,25} After 14 and 28 days, the bending stiffness of the fractured femurs of the

Table 1. Inhibition of 17 β -HSD2 and 17 β -HSD1 by A and 1–16

| Cmpd | X | Y | IC ₅₀ (nM) ^a | | s.f. ^b | IC ₅₀ (nM) ^a | | % inh.@500 nM ^a | metabolic stability <i>t</i> _{1/2} (min) |
|------|-------------------|--------------------------|------------------------------------|---------------------------|-------------------|------------------------------------|---------------------------|----------------------------|---|
| | | | <i>h</i> 17 β -HSD2 | <i>h</i> 17 β -HSD1 | | <i>m</i> 17 β -HSD2 | <i>m</i> 17 β -HSD1 | | human liver S9 |
| A | | | 111 | 21 | 0.2 | n.i. ^c | n.i. ^c | | <5 |
| 1 | 2-CH ₃ | –H | 231 | 306 | 1.3 | n.i. ^c | n.i. ^c | | n.d. ^d |
| 2 | 2-F | –H | 6.9 | 7.2 | 1 | 81.6 | 12 | | n.d. ^d |
| 3 | 2-Cl | –H | 0.9 | 20.3 | 22.5 | 2.7 | 26 | | <5 |
| 4 | 4-Cl | –H | 13.8 | 8.2 | 0.6 | 303.5 | 22 | | n.d. ^d |
| 5 | 2,6-di-F | –H | 5.6 | 1.4 | 0.3 | 30.5 | 43 | | n.d. ^d |
| 6 | 2-F,6-Cl | –H | 8.5 | 1.7 | 0.2 | 8.9 | 54 | | n.d. ^d |
| 7 | 2-Cl,6-F | –H | 6.7 | 15.6 | 2.3 | 2.7 | 25 | | <5 |
| 9 | 2,4,5-tri-F | 4-F | 1.2 | 1.2 | 1 | 27.3 | 24 | | 32 |
| 10 | 2,4,5-tri-F | 4-Cl | 0.4 | 0.7 | 1.8 | 6.2 | 31 | | 40 |
| 11 | 2,4,5-tri-F | 4-CH ₃ | 0.2 | 0.1 | 0.5 | 9.9 | 30 | | 32 |
| 12 | 2,4,5-tri-F | 3-Cl | 0.4 | 0.8 | 2 | 5.6 | 28 | | 42 |
| 13 | 2,4,5-tri-F | 3-CH ₃ | 0.2 | 0.1 | 0.5 | 7.9 | 49 | | 28 |
| 14 | 2,4,5-tri-F | 2-CF ₃ | 1.4 | 4.8 | 3.4 | 11.6 | 30 | | 51 |
| 15 | 2,4,5-tri-F | 2-OCF ₃ | 2.0 | 6.0 | 3 | 24.5 | 25 (1764 nM) ^e | | 60 |
| 16 | 2,4,5-tri-F | 2-OCF ₃ ,4-Br | 1.8 | 2.4 | 1.3 | 14.0 | 30 | | n.d. ^d |

^aMean value of at least two determinations, standard deviation less than 20%. ^bs.f.: selectivity factor = $hIC_{50}(17\beta\text{-HSD1})/hIC_{50}(17\beta\text{-HSD2})$. ^cn.i.: no inhibition @1 μ M. ^dn.d.: not determined. ^e $mIC_{50}(17\beta\text{-HSD1})$. Final concentration of E1 and E2 in *h*17 β -HSD1 and *h*17 β -HSD2 assay: 500 and 500 nM, respectively. Final concentration of E1 and E2 in *m*17 β -HSD1 and *m*17 β -HSD2 assay: 10 and 10 nM, respectively.

vehicle-treated animals was 27.6 and 40.9% of the stiffness determined in the nonfractured femurs of the same animal, respectively. These values are similar to those reported previously in C57BL/6 mice.²⁴ After 14 days, no difference in bending stiffness could be discerned between the 15- and vehicle-treated animals (Figure 1 and Table S1) or in the

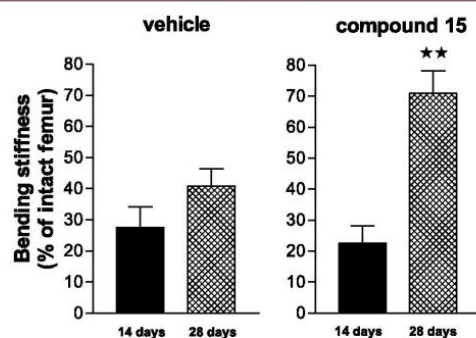


Figure 1. Effect of compound 15 on the bending stiffness of the fractured femurs of C57BL/6 male mice after 14 and 28 days of treatment. **indicates $P < 0.01$ in bone bending stiffness between the vehicle- and 15-treated animals at 28 days (Student's *t* test).

periosteal area of the callus (i.e., the area that represents the newly formed tissue around the fracture) (Figure 2A and Table S1). However, after 28 days, the bending stiffness of the fractured bones in animals treated with 15 was almost twice as high as the bending stiffness of the fractured bones of vehicle-treated animals ($P = 0.005$) (Figure 1 and Table S1). The strong increase in bending stiffness was accompanied with a 61% larger periosteal area of the callus ($P = 0.026$) in 15-treated animals at 28 days (Figure 2A and Table S1). Representative photographs of the callus of healing fractured femurs after 28 days of treatment with 15 and vehicle are shown in Figure 2B.

The periosteal area in the callus of 15-treated animals consisted of a larger bone area than in the vehicle-treated

animals after 28 days (Figure 2C and Table S2, $P = 0.025$), whereas the cartilage and fibrous tissue areas in the periosteal callus area were not different (Table S2). Bone mineralization, that is, the rise in the so-called high-density bone (from ~7% at 14 days to ~18% at 28 days), and increase in bone mineral density (from ~0.24 g/cm³ at 14 days to ~0.32 g/cm³ at 28 days) proceeded normally (Tables S3 and S4). The same holds true for the trabecular number, trabecular thickness, and trabecular separation in the callus (Table S4). Compound 15 does not affect bone mineral density, trabecular number, trabecular thickness, and trabecular separation in the non-fractured (intact) femurs of the animals (Table S5). Compound 15 also does not influence the normal cortical bone distant from the fracture: the diameter measurements of the femurs demonstrate comparable values in the 15-treated animals and vehicle controls (Table S6). These results indicate that 17 β -HSD2 inhibition stimulates bone formation in the callus. As resorption of "old" bone at the fracture site precedes new bone formation, we also investigated whether or not 15 increases the expression of osteoprotegerin (OPG), a biomarker of the inhibition of bone resorption. OPG is an E2-inducible, antiresorptive decoy receptor for the receptor activator of nuclear factor κ B ligand (RANKL), which in turn promotes bone resorption.²⁶ Indeed, treatment with 15 for 14 days increased the expression of OPG in callus by 55% ($P = 0.048$) compared to vehicle treatment, whereas the expression of RANKL in callus did not differ (–1% change). These data are consistent with our working hypothesis that 17 β -HSD2 inhibition leads to both E2-mediated suppression of bone resorption and T-mediated stimulation of bone formation and demonstrate the target engagement of the 17 β -HSD2 inhibitor. These data also demonstrate that despite a lack of change in the bending stiffness of the fractured bone after 14 days (Figure 1), biochemical changes do occur (i.e., increase in OPG expression) within the first 14 days of treatment with 15. The process of remodeling in the 15 group is apparently not completed at day 28 (compared to the vehicle group), as indicated by the still larger callus, which might be because of both these underlying E2- and T-mediated processes.

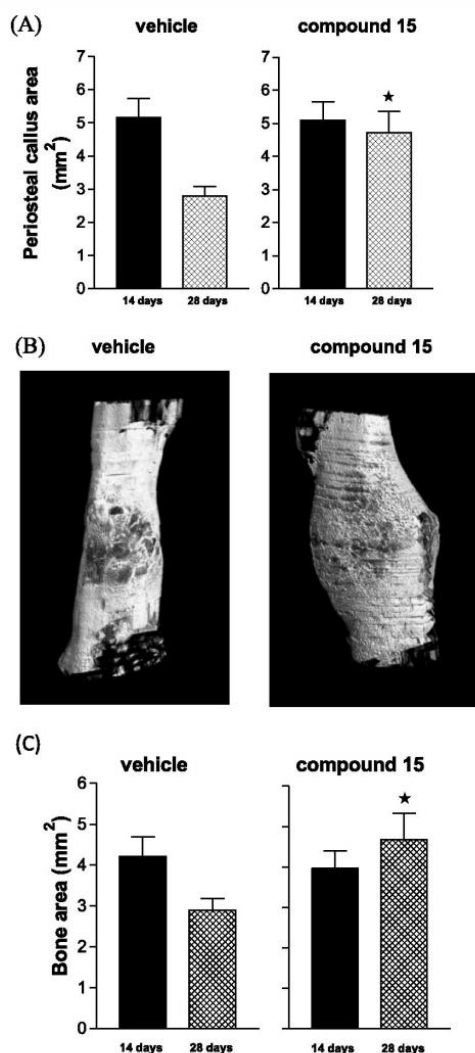


Figure 2. Effect of compound 15 on the periosteal callus area (A), callus size (B), and bone area (C) of the fractured femurs of C57BL/6 male mice after 14 and 28 days of treatment. * indicates $P < 0.05$ regarding the difference in the periosteal callus area and bone area between the vehicle- and 15-treated animals at 28 days (Student's t test).

Notwithstanding the incomplete remodeling at day 28, this target engagement results in a markedly higher biomechanical stability of the healing fracture without affecting the bone quality. Importantly, 28 days of treatment with **15** did not change the plasma concentrations of E2 and T (Table S7). This is in full accordance with the working hypothesis that 17β -HSD2 regulates predominantly intracellular concentrations of E2 and T. In support, the weight of seminal vesicles, which is known to be highly sensitive to the changes in plasma testosterone,^{11,27} was not different between **15**- and vehicle-treated animals after 14 or 28 days (Table S8). We cannot exclude completely that **15** acts via another unknown mechanism, independent of 17β -HSD2, or inhibits an unknown 17β -HSD2 function which is independent of E2 and T. However, this seems highly unlikely. First, our data are

commensurate with 17β -HSD2 inhibition: the plasma concentrations of **15** are sufficiently high (and not too high) to block mouse 17β -HSD2, and our bone E2-inducible biomarker OPG is upregulated in the callus of **15**-treated animals. Second, 17β -HSD2 expression in bone tissue is superior over that of 17β -HSD1, 17β -HSD3, and 17β -HSD4: the enzymes that are structurally and functionally the most similar to 17β -HSD2 and which catalyze the synthesis and degradation of E2 and T. Third, **15** does not markedly bind to E2 receptors, ruling out that **15** acts by stimulating E2 receptors. Fourth, no effects on (control) bone parameters (bone strength and diameter, trabecular number, separation, and thickness), no change in plasma E2 and T, no effect on liver, testicles, seminal vesicles, or body weight (Table S9), and no change in animal behavior during the 28 days of treatment were observed.

CONCLUSIONS

In summary, this study provides for the first time *proof-of-principle* of a 17β -HSD2 inhibitor: inhibition of 17β -HSD2 strongly increases the mechanical stability of the fractured bone because of a larger callus with a newly formed bone without changing the plasma E2 and T concentrations and disturbance of the hypothalamus–pituitary–testes axis. In follow-up studies toward *Proof of Concept* in human patients, compound **15** should be tested for in vivo safety and pharmacokinetic properties in nonrodents, including nonhuman primates (monkeys), and for confirmation of its bone fracture healing efficacy in larger animals. As low-molecular-weight 17β -HSD2 inhibitors shorten the period of immobility during bone fracture healing, 17β -HSD2 inhibitors thus represent a highly attractive, targeted endocrine therapy to treat fractures of fragile bones in patients with osteoporosis and in the elderly.

EXPERIMENTAL SECTION

Chemical Methods. Chemical names follow IUPAC nomenclature. The starting materials were purchased from Aldrich, Acros, Combi-Blocks, or Fluorochem and were used without purification. Gravity-flow column chromatography (CC) was performed on silica gel (70–200 μ m), and the reaction progress was monitored by TLC on Alugram SIL G/UV254 (Macherey-Nagel). Visualization was accomplished with UV light. The ^1H nuclear magnetic resonance (NMR), ^{13}C NMR, and ^{19}F NMR spectra were measured on a Bruker AM500 spectrometer (at 500 MHz, 125, and 470 MHz, respectively) at 300 K and on a Bruker Fourier 300 (at 300 and 75 MHz, respectively) at 300 K. Chemical shifts are reported in δ (parts per million: ppm), by reference to the hydrogenated residues of deuterated solvents as internal standards: 2.05 ppm (^1H NMR) and 29.8 and 206.3 ppm (^{13}C NMR) for acetone- d_6 , 2.50 ppm (^1H NMR) and 39.52 ppm (^{13}C NMR) for dimethyl sulfoxide (DMSO)- d_6 . In case of ^{19}F NMR, trifluoroacetic acid (TFA) was added as an internal standard: δ –76.5 ppm (CF_3TFA). The signals are described as br (broad), s (singlet), d (doublet), t (triplet), dd (doublet of doublets), ddd (doublet of doublet of doublets), dt (doublet of triplets), and m (multiplet). All coupling constants (J) are given in Hertz (Hz). Mass spectrometry was performed on a TSQ Quantum (Thermo Fisher, Dreieich, Germany). The triple quadrupole mass spectrometer was equipped with an electrospray interface. The purity of compounds was determined by liquid chromatography–mass spectrometry (LCMS) using the area percentage method on the UV trace, recorded at a wavelength of 254 nm, and found to be >95%. The Surveyor LC system consisted of a pump, an autosampler, and a PDA detector. The system was operated by the standard software Xcalibur. An RP C18 NUCLEODUR 100-5 (3 mm) column (Macherey-Nagel

GmbH, Düren, Germany) was used as the stationary phase. All solvents were high-pressure liquid chromatography (HPLC) grade. In a gradient run, using acetonitrile and water, the percentage of acetonitrile (containing 0.1% trifluoroacetic acid) was increased from an initial concentration of 0% at 0 min to 100% at 13 min and kept at 100% for 2 min. The injection volume was 15 μ L and the flow rate was set to 800 μ L/min. MS analysis was carried out at a needle voltage of 3000 V and a capillary temperature of 350 °C. Mass spectra were acquired in positive mode, using the electron spray ionization (ESI) method, from 100 to 1000 m/z , and the UV spectra were recorded at the wavelength of 254 nm and in some cases at 360 nm. High-resolution mass spectrometry (HRMS) measurements were recorded on a SpectraSystems-MSQ LCMS system (Thermo Fisher, Dreieich, Germany).

Method A: General Procedure for Friedel–Crafts Acylation. An ice-cooled mixture of arylcarbonyl chloride (1 equiv), monosubstituted thiophene derivative (1.5 equiv), and aluminum trichloride (1 equiv) in anhydrous dichloromethane (10 mL/mmol of arylcarbonyl chloride) was warmed to room temperature and stirred for 2–4 h. A 10 mL of HCl (1 M) was used to quench the reaction. The aqueous layer was extracted with dichloromethane (3 \times 50 mL). The combined organic layers were washed with brine, dried over magnesium sulfate, filtered, and concentrated to dryness. The product was used directly in the subsequent reaction without further purification.

Method B: General Procedure for Suzuki–Miyaura Coupling. A mixture of arylbromide (1 equiv), boronic acid derivative (1.2 equiv), cesium carbonate (4 equiv) and tetrakis(triphenylphosphine) palladium (0.05 equiv) was suspended in an oxygen-free dimethyl ether/water (1:1, v/v, 15 mL/mmol of arylbromide) solution and refluxed under a nitrogen atmosphere. The reaction mixture was cooled to room temperature. The aqueous layer was extracted with ethyl acetate (3 \times 50 mL). The organic layer was washed once with brine and once with water, dried over $MgSO_4$, filtered, and the solution was concentrated under reduced pressure. The product was purified by CC.

Method C: General Procedure for Sulfonamide Coupling. The amino phenyl derivative (1 equiv) was dissolved in absolute pyridine (10 mL/mmol of reactant), and sulfonyl chloride (1.2 equiv) was added. The reaction mixture was stirred overnight at room temperature. The reaction was quenched by adding 10 mL of 2 M HCl and extracted with ethyl acetate (3 \times 50 mL). The organic layers were washed with saturated $NaHCO_3$ and brine, dried over magnesium sulfate, filtered, and concentrated to dryness. The product was used directly in the subsequent reaction without further purification.

Method D: General Procedure for Ether Cleavage. To a solution of respective methoxyaryl compound (1 equiv) in dry dichloromethane (20 mL/mmol of reactant), boron tribromide, 1 M solution in dichloromethane (3 equiv), was added dropwise at 0 °C and stirred overnight at room temperature. After the completion of the reaction, the mixture was diluted with water. The aqueous layer was extracted with dichloromethane (3 \times 50 mL). The combined organic layers were washed with brine, dried over magnesium sulfate, and evaporated to dryness under reduced pressure. The product was purified by CC.

Acetic Acid 3-(5-Bromo-thiophene-2-carbonyl)-2-methyl-phenyl Ester (1b). The title compound was prepared by the reaction of 2-bromothiophene (1150 mg, 7.05 mmol), 3-acetyloxy-2-methylbenzoyl chloride (1000 mg, 4.70 mmol), and aluminum chloride (627 mg, 4.70 mmol) according to method A. The crude product was used directly in the subsequent reaction without further purification [750 mg; MS (ESI) m/z : 338.9 ($M + H$)⁺, $C_{14}H_{12}BrO_3S$ calcd 338.90].

[5-(3-Aminophenyl)thiophen-2-yl](3-hydroxy-2-methylphenyl)-methanone (1a). The title compound was prepared by the reaction of acetic acid 3-(5-bromo-thiophene-2-carbonyl)-2-methyl-phenyl ester (1b) (750 mg, 2.21 mmol), 3-aminophenylboronic acid (365 mg, 2.65 mmol), cesium carbonate (2875 mg, 8.84 mmol), and tetrakis(triphenylphosphine) palladium (128 mg, 111 μ mol) according to method B. The product was purified by CC (petroleum ether/

ethyl acetate 1:1); yield: 33% (230 mg). ¹H NMR (500 MHz, acetone- d_6): δ 8.72 (s, 1H), 7.70 (ddd, J = 11.8, 5.2, 3.2 Hz, 1H), 7.65–7.60 (m, 2H), 7.42 (t, J = 3.9 Hz, 1H), 7.39 (t, J = 3.5 Hz, 1H), 7.19–7.11 (m, 1H), 6.96–6.93 (m, 1H), 6.78–6.68 (m, 1H), 4.89 (s, 2H), 2.17 (s, 3H). MS (ESI) m/z : 310.1 ($M + H$)⁺, $C_{18}H_{16}NO_2S$ calcd 310.0.

N-[3-[5-(3-Hydroxy-2-methylbenzoyl)thiophen-2-yl]phenyl]-benzenesulfonamide (1). The title compound was prepared by the reaction of [5-(3-aminophenyl)thiophen-2-yl](3-hydroxy-2-methylphenyl)methanone (1a) (230 mg, 0.74 mmol) and benzenesulfonyl chloride (156 mg, 0.88 mmol) according to method C. The product was purified by CC (dichloromethane/methanol 99:1); yield: 25% (85 mg). ¹H NMR (500 MHz, acetone- d_6): δ 9.24 (s, 1H), 8.67 (s, 1H), 7.93–7.79 (m, 2H), 7.61 (m, 2H), 7.57–7.52 (m, 2H), 7.51–7.47 (m, 1H), 7.45 (d, J = 4.0 Hz, 1H), 7.41 (d, J = 4.0 Hz, 1H), 7.36 (t, J = 7.9 Hz, 1H), 7.28 (ddt, J = 8.1, 2.0, 0.9 Hz, 1H), 7.19–7.13 (m, 1H), 7.06–7.02 (m, 1H), 6.96 (dd, J = 7.5, 1.1 Hz, 1H), 2.18 (s, 3H). ¹³C NMR (125 MHz, acetone- d_6): δ 190.3, 156.7, 152.9, 144.7, 141.1, 139.7, 137.3, 135.0, 133.9, 133.9, 131.1, 130.0, 128.0, 127.0, 125.7, 123.0, 121.9, 119.8, 118.7, 117.4, 117.3, 12.9. MS (ESI) t_R 8.31 min, m/z : 450.0 ($M + H$)⁺, $C_{24}H_{20}NO_4S_2$ calcd 450.0; HRMS m/z : 450.08099 ($[M + H]^+$, $C_{24}H_{20}NO_4S_2$ calcd 450.08280).

N-[3-[5-(2-Fluoro-3-hydroxy-benzoyl)-thiophen-2-yl]-phenyl]-benzenesulfonamide (2). The title compound was prepared by the reaction of [5-(3-aminophenyl)thiophen-2-yl](2-fluoro-3-methoxyphenyl)methanone (2a) (400 mg, 1.22 mmol) and benzenesulfonyl chloride (259 mg, 1.46 mmol) according to method C. The crude product was reacted with boron tribromide (3 equiv) according to method D. The product was purified by CC (dichloromethane/methanol 99:1); yield over two steps: 14% (80 mg). ¹H NMR (500 MHz, acetone- d_6): δ 9.27 (s, 1H), 9.13 (s, 1H), 7.93–7.82 (m, 2H), 7.60 (dd, J = 10.5, 4.2 Hz, 2H), 7.55 (dt, J = 14.7, 4.4 Hz, 3H), 7.49 (t, J = 6.2 Hz, 2H), 7.37 (t, J = 7.9 Hz, 1H), 7.32–7.27 (m, 1H), 7.23 (td, J = 8.1, 1.7 Hz, 1H), 7.18 (t, J = 7.8 Hz, 1H), 7.09–7.03 (m, 1H). ¹³C NMR (125 MHz, acetone- d_6): δ 184.9, 153.4, 149.3 (d, J = 245.9 Hz), 146.3 (d, J = 12.9 Hz), 143.7, 140.6, 139.8, 137.6, 134.9, 133.9, 131.1, 130.0, 128.7 (d, J = 13.0 Hz), 128.0, 125.9, 125.4 (d, J = 4.2 Hz), 123.0, 122.0, 121.3 (d, J = 2.9 Hz), 120.6, 118.7. MS (ESI) t_R 8.31 min, m/z : 454.0 ($M + H$)⁺, $C_{23}H_{17}FNO_4S_2$ calcd 454.0; HRMS m/z : 454.05588 ($M + H$)⁺, $C_{23}H_{17}FNO_4S_2$ calcd 454.05775.

(5-Bromothiophen-2-yl)(2-chloro-3-methoxyphenyl)methanone (3b). 2-Chloro-3-methoxy-benzoic acid (400 mg, 2.14 mmol, 1 equiv) was dissolved in thionyl chloride (4320 mg, 36.4 mmol, 17 equiv) and stirred under reflux for 1 h. The solution was concentrated in vacuum, and the crude product was reacted with 2-bromothiophene (523 mg, 3.21 mmol) and aluminum chloride (285 mg, 2.14 mmol) according to method A. In slight variation, the mixture was stirred at room temperature overnight. The crude product was used directly in the subsequent reaction without further purification [500 mg; MS (ESI) m/z : 330.96 ($M + H$)⁺, $C_{12}H_9BrClO_2S$ calcd 330.9].

N-[3-[5-(2-Chloro-3-hydroxy-benzoyl)-thiophen-2-yl]-phenyl]-benzenesulfonamide (3). The title compound was prepared by the reaction of [5-(3-aminophenyl)thiophen-2-yl](2-chloro-3-methoxyphenyl)methanone (3a) (450 mg, 1.30 mmol) and benzenesulfonyl chloride (277 mg, 1.57 mmol) according to method C. The crude product was reacted with boron tribromide (3 equiv) according to method D. The product was purified by CC (dichloromethane/methanol 99:1); yield over two steps: 19% (100 mg). ¹H NMR (500 MHz, acetone- d_6): δ 9.26 (s, 1H), 9.22 (s, 1H), 7.87 (ddd, J = 7.0, 3.2, 1.8 Hz, 2H), 7.64–7.58 (m, 2H), 7.57–7.52 (m, 2H), 7.50 (ddd, J = 7.7, 1.7, 1.0 Hz, 1H), 7.47 (d, J = 4.0 Hz, 1H), 7.42 (d, J = 4.0 Hz, 1H), 7.37 (t, J = 7.9 Hz, 1H), 7.33 (dd, J = 8.1, 7.5 Hz, 1H), 7.29 (ddd, J = 8.1, 2.1, 0.9 Hz, 1H), 7.20 (dd, J = 8.2, 1.5 Hz, 1H), 7.03 (dd, J = 7.5, 1.5 Hz, 1H). ¹³C NMR (125 MHz, acetone- d_6): δ 187.0, 154.4, 153.6, 143.3, 140.6, 140.5, 139.8, 137.8, 134.9, 133.9, 131.1, 130.0, 128.7, 128.0, 125.9, 123.0, 122.0, 120.4, 118.9, 118.7, 117.9. MS (ESI) t_R 8.30 min, m/z : 470.0 ($M + H$)⁺, $C_{23}H_{17}ClNO_4S_2$ calcd 470.0; HRMS m/z : 470.02643 ($[M + H]^+$, $C_{23}H_{17}ClNO_4S_2$ calcd 470.02820).

N-[3-[5-(4-Chloro-3-hydroxybenzoyl)thiophen-2-yl]phenyl]-benzenesulfonamide (**4**). The title compound was prepared by the reaction of [5-(3-aminophenyl)thiophen-2-yl](4-chloro-3-methoxyphenyl)methanone (**4a**) (450 mg, 1.30 mmol) and benzenesulfonyl chloride (277 mg, 1.57 mmol) according to method C. The crude product was reacted with boron tribromide (3 equiv) according to method D. The product was purified by CC (dichloromethane/methanol 99:1); yield over two steps: 23% (120 mg). ¹H NMR (500 MHz, acetone-*d*₆): δ 9.36 (s, 1H), 9.28 (s, 1H), 7.90–7.85 (m, 2H), 7.72 (d, *J* = 4.0 Hz, 1H), 7.64–7.59 (m, 2H), 7.57–7.53 (m, 3H), 7.52–7.49 (m, 3H), 7.41–7.35 (m, 2H), 7.28 (ddd, *J* = 8.1, 2.1, 1.0 Hz, 1H). ¹³C NMR (125 MHz, acetone-*d*₆): δ 186.6, 154.0, 152.6, 143.1, 140.6, 139.7, 138.5, 137.0, 134.9, 133.9, 131.1, 131.0, 130.0, 128.0, 125.7, 125.6, 123.0, 122.0, 121.9, 118.7, 117.6. MS (ESI) *t*_R 8.74 min, *m/z*: 470.0 (M + H)⁺, C₂₃H₁₇ClNO₄S₂⁺ calcd 470.0; HRMS *m/z*: 470.02631 ([M + H]⁺), C₂₃H₁₇ClNO₄S₂⁺ calcd 470.02820).

N-[3-[5-(2,6-Difluoro-3-hydroxybenzoyl)thiophen-2-yl]phenyl]-benzenesulfonamide (**5**). The title compound was prepared by the reaction of [5-(3-aminophenyl)thiophene-2-yl](3-methoxy-2,6-difluorophenyl)methanone (**5a**) (390 mg, 0.83 mmol) and benzenesulfonyl chloride (177 mg, 0.99 mmol) according to method C. The crude product was reacted with boron tribromide (3 equiv) according to method D. The product was purified by CC (dichloromethane/methanol 99:1) followed by washing with petroleum ether/diethyl ether 2:1; yield over two steps: 28% (150 mg). ¹H NMR (500 MHz, acetone-*d*₆): δ 9.26 (s, 1H), 9.06 (s, 1H), 7.91–7.84 (m, 2H), 7.65–7.58 (m, 3H), 7.58–7.50 (m, 4H), 7.41–7.36 (m, 1H), 7.30 (ddd, *J* = 8.1, 2.1, 1.0 Hz, 1H), 7.25–7.18 (m, 1H), 7.07–7.00 (m, 1H). ¹³C NMR (125 MHz, acetone-*d*₆): δ 180.6, 154.5, 152.5 (dd, *J* = 240.5, 5.8 Hz), 148.4 (dd, *J* = 245.8, 7.7 Hz), 143.4, 142.6 (dd, *J* = 12.9, 3.1 Hz), 140.6, 139.8, 138.2, 134.7, 133.9, 131.2, 130.0, 128.0, 126.2, 123.1, 122.2, 120.3 (dd, *J* = 9.1, 3.8 Hz), 118.8, 118.0 (dd, *J* = 23.9, 19.7 Hz), 112.4 (dd, *J* = 22.8, 3.9 Hz). MS (ESI) *t*_R 8.37 min, *m/z*: 472.0 (M + H)⁺, C₂₃H₁₆F₂NO₄S₂⁺ calcd 472.0; HRMS *m/z*: 472.04626 ([M + H]⁺), C₂₃H₁₆F₂NO₄S₂⁺ calcd 472.04833).

N-[3-[5-(6-Chloro-2-fluoro-3-hydroxybenzoyl)thiophen-2-yl]phenyl]-benzenesulfonamide (**6**). The title compound was prepared by the reaction of [5-(3-aminophenyl)thiophen-2-yl](6-chloro-2-fluoro-3-methoxyphenyl)methanone (**6a**) (380 mg, 1.05 mmol) and benzenesulfonyl chloride (223 mg, 1.26 mmol) according to method C. The crude product was reacted with boron tribromide (3 equiv) according to method D. The product was purified by CC (dichloromethane/methanol 99:1) followed by washing with petroleum ether/diethyl ether 2:1; yield over two steps: 22% (115 mg). ¹H NMR (500 MHz, acetone-*d*₆): δ 9.38 (s, 1H), 9.27 (s, 1H), 7.91–7.82 (m, 2H), 7.64–7.59 (m, 2H), 7.57–7.50 (m, 5H), 7.38 (dd, *J* = 12.0, 4.2 Hz, 1H), 7.30 (ddd, *J* = 8.1, 2.1, 1.0 Hz, 1H), 7.25 (dd, *J* = 8.8, 1.4 Hz, 1H), 7.19 (t, *J* = 8.9 Hz, 1H). ¹³C NMR (125 MHz, acetone-*d*₆): δ 182.5, 154.5, 149.0 (d, *J* = 244.9 Hz), 145.2 (d, *J* = 12.9 Hz), 142.9, 140.6, 139.8, 138.1, 134.7, 133.9, 131.2, 130.0, 128.4 (d, *J* = 19.6 Hz), 128.0, 126.6 (d, *J* = 3.7 Hz), 126.3, 123.1, 122.2, 120.8 (d, *J* = 4.2 Hz), 120.5 (d, *J* = 3.5 Hz), 118.8. MS (ESI) *t*_R 8.65 min, *m/z*: 488.0 (M + H)⁺, C₂₃H₁₆ClFNO₄S₂⁺ calcd 488.0; HRMS *m/z*: 488.01669 ([M + H]⁺), C₂₃H₁₆ClFNO₄S₂⁺ calcd 488.01878).

N-[3-[5-(2-Chloro-6-fluoro-3-hydroxybenzoyl)thiophen-2-yl]phenyl]-benzenesulfonamide (**7**). The title compound was prepared by the reaction of [5-(3-aminophenyl)thiophen-2-yl](2-chloro-6-fluoro-3-methoxyphenyl)methanone (**7b**) (450 mg, 1.24 mmol) and benzenesulfonyl chloride (264 mg, 1.49 mmol) according to method C. The crude product was reacted with boron tribromide (3 equiv) according to method D. The product was purified by CC (dichloromethane/methanol 99:1) followed by washing with petroleum ether/diethyl ether 2:1; yield: 25% (150 mg). ¹H NMR (500 MHz, acetone-*d*₆): δ 9.28 (s, 1H), 7.91–7.80 (m, 2H), 7.65–7.59 (m, 2H), 7.57–7.49 (m, 5H), 7.38 (t, *J* = 7.9 Hz, 1H), 7.30 (d, *J* = 7.5 Hz, 1H), 7.23–7.15 (m, 2H). ¹³C NMR (125 MHz, acetone-*d*₆): δ 182.6, 154.4, 153.1 (d, *J* = 239.4 Hz), 151.0 (d, *J* = 13.5 Hz),

142.9, 140.6 (d, *J* = 7.5 Hz), 139.8 (d, *J* = 9.6 Hz), 137.9, 134.7, 133.9, 131.2, 130.0, 128.3 (d, *J* = 23.6 Hz), 128.0, 126.2, 123.1 (d, *J* = 1.5 Hz), 122.2 (d, *J* = 3.7 Hz), 118.9 (d, *J* = 11.4 Hz), 118.8 (d, *J* = 3.3 Hz), 116.1, 115.9. MS (ESI) *t*_R 8.44 min, *m/z*: 488.0 (M + H)⁺, C₂₃H₁₆ClFNO₄S₂⁺ calcd 488.0; HRMS *m/z*: 488.01669 ([M + H]⁺), C₂₃H₁₆ClFNO₄S₂⁺ calcd 488.01878).

N-[3-[5-(2,4,5-Trifluoro-3-hydroxy-benzoyl)-thiophen-2-yl]-phenyl]-benzenesulfonamide (**8**). The title compound was prepared by the reaction of [5-(3-aminophenyl)thiophen-2-yl](2,4,5-trifluoro-3-methoxyphenyl)methanone (**8a**) (300 mg, 0.82 mmol) and benzenesulfonyl chloride (177 mg, 0.99 mmol) according to method C. The crude product was reacted with boron tribromide (3 equiv) according to method D. The product was purified by CC (dichloromethane/methanol 99:1) followed by washing with petroleum ether/diethyl ether 2:1; yield over two steps: 25% (100 mg). ¹H NMR (500 MHz, acetone-*d*₆): δ 10.02 (s, 1H), 9.24 (s, 1H), 7.87–7.81 (m, 2H), 7.64 (dd, *J* = 4.0, 1.7 Hz, 1H), 7.61–7.56 (m, 2H), 7.52 (t, *J* = 7.6 Hz, 2H), 7.50–7.46 (m, 2H), 7.35 (t, *J* = 7.9 Hz, 1H), 7.25 (dd, *J* = 8.1, 1.3 Hz, 1H), 7.09 (ddd, *J* = 9.9, 8.2, 5.7 Hz, 1H). ¹³C NMR (125 MHz, acetone-*d*₆): δ 182.8, 154.0, 148.0 (ddd, *J* = 244.2, 11.1, 3.1 Hz), 147.0 (ddd, *J* = 245.1, 12.3, 3.7 Hz), 143.6 (ddd, *J* = 248.3, 15.8, 5.8 Hz), 142.9, 140.6, 139.8, 138.3 (d, *J* = 1.9 Hz), 137.1 (ddd, *J* = 15.8, 12.8, 2.3 Hz), 134.7, 133.9, 131.2, 130.0, 128.0, 126.0, 123.1, 123.2–122.8 (m), 122.1, 118.7, 106.9 (dd, *J* = 21.1, 2.9 Hz). MS (ESI) *t*_R 8.64 min, *m/z*: 490.0 (M + H)⁺, C₂₃H₁₅F₃NO₄S₂⁺ calcd 490.0; HRMS *m/z*: 490.03586 ([M + H]⁺), C₂₃H₁₅F₃NO₄S₂⁺ calcd 490.03891).

4-Fluoro-*N*-[3-[5-(2,4,5-trifluoro-3-hydroxy-benzoyl)-thiophen-2-yl]-phenyl]-benzenesulfonamide (**9**). The title compound was prepared by the reaction of [5-(3-aminophenyl)thiophen-2-yl](2,4,5-trifluoro-3-methoxyphenyl)methanone (**8a**) (300 mg, 0.82 mmol) and 4-fluorobenzene-1-sulfonyl chloride (194 mg, 0.99 mmol) according to method C. The crude product was reacted with boron tribromide (3 equiv) according to method D. The product was purified by CC (dichloromethane/methanol 97:3) followed by washing with petroleum ether/diethyl ether 2:1; yield over two steps: 12% (50 mg). ¹H NMR (500 MHz, acetone-*d*₆): δ 10.00 (s, 1H), 9.27 (s, 1H), 7.97–7.89 (m, 2H), 7.67 (dd, *J* = 4.1, 1.8 Hz, 1H), 7.63 (t, *J* = 1.8 Hz, 1H), 7.53 (ddd, *J* = 5.4, 2.9, 1.9 Hz, 2H), 7.39 (t, *J* = 7.9 Hz, 1H), 7.35–7.30 (m, 2H), 7.29 (ddd, *J* = 8.1, 2.1, 0.9 Hz, 1H), 7.12 (ddd, *J* = 9.9, 8.1, 5.6 Hz, 1H). ¹³C NMR (125 MHz, acetone-*d*₆): δ 181.9, 165.1 (d, *J* = 252.6 Hz), 153.0, 147.1 (ddd, *J* = 244.1, 11.0, 3.1 Hz), 146.1 (ddd, *J* = 244.1, 4.1, 2.9 Hz), 142.7 (ddd, *J* = 248.5, 15.8, 5.8 Hz), 142.1, 138.7, 137.4 (d, *J* = 2.1 Hz), 136.1 (ddd, *J* = 18.2, 12.8, 3.0 Hz), 135.9 (d, *J* = 3.1 Hz), 133.9, 130.3, 130.1 (d, *J* = 9.6 Hz), 125.2, 122.4, 122.1 (ddd, *J* = 15.4, 6.5, 3.8 Hz), 121.4, 118.1, 116.2 (d, *J* = 22.9 Hz), 106.0 (dd, *J* = 21.1, 3.0 Hz). MS (ESI) *t*_R 8.78 min, *m/z*: 508.0 (M + H)⁺, C₂₃H₁₄F₄NO₄S₂⁺ calcd 508.0; HRMS *m/z*: 508.02756 ([M + H]⁺), C₂₃H₁₄F₄NO₄S₂⁺ calcd 508.02949).

4-Chloro-*N*-[3-[5-(2,4,5-trifluoro-3-hydroxy-benzoyl)-thiophen-2-yl]-phenyl]-benzenesulfonamide (**10**). The title compound was prepared by the reaction of [5-(3-aminophenyl)thiophen-2-yl](2,4,5-trifluoro-3-methoxyphenyl)methanone (**8a**) (400 mg, 1.1 mmol) and 4-chlorobenzene-1-sulfonyl chloride (279 mg, 1.32 mmol) according to method C. The crude product was reacted with boron tribromide (3 equiv) according to method D. The product was purified by CC (dichloromethane/methanol 99:1); yield over two steps: 13% (75 mg). ¹H NMR (500 MHz, acetone-*d*₆): δ 9.40 (s, 1H), 7.89–7.84 (m, 2H), 7.66 (dd, *J* = 4.1, 1.8 Hz, 1H), 7.64 (t, *J* = 1.8 Hz, 1H), 7.60–7.56 (m, 2H), 7.54–7.50 (m, 2H), 7.39 (t, *J* = 7.9 Hz, 1H), 7.30 (ddd, *J* = 8.1, 2.1, 1.0 Hz, 1H), 7.11 (ddd, *J* = 9.9, 8.1, 5.6 Hz, 1H). ¹³C NMR (125 MHz, acetone-*d*₆): δ 182.8, 153.9, 148.0 (ddd, *J* = 244.1, 11.0, 3.2 Hz), 147.0 (ddd, *J* = 244.2, 4.2, 2.9 Hz), 143.6 (ddd, *J* = 248.6, 15.8, 5.8 Hz), 143.0, 139.6, 139.5, 139.4, 138.2 (d, *J* = 2.0 Hz), 137.1 (ddd, *J* = 18.0, 12.7, 3.0 Hz), 134.8, 131.2, 130.2, 129.8, 126.1, 123.4, 123.0 (ddd, *J* = 15.4, 6.5, 3.8 Hz), 122.4, 119.0, 106.9 (dd, *J* = 21.1, 3.0 Hz). MS (ESI) *t*_R 9.10 min, *m/z*: 523.9 (M + H)⁺, C₂₃H₁₄ClF₃NO₄S₂⁺ calcd 523.9; HRMS *m/z*: 523.99725 ([M + H]⁺), C₂₃H₁₄ClF₃NO₄S₂⁺ calcd 523.99994).

4-Methyl-N-[3-[5-(2,4,5-trifluoro-3-hydroxy-benzoyl)-thiophen-2-yl]-phenyl]-benzenesulfonamide (11). The title compound was prepared by the reaction of [5-(3-aminophenyl)thiophen-2-yl](2,4,5-trifluoro-3-methoxyphenyl)methanone (**8a**) (400 mg, 1.1 mmol) and 4-methylbenzene-1-sulfonyl chloride (252 mg, 1.32 mmol) according to method C. The crude product was reacted with boron tribromide (3 equiv) according to method D. The product was purified by CC (dichloromethane/methanol 99:1) followed by washing with petroleum ether/diethyl ether 2:1; yield over two steps: 22% (120 mg). ¹H NMR (500 MHz, acetone-*d*₆): δ 10.04 (s, 1H), 9.19 (s, 1H), 7.77–7.73 (m, 2H), 7.67 (dd, *J* = 4.1, 1.8 Hz, 1H), 7.63 (dd, *J* = 2.9, 1.0 Hz, 1H), 7.53–7.49 (m, 2H), 7.40–7.33 (m, 3H), 7.29 (ddd, *J* = 8.1, 2.1, 1.0 Hz, 1H), 7.13 (ddd, *J* = 9.9, 8.1, 5.6 Hz, 1H), 2.35 (s, 3H). ¹³C NMR (125 MHz, acetone-*d*₆): δ 182.8, 154.1, 148.1 (ddd, *J* = 243.9, 11.0, 2.9 Hz), 147.0 (ddd, *J* = 244.1, 4.1, 3.1 Hz), 144.7, 143.6 (ddd, *J* = 248.5, 15.8, 5.9 Hz), 142.9, 140.0, 138.2 (d, *J* = 1.9 Hz), 137.82, 137.0 (ddd, *J* = 18.3, 12.8, 3.1 Hz), 134.7, 131.1, 130.5, 128.0, 126.0, 123.0 (ddd, *J* = 15.9, 6.7, 4.1 Hz), 122.9, 121.9, 118.5, 106.9 (dd, *J* = 21.0, 3.0 Hz), 21.3. MS (ESI) *t*_R 8.90 min, *m/z*: 503.9 (M + H)⁺, C₂₄H₁₇F₃NO₄S₂⁺ calcd 504.0; HRMS *m/z*: 504.05258 ([M + H]⁺, C₂₄H₁₇F₃NO₄S₂⁺ calcd 504.05456).

3-Chloro-N-[3-[5-(2,4,5-trifluoro-3-hydroxy-benzoyl)-thiophen-2-yl]-phenyl]-benzenesulfonamide (12). The title compound was prepared by the reaction of [5-(3-aminophenyl)thiophen-2-yl](2,4,5-trifluoro-3-methoxyphenyl)methanone (**8a**) (300 mg, 0.82 mmol) and 3-chlorobenzene-1-sulfonyl chloride (211 mg, 1.00 mmol) according to method C. The crude product was reacted with boron tribromide (3 equiv) according to method D. The product was purified by CC (dichloromethane/methanol 99:1) followed by washing with petroleum ether/diethyl ether 2:1; yield over two steps: 42% (180 mg). ¹H NMR (500 MHz, acetone-*d*₆): δ 10.10 (s, 1H), 9.35 (s, 1H), 7.70–7.64 (m, 2H), 7.63 (m, 2H), 7.59 (t, *J* = 7.9 Hz, 1H), 7.56 (dd, *J* = 7.8, 0.7 Hz, 1H), 7.53 (d, *J* = 4.0 Hz, 1H), 7.42 (t, *J* = 7.9 Hz, 1H), 7.30 (dd, *J* = 8.1, 1.2 Hz, 1H), 7.13 (ddd, *J* = 9.8, 8.2, 5.7 Hz, 1H). ¹³C NMR (125 MHz, acetone-*d*₆): δ 182.8, 153.8, 148.1 (ddd, *J* = 244.4, 11.1, 3.1 Hz), 148.1–145.9 (m), 144.9–142.5 (m), 143.0, 142.4, 139.3, 138.2 (d, *J* = 2.0 Hz), 137.4–136.7 (m), 135.5, 134.9, 133.9, 131.9, 131.3, 127.7, 126.5, 126.1, 123.5, 123.0 (ddd, *J* = 15.3, 6.6, 3.8 Hz), 122.5, 119.1, 106.9 (dd, *J* = 21.1, 3.0 Hz). MS (ESI) *t*_R 9.07 min, *m/z*: 523.8 (M + H)⁺, C₂₃H₁₄ClF₃NO₄S₂⁺ calcd 523.9; HRMS *m/z*: 523.99823 ([M + H]⁺, C₂₃H₁₄ClF₃NO₄S₂⁺ calcd 523.99994).

3-Methyl-N-[3-[5-(2,4,5-trifluoro-3-hydroxy-benzoyl)-thiophen-2-yl]-phenyl]-benzenesulfonamide (13). The title compound was prepared by the reaction of [5-(3-aminophenyl)thiophen-2-yl](2,4,5-trifluoro-3-methoxyphenyl)methanone (**8a**) (250 mg, 0.68 mmol) and 3-methylbenzene-1-sulfonyl chloride (157 mg, 0.82 mmol) according to method C. The crude product was reacted with boron tribromide (3 equiv) according to method D. The product was purified by CC (dichloromethane/methanol 99:1) followed by washing with petroleum ether/diethyl ether 2:1; yield over two steps: 26% (90 mg). ¹H NMR (500 MHz, acetone-*d*₆): δ 10.00 (s, 1H), 9.21 (s, 1H), 7.70 (s, 1H), 7.69–7.64 (m, 2H), 7.62 (t, *J* = 1.8 Hz, 1H), 7.54–7.49 (m, 2H), 7.45–7.40 (m, 2H), 7.38 (t, *J* = 7.9 Hz, 1H), 7.28 (ddd, *J* = 8.1, 2.1, 0.9 Hz, 1H), 7.16–7.09 (m, 1H), 2.37 (s, 3H). ¹³C NMR (125 MHz, acetone-*d*₆): δ 182.8, 154.1, 149.1–146.9 (m), 148.2–145.9 (m), 143.6 (ddd, *J* = 248.5, 15.8, 5.8 Hz), 142.9, 140.6, 140.2, 139.9, 138.2 (d, *J* = 2.0 Hz), 137.0 (ddd, *J* = 18.1, 12.8, 3.0 Hz), 134.7, 134.5, 131.1, 129.9, 128.3, 126.0, 125.1, 123.3–123.0 (m), 122.98, 122.04, 118.61, 106.9 (dd, *J* = 21.1, 3.0 Hz), 21.24. MS (ESI) *t*_R 8.89 min, *m/z*: 503.9 (M + H)⁺, C₂₄H₁₇F₃NO₄S₂⁺ calcd 504.0; HRMS *m/z*: 504.05252 ([M + H]⁺, C₂₄H₁₇F₃NO₄S₂⁺ calcd 504.05456).

N-[3-[5-(2,4,5-Trifluoro-3-hydroxybenzoyl)thiophen-2-yl]-phenyl]-2-trifluoro-methylbenzenesulfonamide (14). The title compound was prepared by the reaction of [5-(3-aminophenyl)thiophen-2-yl](2,4,5-trifluoro-3-methoxyphenyl)methanone (**8a**) (260 mg, 0.72 mmol) and 2-trifluoromethylbenzenesulfonyl chloride (177 mg, 0.72 mmol) according to method C. The crude product was

reacted with boron tribromide (3 equiv) according to method D. The product was purified by CC (dichloromethane/methanol 99.5:0.5); yield over two steps: 19% (75 mg); ¹H NMR (500 MHz, acetone-*d*₆): δ 9.97 (s, 1H), 9.40 (s, 1H), 8.30–8.23 (m, 1H), 8.04–7.98 (m, 1H), 7.89–7.82 (m, 2H), 7.67 (dd, *J* = 4.1, 1.8 Hz, 1H), 7.66 (t, *J* = 1.8 Hz, 1H), 7.53 (ddd, *J* = 7.8, 1.8, 1.0 Hz, 1H), 7.51 (d, *J* = 4.1 Hz, 1H), 7.40 (t, *J* = 7.9 Hz, 1H), 7.31 (ddd, *J* = 8.1, 2.2, 1.0 Hz, 1H), 7.12 (ddd, *J* = 9.9, 8.1, 5.6 Hz, 1H); ¹³C NMR (125 MHz, acetone-*d*₆): δ 182.8, 153.9, 148.0 (ddd, *J* = 243.6, 11.1, 3.4 Hz), 148.3–145.5 (m), 144.8–142.3 (m), 143.0, 139.1, 138.2 (d, *J* = 2.1 Hz), 137.0 (ddd, *J* = 10.1, 8.0, 5.8 Hz), 134.9, 134.4, 133.8, 132.7, 131.3, 129.5 (q, *J* = 6.4 Hz), 128.4, 128.1, 126.1, 125.0, 123.3, 122.8, 122.0, 118.6, 106.9 (dd, *J* = 21.1, 3.0 Hz). MS (ESI) *t*_R 8.39 min, *m/z*: 558.0 (M + H)⁺, C₂₄H₁₄F₆NO₄S₂⁺ calcd 558.0; HRMS *m/z*: 558.02411 ([M + H]⁺, C₂₄H₁₄F₆NO₄S₂⁺ calcd 558.02629).

N-[3-[5-(2,4,5-Trifluoro-3-hydroxybenzoyl)thiophen-2-yl]-phenyl]-2-trifluoromethoxybenzenesulfonamide (15). The title compound was prepared by the reaction of [5-(3-aminophenyl)thiophen-2-yl](2,4,5-trifluoro-3-methoxyphenyl)methanone (**8a**) (260 mg, 0.72 mmol) and 2-trifluoromethoxybenzenesulfonyl chloride (189 mg, 0.72 mmol) according to method C. The crude product was reacted with boron tribromide (3 equiv) according to method D. The product was purified by CC (dichloromethane/methanol 99.5:0.5); yield over two steps: 38% (154 mg); ¹H NMR (500 MHz, acetone-*d*₆): δ 9.98 (s, 1H), 9.52 (s, 1H), 8.13–8.09 (m, 1H), 7.78 (ddd, *J* = 8.4, 7.5, 1.7 Hz, 1H), 7.66 (ddd, *J* = 4.3, 3.1, 1.1 Hz, 2H), 7.58–7.53 (m, 2H), 7.52–7.50 (m, 2H), 7.38 (td, *J* = 7.9, 0.4 Hz, 1H), 7.31 (ddd, *J* = 8.1, 2.2, 1.0 Hz, 1H), 7.12 (ddd, *J* = 9.9, 8.1, 5.6 Hz, 1H). ¹³C NMR (125 MHz, acetone-*d*₆): δ 181.9, 153.0, 147.1 (ddd, *J* = 244.2, 11.1, 2.9 Hz), 147.0 (ddd, *J* = 244.3, 4.1, 2.9 Hz), 145.9, 142.7 (ddd, *J* = 248.3, 15.7, 5.9 Hz), 142.1, 138.2, 137.3 (d, *J* = 1.5 Hz), 136.1 (ddd, *J* = 17.5, 12.9, 2.8 Hz), 135.4, 133.9, 131.6, 131.3, 130.3, 127.1, 125.1, 122.3, 122.1 (ddd, *J* = 15.6, 6.6, 4.1 Hz), 120.9, 120.6 (d, *J* = 1.3 Hz), 120.3 (q, *J* = 259.2 Hz), 117.5, 106.0 (dd, *J* = 21.1, 2.8 Hz). ¹⁹F NMR (470 MHz, acetone-*d*₆): δ –56.4, –76.5 (CF₃TEA), –138.6, –142.0 to –142.3 (m), –152.5 to –153.5 (m). MS (ESI) *t*_R 10.40 min, *m/z*: 574.0 (M + H)⁺, C₂₄H₁₄F₆NO₅S₂⁺ calcd 574.0; HRMS *m/z*: 574.01880 ([M + H]⁺, C₂₄H₁₄F₆NO₅S₂⁺ calcd 574.02121).

4-Bromo-N-[3-[5-(2,4,5-trifluoro-3-hydroxybenzoyl)thiophen-2-yl]phenyl]-2-trifluoromethoxybenzenesulfonamide (16). The title compound was prepared by the reaction of [5-(3-aminophenyl)thiophen-2-yl](2,4,5-trifluoro-3-methoxyphenyl)methanone (**8a**) (260 mg, 0.72 mmol) and 4-bromo-2-trifluoromethoxybenzenesulfonyl chloride (243 mg, 0.72 mmol) according to method C. The crude product was reacted with boron tribromide (3 equiv) according to method D. The product was purified by CC (dichloromethane/methanol 99.5:0.5); yield over two steps: 41% (190 mg); ¹H NMR (500 MHz, acetone-*d*₆): δ 9.97 (s, 1H), 9.61 (s, 1H), 8.03 (d, *J* = 8.5 Hz, 1H), 7.77 (dd, *J* = 8.5, 1.8 Hz, 1H), 7.74 (d, *J* = 1.6 Hz, 1H), 7.67 (dd, *J* = 4.1, 1.8 Hz, 1H), 7.67–7.65 (m, 1H), 7.54 (ddd, *J* = 7.8, 1.8, 1.0 Hz, 1H), 7.52 (d, *J* = 4.1 Hz, 1H), 7.42–7.37 (m, 1H), 7.31 (ddd, *J* = 8.1, 2.2, 1.0 Hz, 1H), 7.12 (ddd, *J* = 9.9, 8.1, 5.6 Hz, 1H); ¹³C NMR (125 MHz, acetone-*d*₆): δ 182.85, 153.86, 148.10 (ddd, *J* = 244.2, 10.9, 3.2 Hz), 148.23–145.93 (m), 146.95 (d, *J* = 1.8 Hz), 143.65 (ddd, *J* = 248.6, 15.8, 5.8 Hz), 143.09, 138.84, 138.25, 138.23, 137.08 (ddd, *J* = 18.3, 12.9, 3.0 Hz), 134.94, 133.83, 131.82, 131.46, 131.32, 129.11, 126.14, 124.91 (d, *J* = 1.9 Hz), 123.53, 123.07 (ddd, *J* = 15.7, 6.8, 3.9 Hz), 122.07, 118.76, 106.96 (dd, *J* = 21.1, 3.0 Hz). MS (ESI) *t*_R 9.70 min, *m/z*: 651.9 (M + H)⁺, C₂₄H₁₃BrF₆NO₅S₂⁺ calcd 651.9; HRMS *m/z*: 651.92902 ([M + H]⁺, C₂₄H₁₃BrF₆NO₅S₂⁺ calcd 651.93172).

Biochemical Assays. Human and mouse 17β-HSD2 preparations were obtained by isolating the microsomal fractions of human placenta and mouse liver homogenates, respectively, according to the described methods.¹⁹ Incubations were run with [³H]-E2 (human: 500 nM; mouse: 10 nM), cofactor NAD⁺, and inhibitor. Human 17β-HSD1 was prepared from the cytosolic fractions of human placenta, whereas recombinant mouse 17β-HSD1 cDNA (Origene, USA) was transiently expressed in HEK293 cells and prepared by ammonium

sulfate precipitation essentially as described for human 17 β -HSD1 preparation.¹⁹ The enzyme preparations were incubated with [³H]-E1 (human: 500 nM; mouse: 10 nM), cofactor, and inhibitor.¹⁹ The separation and measurement of the substrate and product were accomplished by radio-HPLC. The cellular h17 β -HSD2 inhibitory activity was measured using the breast cancer cell line MDA-MB-231 (17 β -HSD1 activity negligible) with 200 nM [³H]-E2 as the substrate and incubated with **15** for 6 h at 37 °C.²⁹ After ether extraction, the substrate and product were separated and measured as described above. ER α /ER β binding affinity assays, and MTT cell viability assays in HEK293 cells, were performed as described previously.^{19,23} The metabolic stabilities in human and mouse liver S9 fractions were determined in the presence of the cofactors NADPH, UDPGA, and PAPS, as described earlier.²³ Aryl hydrocarbon receptor agonist assays were performed as described earlier.²⁸ Agonist activity on the pregnane X receptor and constitutive androstane receptors were performed at CEREP (now Eurofins) in a cofactor recruitment cell-free assay.

Immunohistochemistry. The expression of 17 β -HSD2 in mouse bone was investigated in 6 μ m longitudinal cryosections of C57BL/6 mouse femur fixed in 4% paraformaldehyde. Immunohistochemistry was performed with the rabbit polyclonal antimouse 17 β -HSD2 antibody M-165 (sc-135042; Santa Cruz Biotechnology, Heidelberg, Germany; 1:50 dilution) as the primary antibody and an Alexa 555-conjugated goat antirabbit IgG (Thermo Fisher, Kandel, Germany; 1:200 dilution) as the secondary antibody. Negative control represents incubation with secondary antibody only. The cell nuclei were stained with 4',6-diamidino-2-phenylindole.

Western Blot Analysis of Biomarkers in Callus Protein. The expression of OPG and RANKL in callus was analyzed in five animals per group after 28 days of treatment following sodium dodecyl sulfate polyacrylamide gel electrophoresis and western blotting using rabbit polyclonal antimouse OPG (1:100, Santa Cruz Biotechnology Inc.) and rabbit polyclonal antimouse RANKL (1:100, Abcam, Cambridge, UK), as described in detail previously.²³ The signals were densitometrically assessed and normalized to β -actin signals to correct for unequal loading.²³ Comparison between the groups was performed using the Student's *t* test. *P* values were calculated using GraphPad Prism QuickCalcs.

E2 and T Plasma Analysis. To determine the effect of 17 β -HSD2 inhibition on the plasma levels of E2 and T, at day 28 after fracture, 100 μ L of plasma was collected from the vena cava for the determination of the plasma levels of E2 and T by ELISA after the extraction of the steroids from the plasma, according to the manufacturer's protocol (DRG, Marburg, Germany).

Animal Procedures. All animal experiments in C57BL/6 mice were approved by the local governmental animal care committee and were conducted in accordance with the European legislation on protection of animals and the NIH Guidelines for the Care and Use of Laboratory Animals (NIH Publication #85-23 Rev. 1985). Experiments were conducted on mature C57BL/6 mice (body weight 27 \pm 3 g, mean \pm SD).

Mouse Subcutaneous Pharmacokinetics. Compound **15** was subcutaneously administered at a dose of 50 mg/kg body weight per animal (*n* = 3). Thirty minutes before administration, suspensions of **15** were freshly prepared in an ultrasonic water bath for 10 minutes. Before the application of the suspension (4 mL/kg body weight), female C57BL/6 mice were anesthetized with 2% isoflurane. At 2, 18, and 24 h, blood samples of 50 μ L were taken from the tail vein and collected in 0.2 mL Eppendorf tubes containing 5 μ L of 106 mM sodium citrate buffer as an anticoagulant. After centrifugation at 5000 rpm at 4 °C, the plasma samples were immediately frozen at -20 °C, and within 24 h, all were stored at -80 °C. For bioanalysis, the plasma samples were thawed, and 10 μ L of plasma was added to 50 μ L of acetonitrile containing diphenhydramine (500 nM) as the internal standard. The samples and calibration standards (in mouse plasma) were centrifuged at 15 000 rpm for 5 min at 4 °C. The solutions were transferred to fresh vials for HPLC-MS/MS analysis (Accucore RP-MS, TSQ Quantum triple quadrupole mass spectrometer, ESI interface). After injection of 10 μ L (performed in duplicate), the

data were analyzed based on the ratio of the peak areas of compound **15** and the internal standard. The detection limit of **15** in plasma was 1.2 nM. In the bone fracture study, the plasma level of **15** was also determined in nine animals at day 28 of treatment (i.e., 24 h after the last dosing at day 27), at sacrifice under anesthetics: the plasma levels of **15** were 498 \pm 81 nM (mean \pm SEM).

Surgical Procedures. Male mice were anesthetized by an intraperitoneal injection of xylazine (15 mg/kg body weight) and ketamine (75 mg/kg body weight) before fracture and surgery. The surgical procedure was performed as described in detail earlier.²³ For analgesia, the mice received tramadol hydrochloride in the drinking water (2.5 mg/100 mL) from day 1 before surgery until day 3 after surgery. The suspensions of **15** in vehicle were made fresh each time during the treatment period of 14 or 28 days. A treatment period of 28 days was chosen because this period covers the most critical (and sensitive) phases in bone fracture healing (i.e., initial inflammation because of tissue injury, callus formation, neovascularization, restoration of bending stiffness, and start of bone remodeling).

Histomorphometrical Analysis. To determine the influence of **15** on the course of bone healing, histomorphometric analysis of the callus was performed at 14 and 28 days of fracture healing after resection of the healed femora and removal of the implant, fixation of the femur in formaldehyde, bone decalcification in ethylenediaminetetraacetic acid, trichrome staining (Masson–Goldner), and light microscopy according to the nomenclature and units of the recommendations of the American Society of Bone and Mineral Research (ASBMR), as described in detail previously.¹⁵

Biomechanical Analysis. For biomechanical analysis, the resected femora were freed from the soft tissue. After removing the implants, the bending stiffness of the callus was measured with a nondestructive bending test using a 3-point bending device, as described in detail previously.¹⁵ To account for the differences in bone stiffness of the individual animals, the nonfractured femora were also analyzed, serving as internal control. All values of the fractured femora are given as percentage of the corresponding nonfractured femora.

Radiological Analysis. At the end of the bone healing period of 14 and 28 days, the complete callus area of the fractured femurs was analyzed using a high-resolution micro-CT imaging system, as described in detail previously.²³ By this method, the following parameters were determined: tissue volume, bone volume, the ratio of bone volume to tissue volume, trabecular thickness, trabecular number, and trabecular separation.

■ ASSOCIATED CONTENT

● Supporting Information

The Supporting Information is available free of charge on the ACS Publications website at DOI: 10.1021/acs.jmedchem.8b01493.

Synthesis of intermediates **2b**, **4b–8b**, and **2a–8a**; NMR spectra, HRMS, and LC–MS of compounds **1–16**, **8a**, and **8b**; and additional biological results of **15** (immunofluorescence microscopy of 17 β -HSD2 expression in mouse cortical bone; ; E2 and T plasma analysis; histomorphometrical, biomechanical, and radiological bone analysis; body, liver, seminal vesicles, testicles weights) (PDF)

Molecular formula strings of all final compounds (CSV)

■ AUTHOR INFORMATION

Corresponding Author

*E-mail: vankoppen@elezopharm.de. Phone: +49 681 910 2893.

ORCID

Ahmed S. Abdelsamie: 0000-0002-5326-4400

Mohamed Salah: 0000-0002-9535-6741

Sandrine Marchais-Oberwinkler: 0000-0001-9941-7233

Martin Frotscher: 0000-0003-1777-8890

Rolf W. Hartmann: 0000-0002-5871-5231

Chris J. van Koppen: 0000-0003-2799-6728

Author Contributions

○A.S.A. and S.H. contributed equally to the work.

Notes

The authors declare the following competing financial interest(s): The authors: Ahmed S. Abdelsamie, Carsten Börger, Lorenz Siebenbürger, Sandrine Marchais-Oberwinkler, Martin Frotscher, Rolf W. Hartmann and Chris J. van Koppen are inventors of a patent application, which covers the respective compound class. ElexoPharm GmbH is the owner of this patent application. Rolf W. Hartmann is the CEO of ElexoPharm GmbH. Chris van Koppen is an employee of ElexoPharm GmbH.

ACKNOWLEDGMENTS

This research was supported by a KMU-innovativ-12 grant of the Bundesministerium für Bildung und Forschung (031A467). We thank Janine Becker and Julia Parakening for excellent technical assistance.

ABBREVIATIONS

E2, estradiol; ER, estrogen receptor; *h*, human; *m*, mouse; T testosterone17 β -HSD, testosterone17 β -HSD17 β -hydroxysteroid dehydrogenase

REFERENCES

- (1) Brunton, L. L.; Chabner, B. A.; Knollmann, B. C. *Goodman & Gilman. The Pharmacological Basis of Therapeutics*, 13th Edition; McGraw-Hill: New York, 2017.
- (2) Edwards, J.; Moore, R. A. Finasteride in the treatment of clinical benign prostatic hyperplasia: a systematic review of randomised trials. *BMC Urol.* **2002**, *2*, 14.
- (3) Hermanowski-Vosatka, A.; Balkovec, J. M.; Cheng, K.; Chen, H. Y.; Hernandez, M.; Koo, G. C.; Le Grand, C. B.; Li, Z.; Metzger, J. M.; Mundt, S. S.; Noonan, H.; Nunes, C. N.; Olson, S. H.; Pikounis, B.; Ren, N.; Robertson, N.; Schaeffer, J. M.; Shah, K.; Springer, M. S.; Strack, A. M.; Strowski, M.; Wu, K.; Wu, T.; Xiao, J.; Zhang, B. B.; Wright, S. D.; Thieringer, R. 11 β -HSD1 inhibition ameliorates metabolic syndrome and prevents progression of atherosclerosis in mice. *J. Exp. Med.* **2005**, *202*, 517–527.
- (4) Saloniemi, T.; Järvensivu, P.; Koskimies, P.; Jokela, H.; Lamminen, T.; Ghaem-Maghami, S.; Dina, R.; Damdimopoulou, P.; Mäkelä, S.; Perheentupa, A.; Kujari, H.; Brosens, J.; Poutanen, M. Novel Hydroxysteroid (17 β) Dehydrogenase 1 Inhibitors Reverse Estrogen-Induced Endometrial Hyperplasia in Transgenic Mice. *Am. J. Pathol.* **2010**, *176*, 1443–1451.
- (5) Aspenberg, P.; Genant, H. K.; Johansson, T.; Nino, A. J.; See, K.; Krohn, K.; García-Hernández, P. A.; Recknor, C. P.; Einhorn, T. A.; Dalsky, G. P.; Mitlak, B. H.; Fierlinger, A.; Lakshmanan, M. C. Teriparatide for acceleration of fracture repair in humans: a prospective, randomized, double-blind study of 102 postmenopausal women with distal radial fractures. *J. Bone Miner. Res.* **2010**, *25*, 404–414.
- (6) Fujita, N.; Matsushita, T.; Ishida, K.; Sasaki, K.; Kubo, S.; Matsumoto, T.; Kurosaka, Y.; Tabata, Y.; Kuroda, R. An analysis of bone regeneration at a segmental bone defect by controlled release of bone morphogenetic protein 2 from a biodegradable sponge composed of gelatin and β -tricalcium phosphate. *J. Tissue Eng. Regen. Med.* **2012**, *6*, 291–298.
- (7) Woo, E. J. Adverse events after recombinant human BMP2 in nonspinal orthopaedic procedures. *Clin. Orthop. Relat. Res.* **2013**, *471*, 1707–1711.
- (8) Bhandari, M.; Jin, L.; See, K.; Burge, R.; Gilchrist, N.; Witvrouw, R.; Krohn, K. D.; Warner, M. R.; Ahmad, Q. I.; Mitlak, B. Does teriparatide improve femoral neck fracture healing: results from a randomized placebo-controlled trial. *Clin. Orthop. Relat. Res.* **2016**, *474*, 1234–1244.
- (9) Wu, L.; Einstein, M.; Geissler, W. M.; Chan, H. K.; Elliston, K. O.; Andersson, S. Expression cloning and characterization of human 17 beta-hydroxysteroid dehydrogenase type 2, a microsomal enzyme possessing 20 alpha-hydroxysteroid dehydrogenase activity. *J. Biol. Chem.* **1993**, *268*, 12964–12969.
- (10) Lu, M.-L.; Huang, Y.-W.; Lin, S.-X. Purification, Reconstitution, and Steady-state Kinetics of the Trans-membrane 17 β -Hydroxysteroid Dehydrogenase 2. *J. Biol. Chem.* **2002**, *277*, 22123–22130.
- (11) Vanderschueren, D.; Vandenput, L.; Boonen, S.; Lindberg, M. K.; Bouillon, R.; Ohlsson, C. Androgens and bone. *Endocr. Rev.* **2004**, *25*, 389–425.
- (12) Purohit, A.; Flanagan, A. M.; Reed, M. J. Estrogen synthesis by osteoblast cell lines. *Endocrinology* **1992**, *131*, 2027–2029.
- (13) Janssen, J. M. M. F.; Bland, R.; Hewison, M.; Coughtrie, M. W. H.; Sharp, S.; Arts, J.; Pols, H. A. P.; van Leeuwen, J. P. T. M. Estradiol formation by human osteoblasts via multiple pathways: relation with osteoblast function. *J. Cell. Biochem.* **1999**, *75*, 528–537.
- (14) Dong, Y.; Qiu, Q. Q.; Debeer, J.; Lathrop, W. F.; Bertolini, D. R.; Tamburini, P. P. 17 β -hydroxysteroid dehydrogenases in human bone cells. *J. Bone Miner. Res.* **1998**, *13*, 1539–1546.
- (15) Bagi, C. M.; Wood, J.; Wilkie, D.; Dixon, B. Effect of 17beta-hydroxysteroid dehydrogenase type 2 inhibitor on bone strength in ovariectomized cynomolgus monkeys. *J. Musculoskelet. Neuronal Interact.* **2008**, *8*, 267–280.
- (16) Holstein, J. H.; Matthys, R.; Histing, T.; Becker, S. C.; Fiedler, M.; Garcia, P.; Meier, C.; Pohlemann, T.; Menger, M. D. Development of a Stable Closed Femoral Fracture Model in Mice. *J. Surg. Res.* **2009**, *153*, 71–75.
- (17) Milewich, L.; Garcia, R. L.; Gerrity, L. W. 17 β -Hydroxysteroid oxidoreductase: A ubiquitous enzyme. Interconversion of estrone and estradiol-17 β in mouse tissues. *Metabolism* **1985**, *34*, 938–944.
- (18) Abdelsamie, A. S.; Bey, E.; Gargano, E. M.; van Koppen, C. J.; Empting, M.; Frotscher, M. Towards the evaluation in an animal disease model: Fluorinated 17 β -HSD1 inhibitors showing strong activity towards both the human and the rat enzyme. *Eur. J. Med. Chem.* **2015**, *103*, 56–68.
- (19) Abdelsamie, A. S.; Bey, E.; Hanke, N.; Empting, M.; Hartmann, R. W.; Frotscher, M. Inhibition of 17 β -HSD1: SAR of bicyclic substituted hydroxyphenylmethanones and discovery of new potent inhibitors with thioether linker. *Eur. J. Med. Chem.* **2014**, *82*, 394–406.
- (20) Miettinen, M. M.; Mustonen, M. V. J.; Poutanen, M. H.; Isomaa, V. V.; Vihko, R. K. Human 17 β -hydroxysteroid dehydrogenase type 1 and type 2 isoenzymes have opposite activities in cultured cells and characteristic cell- and tissue-specific expression. *Biochem. J.* **1996**, *314*, 839–845.
- (21) Speirs, V.; Green, A. R.; Atkin, S. L. Activity and gene expression of 17 β -hydroxysteroid dehydrogenase type I in primary cultures of epithelial and stromal cells derived from normal and tumorous human breast tissue: the role of IL-8. *J. Steroid Biochem. Mol. Biol.* **1998**, *67*, 267–274.
- (22) Huhtinen, K.; Desai, R.; Stähle, M.; Salminen, A.; Handelsman, D. J.; Perheentupa, A.; Poutanen, M. Endometrial and endometriotic concentrations of estrone and estradiol are determined by local metabolism rather than circulating levels. *J. Clin. Endocrinol. Metab.* **2012**, *97*, 4228–4235.
- (23) Abdelsamie, A. S.; van Koppen, C. J.; Bey, E.; Salah, M.; Börger, C.; Siebenbürger, L.; Laschke, M. W.; Menger, M. D.; Frotscher, M. Treatment of estrogen-dependent diseases: Design, synthesis and profiling of a selective 17 β -HSD1 inhibitor with sub-nanomolar IC 50 for a proof-of-principle study. *Eur. J. Med. Chem.* **2017**, *127*, 944–957.
- (24) Histing, T.; Andonyan, A.; Klein, M.; Scheuer, C.; Stenger, D.; Holstein, J. H.; Veith, N. T.; Pohlemann, T.; Menger, M. D. Obesity

does not affect the healing of femur fractures in mice. *Injury* **2016**, *47*, 1435–1444.

(25) Histing, T.; Stenger, D.; Scheuer, C.; Metzger, W.; Garcia, P.; Holstein, J. H.; Klein, M.; Pohlemann, T.; Menger, M. D. Pantoprazole, a proton pump inhibitor, delays fracture healing in mice. *Calcif. Tissue Int.* **2012**, *90*, 507–514.

(26) Bord, S.; Ireland, D. C.; Beavan, S. R.; Compston, J. E. The effects of estrogen on osteoprotegerin, RANKL, and estrogen receptor expression in human osteoblasts. *Bone* **2003**, *32*, 136–141.

(27) Rivero-Müller, A.; Chou, Y.-Y.; Ji, I.; Lajic, S.; Hanyaloglu, A. C.; Jonas, K.; Rahman, N.; Ji, T. H.; Huhtaniemi, I. Rescue of defective G protein-coupled receptor function in vivo by intermolecular cooperation. *Proc. Natl. Acad. Sci. U.S.A.* **2010**, *107*, 2319–2324.

(28) Emmerich, J.; van Koppen, C. J.; Burkhart, J. L.; Hu, Q.; Siebenbürger, L.; Boerger, C.; Scheuer, C.; Laschke, M. W.; Menger, M. D.; Hartmann, R. W. Lead optimization generates CYP11B1 inhibitors of pyridylmethyl isoxazole type with improved pharmacological profile for the treatment of Cushing's disease. *J. Med. Chem.* **2017**, *60*, 5086–5098.

(29) Gargano, E. M.; Allegretta, G.; Perspicace, E.; Carotti, A.; Van Koppen, C.; Frotscher, M.; Marchais-Oberwinkler, S.; Hartmann, R. W. 17 β -Hydroxysteroid Dehydrogenase Type 2 Inhibition: Discovery of Selective and Metabolically Stable Compounds Inhibiting Both the Human Enzyme and Its Murine Ortholog. *PLoS One* **2015**, *10*, No. e0134754.

3.2.III First Structure Activity Relationship of 17 β -Hydroxysteroid Dehydrogenase Type 14 Nonsteroidal Inhibitors and Crystal Structures in Complex with the Enzyme

Florian Braun, Nicole Bertolotti, Gabriele Möller, Jerzy Adamski, Torsten Steinmetzer, **Mohamed Salah**, Ahmed S. Abdelsamie, Chris J. van Koppen, Andreas Heine, Gerhard Klebe, and Sandrine Marchais-Oberwinkler

Reprinted with permission *J. Med. Chem.* 2016, 59 (23), 10719–10737.

DOI: 10.1021/acs.jmedchem.6b01436

Copyright (2016) American Chemical Society

Publication E

Contribution Report

The author planned, performed and interpreted the radiolabeled biological assays. Additionally, he contributed in writing the manuscript.

First Structure–Activity Relationship of 17 β -Hydroxysteroid Dehydrogenase Type 14 Nonsteroidal Inhibitors and Crystal Structures in Complex with the Enzyme

Florian Braun,^{†,Δ} Nicole Bertoletti,^{†,Δ} Gabriele Möller,[‡] Jerzy Adamski,^{‡,§,||} Torsten Steinmetzer,[†] Mohamed Salah,[⊥] Ahmed S. Abdelsamie,^{⊥,#} Chris J. van Koppen,[⊥] Andreas Heine,[†] Gerhard Klebe,^{†,⊙} and Sandrine Marchais-Oberwinkler^{*,†,⊙}

[†]Institute for Pharmaceutical Chemistry, Philipps University Marburg, Marbacher Weg 6, 35032 Marburg, Germany

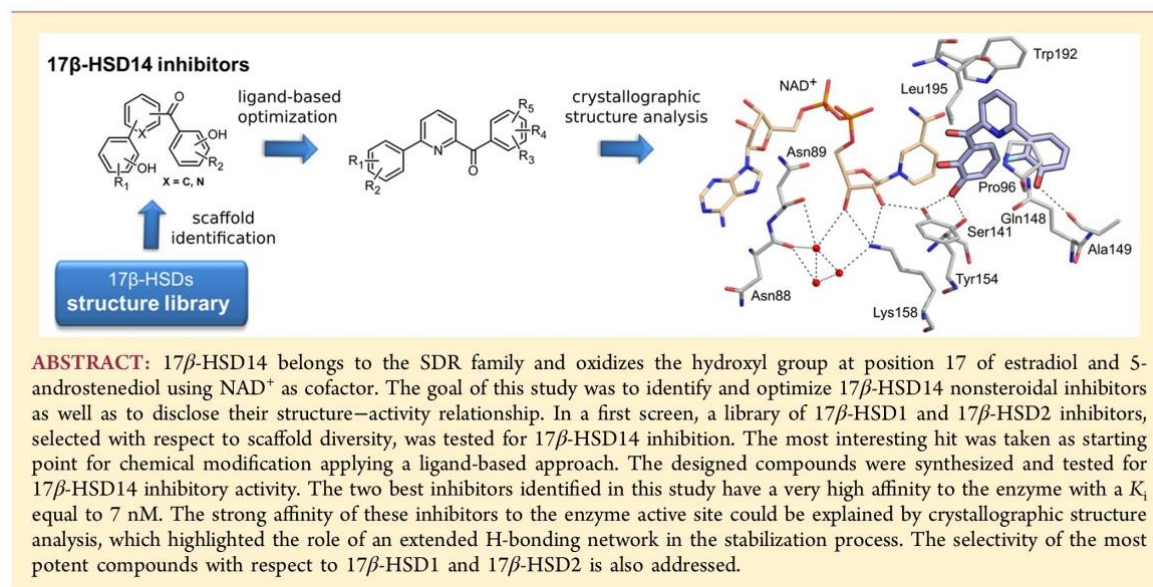
[‡]Genome Analysis Center, Institute of Experimental Genetics, German Research Center for Environmental Health, Helmholtz Zentrum München, 85764 Neuherberg, Germany

[§]Chair of Experimental Genetics, Technical University Munich, 85350 Freising-Weihenstephan, Germany

^{||}German Center for Diabetes Research (DZD), 85764 Neuherberg, Germany

[⊥]ElexoPharm GmbH, Campus A1.2, 66123 Saarbrücken, Germany

S Supporting Information



INTRODUCTION

Human 17 β -hydroxysteroid dehydrogenase type 14 (17 β -HSD14), also called DHRS10 and retSDR3, is an oxidoreductase belonging to the short-chain dehydrogenase-reductase (SDR) family.^{1,2} In vitro, the enzyme oxidizes the hydroxyl group at position 17 of estradiol (E2) and 5-androsten-3 β ,17 β -diol (S-diol) in the presence of the cofactor NAD⁺, however, in vivo, its natural substrate is still unknown.

While Sivik et al.³ described a broad distribution pattern of 17 β -HSD14 across various tissues based on immunohistochemistry studies, Northern blotting experiments showed that the enzyme is predominantly expressed in the brain, liver, and

placenta² as well as in the kidney.⁴ Furthermore, immunofluorescence studies revealed cytosolic localization.²

To understand the function of 17 β -HSD14, the enzyme needs to be further characterized. Inhibitors are useful chemical tools, which can be used not only to characterize the binding site of an enzyme but also to get insight into the physiological role of the latter upon in vivo administration. With the exception of compound 1, which we recently presented,⁵ no inhibitor has been reported for this enzyme.

Received: September 27, 2016

Published: November 9, 2016

The crystal structure of the human 17β -HSD14 has been determined recently as the holo protein (PDB 5JS6 and 5JSF) and as the ternary complex with the nonsteroidal inhibitor **1** (PDB 5ICM). 17β -HSD14 is a tetramer.⁵ The binding cavity was shown to be rather lipophilic with a conical shape. The substrate active site is narrow in the vicinity of the catalytic triad and is solvent exposed at the other end. Tyr253' from the C-terminal chain of the adjacent unit in the tetramer reduces the size of the active site.

Up to now, 14 different 17β -HSD subtypes have been reported.⁶ 17β -HSD1 and 17β -HSD2, the two best characterized subtypes, predominantly catalyze the oxidation and reduction of estrogens and androgens. Inhibitors of these two enzymes have already been reported.^{7–20} While 17β -HSD1 is a cytosolic enzyme and shows a reductive activity in vivo (activation of estrogens), 17β -HSD2 is membrane-bound and catalyzes the oxidation of estrogens and androgens to their less potent analogues similarly to 17β -HSD14. However, 17β -HSD2 and 17β -HSD14 differ in their tissue distribution pattern because, contrary to 17β -HSD14, 17β -HSD2 is not present in the human brain temporal lobe.²¹ The presence of 17β -HSD14 in the brain might indicate that this enzyme is involved in the regulation of active estrogens and androgens in this organ.²

The goal of this work was to identify 17β -HSD14 nonsteroidal inhibitors and to optimize their structures, which led to highly active compounds. The inhibitor optimization was performed following a ligand-based approach. The synthesis and biological evaluation of highly active compounds with a nonsteroidal scaffold together with four new crystal structures of the ternary complexes are reported. Analysis of the crystal structures of the ternary complexes revealed the location of the inhibitor binding sites as well as the resulting protein–inhibitor interactions and a complex pattern of hydrogen bonds (H-bonds) contributing to the strong affinity of these compounds to the enzyme. The physicochemical properties of the new inhibitors as well as selectivity considerations were also addressed.

RESULTS

Design of 17β -HSD14 Inhibitor Candidates. Although 17β -HSDs belong to the same superfamily, they share a low overall sequence identity. Nonetheless, considering the fact that 17β -HSD1 and 17β -HSD2 catalyze the same reaction as 17β -HSD14, the substrate binding site of the three enzymes should exhibit a high structural similarity. On the basis of this idea, it was assumed that some inhibitors developed for 17β -HSD1 and 17β -HSD2 should also bind to 17β -HSD14 and that a common scaffold could be used as starting point to optimize them for 17β -HSD14 binding. In a first screen, a small library of 34 17β -HSD1 and 17β -HSD2 inhibitors, chosen on the basis of structural diversity (Figure 1), was tested for 17β -HSD14 inhibitory activity using a radioactive displacement assay. This assay was performed with the recombinantly expressed enzyme in a bacterial suspension because the pure protein was not available at that time. Thereby sets of active and inactive compounds were identified.

While the series of tested naphthalenes **A** and thiophene amides **B** contained mostly inactive compounds, the dihydroxyphenylbenzenes **C**, -thiophenes and -thiazoles **D** showed examples of low to moderate inhibitory activity against 17β -HSD14 (between 10% and 45% inhibition at 1 μ M). In addition, some of the latter derivatives were also reported to possess very high potency for 17β -HSD1 and/or 17β -HSD2

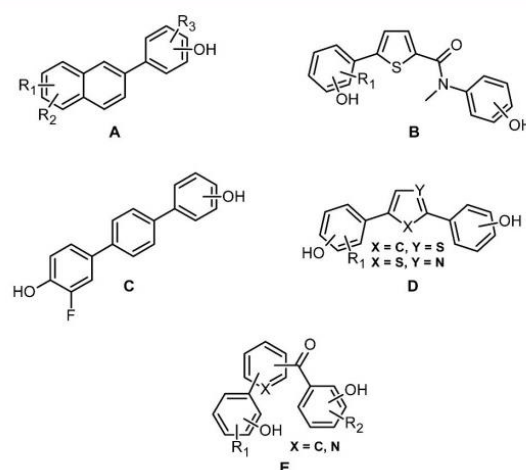


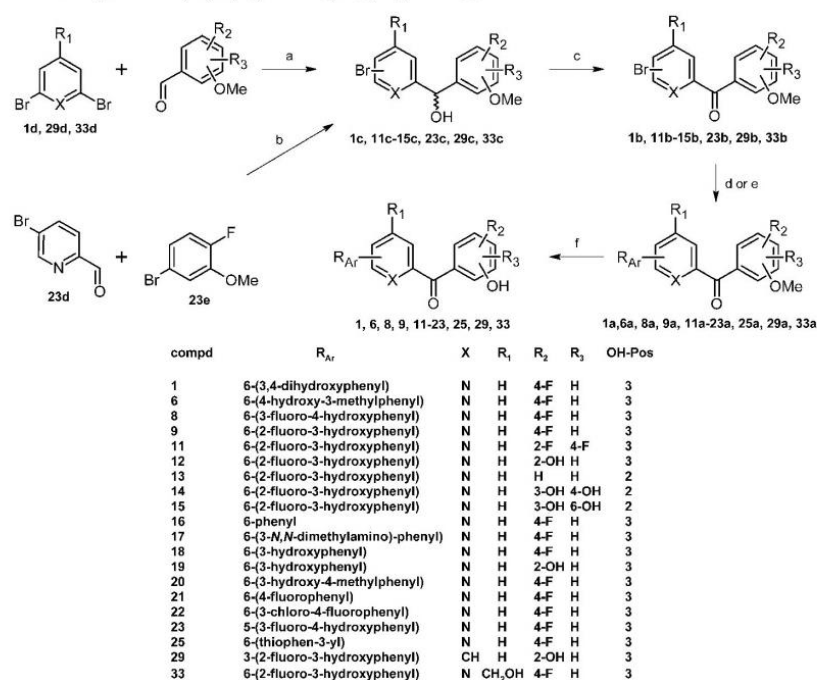
Figure 1. Scaffold of inhibitors from a 17β -HSD1 and 17β -HSD2 library tested for 17β -HSD14 inhibitory activity.

(IC₅₀ in the low nM range), which might lead to difficulties achieving high selectivity for 17β -HSD14. These parent scaffolds were therefore not considered for further optimization. Some members of the pyridine ketone class **E** also showed remarkable inhibitory activity for 17β -HSD14, paralleled by rather low or moderate activity against 17β -HSD1 (Table 1, compound 2), which rendered this class as promising scaffold for further investigations. They were therefore chosen as a starting point for the development of new 17β -HSD14 inhibitors.

Table 1. Most Interesting Compounds Identified in a First Screen

| compd | inhibition of 17β -HSD14 % Inh @ 1 μ M ^a | inhibition of 17β -HSD1 IC ₅₀ (μ M) ^b | inhibition of 17β -HSD2 IC ₅₀ (μ M) ^c |
|-------|---|--|--|
| 2 | 62% | 1.27 | 0.10 |
| 3 | 0% | 5.48 | 0.26 |
| 4 | 19% | 0.29 | 0.04 |
| 5 | 32% | 19.65 | 0.26 |

^aRecombinant 17β -HSD14 enzyme, bacterial suspension, substrate [³H]-E2 [18.3 nM], NAD⁺ [7.5 mM], mean value of three determinations; standard deviation <10%. ^bPlacental 17β -HSD1 enzyme, cytosolic fraction, substrate [³H]-E1 + E1 [500 nM], NADH [0.5 mM], mean value of at least three determinations; standard deviation <20%. ^cPlacental 17β -HSD2 enzyme, microsomal fraction, substrate [³H]-E2 + E2 [500 nM], NAD⁺ [1.5 mM], mean value of at least three determinations; standard deviation <20%.

Scheme 1. Synthesis of Compounds 1, 6, 8, 9, 11–23, 25, 29, and 33^a

^aReagents and conditions: (a) *n*-BuLi, anhydrous THF, −80 °C to room temperature, 1 h; (b) Mg, anhydrous THF, 60 °C, 2 h, 80 °C, 5 h; (c) 2-iodoxybenzoic acid, anhydrous THF, 60 °C, 2–4 h; (d) Cs₂CO₃, Pd(PPh₃)₄, R_{Ar}B(OH)₂, DME/water (2:1), 80 °C, overnight, for compounds 1a, 6a, 8a, 9a, 12a–15a, 17a–20a, 22a, 23a, 25a, 29a, and 33a; (e) Na₂CO₃, Pd(PPh₃)₄, R_{Ar}B(OH)₂, DME/water (2:1), microwave irradiation (60 min, 150 W, 150 °C), for compounds 11a, 16a, and 21a; (f) BBr₃, CH₂Cl₂, −80 °C to room temperature, overnight.

The most interesting hits identified in the preliminary screen are listed in Table 1. The compounds can be categorized into 2,5-(2,3) and 2,6-substituted (5) pyridine ketones and the 1,4-substituted phenyl (4). In the 2,5-compound class, 2 and 3 (62% inhibition at 1 μM vs 0%) differ by the presence/absence of a fluorine atom in *ortho* position to the OH group of the C-ring, suggesting the importance of this atom for inhibitory activity. Furthermore, comparison of 2 with 4 (62% inhibition at 1 μM vs 19%) shows that the pyridine core B is more potent than the phenyl analogue, pointing toward the importance of the nitrogen atom in the B-ring for activity. Concerning the 2,6-compound class, comparison of 5 with 2,5-substituted 3 (32% inhibition at 1 μM vs 0%) shows that moving the A-ring from 5- to 6-position leads to a gain in activity.

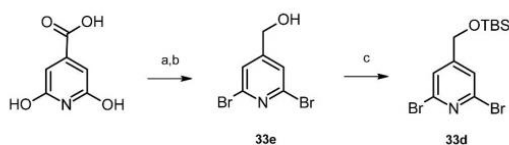
Furthermore, considering the selectivity aspect, the poor inhibitory activity of the 2,6-substituted 5 toward 17β-HSD1 (IC₅₀ = 19.65 μM), compared to the 2,5-substituted analogue 3 (IC₅₀ = 5.48 μM) suggests that the 2,6-substitution pattern might improve selectivity for 17β-HSD14 over 17β-HSD1. Selectivity against 17β-HSD2 does not become obvious with the set of studied test compounds. Consequently, the 2,6-pyridine ketone class was selected for optimization and the derivatives, with modification at the A-ring as well as at the C-ring by substituents with different properties were synthesized. Special attention was paid to the physicochemical properties of the designed compounds in order to focus on compounds which should have a promising bioavailability profile according to the Veber Rules²² and the Lipinski Rules of 5.²³

Chemistry. The synthesis of compounds 1, 6, 8, 9, 11–23, 25, 29, and 33 was achieved in four steps starting from the

dibromopyridine derivatives 1d and 33d and analogous benzene 29d, respectively (Scheme 1). Lithiation with *n*-butyl lithium²⁴ and nucleophilic addition to the appropriate aldehyde provided the alcohol intermediates 1c, 11c–15c, 29c, and 33c. For the synthesis of compound 23 (Scheme 1), aryl bromide 23e was used to prepare the corresponding Grignard reagent. Nucleophilic addition to the carbaldehyde 23d afforded the alcohol intermediate 23c. Oxidation with 2-iodoxybenzoic acid resulted in the corresponding ketones 1b, 11b–15b, 23b, 29b, and 33b. Subsequently, Suzuki couplings²⁵ with different arylboronic acids afforded compounds 1a, 6a, 8a, 9a, 11a–23a, 25a, 29a, and 33a using either standard conditions (Cs₂CO₃, 80 °C, overnight) or microwave irradiations (Na₂CO₃, 150 °C, 60 min, 150 W). Cleavage of the methoxy groups with boron tribromide gave the final compounds 1, 6, 8, 9, 11–23, 25, 29, and 33.

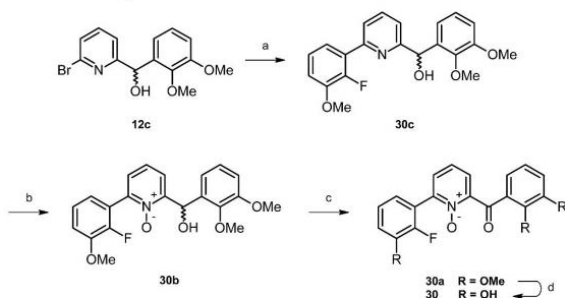
The precursor 33d was prepared starting from citrazinic acid, which was first brominated with commercial phosphorus oxybromide and then reacted with methanol. Reduction of the formed ester²⁶ and protection of the primary alcohol 33e with TBSCl afforded compound 33d (Scheme 2).

The synthesis of the pyridine *N*-oxide 30 was achieved in four steps starting from the previously described alcohol intermediate 12c. The Suzuki coupling reaction with 2-fluoro-3-methoxyphenylboronic acid under standard conditions afforded compound 30c. Oxidation into the pyridine *N*-oxide 30b was performed by means of *meta*-chloroperoxybenzoic acid and further oxidation with 2-iodoxybenzoic acid, resulting in ketone 30a. Cleavage of the methoxy groups with boron trifluoride

Scheme 2. Synthesis of Precursor 33d^a

^aReagents and conditions: (a) (i) POBr₃, 130 °C, 0.5 h, 150 °C, 1.5 h, (ii) MeOH, room temperature, overnight; (b) NaBH₄, EtOH, 85 °C, 3 h; (c) TBSCl, imidazole, DMF, room temperature, 18 h.

dimethylsulfide complex afforded the final pyridine *N*-oxide 30 (Scheme 3).

Scheme 3. Synthesis of *N*-oxide 30^a

^aReagents and conditions: (a) Cs₂CO₃, Pd(PPh₃)₄, 2-fluoro-3-methoxyphenylboronic acid, DME/water (2:1), 80 °C, overnight; (b) *m*-CPBA (77%), CH₂Cl₂, 0 °C to room temperature, overnight; (c) 2-iodoxybenzoic acid, anhydrous THF, 60 °C, 2 h; (d) BF₃·SMe₂, CH₂Cl₂, room temperature, overnight.

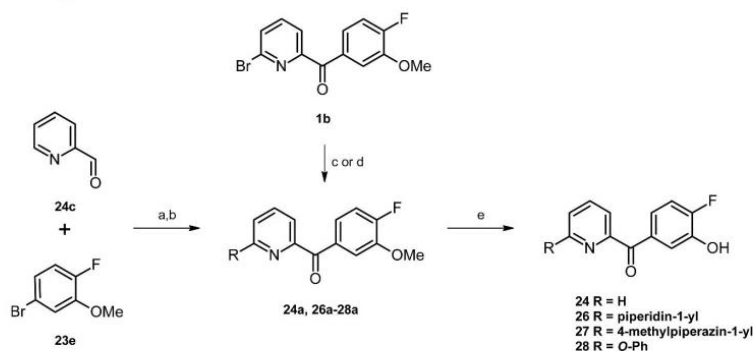
The synthesis of compound 24, lacking the A-ring, was performed by coupling of the pyridine carbaldehyde 24c with the aryl bromide 23e followed by the oxidation to ketone 24a as previously described (Scheme 4). The synthesis of compounds 26 and 27 was realized by amination of 1b with different nonaromatic *N*-heterocycles following the procedure described by Bollinger et al.²⁷ to obtain compounds 26a and 27a. Compound 28, with the A-ring linked via an ether bridge to the pyridine moiety, was synthesized by reacting the 6-

bromopyridine derivative 1b in a copper-catalyzed *O*-arylation using picolinic acid as ligand,²⁸ resulting in compound 28a. All methoxy groups were cleaved with boron tribromide to provide compounds 24 and 26–28 (Scheme 4).

The synthesis of the trisubstituted C-ring derivative 10 was achieved in four steps starting from the 6-bromopyridine-2-carbaldehyde 10d (Scheme 5). Suzuki coupling with 2-fluoro-3-methoxyphenylboronic acid afforded the 6-substituted carbaldehyde 10c. Nucleophilic addition of the in situ formed Grignard reagent of aryl bromide 10e, oxidation of the formed alcohol with 2-iodoxybenzoic acid, and cleavage of the methoxy groups with boron tribromide resulted in the desired compound 10.

The aryl bromide 10e was obtained following a three-step procedure starting from 2-bromo-5-fluorophenol 10h. First, a modified Casiraghi-formylation reaction using paraformaldehyde in the presence of magnesium chloride and triethylamine gave the intermediate 10g.²⁹ Subsequent Dakin reaction with hydrogen peroxide and sodium hydroxide³⁰ followed by protection of the formed dihydroxy compound 10f with methyl iodide afforded compound 10e.

The synthesis of trisubstituted pyridines 31 and 32 was achieved in seven and eight steps, respectively, starting from compound 10d (Scheme 5). Protection of the aldehyde group with trimethyl orthoformate gave the 2-dimethoxy derivative 31f. Iodination with lithium diisopropylamide and iodine³¹ afforded the 5-iodo-6-bromo derivative 31e in moderate yield. For compound 31, subsequent Suzuki coupling with 2.4 equiv of 4-methoxy-3-methylphenylboronic acid provided the 5,6-bisubstituted pyridine 31d. The reaction with 2-fluoro-3-methoxyphenylboronic acid resulted, under the same conditions, selectively in the monocoupled derivative 32e, still brominated in 6-position. Further, a second Suzuki coupling with 4-methoxy-3-methylphenylboronic acid performed on 32e yielded the asymmetric pyridine 32d. Both, 31d and 32d were deprotected with acetic acid to form the aldehydes 31c and 32c. For 31, a nucleophilic reaction with the in situ formed Grignard reagent of compound 23e resulted in the alcohol intermediate 31b. For 32, the corresponding alcohol 32b was obtained after lithiation of aryl bromide 23e with butyl lithium and subsequent nucleophilic reaction. Oxidation with 2-iodoxybenzoic acid and ether cleavage with boron tribromide gave the final compounds 31 and 32.

Scheme 4. Synthesis of Compounds 24 and 26–28^a

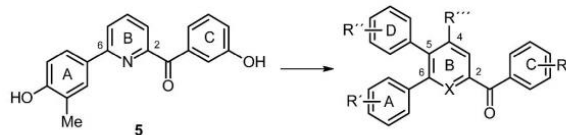
^aReagents and conditions: (a) Mg, anhydrous THF, 60 °C, 2 h, 80 °C, 5 h; (b) 2-iodoxybenzoic acid, anhydrous THF, 60 °C, 3–4 h; (c) *N*-heterocycles, K₃PO₄, 1,4-dioxane, 100 °C, 2–4 d, for compounds 26a and 27a; (d) Cu(I)I, picolinic acid, K₃PO₄, DMSO, 80 °C, 3 d, for compound 28a; (e) BBr₃, CH₂Cl₂, –80 °C to room temperature, overnight.

[illegible]

17 β -HSD14 Inhibitory Activity. Starting from the hit pyridine ketone **5**, modifications were undertaken at the C-ring and A-ring by introduction of different substituents (R, R', Chart 1). These substituents were selected to represent different electronic properties: electron donating or electron withdrawing, H-bond donor, H-bond acceptor, lipophilic, and

hydrophilic. Changes were also performed at the central B-ring by replacement of the nitrogen by a carbon or a N-oxide moiety. An additional phenyl ring (D) with various substituents (R'') were introduced in 5-position as well as a hydroxymethyl group (R''') in 4-position, leading to trisubstituted derivatives.

Chart 1. Modifications Undertaken on the Hit Compound 5



Substituent Variations on the C-Ring. In the first inhibitor screen, it could be shown that in the 2,5-pyridine class (Table 1) the addition of a fluorine atom in *ortho* position to the hydroxyl group at the C-ring (2 compared to 3) resulted in a notable increase in potency of the inhibitor. The analogous fluorinated compound 6 (2,6-substituted pyridine) was therefore synthesized and proved to bind 10 times more potent than the reference compound 5 ($K_i = 245$ nM for 6 vs 26 nM for 5, Table 2). The affinity enhancement caused by the 4-F substituent at the C-ring could also be observed using another substitution pattern at the A-ring: 3-F/4-OH ($K_i = 467$ nM for 7 vs 36 nM for 8, Table 2).

The influence of the substituent pattern used for the C-ring was subsequently studied in more detail with compounds containing a 2-F/3-OH phenyl A-ring motif (compounds 9–15, Table 2). Addition of a 2-OH or a 2-F to the 3-OH/4-F at the C-ring resulted in equipotent compounds ($K_i = 13$, 11, and 9 nM, respectively, for 9, 10, and 11). Replacing the 3-OH/4-F at the C-ring (9) by a 2-OH/3-OH motif (12; $K_i = 64$ nM) led to a slight decrease in affinity. Addition of a 4-OH group (14, $K_i = 405$ nM) or of a 6-OH group at the C-ring (15, $K_i = 796$ nM) resulted in a strong decrease in activity.

The presence of the 3-OMe group at the C-ring (16a, inactive at a concentration of 100 μ M) was detrimental for the inhibitory activity compared to the 3-OH analogue (16, $K_i = 63$ nM).

Substituent Variations on the A-Ring. 2,6-Pyridine derivatives containing the C-ring motif (3-OH/4-F or 2-OH/3-OH) were synthesized with different substituents at varying positions of the A-ring (Table 3).

Compounds with one substituent in the 3- or 4-position (17, 3-NMe₂, $K_i = 7$ nM; 18, 3-OH, $K_i = 7$ nM; 19, 3-OH, $K_i = 44$ nM; and 21, 4-F, $K_i = 221$ nM) showed that their substitution with a polar moiety at 3-position (17, 18, 19) led to stronger binding compared to the one with a lipophilic group at 4-position (21). This effect was confirmed in case the A-ring was disubstituted (22) with the 3-Cl and 4-F substituents, which led to a compound with a similar binding constant as the mono 4-F derivative 21 ($K_i = 190$ and 221 nM for 22 and 21, respectively). These lipophilic groups exerted a detrimental effect on the binding affinity, which was lower compared to the unsubstituted phenyl (16, $K_i = 63$ nM).

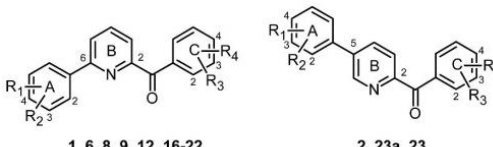
The compounds with two substituents in 2/3- or in 3/4-positions of the A-ring (1, 3-OH/4-OH, $K_i = 7$ nM; 6, 3-Me/4-OH, $K_i = 26$ nM; 8, 3-F/4-OH, $K_i = 36$ nM; 9, 2-F/3-OH, $K_i = 13$ nM) had similar binding constants with the exception of 20 (3-OH/4-Me, $K_i = 47$ nM) with a slightly decreased affinity. No significant difference in activity could be observed between mono- and disubstituted compounds at the A-ring as long as a 3-OH or a 4-OH moiety was present. In summary, the best affinities were achieved in the presence of a 3-OH or a 3-NMe₂ moiety at the A-ring.

In the 2,5-pyridine class, the affinity of 23 ($K_i = 17$ nM) with a 3-F/4-OH substitution pattern at the A-ring was similar to that of compound 2 ($K_i = 24$ nM) with a 3-Me/4-OH substitution pattern at the A-ring and fell into the same range of compounds in the 2,6-class. Furthermore, the methoxy

Table 2. 17 β -HSD14 Inhibitory Activity and Binding Constant (K_i) of 2,6-Pyridine Derivatives with Different Substituents at the C-Ring

| compd | R ₁ | R ₂ | R ₃ | R ₄ | R ₅ | 17 β -HSD14 % inhibition @ 2 μ M ^a | K_i (nM) ^a |
|-------|----------------|----------------|----------------|----------------|----------------|---|-------------------------|
| 5 | 3-Me | 4-OH | H | 3-OH | H | 34 | 245 \pm 21 |
| 6 | 3-Me | 4-OH | H | 3-OH | 4-F | 60 | 26 \pm 3 |
| 7 | 3-F | 4-OH | H | 3-OH | H | 16 | 467 \pm 91 |
| 8 | 3-F | 4-OH | H | 3-OH | 4-F | 67 | 36 \pm 5 |
| 9 | 2-F | 3-OH | H | 3-OH | 4-F | 72 | 13 \pm 5 |
| 10 | 2-F | 3-OH | 2-OH | 3-OH | 4-F | 76 | 11 \pm 3 |
| 11 | 2-F | 3-OH | 2-F | 3-OH | 4-F | 72 | 9 \pm 3 |
| 12 | 2-F | 3-OH | 2-OH | 3-OH | H | 65 | 64 \pm 4 |
| 13 | 2-F | 3-OH | 2-OH | H | H | 66 | 135 \pm 2 |
| 14 | 2-F | 3-OH | 2-OH | 3-OH | 4-OH | 25 | 405 \pm 177 |
| 15 | 2-F | 3-OH | 2-OH | 3-OH | 6-OH | 11 | 796 \pm 122 |
| 16a | H | H | H | 3-OMe | 4-F | ni | nd |
| 16 | H | H | H | 3-OH | 4-F | 57 | 63 \pm 3 |

^aRecombinantly expressed purified 17 β -HSD14 enzyme, fluorimetric assay, substrate E2 [32 μ M], NAD⁺ [1.2 mM], 25 $^{\circ}$ C, mean value of at least two independent experiments each with three technical repeats; ni: no inhibition (<10% inhibition at 100 μ M), nd: not determined.

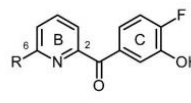
Table 3. 17 β -HSD14 Inhibitory Activity and Binding Constant (K_i) of Pyridine Derivatives with Different Substituents at the A-Ring


| compd | position A-ring | R ₁ | R ₂ | R ₃ | R ₄ | 17 β -HSD14 % inhibition @ 2 μ M ^a | K_i (nM) ^a |
|-------|-----------------|--------------------|----------------|----------------|----------------|---|--------------------------|
| 1 | 6 | 3-OH | 4-OH | 3-OH | 4-F | 69 | 7 \pm 1 |
| 2 | 5 | 3-Me | 4-OH | 3-OH | 4-F | 60 | 24 \pm 9 |
| 6 | 6 | 3-Me | 4-OH | 3-OH | 4-F | 60 | 26 \pm 3 |
| 8 | 6 | 3-F | 4-OH | 3-OH | 4-F | 67 | 36 \pm 5 |
| 9 | 6 | 2-F | 3-OH | 3-OH | 4-F | 72 | 13 \pm 5 |
| 12 | 6 | 2-F | 3-OH | 2-OH | 3-OH | 65 | 64 \pm 4 |
| 16 | 6 | H | H | 3-OH | 4-F | 57 | 63 \pm 3 |
| 17 | 6 | 3-NMe ₂ | H | 3-OH | 4-F | 57 | 7 \pm 1 |
| 18 | 6 | 3-OH | H | 3-OH | 4-F | 65 | 7 \pm 2 |
| 19 | 6 | H | 3-OH | 2-OH | 3-OH | 51 | 44 \pm 3 |
| 20 | 6 | 3-OH | 4-Me | 3-OH | 4-F | 64 | 47 \pm 7 |
| 21 | 6 | H | 4-F | 3-OH | 4-F | 37 | 221 \pm 46 |
| 22 | 6 | 3-Cl | 4-F | 3-OH | 4-F | 44 | 190 \pm 45 |
| 23a | 5 | 3-F | 4-OMe | 3-OMe | 4-F | 12 | 57% \pm 6 ^b |
| 23 | 5 | 3-F | 4-OH | 3-OH | 4-F | 61 | 17 \pm 5 |

^aRecombinantly expressed purified 17 β -HSD14 enzyme, fluorimetric assay, substrate E2 [32 μ M], NAD⁺ [1.2 mM], 25 °C mean value of at least two independent experiments each with three technical repeats; ^bPercent inhibition @ 22.2 μ M

derivative **23a** was less active compared to the hydroxylated analogue **23** as similarly observed for compound **16a**.

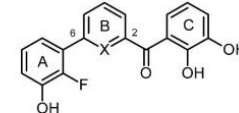
Variation of the A-Ring. To investigate the role of the phenyl A-ring, pyridine derivatives lacking the A-ring (**24**) or derivatives decorated with different heterocycles in 6-position of the B-ring (**25–28**) were designed (Table 4). Comparison of compound **24** (K_i = 1541 nM) with **16** (K_i = 63 nM) showed a decrease in activity. The nonaromatic piperidine **26** (K_i = 407 nM) was also a weaker binder, while the 4-methylpiperazine **27** (K_i = 190 nM) showed a similar inhibitory activity, both compared to **16**.

Table 4. 17 β -HSD14 Inhibitory Activity and Binding Constant (K_i) of 2,6-Pyridine Derivatives with Different Substituents in 6-Position of the Pyridine Ring (Different A-Rings)


| compd | R | 17 β -HSD14 % inhibition @ 2 μ M ^a | K_i (nM) ^a |
|-------|------------------------|---|-------------------------|
| 16 | phenyl | 57 | 63 \pm 3 |
| 24 | H | 13 | 1541 \pm 146 |
| 25 | thiophen-3-yl | 50 | 97 \pm 28 |
| 26 | piperidin-1-yl | 43 | 407 \pm 16 |
| 27 | 4-methylpiperazin-1-yl | 31 | 190 \pm 21 |
| 28 | -O-phenyl | 55 | 50 \pm 0 |

^aRecombinantly expressed purified 17 β -HSD14 enzyme, fluorimetric assay, substrate E2 [32 μ M], NAD⁺ [1.2 mM], 25 °C mean value of at least two independent experiments each with three technical repeats

Variations on the B-Ring. In the design section, it was reported that in the 2,5-pyridine class the central ring played a crucial role in affinity. This aspect was also investigated in the 2,6-class by the synthesis of the phenyl analogue **29** and the corresponding N-oxide **30** (Table 5). Comparison of the biological data of these compounds with the pyridine analogue **12** (K_i = 64 nM) showed that both the phenyl derivative **29** (K_i = 21 nM) and the N-oxide derivative **30** (K_i = 132 nM) had a similar affinity as the pyridine **12**.

Table 5. 17 β -HSD14 Inhibitory Activity and Binding Constant (K_i) for Compounds with Different B-Rings


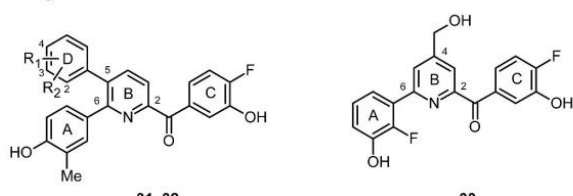
| compd | X | 17 β -HSD14 % inhibition @ 2 μ M ^a | K_i (nM) ^a |
|-------|--------------------------------|---|-------------------------|
| 12 | N | 77 | 64 \pm 4 |
| 29 | C | 60 | 21 \pm 2 |
| 30 | N ⁺ -O ⁻ | 47 | 132 \pm 13 |

^aRecombinantly expressed purified 17 β -HSD14 enzyme, fluorimetric assay, substrate E2 [32 μ M], NAD⁺ [1.2 mM], mean value of at least two independent experiments each with three technical repeats

Trisubstituted Pyridines. On the basis of the hypothesis that the C-ring and the carbonyl group of both the 2,5- and 2,6-pyridines achieve the same interaction as a consequence of binding in the same area, the similarity in affinity of the 2,5-derivative **23** (K_i = 17 nM) and the 2,6-derivative **8** (K_i = 36 nM, Table 3) suggested that the available space for binding the additional ring must be large, even tolerating an A-ring attached to the 5- or 6-position. Trisubstituted pyridines combining

substitutions at the 5- and 6-positions were therefore synthesized (**31** and **32**, Table 6). These trisubstituted compounds turned out to be equipotent (**31**, $K_i = 9$ nM; **32**, $K_i = 15$ nM) with a similar affinity compared to the disubstituted derivatives **6** and **23**.

Table 6. 17 β -HSD14 Inhibitory Activity and Binding Constant (K_i) of Pyridine Derivatives with an Additional D-Ring or a Substituent in 4-Position



| compd | R ₁ | R ₂ | 17 β -HSD14 % inhibition @ 2 μ M ^a | K_i (nM) ^a |
|-------|----------------|----------------|---|-------------------------|
| 6 | | | 60 | 26 \pm 3 |
| 23 | | | 61 | 17 \pm 5 |
| 31 | 3-Me | 4-OH | 71 | 9 \pm 4 |
| 32 | 2-F | 3-OH | 63 | 15 \pm 4 |
| 33 | | | 47 | 86 \pm 7 |

^aRecombinantly expressed purified 17 β -HSD14 enzyme, fluorimetric assay, substrate E2 [32 μ M], NAD⁺ [1.2 mM], mean value of at least two independent experiments each with three technical repeats

Introducing a hydroxymethyl group at the 4-position of the B-ring led to a slight decrease in activity (**33** $K_i = 86$ nM compared to **9** $K_i = 13$ nM, Table 6).

Pan Assay Interference Compounds.³⁷ All the biologically evaluated compounds were tested in silico for nonspecific binding in order to identify false positives using the Pains-remover computer tool.³⁸ From the compounds analyzed, seven did not pass the filter, including **10**, **12**, **14**, **19**, **20**, **29**,

and **30**, suggested as nonspecific binders. They all share as common characteristic a catechol moiety. It is known that catechols can be toxic,³⁹ however, the inhibitory data of these compounds are presented as they are useful to establish a better structure–activity relationship comprehension. In case these compounds turn out to be highly interesting, further assays should be performed to characterize their toxicity.

Crystal Structures Determination. The inhibitors with the highest binding affinity were selected for crystal structure determination in order to get insight into their binding mode. Crystal structures could be obtained for four different inhibitors by co-crystallization of the protein in complex with cofactor and ligands (**6**, PDB 5L7T; **9**, PDB 5L7Y; **10**, PDB 5L7W; **12**, PDB 5EN4). The data collection, processing, and refinement statistics details are reported in the Supporting Information. The crystals were obtained by two different conditions, however, all crystal structures show the same tetragonal space group (I422) with only one monomer present in the asymmetric unit. The crystal structures disclosed that the protein is a homotetramer, in accordance with a previous study.⁵ The structures obtained have a resolution ranging from 1.52 to 2.02 Å. The conformation of the protein in complex with inhibitor **1** (PDB 5ICM) has already been published⁵ and will not be the focus here. It will however be included in the structural comparison.

Description of the Inhibitor Binding Site. The superimposition of all five ternary complexes reveals that binding of the different ligands does not induce conformational changes of the overall geometry of the protein (Figure 2), showing a mean RMSD of 0.15 \pm 0.04 Å between the alignment of the C α atoms of the structures, as calculated with COOT.⁴⁰ The cofactor interacts with the Rossman fold region and experiences similar interactions as already observed for the 17 β -HSD14 holo structure and in complex with inhibitor **1**.⁵ The inhibitor binds into the substrate binding site, which is restricted by two α -helices from the flexible loop (α FG1 and α FG2, residues

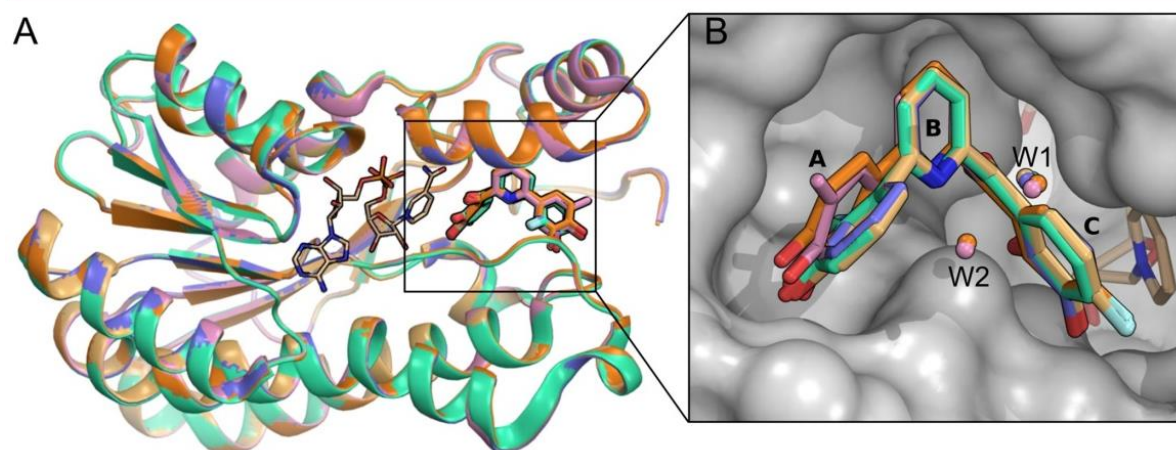


Figure 2. Superimposition of the crystal structures of 17 β -HSD14 obtained in ternary complexes with five inhibitors: **1**, **6**, **9**, **10**, and **12**. (A) The enzyme 17 β -HSD14 is shown as ribbon model (5ICM in orange, 5L7T in pink, 5L7Y in purple–blue, 5L7W in ocher, and 5EN4 in green); inhibitors are shown as stick models. The cofactor NAD⁺ is shown as thin line. (B) Close-up view on the binding pocket. The protein 17 β -HSD14 is displayed by use of the solvent accessible surface. The carbon atoms of the inhibitors are shown for **1** in orange **6** in pink, **9** in purple–blue, **10** in ocher, and **12** in green. Inhibitors are shown as stick models and cofactor as a thin line. The water molecules W1 and W2 are represented in the same color as the corresponding inhibitor of the individual structures. W1 corresponds to water molecule 472 in 5ICM, 518 in 5L7T, 508 in 5L7Y, 496 in 5L7W, and 450 in 5EN4; W2 corresponds to water molecule 530 in 5ICM and 502 in 5L7T in the respective crystal structure. All structural representations were prepared with PyMOL.⁴¹

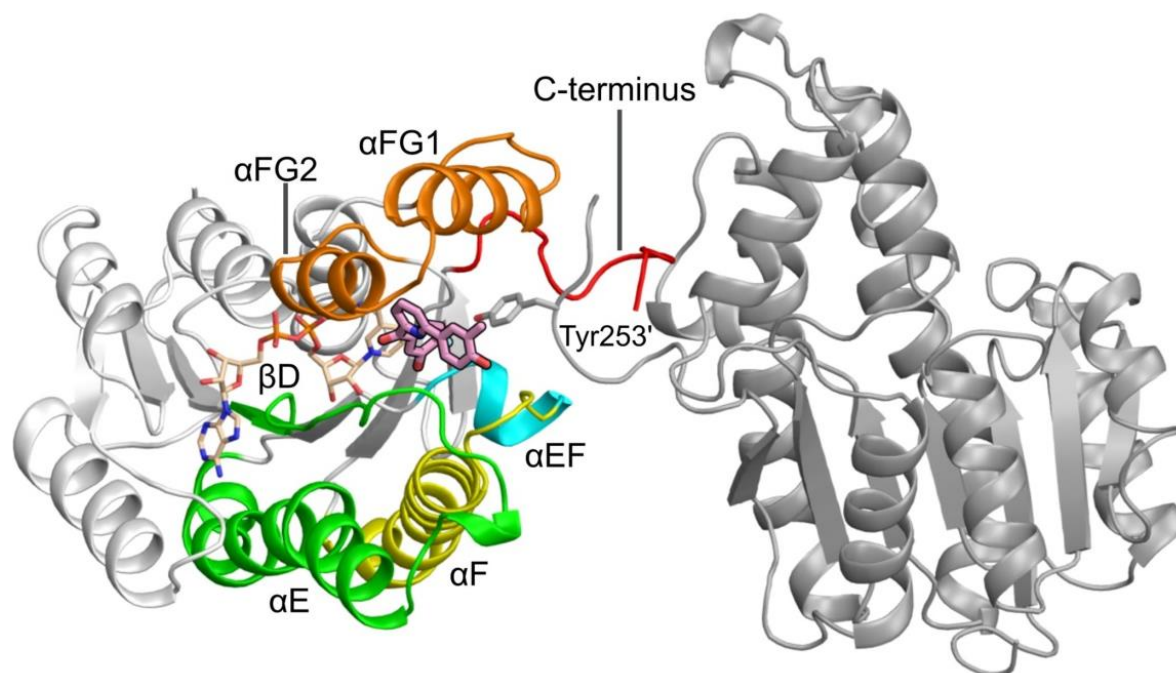


Figure 3. Ribbon representation of inhibitor **6** in complex with the protein 17 β -HSD14 and cofactor NAD⁺. The inhibitor binding site is delimited by α FG1 and α FG2 (orange), α F (the helix containing the catalytic Tyr154 and Lys158, yellow), α EF (cyan), α E and β D (green), and C-terminal tail (red). Inhibitor **6** is shown as stick model, and its carbon atoms are colored in pink. The symmetry equivalent molecule containing Tyr253' is shown in gray on the right-hand side. The cofactor and Tyr253' are shown as thin lines.

189–212, in orange), a portion of the α F helix (containing the catalytic Tyr154, Lys158, in yellow), the short α EF helix (residue 142–146, in cyan), the segment that connects α E with β D (from Asn89 to Arg98, in green), and the C-terminal tail (in red, Figure 3). Furthermore, Tyr253' from the adjacent monomer (in gray on the right-hand side, Figure 3) is pointing toward the inhibitor binding site, reducing the volume of the active site cleft. The annotation of the different helices and β -sheets follows the nomenclature described by Lukacik et al.² The flexible loop is in a conformation that closes the binding pocket, reducing the size of the substrate binding site. Furthermore, the inhibitor binding site is predominantly hydrophobic, with two main hydrophilic regions: the first one corresponds to the two residues of the catalytic triad Tyr154 and Ser141, and the second one is formed by His93 and Gln148 (Figure 4). This second region shapes the binding site in a peculiar form and could be relevant for the achievement of selectivity considering that no other human SDR 17 β -HSDs presents a histidine at this position.

Description of the Binding Mode of Inhibitors in Complex with 17 β -HSD14. In the surface representation, it is obvious that the V-shape of the inhibitor scaffold matches well with the geometry of the active site (Figure 2B). For all five crystallized inhibitors, additional water molecules are observed in the binding pockets: Water W1 is found for all inhibitors in the same position. W1 is localized between the B- and C-ring at an approximate 4 Å distance from the B-ring. W1 establishes an H-bond interaction with the side chain of Asn186 ($d \approx 2.7$ Å). Water W2 is only observed for **1** and **6** (Figure 2B) and found above the plane of the A-ring. W2 interacts with W1 (H-bond contact $d \approx 2.6$ Å). In the case of the other three inhibitors, the

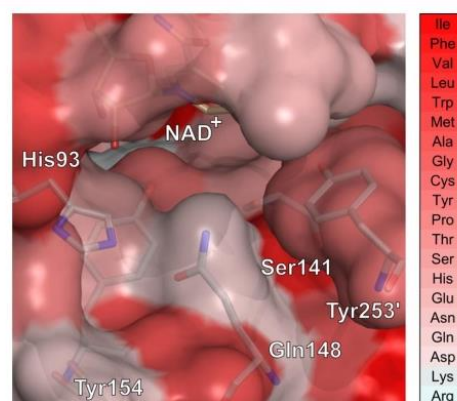


Figure 4. Surface representation of 17 β -HSD14; color coded according to the Eisenberg hydrophobicity scale (from dark-red for highly hydrophobic amino acids to white for highly hydrophilic amino acids).⁴² The cofactor NAD⁺ and amino acids are shown as stick models. The amino acid of the symmetry equivalent molecule is referred as prime (').

orientation of the A-ring plane is shifted, inducing the displacement of W2.

Because of close similarity, only the interactions of **6** and **12**, as representatives of the series, will be described in detail. The structures and details of the interactions of all inhibitors are shown in Figure 5 (A, **6**; B, **12**; C, **9**; D, **10**). Inhibitors **6** and **12** have the same B-ring scaffold (2,6-pyridine) differing in the nature of their A- and C-ring substituents. At the C-ring, the keto group and the pyridine ring of **6** and **12** bind exactly at the

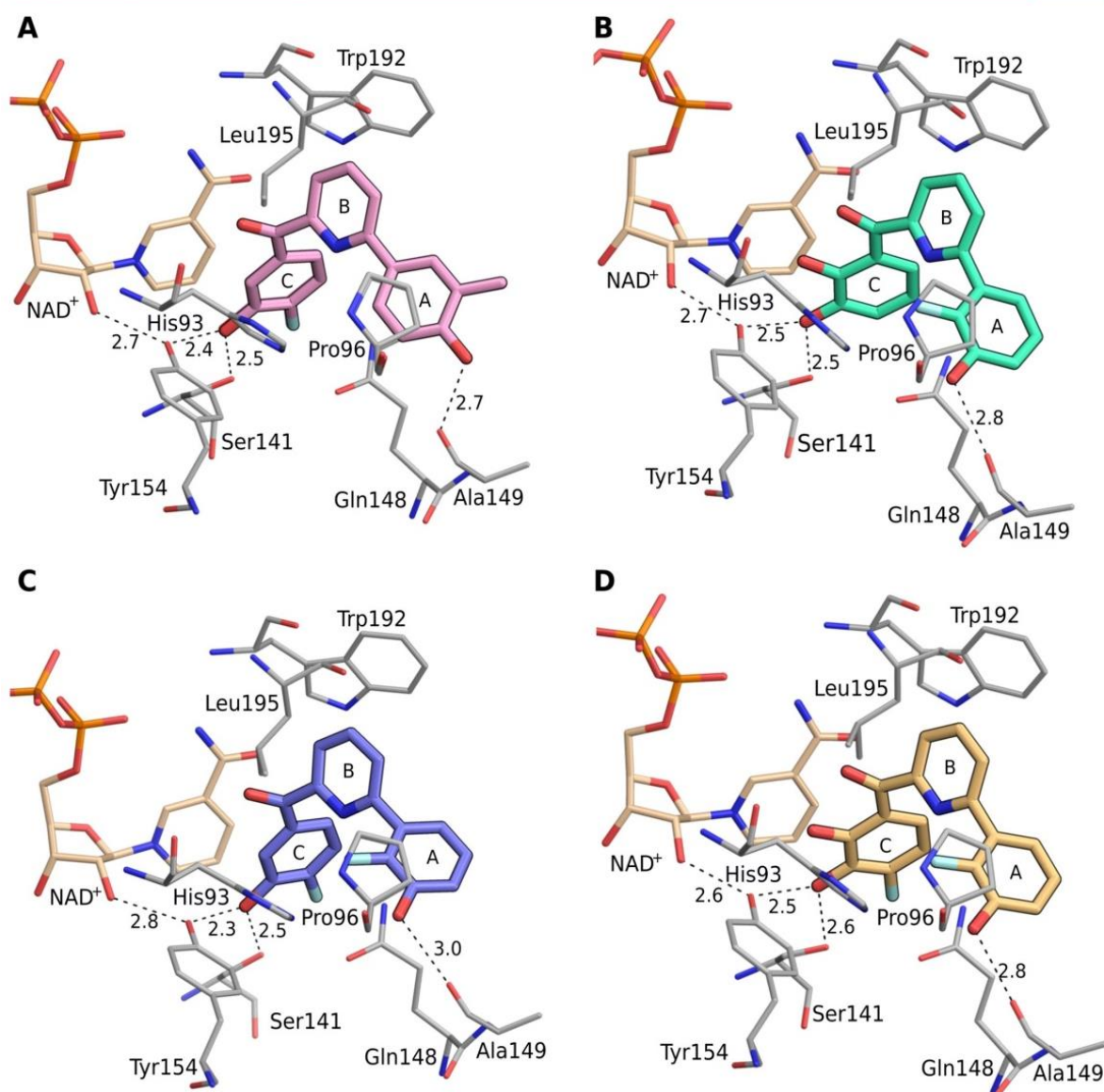


Figure 5. Crystal structures of 17β-HSD14 in complex with cofactor NAD⁺ and inhibitors **6** (in pink, A), **12** (in green, B), **9** (in purple blue, C) and **10** (in ocher, D). The inhibitors are shown as stick models. The amino acids, within a distance of 5 Å, and the cofactor are shown as thin lines. H-bonds are depicted as dotted lines. Distances are given in Å.

same position. The angle between the keto group and the phenyl C-ring is identical in **6** and **12** independent of the presence or absence of the 2-OH group at the C-ring.

The 3-OH groups at the C-ring of **6** and **12** interact via remarkably short H-bond interactions with the side chain of Tyr154 (**6**, $d = 2.4$ Å, **12**, $d = 2.5$ Å) and the side chain of Ser141 (**6**, $d = 2.5$ Å, **12**, $d = 2.5$ Å) from the catalytic triad. The 4-F group at the C-ring of **6** is not involved in any specific interaction.

The phenyl C-ring of **6** and **12** is stabilized by van der Waals contacts with the nicotinamide moiety of NAD⁺. The carbonyl group is not involved in any direct interaction. The central pyridine B-ring is anchored by van der Waals contacts with

Trp192 and Leu195, which wrap around the top part of the pyridine ring. No close contacts are observed with His93.

For **6**, an H-bond interaction is formed between the 4-OH at the A-ring with the carbonyl backbone of Ala149 ($d = 2.7$ Å). The 3-Me group at the A-ring is not involved in any interaction. The aromatic A-ring is not stabilized by any π -stacking interactions, however, van der Waals interactions with Pro96 are observed. No water mediated H-bond interactions are observed; nonetheless, it is remarkable that W1 remains present in this lipophilic environment. In total, 91 van der Waals contacts are achieved by the ligand and its surface is buried to 94.0% (considering only one monomer of the protein, the

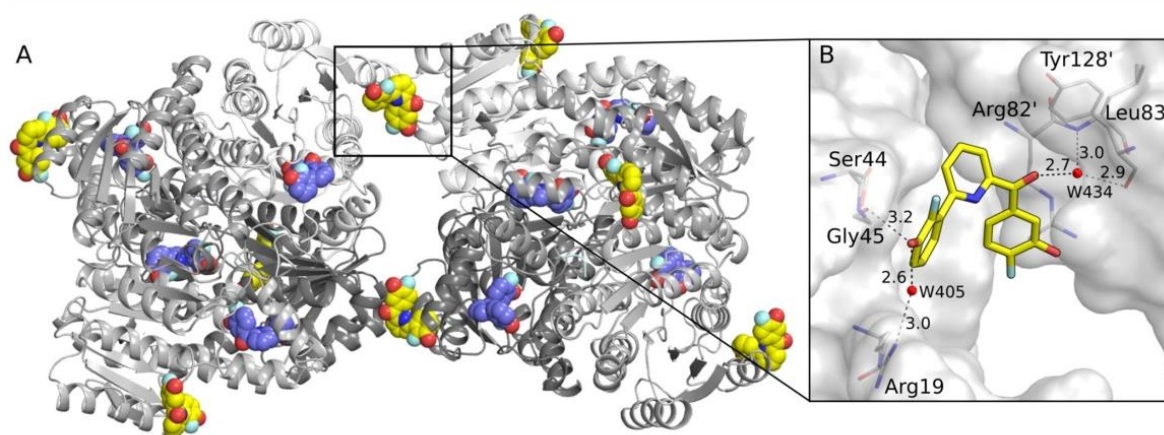


Figure 6. (A) Overall view of the crystal structure of two 17β-HSD14 tetramers in complex with **9**. The protein monomers are shown as ribbon models and colored in gray. The inhibitors are shown as sphere models. The inhibitors located in the substrate binding site are colored in purple-blue, while the inhibitors located between the interfaces of the tetramers are shown in yellow. (B) Close-up view of the second ligand binding site of **9** located at the interface between two tetramers. The enzyme is displayed by use of the solvent accessible surface. Inhibitor **9** is shown as stick model. The amino acids are shown as thin lines. The amino acids of the symmetry equivalent molecule are referred to prime ('). H-bonds are depicted as black dotted lines. Distances are given in Å.

number of van der Waals contacts achieved are summed up to 86 and the buried surface is 87.4%).

In **12**, a rotation of the A-ring plane is observed. Nevertheless, the altered orientation still allows the 3-OH group at the A-ring to be at H-bond distance to Ala149-CO ($d = 2.8$ Å, as observed with **6**). The aromatic A-ring can also establish a van der Waals interaction with the amino acid Pro96. In summary, 82 van der Waals contacts are observed for **12**, with 93.0% of its surface buried in the protein binding pocket (considering only one protein monomer, the ligand achieves 80 van der Waals contacts and its surface is buried to 88.2%).

Interestingly, the crystal structure of **9** in ternary complex with 17β-HSD14 shows the presence of a second inhibitor molecule at the interface between two tetramers (Figure 6A). Close inspection of this interface binding site (Figure 6B) highlights that the inhibitor is stabilized through an H-bond interaction between the 3-OH group at the A-ring to the hydroxyl group of Ser44 side chain ($d = 3.2$ Å) and with a water molecule W405 ($d = 2.6$ Å), which is stabilized by Arg19 ($d = 3.0$ Å). The keto group interacts with the other tetramer through a water molecule W434 ($d = 2.7$ Å), which is also bound to the NH from the backbone of Leu83' ($d = 3.0$ Å) and the carbonyl group of the backbone of Tyr128' ($d = 2.9$ Å). The copy of **9** binding to the interface is placed in a rather hydrophilic environment. The overall geometry of the interface ligand differs from that of the active site ligand: the dihedral angles, for the ligand in the active site and for the ligand binding at the interface, between the keto group and C-ring are -29° and 4° respectively and between the keto group and the B-ring are 129° and -133° , respectively (considering the plane through the keto group as 0°). The dihedral angle between C_2 at the A-ring and the nitrogen at the B-ring is 131° for the ligand in the binding pocket and -60° for the ligand present at the interface. A superimposition of the interface and active site compounds can be seen on Figure 7.

Comparison of the 17β-HSD1, 17β-HSD2, and 17β-HSD14 Structures. The existing crystal structure of 17β-HSD1 in ternary complex with the cofactor NADP⁺ and E2 (PDB

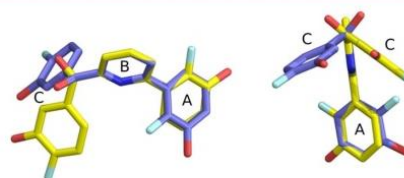


Figure 7. Superimposition of compound **9** based on the pyridine B-rings of the ligand at the interface (in yellow) and active site (in purple-blue).

1FDT) allows the direct comparison with the 17β-HSD14 structure in complex with the cofactor NAD⁺ and estrone (E1, PDB 5HS6). The superimposition reveals a structural conservation of the enzymes only in some regions (22% of sequence identity calculated with COOT,⁴⁰ Figure 8). Small differences in the NAD⁺/NADP⁺ binding site can be observed between type 14 and type 1 (RMSD of 1.6 Å calculated with COOT⁴⁰ based on C_α alignment). This result was expected because both enzymes bind a different cofactor (NAD⁺ for 17β-HSD14 vs NADP⁺ for 17β-HSD1). The flexible loop in 17β-HSD1 restricts the end of the binding cavity, while the corresponding loop in 17β-HSD14 is shifted upward, leaving the binding site widely open. This results in a smaller binding pocket for the type 1 enzyme. Furthermore, while the catalytic triad is conserved in both enzymes, the steroids accommodate in the binding sites with different orientations and achieve distinct interactions.

As no crystal structure is available for 17β-HSD2, the comparison between the structures of type 2 and type 14 is not possible.

Selectivity. Taking into account that the parent scaffold of the new 17β-HSD14 inhibitors was derived from 17β-HSD1 and 17β-HSD2 inhibitors, it was of utmost importance to study their selectivity profile with respect to 17β-HSD1 and 17β-HSD2 binding.

The 17β-HSD1 and 17β-HSD2 inhibition assay was performed using a radioactive assay, quantifying the amount

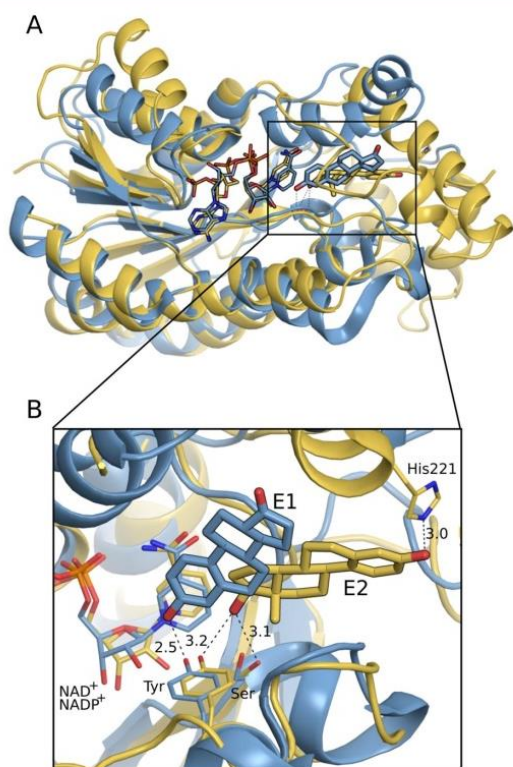


Figure 8. (A) Superimposition of 17 β -HSD1 (yellow, PDB 1FDT) and 17 β -HSD14 (light blue, PDB 5HS6) structures as ternary complexes. (B) Close-up view of the superimposed substrate binding pocket. The proteins are shown as ribbon model. The steroids are shown as stick models. The amino acids, involved in binding of the steroids (Tyr154 for 17 β -HSD14; Tyr155, Ser142 and His 221 for 17 β -HSD1), and the cofactors are shown as thin lines. The carbon atoms of E1 in complex with 17 β -HSD14 are colored in light-blue, and the carbon atoms of (E2) in complex with 17 β -HSD1 are colored in yellow. H-bonds are depicted as black dotted lines. Distances are given in Å.

of [^3H]-labeled E2 (for type 1) and [^3H]-labeled E1 (for type 2) formed after incubation with protein, cofactor, and the inhibitor as previously described.⁴³ The results are shown in Table 7, expressed as percent inhibition when tested at an inhibitor concentration of 1 μM .

As expected, the 2,5-pyridine **23** showed the highest affinity for 17 β -HSD1 (47% inhibition) compared to the 2,6-pyridines (**6–20**, 9–23% inhibition), which were all nearly inactive in 17 β -HSD1.

Inhibition of 17 β -HSD2 was slightly higher than that of 17 β -HSD1 for the compounds with a 2,6-substitution pattern (between 30% and 62% inhibition at 1 μM concentration for **6–20**) and much higher for the 2,5-pyridine ketones (64% and 85% when tested at 1 μM concentration for **23** and **2**, respectively).

A direct comparison of the 17 β -HSD1 and 17 β -HSD2 inhibitory activities with those of 17 β -HSD14 is however problematic as different conditions were used in the assays.

However, under the applied condition in the 17 β -HSD2 inhibition assay, using the Cheng–Prusoff equation for competitive inhibition, a calculated K_i (cK_i) could be estimated:

Table 7. 17 β -HSD14 Binding Constant (K_i) and 17 β -HSD1/17 β -HSD2 Inhibitory Activities (% Inhibition) of the Most Interesting Compounds

| compd | 17 β -HSD14 K_i (nM) ^a | 17 β -HSD1 % inhibition @ 1 μM ^b | 17 β -HSD2 % inhibition @ 1 μM ^c |
|-----------|--|---|---|
| 2 | 24 \pm 9 | 47 | 85 |
| 5 | 245 \pm 21 | 6 | 85 |
| 6 | 26 \pm 3 | 9 | 62 |
| 9 | 13 \pm 5 | 23 | 43 |
| 10 | 11 \pm 3 | 12 | 48 |
| 12 | 64 \pm 4 | 13 | 30 |
| 18 | 7 \pm 2 | 13 | 34 |
| 20 | 47 \pm 7 | 14 | 37 |
| 23 | 17 \pm 5 | 47 | 64 |

^aRecombinant purified 17 β -HSD14 enzyme, fluorimetric assay, substrate E2 [32 μM], NAD⁺ [1.2 mM], 25 $^\circ\text{C}$, mean value of at least two independent experiments each with three technical repeats.

^bPlacental 17 β -HSD1 enzyme, cytosolic fraction, substrate [^3H]-E1 + E1 [500 nM], NADH [0.5 mM], mean value of two determinations; standard deviation <20%. ^cPlacental 17 β -HSD2 enzyme, microsomal fraction, substrate [^3H]-E2 + E2 [500 nM], NAD⁺ [1.5 mM], mean value of two determinations; standard deviation <20%.

for a compound with an IC_{50} of around 1 μM (50% inhibition at 1 μM), a cK_i of about 450 nM was expected (with K_m 17 β -HSD2 = 400 nM in this assay⁴⁴ and $[S] = 500$ nM).

With 48% and 43% inhibition of 17 β -HSD2, compounds **9** and **10** showed a $cK_i \geq 450$ nM. Comparison of their K_i values for 17 β -HSD2 and 17 β -HSD14 binding allowed calculation of a selectivity factor (ratio of $K_i(\text{HSD2})/K_i(\text{HSD14})$), which could be estimated to be around 35 for **9** and ≥ 41 for **10**. Compounds **9** and **10** are relatively selective 17 β -HSD14 inhibitors. The selectivity profile of **12** toward 17 β -HSD2 (with only 30% inhibition at 1 μM) should be even better.

As steroidomimetics, the synthesized compounds might show undesired binding affinity to the estrogen receptors (ERs) α and β . Wetzel et al. reported that the most interesting compounds **2–5**, identified in the first screen, showed very low affinities to both ER subtypes (<0.1%, taking E2 as 100% reference).⁴⁵ It is therefore assumed that the synthesized compounds, which bear the same scaffold, do not bind tightly to the ERs.

DISCUSSION

The combination of the biological results, the crystal structures of the five ligands in ternary complex with the protein and the physicochemical properties provide the basis for the understanding of the structure–activity relationship study of the 2,5- and 2,6-substituted pyridine derivatives.

Focus on the C-Ring Part. The 3-OH group at the C-ring achieves important H-bond interactions with Tyr154 and Ser141, which stabilize the inhibitor in the enzyme binding site. The increase in acidity of this OH moiety, enhanced by the addition of a fluorine atom in *ortho* position to the OH group, correlates with a gain in binding affinity. The crystal structures indicate that the H-bond length between the 3-OH group at the C-ring and Tyr154 is rather short ($d = 2.3–2.5$ Å). This result supports the hypothesis of Hwang et al.,⁴⁶ which describes that in SDR enzymes, the $\text{p}K_a$ of the OH group from the catalytic tyrosine is decreased (through electrostatic interaction with the protonated catalytic Lys-NH₃⁺ and NAD⁺) and that this Tyr-OH is present as deprotonated species in the active site. In our structures, the negatively charged (or at least highly polarized)

carbonyl group of Gln150, as observed in the modeled structure (Supporting Information, Figure S1E). An additional H-bond interaction of N^+-O^- with Gln148 could be gained, but the high desolvation penalty induced by the introduction of the charges might not be compensated, overall resulting in no increase in affinity.

Second Binding Site for Compound 9. For compound 9, a second binding pose at the tetramer interface was observed. The inhibitor was refined to an occupancy of 80% at this additional binding site, suggesting that this ligand exhibits a lower affinity for this region compared to the active site. The binding of the inhibitor in this position might be irrelevant for the inhibitory process. The presence of compound 9 in this place might be an artifact resulting from crystal packing as the binding at the interface does not induce any conformational change of the ternary structure and of the ligand binding site. However, it is striking that Michiels et al.⁴⁸ reported in their NMR studies that phytoestrogens might also bind at the dimer interface of 17 β -HSD1.

Comparison of the 17 β -HSD1, 17 β -HSD2, and 17 β -HSD14 Structures. A positive influence of a fluorine atom in ortho position to a phenolic hydroxyl group was already reported during the development of 17 β -HSD1 dihydroxyphenylthiophenes inhibitors⁴⁹ and 17 β -HSD2 hydroxyphenyl-*N*-methylsulfonamide thiophenes inhibitors.⁵⁰ As no crystal structures of 17 β -HSD1 and 17 β -HSD2 in complex with these nonsteroidal compounds are available, their binding modes remain unclear. As 17 β -HSD type 1, type 2, and type 14 belong to the SDR superfamily, they share similarities in the region in the vicinity of the catalytic triad. The presence of the complex H-bonding network was also identified in the type 1 enzyme after analysis of its crystal structure (PDB ID 1FDT). It could be expected that the 17 β -HSD1 and 17 β -HSD2 inhibitors with an acidic OH-phenyl group have a similar binding mode, interacting with the catalytic triad as observed in the crystal structure of type 14. Therefore, these new 17 β -HSD14 structures in complex with nonsteroidal inhibitors can represent a useful comparative data for 17 β -HSD1 docking studies and 17 β -HSD2 homology modeling.

Basis for Structure-Based Drug Design. On the basis of these results, it should be possible to optimize the current ligands using structure-based drug design. In this compound class, the interactions with the catalytic Tyr154 and Ser141 as well as with Ala149 are very important to anchor the ligand scaffold in the correct position. Specific interactions involving His93 and Gln148 in inhibitor binding should result in an improved activity and selectivity, particularly as His93 is not present in other human SDR 17 β -HSDs. Addressing the water molecule W1 should also lead to an additional interaction with the protein. As the active site is open and solvent exposed, the polar amino acids which are in a close neighborhood to the active site next to the surface could also be targeted by specific interactions.

CONCLUSION

Nonsteroidal 17 β -HSD14 inhibitors have been identified. The initial hits identified in a preliminary screen in the 2,6-substituted pyridine class showed a K_i around 250 nM/300 nM, which was optimized to result in six highly active compounds with $K_i < 15$ nM and two with a K_i of 7 nM. The considerations of substituent effects applied during optimization were successful. It appears that at the C-ring, an acidic 3-OH group is essential to achieve high potency, interacting via strong

H-bond contacts to Tyr154 and Ser141, thereby stabilizing the interaction through an extensive H-bonding network. The structure–activity relationship found for the A-ring shows that a 3-OH or a 4-OH group increases the potency of the inhibition by interacting with Ala149. The crystal structures in complex with the inhibitors confirm the rather large active site, reduced by the C-terminal chain from an adjacent monomer. The new 17 β -HSD14 inhibitors show good physicochemical properties, which should be associated with a good bioavailability profile. They also present a good selectivity profile toward both closely related subtypes 17 β -HSD1 and 17 β -HSD2. The determined crystal structures give important insights not only to characterize the novel protein target but also to understand the binding poses of these nonsteroidal inhibitors and provide the basis for their further structure-based optimization.

EXPERIMENTAL SECTION

1. Chemistry. 1.1. *Chemical Methods.* Chemical names follow IUPAC nomenclature.

Starting materials were purchased from Acros Organics, Alfa Aesar, Combi-Blocks, Roth, and Sigma-Aldrich and were used without further purification. Anhydrous THF was freshly distilled from sodium benzophenone ketyl.

Microwave irradiation experiments were carried out in a CEM-Discover apparatus.

Column chromatography was performed on silica gel (0.04–0.063 mm, Macherey-Nagel), and reaction progress was monitored by TLC on aluminum sheets (Silicagel 60 F254, Merck). Visualization was accomplished with UV light at 254 and 366 nm, respectively.

Preparative HPLC was performed with a Varian PrepStar 218 gradient system using a ProStar 320 detector. A ProntoSIL C18 column (5.0 μ m, 120 Å, 250–32 mm) was used as stationary phase with an acetonitrile/water gradient containing 0.1% TFA at a flow rate of 20 mL/min. All solvents were HPLC grade. Detection was performed at a wavelength of 254 nm.

Mass spectrometry was performed on a Q-Trap 2000 (Applied Biosystems) equipped with an electrospray interface (ESI).

¹H and ¹³C NMR spectra were measured on a JEOL ECX-400 spectrometer (at 400 and 100 MHz, respectively). Chemical shifts are reported in δ (parts per million: ppm), using residual peaks for the deuterated solvents as internal standard:⁵¹ 2.05 ppm (¹H NMR), 29.8 and 206.3 ppm (¹³C NMR), acetone-*d*₆; 7.26 ppm (¹H NMR), 77.2 ppm (¹³C NMR), CDCl₃; 2.50 ppm (¹H NMR), 39.5 ppm (¹³C NMR), DMSO-*d*₆. Signals are described as s, bs, d, t, q, dd, ddd, dt, and m for singlet, broad signal, doublet, triplet, doublet of doublets, doublet of doublet of doublets, doublet of triplets, and multiplet, respectively. All coupling constants (*J*) are given in hertz (Hz).

Infrared spectroscopy was performed on a Bruker ALPHA FT-IR spectrometer as neat sample.

All tested compounds have $\geq 95\%$ chemical purity as evaluated by HPLC. The Shimadzu system consisted of a LC-20AT pump, an SIL-20A autosampler, and a SPD-M20A PDA detector. The system was operated by the standard software LCsolution. A RP C18 NUCLEODUR (125 mm \times 4 mm, 5 μ m) column (Macherey-Nagel) was used as stationary phase. All solvents were HPLC grade. In a gradient run, the percentage of acetonitrile was increased from initial concentration of 30% at 0 min to 90% at 15 min and kept at 90% for 5 min. The injection volume was 20 μ L at a flow rate of 1.00 mL/min. UV spectra were recorded at a wavelength of 254 nm.

Marvin sketch was used for the calculation of the pK_a data (Marvin 15.9.14, 2015, Chemaxon <http://www.chemaxon.com>).

The following compounds were prepared according to previously described procedures: (1a),⁵ (1),⁵ (10g),²⁹ (10f),³⁰ (15d),⁵² (31f),⁵³ (33f)²⁶ (using commercial POBr₃, max temp 150 °C), and (33e).²⁶

1.2. General Chemical Procedures. 1.2.1. *General Procedures for Alcohol Formation.* Method A1: A solution of *n*-BuLi (1.0 eq, 2.5 M in hexane) was diluted with anhydrous THF (0.8 M), and aryl

bromide (1.0 equiv) in anhydrous THF was slowly added at -80°C under argon. The resulting solution was stirred for 15 min at -80°C , then the appropriate aldehyde (1.0 equiv) was added and the reaction solution was stirred for additional 15 min at -80°C followed by room temperature for 2 h. The mixture was quenched with saturated NH_4Cl and extracted with ethyl acetate. The combined organic layer was washed with brine, dried over magnesium sulfate, filtered, and evaporated to dryness under reduced pressure. The product was purified by column chromatography.

Method A2: A mixture of aryl bromide (1.0 equiv), magnesium turnings (1.1 equiv), and a catalytic amount of iodine in anhydrous THF was stirred for 2 h at 60°C under argon. A solution of the appropriate aldehyde in anhydrous THF was added, and the reaction mixture was stirred at 80°C . The end of the reaction was monitored by TLC. The mixture was quenched with brine and extracted with ethyl acetate. The combined organic layer was dried over magnesium sulfate, filtered, and evaporated to dryness under reduced pressure. The product was purified by column chromatography.

1.2.2. General Procedure for Alcohol Oxidation: Method B. 2-Iodoxybenzoic acid (1.2 equiv) was added to a solution of alcohol derivative (1.0 equiv) in THF, and the reaction mixture was stirred at 60°C . After the end of the reaction (monitored by TLC), the mixture was cooled to room temperature, quenched with saturated $\text{Na}_2\text{S}_2\text{O}_3$, and extracted with ethyl acetate. The combined organic layer was washed with water and saturated sodium bicarbonate, dried over magnesium sulfate, filtered, and evaporated to dryness under reduced pressure. The product was purified by column chromatography.

1.2.3. General Procedures for Suzuki Coupling. **Method C1:** A mixture of aryl bromide (1.0 equiv), boronic acid (1.2 equiv), cesium carbonate (4.0 equiv), and tetrakis(triphenylphosphine)palladium (0.02 equiv) was solved in DME/water (2:1) and degassed with argon. The mixture was stirred overnight at 80°C . The reaction mixture was cooled down to room temperature, quenched with water, and extracted with ethyl acetate. The combined organic layer was washed with brine, dried over magnesium sulfate, filtered, and evaporated to dryness under reduced pressure. The product was purified by column chromatography.

Method C2: A mixture of aryl bromide (1.0 equiv), boronic acid (1.2 equiv), sodium carbonate (2.0 equiv), and tetrakis(triphenylphosphine)palladium (0.02 equiv) was solved in DME/water (2:1) and degassed with argon. The mixture was exposed to microwave irradiation (60 min, 150 W, 150°C) and quenched with water after reaching room temperature. The mixture was extracted with ethyl acetate, and the combined organic layer was washed with brine, dried over magnesium sulfate, filtered, and evaporated to dryness under reduced pressure. The product was purified by column chromatography.

1.2.4. General Procedure for Amination of Bromopyridine: Method D. A mixture of bromopyridine (1.0 equiv), appropriate *N*-heterocycle (1.1 equiv), and potassium phosphate (4.0 equiv) in 1,4-dioxane was stirred at 100°C . At the end of the reaction (monitored by TLC), the mixture was cooled to room temperature, quenched with 1 M sodium hydroxide, and extracted with ethyl acetate. The combined organic layer was dried over magnesium sulfate, filtered, and evaporated to dryness under reduced pressure. The product was purified by column chromatography.

1.2.5. General Procedure for Ether Cleavage: Method E. A solution of methoxy derivative (1.0 equiv) in dry dichloromethane was cooled to -80°C , and boron tribromide (1 M in dichloromethane, 5 eq per methoxy function) was slowly added under argon. The reaction mixture was stirred at -80°C for 1 h and then allowed to warm to room temperature overnight. The mixture was cooled in an ice bath, quenched with water, and extracted with ethyl acetate. The combined organic layer was washed with brine, dried over magnesium sulfate, filtered, and evaporated to dryness under reduced pressure. The product was purified by column chromatography.

1.3. Detailed Synthesis Procedures and Compound Characterization. (4-Fluoro-3-hydroxyphenyl)[6-(4-hydroxy-3-methylphenyl)pyridin-2-yl]methanone hydrochloride salt (**6**). According to method E, the title compound was prepared by reaction of (4-fluoro-3-

methoxyphenyl)[6-(4-methoxy-3-methylphenyl)pyridin-2-yl]-methanone (**6a**) (110 mg, 0.31 mmol, 1.0 equiv) with boron tribromide (3.1 mL, 3.1 mmol, 10 equiv) in dichloromethane (6.0 mL). The crude product was purified by column chromatography (cyclohexane/ethyl acetate 3:1), and the hydrochloride salt was prepared by means of 2 M hydrogen chloride solution in ether to give 85 mg (0.24 mmol/75%) of the analytically pure compound $\text{C}_{19}\text{H}_{14}\text{FNO}_3\cdot\text{HCl}$; MW 360; mp $194\text{--}195^{\circ}\text{C}$. ^1H NMR (DMSO- d_6 , 400 MHz): δ 10.29 (bs, 1H), 9.71 (bs, 1H), 8.12–7.96 (m, 2H), 7.85–7.81 (m, 1H), 7.79–7.73 (m, 1H), 7.71 (dd, J = 8.8 Hz, 2.2 Hz, 1H), 7.56 (ddd, J = 8.4 Hz, 4.5 Hz, 2.1 Hz, 1H), 7.33 (dd, J = 11.0 Hz, 8.5 Hz, 1H), 6.89 (d, J = 8.4 Hz, 1H), 2.18 (s, 3H). ^{13}C NMR (DMSO- d_6 , 100 MHz): δ 191.9, 157.1, 155.4, 154.2 (d, J = 248.2 Hz), 154.1, 144.8 (d, J = 12.5 Hz), 138.3, 132.7 (d, J = 3.1 Hz), 129.3, 128.5, 125.6, 124.2, 123.2 (d, J = 7.8 Hz), 121.7, 121.3, 120.0 (d, J = 4.4 Hz), 116.0 (d, J = 19.1 Hz), 114.9, 16.2. IR: 3390, 1661, 1611, 1597, 1583, 1526, 1510, 1427, 1235, 1119, 756 cm^{-1} . MS (ESI): 324 ($\text{M} + \text{H}$) $^{+}$, 7 Hz, 115.8 (d, J = 6.8 Hz), 56.4. MS (ESI): 310, 312 ($\text{M} + \text{H}$) $^{+}$. HPLC analysis: retention time = 12.29 min; peak area, 97.6%.

(4-Fluoro-3-hydroxyphenyl)[6-(3-fluoro-4-hydroxyphenyl)pyridin-2-yl]methanone Hydrochloride Salt (**8**). According to method E, the title compound was prepared by reaction of (4-fluoro-3-methoxyphenyl)[6-(3-fluoro-methoxyphenyl)pyridin-2-yl]-methanone (**8a**) (148 mg, 0.42 mmol, 1.0 equiv) with boron tribromide (4.2 mL, 4.2 mmol, 10 equiv) in dichloromethane (8.0 mL). The crude product was purified by column chromatography (cyclohexane/ethyl acetate 2:1), and the hydrochloride salt was prepared by means of 2 M hydrogen chloride solution in ether to give 92 mg (0.25 mmol/61%) of the analytically pure compound $\text{C}_{19}\text{H}_{14}\text{F}_2\text{NO}_3\cdot\text{HCl}$; MW 364; mp $206\text{--}207^{\circ}\text{C}$. ^1H NMR (acetone- d_6 , 400 MHz): δ 8.16 (dd, J = 8.1 Hz, 1.2 Hz, 1H), 8.11 (dd, J = 8.0 Hz, 7.5 Hz, 1H), 7.93 (dd, J = 8.5 Hz, 1.7 Hz, 1H), 7.90 (dd, J = 3.2 Hz, 1.7 Hz, 1H), 7.88–7.82 (m, 2H), 7.72 (ddd, J = 8.5 Hz, 4.5 Hz, 2.1 Hz, 1H), 7.31 (dd, J = 10.8 Hz, 8.5 Hz, 1H), 7.13 (t, J = 8.7 Hz, 1H). ^{13}C NMR (acetone- d_6 , 100 MHz): δ 192.3, 155.6, 155.4 (d, J = 249.3 Hz), 155.2 (d, J = 2.35 Hz), 152.6 (d, J = 240.0 Hz), 147.2 (d, J = 12.9 Hz), 145.5 (d, J = 13.3 Hz), 139.3, 134.2 (d, J = 3.3 Hz), 131.6 (d, J = 5.9 Hz), 124.8 (d, J = 7.47 Hz), 124.11 (d, J = 3.2 Hz), 123.0, 122.6, 121.3 (d, J = 4.2 Hz), 118.9 (d, J = 3.0 Hz), 116.6 (d, J = 19.2 Hz), 115.3 (d, J = 20.0 Hz). IR: 3380, 1660, 1598, 1582, 1524, 1430, 1235, 754 cm^{-1} . MS (ESI): 328 ($\text{M} + \text{H}$) $^{+}$. HPLC analysis: retention time = 11.63 min; peak area, 98.8%.

(4-Fluoro-3-hydroxyphenyl)[6-(2-fluoro-3-hydroxyphenyl)pyridin-2-yl]methanone Hydrochloride Salt (**9**). According to method E, the title compound was prepared by reaction of (4-fluoro-3-methoxyphenyl)[6-(2-fluoro-3-methoxyphenyl)pyridin-2-yl]-methanone (**9a**) (126 mg, 0.35 mmol, 1.0 equiv) with boron tribromide (3.5 mL, 3.5 mmol, 10 equiv) in dichloromethane (6.0 mL). The crude product was purified by column chromatography (cyclohexane/ethyl acetate 2:1), and the hydrochloride salt was prepared by means of 2 M hydrogen chloride solution in ether to give 117 mg (0.32 mmol/92%) of the analytically pure compound $\text{C}_{18}\text{H}_{11}\text{F}_2\text{NO}_3\cdot\text{HCl}$; MW 364; mp $198\text{--}199^{\circ}\text{C}$. ^1H NMR (DMSO- d_6 , 400 MHz): δ 8.15 (t, J = 7.8 Hz, 1H), 8.00 (ddd, J = 7.9 Hz, 2.1 Hz, 0.9 Hz, 1H), 7.92 (dd, J = 7.7 Hz, 1.0 Hz, 1H), 7.70–7.64 (m, 1H), 7.55 (ddd, J = 8.5 Hz, 4.5 Hz, 2.2 Hz, 1H), 7.31 (dd, J = 11.0 Hz, 8.5 Hz, 1H), 7.29–7.22 (m, 1H), 7.12–7.04 (m, 2H). ^{13}C NMR (DMSO- d_6 , 100 MHz): δ 191.7, 154.6, 154.3 (d, J = 125.5 Hz), 151.9, 149.2 (d, J = 146.2 Hz), 145.6 (d, J = 12.6 Hz), 144.9 (d, J = 12.4 Hz), 138.4, 132.5, 127.3 (d, J = 9.1 Hz), 126.7 (d, J = 8.1 Hz), 124.4 (d, J = 4.1 Hz), 123.3 (d, J = 7.5 Hz), 122.9, 120.2, 119.8 (d, J = 4.5 Hz), 118.5 (d, J = 3.2 Hz), 116.0 (d, J = 19.3 Hz). IR: 3155, 1655, 1593, 1481, 1293, 1225, 750 cm^{-1} . MS (ESI): 328 ($\text{M} + \text{H}$) $^{+}$. HPLC analysis: retention time = 10.82 min; peak area, 98.4%.

[6-(3-(*N,N*-Dimethylamino)-phenyl)pyridin-2-yl][4-fluoro-3-hydroxyphenyl]methanone Trifluoroacetate Salt (**17**). According to method E, the title compound was prepared by reaction of [6-(3-(*N,N*-dimethylamino)-phenyl)pyridin-2-yl] (4-fluoro-3-methoxyphenyl)methanone (**17a**) (105 mg, 0.30 mmol, 1.0 equiv) with boron tribromide (1.5 mL, 1.5 mmol, 5 equiv) in dichloro-

methane (4.0 mL). The crude product was purified by column chromatography (cyclohexane/ethyl acetate 5:1) and preparative HPLC (gradient water/acetonitrile/trifluoroacetic acid 80:20:0.1 \rightarrow 35:65:0.1, in 120 min) to give 75 mg (0.22 mmol/74%) of the analytically pure compound $C_{20}H_{17}FN_2O_3 \cdot TFA$; MW 450; mp 146–147 °C. 1H NMR (acetone- d_6 , 400 MHz [measured as base]): δ 9.06 (s, 1H), 8.17 (dd, J = 8.0 Hz, 1.0 Hz, 1H), 8.09 (t, J = 7.8 Hz, 1H), 8.00–7.92 (m, 2H), 7.82 (ddd, J = 8.5 Hz, 4.6 Hz, 2.1 Hz, 1H), 7.61 (dd, J = 2.5 Hz, 1.7 Hz, 1H), 7.40 (ddd, J = 7.7 Hz, 1.5 Hz, 0.9 Hz, 1H), 7.35–7.26 (m, 2H), 6.85 (ddd, J = 8.2 Hz, 2.7 Hz, 0.8 Hz, 1H), 2.99 (s, 6H). ^{13}C NMR (acetone- d_6 , 100 MHz [measured as base]): δ 192.1, 157.1, 155.3, 155.3 (d, J = 249.3 Hz), 152.1, 145.4, (d, J = 13.0 Hz), 139.6, 139.1, 134.3 (d, J = 3.4 Hz), 130.2, 124.9 (d, J = 7.6 Hz), 123.5, 123.3, 121.6 (d, J = 4.3 Hz), 116.5 (d, J = 19.2 Hz), 115.7, 114.5, 111.7, 40.6. IR: 3400, 1657, 1594, 1529, 1504, 1580, 1434, 764 cm^{-1} . MS (ESI): 337 (M + H) $^+$; HPLC analysis: retention time = 14.62 min; peak area, 98.9%.

2. Biological Methods. **2.1. 17β -HSD14 Inhibition Assay.** In a preliminary study compounds 1–5 were tested using a radioactive displacement assay (procedure A, % of inhibition at a concentration of 1 μ M). The newly synthesized compounds were tested using a fluorimetric assay (procedure B, as percent inhibition at 2 μ M, percent inhibition at the concentration of highest solubility of the compound and K_i). Procedures A and B use the same enzyme source, obtained from a bacterial culture. In procedure A, the assay was performed with a bacterial suspension and in procedure B with the purified form of the enzyme. Because of differences in assay conditions, only results within the same assay can be compared.

2.1.1. Enzyme Expression. The pET-based plasmid containing the coding sequences of the human gene HSD17B14 (using the T205 variant), with a N-terminal 6His-tag and a tobacco etch virus (TEV) protease cleavage site was used for the transfection of *Escherichia coli* BL21 (DE3) pLysS competent cells. The transformed bacteria cells were grown overnight in 100 mL of Terrific Broth medium containing 100 μ g/mL of ampicillin at 37 °C. Subsequently, 25 mL of the overnight culture were transferred in 1 L of the aforementioned medium and allowed to grow at 37 °C until an OD_{600} of 0.4 was reached. Then the temperature was lowered to 15 °C. When the culture reached the OD_{600} of 1.0 the cells were induced with 0.5 mM of IPTG. The bacteria cells were harvested by centrifugation and conserved at –80 °C overnight before proceeding with the purification.

2.1.2. Radioactive Assay Using Procedure A. The bacterial pellet obtained was resuspended in 100 mM phosphate buffer pH 7.7. The bacterial suspension was incubated with [3H]-E2 (final concentration: 18.3 nM) in the presence of the potential inhibitor in DMSO (final concentration in assay: 1 μ M, final DMSO concentration: 1%) at 37 °C. The enzymatic reaction was started by addition of NAD $^+$ (7.5 mM) and incubated for 2 h. The reaction was stopped by addition of 0.21 M ascorbic acid in a methanol/acetic acid mixture (99:1, v/v). Substrate and product were extracted from the reaction mixture by SPE (Strata C18-E columns from Phenomenex on a vacuum device). Separation and quantification of the radioactive steroids was performed with HPLC (Luna 5 μ m C18(2), 125 mm \times 4.00 mm from Phenomenex, with an acetonitrile/water mixture (43:57, v/v), flow rate 1 mL/min). Substrate conversion in % was calculated after integration of the product and substrate peaks. Inhibition was calculated based on conversion without potential inhibitor (DMSO only) which was set to 0% inhibition.

2.1.3. Enzyme Purification and Assay Using Procedure B. Enzyme purification: The cell pellet, previously obtained after IPTG induction, was resuspended in a buffer containing 50 mM Tris, 500 mM NaCl, 0.5 mM TCEP, 250 mM glucose, 1 mM NAD $^+$, 0.5% (v/v) Triton X-100, and cOmplete Protease Inhibitor Cocktail Tablet (Roche, Germany) adjusted at a pH of 8. The cells were disrupted with a high pressure homogenizer (EmulsiFlex-C5, AVESTIN, Mannheim, Germany) and the obtained homogenate was centrifuged at 17700g for 2 h at 4 °C. The supernatant was applied to a Ni-NTA column (5 mL HisTrap FF, GE Healthcare Life Sciences, Freiburg, Germany). Two washing steps were applied: in the first, to remove the DNA, a buffer

composed of 50 mM Tris and 1.5 M NaCl was run against the Ni-column. The second washing step was then performed with a buffer containing 50 mM Tris, 500 mM NaCl, 0.5 mM TCEP, 250 mM glucose, 0.25 mM NAD $^+$, and 21 mM imidazole to remove the unspecific binding proteins. The target protein was eluted by increasing the imidazole concentration in the buffer to 300 mM. TEV protease was added to the protein mixture to cleave the N-6His-tag, and the product solution was dialyzed overnight at 4 °C to reduce the imidazole concentration in the sample (50 mM Tris, 500 mM NaCl, 0.5 mM TCEP, 250 mM glucose, and 0.25 mM NAD $^+$). A second Ni-NTA column was used for separation of the TEV protease from the 17β -HSD14. In this step, the protein was collected from the flow through of the column, while the TEV protease remained on the column. With the goal to increase the purity of the protein, an additional purification step, using a size exclusion chromatography (Superdex 75 26/60, GE Healthcare Life Sciences, Freiburg, Germany) was performed with a running buffer comprising 50 mM Tris, 500 mM NaCl, 0.5 mM TCEP, and 250 mM glucose. To the isolated target protein, an NAD $^+$ solution 0.25 mM (batch for enzymatic assay) or 0.6 mM (batch for crystallization studies) was added. The protein solution was flash-frozen in liquid nitrogen and stored at –80 °C.

Fluorimetric assay using procedure B: The potential inhibitor (in DMSO, final DMSO concentration in assay: 1%) was added to a mixture of NAD $^+$ (1.2 mM) and E2 (32 μ M) in 100 mM phosphate buffer, pH 8. The enzymatic reaction was started by addition of the purified enzyme (1 mg/mL), and the production of the fluorescent NADH formed was measured continuously for 15 min at 25 °C. The fluorimetric assays were recorded on a Tecan Sapphire 2 (λ_{ex} at 340 nm and λ_{em} at 496 nm). The slit width for excitation was 7 nm and for emission 15 nm. Reactions were performed in 200 μ L volumes. The assay was run in 96-well plates in duplicate, each experiment resulting from three technical repeats. A linear relationship between product formation and reaction time was obtained. The slope of the progress curves was calculated by linear regression. The inhibitors do not show fluorescence at the concentrations used in the assay.

The K_i values were calculated using the Morrison equation³⁶ (see Supporting Information). For calculation, three constants were necessary: the substrate concentration (32 μ M), the K_m for 17β -HSD14 with this substrate E2 (6.18 μ M 2), and the concentration in active protein, which was determined experimentally for each experiment (3.2 or 3.3 μ M), using the procedure detailed by Copeland.³⁶ The fitting and data analysis was performed using GraphPad Prism 7.

2.2. 17β -HSD1 and 17β -HSD2 Inhibition Assay. 17β -HSD1 and 17β -HSD2 were partially purified from human placenta according to previously described procedures.⁴³ The enzyme was incubated with NADH (500 μ M) in the 17β -HSD1 assay and with NAD $^+$ (1500 μ M) in the 17β -HSD2 assay in the presence of the potential inhibitor in DMSO (final concentration in assay: 1 μ M, final DMSO concentration: 1%) at 37 °C. The enzymatic reaction was started by addition of the radioactive substrate (either [3H]-E1 (final concentration: 500 nM) in the 17β -HSD1 assay or [3H]-E2 (final concentration: 500 nM) in the 17β -HSD2 assay following a previously described procedure.⁵⁴ Separation and quantification of the radioactive steroids were performed by HPLC coupled to a radiodetector.

3. Protein Co-crystallization with Inhibitors 6, 9, 10, and 12. Protein activity was verified before performing the crystallization studies for each inhibitor. The cocrystallization of 17β -HSD14 in complex with the four inhibitors, 6, 9, 10, and 12, was performed by sitting drop vapor diffusion technique.

For the crystallization of inhibitors 6 and 9 in complex with the protein, an inhibitor stock solution in pure DMSO was added to the protein solution (9.5 mg/mL) containing 0.6 mM NAD $^+$ with a final inhibitor concentration of 0.8 mM and a DMSO concentration of 1%. Then 2 μ L of the mother liquor containing 0.1 M CHES, 1 M trisodium citrate, pH 9.5, was mixed with 2 μ L of the protein solution. After growing for 4 weeks at 18 °C, the crystals were exposed to a cryo buffer composed of the mother liquor with the addition of 20% (w/v) glucose and 0.4 mM of either 6 or 9 and subsequently flash-frozen in liquid nitrogen.

The inhibitors **10** and **12** were crystallized under different conditions. The same concentration of the protein containing 0.6 mM of NAD⁺ was mixed with inhibitor and DMSO to the final concentration of 4 mM of inhibitor and 5% DMSO. Afterward, 2 μ L of this protein–inhibitor solution were mixed with 2 μ L of mother liquor composed of 0.1 M HEPES, 20% (w/v) PEG6000, and 5% (v/v) DMSO, adjusted to pH 7.0. Crystals were grown at a temperature of 18 °C for 4 weeks. The crystals obtained with **10** were exposed to a cryo buffer obtained by the combination of mother liquor with the addition of 20% glucose and successively flash-frozen with liquid nitrogen. The crystals resulting from the complex with **12** were kept at room temperature.

Details about the crystallographic data collection, structure determination, and refinement can be found in the [Supporting Information](#).

■ ASSOCIATED CONTENT

■ Supporting Information

The Supporting Information is available free of charge on the ACS Publications website at DOI: 10.1021/acs.jmedchem.6b01436.

Chemistry: chemical methods; general procedures; detailed synthesis procedures and compound characterization; purity as evaluated by HPLC. Crystallography: data collection and processing; structure determination and refinement; crystallographic table. Physicochemical properties table of the inhibitors. Figures of modeled compounds. Morrison equation ([PDF](#))
Molecular formula strings ([CSV](#))

Accession Codes

Atomic coordinates and experimental data for the co-crystal structures of **6** (PDB 5L7T), **9** (PDB 5L7Y), **10** (PDB 5L7W), **12** (PDB 5EN4) in complex with 17 β -HSD14 will be released upon article publication.

■ AUTHOR INFORMATION

Corresponding Author

*Phone: +49 6421 28 22880. E-mail: marchais@staff.uni-marburg.de.

ORCID

Gerhard Klebe: 0000-0002-4913-390X

Sandrine Marchais-Oberwinkler: 0000-0001-9941-7233

Present Address

#Ahmed S. Abdelsamie Chemistry of Natural and Microbial Products Department, National Research Centre, Dokki, 12622 Cairo, Egypt.

Author Contributions

^ΔF.B. and N.B. contributed equally to the work. The manuscript was written through contributions of all authors. All authors have given approval to the final version of the manuscript.

Notes

The authors declare no competing financial interest.

■ ACKNOWLEDGMENTS

We thank Prof. R.W. Hartmann for providing access to the 17 β -HSD1 and 17 β -HSD2 inhibitors library. HIPS (Helmholtz Institute for Pharmaceutical Sciences, Saarbrücken) is acknowledged for providing the facilities to perform the 17 β -HSD1 and 17 β -HSD2 assays. We are grateful to the Deutsche Forschungsgemeinschaft (MA-5287/1-1 and KL-1204/15-1) for financial support. Part of the research leading to these results

has received funding from the European Community's Seventh Framework Programme (FP7/2007-2013) under BioStruct-X (grant agreement no. 283570). We are also thankful to the beamline staff at Elettra Sincrotrone (Trieste) and PETRA III (EMBL/DESY, Hamburg) for providing outstanding support during data collection. We also thank Laura Sinatra, Lukas Zygalski, Eric Kerste, Laura Toro, Paige Grant, and Andreas Schmidt for help during their internships. We are also grateful to ChemAxon Ltd. for providing free access to Marvin Sketch 15.9.14 for the pK_a calculations and to Dr. Peter Ertl for providing the free access to the PAINS-remover tool. We are grateful to the Chemical Computing Group Inc. for granting no cost academic licenses for their software.⁵⁵

■ ABBREVIATIONS USED

17 β -HSD14, 17 β -hydroxysteroid dehydrogenase type 14; SDR, short-chain dehydrogenase reductase; E2, estradiol; 5-diol, 5-androstene-3 β ,17 β -diol; E1, estrone; H-bond, hydrogen bond

■ REFERENCES

- (1) Lukacik, P.; Kavanagh, K. L.; Oppermann, U. Structure and Function of Human 17 β -Hydroxysteroid Dehydrogenases. *Mol. Cell. Endocrinol.* **2006**, *248*, 61–71.
- (2) Lukacik, P.; Keller, B.; Bunkoczi, G.; Kavanagh, K. L.; Lee, W. H.; Hwa Lee, W.; Adamski, J.; Oppermann, U. Structural and Biochemical Characterization of Human Orphan DHRS10 Reveals a Novel Cytosolic Enzyme with Steroid Dehydrogenase Activity. *Biochem. J.* **2007**, *402*, 419–427.
- (3) Sivik, T.; Vikingsson, S.; Gréen, H.; Jansson, A. Expression Patterns of 17 β -Hydroxysteroid Dehydrogenase 14 in Human Tissues. *Horm. Metab. Res.* **2012**, *44*, 949–956.
- (4) Haeseleer, F.; Palczewski, K. Short-Chain Dehydrogenases/Reductases in Retina. *Methods Enzymol.* **2000**, *316*, 372–383.
- (5) Bertolotti, N.; Braun, F.; Lepage, M.; Möller, G.; Adamski, J.; Heine, A.; Klebe, G.; Marchais-Oberwinkler, S. New Insights into Human 17 β -Hydroxysteroid Dehydrogenase Type 14: First Crystal Structures in Complex with a Steroidal Ligand and with a Potent Non-Steroidal Inhibitor. *J. Med. Chem.* **2016**, *59*, 6961–6967.
- (6) Marchais-Oberwinkler, S.; Henn, C.; Möller, G.; Klein, T.; Negri, M.; Oster, A.; Spadaro, A.; Werth, R.; Wetzel, M.; Xu, K.; Frotscher, M.; Hartmann, R. W.; Adamski, J. 17 β -Hydroxysteroid Dehydrogenases (17 β -HSDs) as Therapeutic Targets: Protein Structures, Functions, and Recent Progress in Inhibitor Development. *J. Steroid Biochem. Mol. Biol.* **2011**, *125*, 66–82.
- (7) Frotscher, M.; Ziegler, E.; Marchais-Oberwinkler, S.; Kruchten, P.; Neugebauer, A.; Fetzter, L.; Scherer, C.; Müller-Vieira, U.; Messinger, J.; Thole, H.; Hartmann, R. W. Design, Synthesis, and Biological Evaluation of (Hydroxyphenyl)naphthalene and -Quinoline Derivatives: Potent and Selective Nonsteroidal Inhibitors of 17 β -Hydroxysteroid Dehydrogenase Type 1 (17 β -HSD1) for the Treatment of Estrogen-Dependent Diseases. *J. Med. Chem.* **2008**, *51*, 2158–2169.
- (8) Bey, E.; Marchais-Oberwinkler, S.; Negri, M.; Kruchten, P.; Oster, A.; Klein, T.; Spadaro, A.; Werth, R.; Frotscher, M.; Birk, B.; Hartmann, R. W. New Insights into the SAR and Binding Modes of Bis(hydroxyphenyl)thiophenes and -Benzenes: Influence of Additional Substituents on 17 β -Hydroxysteroid Dehydrogenase Type 1 (17 β -HSD1) Inhibitory Activity and Selectivity. *J. Med. Chem.* **2009**, *52*, 6724–6743.
- (9) Poirier, D. Inhibitors of 17 Beta-Hydroxysteroid Dehydrogenases. *Curr. Med. Chem.* **2003**, *10*, 453–477.
- (10) Poirier, D.; Boivin, R. P.; Tremblay, M. R.; Bérubé, M.; Qiu, W.; Lin, S.-X. Estradiol-Adenosine Hybrid Compounds Designed to Inhibit Type 1 17 β -Hydroxysteroid Dehydrogenase. *J. Med. Chem.* **2005**, *48*, 8134–8147.
- (11) Maltais, R.; Ayan, D.; Trottier, A.; Barbeau, X.; Lagüe, P.; Bouchard, J.-E.; Poirier, D. Discovery of a Non-Estrogenic Irreversible

- Inhibitor of 17 β -Hydroxysteroid Dehydrogenase Type 1 from 3-Substituted-16 β -(M-Carbamoylbenzyl)-Estradiol Derivatives. *J. Med. Chem.* **2014**, *57*, 204–222.
- (12) Maltais, R.; Trottier, A.; Barbeau, X.; Lagüe, P.; Perreault, M.; Thériault, J.-F.; Lin, S.-X.; Poirier, D. Impact of Structural Modifications at Positions 13, 16 and 17 of 16 β -(M-Carbamoylbenzyl)-Estradiol on 17 β -Hydroxysteroid Dehydrogenase Type 1 Inhibition and Estrogenic Activity. *J. Steroid Biochem. Mol. Biol.* **2016**, *161*, 24–35.
- (13) Lilienkamp, A.; Karkola, S.; Alho-Richmond, S.; Koskimies, P.; Johansson, N.; Huhtinen, K.; Vihko, K.; Wähälä, K. Synthesis and Biological Evaluation of 17beta-Hydroxysteroid Dehydrogenase Type 1 (17beta-HSD1) Inhibitors Based on a thieno[2,3-D]pyrimidin-4(3H)-One Core. *J. Med. Chem.* **2009**, *52*, 6660–6671.
- (14) Allan, G. M.; Lawrence, H. R.; Cornet, J.; Bubert, C.; Fischer, D. S.; Vicker, N.; Smith, A.; Tutill, H. J.; Purohit, A.; Day, J. M.; Mahon, M. F.; Reed, M. J.; Potter, B. V. L. Modification of Estrone at the 6, 16, and 17 Positions: Novel Potent Inhibitors of 17beta-Hydroxysteroid Dehydrogenase Type 1. *J. Med. Chem.* **2006**, *49*, 1325–1345.
- (15) Allan, G. M.; Vicker, N.; Lawrence, H. R.; Tutill, H. J.; Day, J. M.; Huchet, M.; Ferrandis, E.; Reed, M. J.; Purohit, A.; Potter, B. V. L. Novel Inhibitors of 17beta-Hydroxysteroid Dehydrogenase Type 1: Templates for Design. *Bioorg. Med. Chem.* **2008**, *16*, 4438–4456.
- (16) Schuster, D.; Nashev, L. G.; Kirchmair, J.; Laggner, C.; Wolber, G.; Langer, T.; Odermatt, A. Discovery of Nonsteroidal 17beta-Hydroxysteroid Dehydrogenase 1 Inhibitors by Pharmacophore-Based Screening of Virtual Compound Libraries. *J. Med. Chem.* **2008**, *51*, 4188–4199.
- (17) Gobec, S.; Brožič, P.; Lanišnik Rižner, T. Inhibitors of 17beta-Hydroxysteroid Dehydrogenase Type 1. *Curr. Med. Chem.* **2008**, *15*, 137–150.
- (18) Starčević, Š.; Brožič, P.; Turk, S.; Cesar, J.; Lanišnik Rižner, T.; Gobec, S. Synthesis and Biological Evaluation of (6- and 7-Phenyl) Coumarin Derivatives as Selective Nonsteroidal Inhibitors of 17 β -Hydroxysteroid Dehydrogenase Type 1. *J. Med. Chem.* **2011**, *54*, 248–261.
- (19) Wetzel, M.; Marchais-Oberwinkler, S.; Hartmann, R. W. 17 β -HSD2 Inhibitors for the Treatment of Osteoporosis: Identification of a Promising Scaffold. *Bioorg. Med. Chem.* **2011**, *19*, 807–815.
- (20) Xu, K.; Al-Soud, Y. A.; Wetzel, M.; Hartmann, R. W.; Marchais-Oberwinkler, S. Triazole Ring-Opening Leads to the Discovery of Potent Nonsteroidal 17 β -Hydroxysteroid Dehydrogenase Type 2 Inhibitors. *Eur. J. Med. Chem.* **2011**, *46*, 5978–5990.
- (21) Stoffel-Wagner, B.; Watzka, M.; Steckelbroeck, S.; Schramm, J.; Bidlingmaier, J. F.; Klingmüller, D. Expression of 17beta-Hydroxysteroid Dehydrogenase Types 1, 2, 3 and 4 in the Human Temporal Lobe. *J. Endocrinol.* **1999**, *160*, 119–126.
- (22) Veber, D. F.; Johnson, S. R.; Cheng, H.-Y.; Smith, B. R.; Ward, K. W.; Kopple, K. D. Molecular Properties That Influence the Oral Bioavailability of Drug Candidates. *J. Med. Chem.* **2002**, *45*, 2615–2623.
- (23) Lipinski, C. A.; Lombardo, F.; Dominy, B. W.; Feeney, P. J. Experimental and Computational Approaches to Estimate Solubility and Permeability in Drug Discovery and Development Settings. *Adv. Drug Delivery Rev.* **2001**, *46*, 3–26.
- (24) Cai, D.; Hughes, D. L.; Verhoeven, T. R. A Study of the Lithiation of 2,6-Dibromopyridine with Butyllithium, and Its Application to Synthesis of L-739,010. *Tetrahedron Lett.* **1996**, *37*, 2537–2540.
- (25) Miyaura, N.; Suzuki, A. Palladium-Catalyzed Cross-Coupling Reactions of Organoboron Compounds. *Chem. Rev.* **1995**, *95*, 2457–2483.
- (26) Amb, C. M.; Rasmussen, S. C. 6,6'-Dibromo-4,4'-Di-(hexoxymethyl)-2,2'-Bipyridine: A New Solubilizing Building Block for Macromolecular and Supramolecular Applications. *J. Org. Chem.* **2006**, *71*, 4696–4699.
- (27) Bolliger, J. L.; Oberholzer, M.; Frech, C. M. Access to 2-Aminopyridines – Compounds of Great Biological and Chemical Significance. *Adv. Synth. Catal.* **2011**, *353*, 945–954.
- (28) Maiti, D.; Buchwald, S. L. Cu-Catalyzed Arylation of Phenols: Synthesis of Sterically Hindered and Heteroaryl Diaryl Ethers. *J. Org. Chem.* **2010**, *75*, 1791–1794.
- (29) Castro, A.; Depew, K.; Grogan, M.; Holson, E.; Hopkins, B.; Johannes, C.; Keaney, G.; Koney, N.; Liu, T.; Mann, D.; Nevalainen, M.; Peluso, S.; Perez, L.; Snyder, D.; Tibbitts, T. Compounds and Methods for Inhibiting the Interaction of Bcl Proteins with Binding Partners. WO2008024337 (A2), February 28, 2008.
- (30) Eckelbarger, J.; Epp, J.; Fischer, L.; Lowe, C.; Petkus, J.; Roth, J.; Satchivi, N.; Schmitzer, P.; Siddall, T. 4-Amino-6-(heterocyclic)-picolates and 6-Amino-2-(heterocyclic)pyrimidine-4-carboxylates and Their Use As Herbicides. WO2014151008 (A1), September 25, 2014.
- (31) Duan, X.-F.; Li, X.-H.; Li, F.-Y.; Huang, C.-H. A Concise Synthesis of 2,4-Disubstituted Pyridines: A Convenient Synthesis of 2-Bromo-4-Iodopyridine via Halogen Dance and Its Successive One-Pot Disubstitutions. *Synthesis* **2004**, *2004*, 2614–2616.
- (32) Molinspiration; Cheminformatics on the Web, 2016; <http://www.molinspiration.com/> (accessed April 18, 2016).
- (33) Pajouhesh, H.; Lenz, G. R. Medicinal Chemical Properties of Successful Central Nervous System Drugs. *NeuroRx* **2005**, *2*, 541–553.
- (34) Morrison, J. F. The Slow-Binding and Slow, Tight-Binding Inhibition of Enzyme-Catalysed Reactions. *Trends Biochem. Sci.* **1982**, *7*, 102–105.
- (35) Morrison, J. F. Kinetics of the Reversible Inhibition of Enzyme-Catalysed Reactions by Tight-Binding Inhibitors. *Biochim. Biophys. Acta* **1969**, *185*, 269–286.
- (36) Copeland, R. A. *Enzymes: A Practical Introduction to Structure, Mechanism, and Data Analysis*, 2nd ed.; Wiley-VCH: New York, 2000.
- (37) Baell, J. B.; Holloway, G. A. New Substructure Filters for Removal of Pan Assay Interference Compounds (PAINS) from Screening Libraries and for Their Exclusion in Bioassays. *J. Med. Chem.* **2010**, *53*, 2719–2740.
- (38) False Positive Remover; Web-GCB13, 2010; http://Cbligand.org/PAINS/Search_struct.php (accessed July 8, 2016).
- (39) Schweigert, N.; Zehnder, A. J. B.; Eggen, R. I. L. Chemical Properties of Catechols and Their Molecular Modes of Toxic Action in Cells, from Microorganisms to Mammals. *Environ. Microbiol.* **2001**, *3*, 81–91.
- (40) Emsley, P.; Lohkamp, B.; Scott, W. G.; Cowtan, K. Features and Development of Coot. *Acta Crystallogr., Sect. D: Biol. Crystallogr.* **2010**, *66*, 486–501.
- (41) The PyMOL Molecular Graphics System, version 1.7.x; Schrödinger, LLC, 2015.
- (42) Eisenberg, D.; Schwarz, E.; Komaromy, M.; Wall, R. Analysis of Membrane and Surface Protein Sequences with the Hydrophobic Moment Plot. *J. Mol. Biol.* **1984**, *179*, 125–142.
- (43) Kruchten, P.; Werth, R.; Marchais-Oberwinkler, S.; Frotscher, M.; Hartmann, R. W. Development of a Biological Screening System for the Evaluation of Highly Active and Selective 17beta-HSD1-Inhibitors as Potential Therapeutic Agents. *Mol. Cell. Endocrinol.* **2009**, *301*, 154–157.
- (44) Kruchten, P. Entwicklung eines Screeningsystems zur Identifizierung hochaktiver und selektiver Hemmstoffe der 17 β -Hydroxysteroid-Dehydrogenase Typ 1 (17 β HSD1). Dissertation, Saarland University, Saarbrücken, 2009.
- (45) Wetzel, M.; Gargano, E. M.; Hinsberger, S.; Marchais-Oberwinkler, S.; Hartmann, R. W. Discovery of a New Class of Bicyclic Substituted Hydroxyphenylmethanones as 17 β -Hydroxysteroid Dehydrogenase Type 2 (17 β -HSD2) Inhibitors for the Treatment of Osteoporosis. *Eur. J. Med. Chem.* **2012**, *47*, 1–17.
- (46) Hwang, C.-C.; Chang, Y.-H.; Hsu, C.-N.; Hsu, H.-H.; Li, C.-W.; Pon, H.-I. Mechanistic Roles of Ser-114, Tyr-155, and Lys-159 in 3 α -Hydroxysteroid Dehydrogenase/Carbonyl Reductase from *Comamonas testosteroni*. *J. Biol. Chem.* **2005**, *280*, 3522–3528.
- (47) Bissantz, C.; Kuhn, B.; Stahl, M. A Medicinal Chemist's Guide to Molecular Interactions. *J. Med. Chem.* **2010**, *53*, S061–S084.

- (48) Michiels, P. J. A.; Ludwig, C.; Stephan, M.; Fischer, C.; Möller, G.; Messinger, J.; van Dongen, M.; Thole, H.; Adamski, J.; Günther, U. L. Ligand-Based NMR Spectra Demonstrate an Additional Phytoestrogen Binding Site for 17 β -Hydroxysteroid Dehydrogenase Type 1. *J. Steroid Biochem. Mol. Biol.* **2009**, *117*, 93–98.
- (49) Bey, E.; Marchais-Oberwinkler, S.; Negri, M.; Kruchten, P.; Oster, A.; Klein, T.; Spadaro, A.; Werth, R.; Frotscher, M.; Birk, B.; Hartmann, R. W. New Insights into the SAR and Binding Modes of Bis(hydroxyphenyl)thiophenes and -Benzenes: Influence of Additional Substituents on 17 β -Hydroxysteroid Dehydrogenase Type 1 (17 β -HSD1) Inhibitory Activity and Selectivity. *J. Med. Chem.* **2009**, *52*, 6724–6743.
- (50) Perspicace, E.; Giorgio, A.; Carotti, A.; Marchais-Oberwinkler, S.; Hartmann, R. W. Novel N-Methylsulfonamide and Retro-N-Methylsulfonamide Derivatives as 17 β -Hydroxysteroid Dehydrogenase Type 2 (17 β -HSD2) Inhibitors with Good ADME-Related Physicochemical Parameters. *Eur. J. Med. Chem.* **2013**, *69*, 201–215.
- (51) Gottlieb, H. E.; Kotlyar, V.; Nudelman, A. NMR Chemical Shifts of Common Laboratory Solvents as Trace Impurities. *J. Org. Chem.* **1997**, *62* (21), 7512–7515.
- (52) Andrus, M. B.; Meredith, E. L.; Sekhar, B. B. V. S. Synthesis of the Left-Hand Portion of Geldanamycin Using an Anti Glycolate Aldol Reaction. *Org. Lett.* **2001**, *3*, 259–262.
- (53) Hicks, R. G.; Koivisto, B. D.; Lemaire, M. T. Synthesis of Multitopic Verdazyl Radical Ligands. Paramagnetic Supramolecular Synthons. *Org. Lett.* **2004**, *6*, 1887–1890.
- (54) Kruchten, P.; Werth, R.; Marchais-Oberwinkler, S.; Bey, E.; Ziegler, E.; Oster, A.; Frotscher, M.; Hartmann, R. W. Development of Biological Assays for the Identification of Selective Inhibitors of Estradiol Formation from Estrone in Rat Liver Preparations. *C. R. Chim.* **2009**, *12*, 1110–1116.
- (55) *Molecular Operating Environment (MOE)*, 2013.08; Chemical Computing Group Inc.: 1010 Sherbooke St. West, Suite #910, Montreal, QC, Canada, H3A 2R7, 2016.

3.2.IV Inhibitors of 17 β -hydroxysteroid dehydrogenase type 1, 2 and 14: Structures, biological activities and future challenges

Mohamed Salah*, Ahmed S. Abdelsamie*, and Martin Frotscher

Reprinted with permission *Mol. Cell. Endocrinol.* 2018.

DOI: 10.1016/j.mce.2018.10.001

Copyright (2018) ELSEVIER

* These authors contributed equally

Publication F

Contribution Report

The author collected the data for all 17 β -HSD1 inhibitors from literature, and significantly contributed in the selection of the represented candidates of each class. He wrote this part in the review and contributed in the other parts.



Contents lists available at ScienceDirect

Molecular and Cellular Endocrinology

journal homepage: www.elsevier.com

Inhibitors of 17 β -hydroxysteroid dehydrogenase type 1, 2 and 14: Structures, biological activities and future challenges

Mohamed Salah^{a, 1}, Ahmed S. Abdelsamie^{b, c, 1}, Martin Frotscher^{a, *}^a Pharmaceutical and Medicinal Chemistry, Saarland University, Campus C23, D-66123, Saarbrücken, Germany^b Department of Drug Design and Optimization, Helmholtz Institute for Pharmaceutical Research Saarland (HIPS), Campus E81, 66123, Saarbrücken, Germany^c Chemistry of Natural and Microbial Products Department, National Research Centre, Dokki, 12622, Cairo, Egypt

ARTICLE INFO

Keywords:

Steroidogenic enzymes
Hydroxysteroid dehydrogenases
Estrogen dependent diseases
Enzyme inhibitors

ABSTRACT

During the past 25 years, the modulation of estrogen action by inhibition of 17 β -hydroxysteroid dehydrogenase types 1 and 2 (17 β -HSD1 and 17 β -HSD2), respectively, has been pursued intensively. In the search for novel treatment options for estrogen-dependent diseases (EDD) and in order to explore estrogenic signaling pathways, a large number of steroidal and nonsteroidal inhibitors of these enzymes has been described in the literature. The present review gives a survey on the development of inhibitor classes as well as the structural formulas and biological properties of their most interesting representatives. In addition, rationally designed dual inhibitors of both 17 β -HSD1 and steroid sulfatase (STS) as well as the first inhibitors of 17 β -HSD14 are covered.

1. Introduction

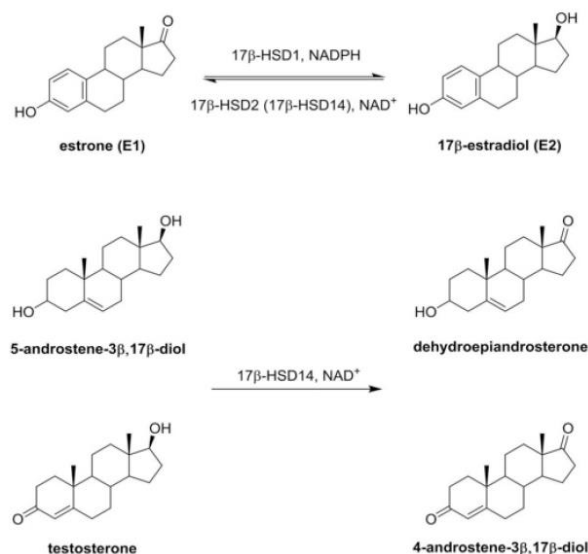
17 β -Hydroxysteroid dehydrogenase type 1 and type 2 (17 β -HSD1 and 17 β -HSD2; EC 1.1.1.62) are oxidoreductases belonging to the short chain dehydrogenase-reductase (SDR) family which interconvert ketones and their corresponding secondary alcohols. Their names are derived from the fact that they catalyze oxidoreductions in the 17 β -position of steroidal substrates, under consumption of the natural cosubstrates NADPH (17 β -HSD1) and NAD⁺ (17 β -HSD2). Thus, 17 β -HSD1 (SDR nomenclature: SDR28C1) catalyzes the reduction of the weakly estrogenic estrone (E1) to the most potent estrogen 17 β -estradiol (E2, Scheme 1) which plays a central role in the etiology of estrogen dependent diseases (EDD). 17 β -HSD2 (SDR2C9), on the other hand, catalyzes the reverse reaction, namely the inactivation of E2 by oxidation to E1. It can therefore be considered as a physiological adversary of the type 1 enzyme. Besides, 17 β -HSD2 is involved in the deactivation of androgens (testosterone, T) and the activation of progestins. Both E1 and E2 exert their physiological effects predominantly by transactivation of the nuclear estrogen receptors (ER) α and β , and the weaker estrogenicity of E1 is due to its lower ER-affinity compared to that of E2.

17 β -HSD1 and 2 display an intracrine mode of action, i.e. they interconvert estrogens within the cells where the estrogenic effects are exerted (Labrie, 1991). The interplay of these two enzymes modulates

estrogen action on a pre-receptor level (Penning, 1997; Duax et al., 2000), depending on the requirements of the cell. 17 β -HSD1 and 2 may therefore be seen as “molecular switches”, as they increase (switch on) and decrease (switch off) ligand occupancy and concomitant transactivation of the ER, respectively (Labrie et al., 2000; Penning, 2003).

In case of EDD, the interplay of 17 β -HSD1 and 2 is disrupted, giving rise to an imbalance between estrogen activation and inactivation. Thus, an increased E2/E1 ratio and high levels of 17 β -HSD1 mRNA are indicative for a crucial role of 17 β -HSD1 e.g. in endometriosis (Šmuc et al., 2007; Huhtinen et al., 2012), endometrial hyperplasia (Saloniemi et al., 2010), endometrial cancer (Cornel et al., 2012, 2017), breast cancer (Jansson, 2009), ovarian tumor (Blomquist et al., 2002) and uterine leiomyoma (Kasai et al., 2004). Inhibition of 17 β -HSD1 is therefore considered as a valuable therapeutic approach for the treatment of these diseases. The validity of this concept is supported by several observations: (1) 17 β -HSD1 inhibition resulted in a decrease of E2 levels in endometriotic specimens (Delvoux et al., 2014); (2) 17 β -HSD1 inhibitors reversed estrogen-induced endometrial hyperplasia in transgenic mice (Saloniemi et al., 2010); (3) Inhibition of 17 β -HSD1 resulted in the reduction of E1-stimulated tumor cell growth *in vitro* and in animal models, suggesting that this target is eligible for the treatment of breast cancer (Husen et al., 2006; Kruchten et al., 2009). The fact that the enzyme catalyzes the final step in estrogen activation

^{*} Corresponding author.Email address: m.frotscher@mx.uni-saarland.de (M. Frotscher)¹ Authors contributed equally.



Scheme 1. Steroid hormone conversions catalyzed by 17β-HSD1, 17β-HSD2 and 17β-HSD14.

makes this approach particularly interesting as it may offer the prospect of few side effects. Osteoporosis is an age-related disease which is connected to decreasing amounts of E2 and T (Vanderschueren et al., 2008). Estrogen replacement therapy proved to be an efficient treatment but led to adverse effects and is no longer recommended. The fact that 17β-HSD2 is present in osteoblasts (Dong et al., 1998) and decreases E2- and T-levels by oxidation to the ketones makes 17β-HSD2 inhibition a promising approach for the treatment of osteoporosis. In an *in vivo* monkey model, a 17β-HSD2 inhibitor led to a decrease of bone resorption and maintenance of bone formation, validating the therapeutic concept (Bagi et al., 2008). As compared to established endocrine treatments of EDD, inhibitors of 17β-HSD1 and 17β-HSD2 should have the advantage to exert little influence on systemic estrogen levels, offering the prospect of fewer side effects.

17β-HSD14 (SDR47C19; synonyms: retSDR3, DHRS10) is another member of the SDR family and the last 17β-HSD that has been identified. *In vitro*, it NAD⁺-dependently oxidizes E2 to E1 (Lukacik et al., 2007) - and thus shows analogy to 17β-HSD2. Moreover, it was found to catalyze the formation of dehydroepiandrosterone and 4-androstene-3,17-dione from 5-androstene-3β,17β-diol and testosterone, respectively (Scheme 1). The physiological role and the native substrate(s) of this enzyme, however, are yet unknown. Therefore, it is still unclear whether this enzyme may serve as a drug target in the future. Recently, the 3D-structures of the cytosolic protein as holo form and as ternary complexes with E1 and with a nonsteroidal inhibitor have been described (Bertoletti et al., 2016; Braun et al., 2016).

2. Inhibitors

Inhibitors of 17β-HSD1 and 2 have been reviewed previously (Poirier, 2003, 2009; Deluca et al., 2005; Brožic et al., 2008; Day et al., 2008, 2010; Marchais-Oberwinkler et al., 2011a). In the following we give a comprehensive overview on inhibitors identified, including recent developments.

2.1. Natural products and parabens as inhibitors of 17β-HSDs

The literature covering effects of phytoestrogens on 17β-HSD enzymes has been reviewed previously (Deluca et al., 2005). In a more recent publication, inhibitory activities of different flavones and related compounds on 17β-HSD enzymes from the fungus *Cochliobolus lunatus* (17β-HSDcl) were reported (Kristan et al., 2005). Flavones hydroxylated at positions 3, 5 and 7 as well as 5-methoxyflavone (Fig. 1, compounds 1–5) led to the strongest inhibition of estradiol oxidation, showing IC₅₀ values in the range of 0.4–1 μM. Their ability to inhibit the reverse reaction (reduction of estrone) was less pronounced (IC₅₀ values from 1.2 μM to 7.4 μM). Coumestrol and kaempferol (Fig. 1, compounds 6 and 7a, respectively) inhibited both reactions unselectively (IC₅₀ values between 2.5 μM and 3.9 μM).

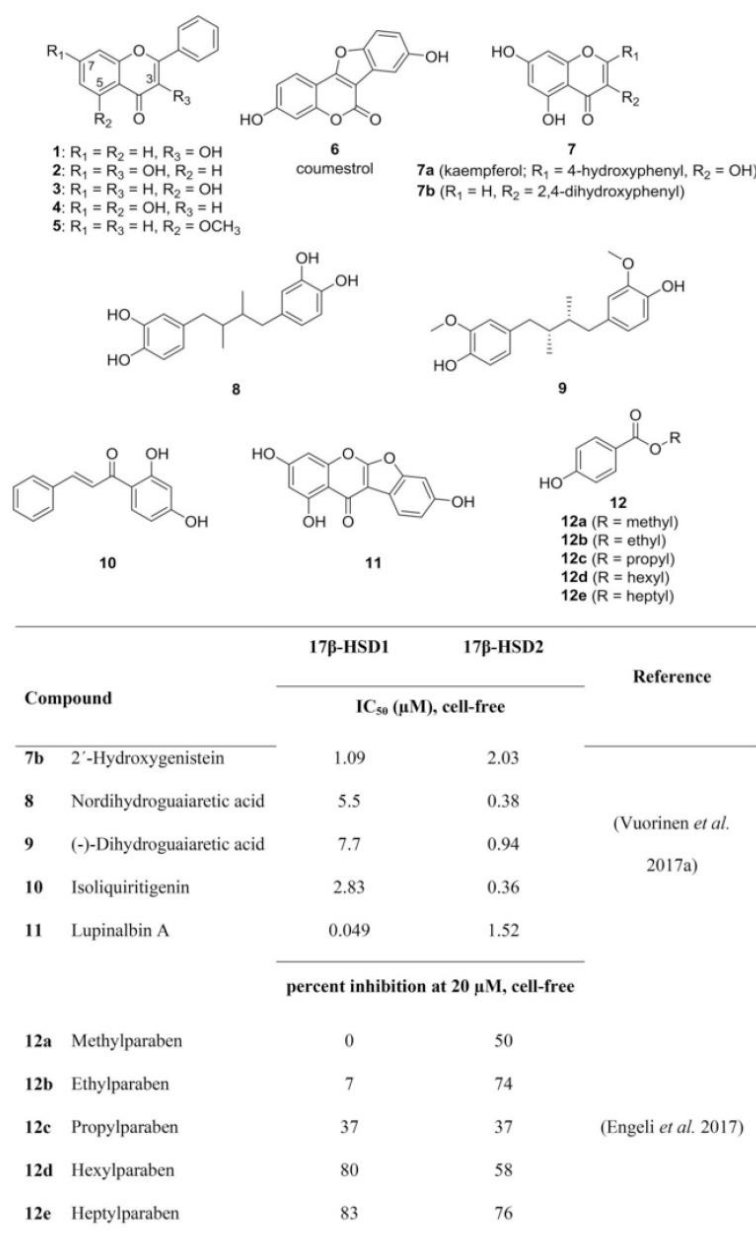
Vuorinen et al. applied a pharmacophore model based on 17β-HSD2 inhibitors to a virtual screening of various databases containing natural products in order to discover new lead structures from nature (Vuorinen et al., 2017a). The work resulted in the identification of new 17β-HSD2 inhibitors and provided information on the binding pocket of the enzyme. The structures and inhibitory data of the most potent compounds 7b and 8–11 are given in Fig. 1.

Parabens (*p*-hydroxybenzoic acid esters) are effective preservatives with high human exposure. In order to investigate possible estrogenic effects exerted by parabens and parabene-like compounds, Engeli et al. addressed their potential interference with local estrogen metabolism by inhibiting 17β-HSD1 and 17β-HSD2 (Engeli et al., 2017). All parabens under investigation moderately inhibited 17β-HSD2. Inhibition of 17β-HSD1 was size-dependent, whereby hexyl- and heptylparaben (Fig. 1, compounds 12d and 12e) were most active. The results suggest that depending on the tissue expression of 17β-HSD1 and 17β-HSD2, parabens might exert pro-estrogenic or anti-estrogenic effects. As smaller parabens (methyl-, ethyl-, propylparaben; compounds 12a–c) are more commonly used than larger parabens, disruption of estrogenic effects through inhibition of 17β-HSD2 is more likely to occur than through inhibition of 17β-HSD1. Regarding the rapid metabolism of the compounds to the inactive *p*-hydroxybenzoic acid (compound 12, R = H), it needs to be determined whether the low micromolar paraben concentrations required for effective disturbance of estrogen action can be reached in target cells *in vivo*.

2.2. Inhibitors of 17β-HSD1

2.2.1. Steroidal inhibitors of 17β-HSD1

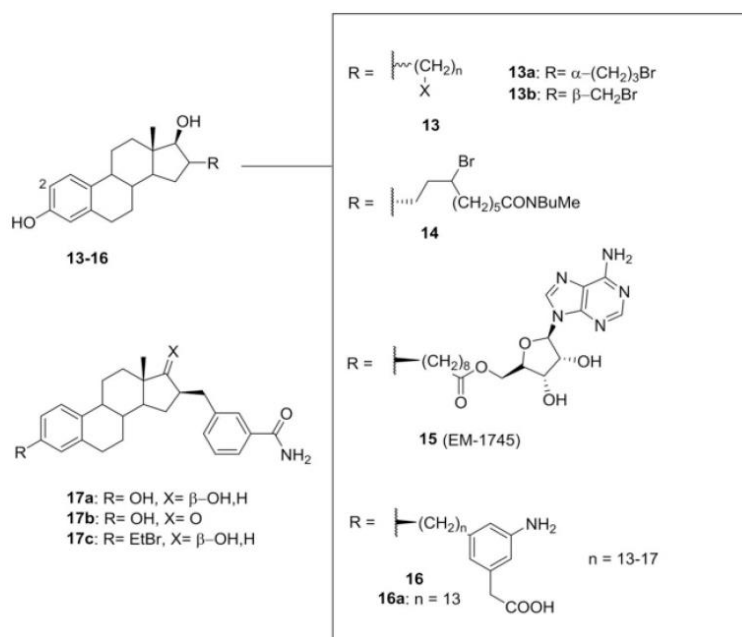
C16 substituted E2 derivatives. Since the 1990s, the Poirier group has been working on C16 substituted estradiol derivatives as inhibitors of 17β-HSD1. First design approaches consisted in the introduction of bromo-substituted aliphatic chains with various lengths (*n* = 1–7) and stereochemistry (*α* or *β*; Fig. 2, structure 13) in the 16-position of the steroidal skeleton (Tremblay et al., 1995; Tremblay and Poirier, 1998; Rouillard et al., 2008). In a cell-free assay, the most potent compounds 13a and 13b displayed IC₅₀ values of 1.3 μM and 1.2 μM, respectively (Rouillard et al., 2008). However, the compounds were found to exert proliferative estrogenic-like effects on the human estrogen dependent breast cancer cell lines ZR-75-1 (Tremblay et al., 1995) and T47D (Rouillard et al., 2008). Two strategies were pursued to eliminate the estrogenic effect: the first strategy consisted in exchanging the bromine atom with chlorine or hydroxy and the introduction of a methoxy group in position 2 (compounds not shown). These modifications, however, reduced potency, and the compounds displayed estrogenic effects towards T47D cells (Rouillard et al., 2008). The second strategy comprised the introduction of a bromopropyl-linker bearing a bulky alkylamide group in the 16α position of estradiol (Fig. 2, compound 14). This modification eliminated estrogenic activity on ZR-75-1 cells but on

Fig. 1. Natural products and parabens showing inhibition of 17 β -HSD1 and 17 β -HSD2.

the expense of inhibitory potency (IC₅₀ under cell-free conditions: 10.4 μ M). Interestingly, compound **14** was found to have antiestrogenic activity as it was able to neutralize the effect of estradiol on ZR-75-1 cells, so it can be considered as a dual-action inhibitor (Pelletier and Poirier, 1996).

In 2002 the same group successfully enhanced the inhibitory activity of C16-substituted E2 derivatives by designing and synthesizing a bifunctional hybrid inhibitor, combining an E2 and an adenosine moiety in a single compound (Fig. 2, EM-1745, compound **15**) which allows for simultaneous occupation of both the substrate and the co-factor binding site (Qiu et al., 2002). Compound **15** showed high inhibitory activity against purified 17 β -HSD1 (IC₅₀ value: 52 nM) (Poirier

et al., 2005). However, two major drawbacks were reported for **15** when used in intact cells or in vivo models, namely cell membrane permeation problems and rapid metabolism, most probably at the ester bond site (Fournier et al., 2008). To overcome the stability problem, two strategies were pursued that focused on simplifying the complex structure of **15**. The first led to a series of compounds which contain a *meta*-substituted aniline as a mimic of the adenosine moiety while the ester bond was replaced by a carbon-carbon bond (Fig. 2, compounds **16**) (Bérubé and Poirier, 2004). The most active compound of this structurally simplified series contained an alkyl chain with 13 carbon atoms (i.e. n = 13) and was slightly less active than compound **15** (Bérubé and Poirier, 2009). The second approach consisted in the par-



| Compound | 17 β -HSD1 | Reference |
|-----------------------|------------------------------|--------------------------------|
| | IC ₅₀ , cell-free | |
| 13a | 1.3 μ M | (Rouillard <i>et al.</i> 2008) |
| 13b | 1.2 μ M | |
| 14 | 10.4 μ M | (Pelletier & Poirier 1996) |
| 15^a | 52 nM | (Poirier <i>et al.</i> 2005) |
| | 8 nM | |
| 16a | 56 nM | (Bérubé & Poirier 2009) |
| 17a | 44 nM in T47D cells | (Laplante <i>et al.</i> 2008) |
| 17b | 171 nM in T47D cells | |
| 17c | 68 nM in T47D cells | (Maltais <i>et al.</i> 2011) |

^aDifferent IC₅₀ values reported in the cited references.

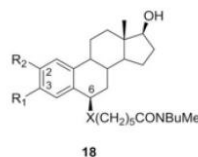
Fig. 2. Steroidal inhibitors of 17 β -HSD1: C16 substituted E2 derivatives.

allel solid phase synthesis of diverse libraries of 16 β -substituted E2 derivatives (not shown) that could serve as bisubstrate inhibitors, however, none of these libraries resulted in compounds that could reach the strong activity of compound **15** (Bérubé *et al.*, 2010).

The introduction of an *m*-carbamoylbenzyl substituent at the 16 β positions of E2 and E1, respectively, led to the highly potent compounds **17a** and **17b** (Fig. 2) with good cellular permeability, displaying IC₅₀ values of 44 and 171 nM, respectively, in an assay using intact T47D cells. In cellular proliferation assays (T47D cells), **17a** was able to inhibit E1-mediated proliferation to a certain extent, without returning to the basal levels of proliferation as **17a** was found to have estrogenic potency itself (Laplante *et al.*, 2008; Mazumdar *et al.*, 2009). Compound **17c**, bearing a 2-bromoethyl side chain at position 3, was devoid of estrogenic properties. Moreover, it showed potent irre-

versible inhibition of 17 β -HSD1 (IC₅₀: 68 nM in intact T47D cells) and it was found to have no effect on 17 β -HSD2, 17 β -HSD7, 17 β -HSD12 and CYP3A4 (Maltais *et al.*, 2011, 2014).

C6 and C2 substituted E2 derivatives. Another approach for the design of steroidal 17 β -HSD1 inhibitors was reported by the Poirier group. The authors described compounds that bear a butyl methyl alkylamide side chain in the C6 position of E2 (Fig. 3, general structure **18**) (Poirier *et al.*, 1998). The 6 β orientation of the thioether linked side chain was found to be essential for activity as compound **18a** (Fig. 3) was 70 times more potent an inhibitor than its 6 α -isomer (not shown; IC₅₀ values 0.17 μ M and 12.0 μ M, respectively) (Poirier *et al.*, 1998). In an attempt to eliminate the estrogen-like effect of this compound, the C3 hydroxy group was replaced with a hydrogen atom (compound **18b**). This modification, however, was not only inadequate to remove



| Compound | X | R ₁ | R ₂ | 17β-HSD1 | Reference |
|------------|-----------------|----------------|----------------|----------------------------------|------------------------|
| | | | | IC ₅₀ (μM), cell free | |
| | | | | 0.17 | (Poirier et al. 1998) |
| 18a | S | OH | H | 82 % ^a | (Cadot et al. 2007) |
| 18b | S | H | H | > 1 | (Tremblay et al. 2005) |
| 18c | CH ₂ | OH | H | 82 % ^a | (Cadot et al. 2007) |
| 18d | CH ₂ | OH | OMe | 32 % ^a | |

^a: percent inhibition at 1 μM in T47D cells

Fig. 3. Steroidal inhibitors of 17β-HSD1: C6 and C2 substituted E2 derivatives.

estrogenicity but also was clearly unfavorable in terms of 17β-HSD1 inhibition (Tremblay et al., 2005). Replacement of the thioether bond by a C—C bond, as exemplified by compound **18c**, led to less estrogenic compounds without affecting inhibition of 17β-HSD1 compared to **18a** (Cadot et al., 2007). The introduction of a 2-methoxy group (compound **18d**) further decreased inhibitory activity without significantly reducing estrogenic effects (Cadot et al., 2007).

C15 substituted E1 derivatives. Messinger et al. introduced another class of 17β-HSD1 inhibitors by synthesizing C15-substituted estrone derivatives (Fig. 4, compounds **19** and **20**) (Messinger et al., 2009). Compound **19** displayed strong and selective inhibition of the target protein in cell-free assay. At a concentration of 1 μM, **19** inhibited recombinant human 17β-HSD2 by 10%. The compound was also found to be cell permeable, as evidenced by its cellular inhibition profile on MCF7 cells (100% inhibition at 1 μM). Moreover, it showed no estrogen receptor mediated effect (Messinger et al., 2009). Compound **19** was shown to strongly reduce E2 levels in human endometrial specimens (decrease of E2 by more than 85% in approx. 70% of the specimens) (Delvoux et al., 2014). The 16β-diastereomer of compound **20** which showed an IC₅₀ value of 194 nM in a cell-free assay (Messinger et al., 2009), was found to inhibit human 17β-HSD1 in transgenic mice expressing human 17β-HSD1 by 85% and 33% in males and females, respectively (Lamminen et al., 2009). Interestingly, the 16α-isomer of compound **20** completely reversed estrogen-induced endometrial hyperplasia in these transgenic mice (Saloniemi et al., 2010).

C2, C6 and C16 substituted E1 derivatives. Potter's group pursued a structure-based drug design strategy using the crystal structure of human 17β-HSD1 to discover new, selective and potent inhibitors (Fig. 4, general structure **21**), with a methyl amide extending from the 16β-position of E1 (Lawrence et al., 2005; Vicker et al., 2006). In this series of compounds, **21a** was the most potent inhibitor of 17β-HSD1 reported, showing selectivity for 17β-HSD1 over 17β-HSD2 (Allan et al., 2006a). The same group also investigated modifications at the 6 and/or 16 position of the steroidal scaffold (Fig. 4, compounds **22a** and **22b**), but none of the compounds showed higher activity than compound **21a** (Allan et al., 2006a).

D- and E-ring modified estrogens. Möller et al. used a computational drug design approach to develop a set of potent 17β-HSD1 inhibitors with a D-homo-E1 scaffold. The 2-phenylethyl derivative (compound **23**, Fig. 5) was the most potent inhibitor of this set with an IC₅₀ value of 15 nM in a cell-free assay (Möller et al., 2009).

Other groups modified the D-ring by annealing an additional ring (E-ring): Poirier's group investigated fused substituted lactones and substituted oxazinone. In intact T47D cells the compounds **24** and **25**

(Fig. 5) showed IC₅₀ values of 1 and 1.4 μM, respectively, and no estrogenic activity. Compound **24** showed a dual action by inhibiting 17β-HSD1 and exerting an antiestrogenic effect on T47D cells (Ouellet et al., 2014). Compound **25** was selective over the 17β-HSD types 2 and 12 (Maltais et al., 2015).

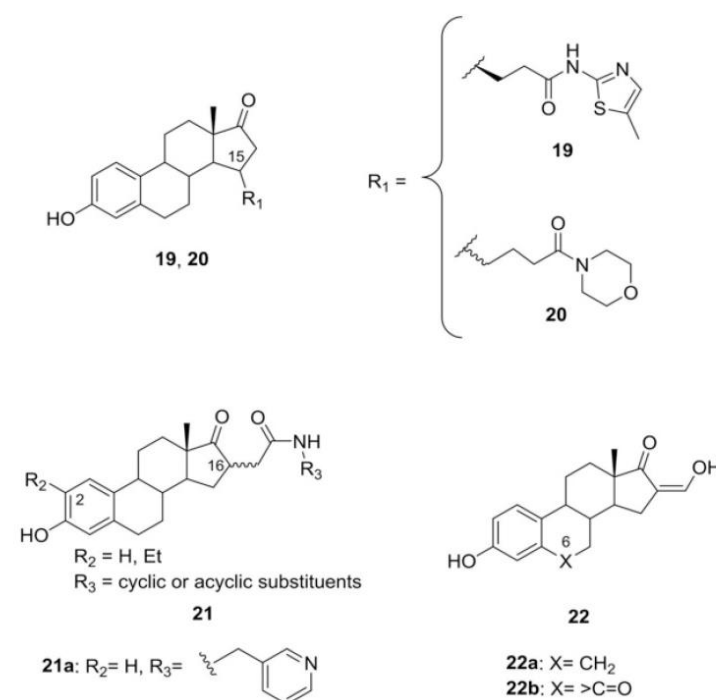
In an extension of their work on the C16 substituted E1 derivatives, the Potter group explored novel E-ring pyrazole derivatives. Compounds **26–28** (Fig. 5) inhibited 17β-HSD1 in T47D cells with IC₅₀ values of 180, 530 and 300 nM, respectively. In addition, they displayed selectivity over 17β-HSD2 and no estrogenic effects (Fischer et al., 2005; Allan et al., 2006a; b).

2.3. Nonsteroidal inhibitors of 17β-HSD1

(Hydroxyphenyl)naphthols. Frotscher et al. described potent and selective 17β-HSD1 inhibitors with a (hydroxyphenyl)naphthol scaffold. Starting point for inhibitor design was a pharmacophore model developed by the group. The model mimics the steroidal substrate with two hydroxyl functions at a distance of about 12 Å from each other, mounted on a hydrophobic core structure (Frotscher et al., 2008).

In cell-free assays, compound **29** (Fig. 6) showed inhibitory activity towards 17β-HSD1, combined with good selectivity over the type 2 enzyme (selectivity factor SF 2/1 = IC₅₀ (17β-HSD2)/IC₅₀ (17β-HSD1) = 48), ERα and β. Thus, it was used as a lead in a further drug design process of this class (Frotscher et al., 2008). The positions of the two hydroxyl-groups were found to be optimum for target inhibition (Marchais-Oberwinkler et al., 2009). Various substituents were introduced on the phenol- and the naphthol-moiety, and only substituents at position 1 of the naphthol system led to more active compounds (e.g. compound **30**: IC₅₀ = 20 nM in cell-free assay) with good selectivity over the type 2 enzyme and ERs) and good pharmacokinetic profile after oral application in rats (Marchais-Oberwinkler et al., 2008). To obtain more drug-like compounds, further structural optimization was performed at the 1-position of the naphthol moiety by introducing different heteroaromatic rings and substituted phenyl groups, and the introduction of a methyl sulfonamide group (compound **31**) was found to be favorable for 17β-HSD1 inhibition in both cell-free and T47D cell assays (Marchais-Oberwinkler et al., 2011b). Further optimization led to the creation of a combinatorial library of substituted sulfonamides. Compound **32** was equiactive to compound **31** with respect to inhibition of human 17β-HSD1 in a cell-free assay, but less potent in a T47D cell assay. With regard to a possible in vivo application, the compound was also tested against marmoset (*Callithrix jacchus*) 17β-HSD1 and showed an inhibition of 19% at 50 nM. Its rigidified analog **33** was the strongest inhibitor of this series towards both marmoset (79% inhibition at 50 nM) and human 17β-HSD1 in cell-free assays, but displayed poor activity in a T47D whole cell assay (IC₅₀ = 1100 nM) (Henn et al., 2012).

Bis(hydroxyphenyl) substituted arenes. Bey et al. introduced bis(hydroxyphenyl) arenes as another inhibitor class based on the above mentioned pharmacophore model (Bey et al., 2008a). Extensive structure activity relationship (SAR) studies (Bey et al., 2008a; b; Al-Soud et al., 2009) revealed that the proper choice of the central ring is crucial for activity: while imidazole and pyrazole resulted in inactive compounds, oxazole, thiazole and thiophene led to strong inhibition of purified human 17β-HSD1 (Fig. 7, compounds **34–36**). In addition, also selectivity could be largely affected by the choice of the central ring: oxazole **34** (Fig. 7) showed selective inhibition of 17β-HSD1 over the type 2 enzyme, whereas the isomeric isoxazole reversed the selectivity (not shown). Inhibitory potency was also dependent on the positions of the two phenolic OH-groups (Bey et al., 2008a; b). In case of compounds **34–36** the favorable positions of the hydroxyl functions (*para/meta*) are implemented. Further improvements in the activity and selectivity were achieved when substituents were introduced to the



| Compound | 17 β -HSD1 IC ₅₀ (nM) | | Reference |
|----------------|---|-----------------------------|--------------------------------|
| | cell-free (nM) | cellular (nM) | |
| 19 | 4 | (100% inhibn. at 1 μ M) | (Messinger <i>et al.</i> 2009) |
| 20(β) | 194 | - | |
| 20(α) | 353 | - | |
| 21a | - | 37 | (Allan <i>et al.</i> 2006a) |
| 22a | - | 110 | |
| 22b | - | 700 | |

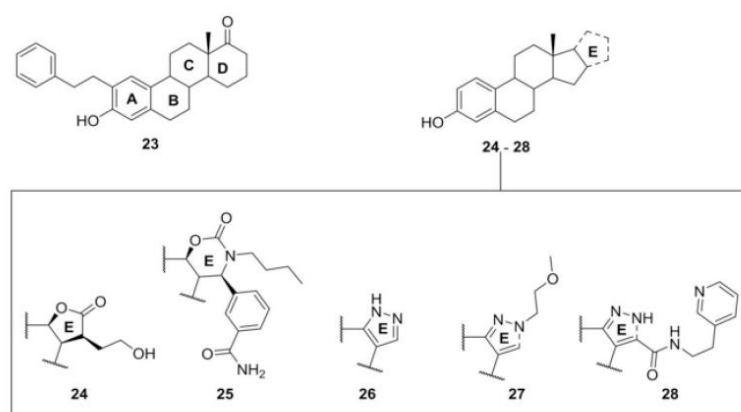
Fig. 4. Steroidal inhibitors of 17 β -HSD1: C2, C6, C15 and C16 substituted E1 derivatives.

p-hydroxy substituted ring (compounds **37a** and **37b**) (Bey *et al.*, 2009). Especially fluorination (compound **37a**) proved to be beneficial, leading to strong target inhibition, pronounced selectivity over 17 β -HSD2 and excellent pharmacokinetic properties in rats after oral application (Bey *et al.*, 2009). Compounds **36** and **37b** were found to neutralize the E1-induced stimulation of proliferation of T47D cells (Kruchten *et al.*, 2009). Some members of this inhibitor class, e.g. compounds **37a** and **37b**, were reported to exert direct antiproliferative activity *in vitro* in cancer cell lines by influencing the cell cycle (Berenyi *et al.*, 2013).

Bicyclic substituted hydroxyphenyl methanones. A structure- and ligand-based pharmacophore model was introduced by the Hartmann group, resulting in novel 17 β -HSD1 inhibitors that were derivatives of bicyclic substituted hydroxyphenylmethanone (Fig. 8, compounds **38a-c**) (Oster *et al.*, 2010a). The influence of changes of the hydroxy-group positions as well as the effects of small substituents introduced at the phenyl ring and of central ring alternatives (thiophene and thiazoles) on inhibitory potency were examined. Compounds **38a-c** were

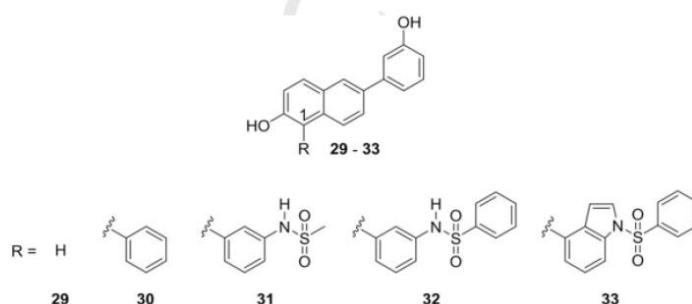
most potent inhibitors with IC₅₀ values in the low nanomolar range in both cell-free and T47D cellular assays, selectivity over 17 β -HSD2, no significant affinity to ER α and ER β , and metabolic stability in human liver microsomes (phase I; $t_{1/2} \geq 100$ min) (Oster *et al.*, 2010a). Structural modifications of the bicyclic system (ring A, Fig. 8) were carried out, paying special attention to the possibility of exchanging the hydroxy function (Oster *et al.*, 2011). This work revealed that the hydroxy function was not essential for activity and could be replaced e.g. with a methylbenzenesulfonamide moiety (compound **39**), resulting in high activity in cell-free and cellular assays at the expense, however, of decreased selectivity over 17 β -HSD2 and metabolic stability ($t_{1/2} = 12.8$ min).

More insight into the SAR of this class was gained by Abdelsamie *et al.* who found that the hydroxyphenyl methanone moiety is important for activity and that its hydroxy function cannot be replaced with possible bioisosteres without complete or significant loss of activity (Abdelsamie *et al.*, 2014). Further structural optimizations were performed to enhance the inhibitory activity against rodent (rat and



| Compound | 17β-HSD1 IC ₅₀ (nM) | | Reference |
|----------|-----------------------------------|----------|------------------------------|
| | Cell-free | Cellular | |
| 23 | 15 | - | (Möller <i>et al.</i> 2009) |
| 24 | - | 1000 | (Ouellet <i>et al.</i> 2014) |
| 25 | - | 1400 | (Maltais <i>et al.</i> 2015) |
| 26 | - | 180 | (Allan <i>et al.</i> 2006a) |
| 27 | - | 530 | (Fischer <i>et al.</i> 2005) |
| 28 | - | 300 | |

Fig. 5. Steroidal inhibitors of 17β-HSD1: D- and E-ring modified estrogens.

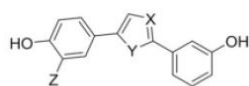


| Compound | 17β-HSD1 IC ₅₀ (nM) | | SF (17β-HSD2/17β-HSD1) | Reference |
|----------|-----------------------------------|----------|---------------------------|--|
| | Cell-free | Cellular | | |
| 29 | 116 | - | 48 | (Frotscher <i>et al.</i> 2008) |
| 30 | 20 | - | 27 | (Marchais-Oberwinkler <i>et al.</i> 2008) |
| 31 | 15 | 71 | 27 | (Marchais-Oberwinkler <i>et al.</i> 2011b) |
| 32 | 15 | 196 | 27 | (Henn <i>et al.</i> 2012) |
| 33 | 32 | 1100 | 12 | |

Fig. 6. Nonsteroidal inhibitors of 17β-HSD1: (Hydroxyphenyl)naphthols.

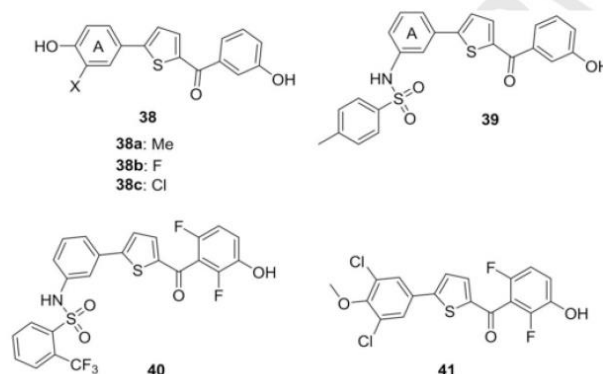
mouse) 17β-HSD1. This goal was achieved by the introduction of fluorine atoms on the benzoyl moiety. Compound 40 (Fig. 8) is one of the most potent inhibitors reported of both human and rat 17β-HSD1 enzymes with IC₅₀ values (purified enzymes) of 2 nM and 97 nM, respectively (Abdelsamie *et al.*, 2015). The main drawback of this compound

was its low selectivity over the type 2 enzymes of human and rat (SF2/1 = 3 and 0.5, respectively). Nevertheless, compound 40 was a lead for further optimizations in order to obtain a suitable candidate for a proof of principle study in a rodent endometriosis model. Thus, compound 41 (Fig. 8) was discovered which is the most potent 17β-HSD1



34 - 37

| Compound | X | Y | Z | 17 β -HSD1 | SF | Reference |
|----------|----|---|-----------------|----------------------------------|-------------------------------------|--------------------|
| | | | | IC ₅₀ (nM), Cell-free | (17 β -HSD2/17 β -HSD1) | |
| 34 | N | O | H | 310 | 56 | (Bey et al. 2008a) |
| 35 | N | S | H | 50 | 80 | |
| 36 | CH | S | H | 69 | 28 | (Bey et al. 2008b) |
| 37a | CH | S | F | 8 | 118 | |
| 37b | CH | S | CH ₃ | 46 | 49 | (Bey et al. 2009) |

Fig. 7. Nonsteroidal inhibitors of 17 β -HSD1: Bis(hydroxyphenyl) substituted arenes.

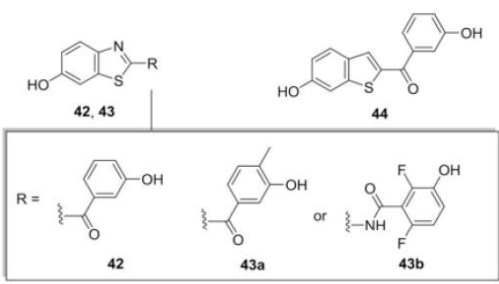
| Compound | 17 β -HSD1 | | SF (17 β -HSD2/17 β -HSD1) | Reference |
|----------|-----------------------|----------|---|---------------------------------|
| | IC ₅₀ (nM) | | | |
| | Cell-free | Cellular | | |
| 38a | 8 | 27 | 48 | (Oster <i>et al.</i> 2010a) |
| 38b | 19 | 17 | 31 | |
| 38c | 5 | 126 | 49 | |
| 39 | 12 | 78 | 14 | (Oster <i>et al.</i> 2011) |
| 40 | 2 | - | 3 | (Abdelsamie <i>et al.</i> 2015) |
| 41 | 0.5 | - | 82 | (Abdelsamie <i>et al.</i> 2017) |

Fig. 8. Nonsteroidal inhibitors of 17 β -HSD1: Bicyclic substituted hydroxyphenyl methanones.

inhibitor known so far, displaying high selectivity over 17 β -HSD2, ER α and β , and a range of hepatic CYP enzymes. A beneficial pharmacokinetic profile in rats makes the compound eligible for a proof of principle study using xenografted immunodeficient rats (Abdelsamie et al., 2017).

Hydroxybenzothiazole and hydroxybenzothiophene derivatives. The Hartmann group developed another pharmacophore model in an approach to design nonsteroidal 17 β -HSD1 inhibitors. The model was based on crystallographic data of the target protein and was used for the virtual screening of a small library of compounds. The virtual hits were experimentally verified, and subsequent structure modifications and rigidification resulted in inhibitors bearing a benzothiazole ring linked to a phenyl system via a keto or amide linker (Spadaro et al., 2012a). In a functional assay using purified human 17 β -HSD1, com-

pound **42** (Fig. 9) displayed an IC₅₀ value of 44 nM. It was selective over the type 2 enzyme, but showed affinity towards the ERs. Inhibitor optimization in terms of selectivity was achieved by introduction of small substituents on the phenyl ring. The methylated benzoyl derivative **43a** and difluoro benzamide derivative **43b** (Fig. 9) were the most selective 17 β -HSD1 inhibitors over the type 2 protein. In addition, they were highly potent inhibitors of 17 β -HSD1 in cell-free and T47D cellular assays (IC₅₀: 258 and 37 nM, respectively), and showed favorable selectivity profiles towards ERs and hepatic CYP enzymes (Spadaro et al., 2012b). A systemic bioisosteric replacement of benzothiazole by other heterocycles resulted in the identification of potent and selective 17 β -HSD1 inhibitors bearing a benzothiophene moiety. Compound **44** (Fig. 9) is more active towards the target enzyme and displayed better



| Compound | 17 β -HSD1 IC ₅₀ (nM) | | SF (17 β -HSD2/17 β -HSD1) | Reference |
|----------|---|----------|---|---------------------------|
| | Cell-free | Cellular | | |
| 42 | 44 | - | 24 | (Spadaro et al. 2012a) |
| 43a | 27 | 258 | 148 | |
| 43b | 13 | 37 | 136 | (Spadaro et al. 2012b) |
| 44 | 13 | - | 40 | (Miralinaghi et al. 2014) |

Fig. 9. Nonsteroidal inhibitors of 17 β -HSD1: Hydroxybenzothiazoles and hydroxybenzothiophenes

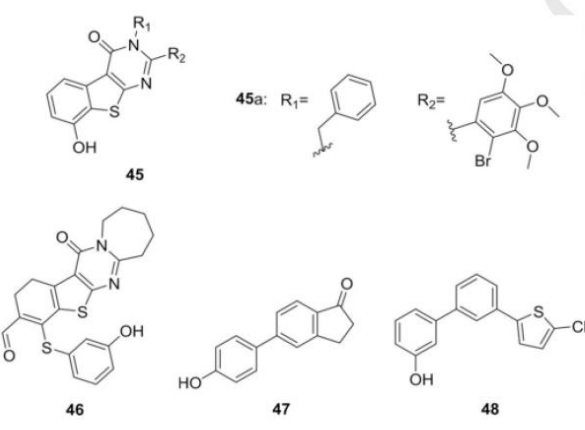
selectivity over 17 β -HSD2 than its benzothiazole analog **42** (Miralinaghi et al., 2014).

Thiophenepyrimidinones. Messinger et al. identified 17 β -HSD1 inhibitors by computer aided drug design starting from a unique nonsteroidal pyrimidinone core (structure **45**, Fig. 10) by optimizing R₁ and R₂. In protein-based inhibition assays compound **45a** displayed an IC₅₀ value of 5 nM against 17 β -HSD1, and selectivity over the type 2 enzyme (8% inhibition at 100 nM). In intact MCF-7 cells, 17 β -HSD1 was

inhibited by 67% when **45** was applied in a concentration of 1 μ M. The compound significantly reduced 17 β -HSD1-dependent tumor growth in a nude mouse model (Messinger et al., 2006). Lilienkamp et al. also reported a potent 17 β -HSD1 inhibitor class derivative of thiophenepyrimidinone that was identified by the screening of a small library of commercially available compounds. Compound **46** (Fig. 10) was the most potent inhibitor of this series with 94% inhibition at 100 nM concentration tested in a cell-free assay at low concentration of E1 (30 nM) (Lilienkamp et al., 2009).

Biphenyl ketones, biphenylols and imidazoles. Several phenylalkyl imidazoles (structures are not shown) and biphenyl ketones were reported as weakly active 17 β -HSD1 inhibitors, showing 10–68% inhibition at a concentration of 100 μ M (Lota et al., 2007; Olusanjo et al., 2008). Allan et al. represented a promising biphenyl ethanone scaffold as a mimic of the E1 template. Structural optimization led to compound **47** (Fig. 10), showing an IC₅₀ value of 1.7 μ M in an assay using T47D cells (Allan et al., 2008). Oster et al. published heterocyclic substituted biphenylols and their aza-analogs with 17 β -HSD1 inhibitory activity (Oster et al., 2010b). The most active compound **48** (Fig. 10) displayed IC₅₀ values of 560 nM (17 β -HSD1) and IC₅₀ 2370 nM (17 β -HSD2) in cell-free assays, and low affinity for ERs α and β .

Flavonoids, cinnamic acid and coumarin derivatives. The inhibitory activity of various flavonoids and cinnamic acid derivatives towards human recombinant 17 β -HSD1 was investigated (Brožič et al., 2009). Diosmetin (Fig. 11, compound **49**) was the most active flavonoid and compound **50** was the most active cinnamic acid derivative with more than 90% and 70% inhibition at 6 μ M, respectively. The same group reported the synthesis of coumarin derivatives as selective nonsteroidal inhibitors of 17 β -HSD1. Compound **51a** (Fig. 11) was the most potent inhibitor in this series with an IC₅₀ value of 270 nM and selectivity towards 17 β -HSD2 and ERs (Starčević et al., 2011a). Recently, Niinivehmas et al. reported on a series of 3-phenylcoumarin analogs as inhibitors of recombinant human 17 β -HSD1 (Niinivehmas et al., 2018). The molecular basis of inhibition was determined by a docking-based SAR analysis, and inhibition of 17 β -HSD2 as well as cross-reactivity against ER α , aromatase, CYP1A2 and monoamine oxidases was evaluated. The most active compound in terms of 17 β -HSD1 inhibition was **51b** (Fig. 11).



| Compound | 17 β -HSD1 IC ₅₀ , cell-free | Reference |
|----------|--|--------------------------|
| 45a | 5 nM | (Messinger et al. 2006) |
| 46 | 94 % inhibition at 100 nM | (Lilienkamp et al. 2009) |
| 47 | 1.7 μ M in T47D cells | (Allan et al. 2008) |
| 48 | 560 nM | (Oster et al. 2010b) |

Fig. 10. Nonsteroidal inhibitors of 17 β -HSD1: Thiophenepyrimidinones, biphenyl ketones and biphenylols.

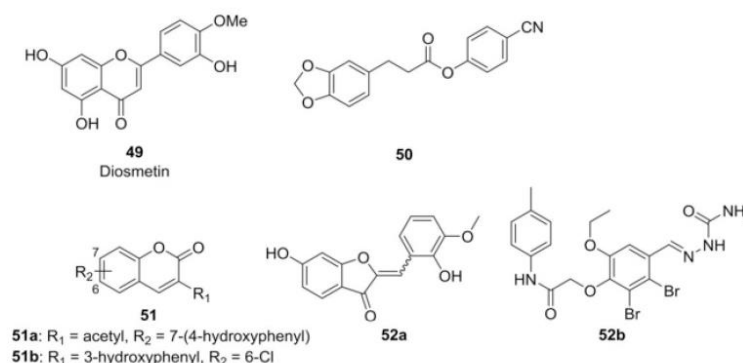


Fig. 11. Nonsteroidal inhibitors of 17β-HSD1: Flavonoids, cinnamic acid, coumarin derivatives and virtual screening candidates 52a and 52b.

Virtual screening candidates. A structure-based high throughput computational screening of a database containing 13 million drug-like molecules resulted in hits that were based on a 2-benzylidenbenzofuranone scaffold. Compound 52a (Fig. 11) was the most potent compound identified, showing an IC₅₀ value of 45 nM for 17β-HSD1 inhibition and selectivity over 17β-HSD2 (Starčević et al., 2011b). Schuster et al. identified nonsteroidal 17β-HSD1 inhibitors by a virtual screening using pharmacophore models built from crystal structures containing steroidal compounds (Schuster et al., 2008). After validation of the most promising model by comparing predicted and experimentally determined inhibitory activities of flavonoids, a virtual library of nonsteroidal compounds was screened. 14 virtual hits were selected for biological testing. Compound 52b (Fig. 11) was the most active one, showing an IC₅₀ value of 5.7 μM and selectivity over the related enzymes tested.

2.4. Dual inhibitors of 17β-HSD1 and steroid sulfatase (STS)

In addition to 17β-HSD1, the local biosynthesis of estrogen involves steroid sulfatase (STS), a key enzyme which converts the inactive estrone sulfate (E1S) - the main transport and storage form of estrogen - into the weakly active E1. The latter in turn is transformed into E2 via action of 17β-HSD1. Recently, the first dual inhibitors of both STS and 17β-HSD1 were reported. Their structures were rationally derived, based on the combination of the SAR for 17β-HSD1 inhibition in the class of bicyclic substituted hydroxyphenyl methanones (e.g. compound 41, Fig. 8) and the sulfamate moiety which is the essential feature for STS inhibition (Potter, 2018). The IC₅₀ values of the dual inhibitor 53 (Fig. 12) in intact T47D cells were 15 nM and 22 nM for STS and 17β-HSD1, respectively, and STS inhibition was found to be irreversible. The compound did not interfere with ERs but efficiently reversed E1S- and E1-induced T47D cell proliferation, without affecting E2-induced proliferation (Salah et al., 2017).

2.5. Inhibitors of 17β-HSD2

2.5.1. Steroidal inhibitors of 17β-HSD2

Spirolactones. In 1994, Auger et al. found that introducing a spiro-γ-lactone at position 17 of E2 provokes a potent inhibition of 17β-HSD2. The first synthetic inhibitor of this type, compound 54 (Fig. 13),

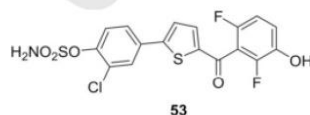


Fig. 12. Dual inhibitor of 17β-HSD1 and steroid sulfatase (STS).

inhibited 17β-HSD2 with an IC₅₀ value of 0.27 μM. Its IC₅₀ towards the type 1 enzyme was reported to be more than 160 times higher, indicating a distinct selectivity (Auger et al., 1994).

The same group described the synthesis and biological evaluation of eleven spiro-γ-lactone analogs containing a steroidal C-18 or C-19 scaffold. Analysis of the inhibitory effect exerted by these compounds on microsomal 17β-HSD activity indicated that compounds containing the C-18 nucleus (exemplified by compound 55, Fig. 13) are more potent 17β-HSD2 inhibitors than C-19 analogs such as compounds 56 and 57 (results shown in figure) (Sam et al., 1995). No compound from this latter study, however, was more potent than compound 54, indicating that combination of a phenolic group and a spiro-γ-lactone moiety was important for efficient 17β-HSD2 inhibition.

In a continuation of this work and based on the obtained SAR, further spirolactones and related compounds were described. Starting from compound 54, structural optimizations were carried out. The resulting 17β-HSD2 inhibitors showed good selectivity over type 1 and type 3 enzymes (compounds 58–61, Fig. 13). Compound 58 was the most potent 17β-HSD2 inhibitor in this series (Poirier et al., 2001).

Starting from compound 58 as a lead, and as an extension of the previous work, Bydal et al. described further E2-based lactone derivatives, aiming at increasing the knowledge on the SAR in this compound class. The most potent compound was the enone 62 (Fig. 13), displaying 74% inhibition of 17β-HSD2 at a concentration of 0.1 μM and 19% inhibition at 0.01 μM (Bydal et al., 2004).

C7-substituted E2 derivatives. Combining the fact that decorating the E2-scaffold with an appropriate lactone moiety provokes 17β-HSD2 inhibition and the finding that an *N*-butyl-*N*-methylundecanamide moiety in 7α-position of E2 leads to anti-estrogenic compounds (63 and 64, Fig. 14) resulted in the design of compound 65 which displayed a selective inhibition of 17β-HSD2. At a concentration of 1 μM, the compound reversed the estrogenic effect induced by 0.1 nM E2 by 87% (Sam et al., 2000).

Fluorine-substituted estrogens. 17-fluorine substituted estratrienes were identified as moderately active inhibitors of various h17β-HSDs. Most of the tested compounds were nonselective inhibitors of h17β-HSD1 and 2. Among them, compounds 66 and 67 (Fig. 14) were shown to be the most potent h17β-HSD2 inhibitors (Deluca et al., 2006).

2.6. Nonsteroidal 17β-HSD2 inhibitors

Disubstituted cis-pyrrolidinones. From a screening effort for novel inhibitors of 17β-HSD2 as potential therapeutics for osteoporosis the 4,5-disubstituted cis-pyrrolidinones 68 and 69 (Fig. 15) were identified as lead compounds. Further 4,5-disubstituted cis-pyrrolidinones were designed and investigated for their ability to inhibit 17β-HSD2. It was

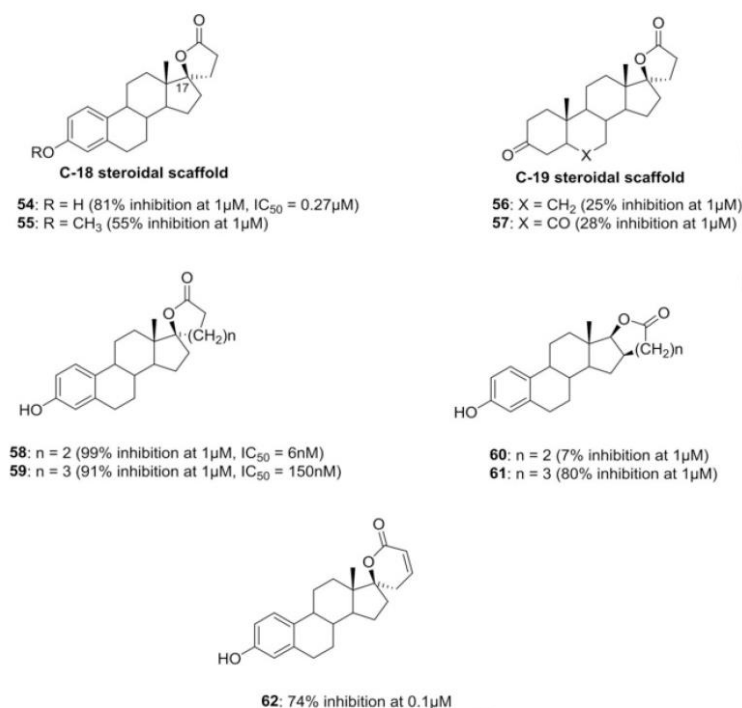


Fig. 13. Steroidal inhibitors of 17β-HSD2: Spirolactones and lactones.

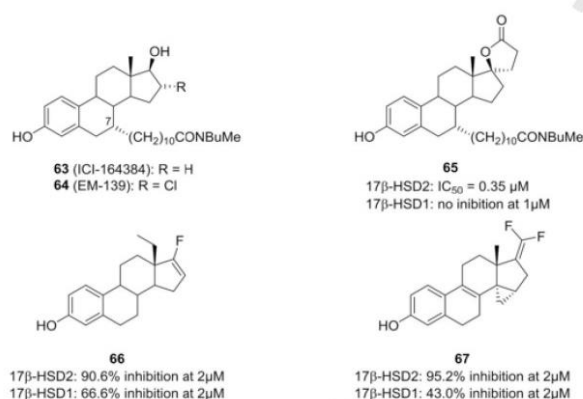


Fig. 14. Steroidal inhibitors of 17β-HSD2: C7-substituted E2 derivatives and fluorine-substituted estrogens.

found that the potency of the initial leads was improved by adding a second aromatic group to the 5-[hydroxy (aryl)methyl] side chain as exemplified by compound **70** (Fig. 15), which was the most potent inhibitor identified in this work (Gunn et al., 2005). Further structural refinements in this compound class focused on the search for an orally active compound eligible for in vivo studies (Wood et al., 2006). Thus, a series of novel 4,5-disubstituted *cis*-pyrrolidinones was synthesized and highly active compounds could be identified, and most of them maintained activity in the cell E2 conversion functional assay. In addition, they did not show appreciable binding to the estrogen, androgen or other steroid receptors and no tangible activity against 11β-HSD2, 17β-HSD1 and 17β-HSD3. Selected enantiomerically pure compounds (**71–74**, Fig. 15), which showed activity in osteoblast MG63 cells (IC₅₀ = 0.03 μM–0.48 μM), were tested for plasma exposure in rats,

and compounds **71–73** were also applied to macaques. Based on its overall *in vitro* profile and the cynomolgus macaque exposure profile, compound **73** was selected for a non-human primate proof-of-concept study (Wood et al., 2006). Ovariectomized cynomolgus monkeys were used as an osteoporosis model to evaluate the efficacy of **73**. After oral application, the compound led to a decrease in bone resorption while bone formation was maintained (Bagi et al., 2008).

Spiro-δ-lactones. Inspired by the molecular structures of steroidal 17β-HSD2 inhibitors described by the Poirier group, nonsteroidal spiro-δ-lactones were designed and tested for 17β-HSD2 inhibition. The compounds were either inactive or showed low activity. In addition, they were chemically unstable which was confirmed and quantified by determination of their half-lives in buffer, precluding further development. In Fig. 16 the most potent representative of this inhibitor class, compound **75**, is displayed (Xu et al., 2011a).

Hydroxyphenylnaphthols. This compound class is also described in the section on nonsteroidal inhibitors of 17β-HSD1 of this review. Interestingly, the selectivity of these compounds can be shifted in favor of 17β-HSD2 inhibition, depending on the substitution pattern. Introduction of hydroxynaphthyl, hydroxyphenyl and (hydroxymethyl)phenyl moieties resulted in inactive or moderately active compounds. The most potent and selective member of this series was compound **76** (Fig. 16) (Wetzel et al., 2011a).

In the further drug optimization process, 21 additional naphthalene-derived compounds were synthesized and evaluated for 17β-HSD2 inhibition and selectivity toward the type 1 enzyme as well as affinity for the estrogen receptors α and β. Compounds with clearly improved properties could be obtained. In cell-free enzyme preparations compound **77** (Fig. 16) showed strong and selective 17β-HSD2 inhibition. In intact T47D cells, **77** displayed an IC₅₀ value of 31 nM for inhibition of 17β-HSD2. In addition, the compound was selective over 17β-HSD4 and 5 (40% and 21% inhibition at 1 μM, respectively) and had low affinity to ERα: its relative binding affinity was less than 0.1% of that

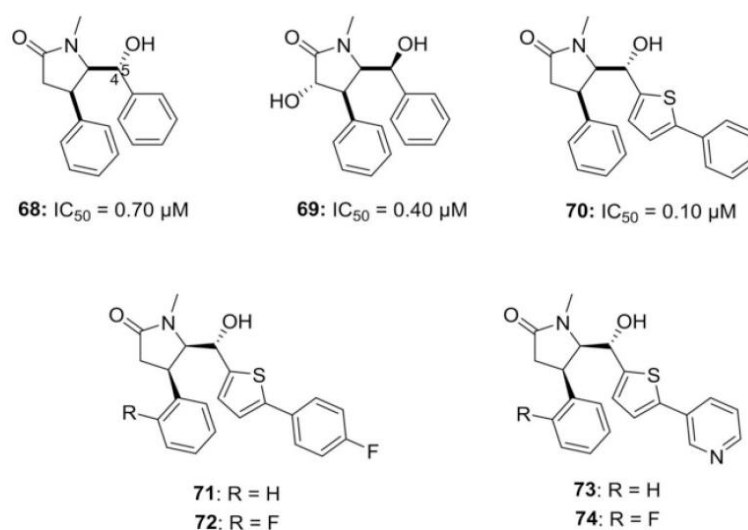
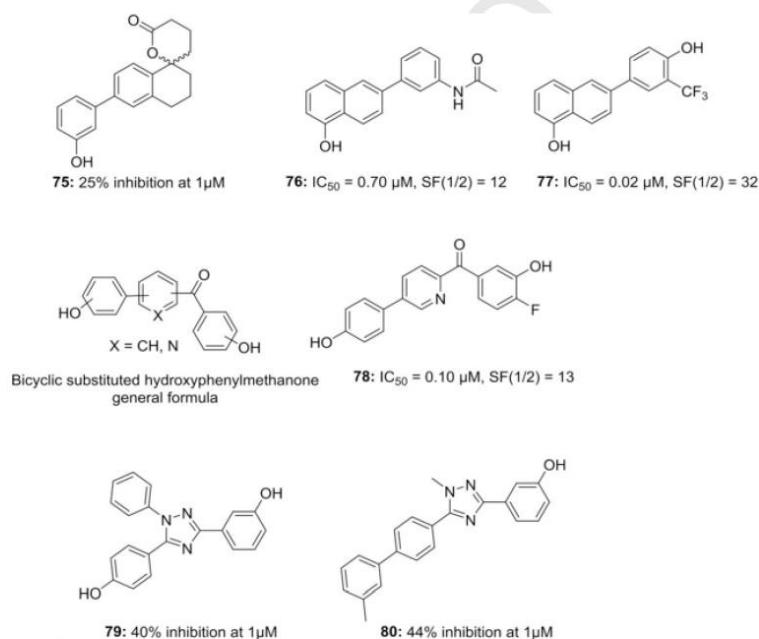
Fig. 15. Nonsteroidal inhibitors of 17β-HSD2: Disubstituted *cis*-pyrrolidinones.

Fig. 16. Nonsteroidal inhibitors of 17β-HSD2: Spiro-δ-lactones, hydroxyphenylnaphthols, bicyclic substituted hydroxyphenylmethanones and (hydroxyphenyl)-1,2,4-triazoles.

of E2. The compound was tested for its inhibition of E1 and E2 formation in rat, mouse and marmoset (*Callithrix jacchus*) tissue preparations (liver or placenta). At 1 μM, it inhibited E1 formation in a rat liver preparation by 77% and E2 formation by 52%. The respective values for the mouse were 72% (reduction of E1 formation) and 52% (reduction of E2 formation) and for the marmoset 99% and 75% (reduction of E1 formation vs reduction of E2 formation). The values obtained for marmoset coincided well with those measured using a human placental preparation (98% and 60%, respectively) (Wetzel et al., 2011b).

Bicyclic substituted hydroxyphenylmethanones. Like the hydroxyphenylnaphthols, bicyclic substituted hydroxyphenylmethanones were originally designed as inhibitors of 17β-HSD1, but could be structurally modified to render them more selective for the type 2 enzyme. This

shift of selectivity was achieved by replacing the thiophene moiety (see Fig. 16) by a six-membered ring (benzene or pyridine). Benzene derivatives were more potent but less selective than their pyridine analogs while the latter showed more favorable combinations of activity and selectivity. The most interesting compound in this work was compound 78 (Wetzel et al., 2012).

(Hydroxyphenyl)-1,2,4-triazoles. Hydroxyphenyl-1,2,4-triazoles constitute a class of 17β-HSD2 inhibitors with moderate activity, displaying selectivity over the type 1 enzyme. Compounds 79 and 80 (Fig. 16) were the most active inhibitors in this compound class (Al-Soud et al., 2009, 2012).

Biphenyl amides and phenylthiophene amides. In 2011, Xu et al. discovered *N*-benzyl-diphenyl-3 (or 4)-carboxamides and *N*-benzyl-thio-

phene-2-carboxamides as potent nonsteroidal 17 β -HSD2 inhibitors (Xu et al., 2011b). Formally, these compounds were derived from the (hydroxyphenyl)-1,2,4-triazoles (see preceding chapter) by replacing the triazole ring with a non-cyclic carboxamide moiety. In the design concept it was hypothesized that the rigidity induced by the triazole ring was responsible for the weak 17 β -HSD2 inhibitory activity. In a cell-free assay, compound **81** (Fig. 17) was the most potent inhibitor in the diphenyl carboxamide class. It is noteworthy that this compound showed a strong selectivity for 17 β -HSD2 over the type 1 enzyme. In addition, it is one of the rare examples for 17 β -HSD2 inhibitors devoid of a phenolic OH-group. In terms of activity and selectivity, the phenylthiophene amide **82** (Fig. 17) was the most interesting compound identified in this study. It showed no binding affinity to the estrogen receptors.

Due to favorable biological properties, the phenylthiophene scaffold was used as a lead for drug optimization studies. In a first approach, the length of the linker between the nitrogen atom of the amide group and the adjacent benzene moiety was varied (Fig. 17, n = 0 and 2) (Marchais-Oberwinkler et al., 2013). While none of the phenethylamides (n = 2) were active, most of the anilides (n = 0) turned out to be moderate or strong inhibitors of 17 β -HSD2. Compounds **83** and **84** (Fig. 17) were the most potent and selective inhibitors in this study, each with an IC₅₀ value of 62 nM in a cell-free assay, similarly strong activities in whole cell assays (T47D) and selectivity over 17 β -HSD1. SAR studies allowed a first characterization of the active site of human 17 β -HSD2. It is quite large and certainly larger than that of 17 β -HSD1. The most potent compounds were investigated regarding their ability to inhibit 17 β -HSD2 from other species (mouse, rat and marmoset). At a concentration of 1 μ M, the hydroxylated compound **82** showed 65% inhibition of E1 formation in mouse liver preparation.

Phenylthiazole amides and structurally modified phenylthiophene amides. A second approach for the optimization of the phenylthiophene-based carboxamides focused on the variation of substitution pattern of the thiophene ring and its replacement with thiazole (Fig. 18). Moreover, the effects of substitution of the amide group with a larger moiety as well as the exchange of the N-methylamide group with possible bioisosteres on the biological properties were investigated. The main aim of this study was the development of novel active and selective 17 β -HSD2 inhibitors with high potency towards both the human protein and its murine ortholog as well as selectivity over the type 1 enzymes of both species, in order to discover compounds eligible for in vivo studies. Very sharp SAR could be observed in this class of compounds. In general, the 2,5-disubstituted thiophene derivatives were less active towards the murine enzyme than towards the human ortholog, except for compound **85** (Fig. 18), which in protein preparations was four times more potent against murine 17 β -HSD2 (IC₅₀ = 54 nM) than against the human enzyme (IC₅₀ = 235 nM) with a strong selectivity over h17 β -HSD1 (SF1/2 = 95) and low affinities to ER α and β (Perspicace et al., 2014).

A major drawback of the aforementioned amides featuring a 2,5-disubstituted thiophene moiety, such as **85** (Fig. 18), was unsatisfactory metabolic stability. Compounds with clearly improved stability towards biotransformation were discovered by structural modifications

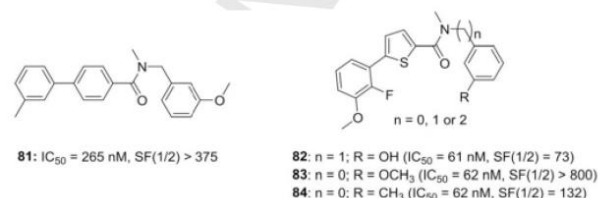


Fig. 17. Nonsteroidal inhibitors of 17 β -HSD2: Biphenyl amides and phenylthiophene amides.

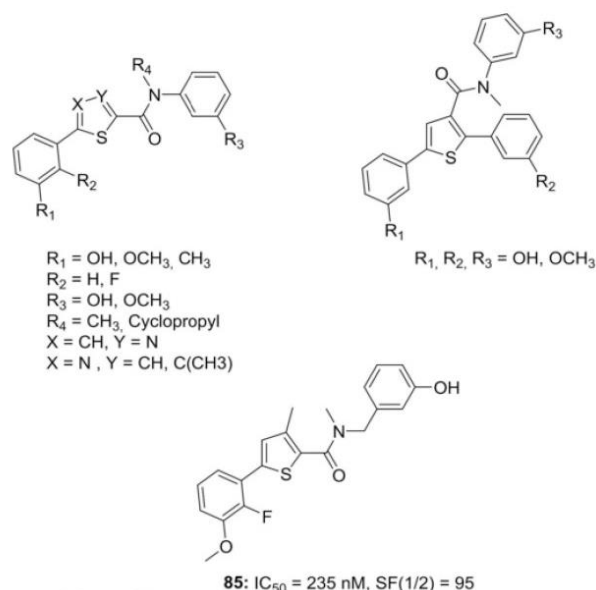


Fig. 18. Nonsteroidal inhibitors of 17 β -HSD2: Phenylthiazole amides and structurally modified phenylthiophene amides. General formulas (upper part) and compound **85**.

and changing lipophilicity (Fig. 19). In addition, an analysis of the main routes of biotransformation of amide-based 2,5-disubstituted thiophenes was performed. Compound **86** (Fig. 19) showed a half-life greater than 120 min in human liver microsomes (S9 fraction), moderate activity towards 17 β -HSD2 and selectivity over 17 β -HSD1 (SF1/2 = 10). In addition, the compound displayed no affinity for the estrogen receptors (Gargano et al., 2014).

Gargano et al. aimed at identifying a compound which can be used for a proof of concept study in a mouse model for osteoporosis beside being a suitable potential therapeutic for treating osteoporosis in humans. For this purpose, 25 previously described inhibitors of human 17 β -HSD2, belonging to the 2,5-thiophene amide, 1,3-phenylene amide and 1,4-phenylene amide classes (Fig. 20), were tested for inhibition of the murine enzyme. From the data obtained, a comparative SAR study was elaborated which was then used to develop a drug optimization

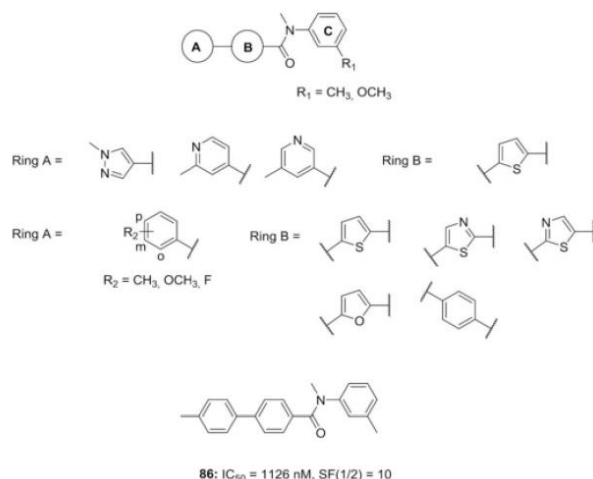


Fig. 19. Nonsteroidal inhibitors of 17 β -HSD2: A- and B-ring modifications in the class of carboxamides, part 1. General formula (upper part) and compound **86**.

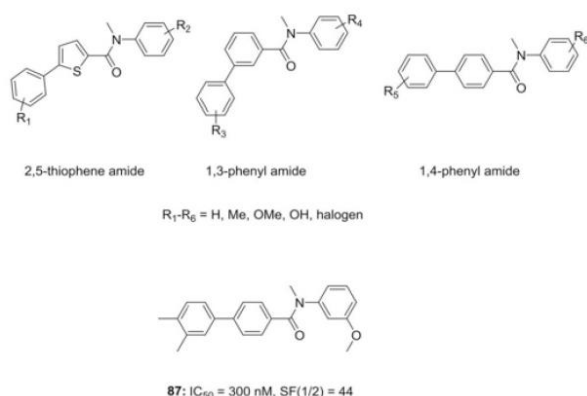


Fig. 20. Nonsteroidal inhibitors of 17 β -HSD2: B-ring modifications in the class of carboxamides, part 2. General formulas (upper part) of the 2,5-thiophene amide (left), 1,3-phenylene amide (middle) and 1,4-phenylene amide classes (right) and compound **87**.

strategy. This rationale led to the discovery of compound **87** (Fig. 20), which was the first 17 β -HSD2 inhibitor to show an appropriate profile for the purposes mentioned above, with strong inhibition of both human and murine 17 β -HSD2 ($IC_{50} = 300 \text{ nM}$ and 140 nM , respectively) and selectivity over the human type 1 enzyme ($SF(1/2) = 44$) and ERs. It also displayed strong inhibitory activity in intact T47D cells (66% inhibition at 250 nM), a half-life of 107 min in human liver microsomes (S9 fraction) and suitable physicochemical parameters ($MW = 345$ and $cLogP = 4.75$) (Gargano et al., 2015).

Unfortunately, compound **87** showed cytotoxic effects in HEK293 cells ($LD_{50} < 6.25 \mu\text{M}$). It was assumed that this property might be attributed to the biphenyl moiety. A successful minimization of cytotoxicity was achieved by replacing the biphenyl system with non-aromatic or angulate moieties (Fig. 21, top). Compound **88** (Fig. 21, bottom) displayed a significantly decreased cytotoxicity ($LD_{50} \approx 25 \mu\text{M}$), improved 17 β -HSD2 inhibitory activity in a cell-free assay and enhanced selectivity over 17 β -HSD1 when compared to **87** (Gargano et al., 2016).

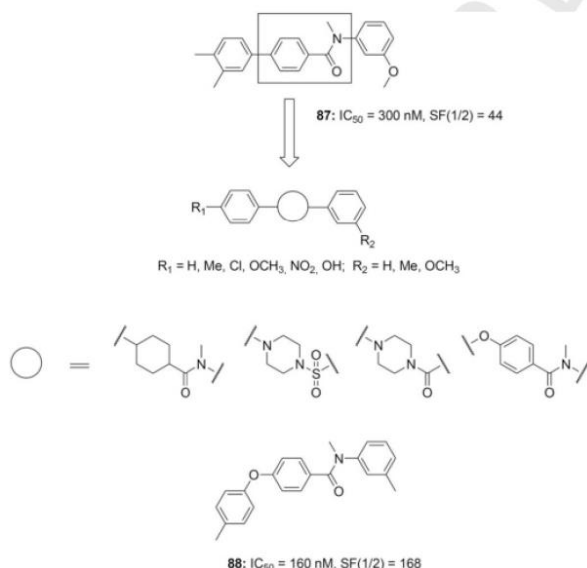


Fig. 21. Nonsteroidal inhibitors of 17 β -HSD2: Replacing the biphenyl system with non-aromatic or angulate moieties. Structural modifications (upper part) and compound **88**.

Thieno[3,2-d]pyrimidinones and related compounds. Rigidification of inhibitors with amidothiophene scaffold (Fig. 17, compounds **83** and **84**; Fig. 18, compound **85**) led to a series of conformationally restricted thieno [3,2-d]pyrimidinones, thieno [3,2-d]pyrimidines and quinazolinones. The compounds showed no or little activity as 17 β -HSD2 inhibitors. However, the two moderately active compounds **89** and **90** (Fig. 22) were discovered, allowing for conclusions concerning the biologically active conformers of the non-rigidified predecessors (Perspicace et al., 2013a).

Biphenyl- and phenylthiophene-sulfonamides. Starting from 17 β -HSD2 inhibitors bearing a biphenylcarboxamide moiety (Fig. 19, compound **86**) another class of biphenyl derivatives was designed by exchanging the carboxamide group with a sulfonamide or a retrosulfonamide group, (Perspicace et al., 2013b). The main goal of this work was to develop new active and selective 17 β -HSD2 inhibitors with a good *in vitro* ADME profile. Inhibitory activity of the retrosulfonamides (with the SO_2 -group linked to the hydroxyphenyl moiety, as seen in compound **91** (Fig. 22) was superior compared to that of the sulfonamides. This property was attributed to the acidity of the phenolic OH-group which is stronger in case of the retrosulfonamides. There was no correlation between the inhibitory potencies of the carboxamides and the analog sulfonamide classes. This fact was attributed to possible different binding modes of the two compound classes in the active site of the enzyme. The most interesting compound identified in this study, compound **91**, showed high inhibitory potency and selectivity over 17 β -HSD1. Moreover, its calculated and experimentally determined ADME parameters ($MW = 373 \text{ g/mol}$, experimentally determined $\log P = 4.42$, $tPSA = 86 \text{ \AA}^2$, 4 rotatable bonds, 2HD, 4HA) predicted a good bioavailability.

Phenylbenzenesulfonamides and -sulfonates. Vuorinen et al. developed specific ligand-based pharmacophore models for 17 β -HSD2 inhibitors. Using these models as virtual screening filters, 7 novel 17 β -HSD2 inhibitors were discovered. An additional search for structurally similar compounds resulted in the biological evaluation of 28 small molecules. In total, 13 new 17 β -HSD2 inhibitors, from which 10 represented phenylbenzene-sulfonamides and -sulfonates, were discovered (general structure given in Fig. 23, left). These inhibitors aided in the development of the SAR-model and -rules for this specific scaffold: in general, 17 β -HSD2 inhibitors require a hydrogen bond donor functionality on one benzene ring, and hydrophobic substituents on the other. The most potent inhibitor discovered was compound **92** (Fig. 23). The compound was selective over the type 1 enzyme (remaining activity of 17 β -HSD1 > 70% at an inhibitor concentration of $20 \mu\text{M}$). Compound **93** showed moderate inhibition of 17 β -HSD2 and no inhibition of the type 1 enzyme (Vuorinen et al., 2014). In continuation of this work, twenty

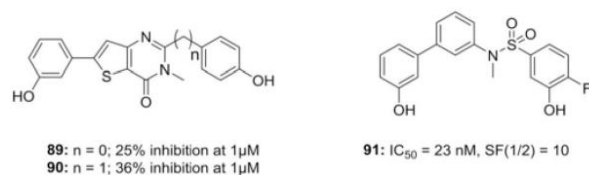


Fig. 22. Nonsteroidal inhibitors of 17 β -HSD2: Thieno [3,2-d]pyrimidinones and biphenyl-sulfonamide

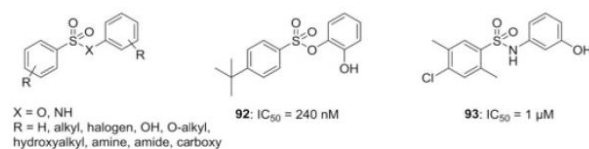


Fig. 23. Nonsteroidal inhibitors of 17 β -HSD2: Phenylbenzenesulfonamides and -sulfonates.

novel compounds representing the phenylbenzenesulfonamide and -sulfonate scaffold were synthesized and tested for their 17 β -HSD2 inhibitory activity. Nine compounds showed IC₅₀-values in the low nanomolar range. Although none of them was more active than **92** they allowed the derivation of more comprehensive SAR-rules for this scaffold (Vuorinen et al., 2017b).

2.7. Inhibitors of 17 β -HSD14

The fact that 17 β -HSD1 and 17 β -HSD2 catalyze the same reaction as 17 β -HSD14 led to the idea that the substrate binding sites of the three enzymes should exhibit a high structural similarity. A small library of 17 β -HSD1 and 17 β -HSD2 inhibitors was tested for 17 β -HSD14 inhibition. Most of the investigated hydroxyphenylmethanones (cf. Figs. 6 and 16) and thiopheneamides (cf. Figs. 17 and 18) were inactive whereas bis(hydroxyphenyl)thiophenes and -thiazoles (Fig. 7) as well as bicyclic substituted hydroxyphenylmethanones containing a pyridine moiety (Fig. 16, general formula, X = N) showed examples of low to moderate inhibitory activity against 17 β -HSD14. Active compounds possessing very high potency for 17 β -HSD1 and/or 17 β -HSD2 were neglected for the subsequent optimization as difficulties in achieving high selectivity for 17 β -HSD14 were anticipated. Starting from the hits **94** and **95** (Fig. 24), approximately thirty compounds were synthesized and tested for 17 β -HSD14 inhibition. In a fluorimetric assay, one of the most active representatives (compound **96**) exhibited a K_i value of 7 nM (Braun et al., 2016). The crystal structure of 17 β -HSD14 in complex with NAD⁺ and **96** is the first to be obtained from a human SDR 17 β -HSD enzyme with a nonsteroidal compound. The inhibitor is embedded in an extended H-bonding network and adopts a V-shaped conformation which corresponds to the active site geometry (Bertoletti et al., 2016).

Very recently, 17 β -HSD14 inhibitors containing a quinoline moiety have been published (Braun et al., 2018). Compound **97** (Fig. 24) is the most interesting inhibitor in this series, showing high affinity to the target protein combined with a good selectivity profile toward the 17 β -HSD types 1, 2 and 10 as well as ER α . In addition, the compound did not display cytotoxicity, good solubility and auspicious predicted bioavailability.

3. Conclusion and outlook

In search of novel treatment options for EDD and in order to explore estrogenic signaling pathways, the possibility to modulate estrogen action by inhibition of 17 β -HSD1 and 17 β -HSD2, respectively, has been pursued intensively within the past 25 years. During this period of time, a considerable number of inhibitors of 17 β -HSD1 and 17 β -HSD2 have been described in the literature. Some of them, such as natural compounds, were discovered in screening approaches. The majority of the inhibitors, however, result from rational drug design approaches, covering both steroidal and nonsteroidal compound classes. An interesting recent evolution is the development of designed multiple ligands which potentially inhibit both STS and 17 β -HSD1. Such dual inhibitors could reduce intracellular E2 levels more effectively than selective inhibitors of 17 β -HSD1 and may thus be superior potential therapeutics, for instance for the treatment of endometriosis where these two proteins are overexpressed.

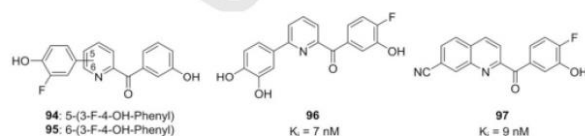


Fig. 24. Inhibitors of 17 β -HSD14.

In spite of the fact that a plethora of potent and selective inhibitors of 17 β -HSD1 and 17 β -HSD2 have been identified in cell-free and cellular assays, only very few compounds have been applied in vivo in pre-clinical studies. No compound has been reported to enter the clinical phase. There are several reasons for this poor outcome. Interspecies differences between the human enzymes and their orthologs from other species, especially rodents, are a main factor that hampered preclinical in vivo evaluation. The problem has been neglected for a long time when research was almost exclusively focused on inhibiting the human enzymes. Whereas the search for 17 β -HSD2 inhibitors by now has generated compounds which provoke potent and selective inhibition of both the human and the rodent enzyme, and may thus be candidates for in vivo evaluation, the development of inhibitors of 17 β -HSD1 was less successful in this respect. In the latter case, transgenic mice expressing the human enzyme have been established to solve this problem. Other approaches relied on primate disease models or xenograft models using immunodeficient mice or rats. Experiments using primates, however, pose high ethical hurdles and are very expensive. Xenograft models bear the drawback to give no information on possible changes of systemic estrogen levels. Insufficient metabolic stability is another issue potentially impeding (pre-)clinical trials, as many inhibitors bear a phenolic OH-group which could entail phase II biotransformation.

It will be a future task to design novel inhibitors of 17 β -HSD2 and especially 17 β -HSD1, combining improved pharmacokinetic and selectivity properties with enhanced inhibitory activities towards rodent orthologs in order to facilitate investigations of their effects in vivo and eventually to accelerate the identification of compounds eligible for clinical evaluation as novel therapeutics.

The situation is different when it comes to 17 β -HSD14 inhibition, which is an emerging research field. As the native substrates of 17 β -HSD14 are unknown, it is presently unclear whether this enzyme may be exploited as a drug target in the future. However, the potent and selective inhibitors which have become available recently could serve as scientific tools, facilitating the elucidation of the physiological role of this protein and allowing conclusions on its druggability.

Author contributions

The manuscript was written through contributions of all authors. All authors have given approval to the final version of the manuscript.

Funding sources

We are grateful to the Deutsche Forschungsgemeinschaft for financial support (FR 3002/1-1) of this work.

References

- Abdelsamie, A.S., Bey, E., Hanke, N., Empting, M., Hartmann, R.W., Frotscher, M., 2014. Inhibition of 17 β -HSD1: SAR of bicyclic substituted hydroxyphenylmethanones and discovery of new potent inhibitors with thioether linker. *Eur. J. Med. Chem.* 82, 394–406. <https://doi.org/10.1016/j.ejmech.2014.05.074>.
- Abdelsamie, A.S., Bey, E., Gargano, E.M., Van Koppen, C.J., Empting, M., Frotscher, M., 2015. Towards the evaluation in an animal disease model: fluorinated 17 β -HSD1 inhibitors showing strong activity towards both the human and the rat enzyme. *Eur. J. Med. Chem.* 103, 56–68. <https://doi.org/10.1016/j.ejmech.2015.08.030>.
- Abdelsamie, A.S., van Koppen, C.J., Bey, E., Salah, M., Börger, C., Siebenbürger, L., Laschke, M.W., Menger, M.D., Frotscher, M., 2017. Treatment of estrogen-dependent diseases: design, synthesis and profiling of a selective 17 β -HSD1 inhibitor with sub-nanomolar IC₅₀ for a proof-of-principle study. *Eur. J. Med. Chem.* 127, 944–957. <https://doi.org/10.1016/j.ejmech.2016.11.004>.
- Al-Soud, Y.A., Bey, E., Oster, A., Marchais-Oberwinkler, S., Werth, R., Kruchten, P., Frotscher, M., Hartmann, R.W., 2009. The role of the heterocycle in bis(hydroxyphenyl)triazoles for inhibition of 17 β -Hydroxysteroid Dehydrogenase (17 β -HSD) type 1 and type 2. *Mol. Cell. Endocrinol.* 301, 212–215. <https://doi.org/10.1016/j.mce.2008.09.012>.
- Al-Soud, Y.A., Marchais-Oberwinkler, S., Frotscher, M., Hartmann, R.W., 2012. Synthesis and biological evaluation of phenyl substituted 1H-1,2,4-Triazoles as non-steroidal

- inhibitors of 17 β -hydroxysteroid dehydrogenase type 2. *Arch. Pharm.* <https://doi.org/10.1002/ardp.201200025>.
- Allan, G.M., Lawrence, H.R., Cornet, J., Bubert, C., Fischer, D.S., Vicker, N., Smith, A., Tutill, H.J., Purohit, A., Day, J.M., et al., 2006a. Modification of estrone at the 6, 16, and 17 positions: novel potent inhibitors of 17 β -hydroxysteroid dehydrogenase type 1. *J. Med. Chem.* 49, 1325–1345. <https://doi.org/10.1021/jm050830t>.
- Allan, G.M., Bubert, C., Vicker, N., Smith, A., Tutill, H.J., Purohit, A., Reed, M.J., Potter, B.V.L., 2006b. Novel, potent inhibitors of 17 β -hydroxysteroid dehydrogenase type 1. *Mol. Cell. Endocrinol.* 248, 204–207. <https://doi.org/10.1016/j.mce.2005.10.021>.
- Allan, G.M., Vicker, N., Lawrence, H.R., Tutill, H.J., Day, J.M., Huchet, M., Ferrandis, E., Reed, M.J., Purohit, A., Potter, B.V.L., 2008. Novel inhibitors of 17 β -hydroxysteroid dehydrogenase type 1: templates for design. *Bioorg. Med. Chem.* 16, 4438–4456. <https://doi.org/10.1016/j.bmc.2008.02.059>.
- Auger, S., Luu-The, V., Sam, K.M., Poirier, D., 1994. 3-Hydroxy-19-nor-17 α -pregna-1,3,5(10)-triene-21,17 β -carbolactone as inhibitor of 17 β -hydroxysteroid dehydrogenase type 2. *Bioorg. Med. Chem. Lett.* 4, 2045–2048. [https://doi.org/10.1016/S0960-894X\(01\)80560-6](https://doi.org/10.1016/S0960-894X(01)80560-6).
- Bagi, C.M., Wood, J., Wilkie, D., Dixon, B., 2008. Effect of 17 β -hydroxysteroid dehydrogenase type 2 inhibitor on bone strength in ovariectomized cynomolgus monkeys. *J. Musculoskelet. Neuronal Interact.* 8, 267–280.
- Berenyi, A., Frotscher, M., Marchais-Oberwinkler, S., Hartmann, R.W., Minorics, R., Ocsosvzki, L., Falkay, G., Zupko, I., 2013. Direct antiproliferative effect of nonsteroidal 17 β -hydroxysteroid dehydrogenase type 1 inhibitors in vitro. *J. Enzym. Inhib. Med. Chem.* 28, 695–703. <https://doi.org/10.3109/14756366.2012.672414>.
- Bertoletti, N., Braun, F., Lepage, M., Möller, G., Adamski, J., Heine, A., Klebe, G., Marchais-Oberwinkler, S., 2016. New insights into human 17 β -hydroxysteroid dehydrogenase type 14: first crystal structures in complex with a steroidal ligand and with a potent nonsteroidal inhibitor. *J. Med. Chem.* 59, 6961–6967. <https://doi.org/10.1021/acs.jmedchem.6b00293>.
- Bérubé, M., Poirier, D., 2004. Synthesis of simplified hybrid inhibitors of type 1 17 β -hydroxysteroid dehydrogenase via cross-metathesis and sonogashira coupling reactions. *Org. Lett.* 6, 3127–3130. <https://doi.org/10.1021/ol048820u>.
- Bérubé, M., Poirier, D., 2009. Design, chemical synthesis, and in vitro biological evaluation of simplified estradiol-adenosine hybrids as inhibitors of 17 β -hydroxysteroid dehydrogenase type 1. *Can. J. Chem.* 87, 1180–1199. <https://doi.org/10.1139/V09-083>.
- Bérubé, M., Delagoutte, F., Poirier, D., 2010. Preparation of 16 β -estradiol derivative libraries as bisubstrate inhibitors of 17 β -hydroxysteroid dehydrogenase type 1 using the multidetachable sulfamate linker. *Molecules* 15, 1590–1631. <https://doi.org/10.3390/molecules15031590>.
- Bey, E., Marchais-Oberwinkler, S., Kruchten, P., Frotscher, M., Werth, R., Oster, A., Algül, O., Neugebauer, A., Hartmann, R.W., 2008a. Design, synthesis and biological evaluation of bis(hydroxyphenyl) azoles as potent and selective non-steroidal inhibitors of 17 β -hydroxysteroid dehydrogenase type 1 (17 β -HSD1) for the treatment of estrogen-dependent diseases. *Bioorg. Med. Chem.* 16, 6423–6435. <https://doi.org/10.1016/j.bmc.2008.04.073>.
- Bey, E., Marchais-Oberwinkler, S., Werth, R., Negri, M., Al-Soud, Y.A., Kruchten, P., Oster, A., Frotscher, M., Birk, B., Hartmann, R.W., 2008b. Design, synthesis, biological evaluation and pharmacokinetics of bis(hydroxyphenyl) substituted azoles, thiophenes, benzenes, and aza-benzenes as potent and selective nonsteroidal inhibitors of 17 β -hydroxysteroid dehydrogenase type 1 (17 β -HSD1). *J. Med. Chem.* 51, 6725–6739. <https://doi.org/10.1021/jm006917>.
- Bey, E., Marchais-Oberwinkler, S., Negri, M., Kruchten, P., Oster, A., Klein, T., Spadaro, A., Werth, R., Frotscher, M., Birk, B., et al., 2009. New insights into the SAR and binding modes of bis(hydroxyphenyl)thiophenes and -benzenes: influence of additional substituents on 17 β -hydroxysteroid dehydrogenase type 1 (17 β -HSD1) inhibitory activity and selectivity. *J. Med. Chem.* 52, 6724–6743. <https://doi.org/10.1021/jm901195w>.
- Blomquist, C.H., Bonenfant, M., McGinley, D.M., Posalaky, Z., Lakatua, D.J., Tuli-Puri, S., Bealka, D.G., Tremblay, Y., 2002. Androgenic and estrogenic 17 β -hydroxysteroid dehydrogenase/17-ketosteroid reductase in human ovarian epithelial tumors: evidence for the type 1, 2 and 5 isoforms. *J. Steroid Biochem. Mol. Biol.* 81, 343–351. [https://doi.org/10.1016/S0960-0760\(02\)00117-6](https://doi.org/10.1016/S0960-0760(02)00117-6).
- Braun, F., Bertoletti, N., Möller, G., Adamski, J., Steinmetzer, T., Salah, M., Abdelsamie, A.S., van Koppen, C.J., Heine, A., Klebe, G., et al., 2016. First structure-activity relationship of 17 β -hydroxysteroid dehydrogenase type 14 nonsteroidal inhibitors and crystal structures in complex with the enzyme. *J. Med. Chem.* 59, 10719–10737. <https://doi.org/10.1021/acs.jmedchem.6b01436>.
- Braun, F., Bertoletti, N., Möller, G., Adamski, J., Frotscher, M., Guragossian, N., Madeira Girio, P.A., Le Borgne, M., Ettouati, L., Falson, P., et al., 2018. Structure-based design and profiling of novel 17 β -HSD14 inhibitors. *Eur. J. Med. Chem.* 155, 61–76. <https://doi.org/10.1016/j.ejmech.2018.05.029>.
- Brožić, P., Lanišnik Rižner, T., Gobec, S., 2008. Inhibitors of 17 β -hydroxysteroid dehydrogenase type 1. *Curr. Med. Chem.* 15, 137–150. <https://doi.org/10.2174/092986708783330629>.
- Brožić, P., Kocbek, P., Sova, M., Kristl, J., Martens, S., Adamski, J., Gobec, S., Lanišnik Rižner, T., 2009. Flavonoids and cinnamic acid derivatives as inhibitors of 17 β -hydroxysteroid dehydrogenase type 1. *Mol. Cell. Endocrinol.* 301, 229–234. <https://doi.org/10.1016/j.mce.2008.09.004>.
- Bydal, P., Auger, S., Poirier, D., 2004. Inhibition of type 2 17 β -hydroxysteroid dehydrogenase by estradiol derivatives bearing a lactone on the D-ring: structure-activity relationships. *Steroids* 69, 325–342. <https://doi.org/10.1016/j.steroids.2004.03.002>.
- Cadot, C., Laplante, Y., Kamal, F., Luu-The, V., Poirier, D., 2007. C6-(N,N-butyl-methyl-heptanamide) derivatives of estrone and estradiol as inhibitors of 17 β -hydroxysteroid dehydrogenase: chemical synthesis and biological evaluation. *Bioorg. Med. Chem.* 15, 714–726. <https://doi.org/10.1016/j.bmc.2006.10.055>.
- Cornel, K.M.C., Kruitwagen, R.F.P.M., Delvoux, B., Visconti, L., Van De Vijver, K.K., Day, J.M., Van Gorp, T., Hermans, R.J.J., Dunselman, G.A., Romano, A., 2012. Overexpression of 17 β -hydroxysteroid dehydrogenase type 1 increases the exposure of endometrial cancer to 17 β -estradiol. *J. Clin. Endocrinol. Metabol.* 97, 591–601. <https://doi.org/10.1210/jc.2011-2994>.
- Cornel, K.M.C., Krakstad, C., Delvoux, B., Xanthouleas, S., Jori, B., Bongers, M.Y., Konings, G.F.J., Kooreman, L.F.S., Kruitwagen, R.F., Salvesen, H.B., et al., 2017. High mRNA levels of 17 β -hydroxysteroid dehydrogenase type 1 correlate with poor prognosis in endometrial cancer. *Mol. Cell. Endocrinol.* 442, 51–57. <https://doi.org/10.1016/j.mce.2016.11.030>.
- Day, J.M., Tutill, H.J., Purohit, A., Reed, M.J., 2008. Design and validation of specific inhibitors of 17 β -hydroxysteroid dehydrogenases for therapeutic application in breast and prostate cancer, and in endometriosis. *Endocr. Relat. Canc.* 15, 665–692. <https://doi.org/10.1677/ERC-08-0042>.
- Day, J.M., Tutill, H.J., Purohit, A., 2010. 17 β -hydroxysteroid dehydrogenase inhibitors. *Minerva Endocrinol.* 35, 87–108.
- Deluca, D., Krazienis, A., Breiting, R., Prehn, C., Möller, G., Adamski, J., 2005. Inhibition of 17 β -hydroxysteroid dehydrogenases by phytoestrogens: comparison with other steroid metabolizing enzymes. *J. Steroid Biochem. Mol. Biol.* 93, 285–292. <https://doi.org/10.1016/j.jsbmb.2004.12.035>.
- Deluca, D., Möller, G., Rosinus, A., Elger, W., Hillisch, A., Adamski, J., 2006. Inhibitory effects of fluorine-substituted estrogens on the activity of 17 β -hydroxysteroid dehydrogenases. *Mol. Cell. Endocrinol.* 248, 218–224. <https://doi.org/10.1016/j.mce.2005.11.037>.
- Delvoux, B., D'Hooghe, T., Kyama, C., Koskimies, P., Hermans, R.J.J., Dunselman, G.A., Romano, A., 2014. Inhibition of type 1 17 β -hydroxysteroid dehydrogenase impairs the synthesis of 17 β -estradiol in endometriosis lesions. *J. Clin. Endocrinol. Metabol.* 99, 276–284.
- Dong, Y., Qiu, Q.Q., Debeer, J., Lathrop, W.F., Bertolini, D.R., Tamburini, P.P., 1998. 17 β -Hydroxysteroid dehydrogenases in human bone cells. *J. Bone Miner. Res.* 13, 1539–1546. <https://doi.org/10.1359/jbmr.1998.13.10.1539>.
- Duax, W.L., Ghosh, D., Pletnev, V., 2000. Steroid dehydrogenase structures, mechanism of action, and disease. *Vitam. Horm.* 58, 121–148. [https://doi.org/10.1016/S0083-6729\(00\)58023-6](https://doi.org/10.1016/S0083-6729(00)58023-6).
- Engeli, R.T., Rohrer, S.R., Vuorinen, A., Herdinger, S., Kaserer, T., Leugger, S., Schuster, D., Odermatt, A., 2017. Interference of paraben compounds with estrogen metabolism by inhibition of 17 β -hydroxysteroid dehydrogenases. *Int. J. Mol. Sci.* 18, <https://doi.org/10.3390/ijms18092007>.
- Fischer, D.S., Allan, G.M., Bubert, C., Vicker, N., Smith, A., Tutill, H.J., Purohit, A., Wood, L., Packham, G., Mahon, M.F., et al., 2005. E-ring modified steroids as novel potent inhibitors of 17 β -hydroxysteroid dehydrogenase type 1. *J. Med. Chem.* 48, 5749–5770. <https://doi.org/10.1021/jm050348a>.
- Fournier, D., Poirier, D., Mazumdar, M., Lin, S.-X., 2008. Design and synthesis of bisubstrate inhibitors of type 1 17 β -hydroxysteroid dehydrogenase: overview and perspectives. *Eur. J. Med. Chem.* 43, 2298–2306. <https://doi.org/10.1016/j.ejmech.2008.01.044>.
- Frotscher, M., Ziegler, E., Marchais-Oberwinkler, S., Kruchten, P., Neugebauer, A., Fetzer, L., Scher, C., Müller-Vieira, U., Messinger, J., Thole, H., et al., 2008. Design, synthesis, and biological evaluation of (hydroxyphenyl)naphthalene and -quinoline derivatives: potent and selective nonsteroidal inhibitors of 17 β -hydroxysteroid dehydrogenase type 1 (17 β -HSD1) for the treatment of estrogen-dependent disease. *J. Med. Chem.* 51, 2158–2169. <https://doi.org/10.1021/jm701447v>.
- Gargano, E.M., Perspicace, E., Hanke, N., Carotti, A., Marchais-Oberwinkler, S., Hartmann, R.W., 2014. Metabolic stability optimization and metabolite identification of 2,5-thiophene amide 17 β -hydroxysteroid dehydrogenase type 2 inhibitors. *Eur. J. Med. Chem.* 87, 203–219. <https://doi.org/10.1016/j.ejmech.2014.09.061>.
- Gargano, E.M., Allegretta, G., Perspicace, E., Carotti, A., Van Koppen, C., Frotscher, M., Marchais-Oberwinkler, S., Hartmann, R.W., 2015. 17 β -Hydroxysteroid dehydrogenase type 2 inhibition: discovery of selective and metabolically stable compounds inhibiting both the human enzyme and its murine ortholog. *PLoS One* 10, 1–19. <https://doi.org/10.1371/journal.pone.0134754>.
- Gargano, E.M., Perspicace, E., Carotti, A., Marchais-Oberwinkler, S., Hartmann, R.W., 2016. Addressing cytotoxicity of 1,4-biphenyl amide derivatives: discovery of new potent and selective 17 β -hydroxysteroid dehydrogenase type 2 inhibitors. *Bioorg. Med. Chem. Lett.* 26, 21–24. <https://doi.org/10.1016/j.bmcl.2015.11.047>.
- Gunn, D., Akuche, C., Baryza, J., Blue, M.L., Brennan, C., Campbell, A.M., Choi, S., Cook, J., Conrad, P., Dixon, B., et al., 2005. 4,5-Disubstituted cis-pyrrolidinones as inhibitors of type II 17 β -hydroxysteroid dehydrogenase. Part 2. SAR. *Bioorg. Med. Chem. Lett.* 15, 3053–3057. <https://doi.org/10.1016/j.bmcl.2005.04.025>.
- Henn, C., Einspanier, A., Marchais-Oberwinkler, S., Frotscher, M., Hartmann, R.W., 2012. Lead optimization of the 17 β -HSD1 inhibitors of the (hydroxyphenyl)naphthol sulfonamide type for the treatment of endometriosis. *J. Med. Chem.* 55, 3307–3318. <https://doi.org/10.1021/jm201735j>.
- Huhtinen, K., Stähle, M., Perheentupa, A., Poutanen, M., 2012. Estrogen biosynthesis and signaling in endometriosis. *Mol. Cell. Endocrinol.* 358, 146–154. <https://doi.org/10.1016/j.mce.2011.08.022>.
- Husen, B., Huhtinen, K., Poutanen, M., Kangas, L., Messinger, J., Thole, H., 2006. Evaluation of inhibitors for 17 β -hydroxysteroid dehydrogenase type 1 in vivo in immunodeficient mice inoculated with MCF-7 cells stably expressing the recombinant human enzyme. *Mol. Cell. Endocrinol.* 248, 109–113. <https://doi.org/10.1016/j.mce.2005.11.042>.

- Jansson, A., 2009. 17 β -hydroxysteroid dehydrogenase enzymes and breast cancer. *J. Steroid Biochem. Mol. Biol.* 114, 64–67. <https://doi.org/10.1016/j.jsbmb.2008.12.012>.
- Kasai, T., Shozu, M., Murakami, K., Segawa, T., Shinohara, K., Nomura, K., Inoue, M., 2004. Increased expression of type I 17 β -hydroxysteroid dehydrogenase enhances in situ production of estradiol in uterine leiomyoma. *J. Clin. Endocrinol. Metabol.* 89, 5661–5668. <https://doi.org/10.1210/jc.2003-032085>.
- Kristan, K., Krajnc, K., Konc, J., Gobec, S., Stojan, J., Rižner, T.L., 2005. Phytoestrogens as inhibitors of fungal 17 β -hydroxysteroid dehydrogenase. *Steroids* 70, 694–703. <https://doi.org/10.1016/j.steroids.2005.02.023>.
- Kruchten, P., Werth, R., Bey, E., Oster, A., Marchais-Oberwinkler, S., Frotscher, M., Hartmann, R.W., 2009. Selective inhibition of 17 β -hydroxysteroid dehydrogenase type 1 (17 β HSD1) reduces estrogen responsive cell growth of T47-D breast cancer cells. *J. Steroid Biochem. Mol. Biol.* 114, 200–206. <https://doi.org/10.1016/j.jsbmb.2009.02.006>.
- Labrie, F., 1991. Intracrinology. *Molecular and Cellular Endocrinology*. vol. 78, C113–C118. [https://doi.org/10.1016/0303-7207\(91\)90116-A](https://doi.org/10.1016/0303-7207(91)90116-A).
- Labrie, F., Luu-The, V., Lin, S.-X., Simard, J., Labrie, C., El-Alfy, M., Pelletier, G., Bélanger, A., 2000. Intracrinology: role of the family of 17 beta-hydroxysteroid dehydrogenases in human physiology and disease. *J. Mol. Endocrinol.* 25, 1–16. <https://doi.org/10.1677/jme.0.0250001>.
- Lamminen, T., Saloniemi, T., Huhtinen, K., Koskimies, P., Messinger, J., Husen, B., Thole, H., Poutanen, M., 2009. In vivo mouse model for analysis of hydroxysteroid (17 β) dehydrogenase 1 inhibitors. *Mol. Cell. Endocrinol.* 301, 158–162. <https://doi.org/10.1016/j.mce.2008.10.034>.
- Laplatte, Y., Cadot, C., Fournier, M.-A., Poirier, D., 2008. Estradiol and estrone C-16 derivatives as inhibitors of type 1 17beta-hydroxysteroid dehydrogenase: blocking of ER+ breast cancer cell proliferation induced by estrone. *Bioorg. Med. Chem.* 16, 1849–1860. <https://doi.org/10.1016/j.bmc.2007.11.007>.
- Lawrence, H.R., Vicker, N., Allan, G.M., Smith, A., Mahon, M.F., Tutill, H.J., Purohit, A., Reed, M.J., Potter, B.V.L., 2005. Novel and potent 17 β -hydroxysteroid dehydrogenase type 1 inhibitors. *J. Med. Chem.* 48, 2759–2762. <https://doi.org/10.1021/jm0494045r>.
- Lilienkamp, A., Karkola, S., Alho-Richmond, S., Koskimies, P., Johansson, N., Huhtinen, K., Vihko, K., Wähälä, K., 2009. Synthesis and biological evaluation of 17-beta-hydroxysteroid dehydrogenase type 1 (17 β HSD1) inhibitors based on a thieno[2,3-d]pyrimidin-4(3H)-one core. *J. Med. Chem.* 52, 6660–6671. <https://doi.org/10.1021/jm900928k>.
- Lota, R.K., Dhanani, S., Owen, C.P., Ahmed, S., 2007. Search for potential non-steroidal inhibitors of 17-hydroxysteroid dehydrogenase (17-HSD) in the treatment of hormone-dependent cancers. *Lett. Drug Des. Discov.* 4, 180–184. <https://doi.org/10.2174/157018007780077417>.
- Lukacik, P., Keller, B., Bunkoczi, G., Kavanagh, K.L., Lee, W.H., Hwa Lee, W., Adamski, J., Oppermann, U., 2007. Structural and biochemical characterization of human orphan DHRS10 reveals a novel cytosolic enzyme with steroid dehydrogenase activity. *Biochem. J.* 402, 419–427. <https://doi.org/10.1042/BJ20061319>.
- Maltais, R., Ayan, D., Poirier, D., 2011. Crucial role of 3-bromoethyl in removing the estrogenic activity of 17beta-HSD1 inhibitor 16beta-(m-Carbamoylbenzyl)estradiol. *ACS Med. Chem. Lett.* 2, 678–681. <https://doi.org/10.1021/ml200093v>.
- Maltais, R., Ayan, D., Trotter, A., Barbeau, X., Lague, P., Bouchard, J.-E., Poirier, D., 2014. Discovery of a non-estrogenic irreversible inhibitor of 17beta-hydroxysteroid dehydrogenase type 1 from 3-substituted-16beta-(m-carbamoylbenzyl)-estradiol derivatives. *J. Med. Chem.* 57, 204–222. <https://doi.org/10.1021/jm401639v>.
- Maltais, R., Trotter, A., Delhomme, A., Barbeau, X., Lague, P., Poirier, D., 2015. Identification of fused 16beta,17beta-oxazinone-estradiol derivatives as a new family of non-estrogenic 17beta-hydroxysteroid dehydrogenase type 1 inhibitors. *Eur. J. Med. Chem.* 93, 470–480. <https://doi.org/10.1016/j.ejmech.2015.01.059>.
- Marchais-Oberwinkler, S., Kruchten, P., Frotscher, M., Ziegler, E., Neugebauer, A., Bhoga, U., Bey, E., Müller-Vieira, U., Messinger, J., Thole, H., et al., 2008. Substituted 6-phenyl-2-naphthols. Potent and selective nonsteroidal inhibitors of 17beta-hydroxysteroid dehydrogenase type 1 (17 β HSD1): design, synthesis, biological evaluation, and pharmacokinetics. *J. Med. Chem.* 51, 4685–4698. <https://doi.org/10.1021/jm800367k>.
- Marchais-Oberwinkler, S., Frotscher, M., Ziegler, E., Werth, R., Kruchten, P., Messinger, J., Thole, H., Hartmann, R.W., 2009. Structure-activity study in the class of 6-(3'-hydroxyphenyl)naphthalenes leading to an optimization of a pharmacophore model for 17 β -hydroxysteroid dehydrogenase type 1 (17 β HSD1) inhibitors. *Mol. Cell. Endocrinol.* 301, 205–211. <https://doi.org/10.1016/j.mce.2008.09.024>.
- Marchais-Oberwinkler, S., Henn, C., Möller, G., Klein, T., Negri, M., Oster, A., Spadaro, A., Werth, R., Wetzel, M., Xu, K., et al., 2011a. 17 β -Hydroxysteroid dehydrogenases (17 β HSDs) as therapeutic targets: protein structures, functions, and recent progress in inhibitor development. *J. Steroid Biochem. Mol. Biol.* 125, 66–82. <https://doi.org/10.1016/j.jsbmb.2010.12.013>.
- Marchais-Oberwinkler, S., Wetzel, M., Ziegler, E., Kruchten, P., Werth, R., Henn, C., Hartmann, R.W., Frotscher, M., 2011b. New drug-like hydroxyphenylnaphthol steroidomimetics as potent and selective 17 β -hydroxysteroid dehydrogenase type 1 inhibitors for the treatment of estrogen-dependent diseases. *J. Med. Chem.* 54, 534–547. <https://doi.org/10.1021/jm1009082>.
- Marchais-Oberwinkler, S., Xu, K., Wetzel, M., Perspice, E., Negri, M., Meyer, A., Odermatt, A., Möller, G., Adamski, J., Hartmann, R.W., 2013. Structural optimization of 2,5-thiophene amides as highly potent and selective 17 β -hydroxysteroid dehydrogenase type 2 inhibitors for the treatment of osteoporosis. *J. Med. Chem.* 56, 167–181. <https://doi.org/10.1021/jm3014053>.
- Mazumdar, M., Fournier, D., Zhu, D.-W., Cadot, C., Poirier, D., Lin, S.-X., 2009. Binary and ternary crystal structure analyses of a novel inhibitor with 17beta-HSD type 1: a lead compound for breast cancer therapy. *Biochem. J.* 424, 357–366. <https://doi.org/10.1042/BJ20091020>.
- Messinger, J., Hirvelä, L., Husen, B., Kangas, L., Koskimies, P., Pentikäinen, O., Saarenketo, P., Thole, H., 2006. New inhibitors of 17 β -hydroxysteroid dehydrogenase type 1. *Mol. Cell. Endocrinol.* 248, 192–198. <https://doi.org/10.1016/j.mce.2005.11.044>.
- Messinger, J., Husen, B., Koskimies, P., Hirvel, L., Kallio, L., Saarenketo, P., Thole, H., 2009. Estrone C15 derivatives-A new class of 17 β -hydroxysteroid dehydrogenase type 1 inhibitors. *Mol. Cell. Endocrinol.* 301, 216–224. <https://doi.org/10.1016/j.mce.2008.10.022>.
- Miralinaghi, P., Schmitt, C., Hartmann, R.W., Frotscher, M., Engel, M., 2014. 6-Hydroxybenzothioephene ketones: potent inhibitors of 17 β -hydroxysteroid dehydrogenase type 1 (17 β HSD1) owing to favorable molecule geometry and conformational preorganization. *ChemMedChem* 9, 2294–2308. <https://doi.org/10.1002/cmdc.201402050>.
- Möller, G., Deluca, D., Gege, C., Rosinus, A., Kowalik, D., Peters, O., Droscher, P., Elger, W., Adamski, J., Hillisch, A., 2009. Structure-based design, synthesis and in vitro characterization of potent 17 β -hydroxysteroid dehydrogenase type 1 inhibitors based on 2-substitutions of estrone and D-homo-estrone. *Bioorg. Med. Chem. Lett* 19, 6740–6744. <https://doi.org/10.1016/j.bmcl.2009.09.113>.
- Niinevehmas, S., Postila, P.A., Rauhamäki, S., Kortet, S., Ahinko, M., Huuskonen, P., Nyberg, N., Lätti, S., Multamäki, E., Juvenon, R.O., et al., 2018. Blocking oestradiol synthesis pathways with potent and selective coumarin derivatives. *J. Enzym. Inhib. Med. Chem.* 33, 743–754. <https://doi.org/10.1080/14756366.2018.1452919>.
- Olusanjo, M.S., Shahid, I., Owen, C.P., Ahmed, S., 2008. Inhibition of 17 β -hydroxysteroid dehydrogenase (17 β HSD) by imida-zole-based compounds. *Lett. Drug Des. Discov.* 5, 48–51. <https://doi.org/10.2174/157018008783406705>.
- Oster, A., Hinsberger, S., Werth, R., Marchais-Oberwinkler, S., Frotscher, M., Hartmann, R.W., 2010a. Bicyclic substituted hydroxyphenylmethanones as novel inhibitors of 17 β -hydroxysteroid dehydrogenase type 1 (17 β HSD1) for the treatment of estrogen-dependent diseases. *J. Med. Chem.* 53, 8176–8186. <https://doi.org/10.1021/jm101073q>.
- Oster, A., Klein, T., Werth, R., Kruchten, P., Bey, E., Negri, M., Marchais-Oberwinkler, S., Frotscher, M., Hartmann, R.W., 2010b. Novel estrone mimetics with high 17 β HSD1 inhibitory activity. *Bioorg. Med. Chem.* 18, 3494–3505. <https://doi.org/10.1016/j.bmc.2010.03.065>.
- Oster, A., Klein, T., Henn, C., Werth, R., Marchais-Oberwinkler, S., Frotscher, M., Hartmann, R.W., 2011. Bicyclic substituted hydroxyphenylmethanone type inhibitors of 17 β -hydroxysteroid dehydrogenase Type1 (17 β HSD1): the role of the bicyclic moiety. *ChemMedChem* 6, 476–487. <https://doi.org/10.1002/cmdc.201000457>.
- Ouellet, J., Ayan, D., Poirier, D., 2014. Synthesis and biological evaluation of estradiol-core derivatives bearing a fused γ -lactone as inhibitors of 17 β -hydroxysteroid dehydrogenase type 1. *Curr. Enzym. Inhib.* 10, 39–52.
- Pelletier, J.D., Poirier, D., 1996. Synthesis and evaluation of estradiol derivatives with 16 α -(bromoalkylamide), 16 α -(bromoalkyl) or 16 α -(bromoalkynyl) side chain as inhibitors of 17 β -hydroxysteroid dehydrogenase type 1 without estrogenic activity. *Bioorg. Med. Chem.* 4, 1617–1628. [https://doi.org/10.1016/0968-0896\(96\)00154-X](https://doi.org/10.1016/0968-0896(96)00154-X).
- Penning, T.M., 1997. Molecular endocrinology of hydroxysteroid dehydrogenases. *Endocr. Rev.* 18, 281–305. <https://doi.org/10.1210/er.18.3.281>.
- Penning, T.M., 2003. Hydroxysteroid dehydrogenases and pre-receptor regulation of steroid hormone action. *Hum. Reprod. Update* 9, 193–205. <https://doi.org/10.1093/humupd/dmg022>.
- Perspice, E., Marchais-Oberwinkler, S., Hartmann, R.W., 2013a. Synthesis and biological evaluation of thieno[3,2-d]-pyrimidinones, thieno[3,2-d]pyrimidines and quinazolinones: conformationally restricted 17 β -hydroxysteroid dehydrogenase type 2 (17 β HSD2) inhibitors. *Molecules* 18, 4487–4509. <https://doi.org/10.3390/molecules18044487>.
- Perspice, E., Giorgio, A., Carotti, A., Marchais-Oberwinkler, S., Hartmann, R.W., 2013b. Novel N-methylsulfonamide and retro-N-methylsulfonamide derivatives as 17 β -hydroxysteroid dehydrogenase type 2 (17 β HSD2) inhibitors with good ADME-related physicochemical parameters. *Eur. J. Med. Chem.* 69, 201–215. <https://doi.org/10.1016/j.ejmech.2013.08.026>.
- Perspice, E., Cozzoli, L., Gargano, E.M., Hanke, N., Carotti, A., Hartmann, R.W., Marchais-Oberwinkler, S., 2014. Novel, potent and selective 17 β -hydroxysteroid dehydrogenase type 2 inhibitors as potential therapeutics for osteoporosis with dual human and mouse activities. *Eur. J. Med. Chem.* 83, 317–337. <https://doi.org/10.1016/j.ejmech.2014.06.036>.
- Poirier, D., 2003. Inhibitors of 17 beta-hydroxysteroid dehydrogenases. *Curr. Med. Chem.* 10, 453–477. <https://doi.org/10.2174/0929867033368222>.
- Poirier, D., 2009. Advances in development of inhibitors of 17beta hydroxysteroid dehydrogenases. *Anti Cancer Agents Med. Chem.* 9, 642–660. <https://doi.org/10.2174/187152009788680000>.
- Poirier, D., Dionne, P., Auger, S., 1998. A 6beta-(thiaheptanamide) derivative of estradiol as inhibitor of 17beta-hydroxysteroid dehydrogenase type 1. *J. Steroid Biochem. Mol. Biol.* 64, 83–90. [https://doi.org/10.1016/S0960-0760\(97\)00136-2](https://doi.org/10.1016/S0960-0760(97)00136-2).
- Poirier, D., Bydal, P., Tremblay, M.R., Sam, K.-M., Luu-The, V., 2001. Inhibitors of type II 17 β -hydroxysteroid dehydrogenase. *Mol. Cell. Endocrinol.* 171, 119–128. [https://doi.org/10.1016/S0303-7207\(00\)00427-5](https://doi.org/10.1016/S0303-7207(00)00427-5).
- Poirier, D., Boivin, R.P., Tremblay, M.R., Berube, M., Qiu, W., Lin, S.-X., 2005. Estradiol-adenosine hybrid compounds designed to inhibit type 1 17beta-hydroxysteroid dehydrogenase. *J. Med. Chem.* 48, 8134–8147. <https://doi.org/10.1021/jm058235e>.

- Potter, B.V.L., 2018. SULFATION PATHWAYS: steroid sulphatase inhibition via aryl sulphamates: clinical progress, mechanism and future prospects. *J. Mol. Endocrinol.* 61, T233–T252. <https://doi.org/10.1530/JME-18-0045>.
- Qiu, W., Campbell, R.L., Gangloff, A., Dupuis, P., Boivin, R.P., Tremblay, M.R., Poirier, D., Lin, S.-X., 2002. A concerted, rational design of type 1 17 β -hydroxysteroid dehydrogenase inhibitors: estradiol-adenosine hybrids with high affinity. *Faseb. J.: Off. Publ. Feder. Am. Soc. Exp. Biol.* 16, 1829–1831. <https://doi.org/10.1096/fj.02-0026fj>.
- Rouillard, F., Lefebvre, J., Fournier, M., Poirier, D., 2008. Chemical synthesis, 17-hydroxysteroid dehydrogenase type 1 inhibitory activity and assessment of in vitro and in vivo estrogenic activities of estradiol derivatives. *Open Enzym. Inhib. J.* 1, 61–71. (doi:1874-9402/08).
- Salah, M., Abdelsamie, A.S., Frotscher, M., 2017. First dual inhibitors of steroid sulfatase (STS) and 17 β -hydroxysteroid dehydrogenase type 1 (17 β -HSD1): designed multiple ligands as novel potential therapeutics for estrogen-dependent diseases. *J. Med. Chem.* 60, 4086–4092. <https://doi.org/10.1021/acs.jmedchem.7b00062>.
- Saloniemi, T., Järvensivu, P., Koskimies, P., Jokela, H., Lamminen, T., Ghaem-Maghamsi, S., Dina, R., Damdimopoulou, P., Mäkelä, S., Perheentupa, A., et al., 2010. Novel hydroxysteroid (17 β) dehydrogenase 1 inhibitors reverse estrogen-induced endometrial hyperplasia in transgenic mice. *Am. J. Pathol.* 176, 1443–1451. <https://doi.org/10.2353/ajpath.2010.090325>.
- Sam, K.M., Auger, S., Luu-The, V., Poirier, D., 1995. Steroidal spiro-gamma-lactones that inhibit 17 beta-hydroxysteroid dehydrogenase activity in human placental microsomes. *J. Med. Chem.* 38, 4518–4528. <https://doi.org/10.1021/jm00022a018>.
- Sam, K., Labrie, F., Poirier, D., 2000. N-Butyl-N-methyl-11-(3'-hydroxy-21',17'-carbolactone-19'-nor-17 α -pregna-1',3',5'(10')-trien-7 α -yl)-undecanamide: an inhibitor of type 2 17 β -hydroxysteroid dehydrogenase that does not have oestrogenic or androgenic activity. *Eur. J. Med. Chem.* 35, 217–225. [https://doi.org/10.1016/S0223-5234\(00\)00124-0](https://doi.org/10.1016/S0223-5234(00)00124-0).
- Schuster, D., Nashev, L.G., Kirchmair, J., Laggner, C., Wolber, G., Langer, T., Odermatt, A., 2008. Discovery of nonsteroidal 17-hydroxysteroid dehydrogenase 1 inhibitors by pharmacophore-based screening of virtual compound libraries. *J. Med. Chem.* 51, 4188–4199. <https://doi.org/10.1021/jm800054h>.
- Šmuc, T., Pucelj, M.R., Šinkovec, J., Husen, B., Thole, H., Lanišnik Rižner, T., 2007. Expression analysis of the genes involved in estradiol and progesterone action in human ovarian endometriosis. *Gynecol. Endocrinol.* 23, 105–111. <https://doi.org/10.1080/09513590601152219>.
- Spadaro, A., Negri, M., Marchais-Oberwinkler, S., Bey, E., Frotscher, M., 2012a. Hydroxybenzothiazoles as new nonsteroidal inhibitors of 17 β -hydroxysteroid dehydrogenase type 1 (17 β -HSD1). *PLoS One* 7, 1–12. <https://doi.org/10.1371/journal.pone.0029252>.
- Spadaro, A., Frotscher, M., Hartmann, R.W., 2012b. Optimization of hydroxybenzothiazoles as novel potent and selective inhibitors of 17 β -HSD1. *J. Med. Chem.* 55, 2469–2473. <https://doi.org/10.1021/jm201711b>.
- Starčević, B., Brožić, P., Turk, S., Cesar, J., Lanišnik Rižner, T., Gobec, S., 2011a. Synthesis and biological evaluation of (6- and 7-Phenyl) coumarin derivatives as selective nonsteroidal inhibitors of 17 β -hydroxysteroid dehydrogenase type 1. *J. Med. Chem.* 54, 248–261. <https://doi.org/10.1021/jm101104z>.
- Starčević, B., Turk, S., Brus, B., Cesar, J., Lanišnik Rižner, T., Gobec, S., 2011b. Discovery of highly potent, nonsteroidal 17 β -hydroxysteroid dehydrogenase type 1 inhibitors by virtual high-throughput screening. *J. Steroid Biochem. Mol. Biol.* 127, 255–261. <https://doi.org/10.1016/j.jsbmb.2011.08.013>.
- Tremblay, M.R., Poirier, D., 1998. Overview of a rational approach to design type I 17-beta-hydroxysteroid dehydrogenase inhibitors without estrogenic activity: chemical synthesis and biological evaluation. *J. Steroid Biochem. Mol. Biol.* 66, 179–191. [https://doi.org/10.1016/S0960-0760\(98\)00043-0](https://doi.org/10.1016/S0960-0760(98)00043-0).
- Tremblay, M.R., Auger, S., Poirier, D., 1995. Synthesis of 16-(bromoalkyl)-estradiols having inhibitory effect on human placental estradiol 17 beta-hydroxysteroid dehydrogenase (17 beta-HSD type 1). *Bioorg. Med. Chem.* 3, 505–523. [https://doi.org/10.1016/0968-0896\(95\)00041-E](https://doi.org/10.1016/0968-0896(95)00041-E).
- Tremblay, M.R., Boivin, R.P., Luu-The, V., Poirier, D., 2005. Inhibitors of type 1 17 β -hydroxysteroid dehydrogenase with reduced estrogenic activity: modifications of the positions 3 and 6 of estradiol. *J. Enzym. Inhib. Med. Chem.* 20, 153–163. <https://doi.org/10.1080/14756360500043307>.
- Vanderschueren, D., Gaytant, J., Boonen, S., Venken, K., 2008. Androgens and bone. *Curr. Opin. Endocrinol. Diabetes Obes.* 15, 250–254. <https://doi.org/10.1097/MED.0b013e3282fe6ca9>.
- Vicker, N., Lawrence, H., Allan, G.M., Bubert, C., Smith, A., Tutill, H.J., Purohit, A., Day, J.M., Mahon, M.F., Reed, M.J., et al., 2006. Focused libraries of 16-substituted estrone derivatives and modified E-ring steroids: inhibitors of 17 β -hydroxysteroid dehydrogenase type 1. *ChemMedChem* 1, 464–481. <https://doi.org/10.1002/cmdc.200500087>.
- Vuorinen, A., Engeli, R., Meyer, A., Bachmann, F., Griesser, U.J., Schuster, D., Odermatt, A., 2014. Ligand-based pharmacophore modeling and virtual screening for the discovery of novel 17 β -hydroxysteroid dehydrogenase 2 inhibitors. *J. Med. Chem.* 57, 5995–6007. <https://doi.org/10.1021/jm5004914>.
- Vuorinen, A., Engeli, R.T., Leugger, S., Bachmann, F., Akram, M., Atanasov, A.G., Waltenberger, B., Temml, V., Stuppner, H., Krenn, L., et al., 2017a. Potential antiosteoporotic natural product lead compounds that inhibit 17 β -hydroxysteroid dehydrogenase type 2. *J. Nat. Prod.* 80, 965–974. <https://doi.org/10.1021/acs.jnatprod.6b00950>.
- Vuorinen, A., Engeli, R.T., Leugger, S., Kreutz, C.R., Schuster, D., Odermatt, A., Matyszczak, B., 2017b. Phenylbenzenesulfonates and -sulfonamides as 17 β -hydroxysteroid dehydrogenase type 2 inhibitors: synthesis and SAR-analysis. *Bioorg. Med. Chem. Lett* 27, 2982–2985. <https://doi.org/10.1016/j.bmcl.2017.05.005>.
- Wetzel, M., Marchais-Oberwinkler, S., Hartmann, R.W., 2011a. 17 β -HSD2 inhibitors for the treatment of osteoporosis: identification of a promising scaffold. *Bioorg. Med. Chem.* 19, 807–815. <https://doi.org/10.1016/j.bmc.2010.12.013>.
- Wetzel, M., Marchais-Oberwinkler, S., Perspicace, E., Möller, G., Adamski, J., Hartmann, R.W., 2011b. Introduction of an electron withdrawing group on the hydroxyphenyl-naphthol scaffold improves the potency of 17 β -hydroxysteroid dehydrogenase type 2 (17 β -HSD2) inhibitors. *J. Med. Chem.* 54, 7547–7557. <https://doi.org/10.1021/jm2008453>.
- Wetzel, M., Gargano, E.M., Hinsberger, S., Marchais-Oberwinkler, S., Hartmann, R.W., 2012. Discovery of a new class of bicyclic substituted hydroxyphenylmethanones as 17 β -hydroxysteroid dehydrogenase type 2 (17 β -HSD2) inhibitors for the treatment of osteoporosis. *Eur. J. Med. Chem.* 47, 1–17. <https://doi.org/10.1016/j.ejmech.2011.09.004>.
- Wood, J., Bagi, C.M., Akuche, C., Bacchiocchi, A., Baryza, J., Blue, M.L., Brennan, C., Campbell, A.M., Choi, S., Cook, J.H., et al., 2006. 4,5-Disubstituted cis-pyrrolidinones as inhibitors of type II 17 β -hydroxysteroid dehydrogenase. Part 3. Identification of lead candidate. *Bioorg. Med. Chem. Lett* 16, 4965–4968. <https://doi.org/10.1016/j.bmcl.2006.06.041>.
- Xu, K., Wetzel, M., Hartmann, R.W., Marchais-Oberwinkler, S., 2011a. Synthesis and biological evaluation of spiro- δ -lactones as inhibitors of 17 β -hydroxysteroid dehydrogenase type 2 (17 β -HSD2). *Lett. Drug Des. Discov.* 8, 406–421. <https://doi.org/10.2174/157018011795514230>.
- Xu, K., Al-Soud, Y.A., Wetzel, M., Hartmann, R.W., Marchais-Oberwinkler, S., 2011b. Triazole ring-opening leads to the discovery of potent nonsteroidal 17 β -hydroxysteroid dehydrogenase type 2 inhibitors. *Eur. J. Med. Chem.* 46, 5978–5990. <https://doi.org/10.1016/j.ejmech.2011.10.010>.

4. Final Discussion

The superior goal of this thesis was the development of the first dual inhibitors of STS and 17 β -HSD1 (DSHIs) that can be used for in vivo proof-of-principle studies using human endometriotic tissues. As previously mentioned in the introduction, STS and 17 β -HSD1 inhibitions play crucial roles in decreasing the local biosynthesis of estrogen inside the endometriosis without affecting the circulating ovarian estrogen in premenopausal women. This offers a novel therapeutic option for the treatment of endometriosis without the common hypo-estrogenic side effects that characterize existing treatment options. In this thesis, two different chemical classes of DSHIs have been introduced. The approach leading to their design, their biological activities and metabolic stabilities will be discussed and compared - whenever possible- in the following chapters. This is followed by a discussion of the pharmacokinetic profiles of the most interesting candidates of the metabolically stable class. For the sake of clarity, compounds mentioned in this section are identified by a capital letter which stands for the respective paper, followed by an arabic number referring to the compound numbering in the respective paper.

4.1 Design rationale of DSHIs

A rational design approach was pursued to imbue STS and 17 β -HSD1 dual inhibitory activity by taking a potent 17 β -HSD1 inhibitor and building the aryl sulfamate pharmacophore which is essential for STS inhibition. This designed multiple ligand approach shall be facilitated by the fact that both target enzymes have very similar natural ligands, E1-S and E1. This tactic was applied successfully on two 17 β -HSD1 inhibitor classes (see figure 9). In the first class of DSHIs, compound **C15** a potent 17 β -HSD1 inhibitor was used as a starting point for building the STS pharmacophore. Extensive structure activity relationship (SAR) studies have been performed on this 17 β -HSD1 inhibitor class which is presented in chapter **3.2.I**. These SAR studies show that the appropriate place to introduce modifications without significantly affecting the 17 β -HSD1 inhibitory activity is ring A as the other part of the scaffold is essential for activity (see figure 9). Therefore, our strategy was to introduce the aryl-O-sulfamate to ring A (results of the first class is presented in chapter **3.1.I**). Similarly, the second class of the DSHIs (results shown in chapter **3.1.II**) was developed, in which compound **B3** was our starting point for the insertion of the sulfamate group on the appropriate ring; in this case it was ring B as a consequence of an existing SAR studies.

4.2 Biological profiling of DSHIs

In general, the introduction of the sulfamate group maintained the 17 β -HSD1 inhibitory activity as anticipated. On the other hand, the STS inhibitory activity was found to be closely linked to the position of the sulfamate on the phenyl ring and the substituents on this ring. The optimization of the sulfamate position on the aryl ring revealed that this group should be in the *meta* or *para* position to the attachment point of the ring (position 3 and 4 on ring A and B in figure 9). In contrast, compounds with *ortho* sulfamate group (position 2 on ring A and B in figure 9) showed no STS inhibition e.g. compounds **A2** and **B7**. In the first class of DSHIs, the presence of an additional group on the phenyl ring was essential for STS inhibitory activity. This was manifested by compounds that lack additional substituents on ring A (**A1** and **A3**), showing no STS inhibition. On the other hand, the presence of electron withdrawing groups (Cl or F) on the aryl system led to the most potent STS inhibition manifested in both classes of inhibitors. This is probably attributed to the enhanced sulfamoyl transfer potential resulting from the increased leaving group ability of the corresponding phenol precursors of the sulfamates. The first class of DSHIs (**A5**, **A6**, **A8** and **A9**) displayed a 3-20 fold higher inhibitory potency against STS when compared to the second class (**B10**, **B11** and **B12**). In the second class, the presence of the methyl group in compounds **B5** and **B6** resulted in a 10-25 fold increase in the 17 β -HSD1 inhibitory activity while maintaining moderate STS inhibitory activity.

17 β -HSD2 has a very beneficial protective role in EDDs by lowering the intracellular levels of E2, making its inhibition undesirable. However, this is a challenging characteristic in 17 β -HSD1 inhibitors as the two enzymes have very similar substrates, namely E1 and E2. Therefore, the selectivity over 17 β -HSD2 of the above mentioned dual inhibitors was evaluated. Generally, the second class displayed higher selectivity over 17 β -HSD2 than the first class. The most selective compounds of the second DSHIs class (**B5**, **B6** and **B12**) showed a 3-7 fold higher selectivity factors in the range of 110-280, compared to **A9** the only selective compound in the first DSHIs class (SF=33).

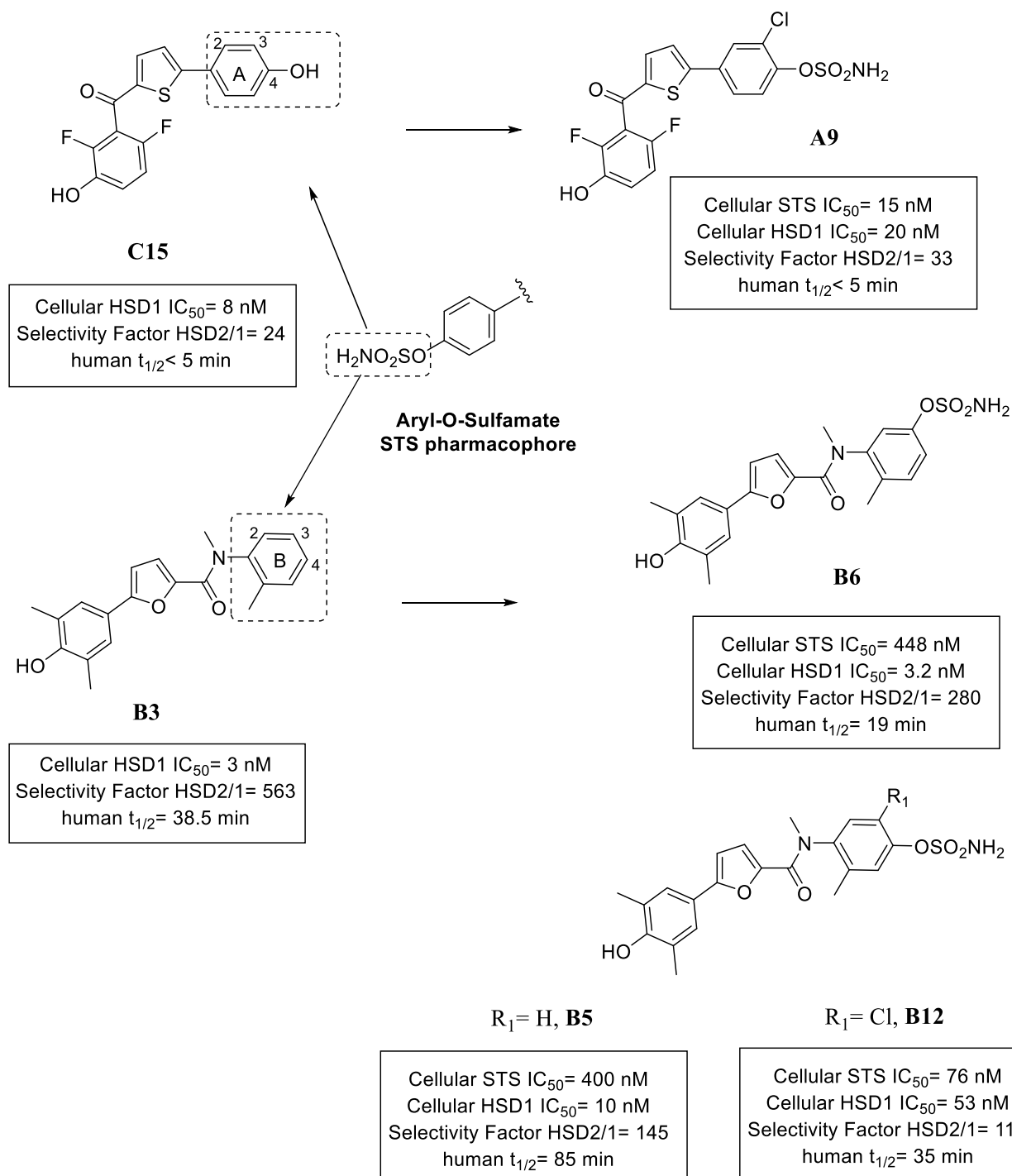


Figure 9 Design rational of DSHIs classes, with the biological data of the most potent representatives

The intracellular inhibitory activity of the most potent candidates from both DSHIs classes using T47D cells which express both target enzymes revealed that the two classes possess good cellular permeability shown by their potent intracellular inhibition for both enzymes. The STS enzyme was found to be irreversibly inhibited by the developed DSHIs of both classes, similar to other sulfamate-containing STS inhibitors.

The biological profiles of the developed DSHIs show that **A9** is the most potent DSHIs from the first class of compounds that poses selectivity over 17 β -HSD2. On the other hand, **B5**, **B6** and **B12** are the most potent and selective candidates of the second class of compounds (see figure 9).

4.3 Effect of DSHIs on estrogen-stimulated growth

After having in hands inhibitors with promising in vitro inhibitory activities towards STS and 17 β -HSD1 even in cellular assays, it was of high interest to evaluate the impact of this inhibition in a more complex assay system. Thus, the effect of **A9** (DSHIs) on E1-S and E1 stimulated growth of T47D cells (ER⁺ breast cancer cells) was evaluated in comparison to single-target inhibitors **A13** and **A14** (17 β -HSD1 inhibitor and STS inhibitor, respectively). **A9** was able to decrease the proliferative effect of E1-S/E1 stimulation in a dose-dependent manner, reaching control levels at concentration of 400 nM. In contrast, the single-target inhibitors did not decrease the stimulated effect of estrogen below 150% and 200% of the control (**A13** and **A14**, respectively). These differences in antiproliferative effects between DSHIs and single-target inhibitors were attributed to the differences in E1 and E2 levels produced in the presence of different inhibitors. It was shown experimentally that in the absence of inhibitors the cells convert E1-S and E1 into E2, which strongly stimulates cell growth. In case of **A9**, no significant conversion of E1-S or E1 was detected, while in case of single-target inhibitors the residual cell proliferation was in agreement with the amounts of E1 and/or E2 produced. Moreover, **A9** showed no influence on non-stimulated or E2-stimulated cell proliferation, indicating that it exerts neither cytotoxic nor estrogenic effects nor estrogen receptor antagonism. Therefore, **A9** (DSHIs) deploys its antiproliferative effect through the inhibition of STS and 17 β -HSD1 which results in the blockage of E2 formation.

4.4 Further in vitro biological evaluation of DSHIs

An important prerequisite for reaching sufficient plasma concentrations for an adequate time interval after in vivo application of the compounds is achieving high in vitro metabolic stability. Therefore, the metabolic stabilities of the compounds with the most beneficial

biological profiles were evaluated. On one hand, compound **A9** the representative of the first class of DSHIs was found to be metabolically unstable with $t_{1/2}$ less than 5 minutes. Upon investigation, it was found that phase II metabolism is the major pathway, which can be strongly linked to the conjugation of the free hydroxy group. Further development of this class was stopped as this hydroxy group is essential for potent 17 β -HSD1 inhibition. On the other hand, the second class of DSHIs was characterized by significantly higher metabolic stability. **B5** showed the best metabolic stability profile of any DSHIs or 17 β -HSD1 inhibitor developed by our group, with $t_{1/2}$ 85 min and 56 min using human and mouse hepatic S9 fractions, respectively. **B6** and **B12** showed acceptable metabolic stability.

Along with their good physiochemical properties and their high safety in cytotoxicity assays performed on selected human cell lines (HEK293 and HepG2 cells), these interesting results of **B5**, **B6** and **B12** constitute important requirements to be eligible for in vivo pharmacokinetic profile evaluation.

4.5 In vivo evaluation of pharmacokinetic profile of DSHIs

In order to select the best candidate from **B5**, **B6** and **B12** for a proof-of-principle study in a xenograft mouse model for endometriosis, their PK profiles had to be evaluated. The plasma levels of the three compounds after single subcutaneous dosing revealed that **B5** had high AUC value (11619 ng.h/mL) which was a 6 fold higher than that's of **B6** and **B12**. Moreover, the plasma concentration of **B5** remained higher than the cellular IC₈₀ values of both target enzymes up to 24 h. After oral application, **B5** showed high plasma levels in first 8 h of the study sufficient for both target enzymes. However, in the following intervals the concentration of **B5** continued declining to reach very low levels that were not sufficient for the inhibition of any of the target enzymes at 24 h. A multiple dose PK study was performed with **B5** in which the compound was administered subcutaneously every day or every second day. After 24 h, the plasma levels were sufficient for inhibition of both target enzymes. The plasma concentrations of **B5** 48 h post-dosing was sufficient for 17 β -HSD1 inhibition but not STS inhibition. However, taking in consideration the irreversible mode of inhibition of STS, these levels could be sufficient but this has to be clinically evaluated. Additionally, a steady state behavior in the plasma level of **B5** was observed which strongly suggest that CYP metabolizing enzymes aren't altered by inhibition or by induction.

4.6 Conclusion

Taken together, a successful design approach for the first DSHIs was implemented, followed by good biological results which demonstrated that the in vitro inhibition of STS and 17 β -HSD1 can be translated into significant anti-proliferative effect for estrogen stimulated cell growth. Additionally, the second class of DSHIs especially compound **B5**, showed very strong inhibition of STS and 17 β -HSD1 in cellular assays along with high selectivity over 17 β -HSD2. The high metabolic stability of **B5** in human and mouse hepatic S9 fractions, besides its good physiochemical properties resulted in admirable PK profile. These findings obviously reflect the suitability of **B5** for future proof-of-principle studies.

As previously shown in the introduction, the HSD enzyme family has a wide range of physiological roles and it is often associated with diseases. In chapter **3.2.II**, a novel targeted intracrine therapy for bone fracture was successfully introduced in a proof-of-principle study using a potent and selective 17 β -HSD2 inhibitor (compound **D15**) in mouse bone fracture model. Moreover, in chapter **3.2.III** the first SAR of 17 β -HSD14 non-steroidal inhibitors was introduced. This will provide the basis for future development of highly potent and selective 17 β -HSD14 inhibitor that could serve as a chemical tool for proper understanding of the enzyme physiological role upon in vivo administration. In this context, a comprehensive review on the inhibitors of 17 β -HSD1, 2 and 14 is included in chapter **3.2.IV**.

4.7 Outlook

The results of the potent dual inhibitor of STS and 17 β -HSD1 **B5**, pave the way for its rational use in future studies to evaluate the efficacy of the DSHIs in proof-of-principle studies for the treatment of endometriosis. In the initial phase, the efficacy of **B5** can be evaluated in vivo using nude mice with xenograft endometrium tissue from endometriotic patients. The parameters to be studied should include:

- Determination of lesion size by ultrasound
- Histological examination of the lesions (incl. neovascularization)
- Determination of STS and 17 β -HSD1 activity in the lesions
- Quantification of plasma steroid hormones (E1-S) and cellular E1-S, E1 and E2 in the lesions

In parallel, an ex vivo study can be performed to compare between the efficacy of the DSHIs (**B5**) and the single inhibitors using human endometriotic tissues. In which the same parameters mentioned in the previous experiment should be monitored.

In case **B5** turned out to be effective in the abovementioned proof-of-principle studies, it could be used as a tool for safety profiling of DSHIs in non-human primate (monkey). Among the parameters that should be monitored:

- Plasma E1-S, E1 and E2
- Ovulation and menstrual cycle disruption
- Bone formation and resorption

5. Supporting information

This section contains the supporting information of the studies presented in chapter 3.1. It contains further experimental details, as well as additional figures and results.

5.1. Supporting information for publication A

5.1.I Chemistry

5.1.I.1 *Chemical methods*

Chemical names follow IUPAC nomenclature.

Starting materials were purchased from Acros Organics, Alfa Aesar, Combi-Blocks, Fluorochem and Sigma Aldrich. Column chromatography was performed on silica gel (0.04-0.063 mm, Macherey-Nagel) and reaction progress was monitored by TLC on aluminum sheets (Silicagel 60 F254, Merck). Visualization was accomplished with UV light at 254 nm.

^1H and ^{13}C NMR spectra were measured on a Bruker-500 (at 500 MHz and 125 MHz, respectively) or Bruker-300 (at 300 MHz). Chemical shifts are reported in δ (parts per million: ppm), using residual peaks of the deuterated solvents as internal standard: $(\text{CD}_3)_2\text{SO}$ (DMSO-*d*6): 2.50 ppm (^1H NMR), 39.52 ppm (^{13}C NMR); $(\text{CD}_3)_2\text{CO}$ (acetone-*d*6): 2.05 ppm (^1H NMR), 29.84 ppm and 206.26 ppm (^{13}C NMR). Signals are described as s, d, t, dd, ddd, dt, td and m for singlet, doublet, triplet, doublet of doublets, doublet of doublet of doublets, doublet of triplets, triplets of doublets and multiplet, respectively. All coupling constants (*J*) are given in Hertz (Hz).

All tested compounds have $\geq 95\%$ chemical purity as evaluated by HPLC. The purity of the compounds was evaluated by LC/MS. The Surveyor®-LC-system consisted of a pump, an auto sampler, and a PDA detector. Mass spectrometry was performed by a TSQ® Quantum (ThermoFisher, Dreieich, Germany). The triple quadrupole mass spectrometer was equipped with an electrospray interface (ESI). The system was operated by the standard software Xcalibur®. A RP C18 NUCLEODUR® 100-5 (3 mm) column (Macherey-Nagel GmbH, Dühren, Germany) was used as stationary phase. All solvents were HPLC grade. In a gradient run the percentage of acetonitrile (containing 0.1 % trifluoroacetic acid) was increased from an initial concentration of 30% at 0 min to 100 % at 12 min and kept at 100 % for 3 min. The injection volume was 25 μL and flow rate was set to 700 $\mu\text{L}/\text{min}$. MS analysis was carried out at a needle voltage of 3000 V and a capillary temperature of 350 °C. Mass spectra were acquired in positive mode from 100 to 1000 m/z and UV spectra were recorded at the wave

length of 254 nm. The melting points were measured using StuartTM melting point apparatus SMP3.

5.1.1.2 *General procedures*

General procedure for Friedel-Crafts acylation (Method A)

An ice-cooled mixture of monosubstituted thiophene derivate (1.5 equiv), 2,6-difluoro-3-methoxybenzoyl chloride (1 equiv), and anhydrous aluminum trichloride (2 equiv) in anhydrous dichloromethane was left for 0.5 h, warmed to room temperature and stirred for 2-4 h, then quenched with 1 M HCl. The aqueous layer was extracted with ethyl acetate. The organic layers were combined, dried over magnesium sulfate and concentrated to dryness under reduced pressure. The product was purified by column chromatography.

General procedure for Suzuki coupling (Method B)

Arylbromide (1 equiv), boronic acid derivative (1.2 equiv), cesium carbonate (4 equiv) and tetrakis(triphenylphosphine) palladium (0.05 equiv) were added to an oxygen-free DME/water (1:1) and refluxed under nitrogen atmosphere for 4 h. The reaction mixture was cooled to room temperature. The aqueous layer was extracted with ethyl acetate. The organic layers were combined, dried over magnesium sulfate and concentrated to dryness under reduced pressure. The product was purified by column chromatography.

General procedure for ether cleavage (Method C)

To a solution of methoxybenzene derivative (1 equiv) in anhydrous dichloromethane at -78 °C (dry ice/acetone bath), boron tribromide in dichloromethane (1 M, 3 equiv per methoxy function) was added dropwise. The reaction mixture was stirred overnight at room temperature under nitrogen atmosphere. The reaction was quenched with water, then the aqueous layer was extracted with ethyl acetate and the combined organic layer was washed with brine, dried over magnesium sulfate, filtered and concentrated to dryness under reduced pressure. The product was purified by column chromatography.

General procedure for Sulfamoylation (Method D)

A solution of phenol derivative (1.0 equiv) in DMA was cooled to 0 °C. A freshly prepared sulfamoyl chloride (5 equiv) was subsequently added over 5 min and the reaction mixture was warmed to room temperature overnight. The reaction was quenched with water, then the aqueous layer was extracted with ethyl acetate. The organic layers were combined, dried over

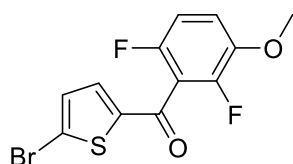
magnesium sulfate and concentrated to dryness under reduced pressure. The product was purified by column chromatography.

Preparation of sulfamoyl chloride (Method E)

A fresh solution was prepared for each reaction. Chlorosulfonyl isocyanate (1 equiv) was cooled to 0 °C. Then formic acid 99% (1 equiv) was then added dropwise to the isocyanate slowly over 10 min. Slow, steady evolution of CO₂ was observed; eventually a white solid was formed. After 10 min, the ice bath was removed and the reaction mixture was warmed to room temperature and then used in the next reaction without further workup.

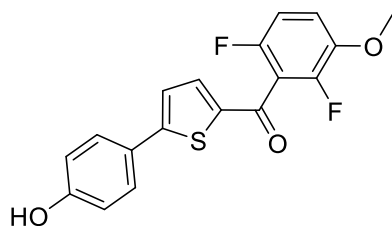
5.1.1.3 Detailed synthesis procedure and compound characterization

(5-Bromothiophen-2-yl)(2,6-difluoro-3-methoxyphenyl)methanone (1a).

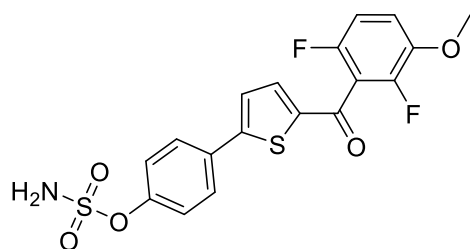


The title compound was prepared according to method A by the reaction of 2,6-difluoro-3-methoxybenzoyl chloride (1.03 g, 5.00 mmol, 1 equiv) and 2-bromothiophene (1.22 g, 7.50 mmol, 1.5 equiv) in the presence of anhydrous aluminium chloride (1.33 g, 10.00 mmol, 2 equiv) in anhydrous dichloromethane (20 ml). The product was purified by column chromatography (cyclohexane/ethylacetate 4:1) to give 1.24 g (3.77 mmol/ 75%) of the analytically pure compound. C₁₂H₇BrF₂O₂S; MW 333; ¹H NMR (300 MHz, (CD₃)₂SO) δ 7.52 (dt, *J* = 4.1, 1.0 Hz, 1H), 7.47 – 7.37 (m, 2H), 7.25 (ddd, *J* = 9.3, 8.8, 1.9 Hz, 1H), 3.89 (s, 3H); MS (ESI): 333.03, 335.04 (M+H)⁺.

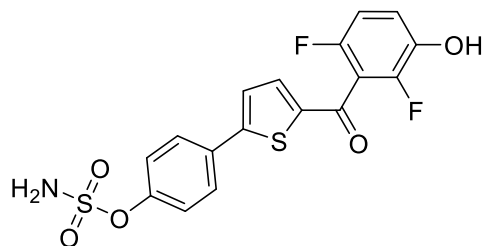
(2,6-Difluoro-3-methoxyphenyl)(5-(4-hydroxyphenyl)thiophen-2-yl)methanone (1b).



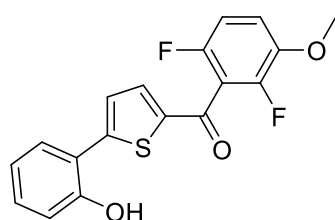
The title compound was prepared according to method B by the reaction of **1a** (0.45 g, 1.50 mmol, 1 equiv) and (4-hydroxyphenyl)boronic acid (0.24 g, 1.80 mmol, 1.2 equiv) in the presence of cesium carbonate (1.95 g, 6.00 mmol, 4 equiv) and tetrakis(triphenylphosphine) palladium (87.00 mg, 0.08 mmol, 0.05 equiv) in DME/water 1:1 (20 ml). The product was purified by column chromatography (dichloromethane) to give 0.39 g (1.12 mmol/ 75%) of the analytically pure compound. C₁₈H₁₂F₂O₃S; MW 346; ¹H NMR (300 MHz, (CD₃)₂SO) δ 9.79 (s, 1H), 7.69 – 7.58 (m, 2H), 7.42 (td, *J* = 9.5, 5.3 Hz, 1H), 7.35 – 7.21 (m, 3H), 7.17 (dd, *J* = 2.3, 1.7 Hz, 1H), 6.88 (ddd, *J* = 7.8, 2.4, 1.4 Hz, 1H), 3.91 (s, 3H); MS (ESI): 347.00 (M+H)⁺.

4-(5-(2,6-Difluoro-3-methoxybenzoyl)thiophen-2-yl)phenyl sulfamate (1c).

The title compound was prepared according to Method D by the reaction of **1b** (0.34 g, 1.00 mmol, 1 equiv) and sulfamoyl chloride (0.58 g, 5.00 mmol, 5 equiv) in DMA (10 ml). The product was purified by column chromatography (cyclohexane/ethylacetate 1:1) to give 0.33 g (0.78 mmol/ 78%) of the analytically pure compound. C₁₈H₁₃F₂NO₅S₂; MW 425; ¹H NMR (300 MHz, (CD₃)₂SO) δ 8.11 (s, 2H), 7.87 – 7.73 (m, 2H), 7.72 (dd, *J* = 3.7, 1.5 Hz, 2H), 7.61 (t, *J* = 8.0 Hz, 1H), 7.45 (dt, *J* = 9.5, 4.8 Hz, 1H), 7.39 (ddd, *J* = 8.2, 2.3, 1.0 Hz, 1H), 7.28 (td, *J* = 9.0, 1.9 Hz, 1H), 3.92 (s, 3H); MS (ESI): 426.03 (M+H)⁺.

4-(5-(2,6-Difluoro-3-hydroxybenzoyl)thiophen-2-yl)phenyl sulfamate (1).

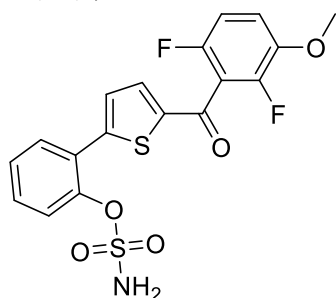
The title compound was prepared according to Method C by the reaction of **1c** (0.21 g, 0.50 mmol, 1 equiv) and boron tribromide (1 M) in dichloromethane (1.50 ml, 1.50 mmol, 3 equiv) in anhydrous dichloromethane (10 ml). The product was purified by column chromatography (dichloromethane/methanol 98.5:1.5) to give 0.10 g (0.25 mmol/ 50%) of the analytically pure compound. C₁₇H₁₁F₂NO₅S₂; MW 411; mp: 176-177; ¹H NMR (500 MHz, (CD₃)₂CO) δ 9.02 (s, 1H), 7.78 (ddd, *J* = 7.8, 1.8, 1.0 Hz, 1H), 7.75 (ddd, *J* = 2.2, 1.8, 0.4 Hz, 1H), 7.67 (dt, *J* = 4.1, 0.8 Hz, 1H), 7.66 (d, *J* = 4.0 Hz, 1H), 7.61 – 7.56 (m, 1H), 7.41 (ddd, *J* = 8.2, 2.3, 1.0 Hz, 1H), 7.25 (s, 2H), 7.23 – 7.18 (m, 1H), 7.04 (ddd, *J* = 9.1, 8.6, 1.9 Hz, 1H); ¹³C NMR (126 MHz, (CD₃)₂CO) δ 180.73, 153.68, 152.53 (dd, *J* = 240.6, 5.7 Hz), 148.40 (dd, *J* = 245.8, 7.7 Hz), 152.18, 143.75, 142.64 (dd, *J* = 12.9, 3.2 Hz), 138.13, 135.45, 131.66, 126.76, 125.46, 124.29, 121.02, 120.40 (dd, *J* = 9.1, 3.9 Hz), 117.95 (dd, *J* = 23.8, 19.6 Hz), 112.44 (dd, *J* = 22.8, 3.8 Hz); MS (ESI): 411.95 (M+H)⁺.

(2,6-Difluoro-3-methoxyphenyl)(5-(2-hydroxyphenyl)thiophen-2-yl)methanone (2b).

The title compound was prepared according to method B by the reaction of **1a** (0.45 g, 1.50 mmol, 1 equiv) and (2-hydroxyphenyl)boronic acid (0.24 g, 1.80 mmol, 1.2 equiv) in the

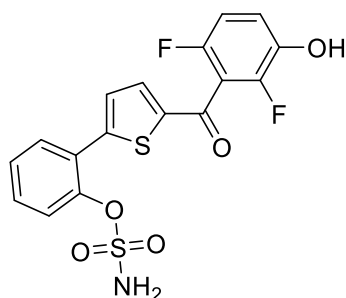
presence of cesium carbonate (1.95 g, 6.00 mmol, 4 equiv) and tetrakis(triphenylphosphine) palladium (87 mg, 0.08 mmol, 0.05 equiv) in DME/water 1:1 (20 ml). The product was purified by column chromatography (cyclohexane/ethylacetate 2:1) to give 0.44 g (1.29 mmol/ 86%) of the analytically pure compound. $C_{18}H_{12}F_2O_3S$; MW 346; 1H NMR (500 MHz, $(CD_3)_2SO$) δ 10.89 (s, 1H), 7.84 (dd, J = 8.0, 1.6 Hz, 1H), 7.77 (d, J = 4.3 Hz, 1H), 7.59 (dd, J = 4.2, 0.9 Hz, 1H), 7.40 (td, J = 9.5, 5.3 Hz, 1H), 7.30 – 7.21 (m, 2H), 7.02 (dd, J = 8.2, 1.2 Hz, 1H), 6.93 (ddd, J = 8.3, 7.2, 1.2 Hz, 1H), 3.90 (s, 3H); MS (ESI): 347.01 ($M+H$) $^+$.

2-(5-(2,6-Difluoro-3-methoxybenzoyl)thiophen-2-yl)phenyl sulfamate (2c).



The title compound was prepared according to Method D by the reaction of **2b** (0.34 g, 1.00 mmol, 1 equiv) and sulfamoyl chloride (0.58 g, 5.00 mmol, 5 equiv) in DMA (10 ml). The product was purified by column chromatography (cyclohexane/ethylacetate 3:2) to give 0.38 g (0.90 mmol/ 90%) of the analytically pure compound. $C_{18}H_{13}F_2NO_5S_2$; MW 425; 1H NMR (500 MHz, $(CD_3)_2SO$) δ 8.37 (s, 2H), 7.93 (dd, J = 7.9, 1.6 Hz, 1H), 7.72 (d, J = 4.2 Hz, 1H), 7.64 (dt, J = 4.3, 0.9 Hz, 1H), 7.61 (dd, J = 8.3, 1.3 Hz, 1H), 7.54 (ddd, J = 8.2, 7.3, 1.6 Hz, 1H), 7.46 – 7.39 (m, 2H), 7.26 (td, J = 9.0, 1.8 Hz, 1H), 3.90 (s, 3H); MS (ESI): 426.04 ($M+H$) $^+$.

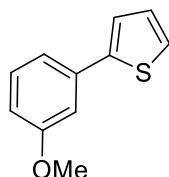
2-(5-(2,6-Difluoro-3-hydroxybenzoyl)thiophen-2-yl)phenyl sulfamate (2).



The title compound was prepared according to Method C by the reaction of **2c** (0.21 g, 0.50 mmol, 1 equiv) and boron tribromide (1 M) in dichloromethane (1.50 ml, 1.50 mmol, 3 equiv) in anhydrous dichloromethane (10 ml). The product was purified by column chromatography (dichloromethane/methanol 98.5:1.5) to give 61.00 mg (0.15 mmol/ 30%) of the analytically pure compound. $C_{17}H_{11}F_2NO_5S_2$; MW 411; mp: 164-165; 1H NMR (500 MHz, $(CD_3)_2CO$) δ 9.06 (d, J = 1.1 Hz, 1H), 7.89 (dd, J = 7.8, 1.7 Hz, 1H), 7.70 (d, J = 4.1 Hz, 1H), 7.68 (dd, J = 8.3, 1.3 Hz, 1H), 7.61 (dt, J = 4.1, 1.0 Hz, 1H), 7.52 (ddd, J = 8.2, 7.4, 1.7 Hz, 1H), 7.48 (s, 2H), 7.44 (td, J = 7.6, 1.3 Hz, 1H), 7.21 (ddd, J = 9.7, 9.1, 5.5 Hz, 1H), 7.04 (ddd, J = 9.1, 8.6, 1.9 Hz, 1H); ^{13}C NMR (126 MHz, $(CD_3)_2CO$) δ 180.99, 152.52 (dd, J = 240.4, 5.9 Hz), 148.40 (dd, J = 245.7, 7.9 Hz), 149.65, 148.28, 144.30, 142.64 (dd, J = 12.9,

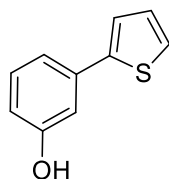
3.2 Hz), 137.32, 131.32, 130.80, 129.13, 127.91, 127.24, 123.56, 120.28 (dd, $J = 9.1, 3.9$ Hz), 118.18 (dd, $J = 24.0, 19.6$ Hz), 112.43 (dd, $J = 22.8, 4.0$ Hz); MS (ESI): 411.95 (M+H)⁺.

2-(3-Methoxyphenyl)thiophene (3a).



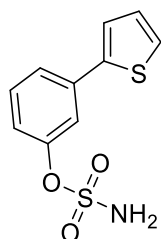
The title compound was prepared according to method B by the reaction of 2-bromothiophene (0.82 g, 5.00 mmol, 1 equiv) and (3-methoxyphenyl)boronic acid (0.91 g, 6.00 mmol, 1.2 equiv) in the presence of cesium carbonate (6.50 g, 20.00 mmol, 4 equiv) and tetrakis(triphenylphosphine) palladium (0.29 g, 0.25 mmol, 0.05 equiv) in DME/water 1:1 (50 ml). The product was purified by column chromatography (cyclohexane/dichloromethane 5:1) to give 0.87 g (4.60 mmol/ 92%) of the analytically pure compound. C₁₁H₁₀OS; MW 190; ¹H NMR (300 MHz, (CD₃)₂SO) δ 7.57 – 7.53 (m, 1H), 7.53 – 7.51 (m, 1H), 7.33 (t, $J = 7.9$ Hz, 1H), 7.24 – 7.20 (m, 1H), 7.19 – 7.17 (m, 1H), 7.13 (dd, $J = 5.0, 3.7$ Hz, 1H), 6.89 (ddd, $J = 8.2, 2.5, 1.0$ Hz, 1H), 3.81 (s, 3H); MS (ESI): 191.02 (M+H)⁺.

3-(Thiophen-2-yl)phenol (3b).



The title compound was prepared according to Method C by the reaction of **3a** (0.76 g, 4.00 mmol, 1 equiv) and boron tribromide (1 M) in dichloromethane (12.00 ml, 12.00 mmol, 3 equiv) in anhydrous dichloromethane (20 ml). The product was purified by column chromatography (cyclohexane/dichloromethane 4:1) to give 0.56 g (3.20 mmol/ 80%) of the analytically pure compound. C₁₀H₈OS; MW 176; ¹H NMR (300 MHz, (CD₃)₂SO) δ 9.55 (s, 1H), 7.51 (dd, $J = 5.1, 1.2$ Hz, 1H), 7.42 (dd, $J = 3.6, 1.2$ Hz, 1H), 7.20 (t, $J = 7.8$ Hz, 1H), 7.11 (dd, $J = 5.1, 3.6$ Hz, 1H), 7.10 – 7.05 (m, 1H), 7.04 – 7.00 (m, 1H), 6.71 (ddd, $J = 8.0, 2.4, 1.0$ Hz, 1H); MS (ESI): 176.98 (M+H)⁺.

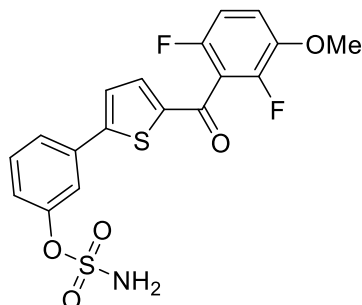
3-(Thiophen-2-yl)phenyl sulfamate (3c).



The title compound was prepared according to Method D by the reaction of **3b** (0.53 g, 3.00 mmol, 1 equiv) and sulfamoyl chloride (1.73 g, 15.00 mmol, 5 equiv) in DMA (20 ml). The product was purified by column chromatography (cyclohexane/ethylacetate 3:2) to give 0.61 g (2.40 mmol/ 80%) of the analytically pure compound. C₁₀H₉NO₃S₂; MW 255; ¹H

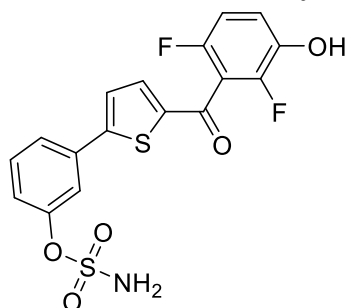
NMR (300 MHz, $(\text{CD}_3)_2\text{SO}$) δ 8.05 (s, 2H), 7.65 – 7.58 (m, 2H), 7.56 (dd, $J = 3.6, 1.2$ Hz, 1H), 7.54 – 7.46 (m, 2H), 7.22 (ddd, $J = 8.1, 2.3, 1.0$ Hz, 1H), 7.17 (dd, $J = 5.1, 3.6$ Hz, 1H); MS (ESI): 256.01 ($\text{M}+\text{H}$)⁺.

3-(5-(2,6-Difluoro-3-methoxybenzoyl)thiophen-2-yl)phenyl sulfamate (3d).



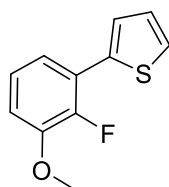
The title compound was prepared according to method by the reaction of 2,6-difluoro-3-methoxybenzoyl chloride (0.41 g, 2.00 mmol, 1 equiv) and **3c** (0.76 g, 3.00 mmol, 1.5 equiv) in the presence of anhydrous aluminium chloride (0.53 g, 4.00 mmol, 2 equiv) in anhydrous dichloromethane (10 ml). The product was purified by column chromatography (cyclohexane/ethylacetate 3:2) to give 0.49 g (1.16 mmol/ 58%) of the analytically pure compound. $\text{C}_{18}\text{H}_{13}\text{F}_2\text{NO}_5\text{S}_2$; MW 425; ^1H NMR (300 MHz, $(\text{CD}_3)_2\text{SO}$) δ 8.10 (s, 2H), 7.85 – 7.76 (m, 1H), 7.76 – 7.68 (m, 3H), 7.60 (t, $J = 8.0$ Hz, 1H), 7.44 (dt, $J = 9.5, 4.7$ Hz, 1H), 7.40 – 7.34 (m, 1H), 7.27 (td, $J = 9.0, 1.9$ Hz, 1H), 3.91 (s, 3H); MS (ESI): 426.00 ($\text{M}+\text{H}$)⁺.

3-(5-(2,6-Difluoro-3-hydroxybenzoyl)thiophen-2-yl)phenyl sulfamate (3).



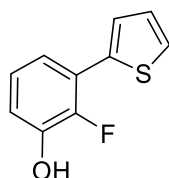
The title compound was prepared according to Method C by the reaction of **3d** (0.21 g, 0.50 mmol, 1 equiv) and boron tribromide (1 M) in dichloromethane (1.50 ml, 1.50 mmol, 3 equiv) in anhydrous dichloromethane (10 ml). The product was purified by column chromatography (dichloromethane/methanol 98.5:1.5) to give 123.00 mg (0.29 mmol/ 58%) of the analytically pure compound. $\text{C}_{17}\text{H}_{11}\text{F}_2\text{NO}_5\text{S}_2$; MW 411; mp: 174-175; ^1H NMR (500 MHz, $(\text{CD}_3)_2\text{CO}$) δ 9.01 (s, 1H), 7.78 (ddd, $J = 7.8, 1.8, 1.0$ Hz, 1H), 7.76 – 7.74 (m, 1H), 7.68 – 7.64 (m, 2H), 7.58 (t, $J = 8.0$ Hz, 1H), 7.41 (ddd, $J = 8.2, 2.3, 1.0$ Hz, 1H), 7.25 (s, 2H), 7.23 – 7.18 (m, 1H), 7.04 (td, $J = 8.9, 1.9$ Hz, 1H); ^{13}C NMR (126 MHz, $(\text{CD}_3)_2\text{CO}$) δ 180.74, 153.69, 152.54 (dd, $J = 240.5, 5.8$ Hz), 152.20, 148.41 (dd, $J = 246.0, 7.7$ Hz), 143.77, 142.66 (dd, $J = 12.8, 3.2$ Hz), 138.14, 135.46, 131.67, 126.78, 125.48, 124.30, 121.04, 120.41 (dd, $J = 9.1, 3.9$ Hz), 117.97 (dd, $J = 23.9, 19.7$ Hz), 112.45 (dd, $J = 22.8, 3.9$ Hz); MS (ESI): 411.95 ($\text{M}+\text{H}$)⁺.

2-(2-Fluoro-3-methoxyphenyl)thiophene (4a).



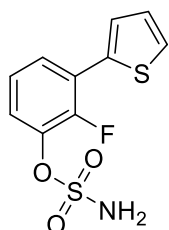
The title compound was prepared according to method B the reaction of 2-bromothiophene (0.82 g, 5.00 mmol, 1 equiv) and (2-fluoro-3-methoxyphenyl)boronic acid (1.02 g, 6.00 mmol, 1.2 equiv) in the presence of cesium carbonate (6.50 g, 20.00 mmol, 4 equiv) and tetrakis(triphenylphosphine) palladium (0.29 g, 0.25 mmol, 0.05 equiv) in DME/water 1:1 (50 ml). The product was purified by column chromatography (cyclohexane/dichloromethane 7:1) to give 1.00 g (4.80 mmol/ 96%) of the analytically pure compound. $C_{11}H_9FOS$; MW 208; 1H NMR (300 MHz, $(CD_3)_2SO$) δ 7.32 – 7.20 (m, 2H), 7.16 (dt, J = 3.7, 1.2 Hz, 1H), 6.94 (ddd, J = 8.0, 7.1, 1.9 Hz, 1H), 6.86 (td, J = 8.0, 1.1 Hz, 1H), 6.76 (ddd, J = 5.2, 3.7, 1.2 Hz, 1H), 3.89 (s, 3H); MS (ESI): 209.03 ($M+H$) $^+$.

2-Fluoro-3-(thiophen-2-yl)phenol (4b).



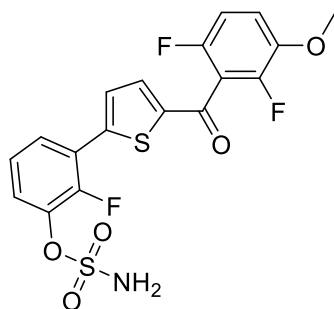
The title compound was prepared according to Method C by the reaction of **4a** (0.83 g, 4.00 mmol, 1 equiv) and boron tribromide (1 M) in dichloromethane (12.00 ml, 12.00 mmol, 3 equiv) in anhydrous dichloromethane (20 ml). The product was purified by column chromatography (cyclohexane/dichloromethane 4:1) to give 0.73 g (3.76 mmol/ 97%) of the analytically pure compound. $C_{10}H_7FOS$; MW 194; 1H NMR (300 MHz, $(CD_3)_2SO$) δ 10.36 (s, 1H), 7.33 – 7.22 (m, 2H), 7.17 (dt, J = 3.7, 1.1 Hz, 1H), 6.95 (ddd, J = 8.0, 7.1, 1.7 Hz, 1H), 6.87 (td, J = 7.9, 1.1 Hz, 1H), 6.77 (ddd, J = 5.1, 3.8, 1.1 Hz, 1H); MS (ESI): 195.01 ($M+H$) $^+$.

2-Fluoro-3-(thiophen-2-yl)phenyl sulfamate (4c).



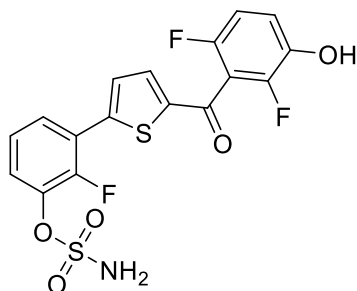
The title compound was prepared according to Method D by the reaction of **4b** (0.58 g, 3.00 mmol, 1 equiv) and sulfamoyl chloride (1.73 g, 15.00 mmol, 5 equiv) in DMA (20 ml). The product was purified by column chromatography (cyclohexane/ethylacetate 3:1) to give 0.44 g (1.60 mmol/ 53%) of the analytically pure compound. $C_{10}H_8FNO_3S_2$; MW 273; 1H NMR (300 MHz, $(CD_3)_2SO$) δ 8.30 (s, 2H), 7.78 – 7.66 (m, 2H), 7.61 (dt, J = 3.7, 1.1 Hz, 1H), 7.39 (ddd, J = 8.1, 7.1, 1.8 Hz, 1H), 7.32 (td, J = 7.9, 1.1 Hz, 1H), 7.22 (ddd, J = 5.0, 3.7, 1.2 Hz, 1H); MS (ESI): 274.00 ($M+H$) $^+$.

3-(5-(2,6-Difluoro-3-methoxybenzoyl)thiophen-2-yl)-2-fluorophenyl sulfamate (4d).



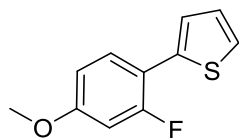
The title compound was prepared according to method A by the reaction of 2,6-difluoro-3-methoxybenzoyl chloride (0.41 g, 2.00 mmol, 1 equiv) and **4c** (0.82 g, 3.00 mmol, 1.5 equiv) in the presence of anhydrous aluminium chloride (0.53 g, 4.00 mmol, 2 equiv) in anhydrous dichloromethane (10 ml). The product was purified by column chromatography (cyclohexane/ethylacetate 3:2) to give 0.60 g (1.35 mmol/ 67%) of the analytically pure compound. $C_{18}H_{12}F_3NO_5S_2$; MW 443; 1H NMR (500 MHz, $(CD_3)_2CO$) δ 8.37 (s, 2H), 7.85 (ddd, J = 8.2, 6.7, 1.6 Hz, 1H), 7.76 – 7.69 (m, 2H), 7.57 (ddd, J = 8.2, 7.4, 1.6 Hz, 1H), 7.40 (td, J = 8.1, 1.4 Hz, 1H), 7.28 – 7.17 (m, 1H), 7.06 (ddd, J = 9.1, 8.5, 1.9 Hz, 1H), 3.91 (s, 3H); MS (ESI): 444.08 (M+H) $^+$.

3-(5-(2,6-Difluoro-3-hydroxybenzoyl)thiophen-2-yl)-2-fluorophenyl sulfamate (4**).**



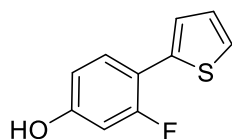
The title compound was prepared according to Method C by the reaction of **4d** (0.22 g, 0.50 mmol, 1 equiv) and boron tribromide (1 M) in dichloromethane (1.50 ml, 1.50 mmol, 3 equiv) in anhydrous dichloromethane (10 ml). The product was purified by column chromatography (dichloromethane/methanol 98.5:1.5) to give 140.00 mg (0.33 mmol/ 66%) of the analytically pure compound. $C_{17}H_{10}F_3NO_5S_2$; MW 429; mp: 176-177; 1H NMR (500 MHz, $(CD_3)_2CO$) δ 9.14 (s, 1H), 7.84 (ddd, J = 8.2, 6.7, 1.6 Hz, 1H), 7.75 – 7.68 (m, 2H), 7.56 (ddd, J = 8.2, 7.4, 1.6 Hz, 1H), 7.52 (s, 2H), 7.39 (td, J = 8.1, 1.4 Hz, 1H), 7.22 (ddd, J = 9.7, 9.2, 5.4 Hz, 1H), 7.05 (ddd, J = 9.1, 8.5, 1.9 Hz, 1H); ^{13}C NMR (126 MHz, $(CD_3)_2CO$) δ 180.99, 152.76 (d, J = 256.1 Hz), 152.51 (dd, J = 240.7, 5.7 Hz), 148.41 (dd, J = 245.9, 7.7 Hz), 146.60 (d, J = 3.5 Hz), 144.54 (d, J = 4.5 Hz), 142.70 (dd, J = 12.8, 3.2 Hz), 139.72 (d, J = 12.8 Hz), 137.37, 129.42 (d, J = 5.3 Hz), 127.84 (d, J = 2.1 Hz), 126.55, 126.04 (d, J = 4.7 Hz), 123.43 (d, J = 10.6 Hz), 120.50 (dd, J = 9.1, 4.0 Hz), 117.94 (dd, J = 23.8, 19.6 Hz), 112.49 (dd, J = 22.7, 3.9 Hz); MS (ESI): 430.09 (M+H) $^+$.

2-(2-Fluoro-4-methoxyphenyl)thiophene (5a**).**



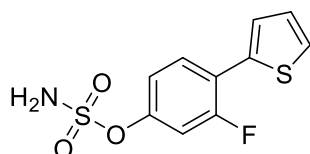
The title compound was prepared according to method B by the reaction of 2-bromothiophene (0.82 g, 5.00 mmol, 1 equiv) and (2-fluoro-4-methoxyphenyl)boronic acid (1.02 g, 6.00 mmol, 1.2 equiv) in the presence of cesium carbonate (6.50 g, 20.00 mmol, 4 equiv) and tetrakis(triphenylphosphine) palladium (0.29 g, 0.25 mmol, 0.05 equiv) in DME/water 1:1 (50 ml). The product was purified by column chromatography (cyclohexane/dichloromethane 7:1) to give 0.84 g (4.05 mmol/ 81%) of the analytically pure compound. C₁₁H₉FOS; MW 208; ¹H NMR (300 MHz, CD₃)₂SO) δ 7.11 (dd, *J* = 12.8, 2.4 Hz, 1H), 7.06 (dd, *J* = 5.2, 1.1 Hz, 1H), 7.01 (dd, *J* = 3.7, 1.1 Hz, 1H), 6.99 – 6.93 (m, 1H), 6.75 (t, *J* = 8.8 Hz, 1H), 6.67 (dd, *J* = 5.2, 3.7 Hz, 1H), 3.42 (s, 3H); MS (ESI): 209.04 (M+H)⁺.

3-Fluoro-4-(thiophen-2-yl)phenol (**5b**).



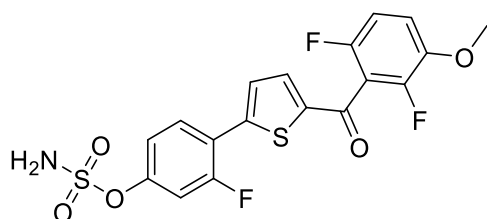
The title compound was prepared according to Method C by the reaction of **5a** (0.83 g, 4.00 mmol, 1 equiv) and boron tribromide (1 M) in dichloromethane (12.00 ml, 12.00 mmol, 3 equiv) in anhydrous dichloromethane (20 ml). The product was purified by column chromatography (cyclohexane/dichloromethane 4:1) to give 0.73 g (3.76 mmol/ 94%) of the analytically pure compound. C₁₀H₇FOS; MW 194; ¹H NMR (300 MHz, CD₃)₂SO) δ 9.55 (s, 1H), 7.13 (dd, *J* = 12.6, 2.3 Hz, 1H), 7.07 (dd, *J* = 5.1, 1.2 Hz, 1H), 7.03 (dd, *J* = 3.8, 1.2 Hz, 1H), 7.00 – 6.90 (m, 1H), 6.85 (t, *J* = 8.7 Hz, 1H), 6.69 (dd, *J* = 5.1, 3.8 Hz, 1H); MS (ESI): 195.03 (M+H)⁺.

3-Fluoro-4-(thiophen-2-yl)phenyl sulfamate (**5c**).



The title compound was prepared according to Method D by the reaction of **5b** (0.58 g, 3.00 mmol, 1 equiv) and sulfamoyl chloride (1.73 g, 15.00 mmol, 5 equiv) in DMA (20 ml). The product was used in the next step without further purification. C₁₀H₈FNO₃S₂; MW 273; MS (ESI): 274.01 (M+H)⁺.

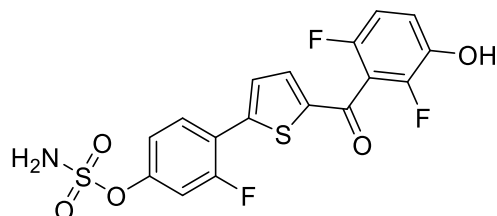
4-(5-(2,6-Difluoro-3-methoxybenzoyl)thiophen-2-yl)-3-fluorophenyl sulfamate (**5d**).



The title compound was prepared according to method A by the reaction of 2,6-difluoro-3-methoxybenzoyl chloride (0.41 g, 2.00 mmol, 1 equiv) and **5c** (0.82 g, 3.00 mmol, 1.5 equiv) in the presence of anhydrous aluminium chloride (0.53 g, 4.00 mmol, 2 equiv) in anhydrous dichloromethane (10 ml). The product was purified by column chromatography

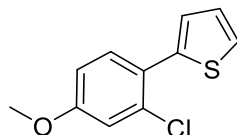
(cyclohexane/ethylacetate 3:2) to give 0.68 g (1.54 mmol/ 77%) of the analytically pure compound. $C_{18}H_{12}F_3NO_5S_2$; MW 443; 1H NMR (500 MHz, $(CD_3)_2CO$) δ 7.99 (t, J = 8.6 Hz, 1H), 7.71 – 7.66 (m, 2H), 7.40 (s, 2H), 7.37 – 7.33 (m, 2H), 7.32 – 7.30 (m, 1H), 7.15 (ddd, J = 9.13, 8.6, 2.0 Hz, 1H), 3.92 (s, 3H); MS (ESI): 444.10 (M+H) $^+$.

4-(5-(2,6-Difluoro-3-hydroxybenzoyl)thiophen-2-yl)-3-fluorophenyl sulfamate (5).



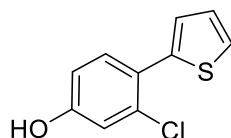
The title compound was prepared according to Method C by the reaction of **5d** (0.22 g, 0.50 mmol, 1 equiv) and boron tribromide (1 M) in dichloromethane (1.50 ml, 1.50 mmol, 3 equiv) in anhydrous dichloromethane (10 ml). The product was purified by column chromatography (dichloromethane/methanol 98.5:1.5) to give 94.00 mg (0.22 mmol/ 44%) of the analytically pure compound. $C_{17}H_{10}F_3NO_5S_2$; MW 429; mp: 172-173; 1H NMR (500 MHz, $(CD_3)_2CO$) δ 9.06 (d, J = 1.3 Hz, 1H), 8.00 (t, J = 8.6 Hz, 1H), 7.73 – 7.67 (m, 2H), 7.42 (s, 2H), 7.37 – 7.31 (m, 2H), 7.25 – 7.18 (m, 1H), 7.05 (ddd, J = 9.1, 8.6, 1.9 Hz, 1H); ^{13}C NMR (126 MHz, $(CD_3)_2CO$) δ 180.91, 159.94 (d, J = 252.6 Hz), 152.63 (d, J = 11.4 Hz), 152.51 (dd, J = 240.7, 5.7 Hz), 148.38 (dd, J = 246.0, 7.8 Hz), 146.70 (d, J = 4.2 Hz), 144.26 (d, J = 4.6 Hz), 142.64 (dd, J = 12.9, 3.2 Hz), 137.45, 130.88 (d, J = 4.0 Hz), 128.90 (d, J = 5.0 Hz), 120.43 (dd, J = 9.1, 3.9 Hz), 120.18 (d, J = 3.7 Hz), 120.05, 117.95 (dd, J = 23.9, 19.4 Hz), 112.46 (dd, J = 22.8, 4.0 Hz), 111.93 (d, J = 25.7 Hz); MS (ESI): 430.12 (M+H) $^+$.

2-(2-Chloro-4-methoxyphenyl)thiophene (6a).



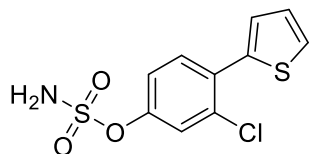
The title compound was prepared according to method B by the reaction of 2-bromothiophene (0.82 g, 5.00 mmol, 1 equiv) and (2-chloro-4-methoxyphenyl)boronic acid (1.11 g, 6.00 mmol, 1.2 equiv) in the presence of cesium carbonate (6.50 g, 20.00 mmol, 4 equiv) and tetrakis(triphenylphosphine) palladium (0.29 g, 0.25 mmol, 0.05 equiv) in DME/water 1:1 (50 ml). The product was purified by column chromatography (cyclohexane/dichloromethane 7:1) to give 1.01 g (4.55 mmol/ 91%) of the analytically pure compound. $C_{11}H_9ClOS$; MW 224; 1H NMR (300 MHz, $(CD_3)_2SO$) δ 7.28 (d, J = 2.4 Hz, 1H), 7.15 (dd, J = 8.7, 2.4 Hz, 1H), 7.08 (dd, J = 5.1, 1.1 Hz, 1H), 7.03 (dd, J = 3.7, 1.1 Hz, 1H), 6.74 (d, J = 8.7 Hz, 1H), 6.67 (dd, J = 5.1, 3.7 Hz, 1H), 3.45 (s, 3H); MS (ESI): 225.03 (M+H) $^+$.

3-Chloro-4-(thiophen-2-yl)phenol (6b).



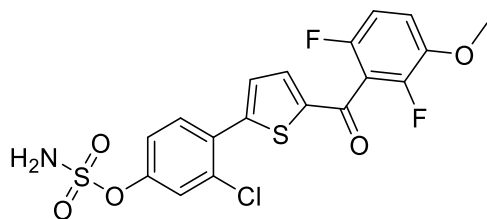
The title compound was prepared according to Method C by the reaction of **6a** (0.90 g, 4.00 mmol, 1 equiv) and boron tribromide (1 M) in dichloromethane (12.00 ml, 12.00 mmol, 3 equiv) in anhydrous dichloromethane (20 ml). The product was purified by column chromatography (cyclohexane/dichloromethane 4:1) to give 0.66 g (3.16 mmol/ 79%) of the analytically pure compound. $C_{10}H_7ClOS$; MW 210; 1H NMR (300 MHz, $(CD_3)_2SO$) δ 9.59 (s, 1H), 7.63 (d, J = 2.3 Hz, 1H), 7.47 (dd, J = 5.1, 1.2 Hz, 1H), 7.43 (dd, J = 8.4, 2.3 Hz, 1H), 7.40 (dd, J = 3.6, 1.2 Hz, 1H), 7.10 (dd, J = 5.1, 3.6 Hz, 1H), 7.01 (d, J = 8.4 Hz, 1H); MS (ESI): 211.05 (M+H) $^+$.

3-Chloro-4-(thiophen-2-yl)phenyl sulfamate (6c).



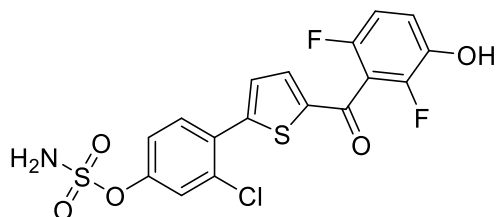
The title compound was prepared according to Method D by the reaction of **6b** (0.63 g, 3.00 mmol, 1 equiv) and sulfamoyl chloride (1.73 g, 15.00 mmol, 5 equiv) in DMA (20 ml). The product was used in the next step without further purification. $C_{10}H_8ClNO_3S_2$; MW 289; MS (ESI): 290.03 (M+H) $^+$.

3-Chloro-4-(5-(2,6-difluoro-3-methoxybenzoyl)thiophen-2-yl)phenyl sulfamate (6d).



The title compound was prepared according to method A by the reaction of 2,6-difluoro-3-methoxybenzoyl chloride (0.41 g, 2.00 mmol, 1 equiv) and **6c** (0.87 g, 3.00 mmol, 1.5 equiv) in the presence of anhydrous aluminium chloride (0.53 g, 4.00 mmol, 2 equiv) in anhydrous dichloromethane (10 ml). The product was purified by column chromatography (cyclohexane/ethylacetate 1:1) to give 0.62 g (1.36 mmol/ 68%) of the analytically pure compound. $C_{18}H_{12}ClF_2NO_5S_2$; MW 459; 1H NMR (500 MHz, $(CD_3)_2CO$) δ 7.84 (d, J = 8.5 Hz, 1H), 7.68 (dt, J = 4.1, 1.0 Hz, 1H), 7.59 (d, J = 2.4 Hz, 1H), 7.57 (d, J = 4.1 Hz, 1H), 7.45 (dd, J = 8.6, 2.4 Hz, 1H), 7.43 (s, 2H), 7.38 (td, J = 9.4, 5.2 Hz, 1H), 7.16 (ddd, J = 9.2, 8.6, 2.0 Hz, 1H), 3.96 (s, 3H); MS (ESI): 460.01 (M+H) $^+$.

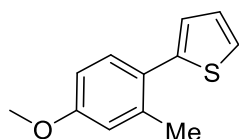
3-Chloro-4-(5-(2,6-difluoro-3-hydroxybenzoyl)thiophen-2-yl)phenyl sulfamate (6e).



The title compound was prepared according to Method C by the reaction of **6d** (0.23 g, 0.50 mmol, 1 equiv) and boron tribromide (1 M) in dichloromethane (1.50 ml, 1.50 mmol,

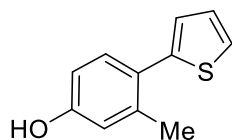
3 equiv) in anhydrous dichloromethane (10 ml). The product was purified by column chromatography (dichloromethane/methanol 98.5:1.5) to give 71.00 mg (0.16 mmol/ 32%) of the analytically pure compound. $C_{17}H_{10}ClF_2NO_5S_2$; MW 445; mp: 160-161; 1H NMR (500 MHz, $(CD_3)_2CO$) δ 9.07 (s, 1H), 7.84 (d, J = 8.5 Hz, 1H), 7.69 (dt, J = 4.0, 1.0 Hz, 1H), 7.59 (d, J = 2.4 Hz, 1H), 7.57 (d, J = 4.1 Hz, 1H), 7.45 (dd, J = 8.6, 2.4 Hz, 1H), 7.43 (s, 2H), 7.22 (ddd, J = 9.7, 9.1, 5.4 Hz, 1H), 7.05 (td, J = 8.9, 1.9 Hz, 1H); ^{13}C NMR (126 MHz, $(CD_3)_2CO$) δ 181.03, 152.50 (dd, J = 240.8, 5.8 Hz), 152.10, 149.86, 148.39 (dd, J = 246.0, 7.8 Hz), 144.89, 142.68 (dd, J = 12.9, 3.4 Hz), 136.99, 133.47, 133.29, 131.04, 130.78, 125.29, 122.74, 120.44 (dd, J = 9.1, 3.9 Hz), 117.89 (dd, J = 23.8, 19.8 Hz), 112.46 (dd, J = 22.8, 4.0 Hz); MS (ESI): 446.10 (M+H) $^+$.

2-(4-Methoxy-2-methylphenyl)thiophene (7a).



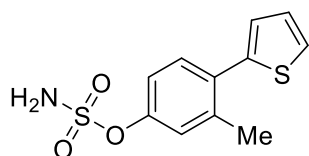
The title compound was prepared according to method B by the reaction of 2-bromothiophene (0.82 g, 5.00 mmol, 1 equiv) and (4-methoxy-2-methylphenyl)boronic acid (0.99 g, 6.00 mmol, 1.2 equiv) in the presence of cesium carbonate (6.50 g, 20.00 mmol, 4 equiv) and tetrakis(triphenylphosphine) palladium (0.29 g, 0.25 mmol, 0.05 equiv) in DME/water 1:1 (50 ml). The product was purified by column chromatography (cyclohexane/dichloromethane 7:1) to give 0.92 g (4.50 mmol/ 90%) of the analytically pure compound. $C_{12}H_{12}OS$; MW 204; 1H NMR (500 MHz, $(CD_3)_2CO$) δ 7.43 (dd, J = 5.2, 1.2 Hz, 1H), 7.30 (d, J = 8.4 Hz, 1H), 7.10 (dd, J = 5.2, 3.5 Hz, 1H), 7.05 (dd, J = 3.5, 1.2 Hz, 1H), 6.88 (d, J = 2.8 Hz, 1H), 6.81 (dd, J = 8.5, 2.7 Hz, 1H), 3.81 (s, 3H), 2.37 (s, 3H); MS (ESI): 205.09 (M+H) $^+$.

3-Methyl-4-(thiophen-2-yl)phenol (7b).



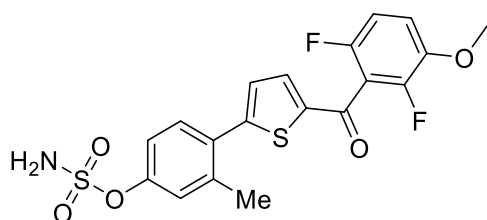
The title compound was prepared according to Method C by the reaction of **7a** (0.82 g, 4.00 mmol, 1 equiv) and boron tribromide (1 M) in dichloromethane (12.00 ml, 12.00 mmol, 3 equiv) in anhydrous dichloromethane (20 ml). The product was purified by column chromatography (cyclohexane/dichloromethane 4:1) to give 0.61 g (3.24 mmol/ 81%) of the analytically pure compound. $C_{11}H_{10}OS$; MW 190; 1H NMR (500 MHz, $(CD_3)_2CO$) δ 8.45 (s, 1H), 7.41 (dd, J = 5.2, 1.2 Hz, 1H), 7.21 (d, J = 8.3 Hz, 1H), 7.08 (dd, J = 5.2, 3.5 Hz, 1H), 7.02 (dd, J = 3.5, 1.2 Hz, 1H), 6.79 (d, J = 2.5 Hz, 1H), 6.72 (dd, J = 8.3, 2.6 Hz, 1H), 2.32 (s, 3H); MS (ESI): 191.10 (M+H) $^+$.

3-Methyl-4-(thiophen-2-yl)phenyl sulfamate (7c).



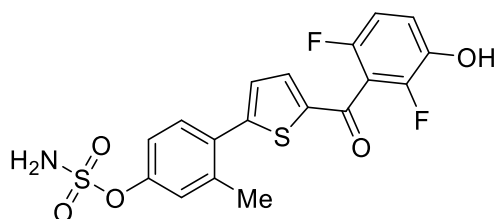
The title compound was prepared according to Method D by the reaction of **7b** (0.57 g, 3.00 mmol, 1 equiv) and sulfamoyl chloride (1.73 g, 15.00 mmol, 5 equiv) in DMA (20 ml). The product was used in the next step without further purification. $C_{11}H_{11}NO_3S_2$; MW 269; MS (ESI): 270.05 (M+H)⁺.

4-(5-(2,6-Difluoro-3-methoxybenzoyl)thiophen-2-yl)-3-methylphenyl sulfamate (7d).

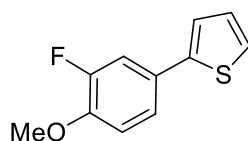


The title compound was prepared according to method A by the reaction of 2,6-difluoro-3-methoxybenzoyl chloride (0.41 g, 2.00 mmol, 1 equiv) and **7c** (0.81 g, 3.00 mmol, 1.5 equiv) in the presence of anhydrous aluminium chloride (0.53 g, 4.00 mmol, 2 equiv) in anhydrous dichloromethane (10 ml). The product was purified by column chromatography (cyclohexane/ethylacetate 2:1) to give 0.65 g (1.48 mmol/ 74%) of the analytically pure compound. $C_{19}H_{15}F_2NO_5S_2$; MW 439; ¹H NMR (500 MHz, (CD₃)₂SO) δ 8.18 (s, 2H), 7.79 (dd, *J* = 2.5, 0.9 Hz, 1H), 7.71 (ddd, *J* = 8.5, 2.5, 0.6 Hz, 1H), 7.65 (d, *J* = 4.1 Hz, 1H), 7.62 (d, *J* = 4.1 Hz, 1H), 7.49 (d, *J* = 8.5 Hz, 1H), 7.26 – 7.18 (m, 1H), 7.05 (td, *J* = 8.9, 1.9 Hz, 1H), 3.89 (s, 3H), 2.43 (s, 3H); MS (ESI): 440.03 (M+H)⁺.

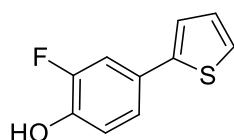
4-(5-(2,6-Difluoro-3-hydroxybenzoyl)thiophen-2-yl)-3-methylphenyl sulfamate (7).



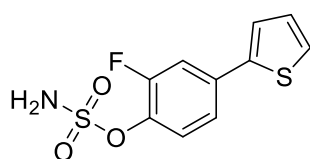
The title compound was prepared according to Method C by the reaction of **7d** (0.22 g, 0.50 mmol, 1 equiv) and boron tribromide (1 M) in dichloromethane (1.50 ml, 1.50 mmol, 3 equiv) in anhydrous dichloromethane (10 ml). The product was purified by column chromatography (dichloromethane/methanol 98.5:1.5) to give 93.00 mg (0.22 mmol/ 44%) of the analytically pure compound. $C_{18}H_{13}F_2NO_5S_2$; MW 425; mp: 166-167; ¹H NMR (500 MHz, (CD₃)₂SO) δ 10.29 (s, 1H), 8.12 (s, 2H), 7.66 (d, *J* = 4.0 Hz, 1H), 7.62 (d, *J* = 8.5 Hz, 1H), 7.40 (d, *J* = 4.0 Hz, 1H), 7.31 (d, *J* = 2.4 Hz, 1H), 7.24 (ddd, *J* = 8.5, 2.5, 0.6 Hz, 1H), 7.20 – 7.13 (m, 1H), 7.13 – 7.07 (m, 1H), 2.45 (s, 3H); ¹³C NMR (126 MHz, (CD₃)₂SO) δ 180.14, 152.44, 150.56, 150.54 (dd, *J* = 239.4, 5.6 Hz), 146.92 (dd, *J* = 246.3, 7.7 Hz), 142.30, 141.91 (dd, *J* = 11.9, 2.8 Hz), 137.86, 137.25, 131.52, 130.50, 129.34, 124.51, 120.14, 119.56 (dd, *J* = 9.2, 3.8 Hz), 116.58 (dd, *J* = 23.6, 19.5 Hz), 111.73 (dd, *J* = 22.4, 3.7 Hz), 20.85; MS (ESI): 426.01 (M+H)⁺.

2-(3-Fluoro-4-methoxyphenyl)thiophene (8a).

The title compound was prepared according to method B by the reaction of 2-bromothiophene (0.82 g, 5.00 mmol, 1 equiv) and (3-fluoro-4-methoxyphenyl)boronic acid (1.02 g, 6.00 mmol, 1.2 equiv) in the presence of cesium carbonate (6.50 g, 20.00 mmol, 4 equiv) and tetrakis(triphenylphosphine) palladium (0.29 g, 0.25 mmol, 0.05 equiv) in DME/water 1:1 (50 ml). The product was purified by column chromatography (cyclohexane/dichloromethane 7:1) to give 0.94 g (4.50 mmol/ 90%) of the analytically pure compound. $C_{11}H_9FOS$; MW 208; 1H NMR (300 MHz, $(CD_3)_2SO$) δ 7.55 (dd, $J = 12.7, 2.3$ Hz, 1H), 7.49 (dd, $J = 5.1, 1.2$ Hz, 1H), 7.45 (dd, $J = 3.6, 1.2$ Hz, 1H), 7.43 – 7.37 (m, 1H), 7.19 (t, $J = 8.8$ Hz, 1H), 7.10 (dd, $J = 5.1, 3.6$ Hz, 1H), 3.86 (s, 3H); MS (ESI): 209.03 (M+H) $^+$.

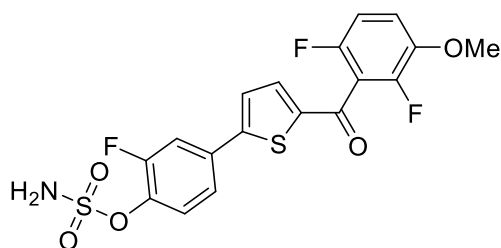
2-Fluoro-4-(thiophen-2-yl)phenol (8b).

The title compound was prepared according to Method C by the reaction of **8a** (0.83 g, 4.00 mmol, 1 equiv) and boron tribromide (1 M) in dichloromethane (12.00 ml, 12.00 mmol, 3 equiv) in anhydrous dichloromethane (20 ml). The product was purified by column chromatography (cyclohexane/dichloromethane 4:1) to give 0.60 g (3.12 mmol/ 78%) of the analytically pure compound. $C_{10}H_7FOS$; MW 194; 1H NMR (300 MHz, $(CD_3)_2SO$) δ 10.32 (s, 1H), 7.56 (dd, $J = 12.8, 2.4$ Hz, 1H), 7.51 (dd, $J = 5.2, 1.3$ Hz, 1H), 7.46 (dd, $J = 3.6, 1.3$ Hz, 1H), 7.42 – 7.38 (m, 1H), 7.20 (t, $J = 8.8$ Hz, 1H), 7.12 (dd, $J = 5.1, 3.6$ Hz, 1H); MS (ESI): 195.04 (M+H) $^+$.

2-Fluoro-4-(thiophen-2-yl)phenyl sulfamate (8c).

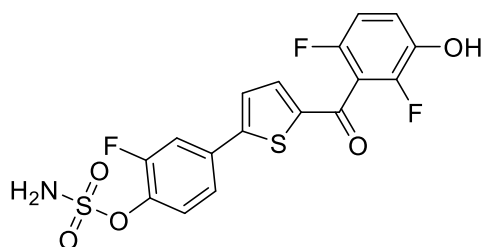
The title compound was prepared according to Method D by the reaction of **8b** (0.58 g, 3.00 mmol, 1 equiv) and sulfamoyl chloride (1.73 g, 15.00 mmol, 5 equiv) in DMA (20 ml). The product was purified by column chromatography (cyclohexane/dichloromethane 1:1) to give 0.49 g (1.8 mmol/ 60%) of the analytically pure compound. $C_{10}H_8FNO_3S_2$; MW 273; 1H NMR (300 MHz, $(CD_3)_2SO$) δ 8.27 (s, 2H), 7.74 (dd, $J = 11.6, 2.1$ Hz, 1H), 7.66 – 7.59 (m, 2H), 7.57 – 7.51 (m, 1H), 7.47 (t, $J = 7.9$ Hz, 1H), 7.17 (dd, $J = 5.0, 3.7$ Hz, 1H); MS (ESI): 273.98 (M+H) $^+$.

4-(5-(2,6-Difluoro-3-methoxybenzoyl)thiophen-2-yl)-2-fluorophenyl sulfamate (8d).



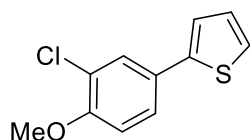
The title compound was prepared according to method A by the reaction of 2,6-difluoro-3-methoxybenzoyl chloride (0.41 g, 2.00 mmol, 1 equiv) and **8c** (0.82 g, 3.00 mmol, 1.5 equiv) in the presence of anhydrous aluminium chloride (0.53 g, 4.00 mmol, 2 equiv) in anhydrous dichloromethane (10 ml). The product was purified by column chromatography (cyclohexane/ethylacetate 1:1) to give 0.69 g (1.56 mmol/ 78%) of the analytically pure compound. $C_{18}H_{12}F_3NO_5S_2$; MW 443; 1H NMR (300 MHz, $(CD_3)_2SO$) δ 8.35 (s, 2H), 7.97 (dd, J = 11.3, 2.2 Hz, 1H), 7.81 – 7.68 (m, 3H), 7.54 (t, J = 8.3 Hz, 1H), 7.43 (td, J = 9.5, 5.3 Hz, 1H), 7.26 (td, J = 9.1, 1.9 Hz, 1H), 3.90 (s, 3H); MS (ESI): 444.09 ($M+H$) $^+$.

4-(5-(2,6-Difluoro-3-hydroxybenzoyl)thiophen-2-yl)-2-fluorophenyl sulfamate (**8**).



The title compound was prepared according to Method C by the reaction of **8d** (0.22 g, 0.50 mmol, 1 equiv) and boron tribromide (1 M) in dichloromethane (1.50 ml, 1.50 mmol, 3 equiv) in anhydrous dichloromethane (10 ml). The product was purified by column chromatography (dichloromethane/methanol 98.5:1.5) to give 124.00 mg (0.29 mmol/ 56%) of the analytically pure compound. $C_{17}H_{10}F_3NO_5S_2$; MW 429; mp: 180-181; 1H NMR (500 MHz, $(CD_3)_2CO$) δ 9.00 (d, J = 1.4 Hz, 1H), 7.80 (dd, J = 11.1, 2.2 Hz, 1H), 7.72 – 7.68 (m, 2H), 7.67 (dt, J = 4.1, 0.9 Hz, 1H), 7.60 (t, J = 8.2 Hz, 1H), 7.48 (s, 2H), 7.21 (ddd, J = 9.6, 9.2, 5.4 Hz, 1H), 7.07 – 7.01 (m, 1H); ^{13}C NMR (126 MHz, $(CD_3)_2CO$) δ 180.77, 155.96 (d, J = 251.3 Hz), 152.58 (d, J = 2.4 Hz), 152.54 (dd, J = 240.6, 5.8 Hz), 148.41 (dd, J = 245.9, 7.6 Hz), 144.12, 142.65 (dd, J = 13.0, 3.2 Hz), 139.36 (d, J = 12.4 Hz), 138.18, 133.84 (d, J = 7.4 Hz), 127.23, 126.64, 123.73 (d, J = 3.6 Hz), 120.45 (dd, J = 9.1, 3.9 Hz), 117.89 (dd, J = 23.9, 19.6 Hz), 115.78 (d, J = 20.7 Hz), 112.46 (dd, J = 22.8, 4.0 Hz); MS (ESI): 430.11 ($M+H$) $^+$.

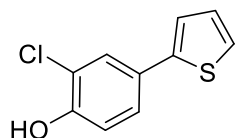
2-(3-Chloro-4-methoxyphenyl)thiophene (**9a**).



The title compound was prepared according to method B by the reaction of 2-bromothiophene (0.82 g, 5 mmol, 1 equiv) and (3-chloro-4-methoxyphenyl)boronic acid (1.11 g, 6.00 mmol, 1.2 equiv) in the presence of cesium carbonate (6.50 g, 20.00 mmol, 4 equiv) and tetrakis(triphenylphosphine) palladium (0.29 g, 0.25 mmol, 0.05 equiv) in DME/water 1:1

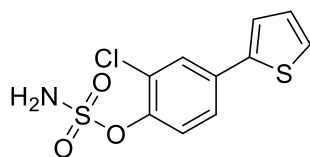
(50 ml). The product was purified by column chromatography (cyclohexane/dichloromethane 7:1) to give 1.01 g (4.50 mmol/ 90%) of the analytically pure compound. $C_{11}H_9ClOS$; MW 224; 1H NMR (300 MHz, $(CD_3)_2SO$) δ 7.72 (d, $J = 2.3$ Hz, 1H), 7.57 (dd, $J = 8.6, 2.3$ Hz, 1H), 7.50 (dd, $J = 5.1, 1.2$ Hz, 1H), 7.47 (dd, $J = 3.6, 1.2$ Hz, 1H), 7.18 (d, $J = 8.6$ Hz, 1H), 7.11 (dd, $J = 5.1, 3.6$ Hz, 1H), 3.88 (s, 3H); MS (ESI): 225.07 (M+H) $^+$.

2-Chloro-4-(thiophen-2-yl)phenol (**9b**).



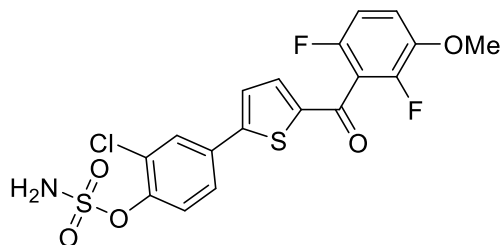
The title compound was prepared according to Method C by the reaction of **9a** (0.90 g, 4.00 mmol, 1 equiv) and boron tribromide (1 M) in dichloromethane (12.00 ml, 12.00 mmol, 3 equiv) in anhydrous dichloromethane (20 ml). The product was purified by column chromatography (cyclohexane/dichloromethane 4:1) to give 0.65 g (3.08 mmol/ 77%) of the analytically pure compound. $C_{10}H_7ClOS$; MW 210; 1H NMR (300 MHz, $(CD_3)_2SO$) δ 10.36 (s, 1H), 7.62 (d, $J = 2.3$ Hz, 1H), 7.46 (dd, $J = 5.1, 1.2$ Hz, 1H), 7.44 – 7.35 (m, 2H), 7.09 (dd, $J = 5.1, 3.6$ Hz, 1H), 7.00 (d, $J = 8.4$ Hz, 1H); MS (ESI): 211.03 (M+H) $^+$.

2-Chloro-4-(thiophen-2-yl)phenyl sulfamate (**9c**).



The title compound was prepared according to Method D by the reaction of **9b** (0.63 g, 3.00 mmol, 1 equiv) and sulfamoyl chloride (1.73 g, 15.00 mmol, 5 equiv) in DMA (20 ml). The product was purified by column chromatography (cyclohexane/ethylacetate 2:1) to give 0.45 g (1.56 mmol/ 52%) of the analytically pure compound. $C_{10}H_8ClNO_3S_2$; MW 289; 1H NMR (300 MHz, $(CD_3)_2SO$) δ 8.29 (s, 2H), 7.88 (d, $J = 2.2$ Hz, 1H), 7.69 (dd, $J = 8.6, 2.3$ Hz, 1H), 7.64 – 7.59 (m, 2H), 7.52 (d, $J = 8.6$ Hz, 1H), 7.16 (dd, $J = 4.9, 3.9$ Hz, 1H); MS (ESI): 290.01 (M+H) $^+$.

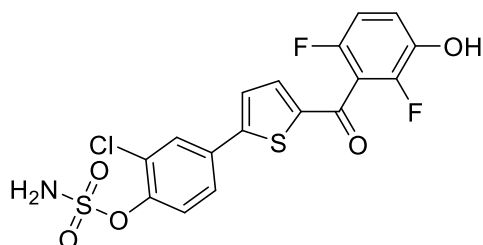
2-Chloro-4-(5-(2,6-difluoro-3-methoxybenzoyl)thiophen-2-yl)phenyl sulfamate (**9d**).



The title compound was prepared according to method A by the reaction of 2,6-difluoro-3-methoxybenzoyl chloride (0.41 g, 2.00 mmol, 1 equiv) and **9c** (0.87 g, 3.00 mmol, 1.5 equiv) in the presence of anhydrous aluminium chloride (0.53 g, 4.00 mmol, 2 equiv) in anhydrous dichloromethane (10 ml). The product was purified by column chromatography (cyclohexane/ethylacetate 1:1) to give 0.59 g (1.30 mmol/ 65%) of the analytically pure

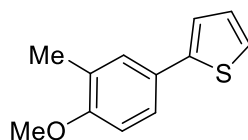
compound. $C_{18}H_{12}ClF_2NO_5S_2$; MW 459; 1H NMR (300 MHz, $(CD_3)_2SO$) δ 8.37 (s, 2H), 8.11 (d, $J = 2.3$ Hz, 1H), 7.88 (dd, $J = 8.6, 2.3$ Hz, 1H), 7.79 (d, $J = 4.1$ Hz, 1H), 7.70 (d, $J = 4.1$ Hz, 1H), 7.59 (d, $J = 8.6$ Hz, 1H), 7.48 – 7.37 (m, 1H), 7.32 – 7.20 (m, 1H), 3.90 (s, 3H); MS (ESI): 459.99 (M+H)⁺.

2-Chloro-4-(5-(2,6-difluoro-3-hydroxybenzoyl)thiophen-2-yl)phenyl sulfamate (9).



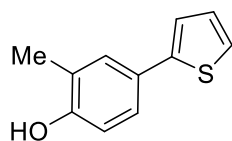
The title compound was prepared according to Method C by the reaction of **9d** (0.23 g, 0.50 mmol, 1 equiv) and boron tribromide (1 M) in dichloromethane (1.50 ml, 1.50 mmol, 3 equiv) in anhydrous dichloromethane (10 ml). The product was purified by column chromatography (dichloromethane/methanol 98.5:1.5) to give 60.00 mg (0.13 mmol/ 27%) of the analytically pure compound. $C_{17}H_{10}ClF_2NO_5S_2$; MW 445; mp: 172-173; 1H NMR (500 MHz, $(CD_3)_2CO$) δ 9.00 (s, 1H), 7.97 (d, $J = 2.3$ Hz, 1H), 7.80 (dd, $J = 8.6, 2.3$ Hz, 1H), 7.67 (d, $J = 4.1$ Hz, 1H), 7.64 – 7.62 (m, 1H), 7.62 (d, $J = 8.5$ Hz, 1H), 7.47 (s, 2H), 7.21 – 7.14 (m, 1H), 7.03 – 6.96 (m, 1H); ^{13}C NMR (126 MHz, $(CD_3)_2CO$) δ 180.76, 152.52 (dd, $J = 240.6, 5.9$ Hz), 152.31, 148.41 (dd, $J = 246.0, 7.6$ Hz), 148.06, 144.15, 142.67 (dd, $J = 12.8, 3.2$ Hz), 138.18, 133.45, 129.05, 129.03, 127.25, 127.04, 125.62, 120.44 (dd, $J = 9.1, 3.9$ Hz), 117.89 (dd, $J = 23.9, 19.6$ Hz), 112.45 (dd, $J = 22.8, 3.9$ Hz); MS (ESI): 446.12 (M+H)⁺.

2-(4-Methoxy-3-methylphenyl)thiophene (10a).



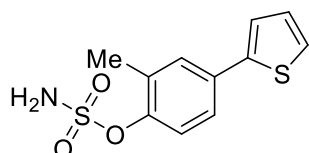
The title compound was prepared according to method B by the reaction of 2-bromothiophene (0.82 g, 5 mmol, 1 equiv) and (4-methoxy-3-methylphenyl)boronic acid (0.99 g, 6 mmol, 1.2 equiv) in the presence of cesium carbonate (6.5 g, 20 mmol, 4 equiv) and tetrakis(triphenylphosphine) palladium (0.29 g, 0.25 mmol, 0.05 equiv) in DME/water 1:1 (50 ml). The product was purified by column chromatography (cyclohexane/dichloromethane 7:1) to give 0.99 g (4.85 mmol/ 97%) of the analytically pure compound. $C_{12}H_{12}OS$; MW 204; 1H NMR (500 MHz, $(CD_3)_2CO$) δ 7.46 – 7.43 (m, 2H), 7.34 (dd, $J = 5.1, 1.2$ Hz, 1H), 7.30 (dd, $J = 3.6, 1.1$ Hz, 1H), 7.06 (dd, $J = 5.1, 3.6$ Hz, 1H), 6.95 – 6.92 (m, 1H), 3.85 (s, 3H), 2.21 (s, 3H); MS (ESI): 347 (M+H); MS (ESI): 205.06 (M+H)⁺.

2-Methyl-4-(thiophen-2-yl)phenol (10b).



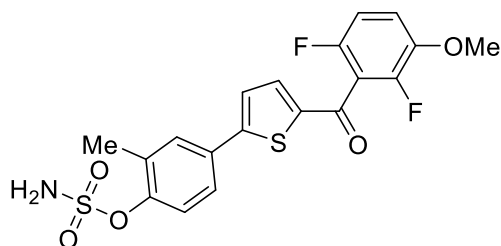
The title compound was prepared according to Method C by the reaction of **10a** (0.82 g, 4.00 mmol, 1 equiv) and boron tribromide (1 M) in dichloromethane (12.00 ml, 12.00 mmol, 3 equiv) in anhydrous dichloromethane (20 ml). The product was purified by column chromatography (cyclohexane/dichloromethane 4:1) to give 0.66 g (3.48 mmol/ 87%) of the analytically pure compound. $C_{11}H_{10}OS$; MW 190; 1H NMR (500 MHz, $(CD_3)_2CO$) δ 8.41 (s, 1H), 7.41 (d, $J = 2.3$ Hz, 1H), 7.33 – 7.29 (m, 2H), 7.25 (dd, $J = 3.6, 1.2$ Hz, 1H), 7.05 (dd, $J = 5.1, 3.6$ Hz, 1H), 6.86 (d, $J = 8.3$ Hz, 1H), 2.24 (s, 3H); MS (ESI): 191.08 (M+H) $^+$.

2-Methyl-4-(thiophen-2-yl)phenyl sulfamate (10c).



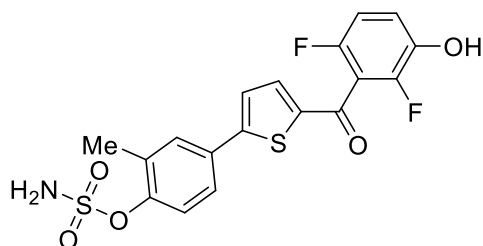
The title compound was prepared according to Method D by the reaction of **10b** (0.57 g, 3.00 mmol, 1 equiv) and sulfamoyl chloride (1.73 g, 15.00 mmol, 5 equiv) in DMA (20 ml). The product was purified by column chromatography (cyclohexane/ethylacetate 4:1) to give 0.72 g (2.67 mmol/ 89%) of the analytically pure compound. $C_{11}H_{11}NO_3S_2$; MW 269; 1H NMR (500 MHz, $(CD_3)_2CO$) δ 7.61 (d, $J = 2.4$ Hz, 1H), 7.53 (dd, $J = 8.4, 2.4$ Hz, 1H), 7.49 – 7.44 (m, 2H), 7.40 (d, $J = 8.4$ Hz, 1H), 7.26 (s, 2H), 7.13 (dd, $J = 5.1, 3.6$ Hz, 1H), 2.38 (s, 3H); MS (ESI): 270.09 (M+H) $^+$.

4-(5-(2,6-Difluoro-3-methoxybenzoyl)thiophen-2-yl)-2-methylphenyl sulfamate (10d).



The title compound was prepared according to method A by the reaction of 2,6-difluoro-3-methoxybenzoyl chloride (0.41 g, 2.00 mmol, 1 equiv) and **10c** (0.81 g, 3.00 mmol, 1.5 equiv) in the presence of anhydrous aluminium chloride (0.53 g, 4.00 mmol, 2 equiv) in anhydrous dichloromethane (10 ml). The product was used in the next step without further purification. $C_{19}H_{15}F_2NO_5S_2$; MW 439; MS (ESI): 440.04 (M+H) $^+$.

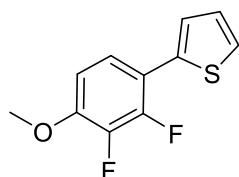
4-(5-(2,6-Difluoro-3-hydroxybenzoyl)thiophen-2-yl)-2-methylphenyl sulfamate (10).



The title compound was prepared according to Method C by the reaction of **10d** (0.22 g, 0.50 mmol, 1 equiv) and boron tribromide (1 M) in dichloromethane (1.50 ml, 1.50 mmol, 3 equiv) in anhydrous dichloromethane (10 ml). The product was purified by column

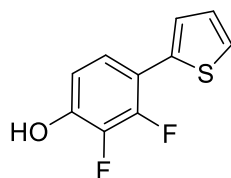
chromatography (dichloromethane/methanol 98.5:1.5) to give 72.00 mg (0.17 mmol/ 34%) of the analytically pure compound. $C_{18}H_{13}F_2NO_5S_2$; MW 425; mp: 190-191; 1H NMR (500 MHz, $(CD_3)_2CO$) δ 9.03 (s, 1H), 7.78 (dd, $J = 2.5, 0.9$ Hz, 1H), 7.70 (ddd, $J = 8.5, 2.5, 0.6$ Hz, 1H), 7.64 (d, $J = 4.1$ Hz, 1H), 7.61 (d, $J = 4.1$ Hz, 1H), 7.49 (d, $J = 8.5$ Hz, 1H), 7.34 (s, 2H), 7.25 – 7.17 (m, 1H), 7.04 (td, $J = 8.9, 1.9$ Hz, 1H), 2.42 (s, 3H); ^{13}C NMR (126 MHz, $(CD_3)_2CO$) δ 180.63, 154.35, 152.49 (dd, $J = 240.3, 5.8$ Hz), 150.93, 148.36 (dd, $J = 245.6, 7.8$ Hz), 143.34, 142.61 (dd, $J = 13.0, 3.4$ Hz), 138.27, 133.68, 132.08, 130.21, 126.25, 125.90, 123.97, 120.28 (dd, $J = 9.1, 3.9$ Hz), 118.02 (dd, $J = 24.2, 19.7$ Hz), 112.41 (dd, $J = 22.8, 3.9$ Hz), 16.59; MS (ESI): 426.03 (M+H) $^+$.

2-(2,3-Difluoro-4-methoxyphenyl)thiophene (11a).



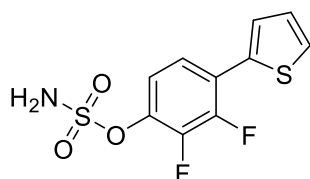
The title compound was prepared according to method B by the reaction of 2-bromothiophene (0.82 g, 5.00 mmol, 1 equiv) and (2,3-difluoro-4-methoxyphenyl)boronic acid (1.13 g, 6.00 mmol, 1.2 equiv) in the presence of cesium carbonate (6.50 g, 20.00 mmol, 4 equiv) and tetrakis(triphenylphosphine) palladium (0.29 g, 0.25 mmol, 0.05 equiv) in DME/water 1:1 (50 ml). The product was used in the next step without further purification. $C_{11}H_8F_2OS$; MW 226; MS (ESI): 227.01 (M+H) $^+$.

2,3-Difluoro-4-(thiophen-2-yl)phenol (11b).



The title compound was prepared according to Method C by the reaction of **11a** (0.80 g, 3.50 mmol, 1 equiv) and boron tribromide (1 M) in dichloromethane (10.50 ml, 10.50 mmol, 3 equiv) in anhydrous dichloromethane (20 ml). The product was purified by column chromatography (cyclohexane/dichloromethane 4:1) to give 0.66 g (3.15 mmol/ 90%) of the analytically pure compound. $C_{10}H_6F_2OS$; MW 212; 1H NMR (300 MHz, $(CD_3)_2CO$) δ 9.46 (s, 1H), 7.58 – 7.49 (m, 2H), 7.46 – 7.40 (m, 1H), 7.19 – 7.12 (m, 1H), 6.96 (dd, $J = 8.8, 1.7$ Hz, 1H); MS (ESI): 213.04 (M+H) $^+$.

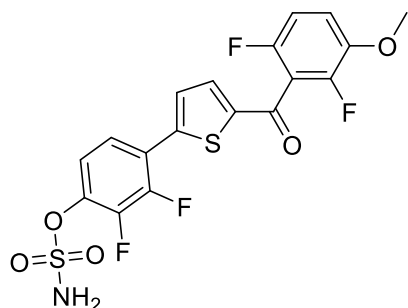
2,3-Difluoro-4-(thiophen-2-yl)phenyl sulfamate (11c).



The title compound was prepared according to Method D by the reaction of **11b** (0.64 g, 3.00 mmol, 1 equiv) and sulfamoyl chloride (1.73 g, 15.00 mmol, 5 equiv) in DMA (20 ml). The product was purified by column chromatography (cyclohexane/ethylacetate 4:1) to give

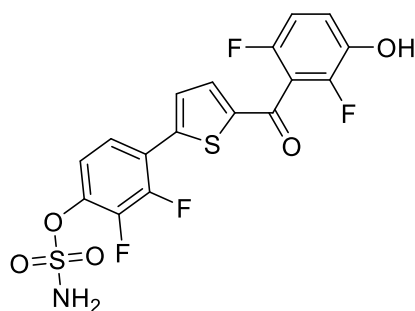
0.50 g (1.74 mmol/ 58%) of the analytically pure compound. $C_{10}H_7F_2NO_3S_2$; MW 291; 1H NMR (300 MHz, $(CD_3)_2SO$) δ 8.42 (s, 2H), 7.89 (t, J = 8.6 Hz, 1H), 7.74 (dd, J = 5.0, 1.2 Hz, 1H), 7.63 (dt, J = 3.7, 1.2 Hz, 1H), 7.44 (dd, J = 8.6, 1.2 Hz, 1H), 7.24 (ddd, J = 5.0, 3.7, 1.2 Hz, 1H); MS (ESI): 292.05 ($M+H$) $^+$.

4-(5-(2,6-Difluoro-3-methoxybenzoyl)thiophen-2-yl)-2,3-difluorophenyl sulfamate (11d).



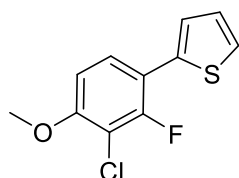
The title compound was prepared according to method A by the reaction of 2,6-difluoro-3-methoxybenzoyl chloride (0.41 g, 2.00 mmol, 1 equiv) and **11c** (0.87 g, 3.00 mmol, 1.5 equiv) in the presence of anhydrous aluminium chloride (0.53 g, 4.00 mmol, 2 equiv) in anhydrous dichloromethane (10 ml). The product was used in the next step without further purification. $C_{18}H_{11}F_4NO_5S_2$; MW 461; MS (ESI): 462.03 ($M+H$) $^+$.

4-(5-(2,6-Difluoro-3-hydroxybenzoyl)thiophen-2-yl)-2,3-difluorophenyl sulfamate (11).



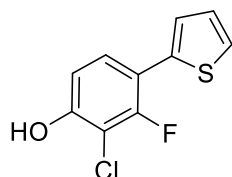
The title compound was prepared according to Method C by the reaction of **11d** (0.23 g, 0.50 mmol, 1 equiv) and boron tribromide (1 M) in dichloromethane (1.50 ml, 1.50 mmol, 3 equiv) in anhydrous dichloromethane (10 ml). The product was purified by column chromatography (dichloromethane/methanol 98.5:1.5) to give 62.00 mg (0.14 mmol/ 28%) of the analytically pure compound. $C_{17}H_9F_4NO_5S_2$; MW 447; mp: 186-187; 1H NMR (500 MHz, $(CD_3)_2CO$) δ 9.15 (s, 1H), 7.77 (ddd, J = 8.9, 7.8, 2.4 Hz, 1H), 7.74 – 7.71 (m, 2H), 7.66 (s, 2H), 7.45 (ddd, J = 9.0, 7.1, 2.1 Hz, 1H), 7.22 (ddd, J = 9.7, 9.1, 5.4 Hz, 1H), 7.04 (ddd, J = 9.1, 8.5, 1.8 Hz, 1H); ^{13}C NMR (126 MHz, $(CD_3)_2CO$) δ 180.99, 152.47 (dd, J = 240.8, 5.7 Hz), 148.37 (dd, J = 246.1, 7.7 Hz), 149.10 (dd, J = 253.6, 12.4 Hz), 145.50, 145.41 (dd, J = 252.9, 14.6 Hz), 144.78 (d, J = 4.2 Hz), 142.67 (dd, J = 12.6, 3.3 Hz), 140.16 (dd, J = 9.7, 2.2 Hz), 137.42, 129.60 (d, J = 5.3 Hz), 124.00 (dd, J = 7.1, 2.4 Hz), 121.84 (d, J = 9.6 Hz), 121.32 (d, J = 3.7 Hz), 120.52 (dd, J = 9.2, 3.9 Hz), 117.78 (dd, J = 23.7, 19.5 Hz), 112.46 (dd, J = 22.7, 3.9 Hz); MS (ESI): 448.01 ($M+H$) $^+$.

2-(3-Chloro-2-fluoro-4-methoxyphenyl)thiophene (12a).



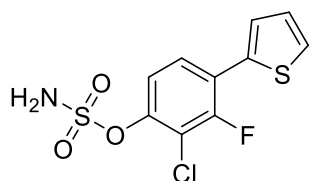
The title compound was prepared according to method B by the reaction of 2-bromothiophene (0.82 g, 5.00 mmol, 1 equiv) and (3-chloro-2-fluoro-4-methoxyphenyl)boronic acid (1.22 g, 6.00 mmol, 1.2 equiv) in the presence of cesium carbonate (6.50 g, 20.00 mmol, 4 equiv) and tetrakis(triphenylphosphine) palladium (0.29 g, 0.25 mmol, 0.05 equiv) in DME/water 1:1 (50 ml). The product was purified by column chromatography (cyclohexane/dichloromethane 7:1) to give 1.10 g (4.55 mmol/ 91%) of the analytically pure compound. $C_{11}H_8ClFOS$; MW 242; 1H NMR (300 MHz, $(CD_3)_2CO$) δ 7.62 (t, $J = 8.8$ Hz, 1H), 7.53 (dd, $J = 5.2, 1.2$ Hz, 1H), 7.48 – 7.42 (m, 1H), 7.16 (ddd, $J = 5.2, 3.7, 1.0$ Hz, 1H), 7.03 (dd, $J = 8.9, 1.7$ Hz, 1H), 3.90 (s, 3H); MS (ESI): 243.03 ($M+H$) $^+$.

2-Chloro-3-fluoro-4-(thiophen-2-yl)phenol (12b).



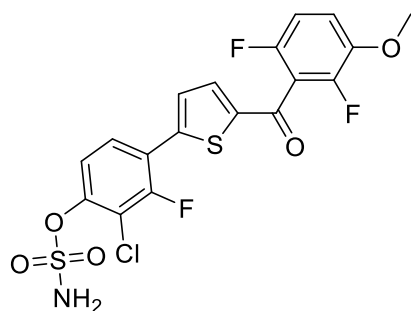
The title compound was prepared according to Method C by the reaction of **12a** (1.00 g, 4.00 mmol, 1 equiv) and boron tribromide (1 M) in dichloromethane (12.00 ml, 12.00 mmol, 3 equiv) in anhydrous dichloromethane (20 ml). The product was purified by column chromatography (cyclohexane/dichloromethane 4:1) to give 0.87 g (3.80 mmol/ 95%) of the analytically pure compound. $C_{10}H_6ClFOS$; MW 228; 1H NMR (300 MHz, $(CD_3)_2CO$) δ 9.44 (s, 1H), 7.56 – 7.47 (m, 2H), 7.44 – 7.40 (m, 1H), 7.14 (ddd, $J = 5.2, 3.7, 1.0$ Hz, 1H), 6.94 (dd, $J = 8.8, 1.7$ Hz, 1H); MS (ESI): 229.05 ($M+H$) $^+$.

2-Chloro-3-fluoro-4-(thiophen-2-yl)phenyl sulfamate (12c).



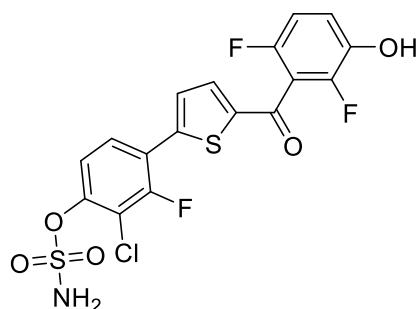
The title compound was prepared according to Method D by the reaction of **12b** (0.68 g, 3.00 mmol, 1 equiv) and sulfamoyl chloride (1.73 g, 15.00 mmol, 5 equiv) in DMA (20 ml). The product was purified by column chromatography (cyclohexane/ethylacetate 4:1) to give 0.90 g (2.94 mmol/ 98%) of the analytically pure compound. $C_{10}H_7ClFNO_3S_2$; MW 307; 1H NMR (300 MHz, $(CD_3)_2SO$) δ 8.44 (s, 2H), 7.86 (t, $J = 8.7$ Hz, 1H), 7.76 (dd, $J = 5.1, 1.2$ Hz, 1H), 7.64 (dt, $J = 3.7, 1.1$ Hz, 1H), 7.43 (dd, $J = 8.9, 1.7$ Hz, 1H), 7.23 (ddd, $J = 5.0, 3.7, 1.2$ Hz, 1H); MS (ESI): 308.00 ($M+H$) $^+$.

2-Chloro-4-(5-(2,6-difluoro-3-methoxybenzoyl)thiophen-2-yl)-3-fluorophenyl sulfamate (12d).



The title compound was prepared according to method A by the reaction of 2,6-difluoro-3-methoxybenzoyl chloride (0.41 g, 2.00 mmol, 1 equiv) and **12c** (0.92 g, 3.00 mmol, 1.5 equiv) in the presence of anhydrous aluminium chloride (0.53 g, 4.00 mmol, 2 equiv) in anhydrous dichloromethane (10 ml). The product was purified by column chromatography (cyclohexane/ethylacetate 3:2) to give 0.89 g (1.88 mmol/ 94%) of the analytically pure compound. $C_{18}H_{11}ClF_3NO_5S_2$; MW 477; 1H NMR (300 MHz, $(CD_3)_2CO$) δ 7.94 (t, J = 8.8 Hz, 1H), 7.77 – 7.68 (m, 2H), 7.61 (s, 2H), 7.55 (dd, J = 8.9, 1.8 Hz, 1H), 7.38 (td, J = 9.4, 5.2 Hz, 1H), 7.15 (ddd, J = 9.3, 8.6, 2.0 Hz, 1H), 3.96 (s, 3H); MS (ESI): 477.99 (M+H) $^+$.

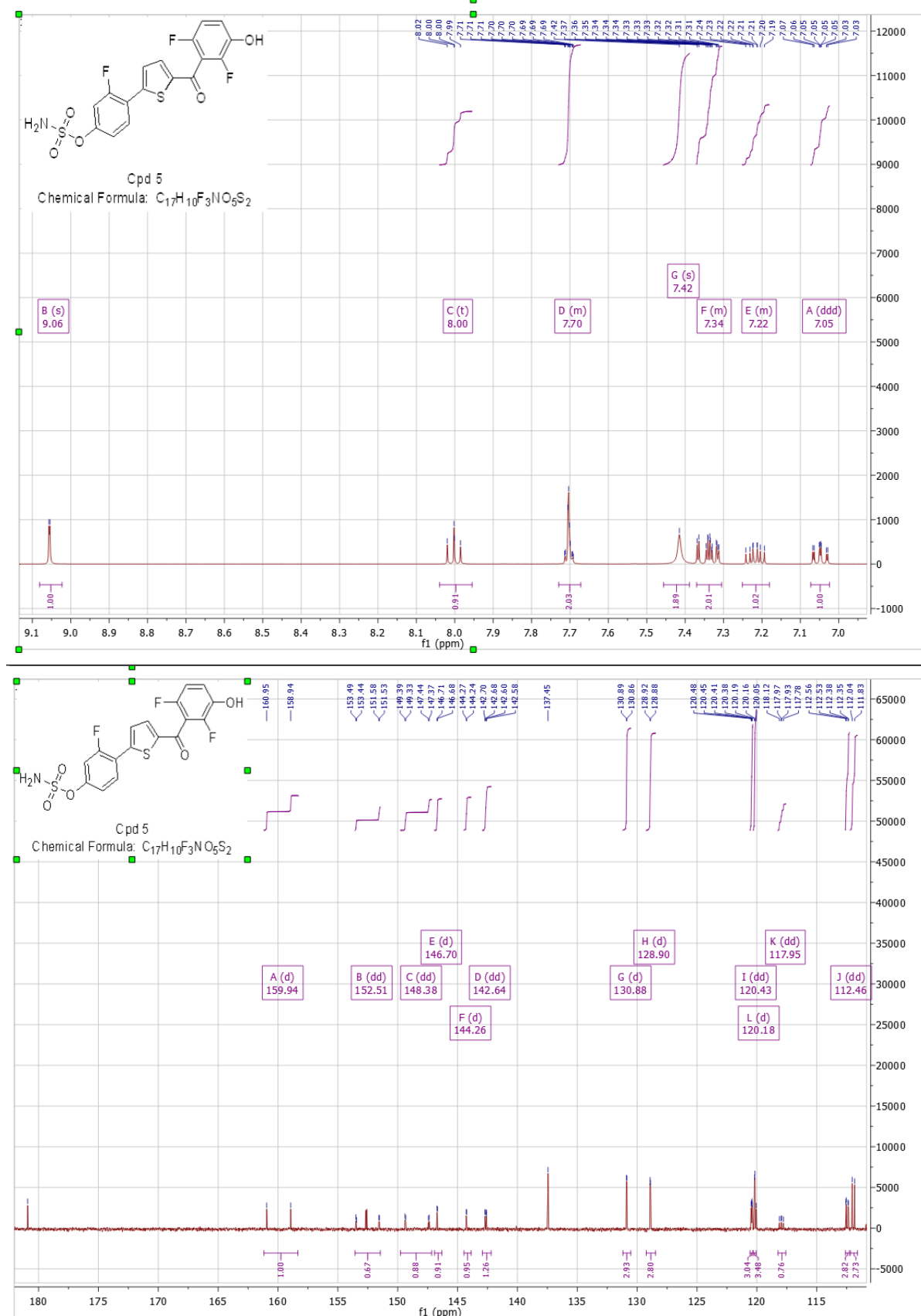
2-Chloro-4-(5-(2,6-difluoro-3-hydroxybenzoyl)thiophen-2-yl)-3-fluorophenyl sulfamate (12).

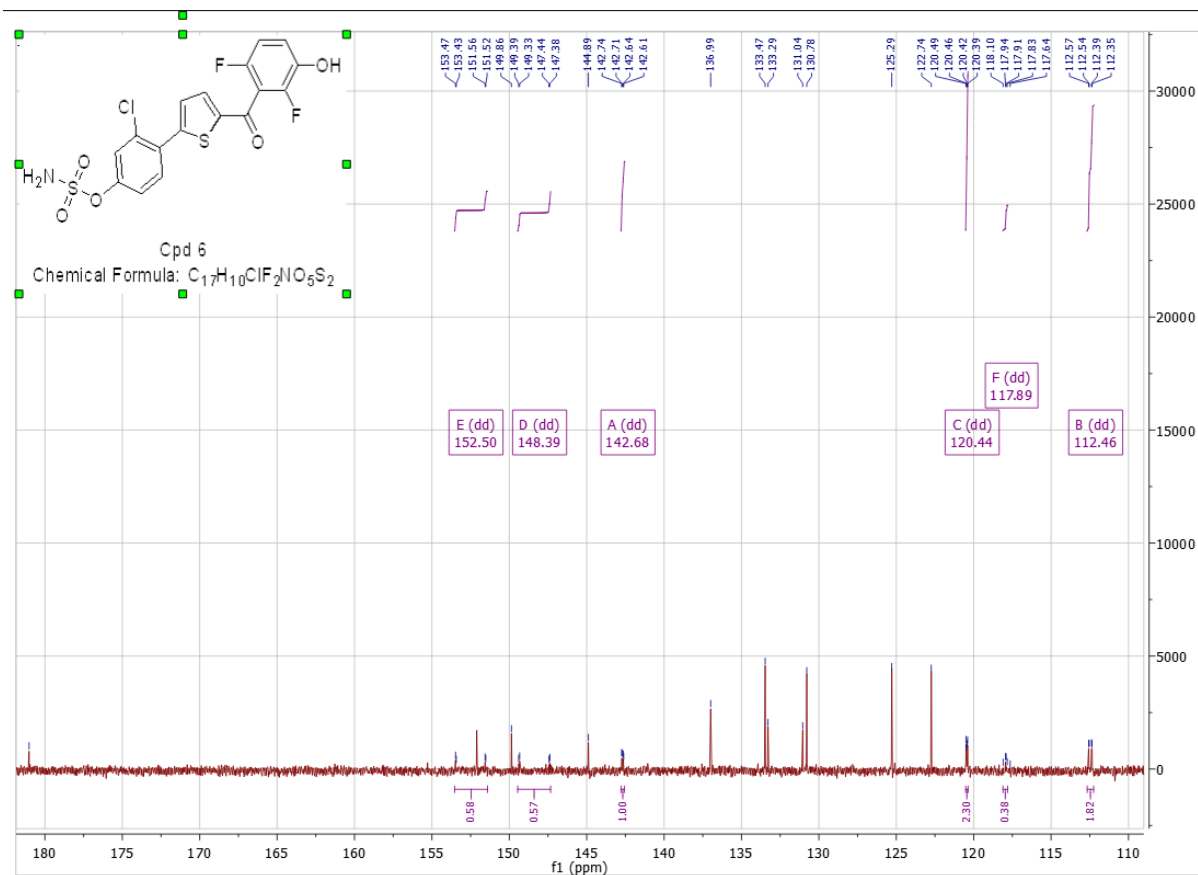
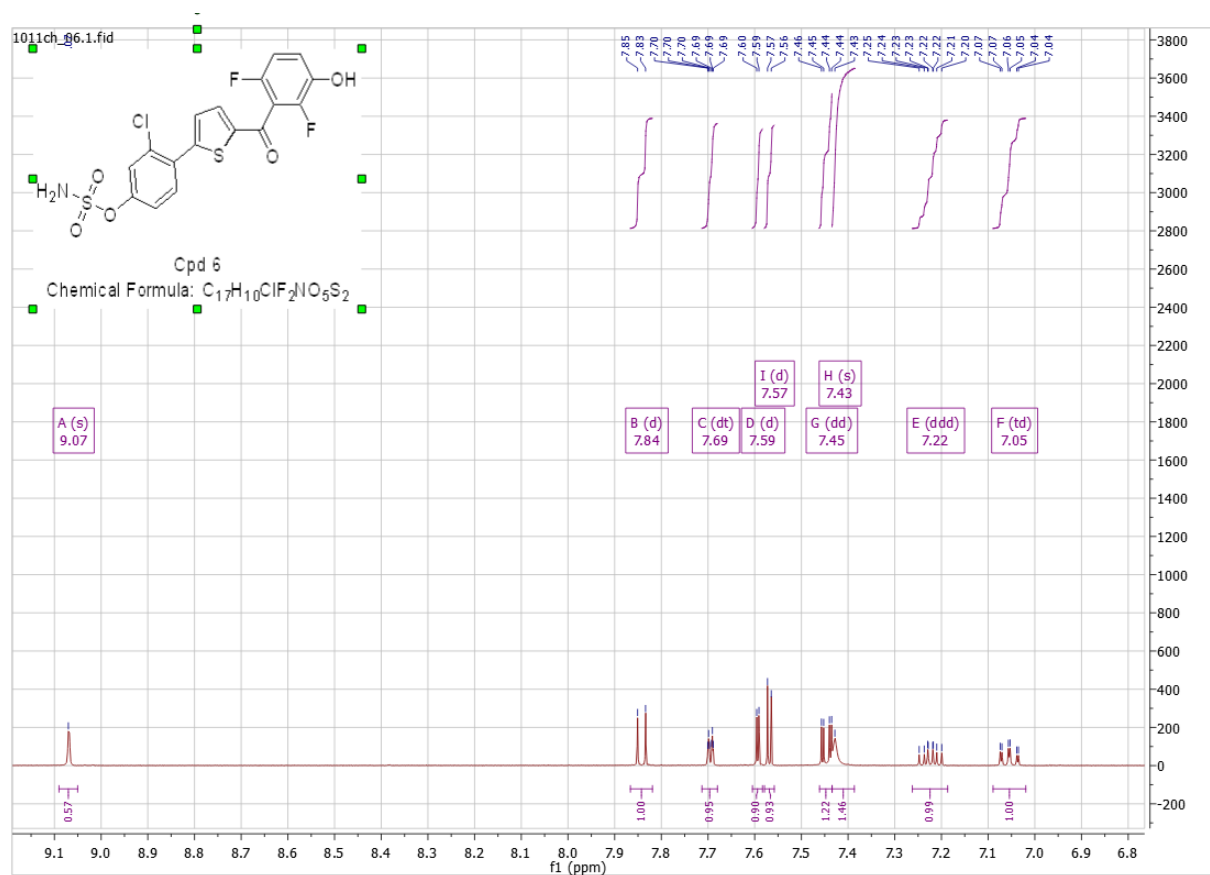


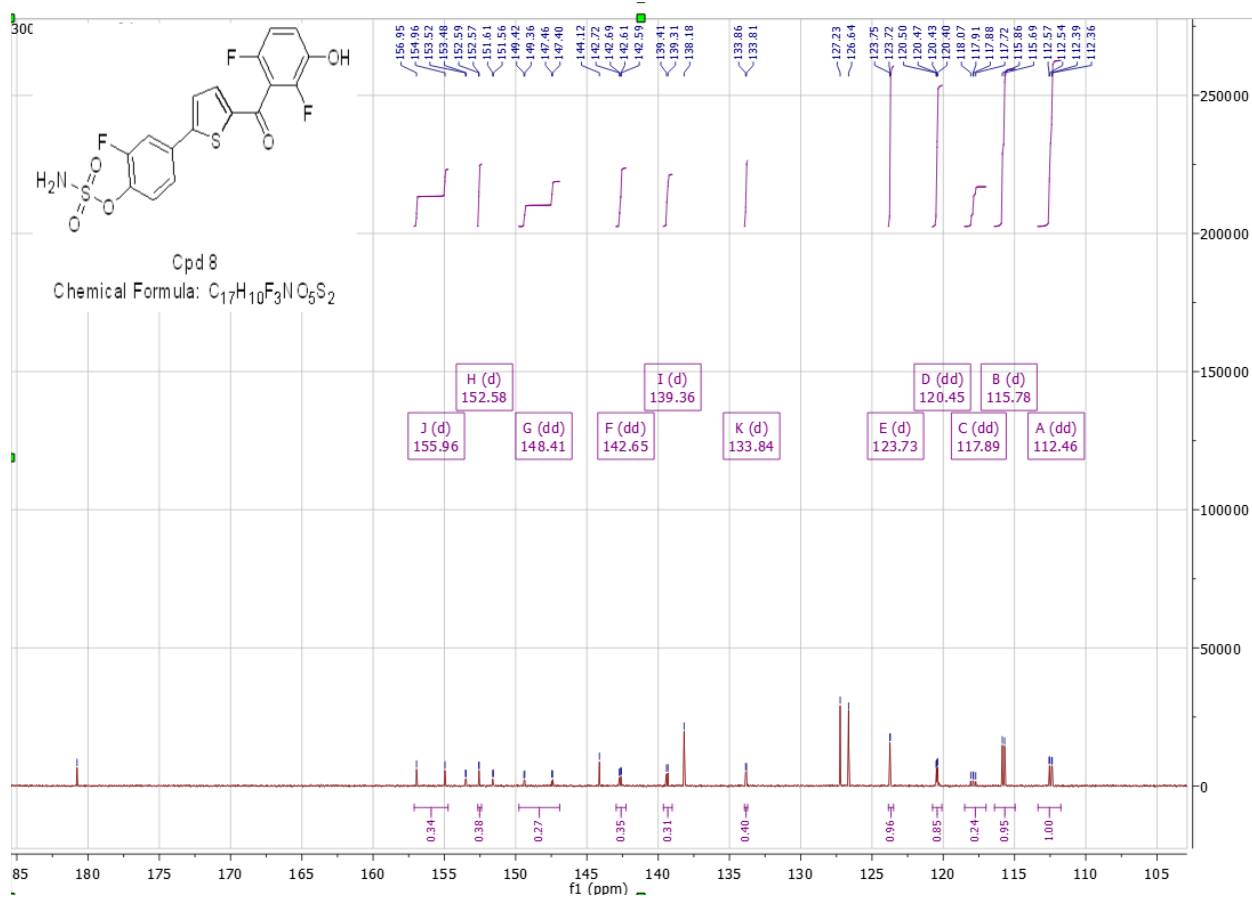
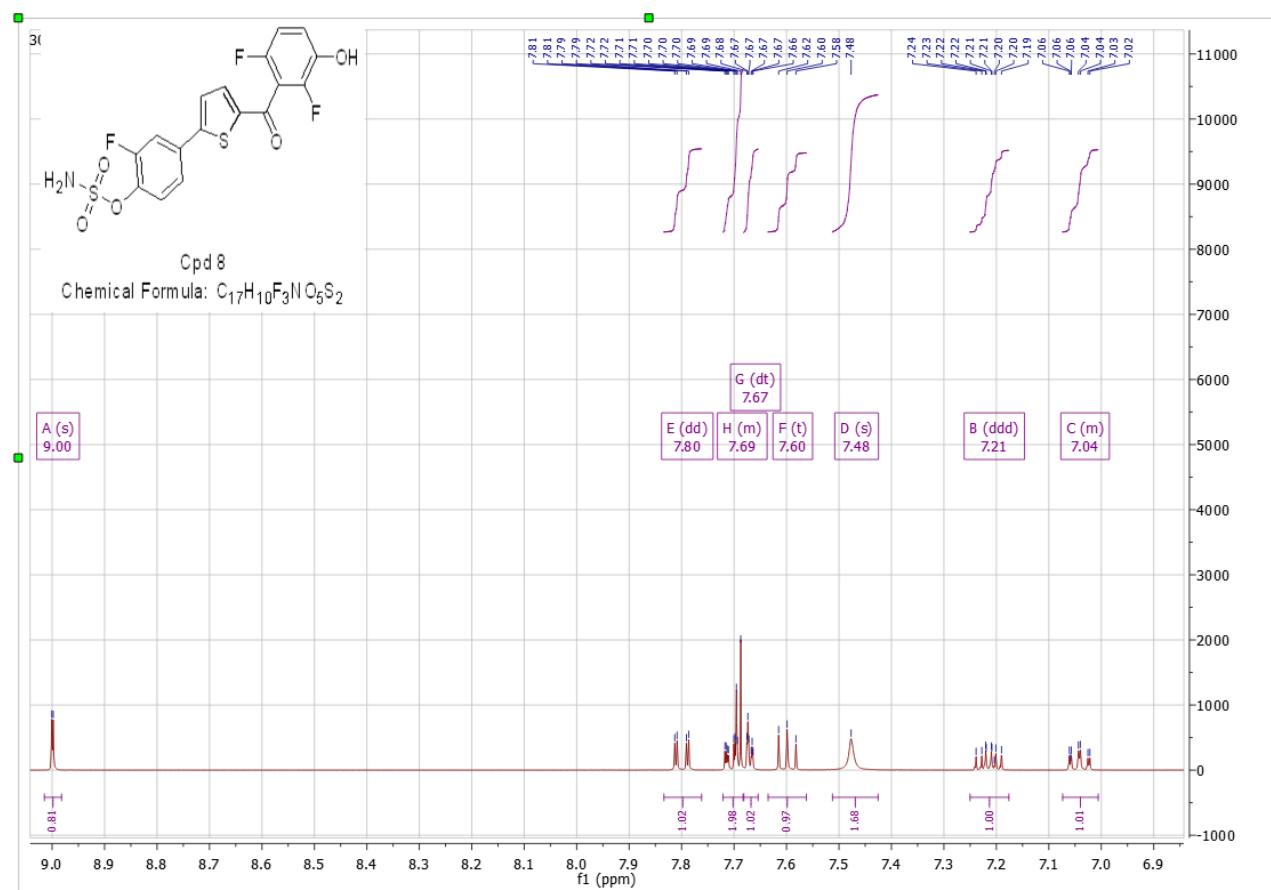
The title compound was prepared according to Method C by the reaction of **12d** (0.24 g, 0.50 mmol, 1 equiv) and boron tribromide (1 M) in dichloromethane (1.50 ml, 1.50 mmol, 3 equiv) in anhydrous dichloromethane (10 ml). The product was purified by column chromatography (dichloromethane/methanol 98.5:1.5) to give 122.00 mg (0.26 mmol/ 53%) of the analytically pure compound. $C_{17}H_9ClF_3NO_5S_2$; MW 463; mp: 179-180; 1H NMR (500 MHz, $(CD_3)_2CO$) δ 9.11 (s, 1H), 7.94 (t, 8.8 Hz, 1H), 7.77 – 7.70 (m, 2H), 7.66 (s, 2H), 7.55 (dd, J = 8.9, 1.8 Hz, 1H), 7.27 – 7.18 (m, 1H), 7.05 (td, J = 8.9, 1.9 Hz, 1H); ^{13}C NMR (126 MHz, $(CD_3)_2CO$) δ 181.02, 156.17 (d, J = 253.5 Hz), 152.51 (dd, J = 240.7, 5.7 Hz), 148.91 (d, J = 1.8 Hz), 148.40 (dd, J = 246.1, 7.7 Hz), 145.77 (d, J = 4.4 Hz), 144.75 (d, J = 4.4 Hz), 142.70 (dd, J = 12.8, 3.2 Hz), 137.46, 129.64 (d, J = 5.2 Hz), 128.21 (d, J = 3.7 Hz), 121.18 (d, J = 12.9 Hz), 120.77 (d, J = 3.8 Hz), 120.54 (dd, J = 9.1, 3.8 Hz), 117.84 (dd, J = 23.7, 19.5 Hz), 117.57 (d, J = 19.9 Hz), 112.51 (dd, J = 22.7, 3.9 Hz); MS (ESI): 464.01 (M+H) $^+$.

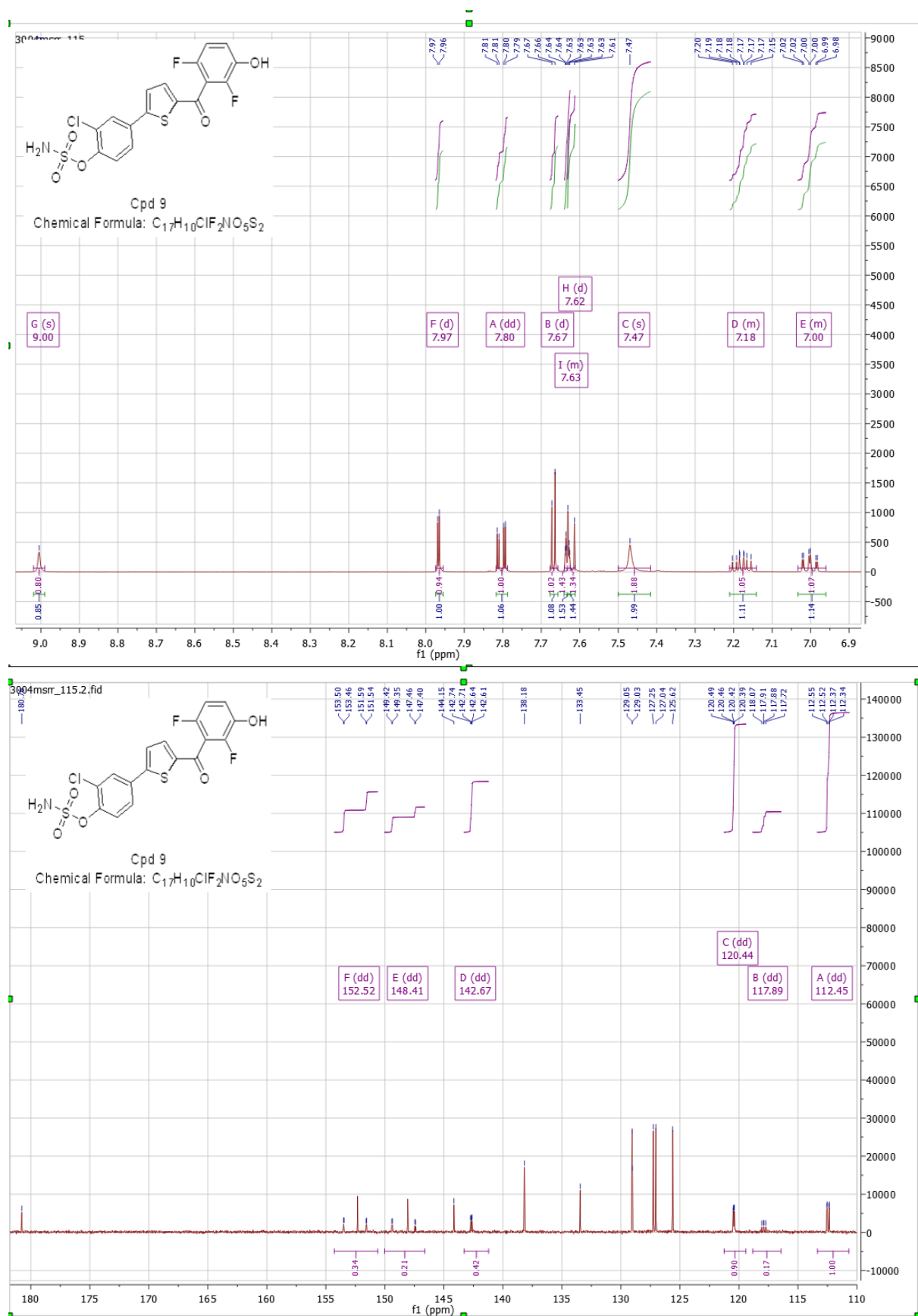
Table S1. Purity of final compounds as evaluated by HPLC

| Compound | R _t (min) | Purity (%) |
|-----------|----------------------|------------|
| 1 | 7.49 | 99.5 |
| 2 | 7.51 | 96.5 |
| 3 | 7.52 | 97.5 |
| 4 | 7.63 | 98.5 |
| 5 | 8.14 | 99.0 |
| 6 | 8.32 | 99.4 |
| 7 | 7.51 | 99.2 |
| 8 | 8.11 | 96.6 |
| 9 | 8.32 | 95.8 |
| 10 | 7.52 | 99.2 |
| 11 | 7.95 | 96.7 |
| 12 | 8.01 | 98.6 |

5.1.1.4 Representative ^1H NMR and ^{13}C NMR spectra

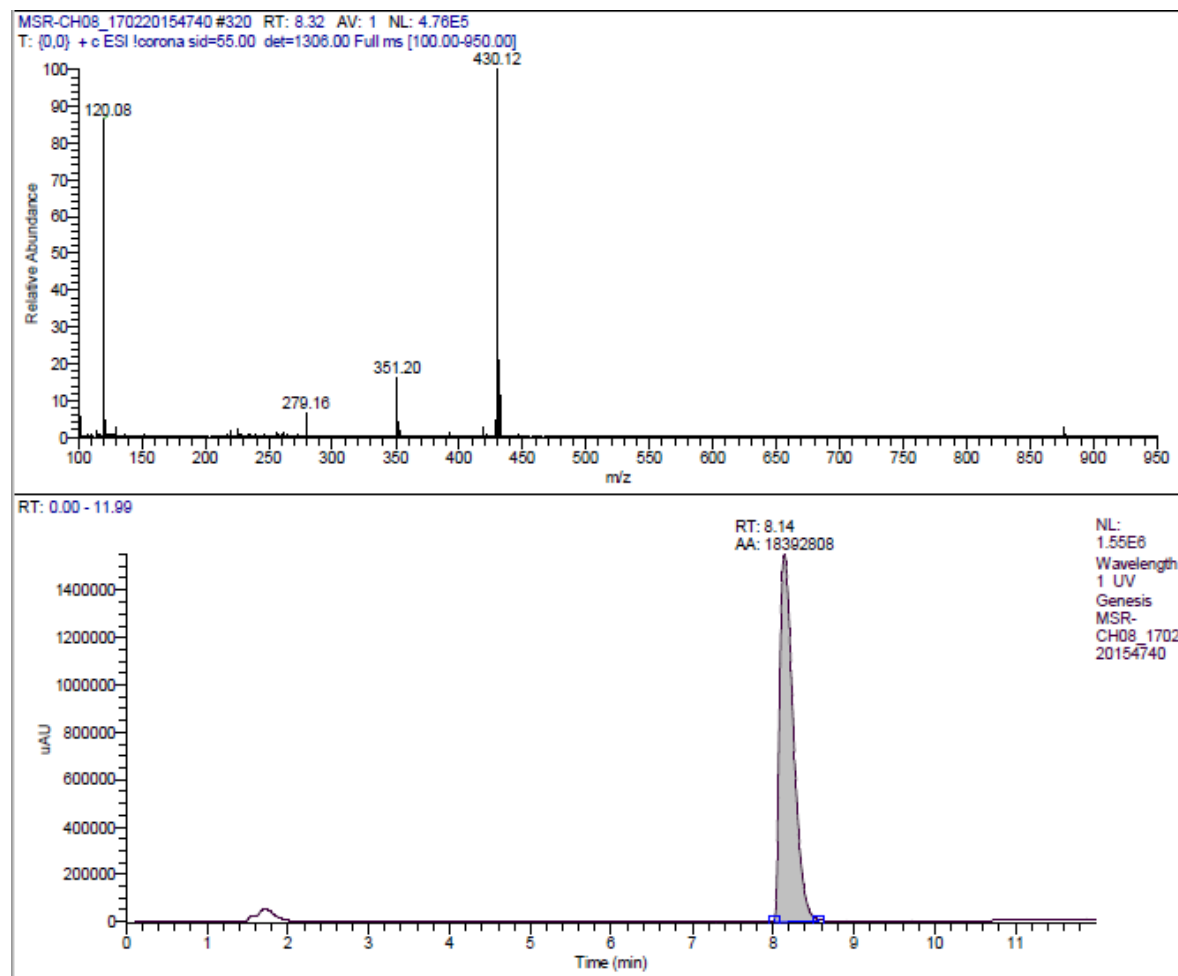


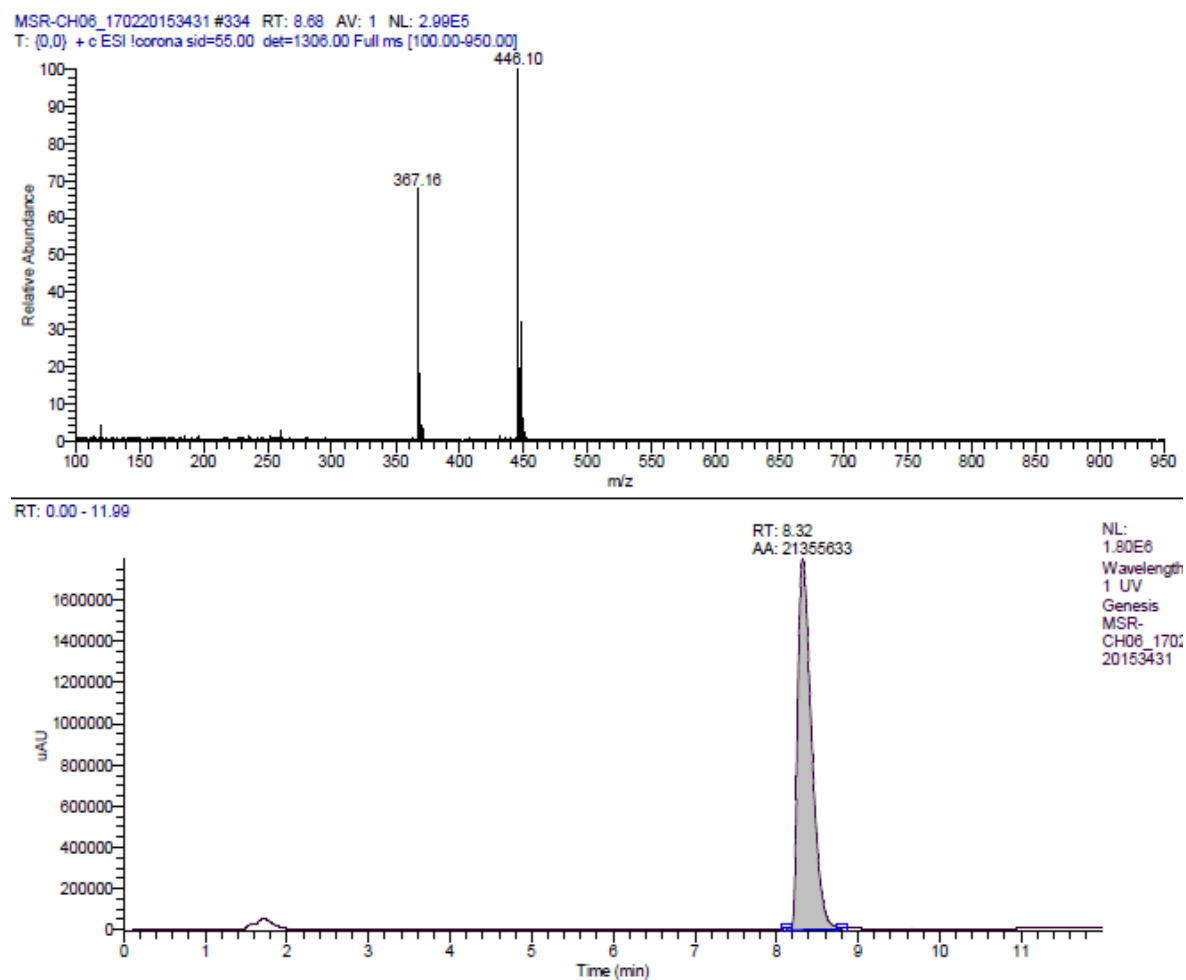


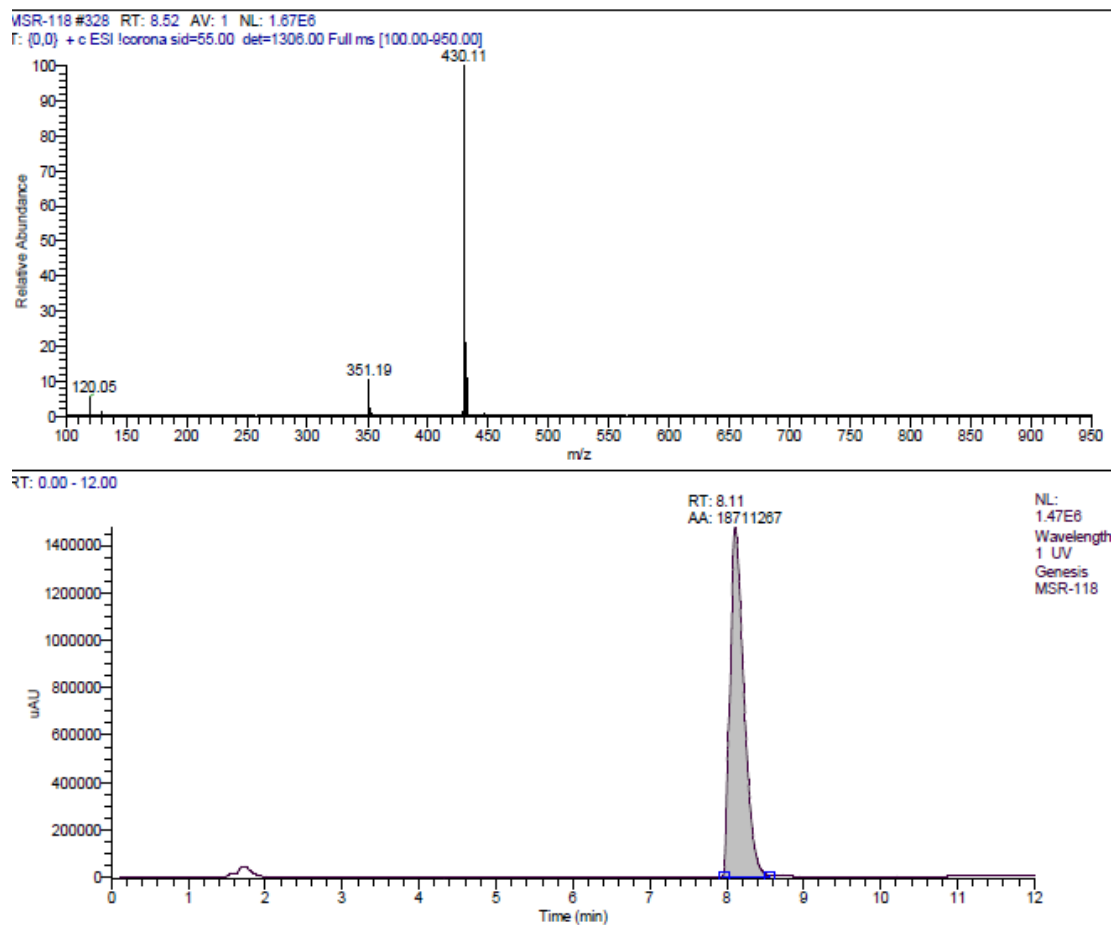


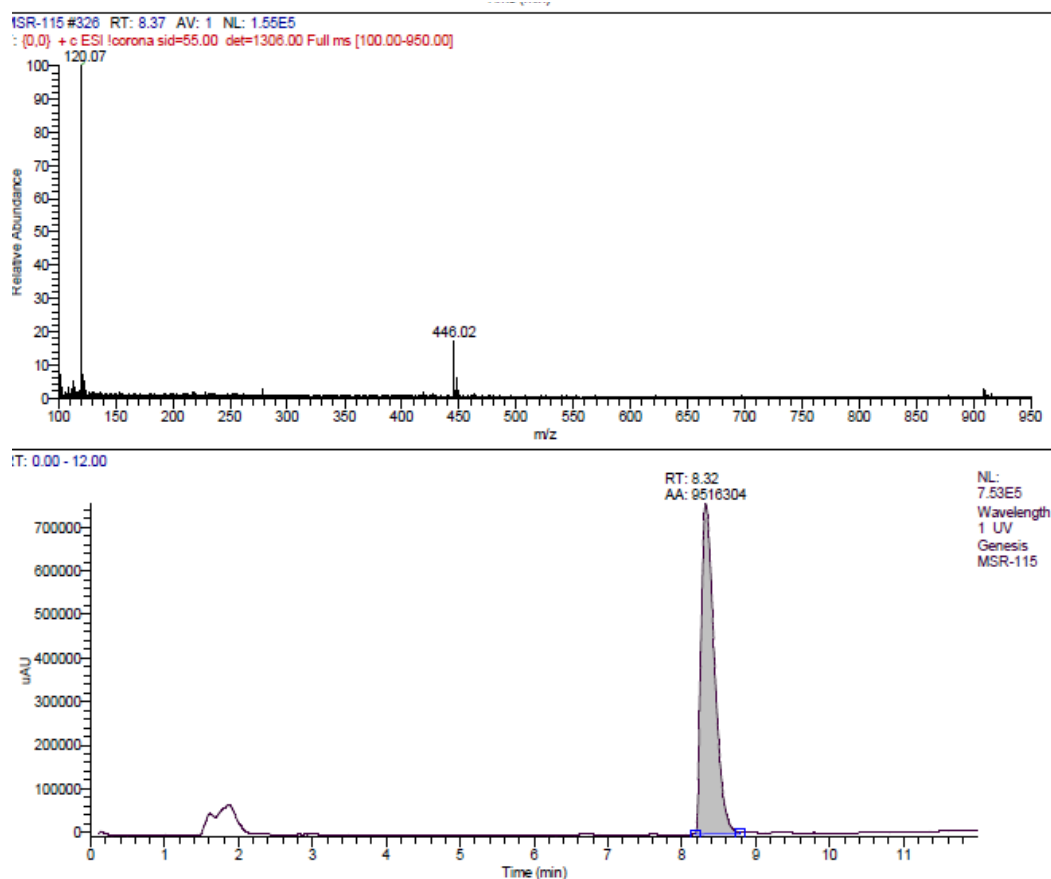
5.1.1.5 *Representative MS spectra*

Compound 5:



Compound 6:

Compound 8:

Compound 9:

5.1.II Biological methods

5.1.II.1 Chemicals

E1-S, E1, E2 and MTT were obtained from Sigma. Radioactively labeled [6,7-³H(N)]-E1-S (40-60 Ci/mmol), [2,4,6,7-³H]-E1 (50-100 Ci/mmol) and [2,4,6,7-³H]-E2 (>110 Ci/mmol) were obtained from Perkin Elmer, Boston. Quickszint Flow 302 scintillator fluid was bought from Zinsser Analytic, Frankfurt. Charcoal-stripped FCS was received from Biowest. Other chemicals were purchased from Sigma, Merck or Gibco.

5.1.II.2 *hSTS cell free inhibition assay*

The human enzyme was partially purified from the microsomal fraction of freshly homogenized human placental tissue according to previously described procedures.^{s1} The enzyme preparation was pre-incubated in Tris-HCl buffer (20 mM, pH= 7.4) for 30 min at 37 °C with DMSO stocks of potential inhibitors (final DMSO concentration in the assay was 1%). Negative and positive controls (vehicle only and **14** at 2 µM, resp.) were present in each assay. Incubation was started by the addition of E1-S (final concentration: 300 nM) for 20 min at 37 °C. Compounds **8** or **14** was added (final concentration: 2 µM) to quench the reaction. The amount of E1 produced was quantified using the competitive Estrone ELISA Kit from DRG Instruments GmbH (Marburg, Germany) according to the instructions of the manufacturer.^{s2} The assay did not show cross-sensitivity for E1-S and E2 in the relevant concentration range. Optical densities were measured with a Polarstar Omega plate reader (BMG Labtech, Ortenberg, Germany) at 450 nm.^{s3} For IC₅₀ determinations, at least two independent measurements were carried out using three different inhibitor concentrations (leading to inhibitions in the range from 30-70%, relative to the uninhibited control). In this assay, the reference compound **14** shows an IC₅₀ value of 15.1 nM, comparable to the value reported in the literature 8 nM.^{s4}

5.1.II.3 *h17β-HSD1 and h17β-HSD2 cell free inhibition assays*

The human enzymes were partially purified from human placental tissue according to previously described procedures.^{s1} Fresh human placenta was homogenized and by fractional centrifugation the cytosolic and microsomal fractions were separated. In case of the *h17β*-HSD1 assay the cytosolic fraction was incubated with NADH (500 µM), while in the case of the *h17β*-HSD2 assay the microsomal fraction was incubated with NAD⁺ (1500 µM) at 37 °C in a phosphate buffer (50 mM) with 20% of glycerol and EDTA (1 mM) in the presence of potential inhibitors which were prepared in DMSO (final DMSO concentration in the assay

was 1%). The enzymatic reaction was started by the addition of a mixture of unlabeled and radiolabeled substrate (final concentration: 500 nM), [^3H]-E1 in the case of *h17 β* -HSD1 assay for 10 min or with [^3H]-E2 in the case of *h17 β* -HSD2 assay for 20 min.^{s1} HgCl_2 (10mM) was used to stop the enzymatic reactions and the steroids were extracted with diethylether. After evaporation, they were dissolved in acetonitrile/water (45:55). E1 and E2 were separated on a C18 reverse phase chromatography column (Nucleodur C₁₈ Isis, Macherey-Nagel) connected to an Agilent 1200 Series (Agilent Technologies) HPLC-system using acetonitrile/water (45:55) as mobile phase. A radioflow detector (Ramona, raytest) was coupled to the HPLC-system for the detection and quantification of the steroids. After the analysis of the resulting chromatograms, the conversion rates were calculated according to the following equation:

$$\%conversion = \left[\frac{\%product}{\%product + \%Substrate} \right] * 100$$

Each value was calculated from at least two independent experiments.

Then the percentage inhibition corresponding to each inhibitor concentration was calculated according to the following equation:

$$\%inhibition = \left[1 - \left(\frac{\%conversion\ of\ the\ inhibitor}{\%conversion\ of\ the\ control\ (DMSO)} \right) \right] * 100$$

At least three different concentrations of each inhibitor leading to inhibitions ranging from 30% to 80% were chosen to deduce the IC₅₀ of each inhibitor. The IC₅₀ of each inhibitor was calculated from at least two independent experiments.

5.1.II.4 *Cell culture*

T47D human mammary cancer cell line was purchased from ECACC, Salisbury. The cells were routinely cultivated in DMEM (Sigma) supplemented with 10% FCS (Sigma) and 100 IU/ml penicillin-streptomycin, and incubated at 37 °C under humidified atmosphere of 5% CO₂. The medium was changed every 2-3 days, and the cells were passed every 9-10 days.

5.1.II.5 *hSTS and h17 β -HSD1 cellular inhibition assays*

The T47D cells were seeded into a 24-well flat-bottom plate at $5 * 10^5$ cells/well in DMEM supplemented with 10% FCS and 100 IU/ml penicillin-streptomycin according to previously described procedures.^{s5,6} After incubation for 24 h of adaptation at 37 °C, the medium was exchanged by a fresh FCS-free DMEM and the test compound dissolved in DMSO was added (final concentration of DMSO was adjusted to 1% in all samples). After 1 h the incubation period was started by the addition of a mixture of unlabeled and radioactive substrate [^3H]-

E1-S (5 nM) for 24 h or [^3H]-E1 (50 nM) for 30 min at 37 °C in case of *h*STS or *h*17 β -HSD1 cellular inhibition assays, respectively. The reaction was stopped by the removal of the supernatant. The supernatant was injected directly (without any further workup) into the same radio-HPLC system mentioned above for *h*17 β -HSD1 and *h*17 β -HSD2 cell free inhibition assays and the IC₅₀s are calculated as described.

5.1.II.6 *Nature of inhibition of STS activity*

In order to investigate the mode of inhibition of STS activity, T47D cells were cultivated as mentioned above but with some changes described by Purohit et al., 1995.^{s7} The cells were pre-incubated with the inhibitors for 2 h at 37 °C, then the medium was removed and the cells were washed 3-4 times with PBS (phosphate buffer saline). The remaining STS activity was assayed as described in the recent procedure by incubating the cells with using [^3H]-E1-S for 24 h at 37 °C, then subsequent quantification of the steroids in the supernatant using HPLC coupled to radiodetector and the IC₅₀s are calculated as described.

5.1.II.7 *Proliferation assay*

In 24-well plates, according to previously described procedures^{s5} the T47D cells were grown for 2 days in RPMI (without phenol red) serum-free medium supplemented with 100 IU/ml penicillin-streptomycin, sodium pyruvate (1 mM) and L-glutamine (2 mM). Then charcoal-stripped FCS 5% (v/v), estrogens and/or the compounds were added after the dilution in ethanol (the final concentration of ethanol was set to 1% of the medium). Every 2-3 days the medium was exchanged with fresh medium containing the same additives. Then the cell viability is evaluated by MTT assay based on the ability of viable cells to convert the yellow water soluble dye 3-(4,5-dimethyl-2-yl)-2,5-diphenyltetrazolium bromide (MTT) to a violet water insoluble formazane. After 7 days of culturing (without passage) in the presence of the respective additives, 100 μl of MTT-solution (5mg/ml in PBS) was added to the medium. After 2 h, the medium was removed and 215 μl of DMSO containing 10% Sodium dodecyl sulphate (SDS) and 0.01 N HCl was added to start the cell lysis and dissolve the blue formazan which was quantified spectrophotometrically at 590 nM using an Omega plate reader spectrometer as described.^{s5} Proliferation in the presence of the vehicle was always arbitrary set to 100%.

5.1.II.8 *Monitoring of estrogens during proliferation assay*

The levels of conversion of the estrogens were monitored by treating the cells as described above in the proliferation assay with some modifications. Radiolabeled estrogens ([^3H]-E1-S

or [^3H]-E1) were used. After 2 days of incubation the supernatant were removed and injected to the radio HPLC for the separation and quantification of the radioactive steroids.

5.1.II.9 *MTT cell viability assay*

In 24-well plates, HEK293 were seeded in DMEM supplemented with 5% FKS and 100 IU/ml penicillin-streptomycin. After 3 h, the incubation was started by the addition of compound 9 at 0.1, 0.2, 0.4 and 1 μM dissolved in ethanol with a final ethanol concentration of 1%. After 48 h, the MTT dye was added and the same procedure as described before was followed. Viability in the presence of the vehicle was arbitrarily set to 100%. For results, see Figure S2.

5.1.III Further results

5.1.III.1 Table S2

Calculated pKa of the phenolic parents of the final compounds and the stability of sulfamate moiety in test buffer

| Compound | cpKa ^a | % ^b |
|-----------|-------------------|----------------|
| 1 | 9.1 | 100 |
| 2 | 9.0 | 100 |
| 3 | 9.4 | 100 |
| 4 | 8.2 | 90 |
| 5 | 8.2 | 100 |
| 6 | 8.2 | 100 |
| 7 | 9.3 | 100 |
| 8 | 7.9 | 90 |
| 9 | 7.8 | 94 |
| 10 | 9.5 | 100 |
| 11 | 6.9 | 28 |
| 12 | 6.7 | 20 |

^a cpKa values of phenolic parent cpd (RO⁻), determined by ACD/Labs Software; ^b % of sulfamated cmpd relative to unsulfamated phenolic parent cpd evaluated at least 2 times (standard deviation less than 10%) using LC-MS after incubating the sulfamated cmpds in 20mM Tris-HCl buffer pH=7.2 for 30min @ 37°C.

5.1.III.2 Table S3

Percentages of remaining STS and *h17β*-HSD1 activities within the T47D cells in the presence of vehicle or *cmpd* 9 after treating it according to the procedure proposed for the determination of the nature of inhibition of STS activity

| Cmpd | % ^a | | | |
|----------------------|---------------------------|-------|---|------|
| | STS activity ^b | | <i>h17β</i> -HSD1 activity ^c | |
| | 24 h | 48h | 24h | 48h |
| Vehicle ^d | 47.4% | 98.5% | 100% | 100% |
| 9 ^e | 0% | 0% | 100% | 100% |

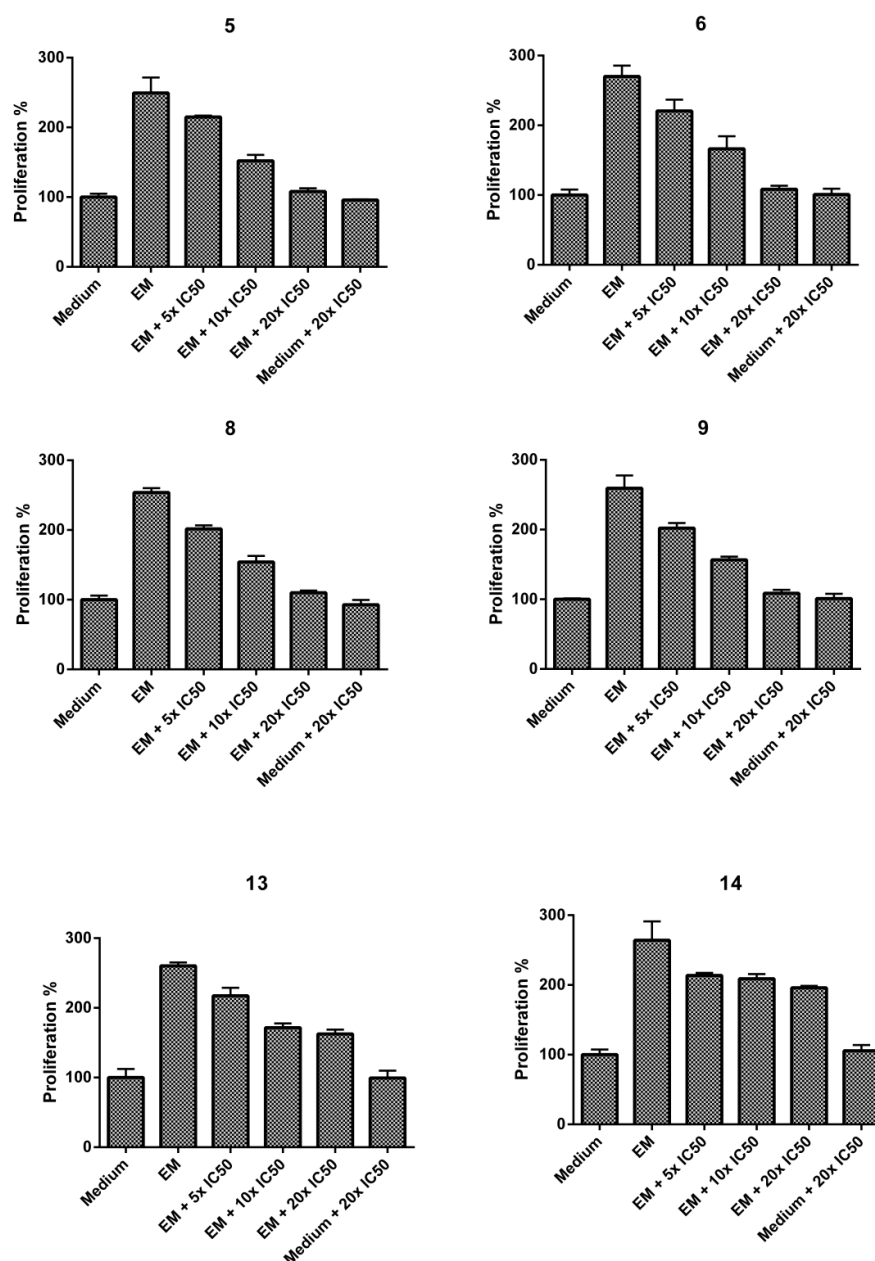
^a Mean value of at least two independent experiments each conducted in triplicates, standard deviation less than 10%; ^b remaining STS activity was assayed by incubating the cells with [³H]-E1-S [5nM] for 24 h and 48 h then quantifying the amount of [³H]-E1 produced relative to the amount of [³H]-E1-S remaining ; ^c remaining *h17β*-HSD1 activity was assayed by incubating the cells with [³H]-E1 [50nM] for 24 h and 48 h then quantifying the amount of [³H]-E2 produced relative to the amount of [³H]-E1 remaining; ^d vehicle: ethanol; ^e *cmpd* 9 [50 nM].

5.1.III.3 Table S2

Inhibitory activities of compounds 9 and 14 towards hSTS in cell-free assay using ELISA kit and radiolabeled [³H]-E1-S

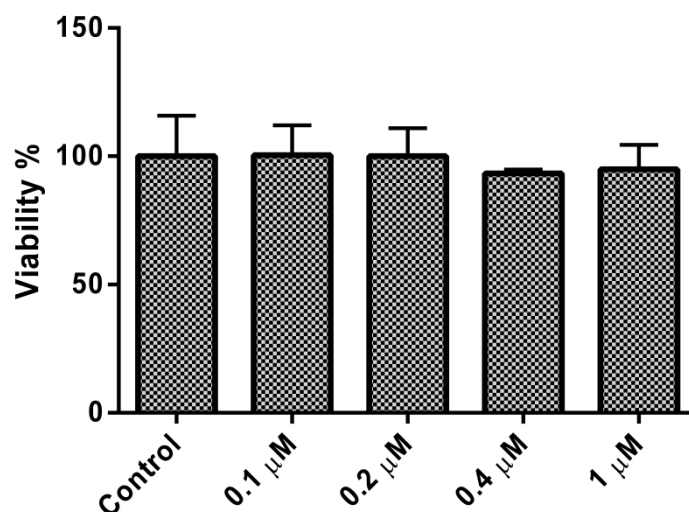
| Cmpd | IC ₅₀ [nM] ^a | |
|------|------------------------------------|-------------------------------------|
| | ELISA detection ^b | Radiolabeled detection ^c |
| | | |
| 9 | 143.1 | 138.8 |
| 14 | 15.1 | 12.2 |

^a Mean value of at least two independent experiments each conducted in duplicates, standard deviation less than 5%; ^b substrate E1-S [300 nM]; ^c exactly the same biochemical steps were followed however the substrate was [³H]-E1-S + E1-S [300 nM], after the quenching step the reaction mixture (without any further workup) was injected into the same radio-HPLC system mentioned above for *h17β*-HSD1 and *h17β*-HSD2 cell free inhibition assays.



5.1.III.4 Figure S1

Concentration dependent inhibition of E1-S- and E1-stimulated cell growth for compounds **5**, **6**, **8**, **9**, **13** and **14** on T47D cells. Cells were grown in phenol red-free RPMI 1640 medium supplemented with 5% stripped FCS. Medium represents cells grown in non-estrogenic medium. EM (estrogenic medium) represents E1-S [50 nM] and E1 [50 nM] treated cells. Compound **5** was tested at 3 different concentrations [200, 400 and 800 nM]. Compound **6** was tested at 3 different concentrations [300, 600 and 1200 nM]. Compounds **8** and **9** were tested at 3 different concentrations [100, 200 and 400 nM]. Compounds **13** and **14** were tested at 3 different concentrations [50, 100 and 200 nM]. Cells were incubated with the respective additives for 7 days without passage. Medium was changed every 2–3 days. Vehicle is ethanol.



5.1.III.5 *Figure S2*

MTT cell viability assay using HEK293 for compound **9**. The cells were seeded in DMEM supplemented with 5% FKS and 100 IU/ml penicillin-streptomycin. After 3 h, the incubation was started by the addition of compound **9** at four different concentrations: 0.1, 0.2, 0.4 and 1 μM dissolved in ethanol with a final concentration 1%. After 48 h, the viability of the cells was evaluated by the addition of MTT dye setting the viability in the presence of the vehicle arbitrary to 100%. Vehicle is ethanol.

5.1.III.6 *Determination of statistical significances*

Statistical analyses of cell proliferation assays were carried using Student's t-test (one-tailed, two samples, same variance). Differences of the mean were classified as insignificant ($p > 0.05$), probable ($p < 0.05$), significant (**, $p < 0.01$) and highly significant (***, $p < 0.001$).

5.1.IV References

- (S1) Kruchten, P.; Werth, R.; Marchais-Oberwinkler, S.; Frotscher, M.; Hartmann, R. W. Development of a Biological Screening System for the Evaluation of Highly Active and Selective 17 β -HSD1-Inhibitors as Potential Therapeutic Agents. *Mol. Cell. Endocrinol.* 2009, 301 (1–2), 154–157.
- (S2) DRG. http://www.drg-diagnostics.de/files/eia-4174_ifu--estrone_2016-12-16_endeitesfr.pdf
- (S3) Mack, J. T.; Brown, C. B.; Garrett, T. E.; Uys, J. D.; Townsend, D. M.; Tew, K. D. Ablation of the ATP-Binding Cassette Transporter, *Abca2* Modifies Response to Estrogen-Based Therapies. *Biomed. Pharmacother.* 2012, 66 (6), 403–408.
- (S4) Woo, L. L.; Purohit, A.; Malini, B.; Reed, M. J.; Potter, B. V. L. Potent Active Site-Directed Inhibition of Steroid Sulphatase by Tricyclic Coumarin-Based Sulphamates. *Chem. Biol.* 2000, 7 (10), 773–791.
- (S5) Kruchten, P.; Werth, R.; Bey, E.; Oster, A.; Marchais-Oberwinkler, S.; Frotscher, M.; Hartmann, R. W. Selective Inhibition of 17 β -Hydroxysteroid Dehydrogenase Type 1 (17 β HSD1) Reduces Estrogen Responsive Cell Growth of T47-D Breast Cancer Cells. *J. Steroid Biochem. Mol. Biol.* 2009, 114 (3–5), 200–206.
- (S6) Chetrite, G. S.; Ebert, C.; Wright, F.; Philippe, A. C.; Pasqualini, J. R. Control of Sulfatase and Sulfotransferase Activities by Medrogestone in the Hormone-Dependent MCF-7 and T-47D Human Breast Cancer Cell Lines. *J. Steroid Biochem. Mol. Biol.* 1999, 70 (1–3), 39–45.
- (S7) Purohit, A.; Williams, G. J.; Howarth, N. M.; Potter, B. V.; Reed, M. J. Inactivation of Steroid Sulfatase by an Active Site-Directed Inhibitor, Estrone-3-O-Sulfamate. *Biochemistry* 1995, 34 (36), 11508–11514.

5.2 Supporting information for Monograph B

5.2.I Chemistry

5.2.I.1 *Chemical methods*

Chemical names follow IUPAC nomenclature.

Starting materials were purchased from Acros Organics, Alfa Aesar, Combi-Blocks, Fluorochem and Sigma Aldrich. Column chromatography was performed on silica gel (0.04-0.063 mm, Macherey-Nagel) and reaction progress was monitored by TLC on aluminum sheets (Silicagel 60 F254, Merck). Visualization was accomplished with UV light at 254 nm.

^1H and ^{13}C NMR spectra were measured on a Bruker-500 (at 500 MHz and 125 MHz, respectively) or Bruker-300 (at 300 MHz). Chemical shifts are reported in δ (parts per million: ppm), using residual peaks of the deuterated solvents as internal standard: $(\text{CD}_3)_2\text{SO}$ (DMSO-*d*6): 2.50 ppm (^1H NMR), 39.52 ppm (^{13}C NMR); $(\text{CD}_3)_2\text{CO}$ (acetone-*d*6): 2.05 ppm (^1H NMR), 29.84 ppm and 206.26 ppm (^{13}C NMR). Signals are described as s, d, t, dd, ddd, dt, td and m for singlet, doublet, triplet, doublet of doublets, doublet of doublet of doublets, doublet of triplets, triplets of doublets and multiplet, respectively. All coupling constants (*J*) are given in Hertz (Hz).

All tested compounds have $\geq 95\%$ chemical purity as evaluated by HPLC. The purity of the compounds was evaluated by LC/MS. The Surveyor®-LC-system consisted of a pump, an auto sampler, and a PDA detector. Mass spectrometry was performed by a TSQ® Quantum (ThermoFisher, Dreieich, Germany). The triple quadrupole mass spectrometer was equipped with an electrospray interface (ESI). The system was operated by the standard software Xcalibur®. A RP C18 NUCLEODUR® 100-5 (3 mm) column (Macherey-Nagel GmbH, Dühren, Germany) was used as stationary phase. All solvents were HPLC grade. In a gradient run the percentage of acetonitrile (containing 0.1 % trifluoroacetic acid) was increased from an initial concentration of 30% at 0 min to 100 % at 12 min and kept at 100 % for 3 min. The injection volume was 25 μL and flow rate was set to 700 $\mu\text{L}/\text{min}$. MS analysis was carried out at a needle voltage of 3000 V and a capillary temperature of 350 °C. Mass spectra were acquired in positive mode from 100 to 1000 *m/z* and UV spectra were recorded at the wavelength of 254 nm. High resolution precise mass spectra were recorded on ThermoFisher Scientific (TF, Dreieich, Germany) Q Exactive Focus system equipped with heated electrospray ionization (HESI)-II source and Xcalibur (version 4.0.27.19) software. Before analysis external mass calibration was done according to the manufacturer's recommendations. The samples were dissolved and diluted in methanol in a concentration of

5 μ M and directly injected onto the Q Exactive Focus using the integrated syringe pump. All the data analyses were done in positive ion mode using voltage scans and the data collected in continuous mode. The melting points were measured using StuartTM melting point apparatus SMP3.

5.2.1.2 General procedures

General procedure for Acyl Chloride formation. (Method A)

A mixture of 5-bromofuran-2-carboxylic acid (5 mmol, 1 equiv), thionylchloride (10 mmol, 2 equiv) and DMF (20 drops) in toluene (30 mL) was refluxed at 110 °C for 4 h. The reaction mixture was cooled to room temperature; the solvent and the excess of thionyl chloride were removed under reduced pressure. The crude product was used in the next step without any further purification.

General procedure for Amide formation. (Method B)

The corresponding aniline (5 mmol, 1 equiv) and Et₃N (7.5 mmol, 1.5 equiv) in CH₂Cl₂ (25 mL) was added at 0 °C under N₂ atmosphere to the acyl chloride. After 30 min at 0 °C, the ice bath was removed and the solution was warmed up and stirred at room temperature overnight. The reaction mixture was extracted twice with ethyl acetate (2 x 15 mL); the organic layer was dried over MgSO₄, filtered and the solution was concentrated under reduced pressure. The residue was purified using flash column chromatography.

General procedure for N-Methylation. (Method C).

After 30 min of ice-cooled stirring for a mixture of benzamide derivatives (4 mmol, 1 equiv) and NaH (60% suspension in mineral oil, 8 mmol, 2 equiv) in DMF (10 mL), iodomethane (8 mmol, 2 equiv) was added and the reaction was left overnight to stir at room temperature. Then the reaction mixture was poured into water. The resulting precipitate was collected, washed with water, dried, and purified by flash column chromatography.

General procedure for ether cleavage (Method D)

A solution of the methoxyaryl compound (1.5 mmol, 1 equiv) in dry DCM (20 mL) was cooled on an ice/water bath. Boron trifluoride dimethyl sulfide complex (30 mmol, 20 equiv) was added dropwise under continuous stirring. The mixture was left to stir overnight at room temperature. After the reaction was finished, the mixture was quenched with methanol and the solvents removed under reduced pressure. The product was purified by flash column chromatography.

General procedure for Suzuki coupling (Method E)

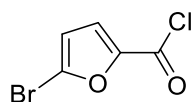
Arylbromide (1 mmol, 1 equiv), boronic acid derivative (1.2 mmol, 1.2 equiv), cesium carbonate (4 mmol, 4 equiv) and tetrakis(triphenylphosphine) palladium (0.05 mmol, 0.05 equiv) were added to an oxygen-free DME/water (1:1) (30 mL) and refluxed at 110 °C under nitrogen atmosphere for 4 h. The reaction mixture was cooled to room temperature. The aqueous layer was extracted with ethyl acetate. The organic layers were combined, dried over magnesium sulfate and concentrated to dryness under reduced pressure. The product was purified by flash column chromatography.

General procedure for Sulfamoylation (Method F)

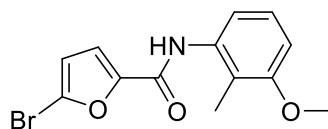
A solution of phenol derivative (0.5 mmol, 1 equiv) in DMA (10 mL) was cooled to 0 °C. A freshly prepared sulfamoyl chloride (5 mmol, 10 equiv) was subsequently added over 5 min and the reaction mixture was warmed to room temperature overnight. The reaction was quenched with water. The resulting precipitate was collected, washed with water, dried, and purified by flash column chromatography.

Preparation of sulfamoyl chloride (Method G)

A fresh solution was prepared for each reaction. Chlorosulfonyl isocyanate (5 mmol, 1 equiv) was cooled to 0 °C. Then formic acid 99% (5 mmol, 1 equiv) was then added dropwise to the isocyanate slowly over 10 min. Slow, steady evolution of CO₂ was observed; eventually a white solid was formed. After 20 min, the ice bath was removed and the reaction mixture was warmed to room temperature and then used in the next reaction without further workup.

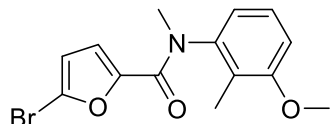
5.2.1.3 Detailed synthesis procedure and compound characterization**5-bromofuran-2-carbonyl chloride**

The title compound was prepared according to method A by the reaction of 5-bromofuran-2-carboxylic acid (0.95 g, 5 mmol, 1 equiv) and thionyl chloride (1.20 g, 10 mmol, 2 equiv) in the presence of dimethyl formamide (20 drops) in toluene (20 ml). The crude product was used in the next step without any further purification.

5-bromo-N-(3-methoxy-2-methylphenyl)furan-2-carboxamide (4a)

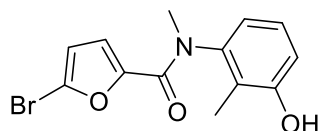
The title compound was prepared according to method B by the reaction of 3-methoxy-2-methylaniline (0.685 g, 5 mmol, 1 equiv) and 5-bromofuran-2-carbonyl chloride (1.05 g, 5 mmol, 1 equiv) in the presence of Et₃N (1.05 ml, 0.76 g, 7.5 mmol, 1.5 equiv) in CH₂Cl₂ (25 ml). The product was purified by flash column chromatography (Petroleum ether/Et₂O, 0 - 50 % EtOAc in 30 min), to give 780 mg (2.51 mmol/ 50% yield) of the analytically pure compound (purity: 97%). C₁₃H₁₂BrNO₃; MW 310.14; ¹H NMR (500 MHz, DMSO-*d*₆) δ 9.91 (s, 1H), 7.32 (d, *J* = 3.6 Hz, 1H), 7.17 (t, *J* = 8.1 Hz, 1H), 6.88 (d, *J* = 8.1 Hz, 2H), 6.82 (d, *J* = 3.5 Hz, 1H), 3.80 (s, 3H), 2.01 (s, 3H); MS (ESI): 310.02, 312.03 (M+H)⁺.

5-bromo-N-(3-methoxy-2-methylphenyl)-N-methylfuran-2-carboxamide (4b)



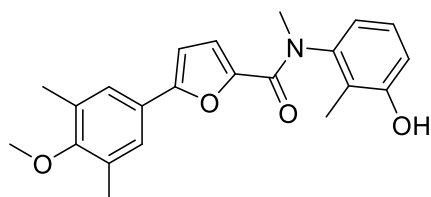
The title compound was prepared by reaction of **4a** (775 mg, 2.50 mmol, 1 equiv), sodium hydride 60 % suspension in mineral oil (200 mg, 6.5 mmol, 2 equiv) and iodomethane (0.31 mL, 5.0 mmol, 2 equiv) in DMF (10 ml) according to method C. The resulting precipitate was purified by flash column chromatography (Petroleum ether/Et₂O, 0 - 50 % EtOAc in 30 min), to give 660 mg (2.03 mmol/ 82% yield) of the analytically pure compound (purity: 99%). C₁₄H₁₄BrNO₃; MW 324.17; ¹H NMR (500 MHz, DMSO-*d*₆) δ 7.27 (t, *J* = 8.1 Hz, 1H), 7.06 (d, *J* = 8.3 Hz, 1H), 6.88 (d, *J* = 7.8 Hz, 1H), 6.48 (d, *J* = 3.6 Hz, 1H), 5.52 (d, *J* = 3.6 Hz, 1H), 3.83 (s, 3H), 3.19 (s, 3H), 1.95 (s, 3H); MS (ESI): 324.03, 326.02 (M+H)⁺.

5-bromo-N-(3-hydroxy-2-methylphenyl)-N-methylfuran-2-carboxamide (4c)



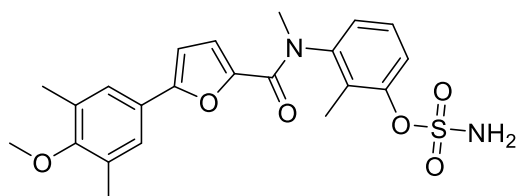
The title compound was prepared by reaction of **4b** (660 mg, 2.0 mmol, 1 equiv) and boron trifluoride dimethyl sulfide (4.2 ml, 40 mmol, 20 equiv) in CH₂Cl₂ (30 ml) according to method D. The resulting product was purified by flash column chromatography (CH₂Cl₂/Methanol, 0 - 5 % methanol in 30 min), to give 400 mg (1.30 mmol/ 65% yield) of the analytically pure compound (purity: 98%). C₁₃H₁₂BrNO₃; MW 310.14; ¹H NMR (500 MHz, DMSO-*d*₆) δ 9.70 (s, 1H), 7.09 (t, *J* = 8.0 Hz, 1H), 6.88 (d, *J* = 8.2 Hz, 1H), 6.71 (d, *J* = 7.8 Hz, 1H), 6.48 (d, *J* = 3.6 Hz, 1H), 5.48 (d, *J* = 3.6 Hz, 1H), 3.18 (s, 3H), 1.90 (s, 3H); MS (ESI): 310.02, 312.03 (M+H)⁺.

N-(3-hydroxy-2-methylphenyl)-5-(4-methoxy-3,5-dimethylphenyl)-N-methylfuran-2-carboxamide (4d)



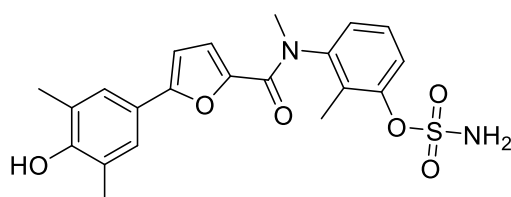
The title compound was prepared by reaction of **4c** (310 mg, 1.0 mmol, 1 equiv), (4-methoxy-3,5-dimethylphenyl)boronic acid (220 mg, 1.2 mmol, 1.2 equiv), cesium carbonate (1300 mg, 4.0 mmol, 4 equiv) and tetrakis(triphenylphosphine)palladium (55 mg, 0.05 mmol, 0.05 equiv) in oxygen-free DME/water (1:1) (30 mL) according to method E. The resulting product was purified by flash column chromatography (CH₂Cl₂/Methanol, 0 - 5 % methanol in 30 min), to give 225 mg (0.62 mmol/ 62% yield) of the analytically pure compound (purity: 95%). C₂₂H₂₃NO₄; MW 365.43; ¹H NMR (500 MHz, DMSO-*d*₆) δ 9.71 (s, 1H), 7.08 (t, *J* = 7.9 Hz, 1H), 6.96 (s, 2H), 6.90 (d, *J* = 8.2 Hz, 1H), 6.75 (d, *J* = 3.6 Hz, 1H), 6.70 (d, *J* = 7.8 Hz, 1H), 6.58 (d, *J* = 3.6 Hz, 1H), 3.63 (s, 3H), 3.20 (s, 3H), 2.20 (s, 6H), 1.97 (s, 3H); MS (ESI): 366.20 (M+H)⁺.

3-(5-(4-methoxy-3,5-dimethylphenyl)-N-methylfuran-2-carboxamido)-2-methylphenyl sulfamate (4e)



The title compound was prepared by reaction of **4d** (220 mg, 0.60 mmol, 1 equiv) and sulfamoyl chloride (600 mg, 6 mmol, 10 equiv) in water-free DMA (10 mL) according to method E. The resulting precipitate was purified by flash column chromatography (CH₂Cl₂/Methanol, 0 - 5 % methanol in 30 min), to give 200 mg (0.45 mmol/ 75% yield) of the analytically pure compound (purity: 98%). C₂₂H₂₄N₂O₆S; MW 444.50; ¹H NMR (500 MHz, DMSO-*d*₆) δ 8.16 (s, 2H), 7.44 (d, *J* = 8.3 Hz, 1H), 7.39 (t, *J* = 8.0 Hz, 1H), 7.27 (d, *J* = 7.7 Hz, 1H), 6.92 (s, 2H), 6.76 (d, *J* = 3.6 Hz, 1H), 6.61 (d, *J* = 3.6 Hz, 1H), 3.63 (s, 3H), 3.24 (s, 3H), 2.20 (s, 6H), 2.16 (s, 3H); MS (ESI): 445.12 (M+H)⁺.

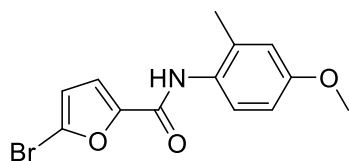
3-(5-(4-hydroxy-3,5-dimethylphenyl)-N-methylfuran-2-carboxamido)-2-methylphenyl sulfamate (4)



The title compound was prepared by reaction of **4e** (200 mg, 0.45 mmol, 1 equiv) and boron trifluoride dimethyl sulfide (0.95 ml, 9.0 mmol, 20 equiv) in CH₂Cl₂ (20 ml) according to method D. The resulting product was purified by flash column chromatography (CH₂Cl₂/Methanol, 0 - 5 % methanol in 30 min), to give 100 mg (0.23 mmol/ 51% yield) of the analytically pure compound (purity: 97%). C₂₁H₂₂N₂O₆S; MW 430.47; mp 138-140 °C; ¹H NMR (500 MHz, DMSO-*d*₆) δ 8.58 (s, 1H), 8.15 (s, 2H), 7.43 (d, *J* = 8.3 Hz, 1H), 7.38 (t, *J* = 8.0 Hz, 1H), 7.26 (d, *J* = 7.7 Hz, 1H), 6.84 (s, 2H), 6.62 (d, *J* = 3.6 Hz, 1H), 6.55 (d, *J* = 3.6 Hz, 1H), 3.23 (s, 3H), 2.15 (s, 3H), 2.14 (s, 6H); ¹³C NMR (126 MHz, DMSO-*d*₆) δ 157.87, 155.54, 154.02, 149.56, 145.29, 144.42, 129.77, 127.43, 126.42, 124.67, 124.16, 122.16.

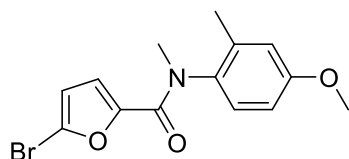
, 120.34 , 119.05 , 104.70 , 37.11 , 16.44 , 11.32 ; HRMS (ESI): calculated 431.127, found 431.123 (M+H)⁺.

5-bromo-N-(4-methoxy-2-methylphenyl)furan-2-carboxamide (5a)



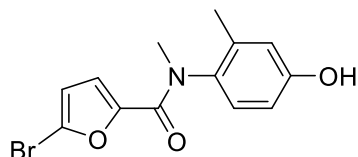
The title compound was prepared according to method B by the reaction of 4-methoxy-2-methylaniline (0.7 g, 5 mmol, 1 equiv) and 5-bromofuran-2-carbonyl chloride (1.05 g, 5 mmol, 1 equiv) in the presence of Et₃N (1.05 ml, 0.76 g, 7.5 mmol, 1.5 equiv) in CH₂Cl₂ (25 ml). The product was purified by flash column chromatography (Petroleum ether/Ethyl acetate, 0 - 30 % EtOAc in 30 min), to give 1.45 g (4.67 mmol/ 94% yield) of the analytically pure compound (purity: 98%). C₁₃H₁₂BrNO₃; MW 310.14; ¹H NMR (300 MHz, DMSO-*d*₆) δ 9.74 (s, 1H), 7.29 (d, *J* = 3.6 Hz, 1H), 7.15 (d, *J* = 8.6 Hz, 1H), 6.84 (d, *J* = 2.9 Hz, 1H), 6.81 (d, *J* = 3.6 Hz, 1H), 6.77 (dd, *J* = 8.6, 2.9 Hz, 1H), 3.74 (s, 3H), 2.16 (s, 3H); MS (ESI): 310.06, 312.07 (M+H)⁺.

5-bromo-N-(4-methoxy-2-methylphenyl)-N-methylfuran-2-carboxamide (5b)

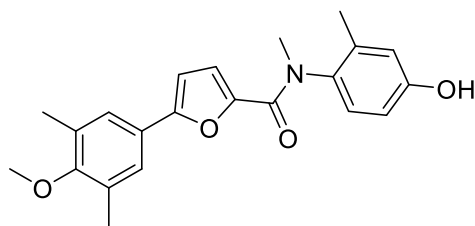


The title compound was prepared by reaction of **5a** (690 mg, 2.2 mmol, 1 equiv), sodium hydride 60 % suspension in mineral oil (186 mg, 4.5 mmol, 2 equiv) and iodomethane (0.28 mL, 4.5 mmol, 2 equiv) in DMF (10 ml) according to method C. The resulting precipitate was purified by flash column chromatography (Petroleum ether/Ethyl acetate, 0 - 50 % EtOAc in 30 min), to give 529 mg (1.63 mmol/ 73% yield) of the analytically pure compound (purity: 99%). C₁₄H₁₄BrNO₃; MW 324.17; ¹H NMR (300 MHz, DMSO-*d*₆) δ 7.18 (d, *J* = 8.6 Hz, 1H), 6.93 (d, *J* = 2.9 Hz, 1H), 6.85 (dd, *J* = 8.6, 3.0 Hz, 1H), 6.48 (d, *J* = 3.6 Hz, 1H), 5.43 (d, *J* = 3.6 Hz, 1H), 3.77 (s, 3H), 3.18 (s, 3H), 2.08 (s, 3H); MS (ESI): 324.10, 326.10 (M+H)⁺.

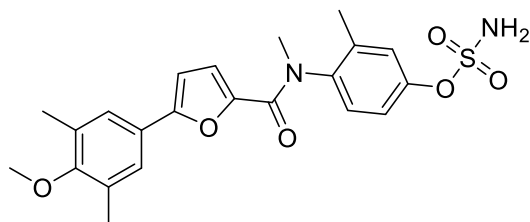
5-bromo-N-(4-hydroxy-2-methylphenyl)-N-methylfuran-2-carboxamide (5c)



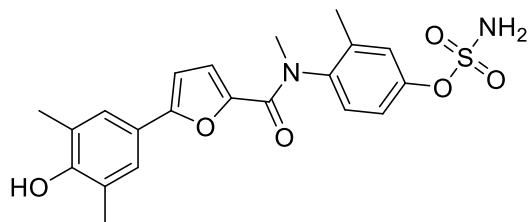
The title compound was prepared by reaction of **5b** (520 mg, 1.6 mmol, 1 equiv) and boron trifluoride dimethyl sulfide (3.15 ml, 30 mmol, 20 equiv) in CH₂Cl₂ (30 ml) according to method D. The resulting product was purified by flash column chromatography (CH₂Cl₂/Methanol, 0 - 5 % methanol in 30 min), to give 350 mg (1.13 mmol/ 70% yield) of the analytically pure compound (purity: 99%). C₁₃H₁₂BrNO₃; MW 310.14; MS (ESI): 310.05, 312.07 (M+H)⁺.

N-(4-hydroxy-2-methylphenyl)-5-(4-methoxy-3,5-dimethylphenyl)-N-methylfuran-2-carboxamide (5d)

The title compound was prepared by reaction of **5c** (350 mg, 1.13 mmol, 1 equiv), (4-methoxy-3,5-dimethylphenyl)boronic acid (250 mg, 1.4 mmol, 1.2 equiv), cesium carbonate (1460 mg, 4.5 mmol, 4 equiv) and tetrakis(triphenylphosphine)palladium (60 mg, 0.06 mmol, 0.05 equiv) in oxygen-free DME/water (1:1) (30 mL) according to method E. The resulting product was purified by flash column chromatography (Petroleum ether/Ethyl acetate, 0 - 50 % EtOAc in 30 min), to give 347 mg (0.95 mmol/ 84% yield) of the analytically pure compound (purity: 95%). $C_{22}H_{23}NO_4$; MW 365.43; 1H NMR (300 MHz, DMSO- d_6) δ 9.62 (s, 1H), 7.06 (d, J = 8.4 Hz, 1H), 7.02 (s, 2H), 6.79 – 6.73 (m, 2H), 6.68 (dd, J = 8.5, 2.8 Hz, 1H), 6.46 (d, J = 3.6 Hz, 1H), 3.64 (s, 3H), 3.19 (s, 3H), 2.21 (s, 6H), 2.04 (s, 3H); MS (ESI): 366.25 (M+H) $^+$.

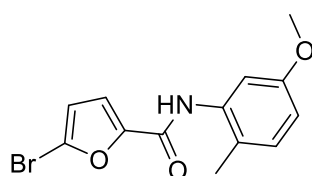
4-(5-(4-methoxy-3,5-dimethylphenyl)-N-methylfuran-2-carboxamido)-3-methylphenyl sulfamate (5e)

The title compound was prepared by reaction of **5d** (340 mg, 0.95 mmol, 1 equiv) and sulfamoyl chloride (1100 mg, 9.5 mmol, 10 equiv) in water-free DMA (10 mL) according to method E. The resulting precipitate was purified by flash column chromatography (CH₂Cl₂/Methanol, 0 - 5 % methanol in 30 min), to give 250 mg (0.56 mmol/ 60% yield) of the analytically pure compound (purity: 95%). $C_{22}H_{24}N_2O_6S$; MW 444.50; 1H NMR (300 MHz, DMSO- d_6) δ 8.1 (s, 2H), 7.41 (d, J = 8.4 Hz, 1H), 7.34 (d, J = 2.7 Hz, 1H), 7.25 (dd, J = 8.5, 2.8 Hz, 1H), 6.95 (s, 2H), 6.79 (d, J = 3.6 Hz, 1H), 6.76 (d, J = 3.6 Hz, 1H), 3.64 (s, 3H), 3.19 (s, 3H), 2.21 (s, 6H), 2.0 (s, 3H); MS (ESI): 445.19 (M+H) $^+$.

4-(5-(4-hydroxy-3,5-dimethylphenyl)-N-methylfuran-2-carboxamido)-3-methylphenyl sulfamate (5)

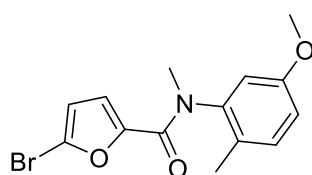
The title compound was prepared by reaction of **SN12** (235 mg, 0.52 mmol, 1 equiv) and boron trifluoride dimethyl sulfide (1.05 ml, 10 mmol, 20 equiv) in CH₂Cl₂ (20 ml) according to method D. The resulting product was purified by flash column chromatography (CH₂Cl₂/Methanol, 0 - 5 % methanol in 30 min), to give 95 mg (0.22 mmol/ 45% yield) of the analytically pure compound (purity: 98%). C₂₁H₂₂N₂O₆S; MW 430.47; mp 192-194 °C; ¹H NMR (500 MHz, DMSO-*d*₆) δ 8.57 (s, 1H), 8.08 (s, 2H), 7.39 (d, *J* = 8.5 Hz, 1H), 7.31 (d, *J* = 2.8 Hz, 1H), 7.23 (dd, *J* = 8.6, 2.8 Hz, 1H), 6.85 (s, 2H), 6.63 (d, *J* = 3.6 Hz, 1H), 6.56 (d, *J* = 3.7 Hz, 1H), 3.23 (s, 3H), 2.17 (s, 3H), 2.14 (s, 6H); ¹³C NMR (75 MHz, Acetone-*d*₆) δ 158.30, 156.09, 154.00, 149.95, 146.18, 141.85, 137.76, 129.47, 124.52, 124.39, 121.41, 121.36, 120.89, 118.68, 104.22, 36.56, 16.87, 15.63; HRMS (ESI): calculated 431.127, found 431.123 (M+H)⁺.

5-bromo-N-(5-methoxy-2-methylphenyl)furan-2-carboxamide (6a)



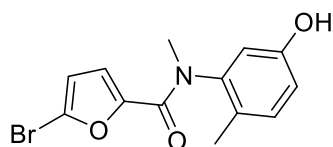
The title compound was prepared according to method B by the reaction of 5-methoxy-2-methylaniline (0.685 g, 5 mmol, 1 equiv) and 5-bromofuran-2-carbonyl chloride (1.05 g, 5 mmol, 1 equiv) in the presence of Et₃N (1.05 ml, 0.76 g, 7.5 mmol, 1.5 equiv) in CH₂Cl₂ (25 ml). The product was purified by flash column chromatography (Petroleum ether/Etyl acetate, 0 - 50 % EtOAc in 30 min), to give 1.05 g (3.38 mmol/ 70% yield) of the analytically pure compound (purity: 95%). C₁₃H₁₂BrNO₃; MW 310.14; ¹H NMR (500 MHz, Acetone-*d*₆) δ 8.94 (s, 1H), δ 7.34 (dd, *J* = 8.4, 2.7 Hz, 1H), 7.22 (d, *J* = 2.7 Hz, 1H), 7.15 (d, *J* = 8.4 Hz, 1H), 6.73 (d, *J* = 3.7 Hz, 1H), 6.72 (d, *J* = 3.8 Hz, 1H), 3.77 (s, 3H), 2.26 (s, 3H); MS (ESI): 310.01, 312.02 (M+H)⁺.

5-bromo-N-(5-methoxy-2-methylphenyl)-N-methylfuran-2-carboxamide (6b)



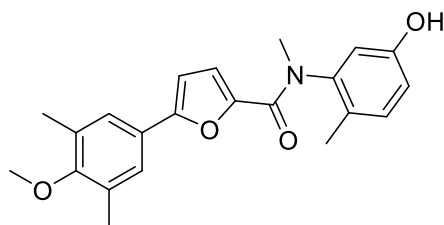
The title compound was prepared by reaction of **6a** (1000 mg, 3.25 mmol, 1 equiv), sodium hydride 60 % suspension in mineral oil (260 mg, 6.5 mmol, 2 equiv) and iodomethane (0.41 mL, 6.5 mmol, 2 equiv) in DMF (10 ml) according to method C. The resulting precipitate was purified by flash column chromatography (Petroleum ether/Etyl acetate, 0 - 50 % EtOAc in 30 min), to give 730 mg (2.25 mmol/ 70% yield) of the analytically pure compound (purity: 95%). C₁₄H₁₄BrNO₃; MW 324.17; ¹H NMR (500 MHz, Acetone-*d*₆) δ 7.25 (d, *J* = 8.4 Hz, 1H), 6.95 (dd, *J* = 8.4, 2.7 Hz, 1H), 6.90 (d, *J* = 2.7 Hz, 1H), 6.35 (d, *J* = 3.6 Hz, 1H), 5.69 (d, *J* = 3.6 Hz, 1H), 3.79 (s, 3H), 3.26 (s, 3H), 2.09 (s, 3H); MS (ESI): 324.04, 326.04 (M+H)⁺.

5-bromo-N-(5-hydroxy-2-methylphenyl)-N-methylfuran-2-carboxamide (6c)



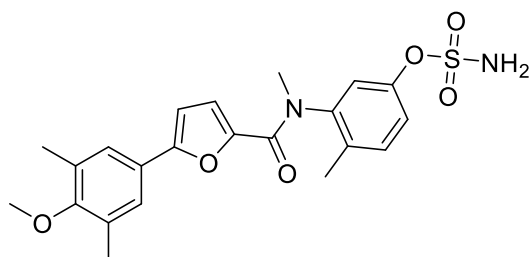
The title compound was prepared by reaction of **6b** (400 mg, 1.25 mmol, 1 equiv) and boron trifluoride dimethyl sulfide (2.7 ml, 25 mmol, 20 equiv) in CH_2Cl_2 (30 ml) according to method D. The resulting product was purified by flash column chromatography (CH_2Cl_2 /Methanol, 0 - 5 % methanol in 30 min), to give 280 mg (0.90 mmol/ 73% yield) of the analytically pure compound (purity: 95%). $\text{C}_{13}\text{H}_{12}\text{BrNO}_3$; MW 310.14; ^1H NMR (500 MHz, $\text{DMSO}-d_6$) δ 9.56 (s, 1H), 7.14 (d, $J = 8.3$ Hz, 1H), 6.77 (dd, $J = 8.4, 2.5$ Hz, 1H), 6.62 (d, $J = 2.5$ Hz, 1H), 6.50 (d, $J = 3.6$ Hz, 1H), 5.53 (d, $J = 3.6$ Hz, 1H), 3.17 (s, 3H), 1.98 (s, 3H); MS (ESI): 310.01, 312.02 ($\text{M}+\text{H}$) $^+$.

N-(5-hydroxy-2-methylphenyl)-5-(4-methoxy-3,5-dimethylphenyl)-N-methylfuran-2-carboxamide (6d)



The title compound was prepared by reaction of **6c** (280 mg, 0.90 mmol, 1 equiv), (4-methoxy-3,5-dimethylphenyl)boronic acid (200 mg, 1.1 mmol, 1.2 equiv), cesium carbonate (1170 mg, 3.6 mmol, 4 equiv) and tetrakis(triphenylphosphine)palladium (50 mg, 0.05 mmol, 0.05 equiv) in oxygen-free DME/water (1:1) (30 mL) according to method E. The resulting product was purified by flash column chromatography (Petroleum ether/Etyl acetate, 0 - 50 % EtOAc in 30 min), to give 180 mg (0.50 mmol/ 55% yield) of the analytically pure compound (purity: 95%). $\text{C}_{22}\text{H}_{23}\text{NO}_4$; MW 365.43; ^1H NMR (500 MHz, $\text{DMSO}-d_6$) δ 9.52 (s, 1H), 7.16 (d, $J = 8.3$ Hz, 1H), 6.98 (s, 2H), 6.79 (dd, $J = 8.4, 2.4$ Hz, 1H), 6.77 (d, $J = 2.6$ Hz, 1H), 6.67 (d, $J = 2.5$ Hz, 1H), 6.60 (d, $J = 3.6$ Hz, 1H), 3.63 (s, 3H), 3.20 (s, 3H), 2.20 (s, 6H), 2.00 (s, 3H); MS (ESI): 366.20 ($\text{M}+\text{H}$) $^+$.

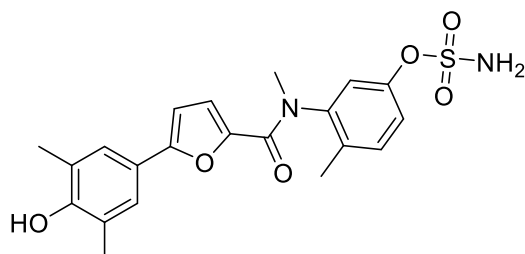
3-(5-(4-methoxy-3,5-dimethylphenyl)-N-methylfuran-2-carboxamido)-4-methylphenyl sulfamate (6e)



The title compound was prepared by reaction of **6d** (180 mg, 0.50 mmol, 1 equiv) and sulfamoyl chloride (500 mg, 5 mmol, 10 equiv) in water-free DMA (10 mL) according to method E. The resulting precipitate was purified by flash column chromatography (CH_2Cl_2 /Methanol, 0 - 5 % methanol in 30 min), to give 130 mg (0.30 mmol/ 60% yield) of

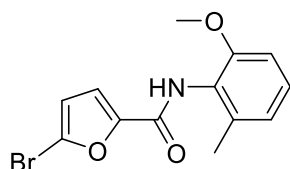
the analytically pure compound (purity: 98%). $C_{22}H_{24}N_2O_6S$; MW 444.50; 1H NMR (500 MHz, DMSO- d_6) δ 8.06 (s, 2H), 7.47 (d, J = 8.3 Hz, 1H), 7.30 (dd, J = 8.1, 2.5 Hz, 1H), 7.28 (d, J = 2.4 Hz, 1H), 6.92 (s, 2H), 6.78 (d, J = 3.6 Hz, 1H), 6.67 (d, J = 3.6 Hz, 1H), 3.63 (s, 3H), 3.26 (s, 3H), 2.20 (s, 6H), 2.12 (s, 3H); MS (ESI): 445.12 (M+H) $^+$.

3-(5-(4-hydroxy-3,5-dimethylphenyl)-N-methylfuran-2-carboxamido)-4-methylphenyl sulfamate (6)

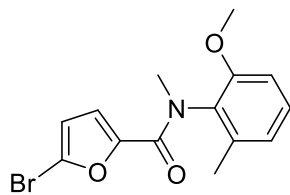


The title compound was prepared by reaction of **6e** (125 mg, 0.28 mmol, 1 equiv) and boron trifluoride dimethyl sulfide (0.6 ml, 5.6 mmol, 20 equiv) in CH_2Cl_2 (20 ml) according to method D. The resulting product was purified by flash column chromatography (CH_2Cl_2 /Methanol, 0 - 5 % methanol in 30 min), to give 80 mg (0.18 mmol/ 66% yield) of the analytically pure compound (purity: 97%). $C_{21}H_{22}N_2O_6S$; MW 430.47; mp 142-144 $^{\circ}C$; 1H NMR (500 MHz, DMSO- d_6) δ 8.58 (s, 1H), 8.05 (s, 2H), 7.45 (d, J = 8.3 Hz, 1H), 7.29 (dd, J = 8.2, 2.5 Hz, 1H), 7.27 (d, J = 2.4 Hz, 1H), 6.84 (s, 2H), 6.64 (d, J = 3.5 Hz, 1H), 6.60 (d, J = 3.7 Hz, 1H), 3.25 (s, 3H), 2.14 (s, 6H), 2.12 (s, 3H); ^{13}C NMR (126 MHz, DMSO- d_6) δ 157.82, 155.53, 154.03, 148.93, 145.35, 143.59, 133.66, 131.88, 124.66, 124.21, 121.70, 121.66, 120.34, 119.07, 104.69, 36.96, 16.53, 16.45; HRMS (ESI): calculated 431.127, found 431.123 (M+H) $^+$.

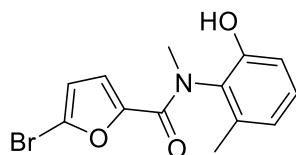
5-bromo-N-(2-methoxy-6-methylphenyl)furan-2-carboxamide (7a)



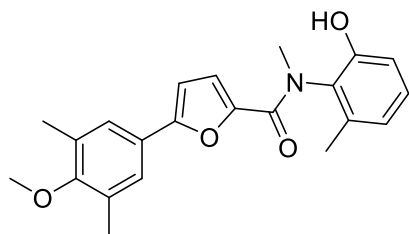
The title compound was prepared according to method B by the reaction of 2-methoxy-6-methylaniline (0.685 g, 5 mmol, 1 equiv) and 5-bromofuran-2-carbonyl chloride (1.05 g, 5 mmol, 1 equiv) in the presence of Et_3N (1.05 ml, 0.76 g, 7.5 mmol, 1.5 equiv) in CH_2Cl_2 (25 ml). The product was purified by flash column chromatography (Petroleum ether/Ethyl acetate, 0 - 30 % EtOAc in 30 min), to give 1300 mg (4.21 mmol/ 84% yield) of the analytically pure compound (purity: 97%). $C_{13}H_{12}BrNO_3$; MW 310.14; 1H NMR (500 MHz, DMSO- d_6) δ 9.56 (s, 1H), 7.31 (d, J = 3.6 Hz, 1H), 7.19 (t, J = 7.9 Hz, 1H), 6.91 (d, J = 8.4 Hz, 1H), 6.86 (d, J = 7.6 Hz, 1H), 6.81 (d, J = 3.5 Hz, 1H), 3.73 (s, 3H), 2.13 (s, 3H); MS (ESI): 310.02, 312.04 (M+H) $^+$.

5-bromo-N-(2-methoxy-6-methylphenyl)-N-methylfuran-2-carboxamide (7b)

The title compound was prepared by reaction of **7a** (1300 mg, 4.20 mmol, 1 equiv), sodium hydride 60 % suspension in mineral oil (340 mg, 8.5 mmol, 2 equiv) and iodomethane (0.31 mL, 5.0 mmol, 2 equiv) in DMF (10 ml) according to method C. The resulting precipitate was purified by flash column chromatography (Petroleum ether/Ethyl acetate, 0 - 50 % EtOAc in 30 min), to give 750 mg (2.31 mmol/ 55% yield) of the analytically pure compound (purity: 99%). $C_{14}H_{14}BrNO_3$; MW 324.17; 1H NMR (500 MHz, DMSO- d_6) δ 7.32 (t, J = 8.0 Hz, 1H), 6.98 (d, J = 8.4 Hz, 1H), 6.94 (d, J = 7.6 Hz, 1H), 6.46 (d, J = 3.6 Hz, 1H), 5.56 (d, J = 3.6 Hz, 1H), 3.71 (s, 3H), 3.11 (s, 3H), 2.11 (s, 3H); MS (ESI): 324.05, 326.06 (M+H) $^+$.

5-bromo-N-(2-hydroxy-6-methylphenyl)-N-methylfuran-2-carboxamide (7c)

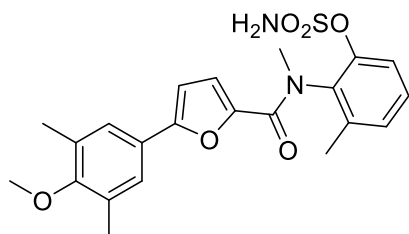
The title compound was prepared by reaction of **7b** (730 mg, 2.25 mmol, 1 equiv) and boron trifluoride dimethyl sulfide (4.75 ml, 45 mmol, 20 equiv) in CH_2Cl_2 (30 ml) according to method D. The resulting product was purified by flash column chromatography (CH_2Cl_2 /Methanol, 0 - 10 % methanol in 30 min), to give 500 mg (1.61 mmol/ 72% yield) of the analytically pure compound (purity: 98%). $C_{13}H_{12}BrNO_3$; MW 310.14; 1H NMR (500 MHz, DMSO- d_6) δ 9.77 (s, 1H), 7.13 (t, J = 7.9 Hz, 1H), 6.78 (d, J = 8.3 Hz, 1H), 6.77 (d, J = 7.7 Hz, 1H), 6.47 (d, J = 3.6 Hz, 1H), 5.54 (d, J = 3.6 Hz, 1H), 3.11 (s, 3H), 2.08 (s, 3H); MS (ESI): 310.02, 312.03 (M+H) $^+$.

N-(2-hydroxy-6-methylphenyl)-5-(4-methoxy-3,5-dimethylphenyl)-N-methylfuran-2-carboxamide (7d)

The title compound was prepared by reaction of **7c** (310 mg, 1.0 mmol, 1 equiv), (4-methoxy-3,5-dimethylphenyl)boronic acid (220 mg, 1.2 mmol, 1.2 equiv), cesium carbonate (1300 mg, 4.0 mmol, 4 equiv) and tetrakis(triphenylphosphine)palladium (55 mg, 0.05 mmol, 0.05 equiv) in oxygen-free DME/water (1:1) (30 mL) according to method E. The resulting product was purified by flash column chromatography (CH_2Cl_2 /Methanol, 0 - 5 % methanol in 30 min), to give 191 mg (0.52 mmol/ 52% yield) of the analytically pure compound (purity:

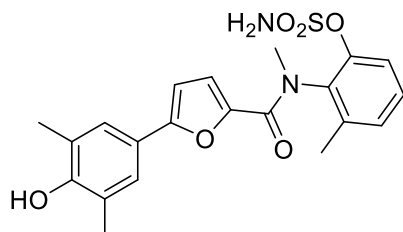
95%). $C_{22}H_{23}NO_4$; MW 365.43; 1H NMR (500 MHz, $DMSO-d_6$) δ 9.67 (s, 1H), 7.15 (t, J = 7.8 Hz, 1H), 6.99 (s, 2H), 6.82 (t, J = 8.2 Hz, 2H), 6.75 (d, J = 3.6 Hz, 1H), 6.54 (d, J = 3.5 Hz, 1H), 3.63 (s, 3H), 3.14 (s, 3H), 2.20 (s, 6H), 2.10 (s, 3H); MS (ESI): 366.22 (M+H) $^+$.

2-(5-(4-methoxy-3,5-dimethylphenyl)-N-methylfuran-2-carboxamido)-3-methylphenyl sulfamate (7e)



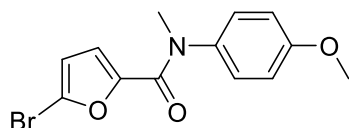
The title compound was prepared by reaction of **7d** (190 mg, 0.50 mmol, 1 equiv) and sulfamoyl chloride (500 mg, 5 mmol, 10 equiv) in water-free DMA (10 mL) according to method E. The resulting precipitate was purified by flash column chromatography (CH_2Cl_2 /Methanol, 0 - 5 % methanol in 30 min), to give 140 mg (0.32 mmol/ 64% yield) of the analytically pure compound (purity: 97%). $C_{22}H_{24}N_2O_6S$; MW 444.50; 1H NMR (500 MHz, $DMSO-d_6$) δ 8.25 (s, 2H), 7.50 – 7.40 (m, 2H), 7.38 – 7.31 (m, 1H), 6.90 (s, 2H), 6.77 (d, J = 3.6 Hz, 1H), 6.69 (d, J = 3.6 Hz, 1H), 3.63 (s, 3H), 3.23 (s, 3H), 2.19 (s, 9H); MS (ESI): 445.13 (M+H) $^+$.

2-(5-(4-hydroxy-3,5-dimethylphenyl)-N-methylfuran-2-carboxamido)-3-methylphenyl sulfamate (7)



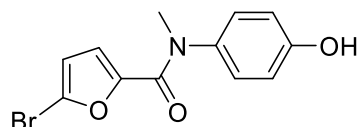
The title compound was prepared by reaction of **7d** (130 mg, 0.30 mmol, 1 equiv) and boron trifluoride dimethyl sulfide (0.70 ml, 6.0 mmol, 20 equiv) in CH_2Cl_2 (20 ml) according to method D. The resulting product was purified by flash column chromatography (CH_2Cl_2 /Methanol, 0 - 5 % methanol in 30 min), to give 30 mg (0.07 mmol/ 24% yield) of the analytically pure compound (purity: 98%). $C_{21}H_{22}N_2O_6S$; MW 430.47; mp 178-180°C; 1H NMR (500 MHz, $DMSO-d_6$) δ 8.56 (s, 1H), 8.25 (s, 2H), 7.51 – 7.40 (m, 2H), 7.33 (dd, J = 7.7, 1.7 Hz, 1H), 6.82 (s, 2H), 6.63 (d, J = 3.7 Hz, 1H), 6.61 (d, J = 3.6 Hz, 1H), 3.22 (s, 3H), 2.19 (s, 3H), 2.14 (s, 6H); ^{13}C NMR (126 MHz, $DMSO$) δ 158.04, 155.34, 153.92, 147.32, 145.63, 137.88, 134.96, 128.73, 128.24, 124.58, 124.19, 120.39, 119.33, 118.53, 104.59, 36.33, 17.23, 16.43; HRMS (ESI): calculated 431.127, found 431.123 (M+H) $^+$.

5-bromo-N-(4-methoxyphenyl)-N-methylfuran-2-carboxamide (8ab)



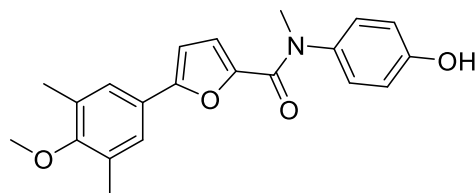
The title compound was prepared according to method B by the reaction of 4-methoxy-N-methylaniline (0.685 g, 5 mmol, 1 equiv) and 5-bromofuran-2-carbonyl chloride (1.05 g, 5 mmol, 1 equiv) in the presence of Et₃N (1.05 ml, 0.76 g, 7.5 mmol, 1.5 equiv) in CH₂Cl₂ (25 ml). The product was purified by flash column chromatography (Petroleum ether/Ethyl acetate, 0 - 30 % EtOAc in 30 min), to give 980 mg (3.16 mmol/ 63% yield) of the analytically pure compound (purity: 95%). C₁₃H₁₂BrNO₃; MW 310.14; ¹H NMR (300 MHz, DMSO-*d*₆) δ 7.25 (d, *J* = 8.9 Hz, 2H), 6.99 (d, *J* = 8.9 Hz, 2H), 6.50 (d, *J* = 3.6 Hz, 1H), 5.67 (d, *J* = 3.6 Hz, 1H), 3.78 (s, 3H), 3.25 (s, 3H); MS (ESI): 310.01, 312.03 (M+H)⁺.

5-bromo-N-(4-hydroxyphenyl)-N-methylfuran-2-carboxamide (8c)



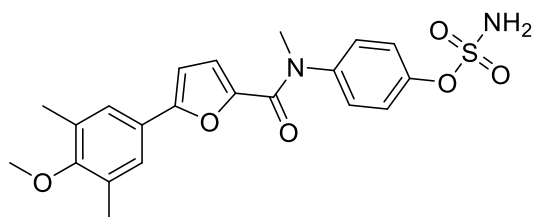
The title compound was prepared by reaction of **8ab** (960 mg, 3.1 mmol, 1 equiv) and boron trifluoride dimethyl sulfide (6.0 ml, 60 mmol, 20 equiv) in CH₂Cl₂ (30 ml) according to method D. The resulting product was purified by flash column chromatography (CH₂Cl₂/Methanol, 0 - 10 % methanol in 30 min), to give 780 mg (2.63 mmol/ 85% yield) of the analytically pure compound (purity: 95%). C₁₂H₁₀BrNO₃; MW 296.12; ¹H NMR (300 MHz, DMSO-*d*₆) δ 9.74 (s, 1H), 7.11 (d, *J* = 8.7 Hz, 2H), 6.80 (d, *J* = 8.7 Hz, 2H), 6.50 (d, *J* = 3.6 Hz, 1H), 5.59 (d, *J* = 3.6 Hz, 1H), 3.23 (s, 3H); MS (ESI): 296.05, 298.05 (M+H)⁺.

N-(4-hydroxyphenyl)-5-(4-methoxy-3,5-dimethylphenyl)-N-methylfuran-2-carboxamide (8d)



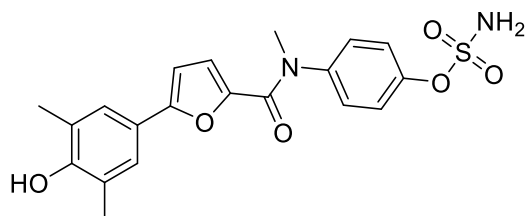
The title compound was prepared by reaction of **8c** (220 mg, 0.75 mmol, 1 equiv), (4-methoxy-3,5-dimethylphenyl)boronic acid (160 mg, 0.9 mmol, 1.2 equiv), cesium carbonate (975 mg, 3.0 mmol, 4 equiv) and tetrakis(triphenylphosphine)palladium (45 mg, 0.04 mmol, 0.05 equiv) in oxygen-free DME/water (1:1) (30 mL) according to method E. The resulting product was purified by flash column chromatography (CH₂Cl₂/Methanol, 0 - 5 % methanol in 30 min), to give 110 mg (0.31 mmol/ 42% yield) of the analytically pure compound (purity: 96%). C₂₁H₂₁NO₄; MW 351.40; ¹H NMR (300 MHz, DMSO-*d*₆) δ 9.69 (s, 1H), 7.13 (d, *J* = 8.7 Hz, 2H), 6.99 (s, 2H), 6.83 (d, *J* = 8.7 Hz, 2H), 6.75 (d, *J* = 3.6 Hz, 1H), 6.56 (d, *J* = 3.6 Hz, 1H), 3.63 (s, 3H), 3.26 (s, 3H), 2.20 (s, 6H); MS (ESI): 352.25 (M+H)⁺.

4-(5-(4-methoxy-3,5-dimethylphenyl)-N-methylfuran-2-carboxamido)phenyl sulfamate (8e)



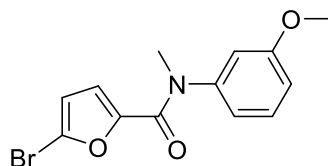
The title compound was prepared by reaction of **8d** (110 mg, 0.31 mmol, 1 equiv) and sulfamoyl chloride (300 mg, 3 mmol, 10 equiv) in water-free DMA (10 mL) according to method E. The resulting precipitate was purified by flash column chromatography (CH_2Cl_2 /Methanol, 0 - 5 % methanol in 30 min), to give 80 mg (0.18 mmol/ 60% yield) of the analytically pure compound (purity: 95%). $\text{C}_{21}\text{H}_{22}\text{N}_2\text{O}_6\text{S}$; MW 430.47; ^1H NMR (300 MHz, $\text{DMSO}-d_6$) δ 8.09 (s, 2H), 7.46 (d, J = 8.9 Hz, 2H), 7.37 (d, J = 8.8 Hz, 2H), 6.93 (s, 2H), 6.79 (d, J = 3.6 Hz, 1H), 6.73 (d, J = 3.6 Hz, 1H), 3.64 (s, 3H), 3.34 (s, 3H), 2.19 (s, 6H); MS (ESI): 431.19 ($\text{M}+\text{H}$) $^+$.

4-(5-(4-hydroxy-3,5-dimethylphenyl)-N-methylfuran-2-carboxamido)phenyl sulfamate (8)



The title compound was prepared by reaction of **8d** (80 mg, 0.18 mmol, 1 equiv) and boron trifluoride dimethyl sulfide (0.40 ml, 4 mmol, 20 equiv) in CH_2Cl_2 (20 ml) according to method D. The resulting product was purified by flash column chromatography (CH_2Cl_2 /Methanol, 0 - 5 % methanol in 30 min), to give 35 mg (0.08 mmol/ 46% yield) of the analytically pure compound (purity: 98%). $\text{C}_{20}\text{H}_{20}\text{N}_2\text{O}_6\text{S}$; MW 416.44; mp 186-188 $^\circ\text{C}$; ^1H NMR (300 MHz, Acetone- d_6) δ 7.57 (s, 1H), 7.49 (d, J = 8.9 Hz, 2H), 7.39 (d, J = 8.8 Hz, 2H), 7.22 (s, 2H), 6.93 (s, 2H), 6.68 (d, J = 3.6 Hz, 1H), 6.57 (d, J = 3.6 Hz, 1H), 3.39 (s, 3H), 2.21 (s, 6H); ^{13}C NMR (75 MHz, Acetone- d_6) δ 159.19 , 156.80 , 154.87 , 150.39 , 146.94 , 144.28 , 129.49 , 125.41 , 125.25 , 124.06 , 122.24 , 119.94 , 105.07 , 38.61 , 16.52; HRMS (ESI): calculated 417.1111, found 417.107 ($\text{M}+\text{H}$) $^+$.

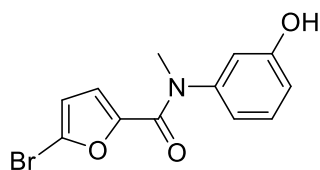
5-bromo-N-(3-methoxyphenyl)-N-methylfuran-2-carboxamide (9ab)



The title compound was prepared according to method B by the reaction of 3-methoxy-N-methylaniline (0.685 g, 5 mmol, 1 equiv) and 5-bromofuran-2-carbonyl chloride (1.05 g, 5 mmol, 1 equiv) in the presence of Et_3N (1.05 ml, 0.76 g, 7.5 mmol, 1.5 equiv) in CH_2Cl_2 (25 ml). The product was purified by flash column chromatography (Petroleum ether/Etyl acetate, 0 - 30 % EtOAc in 30 min), to give 1100 mg (3.60 mmol/ 72% yield) of the analytically pure compound (purity: 99%). $\text{C}_{13}\text{H}_{12}\text{BrNO}_3$; MW 310.14; ^1H NMR (300 MHz, $\text{DMSO}-d_6$) δ 7.33

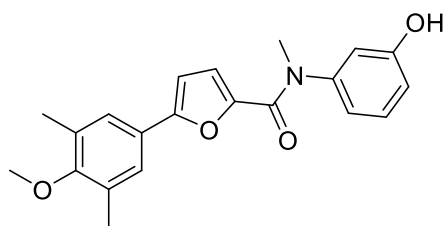
(t, $J = 8.0$ Hz, 1H), 7.02 – 6.91 (m, 2H), 6.90 – 6.81 (m, 1H), 6.52 (d, $J = 3.6$ Hz, 1H), 5.89 (d, $J = 3.6$ Hz, 1H), 3.75 (s, 3H), 3.29 (s, 3H); MS (ESI): 310.05, 312.06 ($M+H$)⁺.

5-bromo-N-(3-hydroxyphenyl)-N-methylfuran-2-carboxamide (9c)



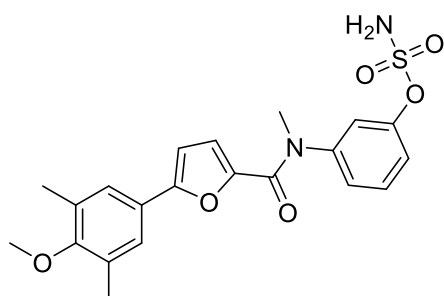
The title compound was prepared by reaction of **9ab** (1100 mg, 3.5 mmol, 1 equiv) and boron trifluoride dimethyl sulfide (7.0 ml, 70 mmol, 20 equiv) in CH_2Cl_2 (30 ml) according to method D. The resulting product was purified by flash column chromatography (CH_2Cl_2 /Methanol, 0 - 10 % methanol in 30 min), to give 800 mg (2.70 mmol/ 77% yield) of the analytically pure compound (purity: 99%). $C_{12}H_{10}BrNO_3$; MW 296.12; 1H NMR (300 MHz, $DMSO-d_6$) δ 9.73 (s, 1H), 7.23 (t, $J = 8.0$ Hz, 1H), 6.79 (ddd, $J = 8.2, 2.4, 1.0$ Hz, 1H), 6.72 (ddd, $J = 7.8, 2.0, 1.0$ Hz, 1H), 6.66 (t, $J = 2.2$ Hz, 1H), 6.53 (d, $J = 3.5$ Hz, 1H), 5.85 (d, $J = 3.6$ Hz, 1H), 3.26 (s, 3H); MS (ESI): 296.03, 298.02 ($M+H$)⁺.

N-(3-hydroxyphenyl)-5-(4-methoxy-3,5-dimethylphenyl)-N-methylfuran-2-carboxamide (9d)



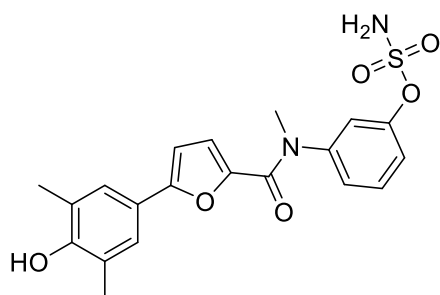
The title compound was prepared by reaction of **9c** (400 mg, 1.35 mmol, 1 equiv), (4-methoxy-3,5-dimethylphenyl)boronic acid (290 mg, 1.62 mmol, 1.2 equiv), cesium carbonate (1755 mg, 5.4 mmol, 4 equiv) and tetrakis(triphenylphosphine)palladium (75 mg, 0.07 mmol, 0.05 equiv) in oxygen-free DME/water (1:1) (30 mL) according to method E. The resulting product was purified by flash column chromatography (CH_2Cl_2 /Methanol, 0 - 5 % methanol in 30 min), to give 270 mg (0.77 mmol/ 56% yield) of the analytically pure compound (purity: 96%). $C_{21}H_{21}NO_4$; MW 351.40; 1H NMR (300 MHz, $DMSO-d_6$) δ 9.70 (s, 1H), 7.24 (t, $J = 8.3$ Hz, 1H), 6.99 – 6.92 (m, 2H), 6.82 (ddd, $J = 8.2, 2.2, 1.1$ Hz, 1H), 6.77 (d, $J = 3.6$ Hz, 1H), 6.74 – 6.69 (m, 3H), 3.63 (s, 3H), 3.29 (s, 3H), 2.19 (s, 6H); MS (ESI): 352.26 ($M+H$)⁺.

3-(5-(4-methoxy-3,5-dimethylphenyl)-N-methylfuran-2-carboxamido)phenyl sulfamate (9e)



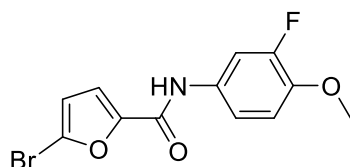
The title compound was prepared by reaction of **9d** (270 mg, 0.60 mmol, 1 equiv) and sulfamoyl chloride (600 mg, 6 mmol, 10 equiv) in water-free DMA (10 mL) according to method E. The resulting precipitate was purified by flash column chromatography (CH₂Cl₂/Methanol, 0 - 5 % methanol in 30 min), to give 190 mg (0.44 mmol/ 73% yield) of the analytically pure compound (purity: 99%). C₂₁H₂₂N₂O₆S; MW 430.47; ¹H NMR (300 MHz, DMSO-*d*₆) δ 8.09 (s, 2H), 7.54 (t, *J* = 8.3 Hz, 1H), 7.36 – 7.29 (m, 2H), 6.96 (s, 1H), 6.92 (s, 2H), 6.77 (d, *J* = 3.5 Hz, 1H), 6.71 (d, *J* = 3.5 Hz, 1H), 3.36 (s, 3H), 2.20 (s, 3H), 2.19 (s, 6H); MS (ESI): 431.19 (M+H)⁺.

3-(5-(4-hydroxy-3,5-dimethylphenyl)-N-methylfuran-2-carboxamido)phenyl sulfamate (9)

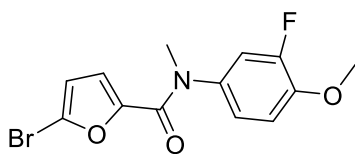


The title compound was prepared by reaction of **9e** (90 mg, 0.21 mmol, 1 equiv) and boron trifluoride dimethyl sulfide (0.40 ml, 4 mmol, 20 equiv) in CH₂Cl₂ (20 ml) according to method D. The resulting product was purified by flash column chromatography (CH₂Cl₂/Methanol, 0 - 5 % methanol in 30 min), to give 35 mg (0.08 mmol/ 39% yield) of the analytically pure compound (purity: 98%). C₂₀H₂₀N₂O₆S; MW 416.44; mp 198-200 °C; ¹H NMR (300 MHz, Acetone-*d*₆) δ 7.57 (s, 1H), 7.54 (t, *J* = 8.3 Hz, 1H), 7.42 – 7.35 (m, 2H), 7.31 (ddd, *J* = 7.9, 2.0, 1.1 Hz, 1H), 7.15 (s, 2H), 6.90 (s, 2H), 6.75 (d, *J* = 3.6 Hz, 1H), 6.57 (d, *J* = 3.6 Hz, 1H), 3.40 (s, 3H), 2.21 (s, 6H); ¹³C NMR (75 MHz, Acetone-*d*₆) δ 159.14 , 156.83 , 154.87 , 152.10 , 147.11 , 146.81 , 131.14 , 126.40 , 125.40 , 125.24 , 122.17 , 122.09, 121.89 , 120.11 , 105.12 , 38.51 , 16.47 ; HRMS (ESI): calculated 417.111, found 417.107 (M+H)⁺.

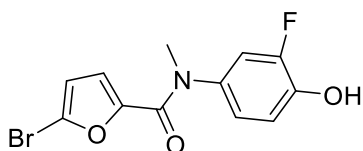
5-bromo-N-(3-fluoro-4-methoxyphenyl)furan-2-carboxamide (MSR208-10a)



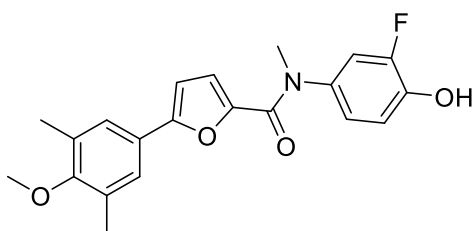
The title compound was prepared according to method B by the reaction of 3-fluoro-4-methoxyaniline (0.705 g, 5 mmol, 1 equiv) and 5-bromofuran-2-carbonyl chloride (1.05 g, 5 mmol, 1 equiv) in the presence of Et₃N (1.05 ml, 0.76 g, 7.5 mmol, 1.5 equiv) in CH₂Cl₂ (25 ml). The product was purified by flash column chromatography (Petroleum ether/Ethyl acetate, 0 - 30 % EtOAc in 30 min), to give 1150 mg (3.66 mmol/ 74% yield) of the analytically pure compound (purity: 97%). C₁₂H₉BrFNO₃; MW 314.11; ¹H NMR (300 MHz, DMSO-*d*₆) δ 10.24 (s, 1H), 7.67 (dd, *J* = 12.5, 2.5 Hz, 1H), 7.46 (ddd, *J* = 9.0, 2.6, 1.5 Hz, 1H), 7.34 (d, *J* = 3.6 Hz, 1H), 7.16 (t, *J* = 9.4 Hz, 1H), 6.84 (d, *J* = 3.6 Hz, 1H), 3.82 (s, 3H); MS (ESI): 314.07, 316.06 (M+H)⁺.

5-bromo-N-(3-fluoro-4-methoxyphenyl)-N-methylfuran-2-carboxamide (10b)

The title compound was prepared by reaction of **10a** (630 mg, 2.0 mmol, 1 equiv), sodium hydride 60 % suspension in mineral oil (167 mg, 4.0 mmol, 2 equiv) and iodomethane (0.25 mL, 4.0 mmol, 2 equiv) in DMF (10 ml) according to method C. The resulting precipitate was purified by flash column chromatography (Petroleum ether/Ethyl acetate, 0 - 40 % EtOAc in 30 min), to give 550 mg (1.66 mmol/ 84% yield) of the analytically pure compound (purity: 99%). $C_{13}H_{11}BrFNO_3$; MW 328.14; 1H NMR (300 MHz, DMSO- d_6) δ 7.36 (dd, J = 12.2, 2.5 Hz, 1H), 7.20 (t, J = 9.0 Hz, 1H), 7.11 (ddd, J = 9.0, 2.5, 1.2 Hz, 1H), 6.54 (d, J = 3.6 Hz, 1H), 5.93 (d, J = 3.6 Hz, 1H), 3.86 (s, 3H), 3.26 (s, 3H); MS (ESI): 328.08, 330.09 (M+H) $^+$.

5-bromo-N-(3-fluoro-4-hydroxyphenyl)-N-methylfuran-2-carboxamide (10c)

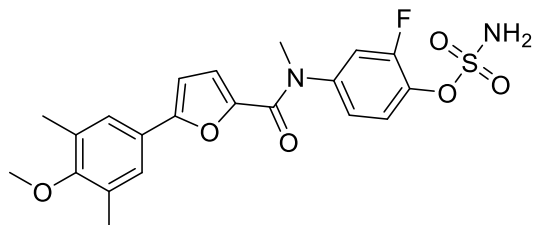
The title compound was prepared by reaction of **10b** (550 mg, 1.7 mmol, 1 equiv) and boron trifluoride dimethyl sulfide (3.5 ml, 35 mmol, 20 equiv) in CH_2Cl_2 (30 ml) according to method D. The resulting product was purified by flash column chromatography (CH_2Cl_2 /Methanol, 0 - 10 % methanol in 30 min), to give 460 mg (1.46 mmol/ 86% yield) of the analytically pure compound (purity: 98%). $C_{12}H_9BrFNO_3$; MW 314.11; 1H NMR (300 MHz, DMSO- d_6) δ 10.18 (s, 1H), 7.39 – 7.12 (m, 1H), 7.12 – 6.82 (m, 2H), 6.53 (d, J = 3.6 Hz, 1H), 5.85 (d, J = 3.5 Hz, 1H), 3.24 (s, 3H); MS (ESI): 314.08, 316.07 (M+H) $^+$.

N-(3-fluoro-4-hydroxyphenyl)-5-(4-methoxy-3,5-dimethylphenyl)-N-methylfuran-2-carboxamide (10d)

The title compound was prepared by reaction of **10c** (460 mg, 1.5 mmol, 1 equiv), (4-methoxy-3,5-dimethylphenyl)boronic acid (300 mg, 1.8 mmol, 1.2 equiv), cesium carbonate (1950 mg, 6.0 mmol, 4 equiv) and tetrakis(triphenylphosphine)palladium (85 mg, 0.075 mmol, 0.05 equiv) in oxygen-free DME/water (1:1) (30 mL) according to method E. The resulting product was purified by flash column chromatography (CH_2Cl_2 /Methanol, 0 - 5 % methanol in 30 min), to give 270 mg (0.73 mmol/ 48% yield) of the analytically pure compound (purity: 99%). $C_{21}H_{20}FNO_4$; MW 369.39; 1H NMR (300 MHz, DMSO- d_6) δ 10.13 (s, 1H), 7.35 – 7.23 (m, 1H), 7.01 (d, J = 8.5 Hz, 1H), 6.97 (s, 2H), 6.94 (d, J = 8.6 Hz, 1H),

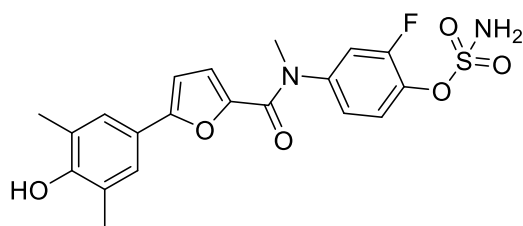
6.79 (d, $J = 3.6$ Hz, 1H), 6.73 (d, $J = 3.6$ Hz, 1H), 3.64 (s, 3H), 3.27 (s, 3H), 2.20 (s, 6H); MS (ESI): 370.21 (M+H)⁺.

2-fluoro-4-(5-(4-methoxy-3,5-dimethylphenyl)-N-methylfuran-2-carboxamido)phenyl sulfamate (10e)



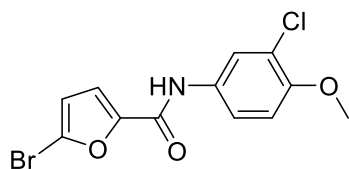
The title compound was prepared by reaction of **10d** (270 mg, 0.70 mmol, 1 equiv) and sulfamoyl chloride (700 mg, 7 mmol, 10 equiv) in water-free DMA (10 mL) according to method E. The resulting precipitate was purified by flash column chromatography (CH₂Cl₂/Methanol, 0 - 5 % methanol in 30 min), to give 183 mg (0.41 mmol/ 58% yield) of the analytically pure compound (purity: 99%). C₂₁H₂₁FN₂O₆S; MW 448.46; ¹H NMR (300 MHz, DMSO-*d*₆) δ 8.32 (s, 2H), 7.63 (dd, $J = 11.2, 2.5$ Hz, 1H), 7.50 (t, $J = 8.7$ Hz, 1H), 7.26 (ddd, $J = 8.7, 2.5, 1.3$ Hz, 1H), 6.95 (s, 2H), 6.86 (d, $J = 3.6$ Hz, 1H), 6.83 (d, $J = 3.6$ Hz, 1H), 3.64 (s, 3H), 3.35 (s, 3H), 2.20 (s, 6H); MS (ESI): 449.18 (M+H)⁺.

2-fluoro-4-(5-(4-hydroxy-3,5-dimethylphenyl)-N-methylfuran-2-carboxamido)phenyl sulfamate (10)



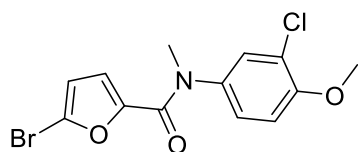
The title compound was prepared by reaction of **SN04** (175 mg, 0.40 mmol, 1 equiv) and boron trifluoride dimethyl sulfide (0.80 ml, 8 mmol, 20 equiv) in CH₂Cl₂ (20 ml) according to method D. The resulting product was purified by flash column chromatography (CH₂Cl₂/Methanol, 0 - 5 % methanol in 30 min), to give 73 mg (0.17 mmol/ 42% yield) of the analytically pure compound (purity: 98%). C₂₀H₁₉FN₂O₆S; MW 434.43; mp 186-188 °C; ¹H NMR (300 MHz, DMSO-*d*₆) δ 8.60 (s, 1H), 8.22 (s, 2H), 7.61 (dd, $J = 11.2, 2.5$ Hz, 1H), 7.49 (t, $J = 8.7$ Hz, 1H), 7.33 – 7.15 (m, 1H), 6.85 (s, 2H), 6.83 (d, $J = 3.7$ Hz, 1H), 6.69 (d, $J = 3.6$ Hz, 1H), 3.34 (s, 3H), 2.14 (s, 6H); ¹³C NMR (126 MHz, Acetone-*d*₆) δ 158.02 (d, $J = 271.7$ Hz), 156.66, 154.82 (d, $J = 37.6$ Hz), 146.75, 145.26 (d, $J = 8.5$ Hz), 137.69 (d, $J = 12.1$ Hz), 125.95, 125.38, 125.27 (d, $J = 9.5$ Hz), 124.67 (d, $J = 3.5$ Hz), 122.17, 120.24, 117.22, 117.06, 105.21, 38.49, 16.54; HRMS (ESI): calculated 435.102, found 435.098 (M+H)⁺.

5-bromo-N-(3-chloro-4-methoxyphenyl)furan-2-carboxamide (11a)



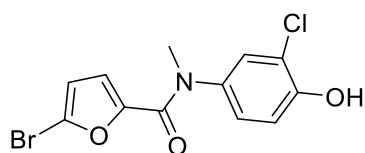
The title compound was prepared according to method B by the reaction of 3-chloro-4-methoxyaniline (0.790 g, 5 mmol, 1 equiv) and 5-bromofuran-2-carbonyl chloride (1.05 g, 5 mmol, 1 equiv) in the presence of Et₃N (1.05 ml, 0.76 g, 7.5 mmol, 1.5 equiv) in CH₂Cl₂ (25 ml). The product was purified by flash column chromatography (Petroleum ether/Ethyl acetate, 0 - 30 % EtOAc in 30 min), to give 1400 mg (4.25 mmol/ 85% yield) of the analytically pure compound (purity: 97%). C₁₂H₉BrClNO₃; MW 330.56; ¹H NMR (300 MHz, DMSO-*d*₆) δ 10.22 (s, 1H), 7.86 (d, *J* = 2.6 Hz, 1H), 7.63 (dd, *J* = 9.0, 2.6 Hz, 1H), 7.33 (d, *J* = 3.6 Hz, 1H), 7.14 (d, *J* = 9.0 Hz, 1H), 6.83 (d, *J* = 3.6 Hz, 1H), 3.84 (s, 3H); MS (ESI): 330.05, 332.05 (M+H)⁺.

5-bromo-N-(3-chloro-4-methoxyphenyl)-N-methylfuran-2-carboxamide (11b)



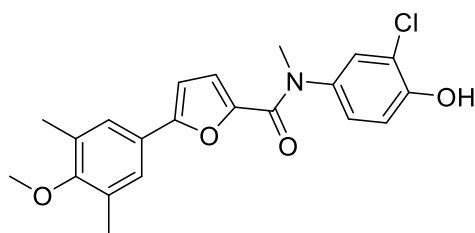
The title compound was prepared by reaction of **11a** (940 mg, 2.9 mmol, 1 equiv), sodium hydride 60 % suspension in mineral oil (240 mg, 5.8 mmol, 2 equiv) and iodomethane (0.35 mL, 5.8 mmol, 2 equiv) in DMF (10 ml) according to method C. The resulting precipitate was purified by flash column chromatography (Petroleum ether/Ethyl acetate, 0 - 40 % EtOAc in 30 min), to give 780 mg (2.26 mmol/ 79% yield) of the analytically pure compound (purity: 97%). C₁₃H₁₁BrClNO₃; MW 344.58; ¹H NMR (300 MHz, DMSO-*d*₆) δ 7.53 (d, *J* = 2.5 Hz, 1H), 7.28 (dd, *J* = 8.7, 2.5 Hz, 1H), 7.18 (d, *J* = 8.8 Hz, 1H), 6.54 (d, *J* = 3.6 Hz, 1H), 5.92 (d, *J* = 3.5 Hz, 1H), 3.88 (s, 3H), 3.26 (s, 3H); MS (ESI): 344.06, 346.07 (M+H)⁺.

5-bromo-N-(3-chloro-4-hydroxyphenyl)-N-methylfuran-2-carboxamide (11c)



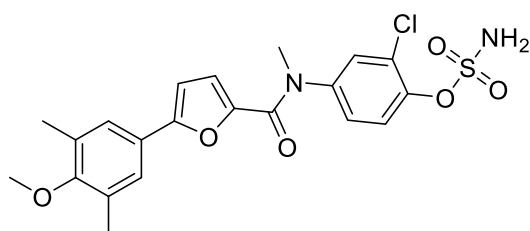
The title compound was prepared by reaction of **11b** (780 mg, 2.3 mmol, 1 equiv) and boron trifluoride dimethyl sulfide (4.5 ml, 46 mmol, 20 equiv) in CH₂Cl₂ (30 ml) according to method D. The resulting product was purified by flash column chromatography (CH₂Cl₂/Methanol, 0 - 10 % methanol in 30 min), to give 614 mg (1.86 mmol/ 81% yield) of the analytically pure compound (purity: 99%). C₁₂H₉BrClNO₃; MW 330.56; ¹H NMR (300 MHz, DMSO-*d*₆) δ 10.48 (s, 1H), 7.41 (d, *J* = 2.5 Hz, 1H), 7.10 (dd, *J* = 8.6, 2.5 Hz, 1H), 6.98 (d, *J* = 8.6 Hz, 1H), 6.54 (d, *J* = 3.6 Hz, 1H), 5.85 (d, *J* = 3.5 Hz, 1H), 3.23 (s, 3H); MS (ESI): 330.05, 332.05 (M+H)⁺.

N-(3-chloro-4-hydroxyphenyl)-5-(4-methoxy-3,5-dimethylphenyl)-N-methylfuran-2-carboxamide (11d)



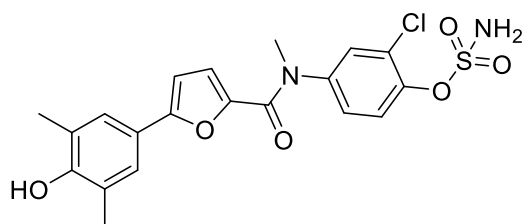
The title compound was prepared by reaction of **11c** (500 mg, 1.5 mmol, 1 equiv), (4-methoxy-3,5-dimethylphenyl)boronic acid (300 mg, 1.8 mmol, 1.2 equiv), cesium carbonate (1950 mg, 6.0 mmol, 4 equiv) and tetrakis(triphenylphosphine)palladium (85 mg, 0.075 mmol, 0.05 equiv) in oxygen-free DME/water (1:1) (30 mL) according to method E. The resulting product was purified by flash column chromatography (CH₂Cl₂/Methanol, 0 - 5 % methanol in 30 min), to give 500 mg (1.29 mmol/ 86% yield) of the analytically pure compound (purity: 99%). C₂₁H₂₀ClNO₄; MW 385.84; ; ¹H NMR (300 MHz, DMSO-*d*₆) δ 10.46 (s, 1H), 7.47 (d, *J* = 2.5 Hz, 1H), 7.08 (dd, *J* = 8.6, 2.5 Hz, 1H), 6.99 (d, *J* = 8.6 Hz, 1H), 6.94 (s, 2H), 6.80 (d, *J* = 3.6 Hz, 1H), 6.78 (d, *J* = 3.6 Hz, 1H), 3.63 (s, 3H), 3.27 (s, 3H), 2.20 (s, 6H); MS (ESI): 386.12 (M+H)⁺.

2-chloro-4-(5-(4-methoxy-3,5-dimethylphenyl)-N-methylfuran-2-carboxamido)phenyl sulfamate (11e)



The title compound was prepared by reaction of **11d** (500 mg, 1.29 mmol, 1 equiv) and sulfamoyl chloride (1300 mg, 13 mmol, 10 equiv) in water-free DMA (10 mL) according to method E. The resulting precipitate was purified by flash column chromatography (CH₂Cl₂/Methanol, 0 - 5 % methanol in 30 min), to give 482 mg (1.04 mmol/ 80% yield) of the analytically pure compound (purity: 99%). C₂₁H₂₁ClN₂O₆S; MW 464.91; ¹H NMR (300 MHz, DMSO-*d*₆) δ 8.35 (s, 2H), 7.79 (d, *J* = 2.5 Hz, 1H), 7.54 (d, *J* = 8.7 Hz, 1H), 7.39 (dd, *J* = 8.7, 2.6 Hz, 1H), 6.92 (s, 2H), 6.90 (d, *J* = 3.6 Hz, 1H), 6.84 (d, *J* = 3.6 Hz, 1H), 3.64 (s, 3H), 3.34 (s, 3H), 2.20 (s, 6H); MS (ESI): 465.18 (M+H)⁺.

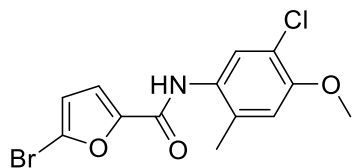
2-chloro-4-(5-(4-hydroxy-3,5-dimethylphenyl)-N-methylfuran-2-carboxamido)phenyl sulfamate (11)



The title compound was prepared by reaction of **SN07** (235 mg, 0.50 mmol, 1 equiv) and boron trifluoride dimethyl sulfide (1.00 ml, 10 mmol, 20 equiv) in CH₂Cl₂ (20 ml) according to method D. The resulting product was purified by flash column chromatography

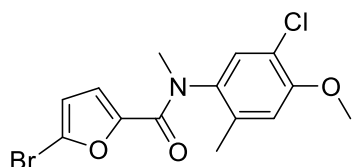
(CH₂Cl₂/Methanol, 0 - 5 % methanol in 30 min), to give 95 mg (0.21 mmol/ 42% yield) of the analytically pure compound (purity: 98%). C₂₀H₁₉ClN₂O₆S; MW 450.89; mp 174-176 °C; ¹H NMR (500 MHz, Acetone-*d*₆) δ 11.62 (s, 1H), 7.67 (d, *J* = 2.6 Hz, 1H), 7.63 (d, *J* = 8.6 Hz, 1H), 7.48 (s, 2H), 7.37 (dd, *J* = 8.7, 2.6 Hz, 1H), 6.91 (s, 2H), 6.85 (d, *J* = 3.7 Hz, 1H), 6.62 (d, *J* = 3.5 Hz, 1H), 3.41 (s, 3H), 2.22 (s, 6H); ¹³C NMR (126 MHz, Acetone-*d*₆) δ 159.11 , 157.07 , 154.98 , 146.73 , 146.45 , 144.84 , 130.29 , 128.36 , 128.03 , 125.39 , 125.32 , 125.17, 122.14 , 120.47 , 105.27 , 38.59 , 16.57; HRMS (ESI): calculated 451.072, found 451.068 (M+H)⁺.

5-bromo-N-(5-chloro-4-methoxy-2-methylphenyl)furan-2-carboxamide (12a)



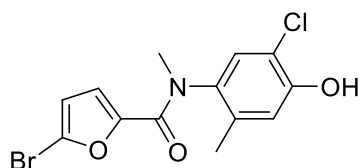
The title compound was prepared according to method B by the reaction of 5-chloro-4-methoxy-2-methylaniline (0.855 g, 5 mmol, 1 equiv) and 5-bromofuran-2-carbonyl chloride (1.05 g, 5 mmol, 1 equiv) in the presence of Et₃N (1.05 ml, 0.76 g, 7.5 mmol, 1.5 equiv) in CH₂Cl₂ (25 ml). The product was purified by flash column chromatography (Petroleum ether/Ethyl acetate, 0 - 30 % EtOAc in 30 min), to give 1200 mg (3.48 mmol/ 70% yield) of the analytically pure compound (purity: 97%). C₁₃H₁₁BrClNO₃; MW 344.59; ¹H NMR (500 MHz, DMSO-*d*₆) δ 9.84 (s, 1H), 7.32 (s, 1H), 7.30 (d, *J* = 3.6 Hz, 1H), 7.07 (s, 1H), 6.83 (d, *J* = 3.5 Hz, 1H), 3.85 (s, 3H), 2.19 (s, 3H); MS (ESI): 344.06, 346.07 (M+H)⁺.

5-bromo-N-(5-chloro-4-methoxy-2-methylphenyl)-N-methylfuran-2-carboxamide (12b)



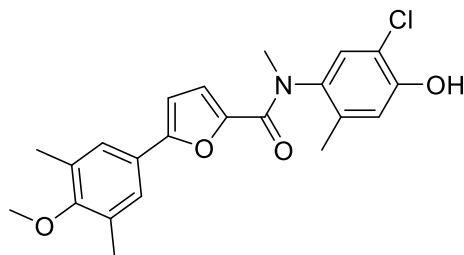
The title compound was prepared by reaction of **12a** (1200 mg, 3.5 mmol, 1 equiv), sodium hydride 60 % suspension in mineral oil (360 mg, 7.0 mmol, 2 equiv) and iodomethane (0.45 mL, 7.0 mmol, 2 equiv) in DMF (10 ml) according to method C. The resulting precipitate was purified by flash column chromatography (Petroleum ether/Ethyl acetate, 0 - 40 % EtOAc in 30 min), to give 920 mg (2.56 mmol/ 73% yield) of the analytically pure compound (purity: 96%). C₁₄H₁₃BrClNO₃; MW 358.61; ¹H NMR (500 MHz, DMSO-*d*₆) δ 7.46 (s, 1H), 7.16 (s, 1H), 6.52 (d, *J* = 3.7 Hz, 1H), 5.64 (d, *J* = 3.7 Hz, 1H), 3.88 (s, 3H), 3.18 (s, 3H), 2.10 (s, 3H); MS (ESI): 358.08, 360.08 (M+H)⁺.

5-bromo-N-(5-chloro-4-hydroxy-2-methylphenyl)-N-methylfuran-2-carboxamide (12c)



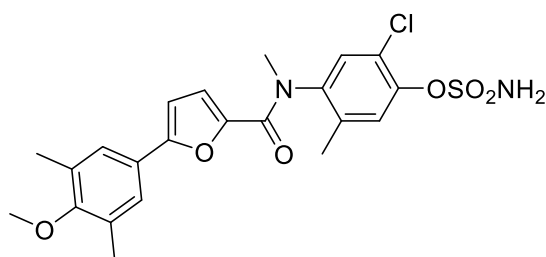
The title compound was prepared by reaction of **12b** (920 mg, 2.6 mmol, 1 equiv) and boron trifluoride dimethyl sulfide (5.5 ml, 50 mmol, 20 equiv) in CH_2Cl_2 (30 ml) according to method D. The resulting product was purified by flash column chromatography (CH_2Cl_2 /Methanol, 0 - 10 % methanol in 30 min), to give 800 mg (2.32 mmol/ 89% yield) of the analytically pure compound (purity: 99%). $\text{C}_{13}\text{H}_{11}\text{BrClINO}_3$; MW 344.58; ^1H NMR (500 MHz, $\text{DMSO}-d_6$) δ 10.47 (s, 1H), 7.34 (s, 1H), 6.90 (s, 1H), 6.52 (d, $J = 3.6$ Hz, 1H), 5.60 (d, $J = 3.6$ Hz, 1H), 3.16 (s, 3H), 2.00 (s, 3H); MS (ESI): 344.04, 346.04 ($\text{M}+\text{H}$) $^+$.

N-(5-chloro-4-hydroxy-2-methylphenyl)-5-(4-methoxy-3,5-dimethylphenyl)-N-methylfuran-2-carboxamide (MSR242-12d)

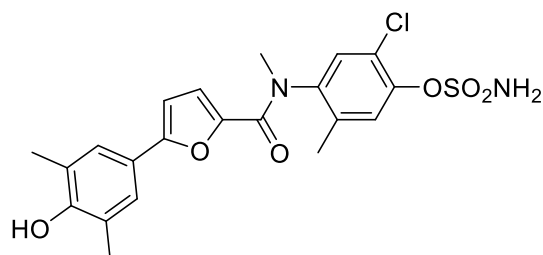


The title compound was prepared by reaction of **12c** (340 mg, 1.0 mmol, 1 equiv), (4-methoxy-3,5-dimethylphenyl)boronic acid (220 mg, 1.2 mmol, 1.2 equiv), cesium carbonate (1300 mg, 4.0 mmol, 4 equiv) and tetrakis(triphenylphosphine)palladium (55 mg, 0.05 mmol, 0.05 equiv) in oxygen-free DME/water (1:1) (30 mL) according to method E. The resulting product was purified by flash column chromatography (CH_2Cl_2 /Methanol, 0 - 5 % methanol in 30 min), to give 300 mg (0.75 mmol/ 75% yield) of the analytically pure compound (purity: 99%). $\text{C}_{22}\text{H}_{22}\text{ClINO}_4$; MW 399.87; ^1H NMR (500 MHz, $\text{DMSO}-d_6$) δ 10.40 (s, 1H), 7.39 (s, 1H), 6.96 (s, 2H), 6.92 (s, 1H), 6.80 (d, $J = 3.6$ Hz, 1H), 6.72 (d, $J = 3.6$ Hz, 1H), 3.63 (s, 3H), 3.20 (s, 3H), 2.21 (s, 6H), 2.00 (s, 3H); MS (ESI): 400.14 ($\text{M}+\text{H}$) $^+$.

2-chloro-4-(5-(4-methoxy-3,5-dimethylphenyl)-N-methylfuran-2-carboxamido)-5-methylphenyl sulfamate (12e)

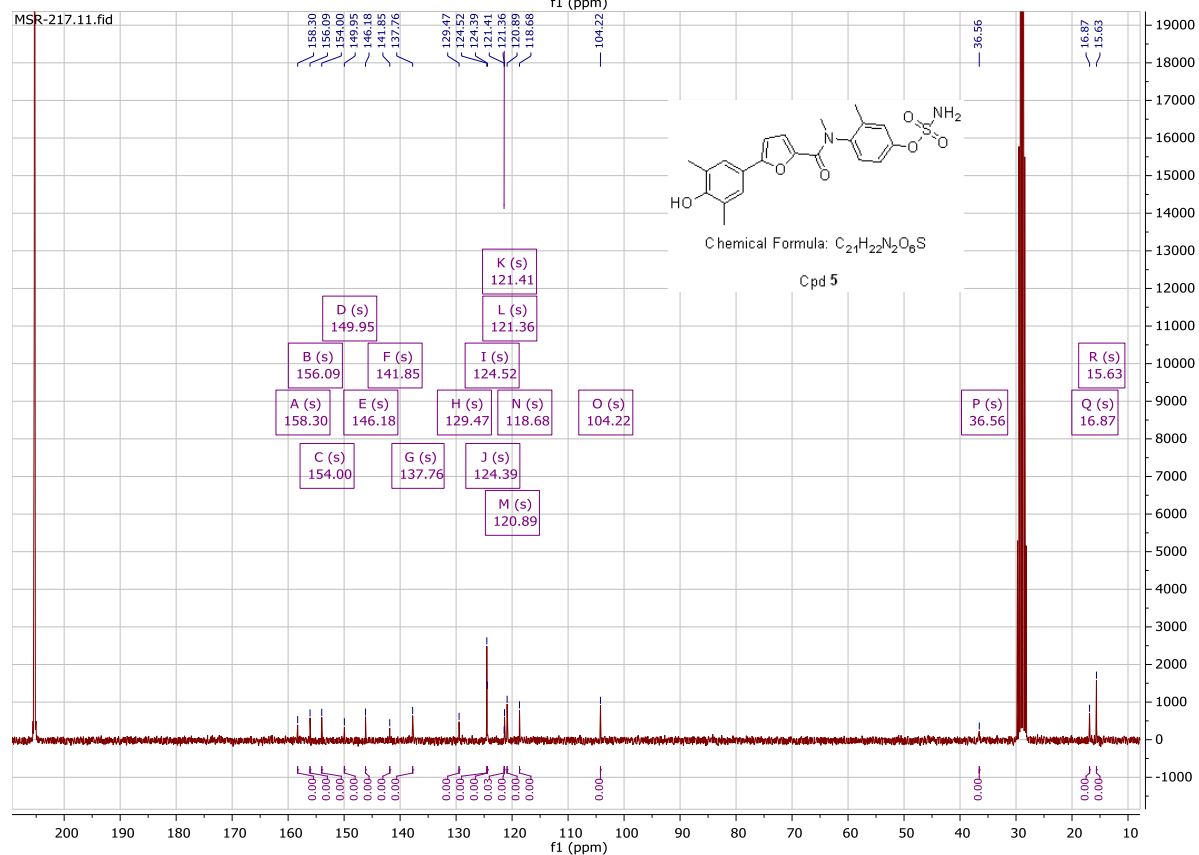
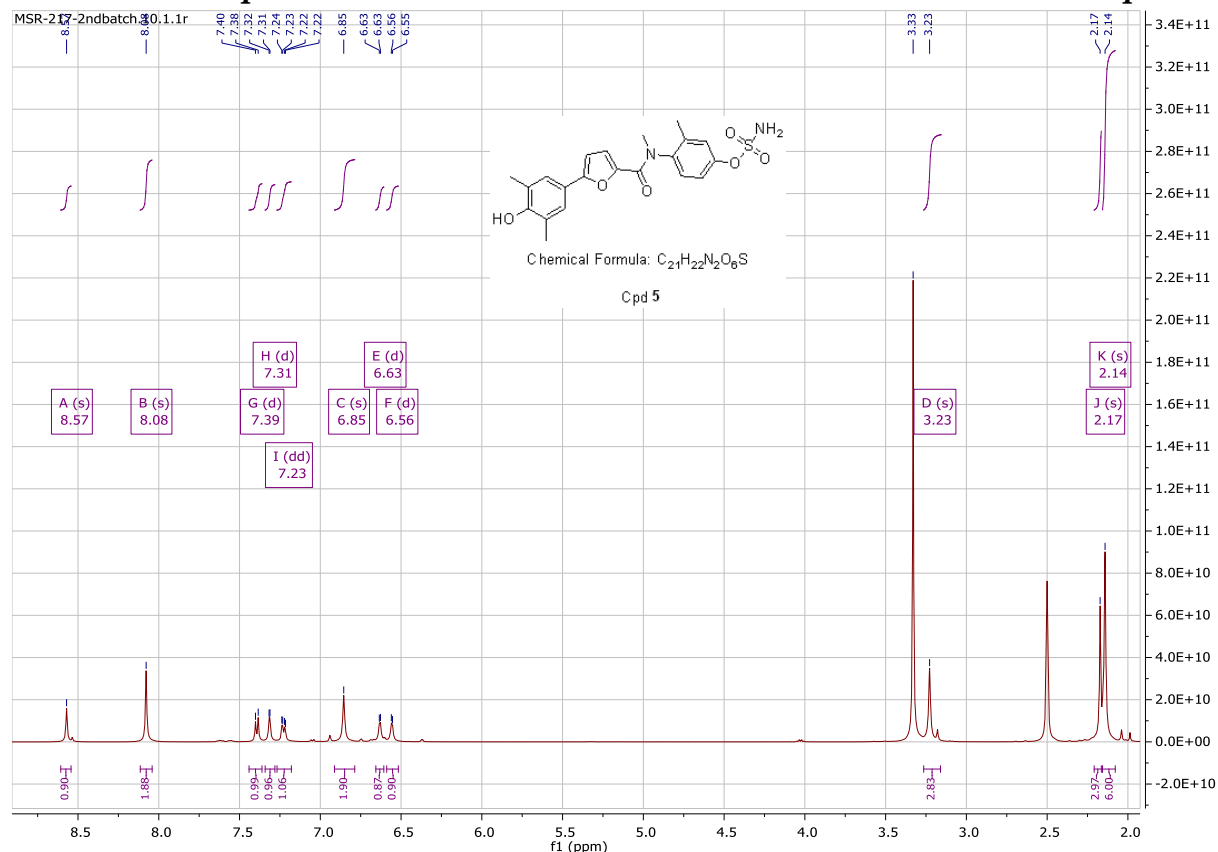


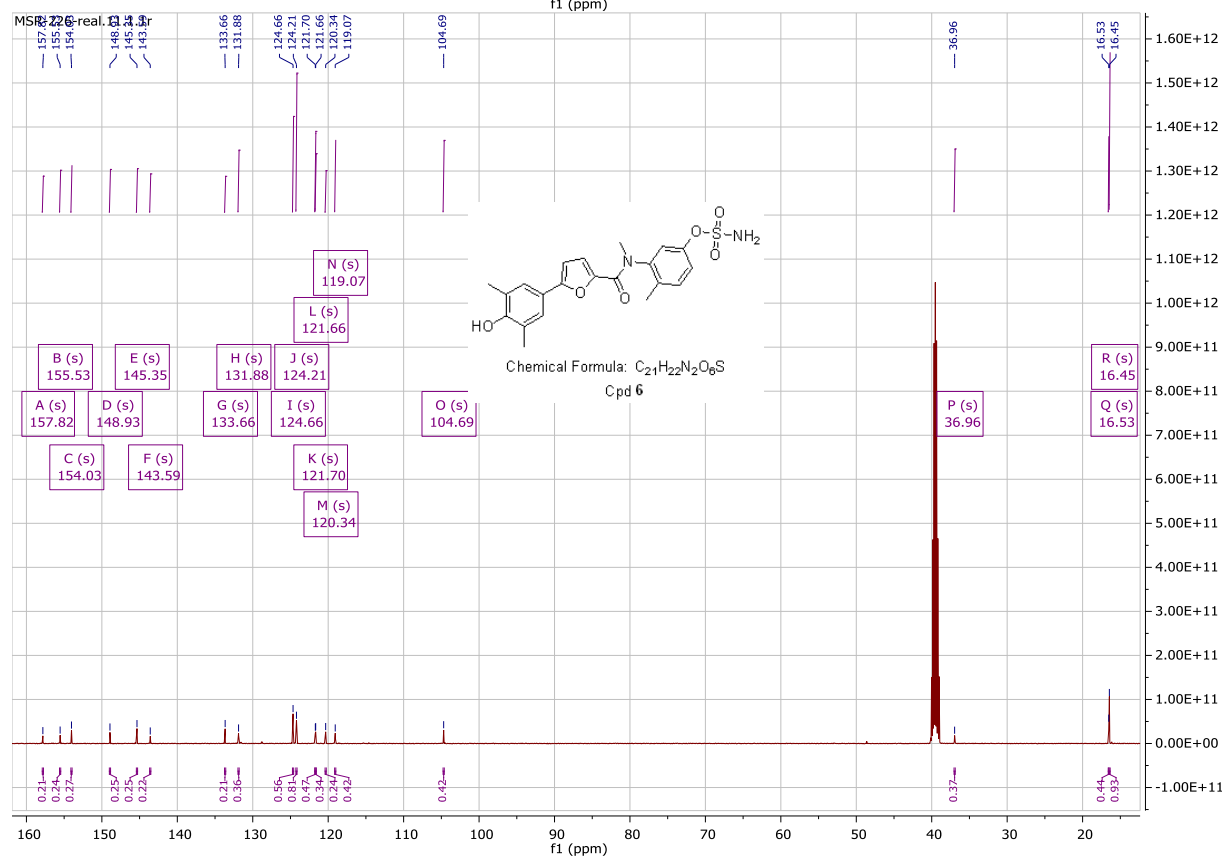
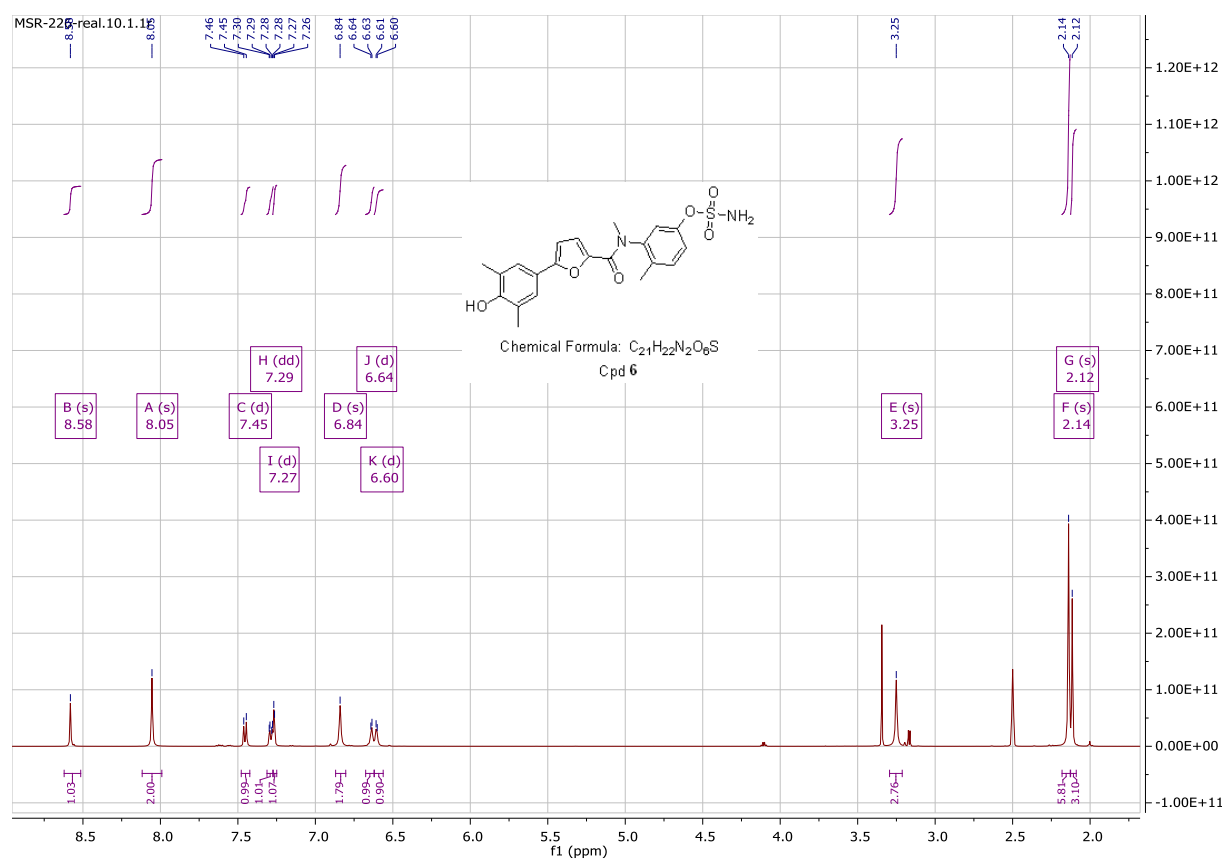
The title compound was prepared by reaction of **12d** (300 mg, 0.75 mmol, 1 equiv) and sulfamoyl chloride (750 mg, 7.5 mmol, 10 equiv) in water-free DMA (10 mL) according to method E. The resulting precipitate was purified by flash column chromatography (CH_2Cl_2 /Methanol, 0 - 5 % methanol in 30 min), to give 210 mg (0.43 mmol/ 59% yield) of the analytically pure compound (purity: 98%). $\text{C}_{22}\text{H}_{23}\text{ClN}_2\text{O}_6\text{S}$; MW 478.94; ^1H NMR (500 MHz, $\text{DMSO}-d_6$) δ 8.35 (s, 2H), 7.75 (s, 1H), 7.52 (s, 1H), 6.91 (s, 2H), 6.83 (d, $J = 3.5$ Hz, 1H), 6.81 (d, $J = 3.8$ Hz, 1H), 3.64 (s, 3H), 3.24 (s, 3H), 2.20 (s, 6H), 2.12 (s, 3H); MS (ESI): 479.20 ($\text{M}+\text{H}$) $^+$.

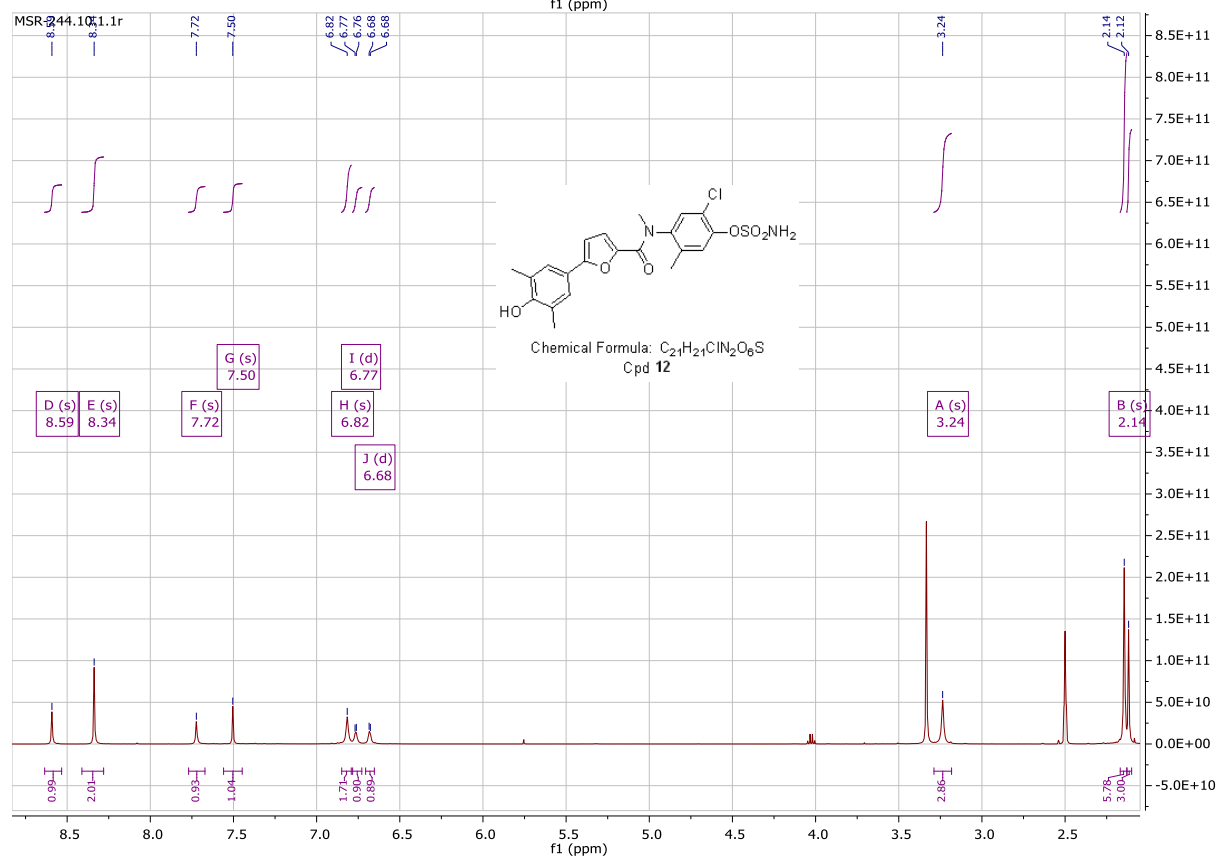
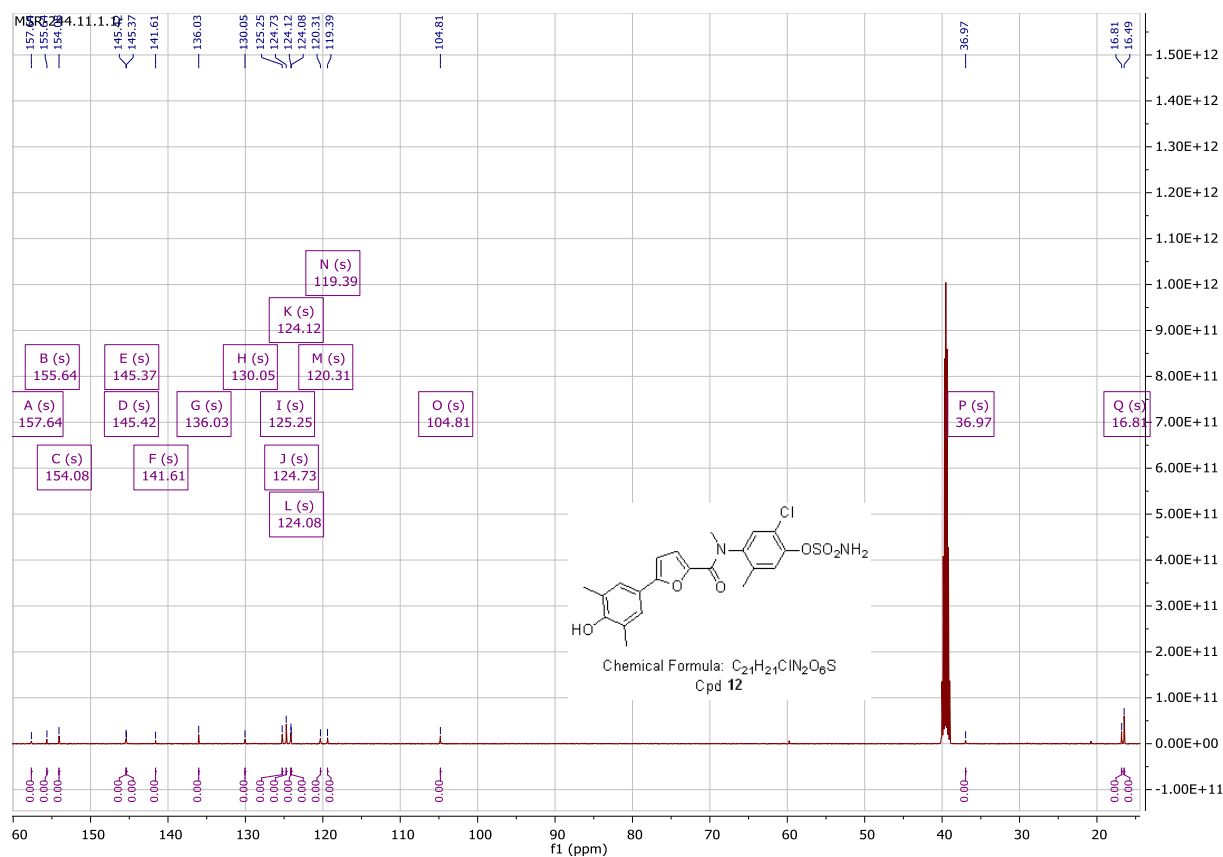
2-chloro-4-(5-(4-hydroxy-3,5-dimethylphenyl)-N-methylfuran-2-carboxamido)-5-methylphenyl sulfamate (12)

The title compound was prepared by reaction of **12e** (200 mg, 0.42 mmol, 1 equiv) and boron trifluoride dimethyl sulfide (0.90 ml, 8.5 mmol, 20 equiv) in CH₂Cl₂ (20 ml) according to method D. The resulting product was purified by flash column chromatography (CH₂Cl₂/Methanol, 0 - 5 % methanol in 30 min), to give 98 mg (0.21 mmol/ 50% yield) of the analytically pure compound (purity: 98%). C₂₁H₂₁ClN₂O₆S; MW 464.91; mp 202-204 °C; ¹H NMR (500 MHz, DMSO-*d*₆) δ 8.59 (s, 1H), 8.34 (s, 2H), 7.72 (s, 1H), 7.50 (s, 1H), 6.82 (s, 2H), 6.77 (d, *J* = 3.9 Hz, 1H), 6.68 (d, *J* = 3.7 Hz, 1H), 3.24 (s, 3H), 2.14 (s, 6H), 2.12 (s, 3H); ¹³C NMR (126 MHz, DMSO) δ 157.64, 155.64, 154.08, 145.42, 145.37, 141.61, 136.03, 130.05, 125.25, 124.73, 124.12, 124.08, 120.31, 119.39, 104.81, 36.97, 16.81, 16.49; HRMS (ESI): calculated 465.088, found 465.084 (M+H)⁺.

5.2.1.4 Representative ^1H NMR and ^{13}C NMR spectra





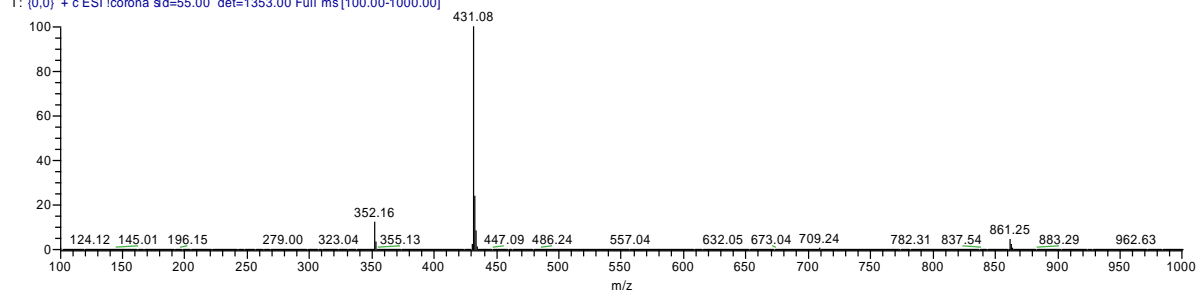


5.2.1.5 Representative MS spectra

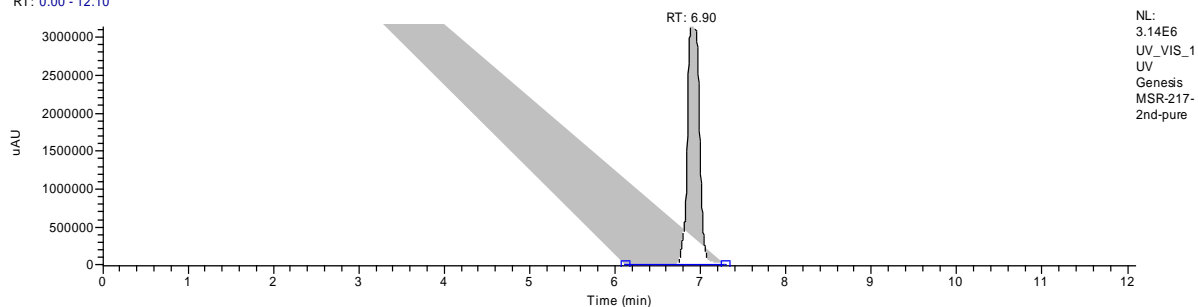
Compound 5:

MSR-217-2nd-pure #345 RT: 7.32 AV: 1 NL: 2.38E7

T: (0,0) + c ESI Icorona sid=55.00 det=1353.00 Full ms [100.00-1000.00]



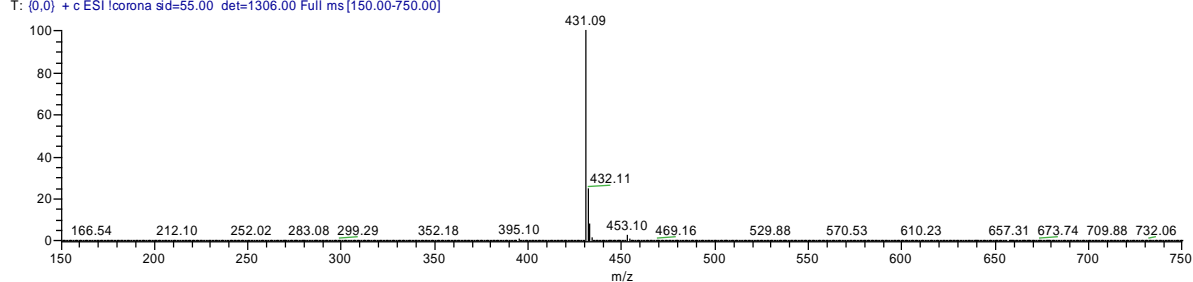
RT: 0.00 - 12.10



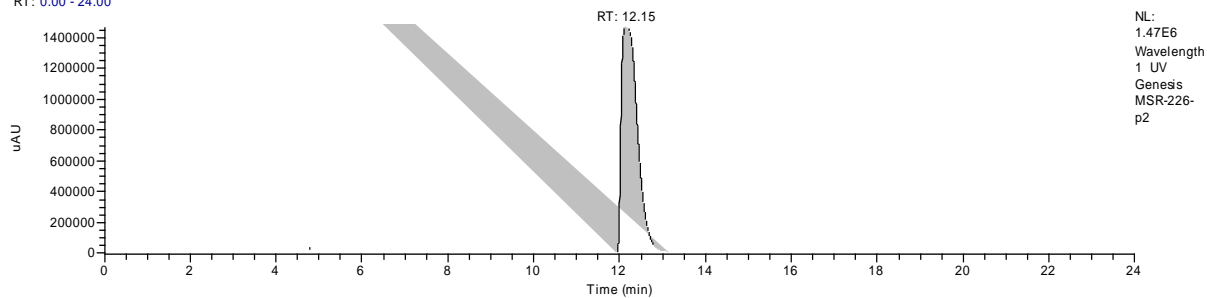
Compound 6:

MSR-226-p2 #582 RT: 12.39 AV: 1 NL: 5.84E6

T: (0,0) + c ESI Icorona sid=55.00 det=1306.00 Full ms [150.00-750.00]

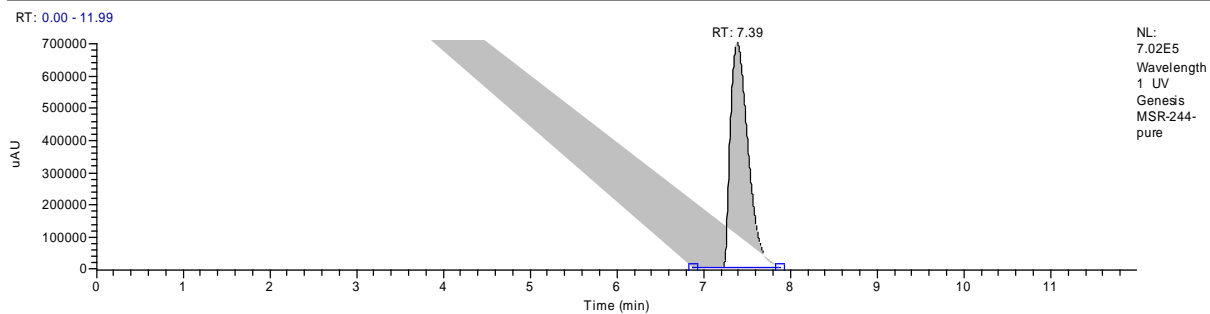
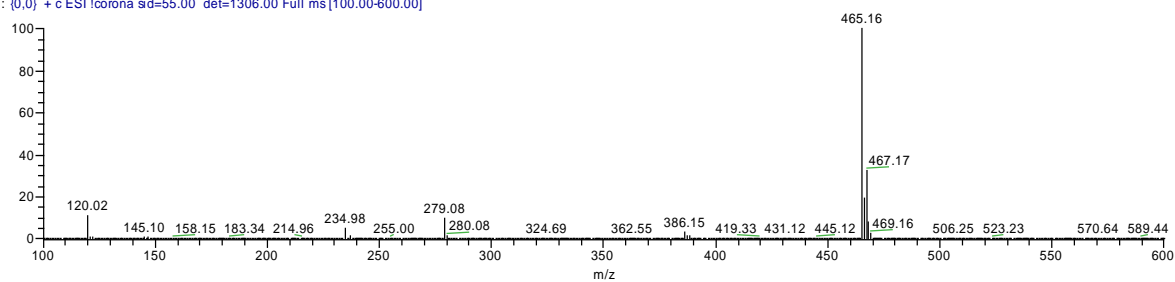


RT: 0.00 - 24.00



Compound 12:

MSR-244-pure #464 RT: 7.56 AV: 1 NL: 2.41E6
T: (0,0) + c ESI Iconora sid=55.00 det=1306.00 Full ms[100.00-600.00]



5.2.II Biological methods

5.2.II.1 Chemicals

E1-S, E1, E2 and MTT were obtained from Sigma. Radioactively labeled [6,7-³H(N)]-E1-S (40-60 Ci/mmol), [2,4,6,7-³H]-E1 (50-100 Ci/mmol) and [2,4,6,7-³H]-E2 (>110 Ci/mmol) were obtained from Perkin Elmer, Boston. Quickszint Flow 302 scintillator fluid was bought from Zinsser Analytic, Frankfurt. Charcoal-stripped FCS was received from Biowest. Other chemicals were purchased from Sigma, Merck or Gibco.

5.2.II.2 *h17β-HSD1 and h17β-HSD2 cell free inhibition assays*

The human enzymes were partially purified from human placental tissue according to previously described procedures.¹ Fresh human placenta was homogenized and by fractional centrifugation the cytosolic and microsomal fractions were separated. In case of the *h17β-HSD1* assay the cytosolic fraction was incubated with NADH (500 μM), while in the case of the *h17β-HSD2* assay the microsomal fraction was incubated with NAD⁺ (1500 μM) at 37 °C in a phosphate buffer (50 mM) with 20% of glycerol and EDTA (1 mM) in the presence of potential inhibitors which were prepared in DMSO (final DMSO concentration in the assay was 1%). The enzymatic reaction was started by the addition of a mixture of unlabeled and radiolabeled substrate (final concentration: 500 nM), [³H]-E1 in the case of *h17β-HSD1* assay for 10 min or with [³H]-E2 in the case of *h17β-HSD2* assay for 20 min.¹ HgCl₂ (10mM) was used to stop the enzymatic reactions and the steroids were extracted with diethylether. After evaporation, they were dissolved in acetonitrile/water (45:55). E1 and E2 were separated on a C18 reverse phase chromatography column (Nucleodur C₁₈ Isis, Macherey-Nagel) connected to an Agilent 1200 Series (Agilent Technologies) HPLC-system using acetonitrile/water (45:55) as mobile phase. A radioflow detector (Ramona, raytest) was coupled to the HPLC-system for the detection and quantification of the steroids. After the analysis of the resulting chromatograms, the conversion rates were calculated according to the following equation:

$$\%conversion = \left[\frac{\%product}{\%product + \% Substrate} \right] * 100$$

Each value was calculated from at least two independent experiments.

Then the percentage inhibition corresponding to each inhibitor concentration was calculated according to the following equation:

$$\%inhibition = \left[1 - \left(\frac{\%conversion\ of\ the\ inhibitor}{\%conversion\ of\ the\ control\ (DMSO)} \right) \right] * 100$$

At least three different concentrations of each inhibitor leading to inhibitions ranging from 30% to 80% were chosen to deduce the IC₅₀ of each inhibitor. The IC₅₀ of each inhibitor was calculated from at least two independent experiments.

5.2.II.3 *Cell culture*

T47D human mammary cancer cell line was purchased from ECACC, Salisbury. The cells were routinely cultivated in DMEM (Sigma) supplemented with 10% FCS (Sigma) and 100 IU/ml penicillin-streptomycin, and incubated at 37 °C under humidified atmosphere of 5% CO₂. The medium was changed every 2-3 days, and the cells were passed every 9-10 days.

5.2.II.4 *hSTS and h17β-HSD1 cellular inhibition assays*

The T47D cells were seeded into a 24-well flat-bottom plate at 5 * 10⁵ cells/well in DMEM supplemented with 10% FCS and 100 IU/ml penicillin-streptomycin according to previously described procedures.^{2,3} After incubation for 24 h of adaptation at 37 °C, the medium was exchanged by a fresh FCS-free DMEM and the test compound dissolved in DMSO was added (final concentration of DMSO was adjusted to 1% in all samples). After 1 h the incubation period was started by the addition of a mixture of unlabeled and radioactive substrate [³H]-E1-S (5 nM) for 24 h or [³H]-E1 (50 nM) for 40 min at 37 °C in case of *hSTS* or *h17β-HSD1* cellular inhibition assays, respectively. The reaction was stopped by the removal of the supernatant. The supernatant was injected directly (without any further workup) into the same radio-HPLC system mentioned above for *h17β-HSD1* and *h17β-HSD2* cell free inhibition assays and the IC₅₀s are calculated as described.

5.2.II.5 *Nature of inhibition of STS activity*

In order to investigate the mode of inhibition of STS activity, T47D cells were cultivated as mentioned above but with some changes described by Purohit et al., 1995.⁴ The cells were pre-incubated with the inhibitors for 2 h at 37 °C, then the medium was removed and the cells were washed 3-4 times with PBS (phosphate buffer saline). The remaining STS activity was assayed as described in the recent procedure by incubating the cells with using [³H]-E1-S for 24 h at 37 °C, then subsequent quantification of the steroids in the supernatant using HPLC coupled to radiodetector and the IC₅₀s are calculated as described.

5.2.II.6 *Metabolic stability in a cell-free assay*

For evaluation of phase I and II metabolic stability 1 μM compound was incubated with 1 mg/ml pooled mammalian (human or mouse) liver S9 fraction (BD Gentest, Heidelberg, Germany), 2 mM NADPH regenerating system, 1 mM UDPGA, 10mM MgCl_2 and 0.1 mM PAPS at 37°C for 0, 5, 15 and 60 minutes at a final volume of 100 μL of 100 mM Potassium hydrogen phosphate buffer pH=7.4. The incubation was stopped by precipitation of S9 enzymes with 2 volumes of cold acetonitrile containing internal standard, then centrifuged for 10 minutes at 4°C and 12500 rpm. For quantification, a calibration curve was developed for each compound assayed by LC-MS/MS (Accucore RP-MS, TSQ Quantum triple quadrupole mass spectrometer, ESI interface) using a serial dilution of 6 standards in the range 10-500 nM. Then, LC-MS/MS was used to analyze the remaining concentration of the test compound at the different time points. The half-life ($t_{1/2}$) was determined using the following equation:

$$t_{1/2} = \frac{\ln(2)}{-K}$$

Where K (decay rate) is the slope of the linear regression from log [test compound] versus time:

$$K = \frac{\ln(\text{Concentration})}{\text{Time}}$$

Then the intrinsic clearance (Cl_{int}) [$\mu\text{L}/\text{min}/\text{mg}$ protein] estimates of the compounds were determined using the following equation:

$$Cl_{int} = K * V * f_u$$

Where: $V = \frac{\text{incubation volume } [\mu\text{L}]}{\text{microsomal protein } [\text{mg}]} = 1000 [\mu\text{L} / \text{mg protein}]$

f_u = unbound fraction of the tested compounds (unknown)= 1

5.2.II.7 *In vivo pharmacokinetic study*

All animal procedures were approved by the local government animal care committee and performed in accordance with the Guide for the Care and Use of Laboratory Animals. The pharmacokinetic study was performed on C57B1/6 mice (body weight 20-25 g) in a group of 3 per compound. Compounds were administered subcutaneously and orally at a dose of 50 mg/kg body weight, and intravenously at a dose of 5 mg/kg body weight. For subcutaneous and oral administrations, the compounds were prepared as a suspension in 0.5% gelatine/5% mannitol (w/w) in water followed by 25 min in an ultrasonic bath 60-90 min before administration (8 μL suspension/gram body weight). For iv administration (4 μL solution/gram

body weight), the compound was dissolved in PEG400/ethanol/water (60/10/30). Before the drug application, the mice were anesthetized with 2% isoflurane. Blood samples of 50 μ l volume were collected from the tail vein into 0.2 mL PCR-tubes containing 10 μ l citrate buffer as an anticoagulant at 0.25, 0.5, 1, 2, 6, 7 and 24 h post-dosing. Plasma was harvested by centrifuging the blood for 5 min at 3000 rpm and 4°C. 10 μ l samples were stored frozen at -80°C until analysis. For bioanalysis, 5 μ l of plasma aliquot was added to 25 μ l of 500 nM diphenhydramine as internal standard in ACN and vortexed for 1 minute using mini-centrifuge. Samples and calibration standards (in mouse plasma) were centrifuged for 5 min at 14000 rpm and 4°C. The supernatant was then transferred into HPLC vial and quantified by LC-MS/MS (Accucore RP-MS, TSQ Quantum triple quadrupole mass spectrometer, ESI interface) as described in the previous section.

5.2.II.8 *Aqueous solubility assay*

Final concentrations of 5, 10, 20, 40, 60, 100 and 200 μ M of the desired compound in phosphate saline buffer (PBS) containing 1% DMSO were prepared, then the solution clarity and potential precipitation of the compound were examined after 1 and 24 h at room temperature (19-24°C).

5.2.II.9 *MTT cell viability assay*

In 24-well plates, HEK293 or HepG2 were seeded in DMEM supplemented with 5% FKS and 100 IU/ml penicillin-streptomycin. After 3 h, the incubation was started by the addition of the tested compound at 100, 50, 40, 25, 20, 12.5, 10 and 5 μ M dissolved in ethanol with a final ethanol concentration of 1%. Then the cell viability is evaluated by MTT assay based on the ability of viable cells to convert the yellow water soluble dye 3-(4,5-dimethyl-2-yl)-2,5-diphenyltetrazolium bromide (MTT) to a violet water insoluble formazane. After incubation time of 72 h in case of HEK293 and 48 h in case of HepG2 cells, 100 μ l of MTT-solution (5mg/ml in PBS) was added to the medium. After 30 min, the medium was removed and 250 μ l of DMSO containing 10% Sodium dodecyl sulphate (SDS) and 0.01 N HCl was added to start the cell lysis and dissolve the blue formazan which was then quantified spectrophotometrically at 590 nM using an Omega plate reader spectrometer as described. Proliferation in the presence of the vehicle was always arbitrary set to 100%.

5.2.II.10 *Aryl hydrocarbon receptor assay*

The AhR activity was evaluated as described before.⁵ The aryl hydrocarbon receptor agonistic activity of compounds was determined in a human hepatocellular carcinoma cell line (HepG2) by measuring the CYP1A1 activity. Cells were split on a 24-well plate (each compound in quadruplicate) and incubated for 16–24 h before compounds or vehicle was added to a final DMSO concentration of 0.1%. After 48 h of incubation with compound (3.16 μ M) or vehicle, cells were washed with 1 mL of warm PBS (37 °C). Then, 500 μ L of 3-cyano-7-ethoxycoumarin (CEC, specific CYP1A1 substrate), which forms a fluorescent product, was added to the cells at a final concentration of 40 μ M in DME medium with 10% fetal calf serum + 1% penicillin + streptomycin (37 °C). After an incubation of 30 min, the fluorescence was measured in the BMG Labtech Clariostar reader (excitation, 409 nm; emission, 460 nm). The increase in fluorescence induced by test compound was expressed relative to the increase induced by the reference compound omeprazole (50 μ M).

5.2.III Oral bioavailability

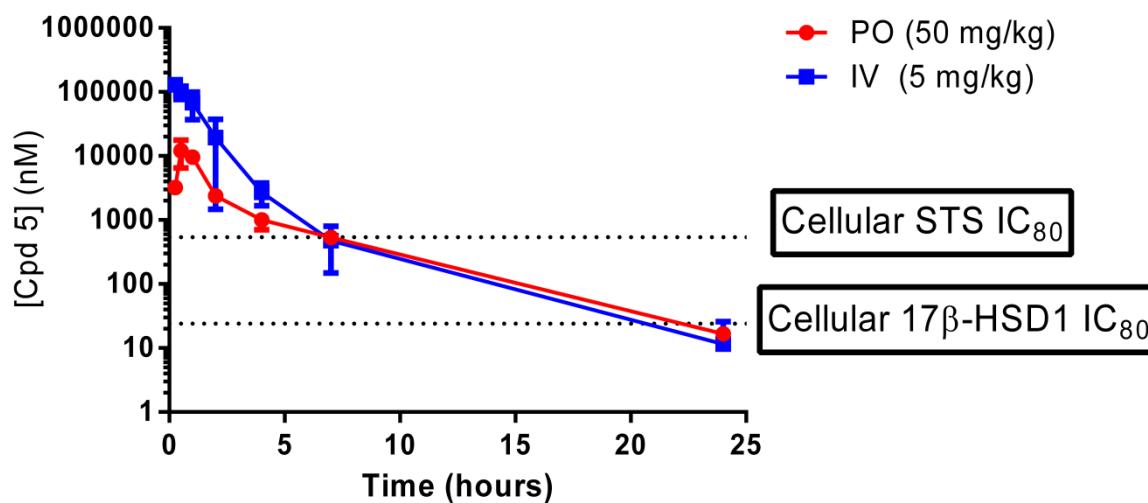


Figure S1. Mean profile (\pm SD) of plasma concentration [nM] in C57B1/6 mice vs time after oral (50 mg/kg) and intravenous (5 mg/kg) application of compounds **5** in single dosing experiments (n=3). Dotted lines represent the cellular IC₈₀ values of STS and 17 β -HSD1 values for compound **5**.

Oral bioavailability (%F) of compound **5**

$$\%F = \frac{AUC_{po} * Dose_{iv}}{AUC_{iv} * Dose_{po}} * 100 = \frac{10350 * 5}{69933 * 50} * 100 = 1.47\%$$

6. References

- (1) Zubeldia-Brenner, L.; Roselli, C. E.; Recabarren, S. E.; Gonzalez Deniselle, M. C.; Lara, H. E. Developmental and Functional Effects of Steroid Hormones on the Neuroendocrine Axis and Spinal Cord. *J. Neuroendocrinol.* **2016**, *28* (7).
- (2) Miller, W. L.; Auchus, R. J. The Molecular Biology, Biochemistry, and Physiology of Human Steroidogenesis and Its Disorders. *Endocr. Rev.* **2011**, *32* (1), 81–151.
- (3) Sugiyama, N.; Barros, R. P. A.; Warner, M.; Gustafsson, J. Å. ER β : Recent Understanding of Estrogen Signaling. *Trends Endocrinol. Metab.* **2010**, *21* (9), 545–552.
- (4) Cui, J.; Shen, Y.; Li, R. Estrogen Synthesis and Signaling Pathways during Aging: From Periphery to Brain. *Trends Mol. Med.* **2013**, *19* (3), 197–209.
- (5) Hall, P. F. Cytochrome P-450 C21sc: One Enzyme with Two Actions: Hydroxylase and Lyase. *J. Steroid Biochem. Mol. Biol.* **1991**, *40* (4–6), 527–532.
- (6) Luu-The, V.; Tremblay, P.; Labrie, F. Characterization of Type 12 17 β -Hydroxysteroid Dehydrogenase, an Isoform of Type 3 17 β -Hydroxysteroid Dehydrogenase Responsible for Estradiol Formation in Women. *Mol. Endocrinol.* **2006**, *20* (2), 437–443.
- (7) Chumsri, S.; Howes, T.; Bao, T.; Sabnis, G.; Brodie, A. Aromatase, Aromatase Inhibitors, and Breast Cancer. *J. Steroid Biochem. Mol. Biol.* **2011**, *125* (1–2), 13–22.
- (8) Robker, R. L.; Richards, J. S. Hormonal Control of the Cell Cycle in Ovarian Cells: Proliferation vs Differentiation. *Biol. Reprod.* **1998**, *59* (3), 476–482.
- (9) Rao, M. C.; Midgley, a R.; Richards, J. S. Proliferation of Ovarian Cellular. *Cell* **1978**, *14* (May), 71–78.
- (10) Richards, J. S. Maturation of Ovarian Follicles: Actions and Interactions of Pituitary and Ovarian Hormones on Follicular Cell Differentiation. *Physiol. Rev.* **1980**, *60* (1).
- (11) Simpson, E. R. Sources of Estrogen and Their Importance. *J. Steroid Biochem. Mol. Biol.* **2003**, *86* (3–5), 225–230.
- (12) Sasano, H.; Okamoto, M.; Mason, J. I.; Simpson, E. R.; Mendelson, C. R.; Sasano, N.; Silverberg, S. G. Immunolocalization of Aromatase, 17 -Hydroxylase and Side-Chain-Cleavage Cytochromes P-450 in the Human Ovary. *Reproduction* **1989**, *85* (1), 163–169.
- (13) Secky, L.; Svoboda, M.; Klameth, L.; Bajna, E.; Hamilton, G.; Zeillinger, R.; Jäger, W.; Thalhammer, T. The Sulfatase Pathway for Estrogen Formation: Targets for the Treatment and Diagnosis of Hormone-Associated Tumors. *J. Drug Deliv.* **2013**, *2013*, 1–13.
- (14) Konings, G.; Brentjens, L.; Delvoux, B.; Linnanen, T.; Cornel, K.; Koskimies, P.; Bongers, M.; Kruitwagen, R.; Xanthouleas, S.; Romano, A. Intracrine Regulation of Estrogen and Other Sex Steroid Levels in Endometrium and Non-Gynecological Tissues; Pathology, Physiology, and Drug Discovery. *Front. Pharmacol.* **2018**, *9*.
- (15) Suzuki, T.; Miki, Y.; Nakamura, Y.; Moriya, T.; Ito, K.; Ohuchi, N.; Sasano, H. Sex Steroid-Producing Enzymes in Human Breast Cancer. *Endocr. Relat. Cancer* **2005**, *12* (4), 701–720.
- (16) Stricker, R.; Eberhart, R.; Chevailler, M. C.; Quinn, F. A.; Bischof, P.; Stricker, R. Establishment of Detailed Reference Values for Luteinizing Hormone, Follicle Stimulating Hormone,

- Estradiol, and Progesterone during Different Phases of the Menstrual Cycle on the Abbott ARCHITECT® Analyzer. *Clin. Chem. Lab. Med.* **2006**, 44 (7), 883–887.
- (17) Labrie, F. All Sex Steroids Are Made Intracellularly in Peripheral Tissues by the Mechanisms of Intracrinology after Menopause. *J. Steroid Biochem. Mol. Biol.* **2015**, 145, 133–138.
- (18) Kotov, A.; Falany, J. L.; Wang, J.; Falany, C. N. Regulation of Estrogen Activity by Sulfation in Human Ishikawa Endometrial Adenocarcinoma Cells. *J. Steroid Biochem. Mol. Biol.* **1999**, 68 (3–4), 137–144.
- (19) Nilsson, S.; Mäkelä, S.; Treuter, E.; Tujague, M.; Thomsen, J.; Andersson, G.; Enmark, E.; Pettersson, K.; Warner, M.; Gustafsson, J.-Å. Mechanisms of Estrogen Action. *Physiol. Rev.* **2001**, 81 (4), 1535–1565.
- (20) Morselli, E.; Santos, R. S.; Criollo, A.; Nelson, M. D.; Palmer, B. F.; Clegg, D. J. The Effects of Oestrogens and Their Receptors on Cardiometabolic Health. *Nat. Rev. Endocrinol.* **2017**, 13 (6), 352–364.
- (21) Jia, M.; Dahlman-Wright, K.; Gustafsson, J.-Å. Estrogen Receptor Alpha and Beta in Health and Disease. *Best Pract. Res. Clin. Endocrinol. Metab.* **2015**, 29 (4), 557–568.
- (22) Drummond, A. E.; Findlay, J. K. The Role of Estrogen in Folliculogenesis. *Mol. Cell. Endocrinol.* **1999**, 151 (November 1998), 57–64.
- (23) Groothuis, P. G.; Dassen, H. H. N. M.; Romano, A.; Punyadeera, C. Estrogen and the Endometrium : Lessons Learned from Gene Expression Profiling in Rodents and Human. **2007**, 13 (4), 405–417.
- (24) Mertens, H. J. M. M.; Heineman, M. J.; Theunissen, P. H. M. H. Androgen , Estrogen and Progesterone Receptor Expression in the Human Uterus during the Menstrual Cycle. *Eur. J. Obstet. Gynecol. Reprod. Biol.* **2001**, 98 (1), 58–65.
- (25) Albrecht, E. D.; Aberdeen, G. W.; Pepe, G. J. The Role of Estrogen in the Maintenance of Primate Pregnancy. *Am. J. Obstet. Gynecol.* **2000**, 182 (2), 432–438.
- (26) Dickson, R. B.; Stancel, G. M. Estrogen Receptor-Mediated Processes in Normal and Cancer Cells. *J. Natl. Cancer Inst. Monogr.* **2000**, 2000 (27), 135–145.
- (27) Gustafsson, J.-Å.; Warner, M. Estrogen Receptor β in the Breast : Role in Estrogen Responsiveness and Development of Breast Cancer. *J. Steroid Biochem. Mol. Biol.* **2000**, 74 (5), 245–248.
- (28) Cauley, J. A.; Robbins, J.; Chen, Z.; Cummings, S. R.; Jackson, R. D.; Lacroix, A. Z.; Leboff, M.; Lewis, C. E.; McGowan, J.; Neuner, J.; Pettinger, M.; Stefanick, M. L.; Wactawski-wende, J. Effects of Estrogen Plus Progestin on Risk of Fracture and Bone Mineral Density. *Jama* **2003**, 290 (13), 1729–1738.
- (29) Turner, R. T.; Riggs, B. L.; Spelsberg, T. C. Skeletal Effects of Estrogen. *Endocr. Rev.* **1994**, 15 (3), 275–300.
- (30) Karas, M. E. M. and R. H. The Protective Effects of Estrogen on the Cardiovascular System. *N. Engl. J. Med.* **1999**, 340 (23), 1801–1811.
- (31) Roof, R. L.; Hall, E. D. Gender Differences in Acute CNS Trauma and Stroke : Neuroprotective Effects of Estrogen and Progesterone. *J. Neurotrauma* **2000**, 17 (5), 367–388.

- (32) Sherwin, B. B. Estrogen and Memory in Women : How Can We Reconcile the Findings ? *Horm. Behav.* **2005**, *47* (3), 371–375.
- (33) Deroo, B. J. Estrogen Receptors and Human Disease. *J. Clin. Invest.* **2006**, *116* (3), 561–570.
- (34) Brown, S. B.; Hankinson, S. E. Endogenous Estrogens and the Risk of Breast, Endometrial, and Ovarian Cancers. *Steroids* **2015**, *99*, 8–10.
- (35) Travis, R. C.; Key, T. J. Oestrogen Exposure and Breast Cancer Risk. *Breast Cancer Res.* **2003**, *5* (5), 239.
- (36) Yager, J. D.; Davidson, N. E. Estrogen Carcinogenesis in Breast Cancer. *N. Engl. J. Med.* **2006**, *354* (3), 270–282.
- (37) Cunat, S.; Hoffmann, P.; Pujol, P. Estrogens and Epithelial Ovarian Cancer. *Gynecol. Oncol.* **2004**, *94* (1), 25–32.
- (38) Rodriguez, C.; Calle, E. E.; Jacob, E. J.; Thun, M. J. And Ovarian Cancer Mortality in a Large Prospective Study of US Women. *Jama* **2013**, *285* (11), 1460–1465.
- (39) GRADY, D.; GEBRETSADIK, T.; KERLIKOWSKE, K.; ERNSTER, V.; PETITTI, D. Hormone Replacement Therapy and Endometrial Cancer Risk: A Meta-Analysis. *Obstet. Gynecol.* **1995**, *85* (2), 304–313.
- (40) Chlebowski, R. T.; Anderson, G. L.; Sarto, G. E.; Haque, R.; Runowicz, C. D.; Aragaki, A. K.; Thomson, C. A.; Howard, B. V.; Wactawski-Wende, J.; Chen, C.; Rohan, T. E.; Simon, M. S.; Reed, S. D.; Manson, J. E. Continuous Combined Estrogen Plus Progestin and Endometrial Cancer: The Women’s Health Initiative Randomized Trial. *J. Natl. Cancer Inst.* **2016**, *108* (3).
- (41) Kitawaki, J.; Kado, N.; Ishihara, H.; Koshiba, H.; Kitaoka, Y.; Honjo, H. Endometriosis: The Pathophysiology as an Estrogen-Dependent Disease. *J. Steroid Biochem. Mol. Biol.* **2002**, *83* (1–5), 149–155.
- (42) Burney, R. O.; Giudice, L. C. Pathogenesis and Pathophysiology of Endometriosis. *Fertil. Steril.* **2012**, *98* (3), 511–519.
- (43) Pacifici, R. Estrogen, Cytokines, and Pathogenesis of Postmenopausal Osteoporosis. *J. Bone Miner. Res.* **1996**, *11* (8), 1043–1051.
- (44) Riggs, B. L.; Khosla, S.; Melton, L. J. A Unitary Model for Involutional Osteoporosis: Estrogen Deficiency Causes Both Type I and Type II Osteoporosis in Postmenopausal Women and Contributes to Bone Loss in Aging Men. *J. Bone Miner. Res.* **1998**, *13* (5), 763–773.
- (45) Black, D. M.; Rosen, C. J. Postmenopausal Osteoporosis. *N. Engl. J. Med.* **2016**, *374* (3), 254–262.
- (46) Giudice, L. C.; Kao, L. C. Endometriosis. *Lancet* **2004**, *364* (9447), 1789–1799.
- (47) Nap, A. W.; Groothuis, P. G.; Demir, A. Y.; Evers, J. L. H.; Dunselman, G. A. J. Pathogenesis of Endometriosis. *Best Practice and Research: Clinical Obstetrics and Gynaecology*. 2004, pp 233–244.
- (48) Berkley, K. J.; Berkley, K. J.; Rapkin, A. J.; Rapkin, A. J.; Papka, R. E.; Papka, R. E. The Pains of Endometriosis. *Science* **2005**, *308* (5728), 1587–1589.
- (49) Nnoaham, K. E.; Hummelshoj, L.; Webster, P.; D’Hooghe, T.; De Cicco Nardone, F.; De Cicco Nardone, C.; Jenkinson, C.; Kennedy, S. H.; Zondervan, K. T. Impact of Endometriosis on

- Quality of Life and Work Productivity: A Multicenter Study across Ten Countries. *Fertil. Steril.* **2011**, *96* (2), 366–373.e8.
- (50) Ferreira, A. L. L.; Bessa, M. M. M.; Drezett, J.; De Abreu, L. C. Quality of Life of the Woman Carrier of Endometriosis: Systematized Review. *Reprod. e Clim.* **2016**, *31* (1), 48–54.
- (51) Giudice, L. C. Endometriosis. *N. Engl. J. Med.* **2010**, *362* (25), 2389–2398.
- (52) Halme, J.; Hammond, M. G.; Hulka, J. F.; Raj, S. G.; Talbert, L. M. Retrograde Menstruation in Healthy Women and in Patients with Endometriosis. *Obstet. Gynecol.* **1984**, *64* (2), 151–154.
- (53) Sasson, I. E.; Taylor, H. S. Stem Cells and the Pathogenesis of Endometriosis. *Ann. N. Y. Acad. Sci.* **2008**, *1127* (1), 106–115.
- (54) Matsuura, K.; Ohtake, H.; Katabuchi, H.; Okamura, H. Coelomic Metaplasia Theory of Endometriosis: Evidence from in Vivo Studies and an in Vitro Experimental Model. *Gynecol. Obstet. Invest.* **1999**, *47* (Suppl. 1), 18–22.
- (55) Bulun, S. E.; Zeitoun, K. M.; Takayama, K.; Sasano, H. Estrogen Biosynthesis in Endometriosis: Molecular Basis and Clinical Relevance. *J. Mol. Endocrinol.* **2000**, *25* (1), 35–42.
- (56) Bulun, S. E. Regulation of Aromatase Expression in Estrogen-Responsive Breast and Uterine Disease: From Bench to Treatment. *Pharmacol. Rev.* **2005**, *57* (3), 359–383.
- (57) Tsai, S.-J.; Wu, M.-H.; Lin, C.-C.; Sun, H. S.; Chen, H.-M. Regulation of Steroidogenic Acute Regulatory Protein Expression and Progesterone Production in Endometriotic Stromal Cells. *J. Clin. Endocrinol. Metab.* **2001**, *86* (12), 5765–5773.
- (58) Attar, E.; Tokunaga, H.; Imir, G.; Yilmaz, M. B.; Redwine, D.; Putman, M.; Gurates, B.; Attar, R.; Yaegashi, N.; Hales, D. B.; Bulun, S. E. Prostaglandin E2 via Steroidogenic Factor-1 Coordinately Regulates Transcription of Steroidogenic Genes Necessary for Estrogen Synthesis in Endometriosis. *J. Clin. Endocrinol. Metab.* **2009**, *94* (2), 623–631.
- (59) Šmuc, T.; Pucelj, M. R.; Šinkovec, J.; Husen, B.; Thole, H.; Lanišnik Rižner, T. Expression Analysis of the Genes Involved in Estradiol and Progesterone Action in Human Ovarian Endometriosis. *Gynecol. Endocrinol.* **2007**, *23* (2), 105–111.
- (60) Dunselman, G. A. J.; Vermeulen, N.; Becker, C.; Calhaz-Jorge, C.; D’Hooghe, T.; De Bie, B.; Heikinheimo, O.; Horne, A. W.; Kiesel, L.; Nap, A.; Prentice, A.; Saridogan, E.; Soriano, D.; Nelen, W. ESHRE Guideline: Management of Women with Endometriosis. *Hum. Reprod.* **2014**, *29* (3), 400–412.
- (61) Ferrero, S.; Evangelisti, G.; Barra, F. Current and Emerging Treatment Options for Endometriosis. *Expert Opin. Pharmacother.* **2018**, *19* (10), 1109–1125.
- (62) Shakiba, K.; Bena, J. F.; McGill, K. M.; Minger, J.; Falcone, T. Surgical Treatment of Endometriosis: A 7-Year Follow-up on the Requirement for Further Surgery. *Obstet. Gynecol.* **2008**, *111* (6), 1285–1292.
- (63) Ferrero, S.; Alessandri, F.; Racca, A.; Leone Roberti Maggiore, U. Treatment of Pain Associated with Deep Endometriosis: Alternatives and Evidence. *Fertil. Steril.* **2015**, *104* (4), 771–792.
- (64) Barra, F.; Scala, C.; Mais, V.; Guerriero, S.; Ferrero, S. Investigational Drugs for the Treatment of Endometriosis, an Update on Recent Developments. *Expert Opin. Investig. Drugs* **2018**, *27* (5), 445–458.

- (65) Huhtinen, K.; Desai, R.; Ståhle, M.; Salminen, A.; Handelsman, D. J.; Perheentupa, A.; Poutanen, M. Endometrial and Endometriotic Concentrations of Estrone and Estradiol Are Determined by Local Metabolism Rather than Circulating Levels. *J. Clin. Endocrinol. Metab.* **2012**, *97* (11), 4228–4235.
- (66) Dassen, H.; Punyadeera, C.; Kamps, R.; Delvoux, B.; Van Langendonck, A.; Donnez, J.; Husen, B.; Thole, H.; Dunselman, G.; Groothuis, P. Estrogen Metabolizing Enzymes in Endometrium and Endometriosis. *Hum. Reprod.* **2007**, *22* (12), 3148–3158.
- (67) Rižner, T. L. Estrogen Metabolism and Action in Endometriosis. *Mol. Cell. Endocrinol.* **2009**, *307* (1–2), 8–18.
- (68) Tosti, C.; Biscione, A.; Morgante, G.; Bifulco, G.; Luisi, S.; Petraglia, F. Hormonal Therapy for Endometriosis: From Molecular Research to Bedside. *Eur. J. Obstet. Gynecol. Reprod. Biol.* **2017**, *209*, 61–66.
- (69) Huhtinen, K.; Ståhle, M.; Perheentupa, A.; Poutanen, M. Estrogen Biosynthesis and Signaling in Endometriosis. *Mol. Cell. Endocrinol.* **2012**, *358* (2), 146–154.
- (70) Borghese, B.; Mondon, F.; Noël, J.-C.; Fayt, I.; Mignot, T.-M.; Vaiman, D.; Chapron, C. Research Resource: Gene Expression Profile for Ectopic Versus Eutopic Endometrium Provides New Insights into Endometriosis Oncogenic Potential. *Mol. Endocrinol.* **2008**, *22* (11), 2557–2562.
- (71) Šmuc, T.; Hevir, N.; Ribič-Pucelj, M.; Husen, B.; Thole, H.; Rižner, T. L. Disturbed Estrogen and Progesterone Action in Ovarian Endometriosis. *Mol. Cell. Endocrinol.* **2009**, *301* (1–2), 59–64.
- (72) Purohit, A.; Fusi, L.; Brosens, J.; Woo, L. W. L.; Potter, B. V. L.; Reed, M. J. Inhibition of Steroid Sulphatase Activity in Endometriotic Implants by 667 COUMATE: A Potential New Therapy. *Hum. Reprod.* **2008**, *23* (2), 290–297.
- (73) Hudelist, G.; Czerwenka, K.; Keckstein, J.; Haas, C.; Fink-Retter, A.; Gschwantler-Kaulich, D.; Kubista, E.; Singer, C. F. Expression of Aromatase and Estrogen Sulfotransferase in Eutopic and Ectopic Endometrium: Evidence for Unbalanced Estradiol Production in Endometriosis. *Reprod. Sci.* **2007**, *14* (8), 798–805.
- (74) Kitawaki, J.; Noguchi, T.; Amatsu, T.; Maeda, K.; Tsukamoto, K.; Yamamoto, T.; Fushiki, S.; Osawa, Y.; Honjo, H. Expression of Aromatase Cytochrome P450 Protein and Messenger Ribonucleic Acid in Human Endometriotic and Adenomyotic Tissues but Not in Normal Endometrium. *Biol. Reprod.* **1997**, *57* (3), 514–519.
- (75) Velasco, I.; J. Rueda; P. Ación. Aromatase Expression in Endometriotic Tissues and Cell Cultures of Patients with Endometriosis. *Mol. Hum. Reprod.* **2006**, *12* (6), 377–381.
- (76) Bukulmez, O.; Hardy, D. B.; Carr, B. R.; Word, R. A.; Mendelson, C. R. Inflammatory Status Influences Aromatase and Steroid Receptor Expression in Endometriosis. *Endocrinology* **2008**, *149* (3), 1190–1204.
- (77) Zeitoun, K.; Takayama, K.; Sasano, H.; Suzuki, T.; Moghrabi, N.; Andersson, S.; Johns, A.; Meng, L.; Putman, M.; Carr, B.; Bulun, S. E. Deficient 17 β -Hydroxysteroid Dehydrogenase Type 2 Expression in Endometriosis: Failure to Metabolize 17 β -Estradiol. *J. Clin. Endocrinol. Metab.* **1998**, *83* (12), 4474–4480.
- (78) Bulun, S.; Cheng, Y.-H.; Pavone, M.; Yin, P.; Imir, G.; Utsunomiya, H.; Thung, S.; Xue, Q.; Marsh, E.; Tokunaga, H.; Ishikawa, H.; Kurita, T.; Su, E. 17 β -Hydroxysteroid Dehydrogenase-2 Deficiency and Progesterone Resistance in Endometriosis. *Semin. Reprod. Med.* **2010**, *28* (01), 044–050.

- (79) Mueller, J. W.; Gilligan, L. C.; Idkowiak, J.; Arlt, W.; Foster, P. A. The Regulation of Steroid Action by Sulfation and Desulfation. *Endocr. Rev.* **2015**, *36* (5), 526–563.
- (80) Hobkirk, R. Steroid Sulfation. *Trends Endocrinol. Metab.* **1993**, *4* (2), 69–74.
- (81) Reed, M. J.; Purohit, A.; Woo, L. W. L.; Newman, S. P.; Potter, B. V. L. Steroid Sulfatase: Molecular Biology, Regulation, and Inhibition. *Endocr. Rev.* **2005**, *26* (2), 171–202.
- (82) Huang, H.; Zhao, M.; Ren, Q.; Yang, Y. Changes in Inhibitory Activity and Secondary Conformation of Soybean Trypsin Inhibitors Induced by Tea Polyphenol Complexation. *J. Sci. Food Agric.* **2009**, *89* (14), 2435–2439.
- (83) Thomas, M. P.; Potter, B. V. L. The Structural Biology of Oestrogen Metabolism. *J. Steroid Biochem. Mol. Biol.* **2013**, *137*, 27–49.
- (84) Hernandez-Guzman, F. G.; Higashiyama, T.; Pangborn, W.; Osawa, Y.; Ghosh, D. Structure of Human Estrone Sulfatase Suggests Functional Roles of Membrane Association. *J. Biol. Chem.* **2003**, *278* (25), 22989–22997.
- (85) Potter, B. V. L. SULFATION PATHWAYS: Steroid Sulphatase Inhibition via Aryl Sulphamates: Clinical Progress, Mechanism and Future Prospects. *J. Mol. Endocrinol.* **2018**, *61* (2), T233–T252.
- (86) Thomas, M. P.; Potter, B. V. L. Discovery and Development of the Aryl O -Sulfamate Pharmacophore for Oncology and Women's Health. *J. Med. Chem.* **2015**, *58* (19), 7634–7658.
- (87) Pasqualini, J. R.; Chetrite, G.; Blacker, C.; Feinstein, M. C.; Delalonde, L.; Talbi, M.; Maloche, C. Concentrations of Estrone, Estradiol, and Estrone Sulfate and Evaluation of Sulfatase and Aromatase Activities in Pre- and Postmenopausal Breast Cancer Patients. *J. Clin. Endocrinol. Metab.* **1996**, *81* (4), 1460–1464.
- (88) Suzuki, M.; Ishida, H.; Shiotsu, Y.; Nakata, T.; Akinaga, S.; Takashima, S.; Utsumi, T.; Saeki, T.; Harada, N. Expression Level of Enzymes Related to in Situ Estrogen Synthesis and Clinicopathological Parameters in Breast Cancer Patients. *J. Steroid Biochem. Mol. Biol.* **2009**, *113* (3–5), 195–201.
- (89) SANTNER, S. J.; FEIL, P. D.; SANTEN, R. J. In Situ Estrogen Production via the Estrone Sulfatase Pathway in Breast Tumors: Relative Importance versus the Aromatase Pathway*. *J. Clin. Endocrinol. Metab.* **1984**, *59* (1), 29–33.
- (90) Utsumi, T.; Yoshimura, N.; Takeuchi, S.; Maruta, M.; Maeda, K.; Harada, N. Elevated Steroid Sulfatase Expression in Breast Cancers. *J. Steroid Biochem. Mol. Biol.* **2000**, *73* (3–4), 141–145.
- (91) Colette, S.; Defrère, S.; Van Kerk, O.; Van Langendonck, A.; Dolmans, M.-M.; Donnez, J. Differential Expression of Steroidogenic Enzymes According to Endometriosis Type. *Fertil. Steril.* **2013**, *100* (6), 1642–1649.
- (92) Šmuc, T.; Ruprecht, R.; Šinkovec, J.; Adamski, J.; Rižner, T. L. Expression Analysis of Estrogen-Metabolizing Enzymes in Human Endometrial Cancer. *Mol. Cell. Endocrinol.* **2006**, *248* (1–2), 114–117.
- (93) Utsunomiya, H.; Ito, K.; Suzuki, T.; Kitamura, T.; Kaneko, C.; Nakata, T.; Niikura, H.; Okamura, K.; Yaegashi, N.; Sasano, H. Steroid Sulfatase and Estrogen Sulfotransferase in Human Endometrial Carcinoma. *Clin. Cancer Res.* **2004**, *10* (17), 5850–5856.
- (94) Hoffmann, F.; Maser, E. Carbonyl Reductases and Pluripotent Hydroxysteroid Dehydrogenases

- of the Short-Chain Dehydrogenase/Reductase Superfamily. *Drug Metab. Rev.* **2007**, *39* (1), 87–144.
- (95) Duax, W. L.; Ghosh, D.; Pletnev, V. Steroid Dehydrogenase Structures, Mechanism of Action, and Disease. *Vitam. Horm.* **2000**, *58*, 121–148.
- (96) Penning, T. M. Hydroxysteroid Dehydrogenases and Pre-Receptor Regulation of Steroid Hormone Action. *Hum. Reprod. Update* **2003**, *9* (3), 193–205.
- (97) Labrie, F.; Luu-The, V.; Lin, S.-X.; Simard, J.; Labrie, C.; El-Alfy, M.; Pelletier, G.; Bélanger, A. Intracrinology: Role of the Family of 17 Beta-Hydroxysteroid Dehydrogenases in Human Physiology and Disease. *J. Mol. Endocrinol.* **2000**, *25* (1), 1–16.
- (98) Moeller, G.; Adamski, J. Multifunctionality of Human 17 β -Hydroxysteroid Dehydrogenases. *Mol. Cell. Endocrinol.* **2006**, *248* (1–2), 47–55.
- (99) Haller, F.; Moman, E.; Hartmann, R. W.; Adamski, J.; Mindnich, R. Molecular Framework of Steroid/Retinoid Discrimination in 17 β -Hydroxysteroid Dehydrogenase Type 1 and Photoreceptor-Associated Retinol Dehydrogenase. *J. Mol. Biol.* **2010**, *399* (2), 255–267.
- (100) Zhongyi, S.; Rantakari, P.; Lamminen, T.; Toppari, J.; Poutanen, M. Transgenic Male Mice Expressing Human Hydroxysteroid Dehydrogenase 2 Indicate a Role for the Enzyme Independent of Its Action on Sex Steroids. *Endocrinology* **2007**, *148* (8), 3827–3836.
- (101) Lukacik, P.; Kavanagh, K. L.; Oppermann, U. Structure and Function of Human 17 β -Hydroxysteroid Dehydrogenases. *Mol. Cell. Endocrinol.* **2006**, *248* (1–2), 61–71.
- (102) Prehn, C.; Möller, G.; Adamski, J. Recent Advances in 17beta-Hydroxysteroid Dehydrogenases. *J. Steroid Biochem. Mol. Biol.* **2009**, *114* (1–2), 72–77.
- (103) Peltoketo, H.; Luu-The, V.; Simard, J.; Adamski, J. 17 β -Hydroxysteroid Dehydrogenase (HSD)/17-Ketosteroid Reductase (KSR) Family; Nomenclature and Main Characteristics of the 17HSD/KSR Enzymes. *J. Mol. Endocrinol.* **1999**, *23* (1), 1–11.
- (104) Persson, B.; Kallberg, Y.; Bray, J. E.; Bruford, E.; Dellaporta, S. L.; Favia, A. D.; Duarte, R. G.; Jörnvall, H.; Kavanagh, K. L.; Kedishvili, N.; Kisiela, M.; Maser, E.; Mindnich, R.; Orchard, S.; Penning, T. M.; Thornton, J. M.; Adamski, J.; Oppermann, U. The SDR (Short-Chain Dehydrogenase/Reductase and Related Enzymes) Nomenclature Initiative. *Chem. Biol. Interact.* **2009**, *178* (1–3), 94–98.
- (105) Vihko, P.; Herrala, A.; Härkönen, P.; Isomaa, V.; Kaija, H.; Kurkela, R.; Pulkka, A. Control of Cell Proliferation by Steroids: The Role of 17HSDs. *Mol. Cell. Endocrinol.* **2006**, *248* (1–2), 141–148.
- (106) Vihko, P.; Herrala, A.; Härkönen, P.; Isomaa, V.; Kaija, H.; Kurkela, R.; Li, Y.; Patrikainen, L.; Pulkka, A.; Soronen, P.; Törn, S. Enzymes as Modulators in Malignant Transformation. *J. Steroid Biochem. Mol. Biol.* **2005**, *93* (2–5), 277–283.
- (107) Langer, L. J.; Engel, L. L. Human Placental Estradiol-17 β Dehydrogenase. *J. Biol. Chem.* **1958**, *233*, 583–588.
- (108) Peltoketo, H.; Isomaa, V.; Mäentausta, O.; Vihko, R. Complete Amino Acid Sequence of Human Placental 17 β -Hydroxysteroid Dehydrogenase Deduced from cDNA. *FEBS Lett.* **1988**, *239* (1), 73–77.
- (109) Ghosh, D.; Pletnev, V. Z.; Zhu, D.-W.; Wawrzak, Z.; Duax, W. L.; Pangborn, W.; Labrie, F.; Lin, S.-X. Structure of Human Estrogenic 17 β -Hydroxysteroid Dehydrogenase at 2.20 Å Resolution.

- Structure* **1995**, 3 (5), 503–513.
- (110) Breton, R.; Housset, D.; Mazza, C.; Fontecilla-Camps, J. C. The Structure of a Complex of Human 17 β -Hydroxysteroid Dehydrogenase with Estradiol and NADP⁺ Identifies Two Principal Targets for the Design of Inhibitors. *Structure* **1996**, 4 (8), 905–915.
- (111) Sawicki, M. W.; Erman, M.; Puranen, T.; Vihko, P.; Ghosh, D. Structure of the Ternary Complex of Human 17 -Hydroxysteroid Dehydrogenase Type 1 with 3-Hydroxyestra-1,3,5,7-Tetraen-17-One (Equilin) and NADP⁺. *Proc. Natl. Acad. Sci.* **1999**, 96 (3), 840–845.
- (112) Sherbet, D. P.; Papari-Zareei, M.; Khan, N.; Sharma, K. K.; Brandmaier, A.; Rambally, S.; Chattopadhyay, A.; Andersson, S.; Agarwal, A. K.; Auchus, R. J. Cofactors, Redox State, and Directional Preferences of Hydroxysteroid Dehydrogenases. *Mol. Cell. Endocrinol.* **2007**, 265–266, 83–88.
- (113) Han, Q.; Campbell, R. L.; Gangloff, A.; Huang, Y.-W.; Lin, S.-X. Dehydroepiandrosterone and Dihydrotestosterone Recognition by Human Estrogenic 17 β -Hydroxysteroid Dehydrogenase: C-18/C-19 STEROID DISCRIMINATION AND ENZYME-INDUCED STRAIN. *J. Biol. Chem.* **2000**, 275 (2), 1105–1111.
- (114) Marchais-Oberwinkler, S.; Henn, C.; Möller, G.; Klein, T.; Negri, M.; Oster, A.; Spadaro, A.; Werth, R.; Wetzel, M.; Xu, K.; Frotscher, M.; Hartmann, R. W.; Adamski, J. 17 β -Hydroxysteroid Dehydrogenases (17 β -HSDs) as Therapeutic Targets: Protein Structures, Functions, and Recent Progress in Inhibitor Development. *J. Steroid Biochem. Mol. Biol.* **2011**, 125 (1–2), 66–82.
- (115) Miyoshi, Y.; Ando, A.; Shiba, E.; Taguchi, T.; Tamaki, Y.; Noguchi, S. Involvement of Up-Regulation of 17 β -Hydroxysteroid Dehydrogenase Type 1 in Maintenance of Intratumoral High Estradiol Levels in Postmenopausal Breast Cancers. *Int. J. Cancer* **2001**, 94 (5), 685–689.
- (116) Jansson, A. 17Beta-Hydroxysteroid Dehydrogenase Enzymes and Breast Cancer. *J. Steroid Biochem. Mol. Biol.* **2009**, 114 (1–2), 64–67.
- (117) Day, J. M.; Foster, P. A.; Tutill, H. J.; Parsons, M. F. C.; Newman, S. P.; Chander, S. K.; Allan, G. M.; Lawrence, H. R.; Vicker, N.; Potter, B. V. L.; Reed, M. J.; Purohit, A. 17 β -Hydroxysteroid Dehydrogenase Type 1, and Not Type 12, Is a Target for Endocrine Therapy of Hormone-Dependent Breast Cancer. *Int. J. Cancer* **2008**, 122 (9), 1931–1940.
- (118) Blomquist, C. H.; Bonenfant, M.; McGinley, D. M.; Posalaky, Z.; Lakatua, D. J.; Tuli-Puri, S.; Bealka, D. G.; Tremblay, Y. Androgenic and Estrogenic 17beta-Hydroxysteroid Dehydrogenase/17-Ketosteroid Reductase in Human Ovarian Epithelial Tumors: Evidence for the Type 1, 2 and 5 Isoforms. *J. Steroid Biochem. Mol. Biol.* **2002**, 81 (4–5), 343–351.
- (119) Saloniemi, T.; Järvensivu, P.; Koskimies, P.; Jokela, H.; Lamminen, T.; Ghaem-Maghami, S.; Dina, R.; Damdimopoulou, P.; Mäkelä, S.; Perheentupa, A.; Kujari, H.; Brosens, J.; Poutanen, M. Novel Hydroxysteroid (17 β) Dehydrogenase 1 Inhibitors Reverse Estrogen-Induced Endometrial Hyperplasia in Transgenic Mice. *Am. J. Pathol.* **2010**, 176 (3), 1443–1451.
- (120) Howarth, N. M.; Purohit, A.; Reed, M. J.; Potter, B. V. L. Estrone Sulfamates: Potent Inhibitors of Estrone Sulfatase with Therapeutic Potential. *J. Med. Chem.* **1994**, 37 (2), 219–221.
- (121) Maltais, R.; Poirier, D. Steroid Sulfatase Inhibitors: A Review Covering the Promising 2000–2010 Decade. *Steroids* **2011**, 76 (10–11), 929–948.
- (122) Ahmed, S.; James, K.; Owen, C. P.; Patel, C. K.; Patel, M. Novel Inhibitors of the Enzyme Estrone Sulfatase (ES). *Bioorg. Med. Chem. Lett.* **2001**, 11 (6), 841–844.

- (123) Purohit, A.; Williams, G. J.; Howarth, N. M.; Potter, B. V.; Reed, M. J. Inactivation of Steroid Sulfatase by an Active Site-Directed Inhibitor, Estrone-3-O-Sulfamate. *Biochemistry* **1995**, *34* (36), 11508–11514.
- (124) Purohit, A.; Williams, G. J.; Roberts, C. J.; Potter, B. V. L.; Reed, M. J. In Vivo Inhibition of Oestrone Sulphatase and Dehydroepiandrosterone Sulphatase by Oestrone-3-O-Sulphamate. *Int. J. Cancer* **1995**, *63* (1), 106–111.
- (125) Elger, W.; Schwarz, S.; Hedden, A.; Reddersen, G.; Schneider, B. Sulfamates of Various Estrogens Are Prodrugs with Increased Systemic and Reduced Hepatic Estrogenicity at Oral Application. *J. Steroid Biochem. Mol. Biol.* **1995**, *55* (3–4), 395–403.
- (126) Woo, L. W. L.; Purohit, A.; Reed, M. J.; Potter, B. V. L. Active Site Directed Inhibition of Estrone Sulfatase by Nonsteroidal Coumarin Sulfamates. *J. Med. Chem.* **1996**, *39* (7), 1349–1351.
- (127) Purohit, A.; Woo, L. W. L.; Potter, B. V. L.; Reed, M. J. In Vivo Inhibition of Estrone Sulfatase Activity and Growth of Nitrosomethylurea-Induced Mammary Tumors by 667 COUMATE. *Cancer Res.* **2000**, *60* (13), 3394–3396.
- (128) Ho, Y. T.; Purohit, A.; Vicker, N.; Newman, S. P.; Robinson, J. J.; Leese, M. P.; Ganeshapillai, D.; Woo, L. W. L.; Potter, B. V. L.; Reed, M. J. Inhibition of Carbonic Anhydrase II by Steroidal and Non-Steroidal Sulphamates. *Biochem. Biophys. Res. Commun.* **2003**, *305* (4), 909–914.
- (129) Ireson, C. R.; Chander, S. K.; Purohit, A.; Parish, D. C.; Woo, L. W. L.; Potter, B. V. L.; Reed, M. J. Pharmacokinetics of the Nonsteroidal Steroid Sulphatase Inhibitor 667 COUMATE and Its Sequestration into Red Blood Cells in Rats. *Br. J. Cancer* **2004**, *91* (7), 1399–1404.
- (130) Poutanen, M.; Miettinen, M.; Vihko, R. Differential Estrogen Substrate Specificities for Transiently Expressed Human Placental 17 Beta-Hydroxysteroid Dehydrogenase and an Endogenous Enzyme Expressed in Cultured COS-M6 Cells. *Endocrinology* **1993**, *133* (6), 2639–2644.
- (131) Geissler, W. M.; Davis, D. L.; Wu, L.; Bradshaw, K. D.; Patel, S.; Mendonca, B. B.; Elliston, K. O.; Wilson, J. D.; Russell, D. W.; Andersson, S. Male Pseudohermaphroditism Caused by Mutations of Testicular 17 β -hydroxysteroid Dehydrogenase 3. *Nat. Genet.* **1994**, *7* (1), 34–39.
- (132) Stanbrough, M.; Bubley, G. J.; Ross, K.; Golub, T. R.; Rubin, M. A.; Penning, T. M.; Febbo, P. G.; Balk, S. P. Increased Expression of Genes Converting Adrenal Androgens to Testosterone in Androgen-Independent Prostate Cancer. *Cancer Res.* **2006**, *66* (5), 2815–2825.
- (133) Jin, Y.; Penning, T. M. Aldo-Keto Reductases and Bioactivation/Detoxication. *Annu. Rev. Pharmacol. Toxicol.* **2007**, *47* (1), 263–292.
- (134) PENNING, T. M.; BURCZYNSKI, M. E.; JEZ, J. M.; HUNG, C.-F.; LIN, H.-K.; MA, H.; MOORE, M.; PALACKAL, N.; RATNAM, K. Human 3 α -Hydroxysteroid Dehydrogenase Isoforms (AKR1C1–AKR1C4) of the Aldo-Keto Reductase Superfamily: Functional Plasticity and Tissue Distribution Reveals Roles in the Inactivation and Formation of Male and Female Sex Hormones. *Biochem. J.* **2000**, *351* (1), 67.
- (135) Haynes, B. P.; Straume, A. H.; Geisler, J.; A'Hern, R.; Helle, H.; Smith, I. E.; Lonning, P. E.; Dowsett, M. Intratumoral Estrogen Disposition in Breast Cancer. *Clin. Cancer Res.* **2010**, *16* (6), 1790–1801.
- (136) Marijanovic, Z.; Laubner, D.; Möller, G.; Gege, C.; Husen, B.; Adamski, J.; Breitling, R. Closing the Gap: Identification of Human 3-Ketosteroid Reductase, the Last Unknown Enzyme of Mammalian Cholesterol Biosynthesis. *Mol. Endocrinol.* **2003**, *17* (9), 1715–1725.

- (137) Krazeisen, A.; Breitling, R.; Imai, K.; Fritz, S.; Möller, G.; Adamski, J. Determination of CDNA, Gene Structure and Chromosomal Localization of the Novel Human 17 β -Hydroxysteroid Dehydrogenase Type 7. *FEBS Lett.* **1999**, *460* (2), 373–379.
- (138) Blanchard, P.-G.; Luu-The, V. Differential Androgen and Estrogen Substrates Specificity in the Mouse and Primates Type 12 17 -Hydroxysteroid Dehydrogenase. *J. Endocrinol.* **2007**, *194* (2), 449–455.
- (139) Moon, Y.-A.; Horton, J. D. Identification of Two Mammalian Reductases Involved in the Two-Carbon Fatty Acyl Elongation Cascade. *J. Biol. Chem.* **2003**, *278* (9), 7335–7343.
- (140) Luu-The, V.; Bélanger, A.; Labrie, F. Androgen Biosynthetic Pathways in the Human Prostate. *Best Pract. Res. Clin. Endocrinol. Metab.* **2008**, *22* (2), 207–221.
- (141) Moghrabi, N.; Andersson, S. 17 β -Hydroxysteroid Dehydrogenases: Physiological Roles in Health and Disease. *Trends Endocrinol. Metab.* **1998**, *9* (7), 265–270.
- (142) Rasiah, K. K.; Gardiner-Garden, M.; Padilla, E. J. D.; Möller, G.; Kench, J. G.; Alles, M. C.; Eggleton, S. A.; Stricker, P. D.; Adamski, J.; Sutherland, R. L.; Henshall, S. M.; Hayes, V. M. HSD17B4 Overexpression, an Independent Biomarker of Poor Patient Outcome in Prostate Cancer. *Mol. Cell. Endocrinol.* **2009**, *301* (1–2), 89–96.
- (143) Fomitcheva, J.; Baker, M. E.; Anderson, E.; Lee, G. Y.; Aziz, N. Characterization of Ke 6, a New 17 β -Hydroxysteroid Dehydrogenase, and Its Expression in Gonadal Tissues. *J. Biol. Chem.* **1998**, *273* (35), 22664–22671.
- (144) He, X.-Y.; Schulz, H.; Yang, S.-Y. A Human Brain L-3-Hydroxyacyl-Coenzyme A Dehydrogenase Is Identical to an Amyloid β -Peptide-Binding Protein Involved in Alzheimer's Disease. *J. Biol. Chem.* **1998**, *273* (17), 10741–10746.
- (145) He, X.-Y.; Merz, G.; Yang, Y.-Z.; Mehta, P.; Schulz, H.; Yang, S.-Y. Characterization and Localization of Human Type10 17 β -Hydroxysteroid Dehydrogenase. *Eur. J. Biochem.* **2001**, *268* (18), 4899–4907.
- (146) Brereton, P.; Suzuki, T.; Sasano, H.; Li, K.; Duarte, C.; Obeyesekere, V.; Haeseleer, F.; Palczewski, K.; Smith, I.; Komesaroff, P.; Krozowski, Z. Pan1b (17 β HSD11)-Enzymatic Activity and Distribution in the Lung. *Mol. Cell. Endocrinol.* **2001**, *171* (1–2), 111–117.
- (147) Chai, Z.; Brereton, P.; Suzuki, T.; Sasano, H.; Obeyesekere, V.; Escher, G.; Saffery, R.; Fuller, P.; Enriquez, C.; Krozowski, Z. 17 β -Hydroxysteroid Dehydrogenase Type XI Localizes to Human Steroidogenic Cells. *Endocrinology* **2003**, *144* (5), 2084–2091.
- (148) Sivik, T.; Vikingsson, S.; Grönlund, H.; Jansson, A. Expression Patterns of 17 β -Hydroxysteroid Dehydrogenase 14 in Human Tissues. *Horm. Metab. Res.* **2012**, *44* (13), 949–956.
- (149) Sivik, T.; Gunnarsson, C.; Fornander, T.; Nordenskjöld, B.; Skoog, L.; Stål, O.; Jansson, A. 17 β -Hydroxysteroid Dehydrogenase Type 14 Is a Predictive Marker for Tamoxifen Response in Oestrogen Receptor Positive Breast Cancer. *PLoS One* **2012**, *7* (7), e40568.
- (150) Lukacik, P.; Keller, B.; Bunkoczi, G.; Kavanagh, K. L.; Lee, W. H.; Hwa Lee, W.; Adamski, J.; Oppermann, U. Structural and Biochemical Characterization of Human Orphan DHRS10 Reveals a Novel Cytosolic Enzyme with Steroid Dehydrogenase Activity. *Biochem. J.* **2007**, *402* (3), 419–427.
- (151) Colette, S.; Defrère, S.; Lousse, J. C.; Van Langendonck, A.; Gotteland, J. P.; Loumaye, E.; Donneze, J. Inhibition of Steroid Sulfatase Decreases Endometriosis in an in Vivo Murine Model.

- Hum. Reprod.* **2011**, *26* (6), 1362–1370.
- (152) Pohl, O.; Bestel, E.; Gotteland, J. P. Synergistic Effects of E2MATE and Norethindrone Acetate on Steroid Sulfatase Inhibition: A Randomized Phase I Proof-of-Principle Clinical Study in Women of Reproductive Age. *Reprod. Sci.* **2014**, *21* (10), 1256–1265.
- (153) PGL2001 Proof of Concept Study in Symptomatic Endometriosis (AMBER)
<https://clinicaltrials.gov/ct2/show/NCT01631981>.
- (154) Stanway, S. J.; Purohit, A.; Woo, L. W. L.; Sufi, S.; Vigushin, D.; Ward, R.; Wilson, R. H.; Stanczyk, F. Z.; Dobbs, N.; Kulinskaya, E.; Elliott, M.; Potter, B. V. L.; Reed, M. J.; Coombes, R. C. Phase I Study of STX 64 (667 Coumate) in Breast Cancer Patients: The First Study of a Steroid Sulfatase Inhibitor. *Clin. Cancer Res.* **2006**, *12* (5), 1585–1592.
- (155) Coombes, R. C.; Cardoso, F.; Isambert, N.; Lesimple, T.; Soulié, P.; Peraire, C.; Fohanno, V.; Kornowski, A.; Ali, T.; Schmid, P. A Phase I Dose Escalation Study to Determine the Optimal Biological Dose of Irosustat, an Oral Steroid Sulfatase Inhibitor, in Postmenopausal Women with Estrogen Receptor-Positive Breast Cancer. *Breast Cancer Res. Treat.* **2013**, *140* (1), 73–82.
- (156) Palmieri, C.; Szydlo, R.; Miller, M.; Barker, L.; Patel, N. H.; Sasano, H.; Barwick, T.; Tam, H.; Hadjiminis, D.; Lee, J.; Shaaban, A.; Nicholas, H.; Coombes, R. C.; Kenny, L. M. IPET Study: An FLT-PET Window Study to Assess the Activity of the Steroid Sulfatase Inhibitor Irosustat in Early Breast Cancer. *Breast Cancer Res. Treat.* **2017**, *166* (2), 527–539.
- (157) Palmieri, C.; Stein, R. C.; Liu, X.; Hudson, E.; Nicholas, H.; Sasano, H.; Guestini, F.; Holcombe, C.; Barrett, S.; Kenny, L.; Reed, S.; Lim, A.; Hayward, L.; Howell, S.; Charles Coombes, R. Correction to: IRIS Study: A Phase II Study of the Steroid Sulfatase Inhibitor Irosustat When Added to an Aromatase Inhibitor in ER-Positive Breast Cancer Patients. *Breast Cancer Res. Treat.* **2018**, *167* (1), 407–407.
- (158) Pautier, P.; Vergote, I.; Joly, F.; Melichar, B.; Kutarska, E.; Hall, G.; Lisyanskaya, A.; Reed, N.; Oaknin, A.; Ostapenko, V.; Zvirbulė, Z.; Chetaille, E.; Geniaux, A.; Shoaib, M.; Green, J. A. A Phase 2, Randomized, Open-Label Study of Irosustat Versus Megestrol Acetate in Advanced Endometrial Cancer. *Int. J. Gynecol. Cancer* **2017**, *27* (2), 258–266.
- (159) Salah, M.; Abdelsamie, A. S.; Frotscher, M. Inhibitors of 17 β -Hydroxysteroid Dehydrogenase Type 1, 2 and 14: Structures, Biological Activities and Future Challenges. *Mol. Cell. Endocrinol.* **2018**.
- (160) Qiu, W.; Campbell, R. L.; Gangloff, A.; Dupuis, P.; Boivin, R. P.; Tremblay, M. R.; Poirier, D.; Lin, S.-X. A Concerted, Rational Design of Type 1 17 β -Hydroxysteroid Dehydrogenase Inhibitors: Estradiol-Adenosine Hybrids with High Affinity. *FASEB J. Off. Publ. Fed. Am. Soc. Exp. Biol.* **2002**, *16* (13), 1829–1831.
- (161) Messinger, J.; Husen, B.; Koskimies, P.; Hirvel, L.; Kallio, L.; Saarenketo, P.; Thole, H. Estrone C15 Derivatives-A New Class of 17 β -Hydroxysteroid Dehydrogenase Type 1 Inhibitors. *Mol. Cell. Endocrinol.* **2009**, *301* (1–2), 216–224.
- (162) Husen, B.; Huhtinen, K.; Poutanen, M.; Kangas, L.; Messinger, J.; Thole, H. Evaluation of Inhibitors for 17 β -Hydroxysteroid Dehydrogenase Type 1 in Vivo in Immunodeficient Mice Inoculated with MCF-7 Cells Stably Expressing the Recombinant Human Enzyme. *Mol. Cell. Endocrinol.* **2006**, *248*, 109–113.
- (163) Delvoux, B.; D’Hooghe, T.; Kyama, C.; Koskimies, P.; Hermans, R. J. J.; Dunselman, G. A.;

- Romano, A. Inhibition of Type 1 17β -Hydroxysteroid Dehydrogenase Impairs the Synthesis of 17β -Estradiol in Endometriosis Lesions. *J. Clin. Endocrinol. Metab.* **2014**, *99* (1), 276–284.
- (164) Company, F. A Study to Investigate the Safety, Tolerability, Food Effect and Pharmacokinetics of FOR-6219 <https://clinicaltrials.gov/ct2/show/NCT03709420>.
- (165) Company, F. TARGETED TREATMENT – HSD17B1 INHIBITOR <https://forendo.com/>.
- (166) HIRVELÄ, L.; Koskimies, P.; Lammintausta, R.; HAKOLA, M.; Eloranta, M. Prodrugs of 17.BETA.-HSD1-Inhibitors, 2015.
- (167) Marchais-Oberwinkler, S.; Wetzel, M.; Ziegler, E.; Kruchten, P.; Werth, R.; Henn, C.; Hartmann, R. W.; Frotscher, M. New Drug-like Hydroxyphenylnaphthol Steroidomimetics as Potent and Selective 17β -Hydroxysteroid Dehydrogenase Type 1 Inhibitors for the Treatment of Estrogen-Dependent Diseases. *J. Med. Chem.* **2011**, *54* (2), 534–547.
- (168) Bey, E.; Marchais-Oberwinkler, S.; Negri, M.; Kruchten, P.; Oster, A.; Klein, T.; Spadaro, A.; Werth, R.; Frotscher, M.; Birk, B.; Hartmann, R. W. New Insights into the SAR and Binding Modes of Bis(Hydroxyphenyl)Thiophenes and -Benzenes: Influence of Additional Substituents on 17β -Hydroxysteroid Dehydrogenase Type 1 (17β -HSD1) Inhibitory Activity and Selectivity. *J. Med. Chem.* **2009**, *52*, 6724–6743.
- (169) Abdelsamie, A. S.; van Koppen, C. J.; Bey, E.; Salah, M.; Börger, C.; Siebenbürger, L.; Laschke, M. W.; Menger, M. D.; Frotscher, M. Treatment of Estrogen-Dependent Diseases: Design, Synthesis and Profiling of a Selective 17β -HSD1 Inhibitor with Sub-Nanomolar IC₅₀ for a Proof-of-Principle Study. *Eur. J. Med. Chem.* **2017**, *127*, 944–957.
- (170) Messinger, J.; Hirvelä, L.; Husen, B.; Kangas, L.; Koskimies, P.; Pentikäinen, O.; Saarenketo, P.; Thole, H. New Inhibitors of 17β -Hydroxysteroid Dehydrogenase Type 1. *Mol. Cell. Endocrinol.* **2006**, *248* (1–2), 192–198.
- (171) Chanplakorn, N.; Chanplakorn, P.; Suzuki, T.; Ono, K.; Chan, M. S. M.; Miki, Y.; Saji, S.; Ueno, T.; Toi, M.; Sasano, H. Increased Estrogen Sulfatase (STS) and 17β hydroxysteroid Dehydrogenase Type I(17β -HSD1) Following Neoadjuvant Aromatase Inhibitor Therapy in Breast Cancer Patients. *Breast Cancer Res. Treat.* **2010**, *120* (3), 639–648.
- (172) Morphy, R.; Rankovic, Z. Designed Multiple Ligands. An Emerging Drug Discovery Paradigm. *J. Med. Chem.* **2005**, *48* (21), 6523–6543.
- (173) Woo, L. W. L.; Bubert, C.; Sutcliffe, O. B.; Smith, A.; Chander, S. K.; Mahon, M. F.; Purohit, A.; Reed, M. J.; Potter, B. V. L. Dual Aromatase-Steroid Sulfatase Inhibitors. *J. Med. Chem.* **2007**, *50* (15), 3540–3560.
- (174) Foster, P. A.; Chander, S. K.; Newman, S. P.; Woo, L. W. L.; Sutcliffe, O. B.; Bubert, C.; Zhou, D.; Chen, S.; Potter, B. V. L.; Reed, M. J.; Purohit, A. A New Therapeutic Strategy against Hormone-Dependent Breast Cancer: The Preclinical Development of a Dual Aromatase and Sulfatase Inhibitor. *Clin. Cancer Res.* **2008**, *14* (20), 6469–6477.

7. Additional publications of the author

7.1 Design and synthesis of conformationally constraint Dyrk1A inhibitors by creating an intramolecular H-bond involving a benzothiazole core

Mohamed Salah*, Mohammad Abdel-Halim* and Matthias Engel

Reprinted with permission *Medchemcomm* 2018, 9 (6), 1045–1053.

DOI: 10.1039/c8md00142a

Copyright (2018) The Royal Chemical Society

* These authors contributed equally

Publication G

Contribution Report

The author contributed significantly to the design concept. He planned, synthesized and characterized all the compounds. He further performed the biological activity assays. The author conceived and wrote the manuscript together with Mohammad Abdel-Halim, who contributed equally.



MedChemComm

RESEARCH ARTICLE

View Article Online
View Journal | View IssueCite this: *Med. Chem. Commun.*,
2018, 9, 1045Received 14th March 2018,
Accepted 27th May 2018

DOI: 10.1039/c8md00142a

rsc.li/medchemcomm

Design and synthesis of conformationally
constraint Dyrk1A inhibitors by creating an
intramolecular H-bond involving a benzothiazole
core†Mohamed Salah, ‡^a Mohammad Abdel-Halim ‡^b and Matthias Engel ‡^{*a}

We present the development of conformationally pre-organised Dyrk1A inhibitors based on the hydroxy-benzothiazole urea scaffold. The modifications introduced to the discovered hit (AHS-211) proved the crucial role of the urea linker to preserve the bioactive conformation and led to the development of compound **b5** as a promising selective Dyrk1A inhibitor.

Introduction

Dyrk1A (the dual-specificity tyrosine phosphorylation-regulated kinase 1A) is a serine/threonine protein kinase that belongs to the DYRK family. The other members in the family are Dyrk1B, Dyrk2, Dyrk3, and Dyrk4. Together with the cyclin-dependent kinases (CDKs), mitogen-activated protein kinases (MAP kinases), glycogen synthase kinases (GSK) and Ccd2-like kinases (CLKs), they compose CMGC super family of kinases.^{1,2}

DYRK1A gene is allocated in the Down syndrome (DS) critical region of chromosome 21. The cognitive impairments and neurofibrillary degeneration seen in DS as well as in Alzheimer's disease (AD) have been found to be associated with Dyrk1A overexpression.^{3–5} Additionally, Dyrk1A was reported to be implicated in numerous biological processes such as T cell regulation,⁶ cell cycle regulation and cell differentiation,^{6,7} stabilization of cytoskeleton,⁸ and brain neurodevelopment.⁹ Drug discovery efforts aim at the development of selective Dyrk1A inhibitors, in particular in light of the putative tumor suppressor activity of the homologous Dyrk2 isoform.¹⁰

In this communication we present 6-hydroxybenzothiazol-2-yl urea as a promising new scaffold for Dyrk1A inhibition that allows pre-organisation of the biologically active conformation. We report some modifications for the scaffold exploration as well as scaffold expansion using an in-house discovered hit (AHS-211, Fig. 1) as a starting compound.

Results and discussion

Compound design

The benzothiazole scaffold was known to be a promising building block for the development of Dyrk1A inhibitors since the discovery of the Dyrk1A/Clk1 inhibitors TG003 and INDY (Fig. 1).^{11,12} The binding mode of the benzothiazole core to the ATP pocket of Dyr1A was determined by X-ray crystallography for INDY;¹² further Dyrk1A co-crystal structures were reported later for acetylated 2-aminobenzothiazole fragments (Fig. 1, structure B).¹³ Both INDY and our previously reported benzothienophene Clk1/Dyrk1A inhibitor¹⁴ (Fig. 1, compound A) contained a hydroxyl group which is important to maintain potency against Dyrk1A. We thought of expanding the hydroxy-benzothiazole scaffold to get potent and selective Dyrk1A inhibitors. To this end, we exploited the benzothiazole ring nitrogen to design and synthesize new derivatives which are rigidized *via* an internal H-bond, avoiding the need to synthesize polycyclic aromatic systems which may have toxicological issues. We envisaged extending the benzothiazole fragment with a urea linker to achieve the desired pseudo 6-membered ring structure

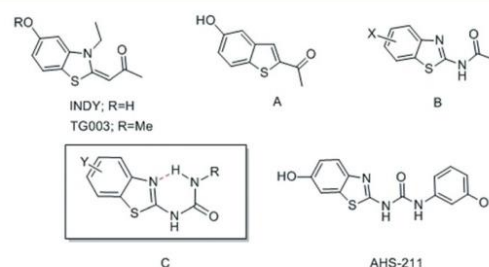


Fig. 1 Previously published benzothiazole- and benzothienophene-based Dyrk1A/Clk1 inhibitors (INDY, TG003, A and B) and new benzothiazole urea derivatives (C and AHS-211).

^a Pharmaceutical and Medicinal Chemistry, Saarland University, Campus C2.3, D-66123 Saarbrücken, Germany.

E-mail: ma.engel@mx.uni-saarland.de; Web: <http://www.pharmmedchem.de>;
Fax: +49 681 302 70308; Tel: +49 681 302 70312

^b Department of Pharmaceutical Chemistry, Faculty of Pharmacy and Biotechnology, German University in Cairo, Cairo 11835, Egypt

† Electronic supplementary information (ESI) available. See DOI: 10.1039/c8md00142a

‡ Both authors contributed equally to this work.

Research Article

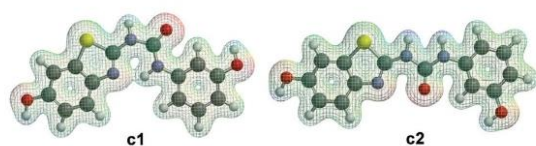


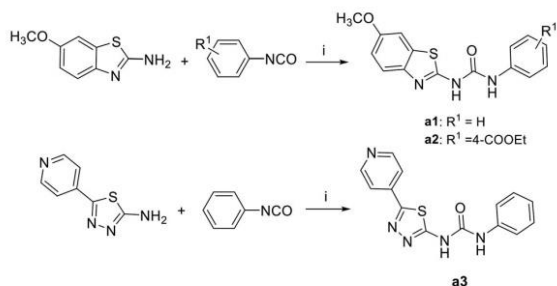
Fig. 2 Lowest energy conformer (**c1**) and the higher energy linear conformer (**c2**) of the benzothiazole urea scaffold, exemplified by hit compound AHS-211, as calculated by the B3LYP density functional method. Shown are the fully coplanar conformers with a mesh displaying the electrostatic potential on an isoelectronic density surface (0.025 e a^{-3}). The intramolecular H-bond that stabilizes a pseudo 6-membered ring in **c1** is indicated by the overlapping electron density in the center. The calculated energy difference between the conformers is 59 kJ mol^{-1} .

between the benzothiazole nitrogen (as HBA) and the distant urea NH (as HBD) as shown in structure **C** Fig. 1. Using *ab initio* calculations, it was corroborated that the suggested benzothiazole urea scaffold showed the proposed pseudo-ring formation in the most stable conformer (conformer **c1**, Fig. 2). In contrast, a considerably higher energy content was calculated for the also coplanar rotamer **c2** ($\Delta E = 59 \text{ kJ mol}^{-1}$, Fig. 2), probably attributable to the lack of the energetically favourable H-bond as well as to the unfavourable polar repulsion between the endocyclic nitrogen and the urea oxygen (*cf.* **c2**, Fig. 2).

Searching in our in-house library for possible hits that may overlap with the designed target urea derivatives revealed the previously published compound AHS-211 as a good candidate. AHS-211 (compound **23** in ref. 15) was previously published as an inactive compound against 17β -hydroxysteroid dehydrogenase type 1 (17β HSD1).¹⁵ Testing AHS-211 against Dyrk1A greatly supported our design concept as it inhibited the recombinant enzyme with an IC_{50} of $0.134 \mu\text{M}$. AHS-211 also inhibited Dyrk1B with an IC_{50} of $0.37 \mu\text{M}$, yielding a selectivity factor of 2.7 for Dyrk1A (Table 2). Furthermore, AHS-211 showed 64.7% inhibition when screened against Dyrk2 at $5 \mu\text{M}$ concentration (Table 2).

Chemistry

The synthesis of the designed urea derivatives was performed mainly through the reaction of the aryl amine derivatives

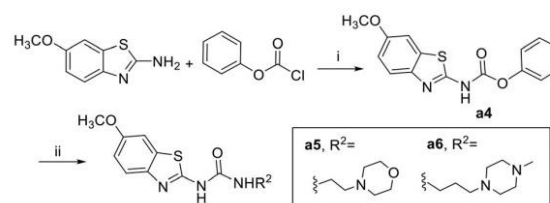


Scheme 1 Synthesis of urea derivatives via isocyanates. Reagents and conditions: (i) DMF, RT, overnight.

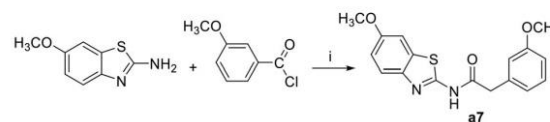
with phenylisocyanates in DMF at room temperature (Scheme 1), or alternatively through the reaction of 2-amino-6-methoxy benzothiazole with phenylchloroformate in the presence of pyridine as a base and dioxane as solvent to give the carbamate compound **a4** which is itself was isolated as the oxygen isostere of urea or further reacted *in situ* with amine derivatives in refluxing dioxane to give the urea compounds (**a5** and **a6**) as shown in Scheme 2. Acylation of 2-amino-6-methoxybenzothiazole was done in acetone in presence of K_2CO_3 to yield the methylene isostere of urea (Scheme 3). Scheme 4 shows the preparation of the amide derivatives starting from the ester **a2** which was hydrolysed to the respective carboxylic acid **a8** under alkaline conditions followed by amide coupling with benzyl amine or 1-methylpiperazine using HBTU as coupling agent. Finally, the methyl ether dealkylation was performed using BBr_3 in dichloromethane (Scheme 5).

Biological evaluation

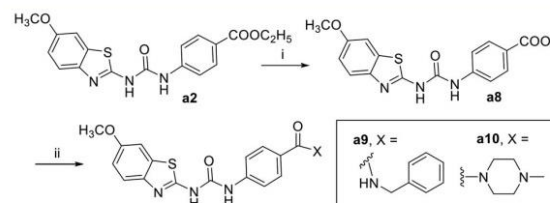
Table 1 shows the screening results of the synthesized methoxy precursors against both Dyrk1A and Dyrk1B while Table 2 shows the screening results for the phenolic analogues against Dyrk1A, Dyrk1B and Dyrk2. As can be seen, the 6-methoxy precursors showed a huge reduction of



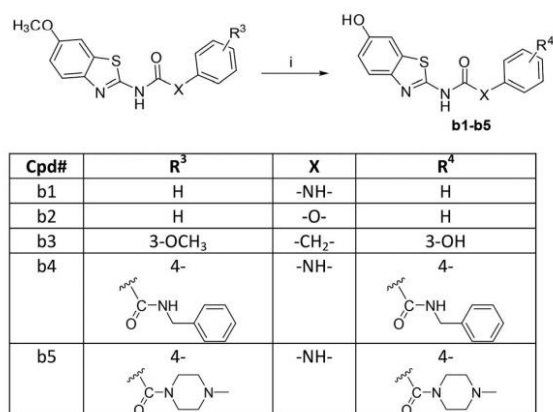
Scheme 2 Synthesis of urea derivatives via carbamates. Reagents and conditions: (i) dioxane, pyridine, RT, 1 h (ii) 1.5 equiv. amine derivative, dioxane, overnight, reflux.



Scheme 3 Synthesis of benzothiazoleamide. Reagents and conditions: (i) acetone, Na_2CO_3 , ice cooling then RT, 1 h.



Scheme 4 Synthesis of the benzamide derivatives. Reagents and conditions: (i) aq. KOH, THF, RT, 14 h (ii) 4 equiv. amine derivative, 1.5 equiv. HBTU, TEA, RT, overnight.



Scheme 5 Ether dealkylation. Reagents and conditions: (i) 15 equiv. BBr₃, CH₂Cl₂, -78 °C then room temperature, 20 h.

potency when compared to their 6-hydroxy analogues, indicating that the 6-hydroxyl (born at the benzothiazole) in AHS-

Table 1 Inhibition of Dyrk1A and Dyrk1B by the methoxy precursors and compound **a3**

| Cpd# | X | Y | Dyrk1A % inhibition at 0.5 μM ^a | Dyrk1B % inhibition at 0.5 μM ^a |
|------|--------------------|---|--|--|
| a1 | -NH- | | 8 | 0 |
| a3 | -NH- | | 19.6 | 12 |
| a4 | -O- | | 13.3 | 0 |
| a5 | -NH- | | 13.8 | 0 |
| a6 | -NH- | | 20.3 | 0 |
| a7 | -CH ₂ - | | 21.2 | 25 |
| a8 | -NH- | | 25.5 | 0 |
| a9 | -NH- | | 30.5 | 0 |
| a10 | -NH- | | 28.1 | 0 |

^a Values are mean values of at least two independent experiments each was done in duplicates; standard deviation <10%. The ATP concentration in the assay was 15 μM.

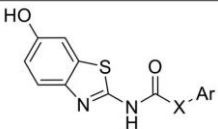
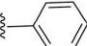
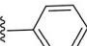
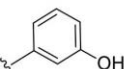
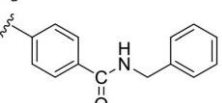
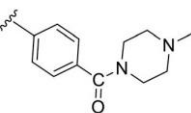
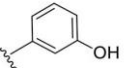
211 has a crucial share in binding to Dyrk1A as HBD function; in fact, none of the 6-methoxy derivatives exhibited more than 31% inhibition at 2 μM of the tested compounds (Table 1). Likewise, compound **a3**, in which the 6-hydroxybenzothiazole moiety was replaced by 5-pyridylthiadiazole, did not show significant activity. In this analogue, the internal H-bond is expected to be conserved and the pyridine nitrogen lies in a similar distance from the urea linker as the 6-methoxy oxygen, thus enabling a similar potential role as HBA; nevertheless, the lack of the HBD impeded the success of this modification.

In contrast, the deletion of the 3-hydroxyl (at the phenyl ring) in AHS-211 almost did not influence the activity, as observed with compound **b1** (IC₅₀ = 0.163 μM against Dyrk1A). Of note, the latter change reduced the potency against Dyrk1B, increasing the selectivity factor to 4.3 toward Dyrk1B, and also reduced the off-target activity against Dyrk2 when compared with the hit AHS-211 (Table 2).

Compounds **b2–b3** were prepared to prove the importance of the urea linker in maintaining the biologically active conformation; in these compounds, the -NH- assumed to act as HBD and help the pseudo ring formation was replaced by the isosteric -O- and -CH₂-, respectively. Compound **b2** gave no inhibition for Dyrk1A and Dyrk1B at 0.5 μM while its urea analogue **b1** showed more than 80% inhibition at the same concentration (Table 2). Since the carbamate-derivative **b2** was least likely to adopt a coplanar conformation similar to **c1** (Fig. 2) because of the electronic repulsion between the oxygen and the ring nitrogen, the complete loss of inhibitory activity supported our hypothesis that the biological activity was associated with a **c1**-like molecule shape. In further accordance, the more neutral electrostatic potential of the methylene bridge in **b3** led to a partial recovery of the inhibitory potency, but failed to reach the potency of AHS-211 due to the lack of the conformation-stabilizing H-bond. Of interest, compound **b3** showed its highest inhibitory potency against Dyrk2 (IC₅₀ ≈ 5 μM, [ATP] = 100 μM), probably due to the additional presence of the *m*-hydroxy function at the phenyl, which also enhanced the Dyrk2 inhibitory activity of AHS-211 (Table 2).

Having proven the crucial role of the urea motif, we envisaged some substantial modifications of compound **b1** to improve potency and selectivity for Dyrk1A; further attempts aimed at optimization of the drug-like properties, such as water solubility and log *P*. To achieve this, two main types of modifications were planned: the first one was to replace the phenyl ring in **b1** with an alkyl chain linked to a basic alicyclic amine like morpholine and *N*-methyl piperazine. This is represented by the 6-methoxy precursors **a5** and **a6**, respectively. Unfortunately, the unsuccessful *O*-demethylation of both compounds hampered testing the effect of such a modification. However, the inhibition noted for these two precursors at 0.5 μM did not indicate a potential advantage over the other modifications presented in Table 1. The second approach was to extend compound **b1** through amide derivatives arising from the phenyl ring. Two amide derivatives

Table 2 Inhibition of Dyrk1A, Dyrk1B and Dyrk2 by the phenolic analogues

|  | | | | | | | | |
|---|--------------------|--|---|--------------------------------------|---|--------------------------------------|---------------------------------|---------------------------------------|
| Cpd# | X | Ar | Dyrk1A | | Dyrk1B | | Selectivity factor ^c | Dyrk2 |
| | | | % inhibition at 0.5 $\mu\text{M}^{a,b}$ | IC_{50} $\mu\text{M}^{a,b}$ | % inhibition at 0.5 $\mu\text{M}^{a,b}$ | IC_{50} $\mu\text{M}^{a,b}$ | | % inhibition at 5 $\mu\text{M}^{a,d}$ |
| b1 | –NH– |  | 80.8 | 0.163 | 43.6 | 0.710 | 4.3 | 40.4 |
| b2 | –O– |  | 0 | ND | 0 | ND | — | 18.6 |
| b3 | –CH ₂ – |  | 37.8 | ND | 0 | ND | — | 50.1 |
| b4 | –NH– |  | 89.8 | 0.063 | 69 | 0.130 | 2.1 | 38.1 |
| b5 | –NH– |  | 99.1 | 0.095 | 21 | 1.513 | 16 | 34.5 |
| AHS-211 | –NH– |  | 74.4 | 0.134 | 54.6 | 0.370 | 2.8 | 64.7 |

^a Values are mean values of at least two independent experiments each was done in duplicates; standard deviation <10%. ^b The assay was carried out at ATP conc. of 15 μM . ^c Selectivity factor: IC_{50} (Dyrk1B)/ IC_{50} (Dyrk1A). ^d The assay was carried out at ATP conc. of 100 μM .

offering diverse possible interactions with the binding site were prepared: the benzyl amide **b4** and the methyl piperazine amide **b5**. Although the extension with the 4-benzyl amide in compound **b4** enhanced the potency toward Dyrk1A (IC_{50} = 0.063 μM) by more than 2-fold compared with **b1** and AHS-211, it did not show any improvement in selectivity over Dyrk1B (Table 2). On the other hand, compound **b5** was almost similar to AHS-211 in potency against Dyrk1A, yet, it showed more than 15 fold selectivity for Dyrk1A over Dyrk1B. Importantly, both **b4** and **b5** displayed superior selectivity for Dyrk1A over Dyrk2 when compared with AHS-211.

As compound **b5** was more selective over Dyrk1B, it was selected for an extended selectivity profiling against all kinases that were frequently reported as being co-inhibited by previously published Dyrk1A inhibitor classes (Table 3).^{16–18} This profiling revealed that our combination of modifications led to a significant increase in selectivity compared with the previously published benzothiazole-based Dyrk1A inhibitors such as INDY, which strongly inhibited, among other kinases, Dyrk2, PIM1 and CK1 δ .¹²

Additionally, **b5** displayed good selectivity for Dyrk1A over Clk1, one of the most common off targets of many reported Dyrk1A inhibitors, with a selectivity factor >7 (IC_{50} of **b5** against Clk1 = 730 nM, [ATP] = 15 μM).

Because of its marked selectivity and good potency, we aimed at analyzing the metabolic stability of **b5** against human hepatic CYP enzymes. Compared to testosterone, which was included as a reference known to be rapidly metabolized, **b5** showed a promising stability (half-life >60 min, Table 4). It is worth mentioning that at 60 min incubation time, 88% of the initial compound concentration could be still detected.

These data were encouraging, suggesting that **b5** might also be applicable in *in vivo* models. As it was expected, compound **b4** exhibited lower, yet, appreciable stability toward hepatic CYP enzymes with a metabolic half-life of 33 min

Table 3 Selectivity profile of **b5** vs. the related kinases^a

| Kinase | % inhibition at 5 μM | Kinase | % inhibition at 5 μM |
|--------------|---------------------------------|----------------|---------------------------------|
| CDK5/p25 | 2 \pm 1 | Haspin | 1 \pm 1 |
| CLK1 | 72 \pm 0.5 | PIM1 | 29 \pm 2.5 |
| CK1 δ | 9 \pm 2 | SRPK1 | 5 \pm 0.5 |
| HIPK1 (Myak) | 50 \pm 0.5 | MLCK (MLCK2) | 45 \pm 3 |
| NTRK2 (TRKB) | 13 \pm 1 | STK17A (DRAK1) | 39 \pm 0 |
| Dyrk1A | 85 \pm 0.5 | | |

^a Values are mean values of at least two duplicates; testing was done at an ATP concentration of 100 μM .

MedChemComm

View Article Online

Research Article

Table 4 Metabolic stability of compounds **4b** and **5b** against human CYP enzymes

| Cpd. | Half-life [min] ^a |
|---------------------------|------------------------------|
| b4 | 33 |
| b5 | >60 |
| Testosterone ^b | 9.6 |

^a Incubation with pooled human liver S9 fraction at 37 °C; samples taken at 0, 15, 30, 60 min, determination of the parent compound by MS. ^b Reference compound with low metabolic stability.

which is mostly attributed to the presence of the unsubstituted benzyl group (Table 4).

Next we aimed at identifying the putative binding mode of **b5** to Dyrk1A in order to explain its high potency and selectivity. To this end, we employed molecular docking to Dyrk1A coordinates derived from a co-crystal structure with a 5-hydroxy benzothiazole fragment (PDB code: 5A3X). Thus, we anticipated that any realistic docking pose should exhibit a significant overlap with the original co-crystallized fragment; this was the case with the docking pose showing the highest score (depicted in Fig. 3). Another criterion for plausibility was that **b5** was binding in the H-bond-stabilized low energy conformation, which was in full agreement with the observed structure–activity relationships and the *ab initio* calculations. The docking model predicts several classical and non-classical H-bonds contributing to the binding affinity inside the ATP pocket (Fig. 3A). Of note, because of the shifted position, the 6-hydroxy function was only acting as an HBD, thus explaining the loss of potency seen with the methoxy precursors.

Noteworthy, Rothweiler *et al.* had identified an alternative binding mode, inverted by 180°, with a 5-methoxy-benzothiazole fragment in the ATP binding pocket of Dyrk1A.¹³ Using the corresponding crystal structure coordinates (PDB: 5A4E) we also evaluated the possibility of an inverted binding mode for our best compound **b5**. Indeed, we found that theoretically, binding of **b5** might also occur in a flipped orientation, with the hydroxyl then forming an H-bond with Asp307 (Fig. S1, ESI†). However, we considered this inverted pose to be less likely, because it did not well explain the drop of potency observed with the methoxy precursor **a10** (28% inhibition at 0.5 μM, Table 1). With **a10**, the H-bond interaction in the hypothetical flipped mode simply switched from Asp307 to Lys188, now with the methoxy oxygen as acceptor (not shown). Thus, the binding pose shown in Fig. S1,† although it cannot be totally ruled out, would predict a comparable potency for **b5** and **a10**, in contrast to our experimental results.

An important structural feature enhancing the selectivity over Dyrk1B was the amide-linked *N*-methyl piperazine extension, which was predicted to engage in an ionic interaction with Asp287 in our model. Although this residue is conserved in Dyrk1B, it could be speculated that its position is slightly shifted in the Dyrk1B 3D structure, thus causing a less efficient ionic interaction. Such a shift in the spatial position of

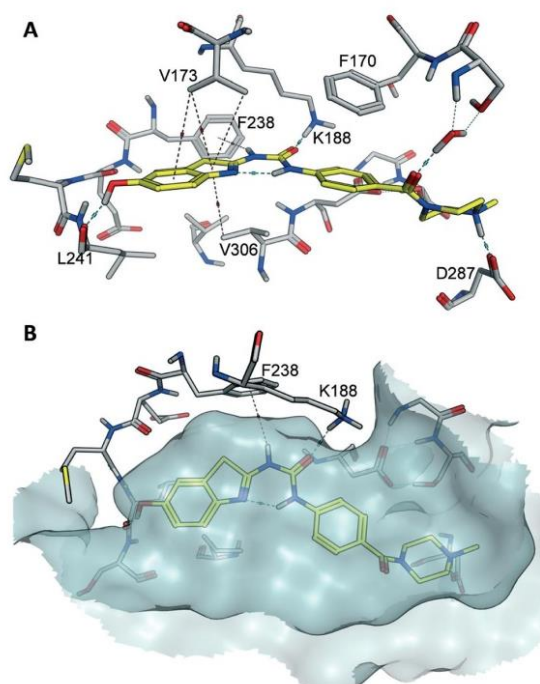


Fig. 3 Predicted binding mode of **b5** in the ATP binding pocket of Dyrk1A. Compound **b5** was docked to the Dyrk1A coordinates derived from the co-crystal structure with 2-acetamido-5-hydroxy benzothiazole (PDB code: 5A3X) using MOE. The pose with the highest score is depicted, showing binding of **b5** (yellow) in the lowest energy conformation of the scaffold (cf. c1, Fig. 2). **A**. Inside the pocket, the ligand is anchored via two crucial H-bonds involving the backbone carbonyl of the hinge region residue Leu241, and the conserved Lys188 as a donor. Several CH–π and an NH–π interaction (with Phe238) additionally enhance the affinity. At the border of the pocket, the protonated piperazine amine is predicted to form a salt bridge with Asp287. H-bonds and ionic bonds are indicated by blue lines and H–π bonds by brown lines. **B**. Top view on the ATP binding pocket visualized by a transparent surface. The ligand is bound as in **A**; through the central pseudo 6-membered ring, ideal shape complementarity to the pocket is achieved.

the corresponding Asp257 can be observed in the X-ray structures of the homologous Dyrk2 (data not shown), however, it cannot be verified with Dyrk1B due to the lack of a published 3D structure.

Conclusion

Our design concept of attaching a urea linker to the benzothiazole core, followed by a scaffold expansion, led to a new class of potent and selective Dyrk1A inhibitors. Of note, the best compound, **b5**, did not appreciably inhibit the homologous Dyrk2 isoform and even showed a remarkable 15 fold selectivity over the most closely related isoform Dyrk1B. In addition, the activity toward the atypical kinase haspin that was strongly inhibited by most of the previously reported Dyrk1A inhibitors was completely abolished with **b5**.

Together with the favorable balance of lipophilic/hydrophilic functions, further testing of **b5** as a potential agent for the treatment of Dyrk1A-related neuropathological disorders can be envisaged.

Experimental section

Chemistry

Solvents and reagents were obtained from commercial suppliers and used as received. A Bruker DRX 500 spectrometer was used to obtain ^1H NMR and ^{13}C NMR spectra, in some cases Bruker Fourier 300 was used. The chemical shifts are referenced to the residual protonated solvent signals. At least 95% purity in all the tested compounds was obtained by means of HPLC coupled with mass spectrometry. Mass spectra (HPLC-ESI-MS) were obtained using a TSQ quantum (Thermo Electron Corporation) instrument prepared with a triple quadrupole mass detector (Thermo Finnigan) and an ESI source. All samples were inserted using an autosampler (Surveyor, Thermo Finnigan) by an injection volume of 10 μL . The MS detection was determined using a source CID of 10 V and carried out at a spray voltage of 4.2 kV, a nitrogen sheath gas pressure of 4.0×10^5 Pa, a capillary temperature of 400 $^\circ\text{C}$, a capillary voltage of 35 V and an auxiliary gas pressure of 1.0×10^5 Pa. The stationary phase used was a RP C18 NUCLEODUR 100-3 (125 \times 3 mm) column (Macherey-Nagel). The solvent system consisted of water containing 0.1% TFA (A) and 0.1% TFA in acetonitrile (B). HPLC-method: flow rate 400 $\mu\text{L min}^{-1}$. The percentage of B started at an initial of 5%, was increased up to 100% during 16 min, kept at 100% for 2 min, and flushed back to 5% in 2 min. High resolution precise mass spectra were recorded on Thermo Fisher Scientific (TF, Dreieich, Germany) Q Exactive Focus system equipped with heated electrospray ionization (HESI)-II source and Xcalibur software (version 4.0.27.19). Before analysis external mass calibration was done according to the manufacturer's recommendations. The samples were dissolved and diluted in methanol in a concentration of 3 μM and directly injected into the Q Exactive Focus using the integrated syringe pump. All the data analyses were done in positive ion mode using voltage scans and the data collected in continuous mode. Melting points were determined using a Mettler FP1 melting point apparatus and are uncorrected.

General procedure for synthesis of urea derivatives

Method A. A solution of the aryl amine (2 mmol) and the respective isocyanate derivative (2.4 mmol) in DMF (10 mL) was left to stir at room temperature for 3 h. The product was precipitated by adding a 50 mL of ice/water mixture then purified with column chromatography.

Method B. To a solution of 6-methoxy-2-aminobenzothiazole (0.36 gm, 2 mmol) in dioxane (6 mL) containing pyridine (179 μL , 2.22 mmol) phenyl chloroformate (0.25 mL, 2 mmol) was added dropwise at room temperature. After 10 min, the carbamate derivative **a4** precipitated, then the corresponding amine derivative (2 mmol) was

added and the reaction mixture was heated to 100 $^\circ\text{C}$ for 5 h. After cooling to room temperature, the reaction mixture was diluted with ethyl acetate and washed with water. The combined organic layers were dried over anhydrous MgSO_4 and concentrated under reduced pressure. The residue was purified with column chromatography to give the desired compounds. Compound **a4** was isolated by filtration in case of the carbamate is needed as a product to be tested or for further demethylation.

Phenyl (6-methoxybenzo[d]thiazol-2-yl)carbamate (a4). The carbamate derivative was isolated by filtration as mentioned above. White solid; yield: 88%; mp >300 $^\circ\text{C}$; ^1H NMR (500 MHz, DMSO) δ 9.34 (s, 1H), 7.63 (d, J = 8.8 Hz, 1H), 7.58 (d, J = 2.6 Hz, 1H), 7.49–7.43 (m, 2H), 7.40 (d, J = 8.8 Hz, 1H), 7.35–7.25 (m, 2H), 7.02 (td, J = 8.7, 2.6 Hz, 1H), 3.80 (s, 3H); MS (ESI): m/z = 301.12 ($\text{M} + \text{H}$) $^+$.

1-(6-Methoxybenzo[d]thiazol-2-yl)-3-phenylurea (a1). The title compound was prepared according to the general procedure for synthesis of urea derivatives (method A) by the reaction of 2-amino-6-methoxybenzothiazole and phenylisocyanate. White solid; yield: 78%; mp 201–202 $^\circ\text{C}$; ^1H NMR (500 MHz, DMSO) δ 10.64 (s, 1H), 9.12 (s, 1H), 7.55 (t, J = 9.2 Hz, 1H), 7.54–7.44 (m, 3H), 7.39–7.25 (m, 2H), 7.08–7.01 (m, 1H), 6.98 (dd, J = 8.8, 2.6 Hz, 1H), 3.80 (s, 3H); ^{13}C NMR (126 MHz, DMSO) δ 157.32, 155.67, 151.73, 142.83138.47, 132.48, 128.91, 122.88, 120.15, 118.75, 114.36, 104.92, 55.58; MS (ESI): m/z = 300.14 ($\text{M} + \text{H}$) $^+$.

Ethyl 4-(3-(6-methoxybenzo[d]thiazol-2-yl)ureido)benzoate (a2). The title compound was prepared according to the general procedure for synthesis of urea derivatives (method A) by the reaction of 2-amino-6-methoxybenzothiazole and 4-(ethoxycarbonyl)phenylisocyanate. White solid; yield: 73%; mp 290–291 $^\circ\text{C}$; ^1H NMR (500 MHz, DMSO) δ 10.73 (s, 1H), 9.51 (s, 1H), 8.02–7.87 (m, 2H), 7.76–7.62 (m, 2H), 7.66 (d, J = 8.5 Hz, 2H), 6.99 (dd, J = 8.8, 2.6 Hz, 1H), 4.29 (q, J = 7.1 Hz, 2H), 3.80 (s, 3H), 1.31 (t, J = 7.1 Hz, 3H); MS (ESI): m/z = 372.02 ($\text{M} + \text{H}$) $^+$.

1-Phenyl-3-(5-(pyridin-4-yl)-1,3,4-thiadiazol-2-yl)urea (a3). The title compound was prepared according to the general procedure for synthesis of urea derivatives (method A) by the reaction of 5-(pyridin-4-yl)-1,3,4-thiadiazol-2-amine and phenylisocyanate. White solid; yield: 88%; mp 153–154.5 $^\circ\text{C}$; ^1H NMR (500 MHz, DMSO) δ 11.34 (s, 1H), 9.11 (s, 1H), 8.72 (dd, J = 4.4, 1.7 Hz, 2H), 7.88 (dd, J = 4.5, 1.7 Hz, 2H), 7.51 (d, J = 7.6 Hz, 2H), 7.42–7.25 (m, 2H), 7.16–6.98 (m, 1H); ^{13}C NMR (126 MHz, DMSO) δ 161.25, 158.83, 151.37, 150.68, 138.21, 137.19, 128.94, 123.19, 120.53, 118.90; MS (ESI): m/z = 297.80 ($\text{M} + \text{H}$) $^+$.

1-(6-Methoxybenzo[d]thiazol-2-yl)-3-(2-morpholinoethyl)urea (a5). The title compound was prepared according to the general procedure for synthesis of urea derivatives (method B) using 4-(2-aminoethyl)morpholine. Beige solid; yield: 68%; mp 179–181 $^\circ\text{C}$; ^1H NMR (500 MHz, DMSO) δ 10.64 (s, 1H), 7.52–7.48 (m, 1H), 7.47 (d, J = 2.6 Hz, 1H), 6.94 (dd, J = 8.8, 2.6 Hz, 1H), 6.77 (s, 1H), 3.78 (s, 3H), 3.64–3.54 (m, 4H), 3.28 (dd, J = 11.8, 6.1 Hz, 2H), 2.46–2.34 (m, 6H); ^{13}C NMR (126

MHz, DMSO) δ 157.87, 155.46, 153.77, 143.22, 132.56, 120.12, 114.07, 104.80, 66.17, 57.27, 55.55, 53.11, 36.15; MS (ESI): m/z = 337.04 ($M + H$)⁺.

1-(6-Methoxybenzo[d]thiazol-2-yl)-3-(3-(4-methylpiperazin-1-yl)propyl)urea (a6). The title compound was prepared according to the general procedure for synthesis of urea derivatives (method B) using 1-(3-aminopropyl)-4-methylpiperazine. White solid; yield: 61%; mp 192–194 °C; ¹H NMR (500 MHz, DMSO) δ 10.76 (s, 1H), 7.47 (dd, J = 15.2, 5.7 Hz, 2H), 7.12 (s, 1H), 6.94 (dd, J = 8.8, 2.6 Hz, 1H), 3.78 (s, 3H), 3.42–3.31 (m, 4H), 3.17 (dd, J = 12.6, 6.5 Hz, 2H), 2.48–2.39 (m, 4H), 2.34 (dd, J = 17.2, 10.0 Hz, 2H), 2.25 (s, 3H), 1.66–1.56 (m, 2H); ¹³C NMR (126 MHz, DMSO) δ 157.78, 155.41, 150.70, 143.22, 132.59, 120.05, 114.01, 104.78, 62.59, 55.55, 54.89, 54.10, 52.01, 44.99, 26.44; MS (ESI): m/z = 363.99 ($M + H$)⁺.

N-(6-Methoxy-benzothiazol-2-yl)-2-(3-methoxy-phenyl)-acetamide (a7). 3-Methoxyphenylacetyl chloride (0.18 g, 1 mmol) was added gradually to a stirred solution of 6-methoxy-2-aminobenzothiazole (0.16 g, 1 mmol) and Na₂CO₃ (0.16 g, 1.5 mmol) in acetone (20 mL) under ice cooling. The mixture was stirred at room temperature under a nitrogen atmosphere for 2 h then added to 100 mL of water/ice mixture, the solid obtained was separated by filtration followed by column chromatography purification to give the title compound as a white solid; yield: 82%; mp 151–152 °C; ¹H NMR (500 MHz, DMSO) δ 12.44 (s, 1H), 7.63 (d, J = 8.8 Hz, 1H), 7.55 (d, J = 2.5 Hz, 1H), 7.25 (t, J = 7.9 Hz, 1H), 7.02 (dd, J = 8.8, 2.6 Hz, 1H), 6.92 (dd, J = 9.4, 4.9 Hz, 2H), 6.84 (dd, J = 7.9, 2.2 Hz, 1H), 3.79 (s, 3H), 3.77 (s, 2H), 3.75 (s, 3H); ¹³C NMR (126 MHz, DMSO) δ 169.72, 159.24, 156.11, 155.83, 142.57, 136.13, 132.71, 129.42, 121.47, 121.10, 115.11, 114.89, 112.23, 104.68, 55.57, 54.97, 41.83; MS (ESI): m/z = 329.19 ($M + H$)⁺.

4-(3-(6-Methoxybenzo[d]thiazol-2-yl)ureido)benzoic acid (a8). The compound was prepared by alkaline ester hydrolysis of compound a2 where 2 M aqueous potassium hydroxide solution (10 mL) was added to a stirred solution of a2 (1 mmol) in THF (50 mL). After stirring at room temperature for 14 h the solvent was evaporated under reduced pressure. The residue was diluted with water (20 mL) and the solution was acidified using 2 M HCl. The product was extracted with ethylacetate (3 × 15 mL). The organic layers were combined and dried over MgSO₄ followed by evaporation of solvent under reduced pressure to give the crude product that was used directly for the next steps without further purification. White solid; yield: 93%; mp 284–286 °C; ¹H NMR (300 MHz, DMSO) δ 11.10 (s, 1H), 10.41 (s, 1H), 7.93 (t, J = 6.0 Hz, 2H), 7.67 (d, J = 8.8 Hz, 2H), 7.59 (d, J = 8.8 Hz, 1H), 7.52 (t, J = 4.0 Hz, 1H), 6.99 (dd, J = 8.8, 2.6 Hz, 1H), 3.81 (s, 3H); MS (ESI): m/z = 343.95 ($M + H$)⁺.

General procedure for amide synthesis

The appropriate amine (4 equiv.) was added dropwise to the solution of the benzoic acid derivative (a8) (0.34 g, 1 mmol), HBTU (0.57 g, 1.5 mmol) and TEA (0.5 mL) in DCM (20 mL).

The reaction mixture was stirred at room temperature overnight. The solvent was evaporated under reduced pressure. The residue was partitioned between 50 mL of ethyl acetate and 20 mL of water, and the aqueous layer was extracted with 20 mL of ethyl acetate (over 3 times). The combined organic extracts were dried over anhydrous MgSO₄, the solvent was removed under reduced pressure, and the product was purified by column chromatography to give the described amide derivative.

N-Benzyl-4-(3-(6-methoxybenzo[d]thiazol-2-yl)ureido)-benzamide (a9). The title compound was prepared according to the general procedure for amide synthesis using benzylamine. White solid; yield: 64%; mp 284–286 °C; ¹H NMR (300 MHz, DMSO) δ 10.76 (s, 1H), 9.39 (s, 1H), 8.94 (t, J = 5.9 Hz, 1H), 7.90 (d, J = 8.7 Hz, 2H), 7.67–7.50 (m, 4H), 7.36–7.30 (m, 4H), 7.25 (dq, J = 6.0, 4.1 Hz, 1H), 7.00 (dd, J = 8.8, 2.6 Hz, 1H), 4.49 (d, J = 6.0 Hz, 2H), 3.81 (s, 3H); MS (ESI): m/z = 433.04 ($M + H$)⁺.

1-(6-Methoxybenzo[d]thiazol-2-yl)-3-(4-(4-methylpiperazine-1-carbonyl)phenyl)urea (a10). The title compound was prepared according to the general procedure for amide synthesis using *N*-methylpiperazine. White solid; yield: 72%; mp 284–286 °C; ¹H NMR (500 MHz, DMSO) δ 10.83 (s, 1H), 9.41 (s, 1H), 7.57 (ddd, J = 11.9, 6.6, 3.6 Hz, 3H), 7.52 (d, J = 2.6 Hz, 1H), 7.41–7.33 (m, 2H), 6.99 (dd, J = 8.8, 2.6 Hz, 1H), 3.79 (s, 3H), 3.48 (s, 4H), 2.35 (s, 4H), 2.22 (s, 3H); ¹³C NMR (126 MHz, DMSO) δ 168.74, 157.74, 155.71, 152.27, 141.75, 139.85, 132.25, 129.78, 128.19, 119.84, 118.11, 114.41, 104.98, 55.58, 54.41, 45.70, 45.43; MS (ESI): m/z = 426.03 ($M + H$)⁺.

General procedure for ether dealkylation

1 M BBr₃ solution in CH₂Cl₂ (15 equiv.) was added dropwise via syringe under nitrogen to a stirred solution of the methyl ether derivative (1 equiv.) in CH₂Cl₂ at –78 °C. Then the reaction was maintained at –78 °C for 1 hour, after that allowed to reach room temperature and stirred for an additional 20 h. The mixture was cooled to 0 °C and H₂O was carefully added (15–25 mL). The product was then repeatedly extracted with EtOAc and the organic layers were dried over anhydrous Na₂SO₄. Upon solvent removal the residue was purified by column chromatography.

1-(6-Hydroxybenzo[d]thiazol-2-yl)-3-phenylurea (b1). The title compound was prepared by demethylation of compound a1 according to the general procedure for ether dealkylation. Off-white solid; yield: 83%; mp 260–262 °C; ¹H NMR (500 MHz, CDCl₃) δ 10.57 (s, 1H), 9.44 (s, 1H), 9.12 (s, 1H), 7.54–7.40 (m, 3H), 7.33 (t, J = 7.9 Hz, 2H), 7.23 (d, J = 2.2 Hz, 1H), 7.03 (dd, J = 17.6, 10.3 Hz, 1H), 6.84 (dd, J = 8.7, 2.4 Hz, 1H); MS (ESI): m/z = 286.08 ($M + H$)⁺; HRMS m/z = 286.0627 (calculated = 286.0645).

Phenyl (6-hydroxybenzo[d]thiazol-2-yl)carbamate (b2). The title compound was prepared by demethylation of compound a4 according to the general procedure for ether dealkylation. White solid; yield: 68%; mp 119–120 °C; ¹H NMR (300 MHz, DMSO) δ 12.36 (s, 1H), 9.52 (s, 1H), 7.53 (d, J = 8.7 Hz, 1H),

7.45 (dt, $J = 10.6, 2.2$ Hz, 2H), 7.35–7.24 (m, 4H), 6.88 (dd, $J = 8.7, 2.5$ Hz, 1H); MS (ESI): $m/z = 286.98$ ($M + H$)⁺; HRMS $m/z = 287.0466$ (calculated = 287.0485).

N-(6-Hydroxybenzo[d]thiazol-2-yl)-2-(3-hydroxyphenyl)-acetamide (b3). The title compound was prepared by demethylation of compound a7 according to the general procedure for ether dealkylation. Beige powder; yield: 70%; mp 227–228 °C; ¹H NMR (500 MHz, DMSO) δ 12.36 (s, 1H), 9.52 (s, 1H), 9.37 (s, 1H), 7.54 (dd, $J = 8.5, 5.9$ Hz, 1H), 7.26 (q, $J = 2.5$ Hz, 1H), 7.09 (dt, $J = 25.2, 12.8$ Hz, 1H), 6.92–6.81 (m, 1H), 6.81–6.71 (m, 2H), 6.65 (ddd, $J = 8.1, 2.3, 1.1$ Hz, 1H), 3.68 (s, 2H); ¹³C NMR (126 MHz, DMSO) δ 169.68, 157.32, 154.93, 154.15, 141.53, 136.04, 132.70, 129.34, 121.07, 119.80, 116.03, 115.19, 113.81, 106.45, 41.85; MS (ESI): $m/z = 301.15$ ($M + H$)⁺; HRMS $m/z = 301.0622$ (calculated = 301.0641).

N-Benzyl-4-(3-(6-hydroxybenzo[d]thiazol-2-yl)ureido)-benzamide (b4). The title compound was prepared by demethylation of compound a9 according to the general procedure for ether dealkylation. Light brown solid; yield: 73%; mp 200–201 °C; ¹H NMR (500 MHz, DMSO) δ 10.75 (s, 1H), 9.47 (s, 1H), 9.42 (s, 1H), 8.95 (t, $J = 6.0$ Hz, 1H), 7.89 (d, $J = 8.8$ Hz, 2H), 7.60 (d, $J = 8.6$ Hz, 2H), 7.53–7.40 (m, 1H), 7.36–7.28 (m, 4H), 7.28–7.19 (m, 2H), 6.85 (dd, $J = 8.7, 2.5$ Hz, 1H), 4.48 (d, $J = 6.0$ Hz, 2H); ¹³C NMR (126 MHz, DMSO) δ 165.60, 154.88, 154.21, 147.81, 140.37, 139.82, 131.12, 128.30, 128.23, 127.17, 126.66, 122.55, 117.72, 115.32, 114.81, 112.70, 106.70, 42.53; MS (ESI): $m/z = 418.97$ ($M + H$)⁺; HRMS $m/z = 419.1149$ (calculated = 419.1172).

1-(6-Hydroxybenzo[d]thiazol-2-yl)-3-(4-(4-methylpiperazine-1-carbonyl)phenyl)urea (b5). The title compound was prepared by demethylation of compound a10 according to the general procedure for ether dealkylation. White solid; yield: 48%; mp 153–155 °C; ¹H NMR (300 MHz, DMSO) δ 10.80 (s, 1H), 9.46 (s, 1H), 9.39 (s, 1H), 7.57 (d, $J = 8.4$ Hz, 2H), 7.46 (d, $J = 8.6$ Hz, 1H), 7.37 (d, $J = 8.5$ Hz, 2H), 7.23 (d, $J = 2.3$ Hz, 1H), 6.84 (dd, $J = 8.6, 2.4$ Hz, 1H), 3.51 (s, 4H), 2.36 (s, 4H), 2.22 (s, 3H); MS (ESI): $m/z = 412.03$ ($M + H$)⁺; HRMS $m/z = 412.1415$ (calculated = 412.1438).

Biological assays

Protein kinase assays were done exactly as described before,¹⁴ except that the ATP concentration were varied as indicated in the legends. Metabolic stability assay is described in the ESI†

Molecular modeling

Ab initio calculations of the equilibrium conformer of AHS-211 and energy levels were carried out as previously described.¹⁹ Molecular docking simulations of the b5 binding to human Dyrk1A (extracted from PDB entries 5A3X or 5A4E, respectively) were performed as previously described.²⁰

Conflicts of interest

The authors declare no competing interest.

Acknowledgements

The support by the Deutsche Forschungsgemeinschaft (DFG) (EN381/2-3) to ME is greatly acknowledged. We thank Mariam G. Tahoun (Helmholtz Institute for Pharmaceutical Research Saarland) for carrying out the metabolic stability studies.

Notes and references

- 1 W. Becker and W. Sippl, *Rev. Geophys.*, 2011, 278, 246–256.
- 2 W. Becker, Y. Weber, K. Wetzel, K. Eirmbter, F. J. Tejedor and H.-G. Joost, *J. Biol. Chem.*, 1998, 273, 25893–25902.
- 3 J. Wegiel, K. Dowjat, W. Kaczmarek, I. Kuchna, K. Nowicki, J. Frackowiak, B. Mazur Kolečka, J. Wegiel, W. P. Silverman, B. Reisberg, M. deLeon, T. Wisniewski, C.-X. Gong, F. Liu, T. Adayev, M.-C. Chen-Hwang and Y.-W. Hwang, *Acta Neuropathol.*, 2008, 116, 391–407.
- 4 F. Liu, Z. Liang, J. Wegiel, Y.-W. Hwang, K. Iqbal, I. Grundke-Iqbal, N. Ramakrishna and C.-X. Gong, *FASEB J.*, 2008, 22, 3224–3233.
- 5 R. Kimura, K. Kamino, M. Yamamoto, A. Nuripa, T. Kida, H. Kazui, R. Hashimoto, T. Tanaka, T. Kudo, H. Yamagata, Y. Tabara, T. Miki, H. Akatsu, K. Kosaka, E. Funakoshi, K. Nishitomi, G. Sakaguchi, A. Kato, H. Hattori, T. Uema and M. Takeda, *Hum. Mol. Genet.*, 2007, 16, 15–23.
- 6 B. Khor, K. L. Conway, R. J. Xavier, J. D. Gagnon, L. N. Aldrich, T. B. Sundberg, M. Schirmer, A. F. Shamji, S. L. Schreiber, G. Goel, M. I. Roche, B. D. Medoff, K. Tran, P. H. Tan, S. Y. Shaw, A. M. Paterson, A. H. Sharpe, S. Mordecai, D. Dombkowski, A. K. Bhan, R. Roychoudhuri, N. P. Restifo and J. J. O'Shea, *eLife*, 2015, 4, e05920.
- 7 U. Soppa, J. Schumacher, T. Pasqualon, W. Becker, O. V. Florencio and F. J. Tejedor, *Cell Cycle*, 2014, 13, 2084–2100.
- 8 K. M. Ori-McKenney, T. Li, S. Meltzer, L. Y. Jan, R. J. McKenney, R. D. Vale, H. H. Huang, A. P. Wiita and Y. N. Jan, *Neuron*, 2016, 90, 551–563.
- 9 F. J. Tejedor and B. Hammerle, *Rev. Geophys.*, 2011, 278, 223–235.
- 10 W. Becker, *Cell Cycle*, 2012, 11, 3389–3394.
- 11 M. Muraki, B. Ohkawara, T. Hosoya, H. Onogi, J. Koizumi, T. Koizumi, K. Sumi, J.-I. Yomoda, M. V. Murray, H. Kimura, K. Furuichi, H. Shibuya, A. R. Krainer, M. Suzuki and M. Hagiwara, *J. Biol. Chem.*, 2004, 279, 24246–24254.
- 12 Y. Ogawa, Y. Nonaka, T. Goto, E. Ohnishi, T. Hiramatsu, I. Kii, M. Yoshida, T. Ikura, H. Onogi, H. Shibuya, T. Hosoya, N. Ito and M. Hagiwara, *Nat. Commun.*, 2010, 1, 86.
- 13 U. Rothweiler, W. Stensen, B. R. O. Brandsdal, J. Isaksson, F. A. Leeson, R. A. Engh and J. S. M. E. Svendsen, *J. Med. Chem.*, 2016, 59, 9814–9824.
- 14 C. Schmitt, P. Miralinaghi, M. Mariano, R. W. Hartmann and M. Engel, *ACS Med. Chem. Lett.*, 2014, 5, 963–967.
- 15 A. Spadaro, M. Negri, S. Marchais-Oberwinkler, E. Bey and M. Frotscher, *PLoS One*, 2012, 7, e29252.
- 16 T. Tahtouh, J. M. Elkins, P. Filippakopoulos, M. Soundararajan, G. Burgy, E. Durieu, C. Cochet, R. S. Schmid, D. C. Lo, F. Delhommel, A. E. Oberholzer, L. H. Pearl, F.

MedChemComm

[View Article Online](#)

Research Article

- Carreaux, J.-P. Bazureau, S. Knapp and L. Meijer, *J. Med. Chem.*, 2012, 55, 9312–9330.
- 17 J. Bain, H. McLauchlan, M. Elliott and P. Cohen, *Biochem. J.*, 2003, 371, 199–204.
- 18 G. D. Cuny, M. Robin, N. P. Ulyanova, D. Patnaik, V. Pique, G. Casano, J.-F. Liu, X. Lin, J. Xian, M. A. Glicksman, R. L. Stein and J. M. G. Higgins, *Bioorg. Med. Chem. Lett.*, 2010, 20, 3491–3494.
- 19 P. Miralinaghi, C. Schmitt, R. W. Hartmann, M. Frotscher and M. Engel, *ChemMedChem*, 2014, 9, 2294–2308.
- 20 A. K. ElHady, M. Abdel-Halim, A. H. Abadi and M. Engel, *J. Med. Chem.*, 2017, 60, 5377–5391.

7.2 Development of novel 2,4-bispyridyl thiophene-based compounds as highly potent and selective Dyrk1A inhibitors. Part I: Benzamide and benzylamide derivatives

Sarah S. Darwish, Mohammad Abdel-Halim, Mohamed Salah, Ashraf H. Abadi, Walter Becker, Matthias Engel

Reprinted with permission *Eur. J. Med. Chem.* 2018, 157, 1031–1050.

DOI: 10.1016/j.ejmech.2018.07.050

Copyright (2018) ELSEVIER

Publication H

Contribution Report

The author performed the kinase inhibition assays as well as the cellular viability assays. He further carried out the in silico physiochemical characterization of the compounds. He contributed in the interpretation of the results.



Contents lists available at ScienceDirect

European Journal of Medicinal Chemistry

journal homepage: <http://www.elsevier.com/locate/ejmech>

Research paper

Development of novel 2,4-bispyridyl thiophene-based compounds as highly potent and selective Dyrk1A inhibitors. Part I: Benzamide and benzylamide derivatives

Sarah S. Darwish^a, Mohammad Abdel-Halim^a, Mohamed Salah^b, Ashraf H. Abadi^a, Walter Becker^c, Matthias Engel^{b,*}^a Department of Pharmaceutical Chemistry, Faculty of Pharmacy and Biotechnology, German University in Cairo, Cairo 11835, Egypt^b Pharmaceutical and Medicinal Chemistry, Saarland University, Campus C2.3, D-66123 Saarbrücken, Germany^c Institute of Pharmacology and Toxicology, Medical Faculty of the RWTH Aachen University, Wendlingweg 2, 52074 Aachen, Germany

ARTICLE INFO

Article history:

Received 14 June 2018

Received in revised form

13 July 2018

Accepted 18 July 2018

Available online 19 July 2018

Keywords:

Dyrk1A

Alzheimer's disease

Bispyridyl thiophene amides

Selectivity

Metabolic stability

ABSTRACT

The protein kinase Dyrk1A modulates several processes relevant to the development or progression of Alzheimer's disease (AD), e. g. through phosphorylation of tau protein, amyloid precursor protein (APP) as well as proteins involved in the regulation of alternative splicing of tau pre-mRNA. Therefore, Dyrk1A has been proposed as a potential target for the treatment of AD. However, the co-inhibition of other closely related kinases of the same family of protein kinases (e.g. Dyrk1B and Dyrk2) or kinases from other families such as Clk1 limits the use of Dyrk1A inhibitors, as this may cause unpredictable side effects especially over long treatment periods. Herein, we describe the design and synthesis of a series of amide functionalized 2,4-bispyridyl thiophene compounds, of which the 4-fluorobenzyl amide derivative (**31b**) displayed the highest potency against Dyrk1A and remarkable selectivity over closely related kinases (IC₅₀: Dyrk1A = 14.3 nM; Dyrk1B = 383 nM, Clk1 > 2 μM). This degree of selectivity over the frequently hit off-targets has rarely been achieved to date. Additionally, **31b** inhibited Dyrk1A in intact cells with high efficacy (IC₅₀ = 79 nM). Furthermore, **31b** displayed a high metabolic stability *in vitro* with a half-life of 2 h. Altogether, the benzamide and benzylamide extension at the 2,4-bispyridyl thiophene core improved several key properties, giving access to compound suitable for future *in vivo* studies.

© 2018 Elsevier Masson SAS. All rights reserved.

1. Introduction

Dual-specificity tyrosine-regulated kinases (Dyrks) are a family of eukaryotic kinases that belong to a larger super family known as the CMGC group [1]. The Dyrk family consists of five mammalian subtypes including Dyrk1A, 1B, 2, 3, and 4 [2]. Dyrk1B is highly expressed in some types of cancers, where it is claimed to exert an anti-apoptotic role in tumour cells by mediating some survival signals [3]. For Dyrk2, several controversial roles were reported in cancer biology: this isoenzyme was found to be amplified and overexpressed in lung and esophageal adenocarcinoma as well as gastrointestinal stromal tumours [4,5]. However, a previous study proposed that Dyrk2 inactivation contributes to the invasiveness of human tumours due to the decreased levels of phosphorylated c-

Jun and c-Myc transcription factors as well as the lowered activation of the p53 tumour suppressor protein [6,7]. Comparably little information exists on the remaining Dyrk isoforms. Dyrk3, which is most closely related to Dyrk2 among the Dyrk family, was shown to attenuate erythropoiesis by efficiently inhibiting NFAT transcriptional activation [8]. Dyrk4, for which few reports exist, was found expressed in human brain during neuronal differentiation [9]. Dyrk1A, the most studied isoform of this family, also has a well-established neurodevelopmental role, as confirmed by the examination of Dyrk1A expression in the developing mouse brain [10]. In humans, Dyrk1A was identified in the Down syndrome (DS) critical region (DSCR) of chromosome 21 [11,12] as a potential candidate gene causing the DS phenotype. DS individuals are characterized by mental retardation, cognitive as well as cranio-facial characteristics, congenital heart disease, an increased risk of childhood leukemia, and an early onset of Alzheimer's Disease (AD) [13]. In DS individuals, the 1.5-fold overexpression of Dyrk1A is believed to cause an imbalance in the neurodevelopmental processes such as

* Corresponding author.

E-mail address: ma.engel@mx.uni-saarland.de (M. Engel).

neurogenesis and neuronal differentiation [14–18], eventually resulting in reduced brain size, neuronal deficits and altered neuronal morphology. Especially the early onset of AD was attributed to an increased phosphorylation of the tau protein and presenilin-1 by Dyrk1A [19].

Importantly, Dyrk1A was found to be involved in the regulation of alternative splicing of pre-mRNA, which is crucial for controlling embryonic development, cell growth and apoptosis [20]. The splicing process is catalyzed by a macromolecular machine called spliceosome which is controlled by protein phosphorylation [21]. Splice site recognition is determined mainly through the interaction of serine-arginine-rich (SR) proteins and heterogeneous nuclear ribonucleoproteins with specific exonic and intronic pre-mRNA sequences [22]. Dyrk1A was reported to phosphorylate several SR proteins, thus modulating their activity [23,24]. In addition, Dyrk1A is known to phosphorylate the non-SR protein SF3b1 which plays an important role in the basic splicing reaction since it is detected only in functional spliceosomes [25].

Among the important SR proteins phosphorylated by Dyrk1A are SRp55, SC35 and ASF, which regulate the inclusion of exon 10 in the tau mRNA in the brain [23,24,26]. Indeed, overexpression of Dyrk1A led to the increase of 3R-tau with incorporated exon 10 in the neonatal brains of Ts65Dn mice, a model of Down syndrome [27]. In the same study, inhibition of Dyrk1A restored the balance of 3R/4R tau protein by preventing the inclusion of exon 10 in the tau mRNA. The relatively increased amount of 3R-tau relative to 4R-tau facilitates tau aggregation, one of the main hallmarks of AD [28]. Not surprisingly, increased Dyrk1A activity in DS brains and Dyrk1A overexpression models was found to change further transcript compositions, e. g. in the mRNAs of neuroligin and of acetylcholinesterase variants, thus producing key synaptic proteins with unusual features [29].

In addition, Dyrk1A was reported to phosphorylate tau protein and APP directly [1,13,30], thus promoting tau aggregation and formation of amyloid plaques, the main molecular hallmarks of sporadic as well as DS-linked AD neurodegeneration [31,32]. A recent study proved that normalization of the gene dosage of Dyrk1A could reduce several phenotypes of AD in a mouse model of DS [33]. Another group showed that Dyrk1A inhibition could improve AD pathologies in mouse model [34]. Altogether, there is ample evidence that Dyrk1A is a promising target in AD [27,33,34] and possibly in splicing-related disorders [35], although the latter indication has scarcely been explored up to now.

Any therapeutic use of Dyrk1A inhibitors requires high selectivity over closely related kinases in the Dyrk family, such as Dyrk1B and Dyrk2, as well as frequently co-inhibited kinases from other families, including Clks, to prevent unwanted adverse effects. However, most of the previously published Dyrk1A inhibitors affected other kinases known to maintain or promote cell proliferation, mainly Clk1/4, haspin, and CK2 [31,36–39]. Indeed, several Dyrk1A inhibitors, including harmine [40], meridianin derivatives [41] and pyrido [2,3-d]pyrimidines [42], were reported to affect cell growth at low μM concentrations, which could well be explained by off-target activities. With respect to cancer, multi-targeted inhibitors might even have advantages over specific ones; for instance, in a study by Zhou et al., 7-azaindole-based compounds that simultaneously targeted Dyrk1A, Dyrk1B and Clk1, efficiently blocked cell proliferation and migration of glioblastoma cells [43]. In contrast, potentially cytotoxic effects of Dyrk inhibitors are expected to limit the therapeutic applicability in neurodegenerative diseases, where the cell viability is already affected by harmful peptide and protein aggregates.

In a previous report, we introduced bispyridyl thiophenes as a novel scaffold for the inhibition of Dyrk and Clk kinases [38]. While the overall selectivity of these inhibitors was promising, they did

not show a pronounced preference among the close homologues Dyrk1A/B, Dyrk2 or Clk1/4; only slight selectivity shifts could be achieved by the introduction of different small substituents; the most potent compound **C29** (compound **29** in Ref. [38]) is depicted in Fig. 1.

In the current study, we present new derivatives of the bispyridyl thiophene scaffold with a crucial amide extension that greatly enhanced the potency and selectivity of the compounds for Dyrk1A as well as the metabolic stability *in vitro*.

2. Results and discussion

2.1. Compound design

We previously described the development of a series of ATP-competitive, bisheterocyclic substituted thiophenes based on the original hit compound **C4** (compound **4** in Ref. [38]), depicted in Fig. 1 (IC_{50}s : Dyrk1A = 300 nM; Dyrk1B = 300 nM; Dyrk2 = 300 nM). The optimized compound **C29** displayed higher potency against Dyrk1A [38], however, still lacked selectivity for Dyrk1A over the closely related kinases Dyrk1B and Dyrk2 as well as Clk1.

Small substituents at one of the pyridine rings of **C4**, such as methyl, methoxy, cyano or halogens effected only a slight modulation of the Dyrk subtype selectivity; however, it was found that particularly at the *meta* position, diverse substituents were tolerated without affecting the potency. Hence we surmised that an amino function, which would give access to a focused library of amides, could also be installed on the pyridine ring. In light of the good physicochemical properties and the low molecular weight (238.31 g/mol) of the core structure **C4**, [38] the attachment of benzamide, sulfonamide and benzylamide moieties was deemed acceptable to enhance binding affinity and selectivity whilst keeping molecular weight and lipophilicity in a drug-like range.

Based on our docking simulation (Fig. 2), the two important hydrogen bonds with the conserved Lys188 and the hinge region residue Leu241 as well as the $\text{CH}-\pi$ interactions involving Lys188, Leu241 and the Phe238 benzene ring were not expected to be compromised by the probe amino function that was added to ring A of **C4**. In accordance, the potency of the resulting compound **2** was even somewhat higher than that of **C4** (Table 1).

Firstly, further aminopyridine derivatives of **C4** were synthesized as probe compounds to identify the optimum position with respect to potency and selectivity. Similar to what was observed with other substituents, the amino function was best tolerated in the 3-position of ring A (Compound **2**, Table 1), however, it did not improve the selectivity over Dyrk1B. Interestingly, the amino function could be introduced at both pyridine rings (ring A and B) with basically the same outcome (cf. compound **35**, Table 1), indicating that it was equally tolerated at each end of the ATP binding pocket or, as also suggested by our docking simulation (Fig. 2), that the inhibitor could flip in the binding site by 180° without loss of affinity due to the rather symmetric shape of the 2,4-bispyridyl scaffold. Shifting the pyridine nitrogen of ring B by incorporating 4-pyridyl (compound **3**) almost abolished the potency, indicating that the added 3-amino did not induce a new binding mode that

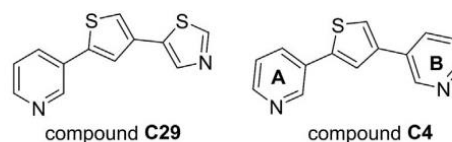


Fig. 1. Previously published Dyrk1A inhibitors.

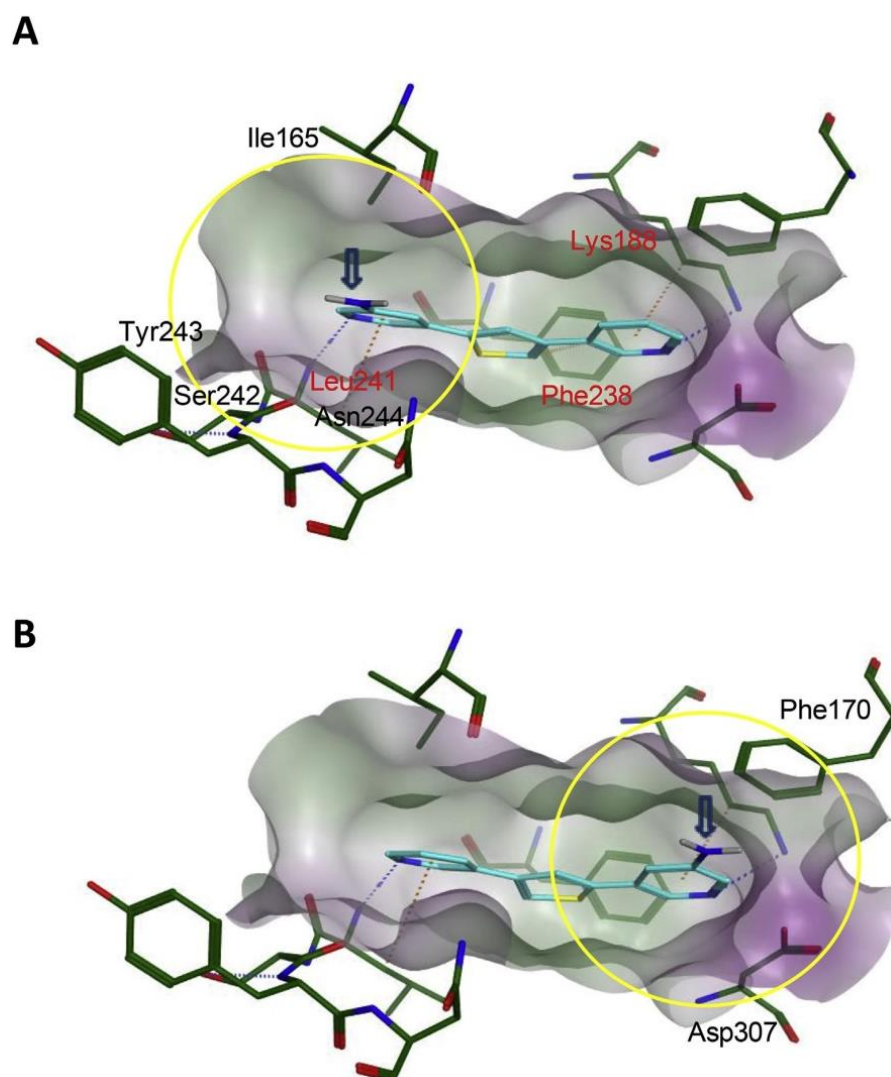


Fig. 2. Extension strategy envisaging amide couplings to probe compound **2**. The amino-functionalized compound **2** (cyan) was docked in the ATP binding pocket of Dyrk1A (derived from PDB entry 3ANR) using MOE. As predicted for the scaffold before [38], **2** showed the crucial hydrogen bond interactions as well as CH- π interactions with amino acid residues Lys188, Leu241 and Phe238 (exemplarily indicated in A, red letters). Because of the rather symmetric shape of the bispyridyl thiophene scaffold, compound **2** and amide derivatives thereof might bind in two different orientations, with the molecule extension being placed either at the hinge region (A) or at the opposite end of the ATP binding pocket (B). As indicated by the yellow circles (a 4 Å radius from probe amino function) in A and B, several H-bond donor/acceptor functions (e.g., from the peptide backbones of Ile165, Ser242 and Tyr243) in addition to an acidic (Asp307), polar (Asn244), and an aromatic function (Phe170) are all located within reach of a putative amide-linked molecule extension. Interactions are indicated by dashed lines. In the colour code of the ATP binding pocket surface, green denotes the most lipophilic and magenta the most hydrophilic areas. (For interpretation of the references to colour in this figure legend, the reader is referred to the Web version of this article.)

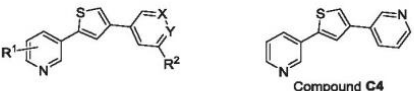
would favour or tolerate another position of the acceptor nitrogen in pyridine ring B (cf. Fig. 1). Eventually, we selected probe compound **2** as basis for further modifications.

Since in both possible binding orientations, the amino function pointed to the borders of the ATP binding pocket, molecule extensions utilizing an amide linkage could potentially address several side chains and/or backbone peptide functions of unexploited residues located at the borders of the ATP binding pocket (encircled in yellow, Fig. 2). These included the Ile165 and Tyr243 side chains at the hinge region side (Fig. 2A) as well as the Phe170 and Asp307 residues located at the opposite edge of the pocket (Fig. 2B). Using a diversification strategy involving an extension of probe compound **2** through amide and sulfonamide couplings, we

aimed at enhancing both the potency towards Dyrk1A and the selectivity over other kinases, in particular Dyrk1B, Dyrk2, Clk1 and haspin.

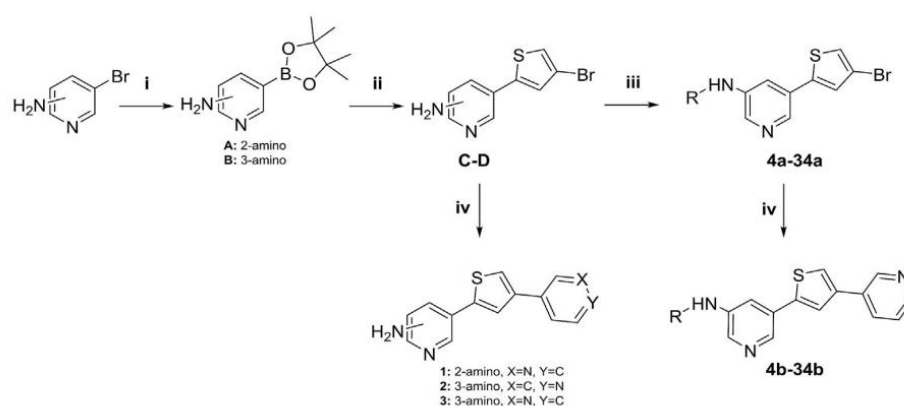
2.2. Chemistry

The synthesis of the planned amide functionalized bispyridyl thiophene compounds was accomplished through a four-step synthesis as summarized in Scheme 1. Firstly, a Miyaura reaction was carried out on 2/3-amino-5-bromopyridine and bis(pinacolato)diboron in presence of potassium acetate and Pd(dppf)Cl₂ as a catalyst to afford the corresponding boronic acid pinacol ester. Next, the produced boronic acid derivative became accessible by a

Table 1Inhibition of Dyrk1A and Dyrk1B kinases (compounds **1–3**, **35**).


| Cpd.No. | R ¹ | X | Y | R ² | Dyrk1A | | Dyrk1B | |
|-----------|-------------------|---|---|-----------------|-------------------------------------|------------------------------------|-------------------------------------|------------------------------------|
| | | | | | % inhibition at 250 nM ^a | IC ₅₀ (nM) ^a | % inhibition at 250 nM ^a | IC ₅₀ (nM) ^a |
| 1 | 2-NH ₂ | N | C | H | 30.5 | 614.3 | 59.5 | 251.4 |
| 2 | 3-NH ₂ | N | C | H | 64.7 | 101 | 65.1 | 154.3 |
| 3 | 3-NH ₂ | C | N | H | 8.4 | ND | 21.7 | ND |
| 35 | H | N | C | NH ₂ | 60 | ND | 67 | 130 |
| C4 | | | | | | 300 | | 300 |

^aValues are mean values of at least two independent experiments, each done in duplicates; standard deviation < 9%; ND: not determined. The ATP concentration in the assay was 15 μ M.



Scheme 1. Reagents and conditions: (i) 4 equiv of CH₃COOK, 4 equiv bis(pinacolato)diboron, 5 mmol% of Pd(dppf)Cl₂ in dioxane, reflux 2 h; (ii) 4 equiv of Cs₂CO₃, 5 mmol% of Pd(PPh₃)₄, 1.2 equiv of 2,4-dibromothiophene in dioxane/water, reflux 3.5 h; (iii) 1.5 equiv Et₃N, 1.2 equiv of the appropriate acid chloride in acetone, room temperature, 2 h; or 2 equiv of benzenesulfonyl chloride in pyridine, 60 °C, overnight; (iv) 4 equiv of Na₂CO₃, 5 mmol% of Pd(dppf)Cl₂, 2 equiv of 3/4-pyridine boronic acid in dioxane/water, reflux, 2 h.

consecutive Suzuki cross coupling reaction with 2,4-dibromothiophene in the presence of Cs₂CO₃ and palladium-tetrakis(triphenylphosphine) to give 4-bromothiophen-2-yl pyridine amines (compounds **C–D**). In the third step and starting from compound **D**, a coupling reaction took place with diverse acid chlorides or benzenesulfonyl chlorides to yield a series of amides in addition to one sulfonamide derivative, respectively. The final reaction was a second Suzuki reaction to synthesize the bispyridyl thiophene functionalized amides (**4b–34b**). This was done using 3-pyridine boronic acid and Pd(dppf)Cl₂ in presence of Na₂CO₃ as a base. It is worth mentioning that the poor yield of the later Suzuki reaction hindered diversification via amide coupling as a last step. Few compounds (**1–3**) were synthesized by direct coupling of the 4-bromothiophen-2-yl pyridine amine intermediates (**C–D**) with 3/4-pyridine boronic acids (Scheme 1). To synthesize the inverted positional isomer of compound **2**, compound **E** was synthesized by coupling 2,4-dibromothiophene with 3-pyridine boronic acid, followed by coupling with compound **B** to yield compound **35** (Scheme 2).

2.3. Biological evaluation

The inhibitory activity of the synthesized compounds was evaluated against recombinant Dyrk1A by screening at 250 nM. For

compounds showing more than 60% inhibition, the IC₅₀ values were determined (Tables 1 and 2). In order to obtain an early indication of the selectivity, all new compounds were tested in parallel against Dyrk1B, the most closely related isoenzyme.

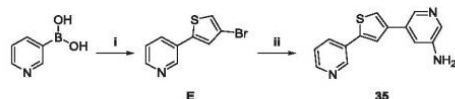
In the present study, we generally focused on the installation of an aromatic system, that could engage in several of the potential interactions with the residues indicated in Fig. 2.

2.3.1. Structure-activity-relationships (SAR)

2.3.1.1. Evaluation of the carboxamide vs. sulfonamide extension. We started with the attachment of a plain phenyl ring through an amide linkage to obtain the benzamide derivative **4b**. When compared to the probe compound **2**, **4b** gave a slightly reduced inhibition without enhancement of selectivity over Dyrk1B (Tables 1 and 2). However, this did not argue for a poor steric fit of the benzoyl moiety, because the amide coupling strongly decreased the mesomeric effect of the amino function on the pyridyl, thus weakening the acceptor strength of the ring nitrogen (cf. Fig. 3A). Considering that this caused a partial loss of affinity, we concluded that the benzoyl moiety was overall tolerated.

In contrast, the substitution of the amide function in **4b** with a sulfonamide moiety yielded a totally inactive analogue (**5b**), clearly indicating that the carboxamide group was much more preferred by the binding site (Table 2).

| Cpd No. | R | No | R |
|---------|---|-----|---|
| 4a | | 20a | |
| 5a | | 21a | |
| 6a | | 22a | |
| 7a | | 23a | |
| 8a | | 24a | |
| 9a | | 25a | |
| 10a | | 26a | |
| 11a | | 27a | |
| 12a | | 28a | |
| 13a | | 29a | |
| 14a | | 30a | |
| 15a | | 31a | |
| 16a | | 32a | |
| 17a | | 33a | |
| 18a | | 34a | |
| 19a | | | |



Scheme 2. Reagents and conditions: (i) 4 equiv of Cs_2CO_3 , 5 mmol% of $\text{Pd}(\text{PPh}_3)_4$, 1.2 equiv of 2,4-dibromothiophene in dioxane/water, reflux 3 h; (ii) 4 equiv of Na_2CO_3 , 5 mmol% of $\text{Pd}(\text{dppf})\text{Cl}_2$, 1.5 equiv of compound **B** in dioxane/water, reflux, 2 h.

2.3.1.2. Evaluation of electron-donating substituents. In an attempt to improve the potency of compound **4b**, different electron-donating as well as electron-withdrawing groups were tested as substituents on the phenyl ring. Firstly, mono-substitution

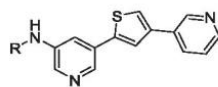
by electron-donating groups was investigated, starting with the addition of the lipophilic methyl group in the *ortho*, *meta* and *para* positions. The *o*- and *m*-toluoyl derivatives (compounds **6b** and **7b**) showed slightly lower inhibitory activity than compound **4b** while the *p*-methyl substitution in **8b** proved to be more favourable ($\text{IC}_{50} = 51.4 \text{ nM}$), raising the potency over that of the probe compound **2** ($\text{IC}_{50} = 101 \text{ nM}$, Table 2). In addition, **8b** retained the selectivity over Dyrk1B. To confirm the optimum substitution position, the more polar and stronger electron-donating methoxy group was explored in the same manner. However, the methoxy group effected leveling of potency between the *ortho*-, *meta*- and *para*-regioisomers, as all of the compounds showed similar degrees of inhibition (compounds **9b–11b**, inhibition between 53.5 and 59.5%, Table 2). There was only a marginal preference for the *para*-position. Altogether, it could be concluded that the *para*-position is superior in case of electron-donating groups, but that the potential activity-enhancing effect of the methoxy substituent might be counteracted by steric clashes. To probe the available space surrounding the *para*-position, the bulky, lipophilic and electron donating *tert*-butyl group was introduced (**12b**); this modification abolished the inhibitory activity against Dyrk1A, suggesting that substituents which are essentially larger than methyl – such as methoxy and particularly *t*-butyl – are likely to produce a steric clash with the ATP binding pocket. Of note, the methoxy-substituted congeners **9b** and **10b** exhibited diminished activity toward Dyrk1B (Table 2), indicating that the variation of substituents at the benzoyl moiety permits to modulate the selectivity.

2.3.1.3. Evaluation of electron-withdrawing substituents. The preference of the benzoyl *para* position, as found with the electron-donating substituents, was not observed when electron-withdrawing groups were explored. In light of the finding described above, we restricted to substituents that did not largely exceed the size of a methyl group. First, we analyzed the effect of a chloro substituent; among the three positional isomers, the *o*-chlorobenzamide analogue **13b** ($\text{IC}_{50} = 90.5 \text{ nM}$, Table 2) was clearly more active than the *m*- or *p*-chloro isomers (**14b** and **15b**, respectively) and represented the most potent mono-substituted benzamide analogue. By examining Dyrk1B inhibition, **13b** showed considerable preference for Dyrk1A over Dyrk1B. Similarly, the smaller fluoro substituent was also tested; on average, the three positional isomers showed a higher activity than the chlorinated analogues (cf. **16b–18b**, Table 2), which might be attributable to the lower steric demand of the fluorine, in particular at the *meta*- and *para*-positions. Additionally, all fluoro derivatives possessed superior selectivity for Dyrk1A over Dyrk1B. However, the most active *o*-fluorobenzamide derivative **16b** ($\text{IC}_{50} = 106.7 \text{ nM}$) did not fully reach the potency level of the chlorinated congener **13b**. Finally, we investigated whether the trifluoromethyl group could boost the activity stronger than fluorine, which was, however, not the case (compounds **19b–21b**, Table 2); all three regioisomers displayed lower inhibitory activity than compound **4b**. Altogether, there was no clear correlation between the inhibitory activity and the modulation of the electron density by the substituents in the benzamide class. Most probably, the influence of the substituents on potency is governed by more than one parameter, e. g. by direct interaction with the binding site, modulation of the electron density, conformational stabilizations, and potential steric interference. Various substituents, in particular methyl, chlorine and fluorine, favourably enhanced the selectivity for Dyrk1A over Dyrk1B, which had not been observed with the unsubstituted benzamide **4b**.

2.3.1.4. Effect of multiple substitutions. Assuming that some of the favourable effects observed with different substituents at several

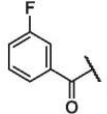
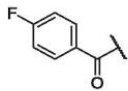
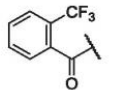
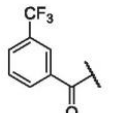
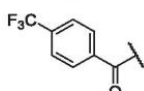
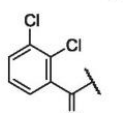
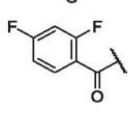
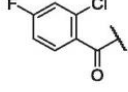
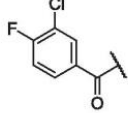
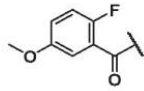
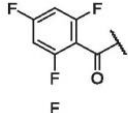
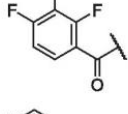
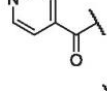
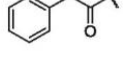
036

S.S. Darwish et al. / European Journal of Medicinal Chemistry 157 (2018) 1031–1050

Table 2
Inhibition of Dyrk1A and Dyrk1B kinases (**4b–34b**).

| Cpd.No. | R | Dyrk1A | | Dyrk1B | |
|------------|---|-------------------------------------|------------------------------------|-------------------------------------|------------------------------------|
| | | % inhibition at 250 nM ^a | IC ₅₀ (nM) ^a | % inhibition at 250 nM ^a | IC ₅₀ (nM) ^a |
| 4b | | 59.5 | ND | 57.6 | ND |
| 5b | | 9.9 | ND | 18.8 | ND |
| 6b | | 50.1 | ND | 39.5 | ND |
| 7b | | 45.2 | ND | 60.5 | ND |
| 8b | | 60.5 | 51.4 | 54.6 | ND |
| 9b | | 57.3 | ND | 15.4 | ND |
| 10b | | 53.5 | ND | 29 | ND |
| 11b | | 59.5 | ND | 25.2 | ND |
| 12b | | 21 | ND | 3.4 | ND |
| 13b | | 72 | 90.5 | 26.3 | ND |
| 14b | | 44.5 | ND | 59.8 | ND |
| 15b | | 25.9 | ND | 52.2 | ND |
| 16b | | 65.1 | 106.7 | 30 | ND |

Table 2 (continued)

| Cpd.No. | R | Dyrk1A | | Dyrk1B | |
|---------|---|-------------------------------------|------------------------------------|-------------------------------------|------------------------------------|
| | | % inhibition at 250 nM ^a | IC ₅₀ (nM) ^a | % inhibition at 250 nM ^a | IC ₅₀ (nM) ^a |
| 17b |  | 59.4 | ND | 26.2 | ND |
| 18b |  | 62.6 | 183.2 | 23.5 | ND |
| 19b |  | 37.7 | ND | 26 | ND |
| 20b |  | 46.7 | ND | 36 | ND |
| 21b |  | 8.5 | ND | 32 | ND |
| 22b |  | 42 | ND | 32 | ND |
| 23b |  | 80.2 | 49 | 41 | ND |
| 24b |  | 54.2 | ND | 33.6 | ND |
| 25b |  | 23.3 | ND | 5.6 | ND |
| 26b |  | 85.2 | 37.3 | 43.8 | ND |
| 27b |  | 93.1 | 23.5 | 38.7 | 298.5 |
| 28b |  | 55.5 | ND | 25.1 | ND |
| 29b |  | 63.7 | 107 | 55.1 | ND |
| 30b |  | 99.6 | 14.9 | 31.2 | 326.3 |

(continued on next page)

Table 2 (continued)

| Cpd.No. | R | Dyrk1A | | Dyrk1B | |
|---------|---|-------------------------------------|------------------------------------|-------------------------------------|------------------------------------|
| | | % inhibition at 250 nM ^a | IC ₅₀ (nM) ^a | % inhibition at 250 nM ^a | IC ₅₀ (nM) ^a |
| 31b | | 86.9 | 14.3 | 36.5 | 383 |
| 32b | | 49.7 | ND | 48.7 | ND |
| 33b | | 49.7 | ND | 49.5 | ND |
| 34b | | 10 | ND | 33.9 | ND |

^aValues are mean values of at least two independent experiments, each performed in duplicates; S.D. < 10%; the assay was carried out at an ATP conc. of 15 μM; ND: not determined.

ring positions could be additive, disubstitution patterns were investigated using combinations of the substituents described above. Initially, disubstitution using identical groups was investigated, starting with the 2,3-dichlorobenzamide analogue (compound **22b**) which led to a decrease in the inhibitory activity compared with the benzamide derivative **4b** and with the *o*-chloro derivative **13b**, confirming the deleterious effect of the *m*-chloro on potency. On the other hand, the 2,4-difluoro congener **23b** showed a great improvement in the inhibitory activity with an IC₅₀ of 49 nM, indicating that the effect of combining two fluorine atoms is indeed additive. However, changing the nature of substituents to 2-chloro-4-fluoro (compound **24b**) decreased the inhibitory activity below that of the unsubstituted analogue **4b**, again confirming that the electron withdrawing properties of the halogens do not play a major role, as they would have been additive. Similarly, the 3-chloro-4-fluoro substitution was detrimental to the activity (compound **25b**). Consequently, the compound design was extended to include a combination of the favourable 2-fluorine with an electron-donating 5-methoxy group (**26b**). **26b** showed a further improved activity with an IC₅₀ of 37.3 nM, indicating that the 2-fluoro substitution can favourably be combined with other substituents to enhance the potency. Fortunately, the resulting disubstituted compounds **23b** and **26b** also exhibited a good selectivity towards Dyrk1A over its closely related isoform Dyrk1B. Prompted by the favourable effects especially by the difluorination, we tested whether a trifluorinated analogue, bearing another fluorine in *ortho*, would even show higher activity. Indeed, compound **27b** with the 2,4,6-trifluoro substitution proved to be the most potent inhibitor among the benzamide series (IC₅₀ = 23.5 nM). Moreover, this improvement of potency of **27b** was accompanied by a remarkable 13-fold increase in selectivity over Dyrk1B. Somewhat unexpectedly, the 3-fluoro in the 2,3,4-trifluoro-substituted isomer (**28b**), completely neutralized the activity-enhancing effects of the other fluorine substituents.

2.3.1.5. Changing the nature of the benzamide ring. To decouple effects of electron withdrawing effects of substituents from potential secondary effects such as steric clashes, we replaced the benzamide phenyl by the electron deficient 4-pyridyl (**29b**), which was supposed to mimic the 4-fluoro substitution in **18b**. Indeed, the inhibitory activity of **29b** followed the same trend as **18b**: Reaching an IC₅₀ of 107 nM, **29b** was more active than the unsubstituted benzamide **4b**, but less active than the 4-methyl-substituted analogue **8b** (IC₅₀ = 51.4 nM). However, since the absence of a *p*-

substituent in **29b** diminished the selectivity toward Dyrk1B (compare with the 4-fluorobenzamide derivative **18b**) no further 4-pyridyl derivatives were synthesized. In many cases, placing substituents at the benzamide favourably reduced the inhibitory activity against Dyrk1B, in particular methoxy (**9b–11b**), 2-chloro (**13b**) and fluoro (**16b–19b**).

2.3.1.6. Insertion of a spacer in some benzamide derivatives (homologation). In our last set of modifications, alkyl spacers were introduced between the amide group and the phenyl ring. Compared with its direct benzamide homologue **4b**, the benzyl amide derivative **30b** displayed a marked improvement in the inhibitory activity to reach an IC₅₀ of 14.9 nM, which was even slightly superior to the most potent benzamide derivative **27b**. However, the introduction of a 4-fluoro substituent (analogous to **18b**) did not further increase the potency toward Dyrk1A (**31b**, IC₅₀ = 14.3 nM), and substitution of the benzyl by the electron-donating 3-methoxy strongly diminished the activity.

The main advantage of the benzylamide vs. the benzamide group was that it did not concomitantly enhance the activity towards Dyrk1B, thus increasing the selectivity factor to almost 27 for **31b** (IC₅₀ ratio Dyrk1B/Dyrk1A). Further elongation of the spacer by one methylene unit to afford compounds **33b** and **34b** did not give any indication that further homologations could be beneficial for the inhibitory activity.

2.3.2. Prediction of the binding mode of **31b** to Dyrk1A

As described above, the addition of a benzamide and especially of a benzylamide moiety to the basic bispyridyl thiophene scaffold led to a boost of potency against Dyrk1A. In order to predict a potential binding mode to the ATP pocket of Dyrk1A, the most potent compound, **31b**, was docked in the coordinates from PDB entry 5A3X [44]. As depicted in Fig. 3A, our docking study predicted two new interactions that are brought about by the benzylamide group: an H-bond between the amide NH and the Asp307 carboxylate, and a CH–π interaction (edge-to-face) between the phenyl ring and Phe170 at the Dyrk1A ATP binding pocket. Moreover, the latter interaction forces the benzyl group to sterically occlude this part of the pocket, thus shielding the H-bond between Asp307 and the amide NH from competing water molecules (Fig. 3B). Taken together, this ensemble of effects might explain the 21-fold increase in potency resulting from the addition of the benzylamide group to the basic scaffold (cf. Table 1).

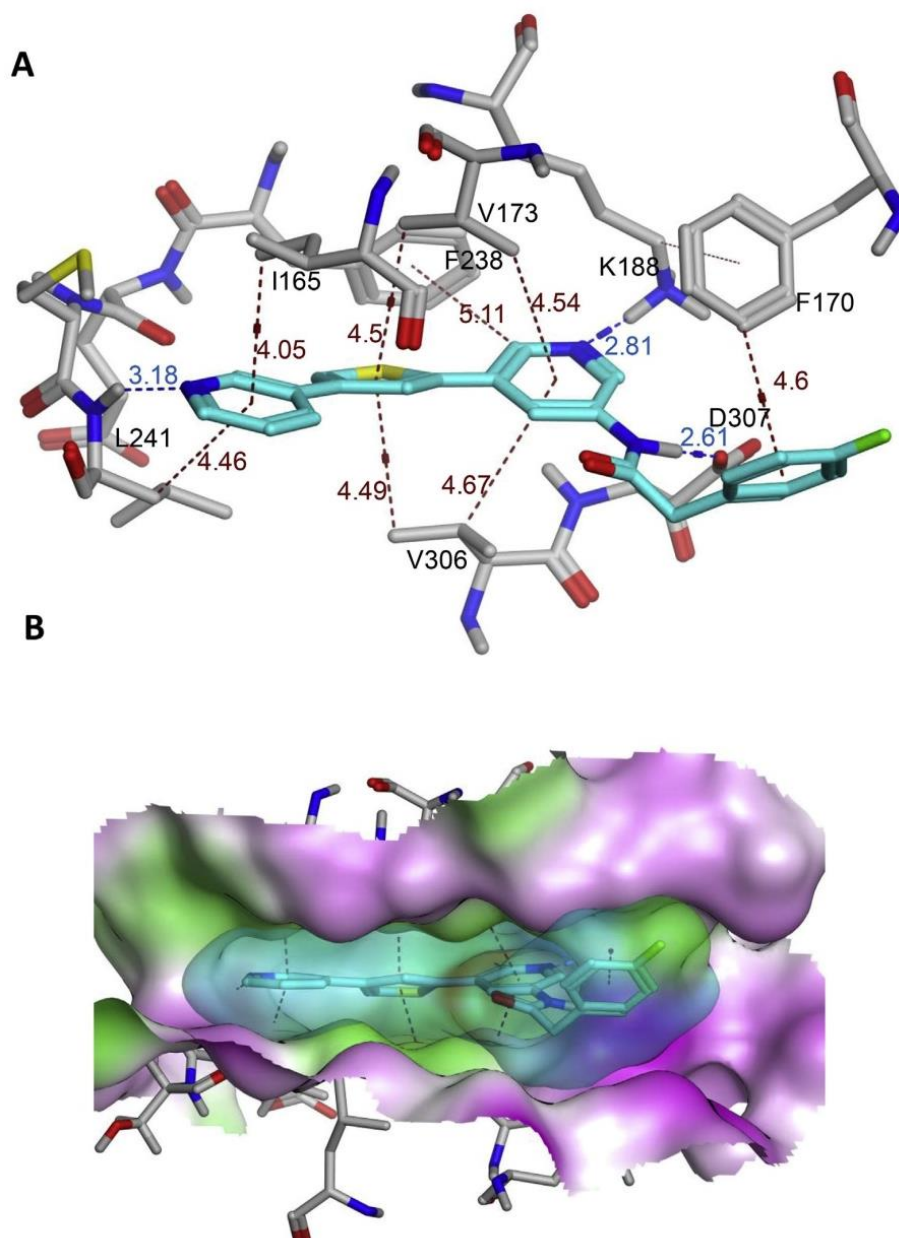


Fig. 3. Predicted binding mode of **31b** in the ATP binding pocket of Dyrk1A. Compound **31b** was docked to the Dyrk1A coordinates derived from the co-crystal structure with harmine (PDB code: 3ANR) using MOE. (A) The pose with the highest score is depicted, showing binding of **31b** (cyan) in the lowest energy conformation of the ligand. Inside the pocket, **31b** is anchored via two crucial H-bonds involving the backbone carbonyl of the hinge region residue Leu241, and the conserved Lys188 as a donor. An additional H-bond is formed between the amide NH and Asp307 (H-bonds are indicated by dashed blue lines). Several CH– π interactions additionally enhance the affinity (indicated by brown dashed lines). The assigned numbers denote the distances in Å. (B) Through the interaction with Phe170, the 4-fluorobenzyl ring (shown with transparent Connolly surface) occludes the right part of the binding pocket, thus shielding the H-bond between Asp307 and the amide NH from competing water molecules. Surface colours indicate lipophilic (green) and hydrophilic (magenta) areas. (For interpretation of the references to colour in this figure legend, the reader is referred to the Web version of this article.)

2.3.3. Extended selectivity profiling of **31b**

As mentioned earlier, one of our major objectives was to improve the selectivity of the previous bispyridyl thiophene compound class for Dyrk1A. After confirming its superior selectivity over Dyrk1B, our most potent inhibitor **31b** was further evaluated for its selectivity against an extended panel of kinases that were frequently reported as being co-inhibited by chemically diverse classes of Dyrk1A inhibitors (Table 3). Of note, **31b** showed only

negligible inhibition of Clk1, which was frequently hit by previous Dyrk1A inhibitors published by us and others [37–39,45–47]. In addition, compound **31b** showed no or only moderate inhibitory activity towards the other frequently reported off-target kinases such as CDK5/p25, CK1 delta, Dyrk2, HIPK1, TRKB, PIM1, MLCK2, SRPK1 and STK17A (Table 3). Also considering the remarkable selectivity towards the closest homologue, Dyrk1B, **31b** was found to be one of the most selective Dyrk1A inhibitors described to date.

Table 3
Selectivity profiling of compound **31b**.

| kinase | % Inhibition at 2 μM^a (IC_{50}) ^b |
|-----------|---|
| CDK5/p25 | 0 |
| Clk1 | 40 |
| Clk2 | 19 |
| CK1 delta | 4 |
| Dyrk1A | 87 (14.3 nM) |
| Dyrk2 | 40 |
| Haspin | 95 (36 nM) |
| HIPK1 | 0 |
| MLCK2 | 9.8 |
| TRKB | 10 |
| PIM1 | 8 |
| SRPK1 | 2 |
| STK17A | 60 |

^aThe screening list was especially composed to include all kinases that were frequently reported as off-targets for diverse chemical classes of Dyrk inhibitors [38,45,57–61]. Screenings were performed as a service at Thermo Fisher Scientific at an ATP concentration of 100 μM . Data represent mean values of duplicates that differed by less than 12%. ^b IC_{50} values were determined for inhibition values > 60% (ATP concentration: 15 μM) and represent mean values of at least two independent experiments, each performed in duplicates; S.D. < 10%.

However, it still inhibited the known off-target haspin, with about 2.5-fold lower potency than Dyrk1A. Haspin is a histone H3 kinase and required for cell proliferation; hence chemical inhibition of intracellular haspin leads to cell growth arrest [48]. However, we did not observe strong effects on HeLa cell proliferation with **31b** (see below for details).

How was selectivity over Clk1 achieved? Of note, while the core compound **C4** had shown the same affinity to both Dyrk1A and Clk1 [38], the benzamide extension decreased the potency of **31b** against Clk1 below that of the parent compound **C4**. Although all residues except Leu167 (corresponds to Ile165 in Dyrk1A) are conserved in Clk1, small spatial shifts of the backbone and the side chains are detectable in the published X-ray structures of the two kinases and may account for the affinity difference. A docking simulation revealed that the small topology differences translated into a less efficient binding of **31b** to Clk1 than to Dyrk1A, as reflected by the reduction in number of CH– π bonds (6 vs. 8) and H-bonds (2 vs. 3) (cf. Fig. S1, Supplementary Information). In accordance with the observed structure–selectivity relationships, the benzyl extension was predicted to have a key role in selectivity tuning towards Dyrk1A: in contrast to that of Dyrk1A, the ATP pocket of Clk1 did not allow favourable interaction of the 4-fluorobenzyl ring with Phe172 (corresponding to Phe170 in Dyrk1A, cf. Fig. 3A) inside the pocket; instead, the CH– π interaction is only possible with Gly170 from the glycine-rich loop, which can only occur at the expense of some interactions inside the pocket (Fig. S1, Supplementary Information).

2.3.4. Inhibition of Dyrk1A by **31b** in HeLa cells

To assess the ability of our most potent analogue **31b** to inhibit Dyrk1A in intact cells, we tested its effect on the Dyrk1A-catalyzed phosphorylation of splicing factor 3b1 (SF3b1). Phosphorylation of SF3b1 on Thr434 correlated with the cellular activity of endogenous Dyrk1A [25]. HeLa cells were transiently transfected with a GFP-SF3b1 expression vector and treated with **31b**. As can be seen in Fig. 4, **31b** inhibited the Dyrk1A-catalyzed phosphorylation of SF3b1 at Thr434 with high efficacy; a significant reduction of phosphorylated SF3b1 was already noted at 30 nM (IC_{50} = 79 nM, Fig. 4).

2.3.5. Evaluation of cytotoxicity in HeLa cells

Selective Dyrk1A inhibitors are not expected to induce cell

growth arrest, since Dyrk1A activity was even reported to diminish cell proliferation in several cell types [49–51]. Therefore, we evaluated our most potent compound, **31b**, for cytotoxicity, which would indicate potential off-target effects or non-specific toxicity. The cell viability assay was performed using HeLa cells, in which the inhibition of intracellular Dyrk1A had been quantified for the same compound (see above). As shown in Table 4, **31b** exerted minimal cytotoxicity up to a concentration of 3 μM , at which almost full inhibition of cellular Dyrk1A was observed before (cf. Fig. 4, IC_{50} = 79 nM). A weak inhibition of cell proliferation was noted at 10 μM ; this could be due to the inhibition of haspin, which might become effective in the cells at this higher concentration. In accordance, chemical inhibition of haspin in HeLa cells was previously shown to induce cell cycle arrest [48]. In the former study, compound HSD972, possessing an IC_{50} of 12 nM against purified haspin, inhibited HeLa cell proliferation with an IC_{50} of 4.8 μM .

Altogether, our results corroborated that – at least in HeLa cells – inhibition of Dyrk1A does not affect cell proliferation. It is therefore likely that the effects of previously published Dyrk1A inhibitors on cell growth of HeLa or other cell lines (e. g. harmine, IC_{50} with HeLa cells: 8 μM [40]) were rather caused by co-inhibition of Dyrk1B, haspin or other kinases.

2.4. Evaluation of the metabolic stability

We further assessed the suitability of two of the most potent analogues (**27b** and **31b**) for a potential application *in vivo*. To this end, we tested their phase I and phase II metabolic stability against S9 fraction from human liver homogenate. Different samples were taken at various time points, and the remaining fraction of parent compound was determined by LC-MS/MS. As shown in Table 5, both **27b** and **31b** exhibited a metabolic half-life of about 2 h. Even considering that the metabolic stability assays with our previous series were performed using rat liver microsomes, this was a substantial improvement to the non-amide extended precursor series; for instance, **C29** (Fig. 1) had shown a half-life of only 27 min [38]. Thus, both the benzamide and the benzylamide modification yielded compounds, **27b** and **31b**, respectively with promising metabolic stability, permitting to test them in future *in vivo* studies.

2.5. Calculation of key physicochemical properties

In order to assess whether the most potent compound **31b** might be able to enter the CNS, we calculated some physicochemical parameters that were found to have a predictive value in retrospective studies [52,53]. In our previous study, the calculated values were found in good agreement with the corresponding experimental values for this compound class [38]. It can be concluded that the values for **31b** (Table 6) are still in a good range with respect to a potential application in the CNS, although the clogP is above the average value found for CNS drugs. However, in general, the lipophilicity reported for CNS drugs tends to be higher than that of non-CNS drugs; for instance, in the survey from Mahar Doan et al. the respective clogP median values were 3.43 for CNS drugs (range 0.16–6.59), and 2.78 for non-CNS drugs (range: –2.81–6.09).

3. Conclusions

The current work presented a series of novel Dyrk1A inhibitors bearing a crucial amide extension. Various benzamide derivatives were synthesized by probing mono-, di- and tri-substitutions with distinct electron-modulating properties. Finally, the insertion of a spacer was tested, which resulted in a dramatic improvement in potency as observed with compounds **30b** and **31b** (IC_{50} = 14.9 nM

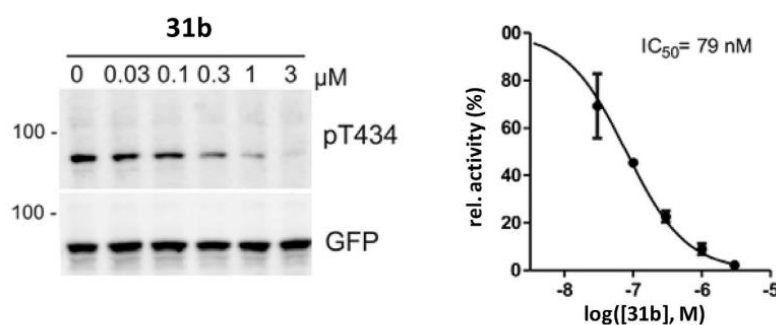


Fig. 4. Inhibition of Dyrk1A activity in cell culture. HeLa cells were transiently transfected with an expression vector for GFP-SF3b1-NT. Cells were treated with variable concentrations of **31b** for 18 h before the phosphorylation of SF3b1 on T434 was measured by immunoblot analysis (left panels). The IC_{50} value for Dyrk1A inhibition was determined from the concentration-response curve fitted to the results of three experiments (means \pm SEM). Dyrk1A activity is shown relative to that in vehicle-treated cells.

Table 4
Effect of **31b** on HeLa cell growth.

| | 1 μ M | 3 μ M | 10 μ M |
|----------------------------|------------|------------|------------|
| 31b | 99 \pm 2 | 97 \pm 5 | 88 \pm 2 |
| Staurosporine ^a | 33 \pm 4 | | |

Viability of treated HeLa cells is given in percent relative to control cells treated with vehicle (means of two experiments with duplicate measurement \pm S.D.). ^a Staurosporine is a known inducer of apoptosis and served as a positive control.

Table 5
Metabolic stability of **27b** and **31b** against human liver S9 fraction^a.

| Cpd No. | Half-life [min] |
|---------------------------|-----------------|
| 27b | 123 |
| 31b | 118 |
| Testosterone ^b | 8.5 |

^a 10 mg/mL, NADP⁺ regenerating system, MgCl₂, UDPGA, PAPS, [inhibitor] = 0.3 μ M, incubation at 37 °C, samples taken at 0, 15, 30, 60, 90 and 120 min, determination of the parent compound by LC-MS/MS. ^b included as a positive control for a rapidly metabolized compound.

Table 6
Calculated physicochemical properties of **31b**.

| Cpd.No. | MW [g/mol] | logP | TPSA [\AA^2] | TPSA [\AA^2] ^b | HBD | HBA |
|------------------------|------------|------|-------------------------|--------------------------------------|-----|-----|
| 31b | 389.45 | 4.11 | 83.1 | 54.88 | 1 | 3 |
| C29^a | 244.34 | 2.48 | 82.3 | 25.8 | 0 | 2 |

^a C29 values are shown for comparison (taken from Ref. [38]). ^b Sulphur was not considered for the calculation of TPSA. Ideal ranges for CNS active drugs: MW: 181–427 g/mol, logP: 0.4–5.1 (median: 2.8), TPSA < 76 \AA^2 , HBD: 0–1; HBA: 2–3 [62].

and 14.3 nM, respectively). Importantly, **31b** also showed a remarkable selectivity over the closely related kinases Dyrk1B and Clk1, which has rarely been reported for previous Dyrk1A inhibitors (IC_{50} : Dyrk1B = 383 nM, Clk1 > 2 μ M). Since Dyrk1A and Clk1 share several splicing factors as substrates, including AF2/ASF, SC35, and SRp55 [23,24,26], our selective inhibitor **31b** will allow to dissect Dyrk1A— from Clk1—mediated splicing regulations; moreover, potential side effects due to a synergistic modulation of SR protein activities through Dyrk1A/Clk1 co-inhibition will be avoided in potential therapeutic trials.

Furthermore, **31b** successfully inhibited Dyrk1A—mediated phosphorylation of SF3b1 in HeLa cells in the two-digit nanomolar range (IC_{50} = 79 nM) while no cytotoxic effects were noted at 3 μ M, and only marginal effects at 10 μ M, thus providing an appropriate

toxicity window for *in vivo* applications. The absence of cytotoxic side effects is especially important when a prolonged treatment of neurodegenerative diseases is envisaged, where the cell viability is already compromised by harmful peptide and protein aggregates.

The metabolic stability was also found to be significantly improved by the new benzamide and benzylamide modification of the previous scaffold. Altogether, the new modification led to an optimization of the key parameters potency, selectivity and metabolic stability, thus allowing to envisage *in vivo* studies in the next step.

4. Experimental section

4.1. Chemistry

Solvents and reagents were obtained from commercial suppliers and used as received. Melting points were determined on a Stuart SMP3 melting point apparatus. All final compounds had a percentage purity of at least 95%, and this could be verified by means of HPLC coupled with mass spectrometry. Mass spectra (HPLC–ESIMS) were obtained using a TSQ quantum (Thermo Electron Corp.) instrument prepared with a triple quadrupole mass detector (Thermo Finnigan) and an ESI source. All samples were injected using an autosampler (Surveyor, Thermo Finnigan) by an injection volume of 10 μ L. The MS detection was determined using a source CID of 10 V and carried out at a spray voltage of 4.2 kV, a nitrogen sheath gas pressure of 4.0×10^5 Pa, a capillary temperature of 400 °C, a capillary voltage of 35 V, and an auxiliary gas pressure of 1.0×10^5 Pa. The stationary phase used was an RP C18 NUCLEODUR 100–3 (125 mm \times 3 mm) column (Macherey & Nagel). The solvent system consisted of water containing 0.1% TFA (A) and 0.1% TFA in acetonitrile (B). The HPLC method used a flow rate of 400 μ L/min. The percentage of B started at 5%, was increased up to 100% during 7 min, was kept at 100% for 2 min, and was flushed back to 5% in 2 min and was kept at 5% for 2 min. A Bruker DRX 500 spectrometer was used to obtain the ¹H NMR and ¹³C NMR spectra. The chemical shifts are referenced to the residual protonated solvent signals.

4.1.1. General synthetic procedures and experimental details

4.1.1.1. Procedure A, procedure for synthesis of compounds A – D. A mixture of 5 mmol of the appropriate amino-5-bromo pyridine and 1.96 gm (20 mmol) of potassium acetate and 0.18 gm (0.25 mmol) of Pd(dppf)Cl₂ and 5.08 gm (20 mmol) of bis(pinacolato)diboron in dioxane was heated to reflux under argon for 2 h to yield compounds **A** and **B**. The mixture was left to attain room temperature and then filtered under vacuum. Without further

purification, a reaction flask containing the filtrate was charged with 6.5 gm (20 mmol) of Cs_2CO_3 , 0.29 gm (0.25 mmol) of palladium-tetrakis(triphenylphosphine) and 6 mmol of 2,4-dibromothiophene together with 30% water in a Suzuki coupling reaction. The reaction was left to reflux under argon for 3.5 h. The mixture was concentrated *in vacuo*. The residue was partitioned between 150 mL ethyl acetate and 50 mL brine solution and then the aqueous layer was re-extracted using 3 portions of 100 mL ethyl acetate. The organic layers were collected and the volume was reduced under reduced pressure. Afterwards the product was purified by CC to yield compounds **C–D**.

4.1.1.2. Procedure B, general procedure for amide synthesis (4a, 6a–34a). A solution of 0.18 gm (0.7 mmol) of compound **D** dissolved in acetone was treated with 0.84 mmol of the appropriate acid chloride followed by the addition of 0.12 gm (1.05 mmol) of TEA. The reaction mixture was left to stir at room temperature for 2 h which was followed by evaporation of solvent *in vacuo* and the product was purified by CC.

4.1.1.3. Procedure C, general procedure for synthesis of compounds 1–3, 4b–34b, 35. The bromo derivative was added to a suspension of 4 equiv of Na_2CO_3 and 5 mmol% of $\text{Pd}(\text{dppf})\text{Cl}_2$ in dioxane/water mixture. This was followed by the addition of the pyridine boronic acid derivative. The reaction was heated to reflux for 2 h under argon atmosphere. The solvent was removed *in vacuo*. Small amount of brine solution was added and extraction was done using ethyl acetate (3 \times 50 mL). The ethyl acetate portions were collected and the volume was reduced *in vacuo*. Afterwards the product was purified by CC.

4.1.1.4. 5-(4-Bromothiophen-2-yl)pyridin-2-amine (C). The compound was synthesized according to procedure **A** using 2-amino-5-bromopyridine: yield: 42%. The product was purified by CC (ethyl acetate/petroleum ether 7:3); ^1H NMR (500 MHz, DMSO) δ 8.23 (d, J = 2.5 Hz, 1H), 7.64 (dd, J = 8.6, 2.6 Hz, 1H), 7.51 (d, J = 1.4 Hz, 1H), 7.32 (d, J = 1.4 Hz, 1H), 6.47 (d, J = 8.7 Hz, 1H), 6.27 (s, 2H); ^{13}C NMR (126 MHz, DMSO) δ 159.71, 144.87, 143.27, 134.41, 123.36, 120.71, 117.24, 109.61, 107.94; MS (ESI) m/z = 254.79 ($\text{M} + \text{H}$) $^+$

4.1.1.5. 5-(4-Bromothiophen-2-yl)pyridin-3-amine (D). The compound was synthesized according to Procedure **A** using 3-amino-5-bromopyridine: yield 80%. The product was purified by CC (ethyl acetate); ^1H NMR (500 MHz, DMSO) δ 8.08 (d, J = 2.0 Hz, 1H), 7.91 (d, J = 2.5 Hz, 1H), 7.70 (d, J = 1.4 Hz, 1H), 7.51 (d, J = 1.5 Hz, 1H), 7.16–7.05 (m, 1H), 5.50 (s, 2H); ^{13}C NMR (126 MHz, DMSO) δ 144.98, 142.31, 136.28, 133.61, 128.34, 126.16, 123.47, 115.68, 109.89; MS (ESI) m/z = 254.82 ($\text{M} + \text{H}$) $^+$

4.1.1.6. 3-(4-Bromothiophen-2-yl)pyridine (E). The title compound was synthesized by reacting 0.5 gm (4 mmol) 3-pyridine boronic acid with 1.2 gm (4.8 mmol) 2,4-dibromothiophene in presence of 5.2 gm (16 mmol) Cs_2CO_3 and 0.14 gm (0.2 mmol) palladium-tetrakis(triphenylphosphine) in dioxane/water. The mixture was left to stir under reflux in inert conditions for 3 h. The solvent was concentrated *in vacuo*, a small amount of brine solution was added to the residue and extracted with ethyl acetate (3 \times 50 mL). The organic layers were collected and the solvent was evaporated *in vacuo*: yield 77%. The product was purified by CC (ethyl acetate/petroleum ether 6:4); ^1H NMR (500 MHz, DMSO) δ 8.92 (dd, J = 2.4, 0.8 Hz, 1H), 8.54 (dd, J = 4.8, 1.5 Hz, 1H), 8.06 (ddd, J = 8.0, 2.4, 1.6 Hz, 1H), 7.78 (d, J = 1.4 Hz, 1H), 7.72 (d, J = 1.5 Hz, 1H), 7.46 (ddd, J = 8.0, 4.8, 0.8 Hz, 1H); ^{13}C NMR (126 MHz, DMSO) δ 149.17, 146.14, 141.14, 132.72, 128.55, 127.15, 124.28, 124.08, 110.15; MS (ESI) = 239.80 ($\text{M} + \text{H}$) $^+$

4.1.1.7. N-(5-(4-bromothiophen-2-yl)pyridin-3-yl)benzamide (4a). The compound was synthesized according to procedure **B** using benzoyl chloride: yield 79%. The product was purified by CC (ethyl acetate/petroleum ether 7:3); ^1H NMR (400 MHz, DMSO) δ 10.59 (s, 1H), 8.94 (d, J = 2.0 Hz, 1H), 8.71 (d, J = 1.9 Hz, 1H), 8.48 (t, J = 2.1 Hz, 1H), 8.05–7.98 (m, 2H), 7.70 (d, J = 1.2 Hz, 1H), 7.66–7.49 (m, 4H); ^{13}C NMR (101 MHz, DMSO) δ 166.51, 141.67, 141.58, 136.57, 134.55, 132.49, 129.50, 129.16, 128.96, 128.20, 127.54, 124.85, 123.73, 110.67; MS (ESI) m/z = 358.85 ($\text{M} + \text{H}$) $^+$

4.1.1.8. N-(5-(4-bromothiophen-2-yl)pyridin-3-yl)benzenesulfonamide (5a). The title compound was synthesized through adding 1.4 mmol of the benzenesulfonyl chloride to a stirred solution of 0.18 gm (0.7 mmol) of compound **B** dissolved in pyridine. The reaction was heated to 60 $^\circ\text{C}$ and left overnight. This was followed by the removal of solvent *in vacuo*: yield 89%. The product was purified by precipitation in ethyl acetate; ^1H NMR (500 MHz, DMSO) δ 10.17 (s, 1H), 8.65 (d, J = 2.0 Hz, 1H), 8.28 (d, J = 2.3 Hz, 1H), 7.72 (t, J = 2.2 Hz, 1H), 7.65 (d, J = 1.5 Hz, 1H), 7.64–7.56 (m, 6H); ^{13}C NMR (126 MHz, DMSO) δ 148.22, 141.33, 140.14, 138.86, 134.95, 133.40, 129.53, 127.67, 126.75, 125.48, 124.92, 123.51, 110.32; MS (ESI) m/z = 387.94 ($\text{M} + \text{H}$) $^+$

4.1.1.9. N-(5-(4-bromothiophen-2-yl)pyridin-3-yl)-2-methylbenzamide (6a). The compound was synthesized according to procedure **B** using *o*-toluoyl chloride: yield 96%. The product was purified by CC (ethyl acetate/petroleum ether 2:3); ^1H NMR (400 MHz, DMSO) δ 10.63 (s, 1H), 8.83 (d, J = 2.1 Hz, 1H), 8.70 (d, J = 2.1 Hz, 1H), 8.47 (s, 1H), 7.80 (d, J = 1.4 Hz, 1H), 7.69 (d, J = 1.3 Hz, 1H), 7.53 (d, J = 7.6 Hz, 1H), 7.47–7.38 (m, 1H), 7.33 (t, J = 7.4 Hz, 2H), 2.41 (s, 3H); ^{13}C NMR (101 MHz, DMSO) δ 168.46, 141.13, 140.99, 140.63, 136.28, 136.19, 135.56, 130.69, 130.09, 128.37, 127.38, 127.12, 125.70, 124.44, 122.55, 110.21, 19.38; MS (ESI) m/z = 372.9 ($\text{M} + \text{H}$) $^+$

4.1.1.10. N-(5-(4-bromothiophen-2-yl)pyridin-3-yl)-3-methylbenzamide (7a). The compound was synthesized according to procedure **B** using *m*-toluoyl chloride: yield 87%. The product was purified by CC (ethyl acetate/petroleum ether 2:3); ^1H NMR (500 MHz, DMSO) δ 10.53 (s, 1H), 8.93 (d, J = 2.3 Hz, 1H), 8.71 (d, J = 2.1 Hz, 1H), 8.46 (t, J = 2.2 Hz, 1H), 7.82 (s, 1H), 7.81 (d, J = 1.4 Hz, 1H), 7.80–7.77 (m, 1H), 7.70 (d, J = 1.4 Hz, 1H), 7.45 (dd, J = 3.9, 1.8 Hz, 2H), 2.42 (s, 3H); ^{13}C NMR (126 MHz, DMSO) δ 166.17, 141.22, 141.15, 141.01, 137.86, 136.15, 134.13, 132.62, 128.42, 128.28, 128.19, 127.09, 124.94, 124.41, 123.28, 110.21, 20.96; MS (ESI) m/z = 372.96 ($\text{M} + \text{H}$) $^+$

4.1.1.11. N-(5-(4-bromothiophen-2-yl)pyridin-3-yl)-4-methylbenzamide (8a). The compound was synthesized according to procedure **B** using *p*-toluoyl chloride: yield 90%. The product was purified by CC (ethyl acetate/petroleum ether 1:1); ^1H NMR (500 MHz, DMSO) δ 10.48 (s, 1H), 8.93 (d, J = 2.3 Hz, 1H), 8.70 (d, J = 2.1 Hz, 1H), 8.47 (t, J = 2.2 Hz, 1H), 7.93 (s, 1H), 7.91 (s, 1H), 7.81 (d, J = 1.4 Hz, 1H), 7.70 (d, J = 1.4 Hz, 1H), 7.37 (d, J = 7.9 Hz, 2H), 2.40 (s, 3H); ^{13}C NMR (126 MHz, DMSO) δ 165.87, 142.19, 141.23, 141.18, 140.95, 136.20, 131.23, 129.05, 128.27, 127.80, 127.09, 124.40, 123.29, 110.21, 21.05; MS (ESI) m/z = 372.89 ($\text{M} + \text{H}$) $^+$

4.1.1.12. N-(5-(4-bromothiophen-2-yl)pyridin-3-yl)-2-methoxybenzamide (9a). The compound was synthesized according to procedure **B** using 2-methoxybenzoyl chloride: yield 60%. The product was purified by CC (ethyl acetate/petroleum ether 3:7); ^1H NMR (500 MHz, DMSO) δ 10.43 (s, 1H), 8.84 (d, J = 2.2 Hz, 1H), 8.69 (d, J = 2.1 Hz, 1H), 8.47 (t, J = 2.1 Hz, 1H), 7.81 (d, J = 1.4 Hz, 1H), 7.70 (d, J = 1.3 Hz, 1H), 7.68 (dd, J = 7.6, 1.7 Hz, 1H), 7.57–7.49 (m, 1H), 7.21 (d, J = 8.4 Hz, 1H), 7.09 (dd, J = 7.7, 7.2 Hz, 1H), 3.92 (s,

3H); ^{13}C NMR (126 MHz, DMSO) δ 165.26, 156.62, 141.11, 140.97, 140.83, 135.94, 132.54, 129.78, 128.38, 127.16, 124.43, 124.12, 122.68, 120.55, 112.08, 110.19, 55.96; MS (ESI) m/z = 388.95 ($\text{M} + \text{H}^+$)

4.1.1.13. *N*-(5-(4-bromothiophen-2-yl)pyridin-3-yl)-3-methoxybenzamide (10a). The compound was synthesized according to procedure **B** using 3-methoxybenzoyl chloride: yield 84%. The product was purified by CC (ethyl acetate/petroleum ether 3:2); ^1H NMR (500 MHz, DMSO) δ 10.53 (s, 1H), 8.92 (d, J = 2.3 Hz, 1H), 8.72 (d, J = 2.1 Hz, 1H), 8.46 (t, J = 2.2 Hz, 1H), 7.81 (d, J = 1.4 Hz, 1H), 7.70 (d, J = 1.4 Hz, 1H), 7.62–7.57 (m, 1H), 7.55–7.52 (m, 1H), 7.49 (t, J = 7.9 Hz, 1H), 7.24–7.14 (m, 1H), 3.85 (s, 3H); ^{13}C NMR (126 MHz, DMSO) δ 165.79, 159.26, 141.30, 141.12, 136.05, 135.50, 129.72, 128.30, 127.13, 124.44, 123.39, 121.54, 119.93, 117.75, 113.06, 110.22, 55.40; MS (ESI) m/z = 388.89 ($\text{M} + \text{H}^+$)

4.1.1.14. *N*-(5-(4-bromothiophen-2-yl)pyridin-3-yl)-4-methoxybenzamide (11a). The compound was synthesized according to procedure **B** using 4-methoxybenzoyl chloride: yield 72%. The product was purified by CC (ethyl acetate/petroleum ether 7:3); ^1H NMR (500 MHz, DMSO) δ 10.46 (s, 1H), 8.93 (d, J = 2.3 Hz, 1H), 8.68 (d, J = 2.1 Hz, 1H), 8.46 (t, J = 2.2 Hz, 1H), 8.02 (s, 1H), 8.00 (s, 1H), 7.80 (d, J = 1.4 Hz, 1H), 7.69 (d, J = 1.4 Hz, 1H), 7.10 (s, 1H), 7.09 (s, 1H), 3.85 (s, 3H); ^{13}C NMR (126 MHz, DMSO) δ 165.41, 162.26, 141.25, 141.23, 140.78, 136.36, 129.78, 128.25, 127.05, 126.12, 124.36, 123.25, 113.74, 110.20, 55.49; MS (ESI) m/z = 388.95 ($\text{M} + \text{H}^+$)

4.1.1.15. *N*-(5-(4-bromothiophen-2-yl)pyridin-3-yl)-4-(tert-butyl)benzamide (12a). The compound was synthesized according to procedure **B** using 4-tert-butylbenzoyl chloride: yield 79%. The product was purified by CC (ethyl acetate/petroleum ether 1:1); ^1H NMR (500 MHz, DMSO) δ 10.49 (s, 1H), 8.92 (d, J = 2.2 Hz, 1H), 8.70 (d, J = 2.1 Hz, 1H), 8.47 (t, J = 2.2 Hz, 1H), 7.94 (d, J = 8.4 Hz, 2H), 7.81 (d, J = 1.4 Hz, 1H), 7.70 (d, J = 1.4 Hz, 1H), 7.58 (d, J = 8.4 Hz, 2H), 1.33 (s, 9H); ^{13}C NMR (126 MHz, DMSO) δ 165.97, 154.96, 141.15, 140.93, 136.19, 131.38, 129.16, 128.26, 127.61, 127.07, 126.43, 125.34, 125.28, 124.39, 123.16, 110.19, 34.73, 30.89; MS (ESI) m/z = 414.92 ($\text{M} + \text{H}^+$)

4.1.1.16. *N*-(5-(4-bromothiophen-2-yl)pyridin-3-yl)-2-chlorobenzamide (13a). The compound was synthesized according to procedure **B** using 2-chlorobenzoyl chloride: yield 59%. The product was purified by CC (ethyl acetate/petroleum ether 3:2); ^1H NMR (500 MHz, DMSO) δ 10.88 (s, 1H), 8.80 (d, J = 2.2 Hz, 1H), 8.73 (d, J = 2.0 Hz, 1H), 8.44 (t, J = 2.1 Hz, 1H), 7.81 (d, J = 1.4 Hz, 1H), 7.74–7.66 (m, 1H), 7.66 (dd, J = 7.5, 1.6 Hz, 1H), 7.62–7.58 (m, 1H), 7.55 (td, J = 7.7, 1.7 Hz, 1H), 7.49 (td, J = 7.4, 1.2 Hz, 1H); ^{13}C NMR (126 MHz, DMSO) δ 165.60, 141.34, 140.97, 140.44, 136.16, 135.85, 131.54, 129.96, 129.79, 129.06, 128.47, 127.35, 127.24, 124.54, 122.43, 110.25; MS (ESI) m/z = 392.9 ($\text{M} + \text{H}^+$)

4.1.1.17. *N*-(5-(4-bromothiophen-2-yl)pyridin-3-yl)-3-chlorobenzamide (14a). The compound was synthesized according to procedure **B** using 3-chlorobenzoyl chloride: yield 65%. The product was purified by CC (ethyl acetate/petroleum ether 3:2); ^1H NMR (500 MHz, DMSO) δ 10.65 (s, 1H), 8.92 (d, J = 2.3 Hz, 1H), 8.73 (d, J = 2.1 Hz, 1H), 8.44 (t, J = 2.2 Hz, 1H), 8.06 (t, J = 1.8 Hz, 1H), 7.98–7.92 (m, 1H), 7.81 (d, J = 1.4 Hz, 1H), 7.71 (qd, J = 2.2, 1.0 Hz, 2H), 7.61 (t, J = 7.9 Hz, 1H); ^{13}C NMR (126 MHz, DMSO) δ 164.61, 141.32, 141.27, 141.04, 136.10, 135.85, 133.32, 131.86, 130.57, 128.33, 127.49, 127.17, 126.62, 124.48, 123.43, 110.24; MS (ESI) m/z = 392.81 ($\text{M} + \text{H}^+$)

4.1.1.18. *N*-(5-(4-bromothiophen-2-yl)pyridin-3-yl)-4-chlorobenzamide (15a). The compound was synthesized according to procedure **B** using 4-chlorobenzoyl chloride: yield 78%. The

product was purified by CC (ethyl acetate/petroleum ether 7:3); ^1H NMR (500 MHz, DMSO) δ 10.62 (s, 1H), 8.91 (d, J = 2.2 Hz, 1H), 8.72 (d, J = 2.0 Hz, 1H), 8.44 (t, J = 2.2 Hz, 1H), 8.03 (d, J = 1.9 Hz, 1H), 8.02 (s, 1H), 7.81 (d, J = 1.3 Hz, 1H), 7.70 (d, J = 1.4 Hz, 1H), 7.66 (d, J = 1.9 Hz, 1H), 7.65 (s, 1H); ^{13}C NMR (126 MHz, DMSO) δ 164.98, 141.28, 141.24, 141.07, 136.92, 135.93, 132.82, 129.72, 128.63, 128.32, 127.15, 124.46, 123.42, 110.23; MS (ESI) m/z = 392.89 ($\text{M} + \text{H}^+$)

4.1.1.19. *N*-(5-(4-bromothiophen-2-yl)pyridin-3-yl)-2-fluorobenzamide (16a). The compound was synthesized according to procedure **B** using 2-fluorobenzoyl chloride: yield 68%. The product was purified by CC (ethyl acetate/petroleum ether 7:3); ^1H NMR (500 MHz, DMSO) δ 11.16 (s, 1H), 9.01 (d, J = 2.0 Hz, 1H), 8.91 (d, J = 1.9 Hz, 1H), 8.66 (s, 1H), 7.89 (d, J = 1.4 Hz, 1H), 7.83 (d, J = 1.4 Hz, 1H), 7.77 (td, J = 7.5, 1.7 Hz, 1H), 7.69–7.62 (m, 1H), 7.39 (dt, J = 12.0, 9.0 Hz, 2H); ^{13}C NMR (126 MHz, DMSO) δ 163.58, 159.09 (d, $J_{\text{C-F}}$ = 250.4 Hz), 139.63, 138.12, 136.94, 136.79, 133.40 (d, $J_{\text{C-F}}$ = 8.5 Hz), 130.10 (d, $J_{\text{C-F}}$ = 2.2 Hz), 129.87, 128.32, 125.57, 125.51, 124.69 (d, $J_{\text{C-F}}$ = 3.5 Hz), 123.62 (d, $J_{\text{C-F}}$ = 14.1 Hz), 116.38 (d, $J_{\text{C-F}}$ = 21.5 Hz), 110.41; MS (ESI) m/z = 376.89 ($\text{M} + \text{H}^+$)

4.1.1.20. *N*-(5-(4-bromothiophen-2-yl)pyridin-3-yl)-3-fluorobenzamide (17a). The compound was synthesized according to procedure **B** using 3-fluorobenzoyl chloride: yield 79%. The product was purified by CC (ethyl acetate/petroleum ether 1:1); ^1H NMR (500 MHz, DMSO) δ 10.63 (s, 1H), 8.92 (d, J = 2.3 Hz, 1H), 8.73 (d, J = 2.1 Hz, 1H), 8.45 (s, 1H), 7.86 (d, J = 7.8 Hz, 1H), 7.83–7.80 (m, 2H), 7.71 (d, J = 1.4 Hz, 1H), 7.63 (td, J = 8.0, 5.9 Hz, 1H), 7.50 (td, J = 8.1, 2.2 Hz, 1H); ^{13}C NMR (126 MHz, DMSO) δ 164.67, 161.94 (d, $J_{\text{C-F}}$ = 244.5 Hz), 141.29 (d, $J_{\text{C-F}}$ = 4.4 Hz), 141.04, 136.40 (d, $J_{\text{C-F}}$ = 7.0 Hz), 135.85, 130.77 (d, $J_{\text{C-F}}$ = 8.0 Hz), 128.32, 127.16, 124.47, 124.01, 123.98, 123.43, 118.97 (d, $J_{\text{C-F}}$ = 21.2 Hz), 114.60 (d, $J_{\text{C-F}}$ = 23.0 Hz), 110.23; MS (ESI) m/z = 377 ($\text{M} + \text{H}^+$)

4.1.1.21. *N*-(5-(4-bromothiophen-2-yl)pyridin-3-yl)-4-fluorobenzamide (18a). The compound was synthesized according to procedure **B** using 4-fluorobenzoyl chloride: yield 98%. The product was purified by CC (ethyl acetate/petroleum ether 3:2); ^1H NMR (500 MHz, DMSO) δ 10.57 (s, 1H), 8.91 (d, J = 2.3 Hz, 1H), 8.72 (d, J = 2.1 Hz, 1H), 8.44 (t, J = 2.2 Hz, 1H), 8.12–8.05 (m, 2H), 7.81 (d, J = 1.4 Hz, 1H), 7.70 (d, J = 1.4 Hz, 1H), 7.41 (t, J = 8.9 Hz, 2H); ^{13}C NMR (126 MHz, DMSO) δ 164.96, 164.34 (d, $J_{\text{C-F}}$ = 249.7 Hz), 141.26, 141.12 (d, $J_{\text{C-F}}$ = 5.1 Hz), 136.03, 132.10 (d, $J_{\text{C-F}}$ = 9.5 Hz), 130.60, 127.13, 124.44, 123.37, 115.62 (d, $J_{\text{C-F}}$ = 22.0 Hz), 115.61, 115.44, 110.23; MS (ESI) m/z = 376.98 ($\text{M} + \text{H}^+$)

4.1.1.22. *N*-(5-(4-bromothiophen-2-yl)pyridin-3-yl)-2-(trifluoromethyl)benzamide fluorobenzamide (19a). The compound was synthesized according to procedure **B** using 2-trifluoromethylbenzoyl chloride: yield 86%. The product was purified by CC (ethyl acetate/petroleum ether 3:2); ^1H NMR (500 MHz, DMSO) δ 10.96 (s, 1H), 8.78 (d, J = 2.3 Hz, 1H), 8.74 (d, J = 2.1 Hz, 1H), 8.40 (s, 1H), 7.89 (d, J = 7.8 Hz, 1H), 7.83–7.81 (m, 2H), 7.76 (ddd, J = 8.2, 7.4, 4.9 Hz, 2H), 7.71 (d, J = 1.4 Hz, 1H); ^{13}C NMR (126 MHz, DMSO) δ 166.24, 141.40, 140.90, 140.45, 135.80, 132.69, 132.62, 131.16, 130.46, 129.64, 128.61, 128.47, 127.23, 126.46 (q, $J_{\text{C-F}}$ = 5.0, 2.2 Hz), 124.52, 122.48, 110.23; MS (ESI) m/z = 426.93 ($\text{M} + \text{H}^+$)

4.1.1.23. *N*-(5-(4-bromothiophen-2-yl)pyridin-3-yl)-3-(trifluoromethyl)benzamide fluorobenzamide (20a). The compound was synthesized according to procedure **B** using 3-trifluoromethylbenzoyl chloride: yield 84%. The product was purified by CC (ethyl acetate/petroleum ether 3:2); ^1H NMR (500 MHz, DMSO) δ 10.78 (s, 1H), 8.93 (d, J = 2.3 Hz, 1H), 8.75 (d, J = 2.1 Hz, 1H), 8.44 (t, J = 2.2 Hz, 1H), 8.30 (d, J = 7.9 Hz, 1H), 8.23 (d, J = 7.8 Hz, 1H),

8.18 (s, 1H), 7.81 (d, $J = 1.4$ Hz, 1H), 7.77 (s, 1H), 7.72 (d, $J = 1.4$ Hz, 1H); ^{13}C NMR (126 MHz, DMSO) δ 166.00, 141.02, 135.78, 135.03, 133.22, 130.10, 129.89, 129.40 (q, $J_{\text{C-F}} = 3.5$ Hz), 128.58 (q, $J_{\text{C-F}} = 7.2$, 3.6 Hz), 128.36, 127.20, 125.50 (q, $J_{\text{C-F}} = 3.9$ Hz), 124.50, 124.35 (q, $J_{\text{C-F}} = 7.7$, 3.9 Hz), 123.60, 122.71, 110.25; MS (ESI) $m/z = 426.88$ (M + H) $^{+}$

4.1.1.24. *N*-(5-(4-bromothiophen-2-yl)pyridin-3-yl)-4-(trifluoromethyl)benzamide fluorobenzamide (21a). The compound was synthesized according to procedure **B** using 4-trifluoromethylbenzoyl chloride: yield 80%. The product was purified by CC (ethyl acetate/petroleum ether 7:3); ^1H NMR (500 MHz, DMSO) δ 10.78 (s, 1H), 8.92 (d, $J = 2.3$ Hz, 1H), 8.74 (d, $J = 2.1$ Hz, 1H), 8.46 (t, $J = 2.2$ Hz, 1H), 8.20 (s, 1H), 8.19 (s, 1H), 7.97 (s, 1H), 7.95 (s, 1H), 7.81 (d, $J = 1.4$ Hz, 1H), 7.71 (d, $J = 1.4$ Hz, 1H); ^{13}C NMR (126 MHz, DMSO) δ 164.93, 141.44, 141.31, 141.01, 137.93, 135.80, 131.87, 128.71, 128.36, 127.21, 126.95, 125.55 (q, $J_{\text{C-F}} = 7.4$, 3.7 Hz), 124.51, 123.49, 110.25; MS (ESI) $m/z = 426.93$ (M + H) $^{+}$

4.1.1.25. *N*-(5-(4-bromothiophen-2-yl)pyridin-3-yl)-2,3-dichlorobenzamide (22a). The compound was synthesized according to procedure **B** using 2,3-dichlorobenzoyl chloride: yield 78%. The product was purified by CC (ethyl acetate/petroleum ether 1:1); ^1H NMR (500 MHz, DMSO) δ 10.98 (s, 1H), 8.76 (dd, $J = 13.1$, 2.2 Hz, 2H), 8.42 (t, $J = 2.2$ Hz, 1H), 7.81 (td, $J = 4.1$, 1.5 Hz, 2H), 7.72 (d, $J = 1.4$ Hz, 1H), 7.64 (dd, $J = 7.6$, 1.5 Hz, 1H), 7.52 (t, $J = 7.8$ Hz, 1H); ^{13}C NMR (126 MHz, DMSO) δ 164.80, 141.52, 140.88, 140.42, 138.40, 135.65, 132.22, 131.75, 128.78, 128.51, 128.16, 127.51, 127.29, 124.57, 122.48, 110.26; MS (ESI) $m/z = 426.78$ (M + H) $^{+}$

4.1.1.26. *N*-(5-(4-bromothiophen-2-yl)pyridin-3-yl)-2,4-difluorobenzamide (23a). The compound was synthesized according to procedure **B** using 2,4-difluorobenzoyl chloride: yield 75%. The product was purified by CC (ethyl acetate/petroleum ether 3:2); ^1H NMR (500 MHz, DMSO) δ 10.75 (s, 1H), 8.81 (d, $J = 2.1$ Hz, 1H), 8.73 (d, $J = 2.1$ Hz, 1H), 8.41 (s, 1H), 7.91–7.78 (m, 2H), 7.71 (d, $J = 1.4$ Hz, 1H), 7.54–7.40 (m, 1H), 7.28 (td, $J = 8.3$, 2.3 Hz, 1H); ^{13}C NMR (126 MHz, DMSO) δ 163.73 (dd, $J_{\text{C-F}} = 251.1$, 12.3 Hz), 162.54, 159.70 (dd, $J_{\text{C-F}} = 253.1$, 13.0 Hz), 141.40, 140.96, 140.74, 135.70, 131.87 (dd, $J_{\text{C-F}} = 10.3$, 4.0 Hz), 128.42, 127.23, 124.52, 122.84, 120.79 (dd, $J_{\text{C-F}} = 14.6$, 3.6 Hz), 112.01 (dd, $J_{\text{C-F}} = 21.8$, 3.5 Hz), 110.24, 104.83 (t, $J_{\text{C-F}} = 26.2$ Hz); MS (ESI) $m/z = 394.87$ (M + H) $^{+}$

4.1.1.27. *N*-(5-(4-bromothiophen-2-yl)pyridin-3-yl)-2-chloro-4-fluorobenzamide (24a). The compound was synthesized according to procedure **B** using 2-chloro-4-fluorobenzoyl chloride: yield 81%. The product was purified by CC (ethyl acetate/petroleum ether 3:2); ^1H NMR (500 MHz, DMSO) δ 10.90 (s, 1H), 8.78 (d, $J = 2.3$ Hz, 1H), 8.74 (d, $J = 2.1$ Hz, 1H), 8.42 (t, $J = 2.2$ Hz, 1H), 7.81 (d, $J = 1.4$ Hz, 1H), 7.76 (dd, $J = 8.6$, 6.1 Hz, 1H), 7.71 (d, $J = 1.4$ Hz, 1H), 7.64 (dd, $J = 9.0$, 2.5 Hz, 1H), 7.40 (td, $J = 8.5$, 2.5 Hz, 1H); ^{13}C NMR (126 MHz, DMSO) δ 164.81, 162.47 (d, $J_{\text{C-F}} = 250.5$ Hz), 141.40, 140.94, 140.46, 135.77, 132.81, 131.53 (d, $J_{\text{C-F}} = 10.9$ Hz), 131.00 (d, $J_{\text{C-F}} = 9.4$ Hz), 128.47, 127.25, 124.55, 122.48, 117.26 (d, $J_{\text{C-F}} = 25.4$ Hz), 114.62 (d, $J_{\text{C-F}} = 21.7$ Hz), 110.26; MS (ESI) $m/z = 410.8$ (M + H) $^{+}$

4.1.1.28. *N*-(5-(4-bromothiophen-2-yl)pyridin-3-yl)-3-chloro-4-fluorobenzamide (25a). The compound was synthesized according to procedure **B** using 3-chloro-4-fluorobenzoyl chloride: yield 82%. The product was purified by CC (ethyl acetate/petroleum ether 1:1); ^1H NMR (500 MHz, DMSO) δ 10.64 (s, 1H), 8.90 (d, $J = 2.2$ Hz, 1H), 8.73 (d, $J = 2.1$ Hz, 1H), 8.42 (t, $J = 2.2$ Hz, 1H), 8.24 (dd, $J = 7.1$, 2.2 Hz, 1H), 8.03 (ddd, $J = 7.0$, 4.4, 1.9 Hz, 1H), 7.81 (d, $J = 1.4$ Hz, 1H), 7.70 (d, $J = 1.3$ Hz, 1H), 7.64 (t, $J = 8.9$ Hz, 1H); ^{13}C NMR (126 MHz, DMSO) δ 163.72, 159.37 (d, $J_{\text{C-F}} = 252.2$ Hz), 141.30 (d, $J_{\text{C-F}} = 14.2$ Hz),

141.02, 135.80, 131.73 (d, $J_{\text{C-F}} = 3.5$ Hz), 130.28, 129.23 (d, $J_{\text{C-F}} = 8.4$ Hz), 128.34, 127.18, 124.49, 123.42, 119.91, 119.76, 117.22 (d, $J_{\text{C-F}} = 21.6$ Hz), 110.25; MS (ESI) $m/z = 410.82$ (M + H) $^{+}$

4.1.1.29. *N*-(5-(4-bromothiophen-2-yl)pyridin-3-yl)-2-fluoro-5-methoxybenzamide (26a). The compound was synthesized according to procedure **B** using 2-fluoro-5-methoxybenzoyl chloride: yield 68%. The product was purified by CC (ethyl acetate/petroleum ether 3:2); ^1H NMR (500 MHz, DMSO) δ 10.72 (s, 1H), 8.83 (d, $J = 2.2$ Hz, 1H), 8.73 (d, $J = 2.1$ Hz, 1H), 8.43 (t, $J = 2.1$ Hz, 1H), 7.81 (d, $J = 1.4$ Hz, 1H), 7.70 (d, $J = 1.4$ Hz, 1H), 7.32 (t, $J = 9.3$ Hz, 1H), 7.24 (dd, $J = 5.5$, 3.2 Hz, 1H), 7.15 (dt, $J = 9.0$, 3.7 Hz, 1H), 3.81 (s, 3H); ^{13}C NMR (126 MHz, DMSO) δ 163.17, 155.30, 155.28, 153.17 (d, $J_{\text{C-F}} = 242.1$ Hz), 141.35, 140.86 (d, $J_{\text{C-F}} = 33.1$ Hz), 135.75, 128.41, 127.22, 124.51, 124.38, 122.79, 118.24 (d, $J_{\text{C-F}} = 8.2$ Hz), 117.21 (d, $J_{\text{C-F}} = 23.8$ Hz), 114.10 (d, $J_{\text{C-F}} = 2.4$ Hz), 110.24, 55.89.

4.1.1.30. *N*-(5-(4-bromothiophen-2-yl)pyridin-3-yl)-2,4,6-trifluorobenzamide (27a). The compound was synthesized according to procedure **B** using 2,4,6-trifluorobenzoyl chloride: yield 69%. The product was purified by CC (ethyl acetate/petroleum ether 3:2); ^1H NMR (500 MHz, DMSO) δ 11.20 (s, 1H), 8.76 (dd, $J = 4.8$, 2.2 Hz, 2H), 8.38 (t, $J = 2.2$ Hz, 1H), 7.82 (d, $J = 1.4$ Hz, 1H), 7.73 (d, $J = 1.4$ Hz, 1H), 7.44 (dd, $J = 9.3$, 7.8 Hz, 2H); MS (ESI) $m/z = 412.81$ (M + H) $^{+}$

4.1.1.31. *N*-(5-(4-bromothiophen-2-yl)pyridin-3-yl)-2,3,4-trifluorobenzamide (28a). The compound was synthesized according to procedure **B** using 2,3,4-trifluorobenzoyl chloride: yield 81%. The product was purified by CC (ethyl acetate/petroleum ether 1:1); ^1H NMR (500 MHz, DMSO) δ 11.03 (s, 1H), 8.83 (d, $J = 2.2$ Hz, 1H), 8.74 (d, $J = 2.1$ Hz, 1H), 8.42 (t, $J = 2.1$ Hz, 1H), 7.81 (d, $J = 1.4$ Hz, 1H), 7.71 (d, $J = 1.4$ Hz, 1H), 7.53–7.47 (m, 1H), 7.25 (td, $J = 9.2$, 1.8 Hz, 1H); MS (ESI) $m/z = 412.80$ (M + H) $^{+}$

4.1.1.32. *N*-(5-(4-bromothiophen-2-yl)pyridin-3-yl)isonicotinamide (29a). The compound was synthesized according to procedure **B** using isonicotinyl chloride: yield 71%. The product was purified by CC (ethyl acetate/MeOH 100:7); ^1H NMR (500 MHz, DMSO) δ 10.83 (s, 1H), 8.91 (d, $J = 2.3$ Hz, 1H), 8.83 (dd, $J = 4.4$, 1.7 Hz, 2H), 8.76 (d, $J = 2.1$ Hz, 1H), 8.45 (t, $J = 2.2$ Hz, 1H), 7.90 (dd, $J = 4.4$, 1.7 Hz, 2H), 7.82 (d, $J = 1.4$ Hz, 1H), 7.72 (d, $J = 1.4$ Hz, 1H); ^{13}C NMR (126 MHz, DMSO) δ 164.61, 150.43, 141.61, 141.32, 141.16, 140.96, 135.59, 128.39, 127.24, 124.54, 123.56, 121.56, 110.27; MS (ESI) $m/z = 459.97$ (M + H) $^{+}$

4.1.1.33. *N*-(5-(4-bromothiophen-2-yl)pyridin-3-yl)-2-phenylacetamide (30a). The compound was synthesized according to procedure **B** using phenylacetyl chloride: yield 81%. The product was purified by CC (ethyl acetate/petroleum ether 3:2); ^1H NMR (500 MHz, DMSO) δ 10.53 (s, 1H), 8.66 (dd, $J = 14.6$, 2.2 Hz, 2H), 8.32 (t, $J = 2.2$ Hz, 1H), 7.78 (d, $J = 1.4$ Hz, 1H), 7.66 (d, $J = 1.4$ Hz, 1H), 7.37–7.31 (m, 4H), 7.26 (ddd, $J = 8.6$, 5.6, 2.7 Hz, 1H), 3.70 (s, 2H); ^{13}C NMR (126 MHz, DMSO) δ 170.01, 141.04, 140.71, 140.05, 136.05, 135.40, 129.21, 128.32, 127.09, 126.65, 124.38, 121.97, 115.90, 110.18, 43.09; MS (ESI) $m/z = 372.98$ (M + H) $^{+}$

4.1.1.34. *N*-(5-(4-bromothiophen-2-yl)pyridin-3-yl)-2-(4-fluorophenyl)acetamide (31a). The compound was synthesized according to procedure **B** using 4-fluorophenyl chloride: yield 84%. The product was purified by CC (ethyl acetate/petroleum ether 3:2); ^1H NMR (500 MHz, DMSO) δ 10.34 (s, 1H), 8.48 (dd, $J = 10.4$, 2.2 Hz, 2H), 8.13 (t, $J = 2.2$ Hz, 1H), 7.60 (d, $J = 1.4$ Hz, 1H), 7.47 (d, $J = 1.4$ Hz, 1H), 7.26–7.09 (m, 2H), 6.97 (ddd, $J = 14.7$, 8.4, 5.2 Hz, 2H), 3.52 (s, 2H); ^{13}C NMR (126 MHz, DMSO) δ 164.59, 161.19 (d, $J_{\text{C-F}}$

δ = 242.3 Hz), 141.06, 140.76, 140.09, 136.04, 131.56 (d, J_{C-F} = 3.0 Hz), 131.16 (d, J_{C-F} = 8.1 Hz), 128.36, 127.12, 124.41, 122.02, 115.04 (d, J_{C-F} = 21.3 Hz), 110.21, 42.06; MS (ESI) m/z = 390.93 (M + H)⁺

4.1.1.35. N-(5-(4-bromothiophen-2-yl)pyridin-3-yl)-2-(3-methoxyphenyl)acetamide (32a). The compound was synthesized according to procedure **B** using 3-methoxyphenyl acetyl chloride: yield 97%. The product was purified by CC (ethyl acetate); ¹H NMR (500 MHz, DMSO) δ 10.52 (s, 1H), 8.68 (d, J = 2.2 Hz, 1H), 8.65 (d, J = 2.1 Hz, 1H), 8.32 (t, J = 2.1 Hz, 1H), 7.78 (d, J = 1.2 Hz, 1H), 7.66 (d, J = 1.2 Hz, 1H), 7.25 (t, J = 8.0 Hz, 1H), 7.01–6.88 (m, 2H), 6.85–6.78 (m, 1H), 3.75 (s, 3H), 3.67 (s, 2H); ¹³C NMR (126 MHz, DMSO) δ 170.39, 159.26, 141.10, 140.77, 140.10, 136.87, 136.11, 129.41, 128.39, 127.16, 124.45, 122.01, 121.46, 115.06, 112.09, 110.26, 59.80, 55.02; MS (ESI) m/z = 404.84 (M + H)⁺

4.1.1.36. N-(5-(4-bromothiophen-2-yl)pyridin-3-yl)-3-(3-methoxyphenyl)propanamide (33a). The compound was synthesized according to procedure **B** using 3-(3-methoxyphenyl)propanoyl chloride: yield 92%. The product was purified by CC (ethyl acetate/petroleum ether 3:2); ¹H NMR (500 MHz, DMSO) δ 10.29 (s, 1H), 8.65 (dd, J = 3.8, 2.2 Hz, 2H), 8.30 (s, 1H), 7.79 (d, J = 1.3 Hz, 1H), 7.66 (d, J = 1.3 Hz, 1H), 7.19 (dd, J = 13.3, 5.2 Hz, 1H), 6.83 (d, J = 6.7 Hz, 2H), 6.76 (dd, J = 8.1, 2.3 Hz, 1H), 3.72 (s, 3H), 2.91 (t, J = 7.7 Hz, 2H), 2.68 (t, J = 7.7 Hz, 2H); ¹³C NMR (126 MHz, DMSO) δ 171.35, 159.31, 142.56, 141.14, 140.05, 136.07, 129.41, 128.37, 127.10, 124.43, 121.94, 120.48, 113.95, 113.91, 111.47, 110.25, 54.91, 35.17, 30.64; MS (ESI) m/z = 416.9 (M + H)⁺

4.1.1.37. N-(5-(4-bromothiophen-2-yl)pyridin-3-yl)-3-(pyridin-3-yl)propanamide (34a). The compound was synthesized according to procedure **B** using 3-(pyridin-3-yl)propanoyl chloride: yield 82%. The product was purified by CC (DCM/MeOH 100:5); ¹H NMR (500 MHz, DMSO) δ 10.31 (s, 1H), 8.64 (d, J = 2.1 Hz, 2H), 8.49 (d, J = 1.7 Hz, 1H), 8.41 (dd, J = 4.8, 1.6 Hz, 1H), 8.28 (t, J = 2.2 Hz, 1H), 7.79 (d, J = 1.4 Hz, 1H), 7.72–7.58 (m, 2H), 7.32 (ddd, J = 7.8, 4.8, 0.8 Hz, 1H), 2.95 (t, J = 7.5 Hz, 2H), 2.72 (t, J = 7.6 Hz, 2H); ¹³C NMR (126 MHz, DMSO) δ 171.02, 149.59, 147.37, 141.09, 140.65, 140.04, 136.38, 135.96, 135.84, 128.36, 127.09, 124.40, 123.45, 121.97, 110.21, 37.25, 27.63; MS (ESI) m/z = 387.94 (M + H)⁺

4.1.1.38. 5-(4-(Pyridin-3-yl)thiophen-2-yl)pyridin-2-amine (1). The compound was synthesized according to procedure **C** to give a yellow solid: yield 12%. The product was purified by CC (DCM/MeOH 100:3); mp 161.8–162.8 °C; ¹H NMR (500 MHz, DMSO) δ 9.45 (d, J = 1.7 Hz, 1H), 8.96 (dd, J = 4.7, 1.5 Hz, 1H), 8.83 (d, J = 2.1 Hz, 1H), 8.55 (ddd, J = 7.9, 2.3, 1.6 Hz, 1H), 8.23–8.20 (m, 2H), 8.19 (d, J = 1.5 Hz, 1H), 7.86 (ddd, J = 7.9, 4.8, 0.8 Hz, 1H), 7.08 (dd, J = 8.6, 0.7 Hz, 1H), 6.13 (s, 2H); ¹³C NMR (126 MHz, DMSO) δ 170.13, 158.84, 158.00, 155.85, 154.00, 150.13, 145.26, 143.55, 141.88, 134.19, 130.78, 130.03, 129.84, 118.52; MS (ESI) m/z = 253.93 (M + H)⁺

4.1.1.39. 5-(4-(Pyridin-3-yl)thiophen-2-yl)pyridin-3-amine (2). The compound was synthesized according to procedure **C** to give a dark brown solid: yield 32%. The product was purified by CC (DCM/MeOH 100:5); mp 134.7–135 °C; ¹H NMR (500 MHz, DMSO) δ 9.04 (d, J = 1.7 Hz, 1H), 8.52 (dd, J = 4.7, 1.5 Hz, 1H), 8.20–8.16 (m, 2H), 8.06 (d, J = 1.5 Hz, 1H), 8.05 (d, J = 1.5 Hz, 1H), 7.91 (d, J = 2.3 Hz, 1H), 7.46 (ddd, J = 8.0, 4.8, 0.8 Hz, 1H), 7.20–7.17 (m, 1H), 5.51 (s, 2H); ¹³C NMR (126 MHz, DMSO) δ 148.28, 147.17, 144.98, 142.00, 139.14, 135.91, 133.85, 133.22, 130.55, 129.27, 123.88, 122.80, 122.06, 115.90; MS (ESI) m/z = 253.94 (M + H)⁺

4.1.1.40. 5-(4-(Pyridin-4-yl)thiophen-2-yl)pyridin-3-amine (3). The compound was synthesized according to procedure **C** to give a

light brown solid: yield 23%. The product was purified by CC (DCM/MeOH 100:3); mp 199.2–202 °C; ¹H NMR (500 MHz, DMSO) δ 8.62 (s, 2H), 8.23 (s, 1H), 8.20 (s, 1H), 8.09 (d, J = 1.0 Hz, 1H), 7.92 (s, 1H), 7.80 (s, 2H), 7.19 (s, 1H), 5.52 (s, 2H); ¹³C NMR (126 MHz, DMSO) δ 150.28, 145.04, 142.19, 141.51, 139.69, 136.00, 133.83, 129.19, 124.12, 122.66, 120.51, 115.90; MS (ESI) m/z = 253.96 (M + H)⁺

4.1.1.41. N-(5-(4-(pyridin-3-yl)thiophen-2-yl)pyridin-3-yl)benzamide (4b). The compound was synthesized according to procedure **C** to give a red solid: yield 29%. The product was purified by CC (DCM/MeOH 100:3); mp 88.2–90.5 °C; ¹H NMR (500 MHz, DMSO) δ 10.59 (s, 1H), 9.08 (s, 1H), 8.87 (dd, J = 53.6, 1.9 Hz, 2H), 8.54 (dd, J = 5.1, 2.9 Hz, 2H), 8.25–8.12 (m, 3H), 8.07–7.96 (m, 2H), 7.67–7.61 (m, 1H), 7.58 (ddt, J = 8.2, 6.7, 1.3 Hz, 2H), 7.48 (dd, J = 7.8, 4.7 Hz, 1H); ¹³C NMR (126 MHz, DMSO) δ 166.08, 148.39, 147.20, 141.19, 140.92, 140.82, 139.41, 136.12, 134.17, 133.28, 132.05, 130.43, 129.26, 128.54, 127.77, 123.92, 123.74, 123.49, 122.94; MS (ESI) m/z = 358.05 (M + H)⁺

4.1.1.42. N-(5-(4-(pyridin-3-yl)thiophen-2-yl)pyridin-3-yl)benzenesulfonamide (5b). The compound was synthesized according to procedure **C** to give a white solid: yield 29%. The product was purified by CC (DCM/MeOH 100:4); mp 213.4–214.7 °C; ¹H NMR (500 MHz, DMSO) δ 10.74 (s, 1H), 9.06 (s, 1H), 8.73 (s, 1H), 8.54 (s, 1H), 8.16 (dd, J = 19.5, 8.3 Hz, 4H), 7.83 (d, J = 7.5 Hz, 2H), 7.73 (s, 1H), 7.63 (d, J = 7.2 Hz, 1H), 7.58 (t, J = 7.4 Hz, 2H), 7.48 (s, 1H); ¹³C NMR (126 MHz, DMSO) δ 148.41, 147.19, 141.94, 140.47, 140.00, 139.47, 138.93, 134.71, 133.34, 133.27, 130.32, 129.64, 129.51, 126.73, 124.12, 123.88, 123.28, 123.22; MS (ESI) m/z = 393.92 (M + H)⁺

4.1.1.43. 2-Methyl-N-(5-(4-(pyridin-3-yl)thiophen-2-yl)pyridin-3-yl)benzamide (6b). The compound was synthesized according to procedure **C** to give a brown solid: yield 47%. The product was purified by CC (DCM/MeOH 100:2.5); mp 171.6–173.4 °C; ¹H NMR (500 MHz, DMSO) δ 10.65 (s, 1H), 9.08 (d, J = 1.5 Hz, 1H), 8.83 (s, 1H), 8.81 (d, J = 1.7 Hz, 1H), 8.54 (d, J = 2.4 Hz, 2H), 8.27–8.20 (m, 2H), 8.16 (d, J = 1.4 Hz, 1H), 7.55 (d, J = 7.6 Hz, 1H), 7.49 (dd, J = 7.7, 4.7 Hz, 1H), 7.43 (dd, J = 10.7, 4.3 Hz, 1H), 7.34 (t, J = 7.3 Hz, 2H), 2.43 (s, 3H); ¹³C NMR (126 MHz, DMSO) δ 168.45, 148.27, 147.09, 141.09, 140.82, 140.27, 139.35, 136.34, 136.20, 135.56, 133.41, 130.69, 130.47, 130.07, 129.32, 127.39, 125.70, 123.95, 123.74, 122.99, 122.71, 19.39; MS (ESI) m/z = 372.08 (M + H)⁺

4.1.1.44. 3-Methyl-N-(5-(4-(pyridin-3-yl)thiophen-2-yl)pyridin-3-yl)benzamide (7b). The compound was synthesized according to procedure **C** to give a dark grey solid: yield 26%. The product was purified by CC (DCM/MeOH 100:3); mp 103–103.7 °C; ¹H NMR (500 MHz, CDCl₃) δ 9.19 (s, 1H), 8.96 (d, J = 10.0 Hz, 3H), 8.91 (s, 1H), 8.87 (s, 1H), 8.21 (d, J = 7.8 Hz, 1H), 8.06 (s, 1H), 8.04 (s, 1H), 7.95 (s, 1H), 7.84 (s, 1H), 7.69 (d, J = 4.5 Hz, 2H), 7.67 (d, J = 7.0 Hz, 1H), 2.73 (s, 3H); ¹³C NMR (126 MHz, CDCl₃) δ 166.78, 148.58, 147.57, 142.35, 141.59, 140.50, 139.95, 138.98, 135.52, 134.14, 133.72, 133.28, 131.37, 130.41, 128.90, 128.10, 124.39, 124.31, 123.91, 123.51, 122.28, 24.98; MS (ESI) m/z = 372.08 (M + H)⁺

4.1.1.45. 4-Methyl-N-(5-(4-(pyridin-3-yl)thiophen-2-yl)pyridin-3-yl)benzamide (8b). The compound was synthesized according to procedure **C** to give a dark grey solid: yield 45%. The product was purified by CC (DCM/MeOH 100:3); mp 185.9–186.9 °C; ¹H NMR (500 MHz, DMSO) δ 10.50 (s, 1H), 9.09 (s, 1H), 8.94 (s, 1H), 8.82 (s, 1H), 8.54 (s, 2H), 8.22 (d, J = 13.0 Hz, 2H), 8.16 (s, 1H), 7.94 (d, J = 7.9 Hz, 2H), 7.48 (s, 1H), 7.38 (d, J = 7.8 Hz, 2H), 2.40 (s, 3H); ¹³C NMR (126 MHz, DMSO) δ 165.83, 148.33, 147.15, 142.12, 141.01, 140.87, 140.84, 139.39, 136.21, 134.38, 133.23, 131.24, 130.48, 129.01, 127.77, 123.93, 123.68, 123.42, 122.88, 21.02; MS (ESI) m/z = 372.02

(M + H)⁺

4.1.1.46. 2-Methoxy-N-(5-(4-(pyridin-3-yl)thiophen-2-yl)pyridin-3-yl)benzamide (9b). The compound was synthesized according to procedure **C** to give a greyish white solid; yield 44%. The product was purified by CC (DCM/MeOH 100:3); mp 185.9–186.9 °C; ¹H NMR (500 MHz, DMSO) δ 10.44 (s, 1H), 9.10 (s, 1H), 8.81 (s, 2H), 8.55 (s, 2H), 8.22 (s, 2H), 8.15 (s, 1H), 7.69 (d, *J* = 6.2 Hz, 1H), 7.54 (s, 1H), 7.49 (s, 1H), 7.21 (d, *J* = 7.9 Hz, 1H), 7.10 (d, *J* = 6.8 Hz, 1H), 3.93 (s, 3H); ¹³C NMR (126 MHz, DMSO) δ 165.24, 156.59, 148.35, 147.17, 141.06, 140.78, 140.46, 139.37, 134.39, 133.25, 132.47, 130.44, 129.74, 129.33, 124.19, 123.92, 123.76, 122.92, 122.80, 120.52, 112.04, 55.94; MS (ESI) *m/z* = 388.03 (M + H)⁺

4.1.1.47. 3-Methoxy-N-(5-(4-(pyridin-3-yl)thiophen-2-yl)pyridin-3-yl)benzamide (10b). The compound was synthesized according to procedure **C** to give a white solid; yield 47%. The product was purified by CC (DCM/MeOH 100:2); mp 170.5–171.3 °C; ¹H NMR (500 MHz, DMSO) δ 10.54 (s, 1H), 9.07 (s, 1H), 8.92 (s, 1H), 8.82 (s, 1H), 8.53 (d, *J* = 1.9 Hz, 2H), 8.28–8.18 (m, 2H), 8.15 (s, 1H), 7.61 (d, *J* = 7.5 Hz, 1H), 7.55 (s, 1H), 7.48 (dd, *J* = 14.3, 6.4 Hz, 2H), 7.21 (d, *J* = 8.2 Hz, 1H), 3.86 (s, 3H); ¹³C NMR (126 MHz, DMSO) δ 165.77, 159.26, 148.39, 147.20, 141.22, 140.97, 140.80, 139.40, 136.04, 135.54, 133.27, 130.42, 129.71, 129.24, 123.90, 123.74, 123.55, 122.93, 119.94, 117.74, 113.06, 55.40; MS (ESI) *m/z* = 388.09 (M + H)⁺

4.1.1.48. 4-Methoxy-N-(5-(4-(pyridin-3-yl)thiophen-2-yl)pyridin-3-yl)benzamide (11b). The compound was synthesized according to procedure **C** to give a dark brown solid; yield 32%. The product was purified by CC (DCM/MeOH 100:4); mp 210.5–210.8 °C; ¹H NMR (500 MHz, DMSO) δ 10.41 (s, 1H), 9.07 (s, 1H), 8.92 (s, 1H), 8.79 (s, 1H), 8.53 (s, 2H), 8.21 (d, *J* = 9.4 Hz, 2H), 8.15 (s, 1H), 8.02 (d, *J* = 8.5 Hz, 2H), 7.50–7.37 (m, 1H), 7.10 (d, *J* = 8.5 Hz, 2H), 3.86 (s, 3H); ¹³C NMR (126 MHz, DMSO) δ 165.39, 162.25, 148.38, 147.19, 140.93, 140.89, 139.38, 136.29, 133.26, 130.62, 130.43, 129.77, 129.20, 126.14, 123.90, 123.67, 123.42, 122.88, 113.75, 55.49; MS (ESI) *m/z* = 388.1 (M + H)⁺

4.1.1.49. 4-(tert-Butyl)-N-(5-(4-(pyridin-3-yl)thiophen-2-yl)pyridin-3-yl)benzamide (12b). The compound was synthesized according to procedure **C** to give a white solid; yield 51%. The product was purified by CC (DCM/MeOH 100:3); mp 205.4–205.9 °C; ¹H NMR (500 MHz, DMSO) δ 10.50 (s, 1H), 9.07 (d, *J* = 1.8 Hz, 1H), 8.92 (d, *J* = 2.3 Hz, 1H), 8.80 (d, *J* = 2.1 Hz, 1H), 8.57–8.51 (m, 2H), 8.25–8.19 (m, 2H), 8.16 (d, *J* = 1.4 Hz, 1H), 7.96 (d, *J* = 1.8 Hz, 1H), 7.95 (d, *J* = 1.8 Hz, 1H), 7.59 (d, *J* = 1.8 Hz, 1H), 7.58 (d, *J* = 1.8 Hz, 1H), 7.51–7.44 (m, 1H), 1.33 (s, 9H); ¹³C NMR (126 MHz, DMSO) δ 165.98, 154.95, 148.39, 147.20, 141.07, 140.84, 139.40, 136.20, 134.42, 133.27, 131.45, 130.42, 129.22, 127.65, 125.30, 123.90, 123.71, 123.35, 122.91, 34.75, 30.91; MS (ESI) *m/z* = 414.04 (M + H)⁺

4.1.1.50. 2-Chloro-N-(5-(4-(pyridin-3-yl)thiophen-2-yl)pyridin-3-yl)benzamide (13b). The compound was synthesized according to procedure **C** to give a brown solid; yield 53%. The product was purified by CC (DCM/MeOH 100:3); mp 159–159.6 °C; ¹H NMR (500 MHz, DMSO) δ 10.89 (s, 1H), 9.08 (s, 1H), 8.82 (d, *J* = 17.7 Hz, 2H), 8.53 (d, *J* = 12.2 Hz, 2H), 8.26–8.18 (m, 2H), 8.16 (s, 1H), 7.67 (d, *J* = 7.4 Hz, 1H), 7.55 (t, *J* = 6.8 Hz, 2H), 7.49 (d, *J* = 7.3 Hz, 2H); ¹³C NMR (126 MHz, DMSO) δ 165.59, 149.14, 148.38, 147.78, 147.20, 141.43, 140.66, 140.09, 139.44, 136.22, 134.41, 133.28, 131.50, 129.96, 129.78, 129.06, 127.34, 123.91, 123.86, 123.03, 122.56; MS (ESI) *m/z* = 391.96 (M + H)⁺

4.1.1.51. 3-Chloro-N-(5-(4-(pyridin-3-yl)thiophen-2-yl)pyridin-3-yl)benzamide (14b). The compound was synthesized according to

procedure **C** to give a dark grey solid; yield 56%. The product was purified by CC (DCM/MeOH 100:3); mp 98.5–100.5 °C; ¹H NMR (500 MHz, DMSO) δ 10.66 (s, 1H), 9.08 (s, 1H), 8.93 (s, 1H), 8.84 (s, 1H), 8.54 (s, 1H), 8.51 (s, 1H), 8.23 (s, 1H), 8.20 (d, *J* = 8.0 Hz, 1H), 8.16 (s, 1H), 8.07 (s, 1H), 7.97 (d, *J* = 7.8 Hz, 1H), 7.71 (d, *J* = 8.0 Hz, 1H), 7.61 (t, *J* = 7.9 Hz, 1H), 7.48 (dd, *J* = 7.6, 4.8 Hz, 1H); ¹³C NMR (126 MHz, DMSO) δ 164.58, 148.36, 147.17, 141.40, 140.91, 140.72, 139.41, 136.12, 135.88, 133.31, 133.26, 131.83, 130.54, 130.44, 129.30, 127.49, 126.61, 123.92, 123.77, 123.55, 122.97; MS (ESI) *m/z* = 391.97 (M + H)⁺

4.1.1.52. 4-Chloro-N-(5-(4-(pyridin-3-yl)thiophen-2-yl)pyridin-3-yl)benzamide (15b). The compound was synthesized according to procedure **C** to give a dark grey solid; yield 46%. The product was purified by CC (DCM/MeOH 100:3); mp 196–196.4 °C; ¹H NMR (500 MHz, DMSO) δ 10.63 (s, 1H), 9.07 (s, 1H), 8.91 (s, 1H), 8.82 (s, 1H), 8.60–8.47 (m, 2H), 8.29–8.17 (m, 2H), 8.15 (s, 1H), 8.04 (d, *J* = 8.4 Hz, 2H), 7.65 (d, *J* = 8.4 Hz, 2H), 7.48 (dd, *J* = 7.7, 4.8 Hz, 1H); ¹³C NMR (126 MHz, DMSO) δ 164.95, 148.37, 147.18, 141.33, 140.93, 140.74, 139.41, 136.89, 135.93, 133.25, 132.85, 130.42, 129.72, 129.27, 128.61, 123.90, 123.76, 123.56, 122.95; MS (ESI) *m/z* = 392.02 (M + H)⁺

4.1.1.53. 2-Fluoro-N-(5-(4-(pyridin-3-yl)thiophen-2-yl)pyridin-3-yl)benzamide (16b). The compound was synthesized according to procedure **C** to give a grey solid; yield 52%. The product was purified by CC (DCM/MeOH 100:3); mp 169.3–169.6 °C; ¹H NMR (500 MHz, DMSO) δ 10.53 (s, 1H), 9.08 (s, 1H), 8.94 (s, 1H), 8.82 (s, 1H), 8.53 (t, *J* = 2.2 Hz, 2H), 8.25–8.19 (m, 2H), 8.15 (d, *J* = 1.4 Hz, 1H), 7.84 (s, 1H), 7.82–7.79 (m, 1H), 7.52–7.47 (m, 1H), 7.47–7.42 (m, 2H); ¹³C NMR (126 MHz, DMSO) δ 163.44, 159.00 (d, *J*_{C-F} = 249.5 Hz), 149.15, 147.19, 141.45, 140.69, 140.35, 139.43, 135.82, 133.31, 133.07 (d, *J*_{C-F} = 8.4 Hz), 130.04 (d, *J*_{C-F} = 2.5 Hz), 130.43, 129.39, 123.93, 124.69 (d, *J*_{C-F} = 3.3 Hz), 124.20 (d, *J*_{C-F} = 14.6 Hz), 123.86, 123.03, 122.90, 123.16 (d, *J*_{C-F} = 21.6 Hz); MS (ESI) *m/z* = 376.05 (M + H)⁺

4.1.1.54. 3-Fluoro-N-(5-(4-(pyridin-3-yl)thiophen-2-yl)pyridin-3-yl)benzamide (17b). The compound was synthesized according to procedure **C** to give a dark brown solid; yield 41%. The product was purified by CC (DCM/MeOH 100:3); mp 152.1–152.2 °C; ¹H NMR (500 MHz, DMSO) δ 10.63 (s, 1H), 9.08 (s, 1H), 8.92 (s, 1H), 8.83 (s, 1H), 8.52 (s, 2H), 8.30–8.17 (m, 2H), 8.16 (s, 1H), 7.85 (dd, *J* = 20.5, 8.6 Hz, 2H), 7.64 (dd, *J* = 13.8, 7.5 Hz, 1H), 7.53–7.45 (m, 2H); ¹³C NMR (126 MHz, DMSO) δ 164.66, 161.94 (d, *J*_{C-F} = 244.5 Hz), 148.38, 147.18, 141.40, 140.92, 140.71, 139.41, 136.44 (d, *J*_{C-F} = 6.9 Hz), 135.86, 133.26, 130.79, 130.75 (d, *J*_{C-F} = 8.1 Hz), 129.28, 124.00 (d, *J*_{C-F} = 2.6 Hz), 123.90, 123.78, 123.57, 122.97, 118.94 (d, *J*_{C-F} = 21.1 Hz), 114.60 (d, *J*_{C-F} = 23.0 Hz); MS (ESI) *m/z* = 376.06 (M + H)⁺

4.1.1.55. 4-Fluoro-N-(5-(4-(pyridin-3-yl)thiophen-2-yl)pyridin-3-yl)benzamide (18b). The compound was synthesized according to procedure **C** to give a brown solid; yield 34%. The product was purified by CC (DCM/MeOH 100:3); mp 175.1–176 °C; ¹H NMR (500 MHz, DMSO) δ 10.58 (s, 1H), 9.07 (d, *J* = 1.9 Hz, 1H), 8.91 (d, *J* = 2.2 Hz, 1H), 8.81 (d, *J* = 2.0 Hz, 1H), 8.53 (dd, *J* = 4.7, 1.3 Hz, 1H), 8.51 (t, *J* = 2.1 Hz, 1H), 8.21 (dd, *J* = 7.9, 4.7 Hz, 2H), 8.15 (d, *J* = 1.3 Hz, 1H), 8.10 (dd, *J* = 8.8, 5.5 Hz, 2H), 7.47 (dd, *J* = 7.9, 4.7 Hz, 1H), 7.41 (t, *J* = 8.8 Hz, 2H); ¹³C NMR (126 MHz, DMSO) δ 164.94, 164.32 (d, *J*_{C-F} = 249.8 Hz), 148.37, 147.19, 141.24, 140.85 (d, *J*_{C-F} = 19.3 Hz), 139.40, 136.01, 133.26, 130.62, 130.52 (d, *J*_{C-F} = 26.4 Hz), 130.41, 129.24, 123.88, 123.73, 123.54, 122.92, 115.59, 115.41; MS (ESI) *m/z* = 376.08 (M + H)⁺

4.1.1.56. N-(5-(4-(pyridin-3-yl)thiophen-2-yl)pyridin-3-yl)-2-(trifluoromethyl)benzamide (19b). The compound was synthesized

according to procedure **C** to give grey solid: yield 53%. The product was purified by CC (DCM/MeOH 100:3); mp 81.4–83.1 °C; ¹H NMR (500 MHz, DMSO) δ 10.96 (s, 1H), 9.08 (d, *J* = 2.0 Hz, 1H), 8.84 (d, *J* = 1.9 Hz, 1H), 8.78 (d, *J* = 2.1 Hz, 1H), 8.59–8.51 (m, 1H), 8.47 (t, *J* = 2.1 Hz, 1H), 8.22 (dd, *J* = 7.1, 4.7 Hz, 2H), 8.16 (d, *J* = 1.2 Hz, 1H), 7.90 (d, *J* = 7.9 Hz, 1H), 7.87–7.78 (m, 2H), 7.76 (t, *J* = 7.6 Hz, 1H), 7.48 (dd, *J* = 7.9, 4.8 Hz, 1H); ¹³C NMR (126 MHz, DMSO) δ 166.23, 148.34, 147.16, 141.50, 140.59, 140.09, 139.41, 135.81, 135.42, 133.31, 132.69, 130.45, 130.39, 129.43, 128.63, 126.45 (q, *J*_{C-F} = 8.9, 4.1 Hz), 125.76, 124.79, 123.88, 123.86, 123.04, 122.61; MS (ESI) *m/z* = 425.97 (M + H)⁺

4.1.1.57. N-(5-(4-(pyridin-3-yl)thiophen-2-yl)pyridin-3-yl)-3-(trifluoromethyl)benzamide (20b). The compound was synthesized according to procedure **C** to give light brown solid: yield 47%. The product was purified by CC (DCM/MeOH 100:3); mp 185.6–186.4 °C; ¹H NMR (500 MHz, DMSO) δ 10.79 (s, 1H), 9.08 (s, 1H), 8.93 (s, 1H), 8.85 (s, 1H), 8.54 (d, *J* = 3.9 Hz, 1H), 8.51 (s, 1H), 8.36 (s, 1H), 8.32 (d, *J* = 7.9 Hz, 1H), 8.24 (s, 1H), 8.21 (d, *J* = 8.1 Hz, 1H), 8.16 (s, 1H), 8.02 (d, *J* = 7.5 Hz, 1H), 7.83 (t, *J* = 7.7 Hz, 1H), 7.48 (dd, *J* = 7.7, 4.8 Hz, 1H); ¹³C NMR (126 MHz, DMSO) δ 164.57, 141.28 (d, *J*_{C-F} = 61.5 Hz), 148.39, 147.19, 140.68, 139.42, 135.78, 135.06, 133.26, 131.96, 130.41, 129.89, 129.30, 129.28 (d, *J*_{C-F} = 32.2 Hz), 128.57 (d, *J*_{C-F} = 3.3 Hz), 125.02, 124.35 (q, *J*_{C-F} = 7.6, 3.8 Hz), 123.90, 123.81, 123.73, 122.99, 122.86; MS (ESI) *m/z* = 426.03 (M + H)⁺

4.1.1.58. N-(5-(4-(pyridin-3-yl)thiophen-2-yl)pyridin-3-yl)-4-(trifluoromethyl)benzamide (21b). The compound was synthesized according to procedure **C** to give a greyish white solid: yield 34%. The product was purified by CC (DCM/MeOH 100:3); mp 208.8–210.1 °C; ¹H NMR (500 MHz, DMSO) δ 10.78 (s, 1H), 9.07 (s, 1H), 8.92 (s, 1H), 8.84 (s, 1H), 8.53 (s, 2H), 8.27–8.18 (m, 4H), 8.16 (s, 1H), 7.97 (s, 1H), 7.95 (s, 1H), 7.47 (dd, *J* = 7.6, 4.8 Hz, 1H); ¹³C NMR (126 MHz, DMSO) δ 164.89, 148.38, 147.18, 141.52, 141.52, 140.95, 140.68, 139.41, 137.95, 135.77, 133.25, 131.85, 130.39, 129.29, 128.69, 125.52 (q, *J*_{C-F} = 3.7 Hz), 123.88, 123.80, 123.62, 122.97; MS (ESI) *m/z* = 426 (M + H)⁺

4.1.1.59. 2,3-Dichloro-N-(5-(4-(pyridin-3-yl)thiophen-2-yl)pyridin-3-yl)benzamide (22b). The compound was synthesized according to procedure **C** to give dark brown semi-solid: yield 58%. The product was purified by CC (DCM/MeOH 100:3); ¹H NMR (500 MHz, DMSO) δ 11.01 (s, 1H), 9.18 (s, 1H), 8.92 (s, 2H), 8.64 (s, 1H), 8.51 (d, *J* = 9.2 Hz, 1H), 8.25–8.20 (m, 2H), 8.17 (s, 1H), 7.82 (dd, *J* = 8.1, 1.3 Hz, 1H), 7.66 (dd, *J* = 7.6, 1.2 Hz, 1H), 7.53 (t, *J* = 7.8 Hz, 2H); ¹³C NMR (126 MHz, DMSO) δ 164.79, 148.30, 147.12, 141.51, 140.61, 140.01, 139.49, 138.45, 134.38, 133.24, 132.20, 131.82, 131.71, 130.53, 128.76, 128.15, 127.50, 126.60, 123.93, 123.08, 122.55; MS (ESI) *m/z* = 426.07 (M + H)⁺

4.1.1.60. 2,4-Difluoro-N-(5-(4-(pyridin-3-yl)thiophen-2-yl)pyridin-3-yl)benzamide (23b). The compound was synthesized according to procedure **C** to give brown solid: yield 56%. The product was purified by CC (DCM/MeOH 100:3); mp 210–212.8 °C; ¹H NMR (500 MHz, DMSO) δ 10.77 (s, 1H), 9.08 (s, 1H), 8.83 (d, *J* = 11.0 Hz, 2H), 8.54 (s, 1H), 8.49 (s, 1H), 8.24 (d, *J* = 1.3 Hz, 1H), 8.21 (d, *J* = 8.0 Hz, 1H), 8.16 (d, *J* = 1.3 Hz, 1H), 7.84 (dd, *J* = 15.1, 8.4 Hz, 1H), 7.52–7.45 (m, 2H), 7.28 (td, *J* = 8.5, 2.4 Hz, 1H); ¹³C NMR (126 MHz, DMSO) δ 163.70 (dd, *J*_{C-F} = 250.8, 12.2 Hz), 159.70 (dd, *J*_{C-F} = 252.7, 13.0 Hz), 162.52, 149.11, 148.36, 147.75, 147.17, 141.47, 140.62, 140.36, 139.42, 134.39, 133.25, 131.85 (dd, *J*_{C-F} = 10.5, 4.1 Hz), 123.85, 123.00, 122.96, 120.83 (dd, *J*_{C-F} = 14.5, 3.6 Hz), 111.98 (dd, *J*_{C-F} = 21.5, 3.5 Hz), 105.02, 104.81 (d, *J*_{C-F} = 52.5 Hz); MS (ESI) *m/z* = 394 (M + H)⁺

4.1.1.61. 2-Chloro-4-fluoro-N-(5-(4-(pyridin-3-yl)thiophen-2-yl)pyridin-3-yl)benzamide (24b). The compound was synthesized according to procedure **C** to give dark grey solid: yield 50%. The product was purified by CC (DCM/MeOH 100:3); mp 166.6–169 °C; ¹H NMR (500 MHz, DMSO) δ 10.90 (s, 1H), 9.08 (s, 1H), 8.84 (s, 1H), 8.79 (s, 1H), 8.54 (s, 1H), 8.50 (d, *J* = 1.9 Hz, 1H), 8.22 (dd, *J* = 12.9, 4.6 Hz, 2H), 8.16 (d, *J* = 1.2 Hz, 1H), 7.77 (dd, *J* = 8.5, 6.1 Hz, 1H), 7.64 (dd, *J* = 9.0, 2.4 Hz, 1H), 7.48 (dd, *J* = 7.7, 4.8 Hz, 1H), 7.40 (td, *J* = 8.5, 2.4 Hz, 1H); ¹³C NMR (126 MHz, DMSO) δ 164.78, 162.43 (d, *J*_{C-F} = 250.5 Hz), 148.36, 147.17, 141.47, 140.60, 140.08, 139.42, 135.77, 134.40, 133.27, 132.87, 131.51 (d, *J*_{C-F} = 11.0 Hz), 130.98 (d, *J*_{C-F} = 9.3 Hz), 130.40, 123.91, 123.85, 123.03, 122.58, 117.24 (d, *J*_{C-F} = 25.2 Hz), 114.60 (d, *J*_{C-F} = 21.6 Hz); MS (ESI) *m/z* = 409.95 (M + H)⁺

4.1.1.62. 3-Chloro-4-fluoro-N-(5-(4-(pyridin-3-yl)thiophen-2-yl)pyridin-3-yl)benzamide (25b). The compound was synthesized according to procedure **C** to give a brown solid: yield 44%. The product was purified by CC (DCM/MeOH 100:3); mp 126.8–127.7 °C; ¹H NMR (500 MHz, DMSO) δ 10.66 (s, 1H), 9.15 (s, 1H), 8.93 (d, *J* = 36.4 Hz, 2H), 8.61 (s, 1H), 8.49 (s, 1H), 8.26 (dd, *J* = 7.1, 2.1 Hz, 1H), 8.21 (d, *J* = 11.4 Hz, 2H), 8.15 (s, 1H), 8.05 (ddd, *J* = 8.3, 4.6, 2.2 Hz, 1H), 7.64 (t, *J* = 8.9 Hz, 1H), 7.51 (s, 1H); ¹³C NMR (126 MHz, DMSO) δ 163.64, 159.29 (d, *J*_{C-F} = 252.4 Hz), 148.25, 147.07, 141.31, 141.30, 141.26, 140.80, 140.69, 140.68, 139.42, 133.17, 131.70, 131.69 (d, *J*_{C-F} = 3.4 Hz), 129.19, 129.16 (d, *J*_{C-F} = 8.5 Hz), 123.75, 123.45, 122.94, 119.77 (d, *J*_{C-F} = 18.0 Hz), 117.14 (d, *J*_{C-F} = 21.5 Hz); MS (ESI) *m/z* = 409.94 (M + H)⁺

4.1.1.63. 2-Fluoro-5-methoxy-N-(5-(4-(pyridin-3-yl)thiophen-2-yl)pyridin-3-yl)benzamide (26b). The compound was synthesized according to procedure **C** to give white solid: yield 49%. The product was purified by CC (DCM/MeOH 100:3); mp 181.6–182.9 °C; ¹H NMR (500 MHz, DMSO) δ 10.73 (s, 1H), 9.07 (d, *J* = 1.9 Hz, 1H), 8.83 (d, *J* = 1.9 Hz, 2H), 8.53 (dd, *J* = 4.7, 1.4 Hz, 1H), 8.50 (s, 1H), 8.22 (ddd, *J* = 8.0, 4.6, 1.5 Hz, 2H), 8.16 (d, *J* = 1.3 Hz, 1H), 7.48 (dd, *J* = 7.9, 4.8 Hz, 1H), 7.33 (t, *J* = 9.3 Hz, 1H), 7.26 (dd, *J* = 5.5, 3.2 Hz, 1H), 7.18–7.13 (m, 1H), 3.82 (s, 3H); ¹³C NMR (126 MHz, DMSO) δ 163.16, 153.19 (d, *J*_{C-F} = 242.2 Hz), 149.14, 148.37, 147.78, 147.18, 141.46, 140.67, 140.39, 139.41, 135.75, 133.31, 130.41, 129.35, 124.50 (d, *J*_{C-F} = 16.5 Hz), 123.91, 123.84, 122.98 (d, *J*_{C-F} = 11.1 Hz), 118.22 (d, *J*_{C-F} = 8.0 Hz), 117.21 (d, *J*_{C-F} = 23.8 Hz), 114.11 (d, *J*_{C-F} = 2.5 Hz), 55.87; MS (ESI) *m/z* = 405.99 (M + H)⁺

4.1.1.64. 2,4,6-Trifluoro-N-(5-(4-(pyridin-3-yl)thiophen-2-yl)pyridin-3-yl)benzamide (27b). The compound was synthesized according to procedure **C** to give dark grey solid: yield 59%. The product was purified by CC (DCM/MeOH 100:3); mp 168.2–170.5 °C; ¹H NMR (500 MHz, DMSO) δ 11.22 (s, 1H), 9.15 (s, 1H), 8.91 (s, 1H), 8.60 (s, 1H), 8.46 (s, 1H), 8.26 (s, 1H), 8.22 (d, *J* = 7.7 Hz, 1H), 8.17 (s, 1H), 7.58–7.50 (m, 2H), 7.44 (t, *J* = 8.7 Hz, 2H); MS (ESI) *m/z* = 411.95 (M + H)⁺

4.1.1.65. 2,3,4-Trifluoro-N-(5-(4-(pyridin-3-yl)thiophen-2-yl)pyridin-3-yl)benzamide (28b). The compound was synthesized according to procedure **C** to give a grey solid: yield 49%. The product was purified by CC (DCM/MeOH 100:3); mp 161.6–161.9 °C; ¹H NMR (500 MHz, DMSO) δ 10.89 (s, 1H), 9.08 (s, 1H), 8.83 (d, *J* = 23.4 Hz, 2H), 8.54 (s, 1H), 8.47 (s, 1H), 8.24 (d, *J* = 1.2 Hz, 1H), 8.21 (d, *J* = 8.0 Hz, 1H), 8.16 (d, *J* = 1.2 Hz, 1H), 7.66 (dd, *J* = 13.5, 6.2 Hz, 1H), 7.57–7.51 (m, 1H), 7.48 (dd, *J* = 7.7, 5.0 Hz, 1H); MS (ESI) *m/z* = 412.13 (M + H)⁺

4.1.1.66. N-(5-(4-(pyridin-3-yl)thiophen-2-yl)pyridin-3-yl)isonicotinamide (29b). The compound was synthesized according to

procedure **C** to give a white solid: yield 35%. The product was purified by CC (DCM/MeOH 100:8); mp 152.1–152.3 °C; ^1H NMR (500 MHz, DMSO) δ 10.87 (s, 1H), 8.53 (s, 1H), 8.36 (s, 1H), 8.25 (s, 1H), 8.22 (d, J = 7.9 Hz, 1H), 8.17 (s, 1H), 7.96 (s, 2H), 7.58 (s, 1H), 7.50 (s, 2H), 7.17 (s, 1H), 6.56 (s, 2H); ^{13}C NMR (126 MHz, DMSO) δ 164.59, 150.34, 148.32, 148.18, 147.12, 147.07, 141.61, 141.49, 141.12, 140.93, 140.64, 139.45, 133.24, 123.86, 123.65, 123.04, 121.79, 121.71; MS (ESI) m/z = 359.09 ($\text{M} + \text{H}$) $^+$

4.1.1.67. 2-Phenyl-N-(5-(4-(pyridin-3-yl)thiophen-2-yl)pyridin-3-yl)acetamide (30b). The compound was synthesized according to procedure **C** to give dark grey: yield 30%. The product was purified by CC (DCM/MeOH 100:3); mp 90.5–91.8 °C; ^1H NMR (500 MHz, DMSO) δ 10.58 (s, 1H), 9.11 (s, 1H), 8.76 (d, J = 27.7 Hz, 2H), 8.58 (s, 1H), 8.40 (s, 1H), 8.20 (dd, J = 12.7, 4.6 Hz, 2H), 8.14 (d, J = 1.2 Hz, 1H), 7.49 (d, J = 7.1 Hz, 1H), 7.39–7.31 (m, 4H), 7.29–7.18 (m, 1H), 3.72 (s, 2H); ^{13}C NMR (126 MHz, DMSO) δ 170.00, 148.16, 146.99, 140.78, 140.74, 139.65, 139.34, 135.46, 134.48, 133.39, 131.02, 130.71, 129.22, 128.33, 126.65, 124.14, 123.72, 122.97, 122.10, 43.11; MS (ESI) m/z = 372.04 ($\text{M} + \text{H}$) $^+$

4.1.1.68. 2-(4-Fluorophenyl)-N-(5-(4-(pyridin-3-yl)thiophen-2-yl)pyridin-3-yl)acetamide (31b). The compound was synthesized according to procedure **C** to give a yellowish white solid: yield 34%. The product was purified by CC (DCM/MeOH 100:3.5); mp 172.5–175.1 °C; ^1H NMR (500 MHz, DMSO) δ 10.54 (s, 1H), 9.06 (s, 1H), 8.75 (s, 1H), 8.68 (s, 1H), 8.53 (d, J = 4.0 Hz, 1H), 8.39 (t, J = 2.1 Hz, 1H), 8.23–8.16 (m, 2H), 8.13 (d, J = 1.4 Hz, 1H), 7.47 (dd, J = 7.9, 4.8 Hz, 1H), 7.43–7.35 (m, 2H), 7.22–7.12 (m, 2H), 3.72 (s, 2H); ^{13}C NMR (126 MHz, DMSO) δ 169.92, 161.19 (d, $J_{\text{C-F}}$ = 242.3 Hz), 148.33, 147.15, 140.80 (d, $J_{\text{C-F}}$ = 14.6 Hz), 139.71, 139.38, 136.05, 133.30, 131.59, 131.62, 131.17 (d, $J_{\text{C-F}}$ = 8.1 Hz), 130.41, 129.31, 123.91, 123.73, 122.93, 122.14, 115.04 (d, $J_{\text{C-F}}$ = 21.2 Hz), 42.08; MS (ESI) m/z = 390.02 ($\text{M} + \text{H}$) $^+$

4.1.1.69. 2-(3-Methoxyphenyl)-N-(5-(4-(pyridin-3-yl)thiophen-2-yl)pyridin-3-yl)acetamide (32b). The compound was synthesized according to procedure **C** to give a white solid: yield 26%. The product was purified by CC (DCM/MeOH 100:3); mp 156.9–157.4 °C; ^1H NMR (500 MHz, DMSO) δ 10.53 (s, 1H), 9.06 (d, J = 1.7 Hz, 1H), 8.75 (d, J = 1.9 Hz, 1H), 8.68 (d, J = 2.0 Hz, 1H), 8.52 (d, J = 3.7 Hz, 1H), 8.39 (t, J = 2.0 Hz, 1H), 8.22–8.17 (m, 2H), 8.14 (d, J = 1.2 Hz, 1H), 7.46 (dd, J = 7.9, 4.8 Hz, 1H), 7.25 (t, J = 8.0 Hz, 1H), 7.00–6.88 (m, 2H), 6.88–6.79 (m, 1H), 3.75 (s, 3H), 3.68 (s, 2H); ^{13}C NMR (126 MHz, DMSO) δ 169.85, 159.20, 148.40, 147.16, 140.81, 140.71, 139.67, 139.36, 136.85, 136.05, 133.24, 130.36, 129.36, 129.27, 123.87, 123.70, 122.89, 122.07, 121.42, 115.03, 112.02, 54.96, 43.17; MS (ESI) m/z = 402.02 ($\text{M} + \text{H}$) $^+$

4.1.1.70. 2-(3-Methoxyphenyl)-N-(5-(4-(pyridin-3-yl)thiophen-2-yl)pyridin-3-yl)acetamide (33b). The compound was synthesized according to procedure **C** to give a beige solid: yield 26%. The product was purified by CC (DCM/MeOH 100:3); mp 154.3–155.7 °C; ^1H NMR (500 MHz, DMSO) δ 10.30 (s, 1H), 9.06 (d, J = 2.1 Hz, 1H), 8.70 (dd, J = 45.9, 2.1 Hz, 2H), 8.53 (dd, J = 4.7, 1.4 Hz, 1H), 8.37 (t, J = 2.1 Hz, 1H), 8.22–8.18 (m, 2H), 8.14 (d, J = 1.2 Hz, 1H), 7.47 (dd, J = 7.9, 4.8 Hz, 1H), 7.20 (t, J = 8.1 Hz, 1H), 6.84 (d, J = 6.8 Hz, 2H), 6.76 (dd, J = 8.3, 2.2 Hz, 1H), 3.72 (s, 3H), 2.92 (t, J = 7.7 Hz, 2H), 2.69 (t, J = 7.7 Hz, 2H); ^{13}C NMR (126 MHz, DMSO) δ 171.27, 159.26, 148.36, 147.17, 142.54, 140.77, 140.67, 139.63, 139.37, 136.02, 133.25, 130.37, 129.36, 129.26, 123.87, 123.66, 122.88, 122.05, 120.44, 113.87, 111.42, 54.86, 37.70, 30.61; MS (ESI) m/z = 415.96 ($\text{M} + \text{H}$) $^+$

4.1.1.71. 3-(Pyridin-3-yl)-N-(5-(4-(pyridin-3-yl)thiophen-2-yl)pyridin-3-yl)propanamide (34b). The compound was synthesized

according to procedure **C** to give a brown solid: yield 10%. The product was purified by CC (DCM/MeOH/TEA 100:3:1); mp 92.8–94.2 °C; ^1H NMR (500 MHz, DMSO) δ 10.25 (s, 1H), 8.79 (s, 1H), 8.42 (d, J = 30.0 Hz, 2H), 8.34 (s, 1H), 8.25 (dd, J = 13.8, 4.6 Hz, 2H), 8.09 (s, 1H), 7.97 (d, J = 8.1 Hz, 1H), 7.89 (d, J = 13.1 Hz, 2H), 7.67 (d, J = 7.7 Hz, 1H), 7.24 (dd, J = 12.8, 5.5 Hz, 2H), 2.21 (s, 4H); ^{13}C NMR (126 MHz, DMSO) δ 170.94, 147.81, 147.15, 146.55, 145.05, 140.81, 140.64, 139.62, 139.13, 138.94, 137.85, 136.06, 134.00, 130.67, 129.35, 124.48, 124.19, 123.74, 123.22, 122.23, 36.92, 27.55; MS (ESI) m/z = 387.03 ($\text{M} + \text{H}$) $^+$

4.1.1.72. 5-(5-(Pyridin-3-yl)thiophen-3-yl)pyridin-3-amine (35). The compound was synthesized according to procedure **C** using **compound B** to give a brown solid: yield 19%. The product was purified by CC (DCM/MeOH 100:4); mp 142.2–142.3 °C; ^1H NMR (500 MHz, DMSO) δ 8.98 (dd, J = 2.4, 0.8 Hz, 1H), 8.53 (dd, J = 4.7, 1.5 Hz, 1H), 8.19 (d, J = 1.9 Hz, 1H), 8.12 (ddd, J = 8.0, 2.4, 1.6 Hz, 1H), 8.06 (d, J = 1.5 Hz, 1H), 7.91 (dd, J = 3.9, 2.0 Hz, 2H), 7.47 (ddd, J = 8.0, 4.8, 0.9 Hz, 1H), 7.23 (dd, J = 2.5, 2.1 Hz, 1H), 5.39 (s, 2H); ^{13}C NMR (126 MHz, DMSO) δ 148.70, 146.20, 144.84, 140.48, 140.28, 135.62, 135.03, 132.67, 130.41, 129.58, 124.08, 123.81, 122.09, 116.71; MS (ESI) m/z = 253.84 ($\text{M} + \text{H}$) $^+$

4.2. Biological assays

4.2.1. Protein kinases and inhibition assays

Human Dyrk1A was expressed and purified as described earlier [38]. Dyrk1B and Clk1 were purchased from Life Technologies (lot no. 877059G, Catalog no. PV4649 and lot no. 1095729A, catalog no. PV3315). Woodtide substrate peptide for Dyrk1A and Dyrk1B (KKISGRSLSPIMTEQ) and RS repeat substrate peptide for Clk1 (GRSRSRSRSRSRSR) were custom synthesized at the Department of Medical Biochemistry and Molecular Biology, Saarland University, Homburg, Germany. Kinase inhibition assays for Dyrk1A, Dyrk1B, Clk1 were performed as described previously, in the presence of 15 μM ATP [38]. The calculated IC_{50} values are representative of at least two independent determinations. The larger panel of kinases shown in Table 3 was screened by the SelectScreen Kinase Profiling Service, Thermo Fisher Scientific, Paisley, U.K.

4.2.2. Cell-based assays

Stock solutions of the inhibitors were prepared in dimethylsulfoxide (DMSO). All effects were compared to vehicle controls which contained DMSO at the respective final concentration in growth medium. Protein kinase activity of endogenous Dyrk1A in HeLa cells was assayed by measuring the phosphorylation of T434 in overexpressed GFP-SF3b1-NT as described previously [54]. Briefly, HeLa cells were transiently transfected in 6-well plates and treated with test compounds for 18 h. Total cellular lysates were subjected to Western blot analysis with the help of a custom-made rabbit antibody for phosphorylated T434 in SF3b1 and a commercial goat antibody for GFP (no. 600-101-215, Rockland Immunochemicals, Gilbertsville, PA, USA). Blots were developed using horseradish peroxidase (HRP)-conjugated secondary antibodies and enhanced chemiluminescent substrates. Signals were quantified using the AIDA Image Analyzer 5.0 program (Raytest, Straubenhardt, Germany). pT434 signals were normalised to total protein levels as determined from GFP immunoreactivity. GraphPad Prism 5.0 (GraphPad Software, La Jolla, CA, USA) was used for non-linear curve fitting (Hill slope –1).

Viability assays were performed using a 96-well plate format (20,000–30,000 cells per well). Cells were cultivated for 3 days before cell viability was assessed with the help of a tetrazolium dye assay (XTT assay, AppliChem GmbH, Darmstadt, Germany).

4.3. Molecular docking studies

Molecular docking was performed as previously described using MOE [55].

4.4. Metabolic stability in a cell free assay

Evaluation of metabolic stability and determination of half-lives was carried out using human S9 fraction as described previously [56].

4.5. Physicochemical properties calculation

Calculation of key physicochemical properties was performed using ACD/Labs software (ACD/Percepta, 2012, Advanced Chemistry Development, Inc) as described previously [38].

Notes

The authors declare no competing financial interest.

Acknowledgements

The excellent technical assistance of Simone Bamberg-Lemper is gratefully acknowledged. The authors would like to thank Prof. Dr. R. W. Hartmann and Prof. Dr. Christian Ducho for generously providing lab facilities to the M.E. group. S.S.D. and M.A.-H. acknowledge The Science & Technology Development Fund in Egypt (STDF) for funding through the GE-SEED, Project 17391. We are also grateful to the DAAD for the travelling support to S.S.D. through GradUS Global 2017 and GERSS 2015 funds. The support by the DAAD in the framework "PPP Ägypten 15" (Project-ID 57190395) to M.E. is highly appreciated. Also, the support by the Deutsche Forschungsgemeinschaft (DFG) (Grant EN381/2-3) to M.E. is greatly acknowledged. We are also thankful for Dr. Mostafa M. Hamed and Mariam G. Tahoun (Helmholtz Institute for Pharmaceutical Research Saarland) for carrying out the metabolic stability studies.

Appendix A. Supplementary data

Supplementary data related to this article can be found at <https://doi.org/10.1016/j.ejmech.2018.07.050>.

Abbreviations Used

| | |
|-------------------------|--|
| AD | Alzheimer's disease |
| APP | Amyloid precursor protein |
| ASF | Alternative splicing factor |
| CC | Column chromatography |
| CDK | Cyclin dependant kinases |
| CID | collision induced dissociation |
| CK | Casein kinase |
| Clk | cdc-like kinase |
| DS | Down's syndrome |
| Dyrk | Dual specificity tyrosine regulated kinase |
| GFP | Green fluorescent protein |
| HBA | Hydrogen bond acceptor |
| HBD | Hydrogen bond donor |
| HIPK1 | Homeodomain-interacting protein kinase 1 |
| IC ₅₀ | Half maximal inhibitory concentration |
| MLCK2 | Myosin light chain kinase 2 |
| NFAT | Nuclear factor of activated T cells |
| Pd(dppf)Cl ₂ | [1, 1'- Bis(diphenylphosphino)ferrocene] dichloropalladium(II) |

| | |
|--------|---|
| PIM1 | Proviral integration site for Moloney murine leukemia virus-1 |
| TRKB | Tropomyosin receptor kinase B |
| SF3b1 | Splicing factor 3b1 |
| SRPK1 | Serine/arginine-rich protein kinase 1 |
| STK17A | Serine/threonine kinase 17A |

References

- [1] B. Smith, F. Medda, V. Gokhale, T. Duncley, C. Hulme, Recent advances in the design, synthesis, and biological evaluation of selective DYRK1A inhibitors: a new avenue for a disease modifying treatment of Alzheimer's? *ACS Chem. Neurosci.* 3 (2012) 857–872.
- [2] A. Ionescu, F. Dufrasne, M. Gelbcke, I. Jabin, R. Kiss, D. Lamoral-Theys, DYRK1A kinase inhibitors with emphasis on cancer, *Mini Rev. Med. Chem.* 12 (2012) 1315–1329.
- [3] S.E. Mercer, E. Friedman, Mirk/Dyrk1B: a multifunctional dual-specificity kinase involved in growth arrest, differentiation, and cell survival, *Cell Biochem. Biophys.* 45 (2006) 303–315.
- [4] C.T. Miller, S. Aggarwal, T.K. Lin, S.L. Dagenais, J.I. Contreras, M.B. Orringer, T.W. Glover, D.G. Beer, L. Lin, Amplification and overexpression of the dual-specificity tyrosine-(Y)-phosphorylation regulated kinase 2 (DYRK2) gene in esophageal and lung adenocarcinomas, *Canc. Res.* 63 (2003) 4136–4143.
- [5] N. Koon, R. Schneider-Stock, M. Sarlomo-Rikala, J. Lasota, M. Smolkin, G. Petroni, A. Zaika, C. Boltze, F. Meyer, L. Andersson, S. Knuutila, M. Miettinen, W. El-Rifai, Molecular targets for tumour progression in gastrointestinal stromal tumours, *Gut* 53 (2004) 235–240.
- [6] N. Taira, R. Mimoto, M. Kurata, T. Yamaguchi, M. Kitagawa, Y. Miki, K. Yoshida, DYRK2 priming phosphorylation of c-Jun and c-Myc modulates cell cycle progression in human cancer cells, *J. Clin. Invest.* 122 (2012) 859–872.
- [7] N. Taira, K. Nihira, T. Yamaguchi, Y. Miki, K. Yoshida, DYRK2 is targeted to the nucleus and controls p53 via Ser46 phosphorylation in the apoptotic response to DNA damage, *Mol. Cell* 25 (2007) 725–738.
- [8] O. Bogacheva, O. Bogachev, M. Menon, A. Dev, E. Houde, E.I. Valoret, H.M. Prosser, C.L. Creasy, S.J. Pickering, E. Grau, K. Rance, G.P. Livi, V. Karur, C.L. Erickson-Miller, D.M. Wojchowski, DYRK3 dual-specificity kinase attenuates erythropoiesis during anemia, *J. Biol. Chem.* 283 (2008) 36665–36675.
- [9] T.I. Slepak, L.D. Salay, V.P. Lemmon, J.L. Bixby, Dyrk kinases regulate phosphorylation of doublecortin, cytoskeletal organization, and neuronal morphology, *Cytoskeleton (Hoboken)* 69 (2012) 514–527.
- [10] B. Hammerle, C. Elizalde, F.J. Tejedor, The spatio-temporal and subcellular expression of the candidate Down syndrome gene Mnb/Dyrk1A in the developing mouse brain suggests distinct sequential roles in neuronal development, *Eur. J. Neurosci.* 27 (2008) 1061–1074.
- [11] J. Guimera, C. Casas, C. Pucharcos, A. Solans, A. Domenech, A.M. Planas, J. Ashley, M. Lovett, X. Estivill, M.A. Pritchard, A human homologue of Drosophila minibrain (MNB) is expressed in the neuronal regions affected in Down syndrome and maps to the critical region, *Hum. Mol. Genet.* 5 (1996) 1305–1310.
- [12] W.J. Song, L.R. Sternberg, C. Kasten-Sportes, M.L. Keuren, S.H. Chung, A.C. Slack, D.E. Miller, T.W. Glover, P.W. Chiang, L. Lou, D.M. Kurnit, Isolation of human and murine homologues of the Drosophila minibrain gene: human homologue maps to 21q22.2 in the Down syndrome "critical region", *Genomics* 38 (1996) 331–339.
- [13] W. Becker, U. Soppa, F.J. Tejedor, DYRK1A: a potential drug target for multiple Down syndrome neuropathologies, *CNS Neurol. Disord. - Drug Targets* 13 (2014) 26–33.
- [14] J.T. Coyle, M.L. Oster-Granite, J.D. Gearhart, The neurobiologic consequences of Down syndrome, *Brain Res. Bull.* 16 (1986) 773–787.
- [15] A. Contestabile, F. Benfenati, L. Gasparini, Communication breaks-Down: from neurodevelopment defects to cognitive disabilities in Down syndrome, *Prog. Neurobiol.* 91 (2010) 1–22.
- [16] K. Gardiner, Y. Herault, I.T. Lott, S.E. Antonarakis, R.H. Reeves, M. Dierssen, Down syndrome: from understanding the neurobiology to therapy, *J. Neurosci.* 30 (2010) 14943–14945.
- [17] T.F. Haydar, R.H. Reeves, Trisomy 21 and early brain development, *Trends Neurosci.* 35 (2012) 81–91.
- [18] J. Wegiel, C.X. Gong, Y.W. Hwang, The role of DYRK1A in neurodegenerative diseases, *FEBS J.* 278 (2011) 236–245.
- [19] S.R. Ryoo, H.K. Jeong, C. Radnaabazar, J.J. Yoo, H.J. Cho, H.W. Lee, I.S. Kim, Y.H. Cheon, Y.S. Ahn, S.H. Chung, W.J. Song, DYRK1A-mediated hyperphosphorylation of Tau. A functional link between Down syndrome and Alzheimer disease, *J. Biol. Chem.* 282 (2007) 34850–34857.
- [20] O. Kelemen, P. Convertini, Z. Zhang, Y. Wen, M. Shen, M. Falaleeva, S. Stamm, Function of alternative splicing, *Gene* 514 (2013) 1–30.
- [21] M.L. Hastings, A.R. Krainer, Pre-mRNA splicing in the new millennium, *Curr. Opin. Cell Biol.* 13 (2001) 302–309.
- [22] Z. Zhou, X.D. Fu, Regulation of splicing by SR proteins and SR protein-specific kinases, *Chromosoma* 122 (2013) 191–207.
- [23] X. Yin, N. Jin, J. Gu, J. Shi, J. Zhou, C.X. Gong, K. Iqbal, I. Grundke-Iqbal, F. Liu, Dual-specificity tyrosine phosphorylation-regulated kinase 1A (Dyrk1A) modulates serine/arginine-rich protein 55 (SRP55)-promoted Tau exon 10

- inclusion, *J. Biol. Chem.* 287 (2012) 30497–30506.
- [24] W. Qian, H. Liang, J. Shi, N. Jin, I. Grundke-Iqbal, K. Iqbal, C.X. Gong, F. Liu, Regulation of the alternative splicing of tau exon 10 by SC35 and Dyrk1A, *Nucleic Acids Res.* 39 (2011) 6161–6171.
- [25] K. de Graaf, H. Czajkowska, S. Rottmann, L.C. Packman, R. Lilischkis, B. Luscher, W. Becker, The protein kinase DYRK1A phosphorylates the splicing factor SF3b1/SAP155 at Thr434, a novel *in vivo* phosphorylation site, *BMC Biochem.* 7 (2006) 7.
- [26] J. Shi, T. Zhang, C. Zhou, M.O. Chohan, X. Gu, J. Wegiel, J. Zhou, Y.W. Hwang, K. Iqbal, I. Grundke-Iqbal, C.X. Gong, F. Liu, Increased dosage of Dyrk1A alters alternative splicing factor (ASF)-regulated alternative splicing of tau in Down syndrome, *J. Biol. Chem.* 283 (2008) 28660–28669.
- [27] X. Yin, N. Jin, J. Shi, Y. Zhang, Y. Wu, C.X. Gong, K. Iqbal, F. Liu, Dyrk1A overexpression leads to increase of 3R-tau expression and cognitive deficits in Ts65Dn Down syndrome mice, *Sci. Rep.* 7 (2017) 12.
- [28] K. Iqbal, F. Liu, C.X. Gong, Tau and neurodegenerative disease: the story so far, *Nat. Rev. Neurol.* 12 (2016) 15–27.
- [29] D. Toiber, G. Azkona, S. Ben-Ari, N. Toran, H. Soreq, M. Dierssen, Engineering DYRK1A overexpression yields Down syndrome-characteristic cortical splicing aberrations, *Neurobiol. Dis.* 40 (2010) 348–359.
- [30] J. Wegiel, W. Kaczmarek, M. Barua, I. Kuchna, K. Nowicki, K.C. Wang, S.M. Yang, J. Frackowiak, B. Mazur-Kolecka, W.P. Silverman, B. Reisberg, I. Monteiro, M. de Leon, T. Wisniewski, A. Dalton, F. Lai, Y.W. Hwang, T. Adayev, F. Liu, K. Iqbal, I.G. Iqbal, C.X. Gong, Link between DYRK1A overexpression and several-fold enhancement of neurofibrillary degeneration with 3-repeat tau protein in Down syndrome, *J. Neuropathol. Exp. Neurol.* 70 (2011) 36–50.
- [31] S. Coutadeur, H. Benyammine, L. Delalande, C. de Oliveira, B. Leblond, A. Foucourt, T. Besson, A.S. Casagrande, T. Tavernier, A. Girard, M.P. Pando, L. Desire, A novel DYRK1A (dual specificity tyrosine phosphorylation-regulated kinase 1A) inhibitor for the treatment of Alzheimer's disease: effect on Tau and amyloid pathologies *in vitro*, *J. Neurochem.* 133 (2015) 440–451.
- [32] D. Frost, B. Meechooet, T. Wang, S. Gately, M. Giorgetti, I. Shcherbakova, T. Duncley, Beta-carboline compounds, including harmine, inhibit DYRK1A and tau phosphorylation at multiple Alzheimer's disease-related sites, *PLoS One* 6 (2011), e19264.
- [33] S. Garcia-Cerro, N. Rueda, V. Vidal, S. Lantigua, C. Martinez-Cue, Normalizing the gene dosage of Dyrk1A in a mouse model of Down syndrome rescues several Alzheimer's disease phenotypes, *Neurobiol. Dis.* 106 (2017) 76–88.
- [34] C. Branca, D.M. Shaw, R. Belfiore, V. Gokhale, A.Y. Shaw, C. Foley, B. Smith, C. Hulme, T. Duncley, B. Meechooet, A. Caccamo, S. Oddo, Dyrk1 inhibition improves Alzheimer's disease-like pathology, *Aging Cell* 16 (2017) 1146–1154.
- [35] D. Dowling, S. Nasr-Esfahani, C.H. Tan, K. O'Brien, J.L. Howard, D.A. Jans, D.F. Purcell, C.M. Stoltzfus, S. Sonza, HIV-1 infection induces changes in expression of cellular splicing factors that regulate alternative viral splicing and virus production in macrophages, *Retrovirology* 5 (2008) 18.
- [36] A.G. Golub, O.Y. Yakovenko, A.O. Prykhod'ko, S.S. Lukashov, V.G. Bdzhola, S.M. Yarmoluk, Evaluation of 4,5,6,7-tetrahalogeno-1H-isindole-1,3(2H)-diones as inhibitors of human protein kinase CK2, *Biochim. Biophys. Acta* 1784 (2008) 143–149.
- [37] Y. Ogawa, Y. Nonaka, T. Goto, E. Ohnishi, T. Hiramatsu, I. Kii, M. Yoshida, T. Ikura, H. Onogi, H. Shibuya, T. Hosoya, N. Ito, M. Hagiwara, Development of a novel selective inhibitor of the Down syndrome-related kinase Dyrk1A, *Nat. Commun.* 1 (2010) 86.
- [38] C. Schmitt, D. Kail, M. Mariano, M. Empting, N. Weber, T. Paul, R.W. Hartmann, M. Engel, Design and synthesis of a library of lead-like 2,4-bis(heterocyclic) substituted thiophenes as selective Dyrk/Clk inhibitors, *PLoS One* 9 (2014), e87851.
- [39] K. Ruben, A. Wurzbauer, A. Walte, W. Sippl, F. Bracher, W. Becker, Selectivity profiling and biological activity of novel beta-carbolines as potent and selective DYRK1 kinase inhibitors, *PLoS One* 10 (2015), e0132453.
- [40] Y. Song, D. Kesuma, J. Wang, Y. Deng, J. Duan, J.H. Wang, R.Z. Qi, Specific inhibition of cyclin-dependent kinases and cell proliferation by harmine, *Biochem. Biophys. Res. Commun.* 317 (2004) 128–132.
- [41] F. Giraud, G. Alves, E. Debiton, L. Nauton, V. Thery, E. Durieu, Y. Ferandin, O. Lozach, L. Meijer, F. Anizon, E. Pereira, P. Moreau, Synthesis, protein kinase inhibitory potencies, and *in vitro* antiproliferative activities of meridianin derivatives, *J. Med. Chem.* 54 (2011) 4474–4489.
- [42] K. Anderson, Y. Chen, Z. Chen, R. Dominique, K. Glenn, Y. He, C. Janson, K.C. Luk, C. Lukacs, A. Polonskaia, Q. Qiao, A. Railkar, P. Rossman, H. Sun, Q. Xiang, M. Vilenchik, P. Wovkulich, X. Zhang, Pyrido[2,3-d]pyrimidines: discovery and preliminary SAR of a novel series of DYRK1B and DYRK1A inhibitors, *Bioorg. Med. Chem. Lett.* 23 (2013) 6610–6615.
- [43] Q. Zhou, A.F. Phoa, R.H. Abbassi, M. Hoque, T.A. Reekie, J.S. Font, R.M. Ryan, B.W. Stringer, B.W. Day, T.G. Johns, L. Munoz, M. Kassiou, Structural optimization and pharmacological evaluation of inhibitors targeting dual-specificity tyrosine phosphorylation-regulated kinases (DYRK) and cdc-like kinases (CLK) in glioblastoma, *J. Med. Chem.* 60 (2017) 2052–2070.
- [44] U. Rothweiler, W. Stensen, B.O. Brandsdal, J. Isaksson, F.A. Leeson, R.A. Engh, J.S. Svendsen, Probing the ATP-binding pocket of protein kinase DYRK1A with benzothiazole fragment molecules, *J. Med. Chem.* 59 (2016) 9814–9824.
- [45] C. Schmitt, P. Miralinaghi, M. Mariano, R.W. Hartmann, M. Engel, Hydroxybenzothiofene ketones are efficient Pre-mRNA splicing modulators due to dual inhibition of Dyrk1A and Clk1/4, *ACS Med. Chem. Lett.* 5 (2014) 963–967.
- [46] Y. Loidreau, P. Marchand, C. Dubouilh-Benard, M.R. Nourrisson, M. Duflos, N. Loaec, L. Meijer, T. Besson, Synthesis and biological evaluation of N-aryl-7-methoxybenzo[b]furo[3,2-d]pyrimidin-4-amine and their N-arylbenzo[b]thieno[3,2-d]pyrimidin-4-amine analogues as dual inhibitors of CLK1 and DYRK1A kinases, *Eur. J. Med. Chem.* 59 (2013) 283–295.
- [47] M. Debdab, F. Carreaux, S. Renault, M. Soundararajan, O. Fedorov, P. Filippakopoulos, O. Lozach, L. Babault, T. Tahtouh, B. Baratte, Y. Ogawa, M. Hagiwara, A. Eisenreich, U. Rauch, S. Knapp, L. Meijer, J.P. Bazureau, Leucettines, a class of potent inhibitors of cdc2-like kinases and dual specificity, tyrosine phosphorylation regulated kinases derived from the marine sponge leucettamine B: modulation of alternative pre-RNA splicing, *J. Med. Chem.* 54 (2011) 4172–4186.
- [48] C. Opoku-Temeng, N. Dayal, M. Afkari Soorreshjani, H.O. Sintim, 3H-pyrazolo [4,3-f]quinoline haspin kinase inhibitors and anticancer properties, *Bioorg. Chem.* 78 (2018) 418–426.
- [49] J. Park, Y. Oh, L. Yoo, M.S. Jung, W.J. Song, S.H. Lee, H. Seo, K.C. Chung, Dyrk1A phosphorylates p53 and inhibits proliferation of embryonic neuronal cells, *J. Biol. Chem.* 285 (2010) 31895–31906.
- [50] Q. Liu, N. Liu, S. Zang, H. Liu, P. Wang, C. Ji, X. Sun, Tumor suppressor DYRK1A effects on proliferation and chemoresistance of AML cells by downregulating c-Myc, *PLoS One* 9 (2014), e98853.
- [51] W. Shen, B. Taylor, Q. Jin, V. Nguyen-Tran, S. Meeusen, Y.Q. Zhang, A. Kamireddy, A. Swafford, A.F. Powers, J. Walker, J. Lamb, B. Bursallaya, M. DiDonato, G. Harb, M. Qiu, C.M. Filippi, L. Deaton, C.N. Turk, W.L. Suarez-Pinzon, Y. Liu, X. Hao, T. Mo, S. Yan, J. Li, A.E. Herman, B.J. Hering, T. Wu, H. Martin Seidel, P. McNamara, R. Glynn, B. Laffitte, Inhibition of DYRK1A and GSK3B induces human beta-cell proliferation, *Nat. Commun.* 6 (2015) 8372.
- [52] K.M. Mahar Doan, J.E. Humphreys, L.O. Webster, S.A. Wring, L.J. Shampine, C.J. Serabjit-Singh, K.K. Adkison, J.W. Polli, Passive permeability and P-glycoprotein-mediated efflux differentiate central nervous system (CNS) and non-CNS marketed drugs, *J. Pharmacol. Exp. Therapeut.* 303 (2002) 1029–1037.
- [53] H. Pajouhesh, G.R. Lenz, Medicinal chemical properties of successful central nervous system drugs, *NeuroRx* 2 (2005) 541–553.
- [54] N. Gockler, G. Joffre, C. Papadopoulos, U. Soppe, F.J. Tejedor, W. Becker, Harmine specifically inhibits protein kinase DYRK1A and interferes with neurite formation, *FEBS J.* 276 (2009) 6324–6337.
- [55] A.K. ElHady, M. Abdel-Halim, A.H. Abadi, M. Engel, Development of selective Clk1 and -4 inhibitors for cellular depletion of cancer-relevant proteins, *J. Med. Chem.* 60 (2017) 5377–5391.
- [56] E.M. Gargano, E. Perspicace, N. Hanke, A. Carotti, S. Marchais-Oberwinkler, R.W. Hartmann, Metabolic stability optimization and metabolite identification of 2,5-thiophene amide 17beta-hydroxysteroid dehydrogenase type 2 inhibitors, *Eur. J. Med. Chem.* 87 (2014) 203–219.
- [57] T. Tahtouh, J.M. Elkins, P. Filippakopoulos, M. Soundararajan, G. Burgy, E. Durieu, C. Cochet, R.S. Schmid, D.C. Lo, F. Delhommel, A.E. Oberholzer, L.H. Pearl, F. Carreaux, J.P. Bazureau, S. Knapp, L. Meijer, Selectivity, cocrystal structures, and neuroprotective properties of leucettines, a family of protein kinase inhibitors derived from the marine sponge alkaloid leucettamine B, *J. Med. Chem.* 55 (2012) 9312–9330.
- [58] J. Bain, H. McLauchlan, M. Elliott, P. Cohen, The specificities of protein kinase inhibitors: an update, *Biochem. J.* 371 (2003) 199–204.
- [59] T. Anastassiadis, S.W. Deacon, K. Devarajan, H. Ma, J.R. Peterson, Comprehensive assay of kinase catalytic activity reveals features of kinase inhibitor selectivity, *Nat. Biotechnol.* 29 (2011) 1039–1045.
- [60] M.A. Pagano, J. Bain, Z. Kazimierzczuk, S. Sarno, M. Ruzzene, G. Di Maira, M. Elliott, A. Orzeszko, G. Cozza, F. Meggio, L.A. Pinna, The selectivity of inhibitors of protein kinase CK2: an update, *Biochem. J.* 415 (2008) 353–365.
- [61] G.D. Cuny, M. Robin, N.P. Ulyanova, D. Patnaik, V. Pique, G. Casano, J.F. Liu, X. Lin, J. Xian, M.A. Glicksman, R.L. Stein, J.M. Higgins, Structure-activity relationship study of acridine analogs as haspin and DYRK2 kinase inhibitors, *Bioorg. Med. Chem. Lett.* 20 (2010) 3491–3494.
- [62] A.K. Ghose, T. Herbertz, R.L. Hudkins, B.D. Dorsey, J.P. Mallamo, Knowledge-based, central nervous system (CNS) lead selection and lead optimization for CNS drug discovery, *ACS Chem. Neurosci.* 3 (2012) 50–68.

7.3 Development of novel amide-derivatized 2,4-bispyridyl thiophenes as highly potent and selective Dyrk1A inhibitors. Part II: Identification of the cyclopropylamide moiety as a key modification

Sarah S. Darwish, Mohammad Abdel-Halim, Ahmed K. ElHady, Mohamed Salah, Ashraf H. Abadi, Walter Becker, Matthias Engel

Reprinted with permission *Eur. J. Med. Chem.* 2018, 158, 270–285.

DOI: 10.1016/j.ejmech.2018.08.097

Copyright (2018) ELSEVIER

Publication I

Contribution Report

The author significantly contributed in the kinase inhibition assays as well as the cellular viability assays. He further carried out the in silico physiochemical characterization of the compounds. He contributed in the interpretation of the results.



Contents lists available at ScienceDirect

European Journal of Medicinal Chemistry

journal homepage: <http://www.elsevier.com/locate/ejmech>

Research paper

Development of novel amide–derivatized 2,4-bispyridyl thiophenes as highly potent and selective Dyrk1A inhibitors. Part II: Identification of the cyclopropylamide moiety as a key modification



Sarah S. Darwish^a, Mohammad Abdel-Halim^a, Ahmed K. ElHady^a, Mohamed Salah^b, Ashraf H. Abadi^a, Walter Becker^c, Matthias Engel^{b,*}

^a Department of Pharmaceutical Chemistry, Faculty of Pharmacy and Biotechnology, German University in Cairo, Cairo, 11835, Egypt

^b Pharmaceutical and Medicinal Chemistry, Saarland University, Campus C2.3, D-66123, Saarbrücken, Germany

^c Institute of Pharmacology and Toxicology, Medical Faculty of the RWTH Aachen University, Wendlingweg 2, 52074, Aachen, Germany

ARTICLE INFO

Article history:

Received 14 June 2018

Received in revised form

29 August 2018

Accepted 31 August 2018

Available online 3 September 2018

Keywords:

Dyrk1A

Neurodegenerative diseases

Cyclopropyl amide

SF3b1 phosphorylation

CNS penetration

ABSTRACT

Dual-specificity tyrosine phosphorylation-regulated kinase 1A (Dyrk1A) is a potential target in Alzheimer's disease (AD) because of the established correlation between its over-expression and generation of neurofibrillary tangles (NFT) as well as the accumulation of amyloid plaques. However, the use of Dyrk1A inhibitors requires a high degree of selectivity over closely related kinases. In addition, the physicochemical properties of the Dyrk1A inhibitors need to be controlled to enable CNS permeability. In the present study, we optimized our previously published 2,4-bispyridyl thiophene class of Dyrk1A inhibitors by the synthesis of a small library of amide derivatives, carrying alkyl, cycloalkyl, as well as acidic and basic residues. Among this library, the cyclopropylamido modification (compound **4b**) was identified as being highly beneficial for several crucial properties. **4b** displayed high potency and selectivity against Dyrk1A over closely related kinases in cell-free assays (IC₅₀: Dyrk1A = 3.2 nM; Dyrk1B = 72.9 nM and Clk1 = 270 nM) and inhibited the Dyrk1A activity in HeLa cells with high efficacy (IC₅₀: 43 nM), while no significant cytotoxicity was observed. In addition, the cyclopropylamido group conferred high metabolic stability and maintained the calculated physicochemical properties in a range compatible with a potential CNS activity. Thus, based on its favourable properties, **4b** can be considered as a candidate for further *in vivo* testing in animal models of AD.

© 2018 Elsevier Masson SAS. All rights reserved.

1. Introduction

Dual-specificity tyrosine-regulated kinases (Dyrks) belong to the larger human kinome family known as the CMGC group [1] which includes cyclin-dependent kinases (CDKs), mitogen-activated protein kinase (MAPKs), glycogen synthase kinases (GSKs), and cdc-like kinases (Clks) [2]. The Dyrk family comprises the mammalian subtypes 1A, 1B, 2, 3, and 4 [3]. As their name implies, dual specificity kinases are capable of catalyzing their self-activation by autophosphorylation at a conserved tyrosine residue, whereas the resulting mature forms of the kinases can only phosphorylate exogenous protein substrates at serine or threonine residues [1,2]. Due to its location in the Down Syndrome (DS)

critical region on human chromosome 21, Dyrk1A is the most studied isoform in its family [4–6]. During embryonic development, Dyrk1A plays an important role in neurogenesis as well as neuronal differentiation [7], hence its about 1.5 fold overexpression in DS-affected individuals (trisomy 21) is believed to contribute to the neurodevelopmental alterations associated with DS. Moreover, dysregulated Dyrk1A activity was shown to play a pathogenic role in the development of Alzheimer's disease (AD) in DS individuals [1,8]. The main hallmarks of AD include neurofibrillary tangles (NFT) as well as the accumulation of amyloid plaques [9]. *In vitro* studies showed that Dyrk1A directly phosphorylates tau protein, leading to the loss of tau biological function as well as sequestration of normal tau and neurofibrillary degeneration [10–12]. Additionally, Dyrk1A was found associated with NFTs in individuals with DS in the age group of 38–51 years, suggesting that Dyrk1A contributes to the early onset of neurofibrillary degeneration [13]. Furthermore, over-expressed Dyrk1A hyperphosphorylates

* Corresponding author.

E-mail address: ma.engel@mx.uni-saarland.de (M. Engel).

amyloid precursor protein (APP) which enhances the production of amyloid- β , the main component of amyloid plaques [9,13,14].

More recently, evidence has accumulated that Dyrk1A can also contribute to α -synuclein aggregation and fibrillization in Lewy bodies in Parkinson's disease (PD) and Lewy body dementia [15–19]. Dyrk1A binds to and phosphorylates α -synuclein at Ser87 [15]. In addition, Dyrk1A phosphorylates the neurodegeneration-related septin 4 [16], and complexes of these proteins may contribute to the cytoplasmic aggregation/fibrillization observed in PD, Lewy body dementia and multiple-system atrophy [17,18]. Moreover, parkin was reported to co-localize and bind to Dyrk1A [19]. Dyrk1A directly phosphorylates parkin at Ser-131, causing the inhibition of its E3 ubiquitin ligase activity, which may also contribute to the pathogenesis of PD.

Furthermore, both AD and PD are also driven by aberrant splicing events which may be co-regulated by Dyrk1A, too [20–23]. Dyrk1A was reported to phosphorylate SR proteins which are considered among the main determinants of splice site recognition in pre-mRNA [24]. Dyrk1A is additionally known to catalyze the phosphorylation of the non-SR protein SF3b1 which is an important modulator of splicing reactions [25]. In AD, a misbalance of the two splicing-dependent 3R and 4R tau isoforms was shown to be caused by Dyrk1A in a mouse model [26]. This imbalance can be linked to the ability of Dyrk1A to phosphorylate relevant SR proteins such as SRp55, SC35 and ASF [20–22]. Besides the proven influence on the 3R/4R tau protein ratio, Dyrk1A over-dosage models also showed changes in the neuroigin mRNAs transcript composition as well as changes in the splicing pattern of acetylcholinesterase (AChE), leading to different AChE mRNA variants [27].

Thus, pharmacological inhibition of Dyrk1A might not only suppress the pathogenic hyperphosphorylation of neuroproteins, it may also restore the normal pattern of splicing products of the respective proteins. In light of these pleiotropic functions of Dyrk1A, potential pharmacological inhibitors of Dyrk1A should be highly selective to avoid the accumulation of adverse side effects due to additional off target inhibitions. Although many published Dyrk1A inhibitors, including harmine [28], INDY [29], leucettine L41 [30], EHT 5372 [31], and 7-chloro-2-phenyl-1*H*-indole-3-carbonitrile [32] exhibited a good overall selectivity in a larger kinase screening panel, they still showed co-inhibition of at least one of the off-targets Dyrk1B, Clk1 and/or haspin, all of which show a high degree of similarity with Dyrk1A in their ATP binding site. The catalytic domain of Dyrk1A and Dyrk1B possess a sequence identity of 85%, and their ATP binding sites differ by only one amino acid residue: Met240 of Dyrk1A is replaced by Leu192 in Dyrk1B [32]. Dyrk1B was proposed as an anticancer target [33–35], however, in the CNS, it was shown to be implicated in the regulation of astrocyte activation [36] which can have pro-inflammatory and neurotoxic but also neuroprotective roles [37–39]. In addition, prolonged inhibition of Dyrk1B may trigger or aggravate metabolic syndrome as a side effect, since the loss of Dyrk1B activity due to a point mutation that decreased the protein stability was shown to cause an autosomal-dominant form of metabolic syndrome [40]. Clk1 is involved in the regulation of alternative splicing [41], too, hence co-inhibition of Dyrk1A and Clk1 might potentiate the effects on alternative splicing of numerous pre-mRNAs, which could be poorly tolerated during prolonged treatments. Finally, haspin is indispensable for cell division [42], and its inhibition is expected to interfere with normal cell proliferation.

In a previous study, we introduced the 2,4-bispyridyl thiophene core as a favourable scaffold for Dyrk1A inhibition [43]. The selectivity of this scaffold over some of the common off target kinases was increased in a subsequent study using an amide-linked structural extension [44]. In the current work, we present new

derivatives of the 2,4-bispyridyl thiophene amides with further improved selectivity profiles and physicochemical properties.

2. Results and discussion

2.1. Design strategy

In our previous attempt to improve the selectivity towards Dyrk1A, we extended the bispyridyl thiophene scaffold by introducing an additional amino function on the pyridine at the thiophene-2 position, yielding compound **1** (compound **2** in Ref. [44], Fig. 1). Its increased potency prompted us to attach a variety of side chains through amide linkage. In the library thus generated, we had identified Compound **II** (compound **31b** in Ref. [44]) as the most potent inhibitor of that series. It also showed a great improvement in selectivity towards Dyrk1B and Clk1 (IC_{50} : Dyrk1B = 383 nM, Clk1 > 2 μ M, [ATP] = 15 μ M), however, we noticed that **II** still showed significant cross reactivity with haspin (IC_{50} = 36 nM). In addition, the clogP value of the benzylamide derivative **II** (clogP = 4.11) was above the optimal average range reported for CNS active compounds, which is about 2.8 [45].

Therefore, it seemed straightforward to extend our diversification strategy by including mainly non aromatic and polar amide moieties, in order to enable alternative interactions with pocket side chains and decrease the lipophilicity. We selected different alkyl, cycloalkyl, as well as acidic and basic amide side chain extensions, which could potentially address pocket residues located at the hinge region of the ATP binding site (e.g., Tyr243 and Ile165) but also at the opposite side (e.g. Asp307, Phe170). We used the previously reported compound **I** as our extendable hit (Fig. 1).

2.2. Chemistry

The main synthetic scheme for attaining the planned amide functionalized 2,4-bispyridyl thiophenes amide derivatives constitutes four steps (Scheme 1). Primarily, a Miyaura reaction was carried out on 3-amino-5-bromopyridine and bis(pinacolato)diboron in the presence of potassium acetate and Pd (dppf)Cl₂ as a catalyst to yield the corresponding boronic acid pinacol ester (Compound **A**). In the second step, Suzuki cross coupling reaction with 2,4-dibromothiophene in the presence of Cs₂CO₃ and palladium-tetrakis (triphenylphosphine) to give 4-bromothiophen-2-yl pyridine amines takes place to yield compound **B**. Afterwards, the amino group in compound **B** undergoes a coupling reaction with diverse carboxylic acids and methylsulfonyl chloride to yield a series of amides and sulfonamide, respectively. Finally, the free bromo in the previous amides/sulfonamides make the compounds accessible for a second Suzuki reaction with 3-pyridine boronic acid to synthesize the bispyridyl thiophene functionalized amides (**1b–8b**). Alkylation of the secondary amide of compound **4a** was done by deprotonation of the amide with KH followed by the reaction with the respective alkyl iodide then the product was coupled with 3-pyridine boronic acid to yield compounds **9–10** (Scheme 1). To have an amide with basic side chains, either an additional BOC deprotection was performed on compound **7b** using TFA to release compound **11** (Scheme 2) or the chloroacetamide derivative (compound **E**) was reacted with the appropriate alicyclic amines followed by subsequent Suzuki coupling to yield compounds **12–13** (Scheme 3). In order to omit the terminal pyridyl of compound **4b**, compound **B** was coupled with 2-bromothiophene, followed by amide coupling with cyclopropyl carboxylic acid to give compound **14** (Scheme 4). In addition to the compounds mentioned above, a second unique cluster of compounds was synthesized by linking the pyrazol-4-yl moiety to position 4 of the thiophene core of compound **4a**. In compounds **17–19**, the 4-pyrazoleboronic acid

272

S.S. Darwish et al. / European Journal of Medicinal Chemistry 158 (2018) 270–285

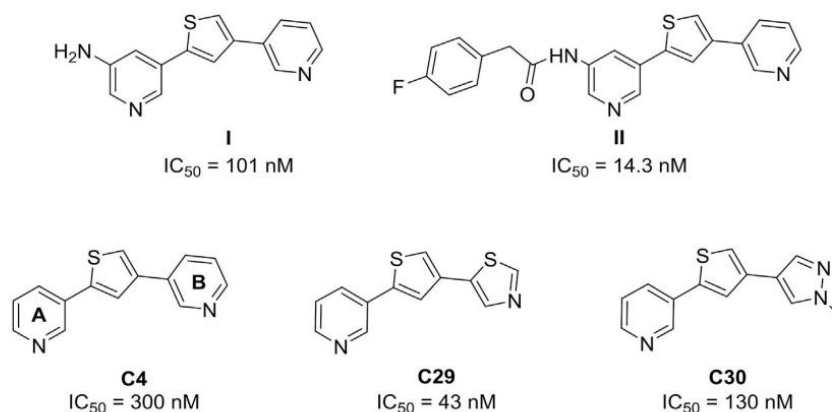
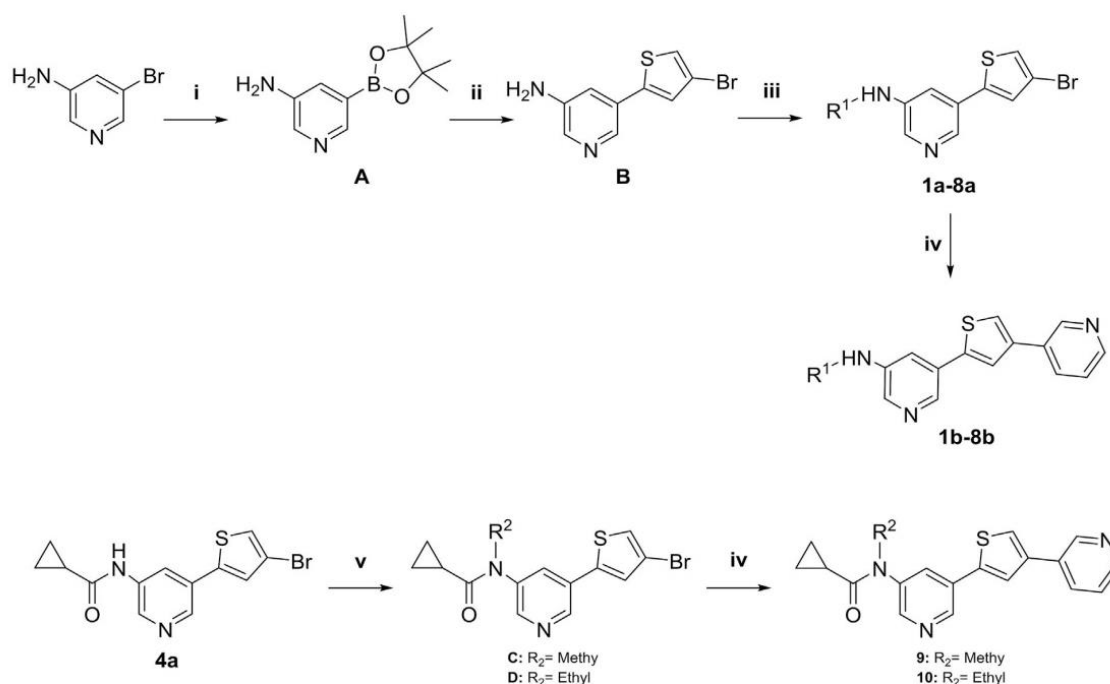


Fig. 1. Previously published Dyrk1A inhibitors derived from the basic 2,4-bispyridyl thiophene scaffold C4. The IC_{50} values against Dyrk1A are indicated (determined at $15 \mu\text{M}$ ATP).



Scheme 1. Reagents and conditions: (i) 4 equiv of potassium acetate, 4 equiv bis(pinacolato)diboron, 5 mmol% of Pd(dppf)Cl₂ in dioxane, reflux 2 h; (ii) 4 equiv of Cs₂CO₃, 5 mmol% of palladium-tetrakis(triphenylphosphine), 1.2 equiv of 2,4-dibromothiophene in dioxane/water, reflux 3.5 h; (iii) 1.5 equiv of HBTU (or HATU), 4 equiv of DIPEA, 3 equiv of the appropriate acid in DCM, room temperature, overnight; or 2 equiv of the appropriate sulfonyl chloride in pyridine, 60 °C, overnight; (iv) 4 equiv of Na₂CO₃, 5 mmol% of Pd(dppf)Cl₂, 2 equiv of 3-pyridine boronic acid in dioxane/water, reflux, 2 h; (v) 10 equiv of KH, 1 equiv of the appropriate alkyl iodide in DMF, room temperature, 2 days.

pinacol ester was initially alkylated by its reaction with the corresponding alkyl iodides in the presence of Cs₂CO₃ as a base (Scheme 5).

2.3. Biological evaluation

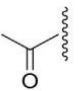
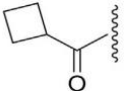
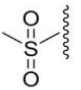
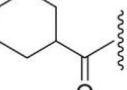
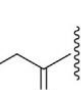
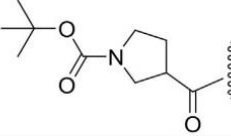
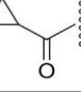
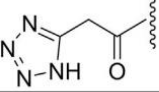
2.3.1. Investigation of the amide linker

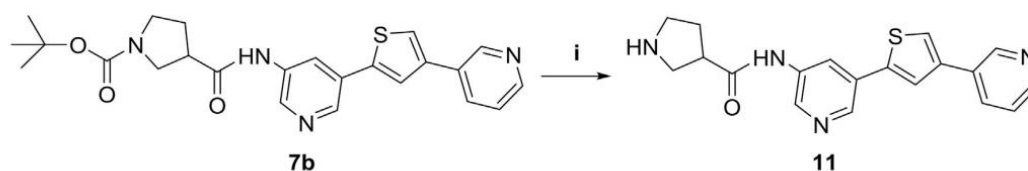
Firstly, we investigated which type of amide was preferred as linking functionality with small alkyl groups. Comparing the methyl amide and the methyl sulfonamide derivatives (compounds 1b and 2b, respectively) of precursor compound I (Fig. 1), we found that the amide linkage was better tolerated (Table 1), although the activity of 1b fell below that of I. However, an initial loss of potency

was not unexpected for the simple amide derivative, because the mesomeric effect of the former amine was strongly diminished, thus lowering the electron density and H-bond acceptor strength at the pyridine nitrogen.

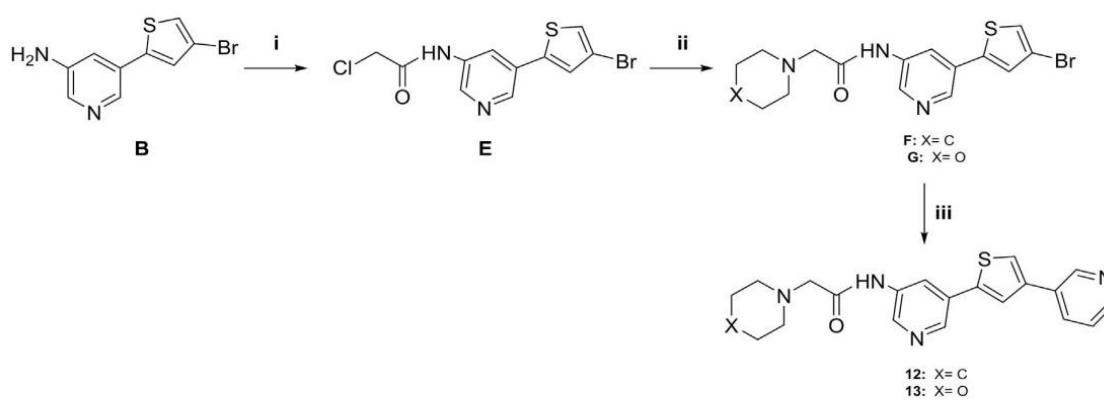
2.3.2. The effect of alkylamido extensions

Since the Dyrk1A inhibitory activity was totally abolished with the methyl sulfonamide (2b, Table 1), further alkyl extensions were subsequently introduced via the carboxamide linker, hoping to over-compensate the drop of potency brought about this functional group. While a simple homologation did not seem promising, as indicated by the lack of potency gain with the ethyl amide derivative 3b (Table 1), the cyclopropyl substituent in compound 4b

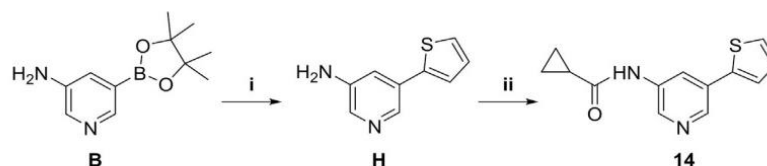
| No | R ¹ | No | R ¹ |
|----|---|----|---|
| 1a |  | 5a |  |
| 2a |  | 6a |  |
| 3a |  | 7a |  |
| 4a |  | 8a |  |



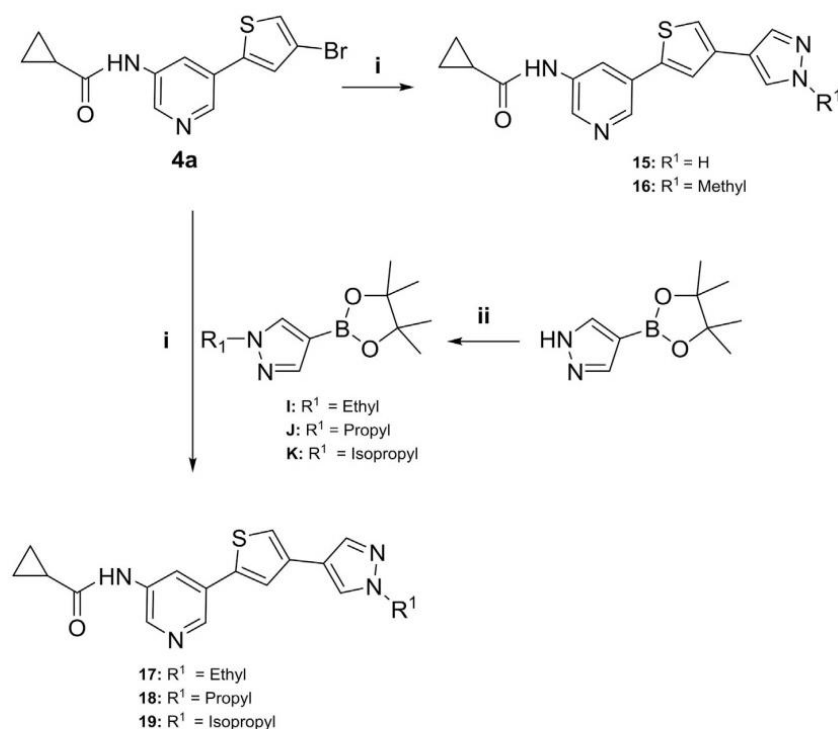
Scheme 2. Reagents and conditions: (i) TFA in DCM, room temperature, overnight.



Scheme 3. Reagents and conditions: (i) 1.5 equiv of HBTU, 4 equiv of DIPEA, 3 equiv of chloroacetic acid, room temperature, overnight; (ii) 10 equiv of the appropriate alicycle in methanol, reflux, 2 h; (iii) 4 equiv of Na₂CO₃, 5 mmol% of Pd (dppf)Cl₂, 2 equiv of 3-pyridine boronic acid in dioxane/water, reflux, 2 h.



Scheme 4. Reagents and conditions: (i) 4 equiv of Cs₂CO₃, 5 mmol% of palladium-tetrakis (triphenylphosphine), 1.2 equiv of 2-bromothiophene in dioxane/water, reflux 3 h; (ii) 1.5 equiv of HBTU, 4 equiv of DIPEA, 3 equiv cyclopropanecarboxylic acid in DCM, room temperature, overnight.



Scheme 5. Reagents and conditions: (i) 4 equiv of Na₂CO₃, 5 mmol% of Pd (dppf)Cl₂, 2 equiv of the appropriate pyrazole boronic acid in dioxane/water, reflux, 2 h; (ii) 2 equiv of Cs₂CO₃, 2 equiv of the appropriate alkyl iodide in acetone, reflux, overnight.

caused a dramatic and unexpected increase in activity, lowering the IC₅₀ to 3.2 nM. Interestingly, a one-atom ring expansion through the use of cyclobutyl in compound **5b** reduced the inhibitory activity by more than 18-fold (Table 1). This trend was confirmed with larger cycloalkyl ring expansions, e. g., with the cyclohexyl derivative **6b** (40.3% inhibition at 250 nM), indicating that the cyclopropyl amide moiety in **4b** had the optimal size. It is likely that larger cycloalkyl rings caused steric clashes with the predicted binding site at the ATP binding pocket (cf. below and Fig. 2).

2.3.3. The effect of polar and ionizable amide extensions

Despite the large boost of potency observed with the cyclopropyl moiety, our further attempts focused on establishing polar interactions with the hydrophilic amino acid residues at the pocket border. Especially the introduction of basic moieties seemed worthwhile with respect to a potential enhancement of the CNS availability of our inhibitors – besides a general improvement of drug-like characteristics. The pyrrolidine-3-carboxamide derivative **11**, in which a secondary amine was integrated in the cycloalkylamide moiety, indicated some degree of tolerance toward basic functions, but did not reach by far the potency of the best compound, **4b** (Table 1). Shifting the position of the protonable nitrogen and introducing a methylene spacer, as in the piperidinylacetamide **12**, decreased the biological activity against Dyrk1A to the level of the cyclohexane carboxamide **6b**. The morpholino analogue **13** exhibited a further drop of activity, indicating that multiple polar atoms are not tolerated. A tetrazolyl acetamide derivative with reversed, partially anionic charge was also synthesized and tested (**8b**); its low inhibitory activity (24% at 250 nM) suggested that an anionic charge cannot compensate for the unfavourable influence of increased polarity (Table 1). Compound **7b**, the protected synthetic precursor of **11**, was also tested to probe

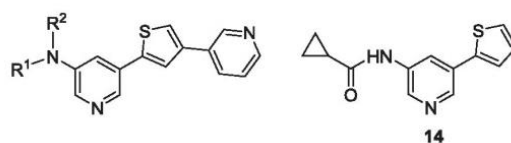
whether a further structural extension by bulky side chains could be promising; however, this was not the case, as indicated by the total loss of activity with **7b**.

2.3.4. The effect of N-alkylation of the cyclopropylamide moiety

Two more derivatives were synthesized by the N-alkylation of our most potent compound **4b** to afford the N-methyl and N-ethyl derivatives (compounds **9** and **10**, respectively). Both tertiary amide derivatives almost lost the Dyrk1A inhibitory activity (Table 1). N-alkylation of an amide function not only removes the H-bond acceptor hydrogen, but also has a considerable impact on the preferred conformation, hydrophobicity and rotational flexibility of the respective molecule part. Most likely, the N-alkyl caused the carboxamide function to rotate out of the pyridine ring plane, due to steric hindrance between the alkyl and the *ortho* H atoms, thus stabilizing a biologically less active conformation. In our binding model, compound **4b** bound with a coplanar carboxamide–pyridine conformation (cf. Fig. 2). On the other hand, the loss of the HBD function did not play a role, at least according to our predicted binding model. Nevertheless, to exclude experimentally that an alternative binding mode could be formed, involving tandem H-bonding of the pyridine N and the amide carbonyl or NH to the hinge region, we synthesized the truncated derivative **14**, which should adopt this hypothetical binding mode more easily than the full length parent compound **4b**. As indicated by the complete loss of activity of **14**, the compounds did not switch to a new binding mode driven by tandem H-bonding to the hinge region, rather the 4-pyridyl ring was still essential, probably interacting with Lys188 as illustrated in Fig. 2.

2.3.5. Replacement of the 4-pyridyl in **4b** by pyrazole

With the last set of compounds, we investigated whether the

Table 1Inhibition of Dyrk1A and Dyrk1B by the (bis)pyridine thiophene derivatives **1b–8b**, **9–14**.

| Cpd.No. | R ¹ | R ² | Dyrk1A | | Dyrk1B | |
|-----------|----------------|----------------|-------------------------------------|------------------------------------|-------------------------------------|------------------------------------|
| | | | % inhibition at 250 nM ^a | IC ₅₀ (nM) ^a | % inhibition at 250 nM ^a | IC ₅₀ (nM) ^a |
| 1b | | H | 17.6 | ND | 40.3 | ND |
| 2b | | H | 0 | ND | 23.5 | ND |
| 3b | | H | 18.6 | ND | 49.3 | ND |
| 4b | | H | 73.1 | 3.2 | 40 | 72.9 |
| 5b | | H | 65.7 | 57.8 | 81 | 218.8 |
| 6b | | H | 40.3 | ND | 51 | ND |
| 7b | | H | 0 | ND | 34.9 | ND |
| 8b | | H | 24.4 | ND | 38.5 | ND |
| 9 | | methyl | 19.4 | ND | 0.9 | ND |
| 10 | | ethyl | 24.9 | ND | 14.6 | ND |
| 11 | | H | 57.4 | ND | 62.7 | 131.7 |
| 12 | | H | 47.3 | ND | 51.8 | ND |
| 13 | | H | 21.8 | ND | 13.9 | ND |
| 14 | | | 0 | ND | 0 | ND |

^a Values are mean values of at least two experiments; standard deviation < 9%; the assay was carried out at an ATP conc. of 15 μM; ND: not determined.

nitrogen in a heteroaromatic five-membered ring could further increase the potency. In our previously reported series, the methyl pyrazole moiety proved to be a good surrogate of ring B as shown in compound **C30** in Fig. 1 (compound **30** in Ref. [43]), since it mediated a higher potency towards Dyrk1A than the 4-pyridyl in **C4** (compound **4** in Ref. [43], Fig. 1) (IC₅₀'s: 130 nM vs. 300 nM). Hence, it was straightforward to combine the favourable cyclopropylamide feature (this work) with the methyl pyrazolyl ring (previous work).

The resulting compound **16** was also potent against Dyrk1A (IC₅₀ = 42.6 nM, Table 2), still exhibiting a 3-fold increase in potency compared to compound **C30** due to the cyclopropyl amide extension. However, when compared to **4b**, compound **16** was almost 13-fold less potent, indicating that in the presence of the cyclopropylamide extension, pyridine was preferred as ring B (cf. Fig. 1) over N-methyl pyrazole. This was partially attributable to a steric hindrance of the N-methyl group in **16**, because the

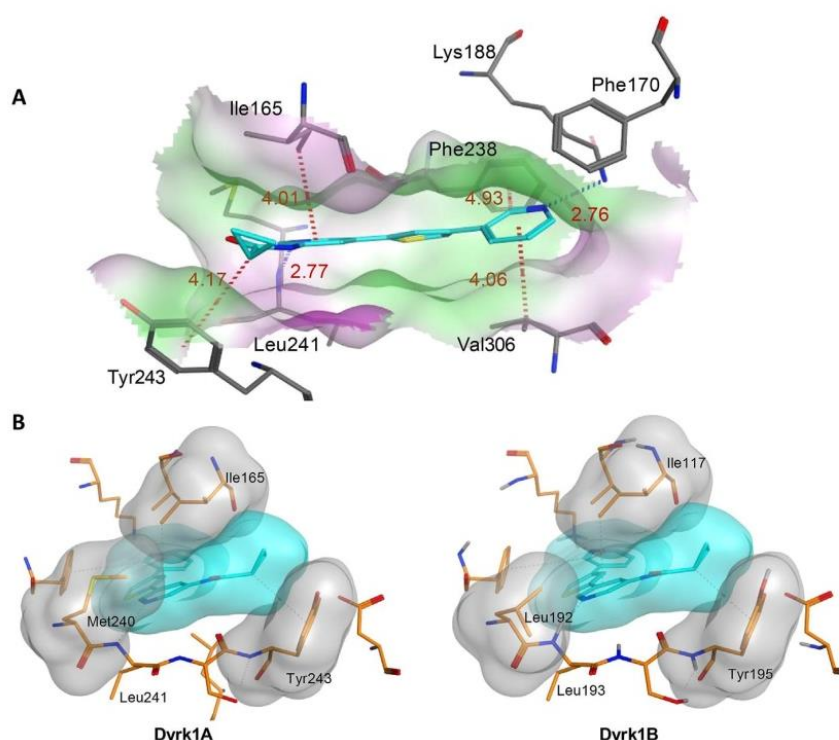
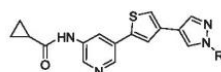


Fig. 2. (A) Binding model for the interaction between compound **4b** and the ATP binding pocket of Dyrk1A (PDB code: 3ANR). **4b** (cyan) was docked into the ATP pocket of Dyrk1A using MOE. In the binding model, compound **4b** is anchored between the conserved Lys188 and the hinge region residue Leu241 through two hydrogen bonds with the two pyridine rings. In addition, we found three CH- π interactions involving Lys188, Phe238 and Ile165. The cyclopropyl extension was proven beneficial by performing an extra Van der Waals interaction with the benzene ring of Tyr243. Interactions are indicated by dashed lines (blue; hydrogen bonds, red; CH- π interactions), and distances between the heavy atoms are given in Å. In the color code of the ATP binding pocket surface, green denotes the most lipophilic and magenta the most hydrophilic areas. (B) Met240 in Dyrk1A is expected to perform van der Waals interaction with the pyridine ring that is H-bonded to Leu241 in the Dyrk1A ATP pocket, possibly anchoring the pyridine ring at this position. Interactions with Ile165 additionally stabilize the complex. In contrast, the van der Waals interaction surface to the corresponding Leu192 (right panel, Dyrk1B) is considerably smaller. (For interpretation of the references to color in this figure legend, the reader is referred to the Web version of this article.)

Table 2

Inhibition of Dyrk1A and Dyrk1B by the pyrazole analogues **15**–**19**.



| Cpd.No. | R | Dyrk1A | | Dyrk1B | |
|-----------|-----------|-------------------------------------|------------------------------------|-------------------------------------|------------------------------------|
| | | % inhibition at 250 nM ^a | IC ₅₀ (nM) ^a | % inhibition at 250 nM ^a | IC ₅₀ (nM) ^a |
| 15 | H | 85.7 | 18 | 58.1 | 138 |
| 16 | methyl | 70.4 | 42.6 | 78.6 | 67.1 |
| 17 | ethyl | 78.8 | 29.7 | 57 | ND |
| 18 | propyl | 68 | 76 | 65.7 | 98.8 |
| 19 | isopropyl | 10.1 | ND | 0.7 | ND |

^a Values are mean values of at least two experiments; standard deviation < 10%; the assay was carried out at an ATP conc. of 15 μ M; ND: not determined.

demethylated 1H-pyrazolyl derivative **15** was clearly more potent (IC₅₀ = 18 nM, Table 2).

Nevertheless, we aimed at exploring the possibility of utilizing the pyrazole nitrogen as a convenient attachment point for further molecule extensions. Therefore, we probed the effect of installing ethyl, propyl and isopropyl groups at the pyrazole N1 (compounds **17**, **18** and **19**, respectively). Interestingly, placing an ethyl group instead of the methyl in compound **16** slightly improved the inhibitory potency (compound **17**, IC₅₀ = 29.7 nM), suggesting that an enhancement of the hydrophobic effect partially compensated

for the steric hindrance. However, further elongation of the alkyl chain to n-propyl (**18**) reduced the inhibitory activity again (IC₅₀ = 76 nM). Moreover, the branched isopropyl derivative (**19**) was almost inactive against Dyrk1A. These data suggested that pyrazole N1 in **15** was not suitable for molecule extensions because of the unfavourable vector, probably causing steric clashes of the substituents inside the binding pocket. In addition, a further disadvantage of the pyrazole containing scaffold was noted with respect to the selectivity. In general, the scaffold was better tolerated by Dyrk1B, thus lowering the selectivity factor for Dyrk1A over

Dyrk1B to 8 for **15** (compared with 24 for **4b**), while the selectivity was even lost with the N-alkylated derivatives **16–18**. Fig. 3 summarizes the structure activity relationships of the current series toward Dyrk1A.

2.3.6. Predicted binding mode of **4b** to Dyrk1A

4b showed a remarkable boost of potency, which was attributable to the rather small cyclopropylamide moiety. To identify the binding mode of **4b** and the particular interactions of the cyclopropylamide extension, we performed docking simulations to the ATP binding pocket using the coordinates from PDB entry 3ANR (human Dyrk1A/harmine complex). While in theory, binding in two different orientations was conceivable, each with the pyridine nitrogens forming H-bonds with Lys188 and the Leu241 NH, only one of the binding orientations placed the key cyclopropylamide group close to a pocket side chain with which it could interact (Fig. 2A). In this binding model, a CH- π interaction between the hinge region residue Tyr243 and the cyclopropyl carbon in **4b** was observed. Furthermore, the cyclopropyl moiety showed packing against the Ile165 side chain, leading to additional hydrophobic interactions (Fig. 2B). Thus, the notable impact of the cyclopropyl may arise from a combination of CH- π and hydrophobic interactions with different side chains, leading to a synergistic enhancement of binding affinity. Such a cooperativity between different simultaneous interactions, also including hydrophobic interactions, is common in protein–ligand binding and has been experimentally confirmed [46]. Hence, if one of the specific interactions is weakened, the total binding affinity is over-proportionally affected. This might explain the low activity of **1b**; according to our docking model, the methyl at the amide function could also engage in CH- π interaction with Tyr243 but cannot reach Ile165 (see Fig. S1, Supplementary Information).

2.3.7. Selectivity against Dyrk1B and other selected kinases

The selectivity of all new compounds was initially evaluated against Dyrk1B, the isoform most closely related to Dyrk1A, by screening at 250 nM, as shown in Tables 1 and 2. All of the new potent compounds were clearly more active against Dyrk1A, similar to what we observed with the benzamide and benzylamide derivatives [44]. The most potent cycloalkylamide derivatives of bispyridyl thiophene, **4b** and **5b**, showed selectivity factors (Dyrk1A over -1B) of approximately 24- and 4-fold, respectively. While the pyrazole analogue **15** also exhibited a significant 8-fold selectivity toward Dyrk1A, this was lost with the N1-alkylated congeners (see above). Altogether, **4b** possessed the greatest selectivity for Dyrk1A in the present series, nearly approximating the 27 fold selectivity observed with the previous 4-fluorobenzyl amide derivative **II** (depicted in Fig. 1). To further examine the selectivity of **4b**, it was additionally tested against a panel of kinases (Table 3) which are supposed to have structurally similar ATP

Table 3
Selectivity profiling of compound **4b**.

| kinase | % Inhibition at 1.25 μ M ^a (IC ₅₀) ^b |
|-----------|--|
| CDK5/p25 | 1 |
| Clk1 | n.d. (270 nM) |
| Clk2 | 21 |
| CK1 delta | 4 |
| Dyrk1A | 89 (3.2 nM) |
| Haspin | 72 (76.3 nM) |
| HIPK1 | 1 |
| MLCK2 | 12.1 |
| TRKB | 8 |
| PIM1 | n.i. |
| SRPK1 | 2 |
| STK17A | 51.3 |

^a The screening list was especially composed to include all kinases that were frequently reported as off-targets for diverse chemical classes of Dyrk inhibitors [30,43,54–58]. Screenings were performed as a service at Thermo Fisher Scientific at an ATP concentration of 100 μ M n. i., no inhibition. n. d. not determined. Data represent mean values of duplicates that differed by less than 11%.

^b IC₅₀ value was determined for inhibition values > 60% at an ATP concentration of 15 μ M.

binding pockets and were frequently reported to show cross reactivity with diverse Dyrk1A inhibitors. As can be seen in Tables 3, **4b** displayed a remarkable selectivity in this crucial selection of kinases, ranking **4b** among the most selective Dyrk1A inhibitors published so far. Even haspin, a kinase which was still slightly co-inhibited by the previous compound **II**, was 24 times less strongly inhibited by **4b** than the target Dyrk1A.

How was the selectivity over the most closely related isoform Dyrk1B achieved?

Despite the high sequence similarity between Dyrk1A and Dyrk1B, our most potent compound **4b** showed a remarkable 24-fold selectivity towards Dyrk1A. Indeed, the ATP binding sites of two closely related homologues differ only by a single amino acid (Met240 in Dyrk1A corresponds to Leu192 in Dyrk1B). Our docking model gave a hint on how this difference might translate into reduced affinity to Dyrk1B. Although the Met240 side chain in Dyrk1A is not directly facing the ATP binding pocket, it could be attracted by a hydrophobic patch created or enhanced upon binding of the inhibitor, thereby engaging in van der Waals and hydrophobic interactions with the pyridine ring in **4b** which is H-bonded to Leu241. The latter interactions could possibly contribute to anchoring the pyridine ring at this position in Dyrk1A, and might explain, at least partially, the lower potency of **4b** against Dyrk1B, where the van der Waals interaction surface to the corresponding Leu192 is considerably smaller (see Fig. 2B). Concomitantly, the essential H-bond of the pyridine N to the hinge region NH might be less effectively shielded from water molecules in Dyrk1B. Furthermore, attractive interactions between aliphatic sulfur and pyridine

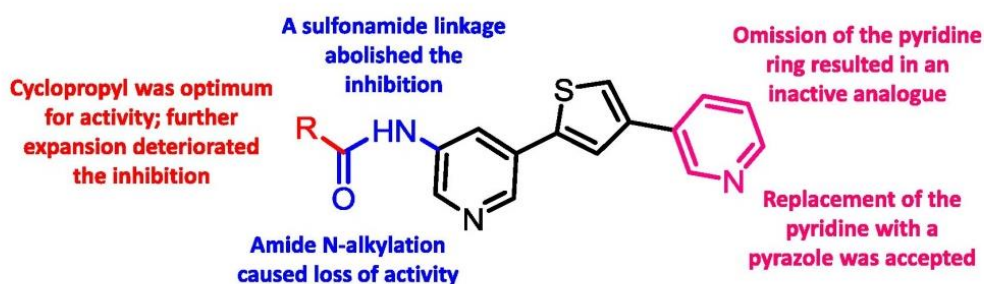


Fig. 3. Summary of the structure activity relationship for Dyrk1A inhibition.

nitrogen are well documented [47] and might play a role with Dyrk1A, but would be absent with Dyrk1B.

2.3.8. Inhibition of Dyrk1A in HeLa cells

To evaluate the potency of **4b** against Dyrk1A in intact cells, we analyzed the effects on the intracellular phosphorylation of the splicing factor 3b1 (SF3b1) using western blot analysis (Fig. 4). The phosphorylation of Thr434 on SF3b1 was previously shown to be solely dependent on Dyrk1A activity in HeLa cells [25]. The inactive analogue **9** served as a negative control. In this assay, treatment of HeLa cells with **4b** reduced the pT343-signal in a concentration-dependent manner with an IC₅₀ value of 43 nM (Fig. 4). These results were in good agreement with the strong Dyrk1A inhibition observed in the cell free assay.

In parallel, we assessed the potential cytotoxicity of our most potent compound **4b** with the same cell line. As can be seen in Table 4, our test compounds showed minimal cytotoxicity on HeLa cells up to a concentration of 3 μ M, which ensures the safety of our inhibitor in concentrations that fully inhibit Dyrk1A in cells.

2.4. Evaluation of CNS drug like properties

Since the major indication for Dyrk1A inhibitors is the treatment of neurodegenerative diseases, it was straightforward to assess the ability of our novel analogues to cross the BBB. A set of physicochemical properties has been previously reported in literature to be associated with high probability of CNS penetration [45]. CNS-active drug candidates are assumed to have definite attributes exemplified in molecular weight: 181–427, logP: 0.4–5.1 (median: 2.8) [45], HBA: 2–3, HBD: 0–1, and TPSA (topological polar surface area) < 76 Å² [48]. Accordingly, we calculated different physicochemical parameters using ACD/Labs software for our most potent inhibitors (**4b** and **15b**) to estimate the CNS drug-likeness of the current series (Table 5). Most of the calculated parameters for both inhibitors were in good agreement with the ideal ranges for brain penetration as reported in literature. In comparison to the analogue from the previous series, **II**, Compounds **4b** and **15** showed more favourable characteristics, such as reduced logP and molecular weight, thus increasing the likeliness to penetrate the BBB. With respect to the TPSA values which exceeded the limit of 76 Å², it should be mentioned that this depends on whether the thiophene sulphur is included in the calculation or not. Sulphur actually shows little polarity in the aromatic ring system, and thiophene is therefore often employed as bioisosteric replacement for benzene. Without counting the thiophene sulphur, the TPSA values for **4b**

Table 4
Effect of **1b** and **4b** on HeLa cell growth.

| | 1 μ M | 3 μ M | 10 μ M |
|----------------------------|------------|-------------|------------|
| 4b | 98 \pm 2 | 95 \pm 4 | 83 \pm 3 |
| 1b | 99 | 102 \pm 3 | 98 \pm 3 |
| Staurosporine ^a | 33 \pm 4 | | |

Values denote the viability of treated HeLa cells is given in percent relative to control cells treated with vehicle (means of two separate experiments with duplicate measurements \pm S.D.).

^a Staurosporine is a known inducer of apoptosis and served as a positive control.

Table 5
Calculated physicochemical properties of the most potent compounds **4b** and **15**.

| Cpd.No. | MW [gm/mol] | logP | TPSA [Å ²] | TPSA [Å ²] ^b | HBD | HBA |
|------------------------|-------------|------|------------------------|-------------------------------------|-----|-----|
| 4b | 321.40 | 2.69 | 83.1 | 54.9 | 1 | 3 |
| 15 | 310.38 | 2.6 | 98.9 | 70.7 | 2 | 3 |
| C29^a | 244.34 | 2.48 | 82.3 | 25.8 | 0 | 2 |

^a C29 values are shown for comparison (taken from Ref. [43]).

^b Sulphur was not considered for the calculation of TPSA. Ideal ranges for CNS active drugs: MW: 181–427 g/mol, logP 0.4–5.1 (median: 2.8) [45], TPSA < 76 Å², HBD: 0–1; HBA: 2–3 [48].

and **15** are 54.9 and 70.7 Å², respectively.

Interestingly, searching the literature for structurally similar compounds that had shown high brain penetration *in vivo*, we found a series of pyridine-containing glutamate receptor antagonists, e. g., 2-[2-[3-(pyridin-3-yloxy)phenyl]-2H-tetrazol-5-yl]pyridine [49], that even showed a larger polar surface due to the central tetrazole core. Altogether, our assessment suggested a high probability of CNS penetration for our most potent compounds **4b** and **15**.

2.5. Evaluation of metabolic stability

To further assess whether **4b** and **15** are suitable for *in vivo* studies, the phase I and phase II metabolic stability were measured using human hepatic liver S9 fractions. A definite set of samples were taken at defined time points, and the remaining percentage of parent compound was determined by LC-MS/MS. The calculated half-life times almost reached 2.5 h for **4b** and **15** (Table 6), indicating a high metabolic stability, which exceeded that of the previous benzamide-extended compound **II** (half-life against human S9 fraction: 118 min [44], tested in parallel).

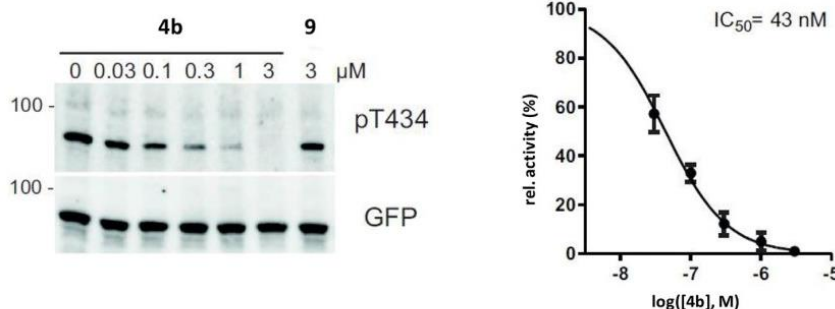


Fig. 4. Inhibition of SF3b1 phosphorylation by Dyrk1A inhibition in HeLa cells using **4b**. HeLa cells expressing GFP-SF3b1-NT were treated with the indicated compounds for 18 h at the shown concentrations. Phosphorylation of SF3b1 was quantitated by immunoblotting with pT434 antibody (left panels). Compound **9** from present work was used as a negative control as it did not inhibit Dyrk1A in the primary kinase screening. Quantitative evaluation of the results was performed to calculate the indicated IC₅₀ which was deduced from the dose-response curve fitted to the results of three experiments (means \pm SEM). All data were standardized to the level of phosphorylation in cells untreated with inhibitors.

Table 6
Metabolic stability of **4b** and **15** against human S9 fraction.^a

| Cpd No. | Half-life [min] |
|---------------------------|-----------------|
| 4b | 144 |
| 15 | 147 |
| Testosterone ^b | 8.5 |

^a 10 mg/mL, NADP⁺ regenerating system, MgCl₂, UDPGA, PAPS, [inhibitor] = 0.3 μM, incubation at 37 °C, samples taken at 0, 15, 30, 60, 90 and 120 min, determination of the parent compound by LC-MS/MS.

^b Included as a positive control for a rapidly metabolized compound.

3. Conclusions

We developed a novel Dyrk1A inhibitor series of amide-functionalized bispyridyl thiophenes carrying different alkyl, cycloalkyl and polar side chains. In this series, the cyclopropyl amide in compound **4b** was identified as a key modification, which led to an enhancement of several essential properties. Firstly, **4b** exhibited the most potent Dyrk1A inhibition with an IC₅₀ of 3.2 nM. In addition, the cyclopropyl amide modification effected a significant increase in selectivity over closely related kinases including haspin (selectivity factor: 24), which was often found to be co-inhibited even by some of the most selective Dyrk1A inhibitors, such as TG003 and harmine [50,51]. Of note, the benzylamide-modified previous inhibitor **II** had only achieved a moderate 2.5 fold selectivity over haspin [44]. The cyclopropylamide modification did not only increase potency and selectivity, but moreover, it also enhanced the metabolic stability against human liver S9 fractions, leading to a half-life of almost 2.5 h.

As anticipated by the high cell free potency, **4b** inhibited Dyrk1A in HeLa cells with an IC₅₀ of only 43 nM. This cellular potency, in combination with the high selectivity, low cytotoxicity and high metabolic stability render **4b** a promising candidate for *in vivo* studies using models of neurodegenerative diseases.

4. Experimental section

4.1. Chemistry

Solvents and reagents were obtained from commercial suppliers and used as received. Melting points were determined on a Stuart SMP3 melting point apparatus. All final compounds had a percentage purity of at least 95%, and this could be verified by means of HPLC coupled with mass spectrometry. Mass spectra (HPLC–ESIMS) were obtained using a TSQ quantum (Thermo Electron Corp.) instrument prepared with a triple quadrupole mass detector (Thermo Finnigan) and an ESI source. All samples were injected using an autosampler (Surveyor, Thermo Finnigan) by an injection volume of 10 μL. The MS detection was determined using a source CID of 10 V and carried out at a spray voltage of 4.2 kV, a nitrogen sheath gas pressure of 4.0×10^5 Pa, a capillary temperature of 400 °C, a capillary voltage of 35 V, and an auxiliary gas pressure of 1.0×10^5 Pa. The stationary phase used was an RP C18 NUCLEODUR 100–3 (125 mm × 3 mm) column (Macherey & Nagel). The solvent system consisted of water containing 0.1% TFA (A) and 0.1% TFA in acetonitrile (B). The HPLC method used a flow rate of 400 μL/min. The percentage of B started at 5%, was increased up to 100% during 7 min, was kept at 100% for 2 min, and was flushed back to 5% in 2 min and was kept at 5% for 2 min. A Bruker DRX 500 spectrometer was used to obtain the ¹H NMR and ¹³C NMR spectra. The chemical shifts are referenced to the residual protonated solvent signals.

4.1.1. General synthetic procedures and experimental details

4.1.1.1. Procedure A, procedure for synthesis of compounds A–B, H. A mixture of 5 mmol of the 3-amino-5-bromo pyridine and 1.96 g (20 mmol) of potassium acetate and 0.18 g (0.25 mmol) of Pd(dppf)Cl₂ and 5.08 g (20 mmol) of bis(pinacolato)diboron in dioxane was heated to reflux under argon for 2 h to yield compounds **A**. The mixture was left to attain room temperature and then filtered under vacuum. Without further purification, a reaction flask containing the filtrate was charged with 6.5 g (20 mmol) of Cs₂CO₃, 0.29 g (0.25 mmol) of palladium-tetrakis(triphenylphosphine) and 6 mmol of the appropriate bromothiophene together with 30% water in a Suzuki coupling reaction. The reaction was left to reflux under argon for 3.5 h. The mixture was concentrated *in vacuo*. The residue was partitioned between 150 mLs ethyl acetate and 50 mLs brine solution and then the aqueous layer was re-extracted using 3 portions of 100 mLs ethyl acetate. The organic layers were collected and the volume was reduced under reduced pressure. Afterwards the product was purified by CC to yield compounds **B, H**.

4.1.1.2. Procedure B, general procedure for the amide synthesis of compounds 1a, 3a – 8a, E, 14. 0.18 g (0.7 mmol) of compound **D** was added to a mixture of 0.4 g (1.05 mmol) of HBTU (in compounds **1a, 3a–7a, E, 14**) or 0.4 g (1.05 mmol) HATU (in compounds **8a**) and 0.36 g (1.05 mmol) of DIPEA together with 2.1 mmol of the appropriate acid in DCM. The mixture was left to stir at room temperature overnight, and afterwards, the solvent was evaporated *in vacuo* and the product was purified by CC.

4.1.1.3. Procedure C, general procedure for amide alkylation (C–D). 0.14 g (3.5 mmol) KH was added gradually to stirred solution of 0.23 g (0.35 mmol) of compound **4a** in 2 mLs DMF under ice cooling. The reaction mixture was left to stir for 1 h and then 1 equiv of the appropriate alkyl iodide was added to the reaction vessel and the mixture was left to stir for 2 days at room temperature. The mixture was partitioned between aqueous brine solution and ethyl acetate layers and the aqueous layer was extracted by three 50-mL portions of ethyl acetate. The organic layers were collected and the solvent was removed under vacuum, this was followed by purification of the desired products using CC.

4.1.1.4. Procedure D, general procedure for synthesis of compounds F – G. 0.27 g (0.7 mmol) of compound **E** was added to a solution of 7 mmol of the appropriate alicyclic amine dissolved in methanol. The reaction mixture was heated to reflux for 1 h. Afterwards, the solvent was removed *in vacuo* and the produced residue was purified using CC.

4.1.1.5. Procedure E, general procedure for synthesis of compounds 1b–8b, 9–10, 12–13, 15–19. The bromo derivative was added to a suspension of 4 equiv of Na₂CO₃ and 5 mmol% of Pd(dppf)Cl₂ in dioxane/water mixture. This was followed by the addition of the pyridine/pyrazole boronic acid derivative. The reaction was heated to reflux for 2 h under argon atmosphere. The solvent was removed *in vacuo*. Small amount of brine solution was added and extraction was done using ethyl acetate (3 × 50 mLs). The ethyl acetate portions were collected and the volume was reduced *in vacuo*. Afterwards the product was purified by CC.

4.1.1.6. Procedure F, general procedure for pyrazole alkylation (compounds I, J, K). To a solution of 4-pyrazoleboronic acid pinacol ester dissolved in acetone, 2 equiv of Cs₂CO₃ and 2 equiv of the appropriate alkyl iodide were added. The reaction mixture was left to reflux overnight. The solvent was evaporated *in vacuo* and the product entered the following reaction without further purification.

4.1.1.7. 5-(4-Bromothiophen-2-yl)pyridin-3-amine (B). The compound was synthesized according to Procedure A: yield 80%. The product was purified by CC (ethyl acetate); ^1H NMR (500 MHz, DMSO) δ 8.08 (d, J = 2.0 Hz, 1H), 7.91 (d, J = 2.5 Hz, 1H), 7.70 (d, J = 1.4 Hz, 1H), 7.51 (d, J = 1.5 Hz, 1H), 7.16–7.05 (m, 1H), 5.50 (s, 2H); ^{13}C NMR (126 MHz, DMSO) δ 144.98, 142.31, 136.28, 133.61, 128.34, 126.16, 123.47, 115.68, 109.89; MS (ESI) m/z = 254.82 ($\text{M} + \text{H}$) $^+$

4.1.1.8. N-(5-(4-bromothiophen-2-yl)pyridin-3-yl)-N-methylcyclopropanecarboxamide (C). The compound was synthesized according to Procedure C using methyl iodide: yield 83%. The product was purified by CC (DCM/MeOH 100:1.5); ^1H NMR (500 MHz, DMSO) δ 8.86 (s, 1H), 8.57 (d, J = 1.9 Hz, 1H), 8.19 (s, 1H), 7.83 (d, J = 1.4 Hz, 1H), 7.81 (d, J = 1.3 Hz, 1H), 3.34 (s, 3H), 1.54–1.37 (m, 1H), 0.86–0.82 (m, 2H), 0.69 (t, J = 4.3 Hz, 2H); ^{13}C NMR (126 MHz, DMSO) δ 172.32, 147.61, 144.17, 140.69, 140.12, 130.89, 129.22, 127.99, 124.84, 110.20, 36.93, 12.39, 8.24; MS (ESI) m/z = 336.91 ($\text{M} + \text{H}$) $^+$

4.1.1.9. N-(5-(4-bromothiophen-2-yl)pyridin-3-yl)-N-ethylcyclopropanecarboxamide (D). The compound was synthesized according to Procedure C using ethyl iodide: yield 79%. The product was purified by CC (DCM/MeOH 100:1); ^1H NMR (500 MHz, DMSO) δ 8.88 (s, 1H), 8.51 (s, 1H), 8.15 (s, 1H), 7.83 (t, J = 1.8 Hz, 2H), 3.75 (s, 2H), 1.25–1.13 (m, 1H), 1.04 (t, 3H), 0.88–0.77 (m, 2H), 0.66 (s, 2H); ^{13}C NMR (126 MHz, DMSO) δ 171.69, 148.59, 144.64, 140.00, 139.00, 131.89, 129.40, 128.11, 124.86, 110.22, 43.53, 12.98, 12.62, 8.17; MS (ESI) m/z = 350.89 ($\text{M} + \text{H}$) $^+$

4.1.1.10. N-(5-(4-bromothiophen-2-yl)pyridin-3-yl)acetamide (1a). The compound was synthesized according to procedure B using acetic acid: yield 98%. The product was purified by CC (ethyl acetate); ^1H NMR (500 MHz, DMSO) δ 10.30 (s, 1H), 8.64 (dd, J = 3.1, 2.4 Hz, 2H), 8.29 (t, J = 2.2 Hz, 1H), 7.79 (d, J = 1.4 Hz, 1H), 7.66 (d, J = 1.4 Hz, 1H), 2.10 (s, 3H); ^{13}C NMR (126 MHz, DMSO) δ 169.23, 141.17, 140.57, 140.02, 136.16, 128.35, 127.07, 124.41, 121.90, 110.23, 23.95; MS (ESI) m/z = 297.95 ($\text{M} + \text{H}$) $^+$

4.1.1.11. N-(5-(4-bromothiophen-2-yl)pyridin-3-yl)methanesulfonamide (2a). The title compound was synthesized through adding 1.4 mmol of the methanesulfonyl chloride to a stirred solution of 0.18 g (0.7 mmol) of compound B dissolved in pyridine. The reaction was heated to 60 °C and left overnight. This was followed by the removal of solvent *in vacuo*: yield 69.1%. The product was purified by CC (ethyl acetate); ^1H NMR (500 MHz, DMSO) δ 10.16 (s, 1H), 8.68 (d, J = 2.0 Hz, 1H), 8.39 (d, J = 2.4 Hz, 1H), 7.81 (d, J = 1.4 Hz, 1H), 7.77 (t, J = 2.2 Hz, 1H), 7.71 (d, J = 1.5 Hz, 1H), 3.13 (s, 3H); ^{13}C NMR (126 MHz, DMSO) δ 141.43, 140.71, 135.35, 133.06, 128.82, 127.53, 124.65, 122.78, 110.19, 40.11; MS (ESI) m/z = 331.69 (M) $^+$

4.1.1.12. N-(5-(4-bromothiophen-2-yl)pyridin-3-yl)propionamide (3a). The compound was synthesized according to procedure B using propionic acid: yield 64%. The product was purified by CC (ethyl acetate/petroleum ether 8:2); ^1H NMR (500 MHz, DMSO) δ 10.36 (s, 1H), 8.69 (s, 1H), 8.63 (s, 1H), 8.34 (t, J = 2.2 Hz, 1H), 7.79 (d, J = 1.4 Hz, 1H), 7.66 (d, J = 1.4 Hz, 1H), 2.39 (q, J = 7.5 Hz, 2H), 1.10 (t, J = 7.5 Hz, 3H). MS (ESI) m/z = 310.99 ($\text{M} + \text{H}$) $^+$

4.1.1.13. N-(5-(4-bromothiophen-2-yl)pyridin-3-yl)cyclopropanecarboxamide (4a). The compound was synthesized according to procedure B using cyclopropanecarboxylic acid: yield 94%. The product was purified by CC (ethyl acetate/petroleum ether 6:4); ^1H NMR (500 MHz, DMSO) δ 10.57 (d, J = 1.2 Hz, 1H), 8.66 (d,

J = 2.3 Hz, 1H), 8.63 (d, J = 2.1 Hz, 1H), 8.32 (t, J = 2.2 Hz, 1H), 7.79 (d, J = 1.4 Hz, 1H), 7.66 (d, J = 1.4 Hz, 1H), 1.80 (dd, J = 12.4, 6.3 Hz, 1H), 1.46 (m, J = 21.2, 15.9, 10.8, 6.4 Hz, 2H), 1.30–1.11 (m, 2H); ^{13}C NMR (126 MHz, DMSO) δ 175.51, 141.14, 140.41, 139.93, 136.13, 128.31, 127.02, 124.33, 121.86, 110.16, 14.56, 7.65; MS (ESI) m/z = 322.93 ($\text{M} + \text{H}$) $^+$

4.1.1.14. N-(5-(4-bromothiophen-2-yl)pyridin-3-yl)cyclobutanecarboxamide (5a). The compound was synthesized according to procedure B using cyclobutanecarboxylic acid: yield 94.6%. The product was purified by CC (ethyl acetate/petroleum ether 7:3); ^1H NMR (400 MHz, DMSO) δ 10.15 (s, 1H), 8.69 (d, J = 1.9 Hz, 1H), 8.63 (d, J = 1.9 Hz, 1H), 8.35 (s, 1H), 7.79 (d, J = 1.1 Hz, 1H), 7.66 (d, J = 1.2 Hz, 1H), 3.09–2.99 (m, 1H), 1.10–1.00 (m, 2H), 0.97 (td, J = 7.0, 1.7 Hz, 2H), 0.82 (dd, J = 15.2, 7.5 Hz, 2H); ^{13}C NMR (101 MHz, DMSO) δ 173.82, 141.21, 140.44, 140.13, 136.26, 128.30, 127.04, 121.99, 116.94, 110.22, 24.59, 17.73; MS (ESI) m/z = 337 ($\text{M} + \text{H}$) $^+$

4.1.1.15. N-(5-(4-bromothiophen-2-yl)pyridin-3-yl)cyclohexanecarboxamide (6a). The compound was synthesized according to procedure B using cyclohexanecarboxylic acid: yield 51%. The product was purified by CC (ethyl acetate/petroleum ether 6:4); ^1H NMR (500 MHz, DMSO) δ 10.17 (s, 1H), 8.67 (d, J = 2.3 Hz, 1H), 8.62 (d, J = 2.1 Hz, 1H), 8.35 (t, J = 2.2 Hz, 1H), 7.78 (d, J = 1.4 Hz, 1H), 7.65 (d, J = 1.5 Hz, 1H), 2.36 (ddd, J = 11.6, 8.1, 3.5 Hz, 1H), 1.83 (d, J = 11.8 Hz, 2H), 1.80–1.73 (m, 2H), 1.41 (m, J = 12.4, 2.9 Hz, 2H), 1.34–1.11 (m, 4H); ^{13}C NMR (126 MHz, DMSO) δ 175.14, 141.21, 140.40, 140.07, 136.33, 128.28, 127.01, 124.34, 121.88, 110.19, 44.82, 29.01, 25.36, 25.16; MS (ESI) m/z = 364.97 ($\text{M} + \text{H}$) $^+$

4.1.1.16. tert-Butyl 3-((5-(4-bromothiophen-2-yl)pyridin-3-yl)carbamoyl)pyrrolidine-1-carboxylate (7a). The compound was synthesized according to procedure B using *N*-Boc-pyrrolidine-3-carboxylic acid: yield 88%. The product was purified by CC (DCM/MeOH 100:3); ^1H NMR (500 MHz, DMSO) δ 10.40 (s, 1H), 8.66 (dd, J = 6.6, 2.2 Hz, 2H), 8.32 (t, J = 2.2 Hz, 1H), 7.79 (d, J = 1.4 Hz, 1H), 7.67 (d, J = 1.4 Hz, 1H), 3.03 (dd, J = 16.4, 8.6 Hz, 2H), 2.13 (d, J = 2.9 Hz, 1H), 2.03 (s, 2H), 2.00–1.90 (m, 2H), 1.41 (s, 9H); ^{13}C NMR (126 MHz, DMSO) δ 153.35, 141.06, 140.77, 140.20, 135.94, 132.94, 128.34, 127.11, 124.41, 122.19, 110.21, 78.34, 54.89, 53.55, 41.81, 28.16, 28.14; MS (ESI) m/z = 453.84 ($\text{M} + \text{H}$) $^+$

4.1.1.17. N-(5-(4-bromothiophen-2-yl)pyridin-3-yl)-2-(1H-tetrazol-5-yl)acetamide (8a). The compound was synthesized according to procedure B using 1H-Tetrazole-5-acetic acid: yield 97%. The product was purified by extraction with 2 M NaOH and ethyl acetate (3 \times 50 mLs). The aqueous layer was normalised using 1 M HCl and dried *in vacuo*; ^1H NMR (500 MHz, DMSO) δ 10.78 (s, 1H), 8.68 (d, J = 2.3 Hz, 1H), 8.61 (d, J = 2.1 Hz, 1H), 8.33 (t, J = 2.2 Hz, 1H), 7.77 (d, J = 1.4 Hz, 1H), 7.64 (d, J = 1.4 Hz, 1H), 3.77 (s, 2H), 3.42 (s, 1H); ^{13}C NMR (126 MHz, DMSO) δ 169.31, 155.55, 141.19, 140.54, 140.13, 136.22, 128.34, 127.08, 124.39, 121.97, 110.19, 34.83; MS (ESI) m/z = 364.90 ($\text{M} + \text{H}$) $^+$

4.1.1.18. 2-(Piperidin-1-yl)-N-(5-(4-(pyridin-3-yl)thiophen-2-yl)pyridin-3-yl)acetamide (F). The compound was synthesized according to procedure D using piperidine: yield 83.8%. The product was purified by CC (ethyl acetate/MeOH 100:1); ^1H NMR (500 MHz, DMSO) δ 9.81 (s, 1H), 8.61 (d, J = 2.3 Hz, 1H), 8.46 (d, J = 2.1 Hz, 1H), 8.16 (t, J = 2.2 Hz, 1H), 7.61 (d, J = 1.4 Hz, 1H), 7.49 (d, J = 1.4 Hz, 1H), 2.94 (s, 2H), 2.35–2.30 (m, 4H), 1.39 (m, J = 11.1, 5.6 Hz, 4H), 1.22 (d, J = 4.2 Hz, 2H); ^{13}C NMR (126 MHz, DMSO) δ 164.59, 141.07, 140.84, 140.67, 135.52, 128.31, 127.14, 124.40, 122.64, 110.17, 62.55, 54.11, 25.32, 23.51; MS (ESI) = 379.96 ($\text{M} + \text{H}$) $^+$

4.1.1.19. *N*-(5-(4-bromothiophen-2-yl)pyridin-3-yl)-2-morpholinoacetamide (G**).** The compound was synthesized according to procedure **D** using morpholine: yield 83.3%. The product was purified by CC (ethyl acetate/MeOH 100:3); ^1H NMR (500 MHz, DMSO) δ 10.07 (s, 1H), 8.78 (d, $J = 2.2$ Hz, 1H), 8.66 (d, $J = 2.1$ Hz, 1H), 8.34 (t, $J = 2.2$ Hz, 1H), 7.79 (d, $J = 1.4$ Hz, 1H), 7.68 (d, $J = 1.4$ Hz, 1H), 3.69–3.62 (m, 4H), 3.20 (d, $J = 15.9$ Hz, 2H), 2.52 (m, 4H); ^{13}C NMR (126 MHz, DMSO) δ 169.13, 164.60, 141.06, 140.91, 135.51, 128.31, 127.14, 124.42, 122.73, 110.19, 66.02, 61.95, 53.18; MS (ESI) $m/z = 383.86$ (M + H) $^+$

4.1.1.20. 5-(Thiophen-2-yl)pyridin-3-amine (H**).** The compound was synthesized according to Procedure **A** using 2-bromothiophene: yield 89%. The product was purified by CC (ethyl acetate/petroleum ether 9:1); ^1H NMR (500 MHz, DMSO) δ 8.07 (d, $J = 1.7$ Hz, 1H), 7.87 (d, $J = 2.3$ Hz, 1H), 7.57 (d, $J = 5.0$ Hz, 1H), 7.46 (d, $J = 3.2$ Hz, 1H), 7.20–7.09 (m, 2H), 5.47 (s, 2H); ^{13}C NMR (126 MHz, DMSO) δ 144.95, 140.69, 135.61, 133.80, 129.50, 128.47, 126.03, 124.03, 115.94.

4.1.1.21. *N*-(5-(4-(pyridin-3-yl)thiophen-2-yl)pyridin-3-yl)acetamide (1b**).** The compound was synthesized according to procedure **E** to give a brown solid: yield 13.8%. The product was purified by CC (DCM/MeOH/TEA 100:5:1); mp 151.3–153.2 °C; ^1H NMR (500 MHz, DMSO) δ 10.50 (s, 1H), 9.06 (d, $J = 1.7$ Hz, 1H), 8.74 (d, $J = 1.8$ Hz, 1H), 8.69 (d, $J = 2.0$ Hz, 1H), 8.53 (d, $J = 3.6$ Hz, 1H), 8.38 (s, 1H), 8.19 (dd, $J = 8.3, 4.6$ Hz, 2H), 8.15 (s, 1H), 7.47 (dd, $J = 7.9, 4.8$ Hz, 1H), 2.11 (s, 3H); ^{13}C NMR (126 MHz, DMSO) δ 169.25, 148.41, 147.21, 140.87, 140.64, 139.70, 139.39, 136.23, 133.31, 130.43, 129.27, 123.94, 123.68, 122.93, 122.09, 23.93; MS (ESI) $m/z = 296.02$ (M + H) $^+$

4.1.1.22. *N*-(5-(4-(pyridin-3-yl)thiophen-2-yl)pyridin-3-yl)methanesulfonamide (2b**).** The compound was synthesized according to procedure **E** to give a white solid: yield 45.4%. The product was purified by extraction with water and ethyl acetate (3 \times 50 mLs) the organic layers were collected and the solvent was removed *in vacuo*; mp > 280 °C; ^1H NMR (500 MHz, DMSO) δ 10.37 (s, 1H), 9.06 (s, 1H), 8.76 (d, $J = 1.9$ Hz, 1H), 8.53 (d, $J = 3.4$ Hz, 1H), 8.43 (d, $J = 2.1$ Hz, 1H), 8.21 (s, 2H), 8.17 (s, 1H), 7.89 (s, 1H), 7.47 (dd, $J = 7.9, 4.6$ Hz, 1H), 3.11 (s, 3H); ^{13}C NMR (126 MHz, DMSO) δ 148.40, 147.19, 141.33, 140.68, 140.40, 139.53, 139.36, 135.86, 133.30, 130.37, 129.70, 124.06, 123.90, 123.17; MS (ESI) $m/z = 331.79$ (M + H) $^+$

4.1.1.23. *N*-(5-(4-(pyridin-3-yl)thiophen-2-yl)pyridin-3-yl)propionamide (3b**).** The compound was synthesized according to procedure **E** to give a beige solid: yield 9.1%. The product was purified by CC (DCM/MeOH 100:5); mp 211.6–212.4 °C; ^1H NMR (500 MHz, DMSO) δ 10.21 (s, 1H), 9.06 (d, $J = 1.7$ Hz, 1H), 8.73 (d, $J = 2.1$ Hz, 1H), 8.67 (d, $J = 2.2$ Hz, 1H), 8.53 (dd, $J = 4.7, 1.5$ Hz, 1H), 8.39 (t, $J = 2.2$ Hz, 1H), 8.19 (ddd, $J = 8.0, 2.3, 1.6$ Hz, 1H), 8.17 (d, $J = 1.5$ Hz, 1H), 8.13 (d, $J = 1.4$ Hz, 1H), 7.47 (ddd, $J = 7.9, 4.8, 0.8$ Hz, 1H), 2.39 (q, $J = 7.5$ Hz, 2H), 1.12 (t, $J = 7.5$ Hz, 3H); ^{13}C NMR (126 MHz, DMSO) δ 172.79, 148.34, 147.17, 140.85, 140.53, 139.68, 139.36, 136.16, 133.24, 130.39, 129.23, 123.85, 123.61, 122.82, 122.07, 29.39, 9.37; MS (ESI) $m/z = 310.08$ (M + H) $^+$

4.1.1.24. *N*-(5-(4-(pyridin-3-yl)thiophen-2-yl)pyridin-3-yl)cyclopropanecarboxamide (4b**).** The compound was synthesized according to procedure **E** to give a brick red solid: yield 8.5%. The product was purified by CC (DCM/MeOH 100:5); mp 194–195.8 °C; ^1H NMR (500 MHz, DMSO) δ 10.58 (s, 1H), 9.06 (d, $J = 1.9$ Hz, 1H), 8.69 (dd, $J = 37.5, 2.1$ Hz, 2H), 8.52 (dd, $J = 4.7, 1.4$ Hz, 1H), 8.39 (t, $J = 2.2$ Hz, 1H), 8.23–8.16 (m, 2H), 8.13 (d, $J = 1.4$ Hz, 1H), 7.47 (dd, $J = 7.9, 4.8$ Hz, 1H), 1.85–1.78 (m, 1H), 0.95–0.79 (m, 4H); ^{13}C NMR (126 MHz, DMSO) δ 172.53, 148.35, 147.15, 140.82, 140.52, 139.57,

139.35, 136.13, 133.24, 130.38, 129.26, 123.87, 123.63, 122.85, 122.03, 14.56, 7.56; MS (ESI) $m/z = 321.93$ (M + H) $^+$

4.1.1.25. *N*-(5-(4-(pyridin-3-yl)thiophen-2-yl)pyridin-3-yl)cyclobutanecarboxamide (5b**).** The compound was synthesized according to procedure **E** to give an off-white solid: yield 17%. The product was purified by CC (DCM/MeOH 100:4); mp 213–214.2 °C; ^1H NMR (500 MHz, DMSO) δ 10.09 (s, 1H), 9.06 (s, 1H), 8.73 (s, 1H), 8.68 (s, 1H), 8.53 (d, $J = 4.0$ Hz, 1H), 8.41 (s, 1H), 8.20 (d, $J = 8.7$ Hz, 2H), 8.14 (s, 1H), 7.47 (dd, $J = 7.7, 4.7$ Hz, 1H), 3.31–3.22 (m, 1H), 2.32–2.19 (m, 2H), 2.14 (d, $J = 8.6$ Hz, 2H), 1.96 (dd, $J = 19.0, 9.3$ Hz, 1H), 1.83 (d, $J = 9.8$ Hz, 1H); ^{13}C NMR (126 MHz, DMSO) δ 173.76, 148.38, 147.20, 140.87, 140.57, 139.78, 139.38, 136.21, 133.27, 130.42, 129.24, 123.89, 123.65, 122.86, 122.16, 24.58, 17.71; MS (ESI) $m/z = 336.08$ (M + H) $^+$

4.1.1.26. *N*-(5-(4-(pyridin-3-yl)thiophen-2-yl)pyridin-3-yl)cyclohexanecarboxamide (6b**).** The compound was synthesized according to procedure **E** to give a beige solid: yield 14%. The product was purified by CC (DCM/MeOH 100:3); mp 182–184 °C; ^1H NMR (500 MHz, DMSO) δ 10.17 (s, 1H), 9.06 (s, 1H), 8.72 (s, 1H), 8.67 (s, 1H), 8.53 (d, $J = 3.7$ Hz, 1H), 8.42 (s, 1H), 8.23–8.15 (m, 2H), 8.13 (s, 1H), 7.53–7.42 (m, 1H), 2.38 (t, $J = 11.4$ Hz, 1H), 1.85 (d, $J = 12.2$ Hz, 2H), 1.77 (d, $J = 11.9$ Hz, 2H), 1.66 (d, $J = 12.0$ Hz, 1H), 1.43 (d, $J = 12.2$ Hz, 2H), 1.26 (dd, $J = 23.2, 10.8$ Hz, 2H), 1.22–1.16 (m, 1H); ^{13}C NMR (126 MHz, DMSO) δ 175.08, 148.33, 147.16, 140.87, 140.49, 139.70, 139.35, 136.30, 133.25, 130.40, 129.20, 123.86, 123.59, 122.82, 122.03, 44.79, 29.00, 25.35, 25.15; MS (ESI) $m/z = 364.03$ (M + H) $^+$

4.1.1.27. *tert*-Butyl 3-((5-(4-(pyridin-3-yl)thiophen-2-yl)pyridin-3-yl)carbamoyl)pyrrolidine-1-carboxylate (7b**).** The compound was synthesized according to procedure **E** to give a yellow semi-solid: yield 34%. The product was purified by CC (DCM/MeOH/TEA 100:4:1); ^1H NMR (500 MHz, DMSO) δ 10.49 (s, 1H), 9.08 (s, 1H), 8.73 (dd, $J = 32.1, 1.9$ Hz, 2H), 8.55 (d, $J = 3.5$ Hz, 1H), 8.41 (t, $J = 2.1$ Hz, 1H), 8.27–8.21 (m, 1H), 8.20 (d, $J = 1.4$ Hz, 1H), 8.16 (d, $J = 1.4$ Hz, 1H), 7.51 (dd, $J = 7.9, 4.8$ Hz, 1H), 3.54 (dd, $J = 20.8, 11.7$ Hz, 2H), 3.25–3.16 (m, 2H), 2.10 (dd, $J = 29.5, 14.7$ Hz, 2H), 1.41 (s, 9H), 1.23 (d, $J = 1.2$ Hz, 1H); ^{13}C NMR (126 MHz, DMSO) δ 177.88, 153.34, 147.97, 146.77, 140.80, 139.80, 139.22, 133.72, 130.57, 129.47, 129.15, 128.07, 124.07, 123.74, 123.10, 122.35, 78.38, 61.17, 45.66, 45.59, 28.20, 28.17; MS (ESI) $m/z = 451.35$ (M + H) $^+$

4.1.1.28. *N*-(5-(4-(pyridin-3-yl)thiophen-2-yl)pyridin-3-yl)-2-(1H-tetrazol-5-yl)acetamide (8b**).** The compound was synthesized according to procedure **E** to give an off-white solid: yield 55.4%. The product was purified by CC (DCM/MeOH/TEA 100:11:3); mp 119.2–122.7 °C; ^1H NMR (500 MHz, DMSO) δ 10.80 (s, 1H), 9.14–8.99 (m, 1H), 8.73 (d, $J = 2.1$ Hz, 1H), 8.69 (d, $J = 2.2$ Hz, 1H), 8.52 (dd, $J = 4.7, 1.6$ Hz, 1H), 8.40 (t, $J = 2.2$ Hz, 1H), 8.22–8.16 (m, 2H), 8.14 (d, $J = 1.4$ Hz, 1H), 7.50–7.43 (m, 1H), 5.32 (s, 1H), 3.86 (s, 2H); ^{13}C NMR (126 MHz, DMSO) δ 172.10, 168.73, 148.35, 147.19, 140.80, 140.73, 139.73, 139.37, 136.12, 133.28, 130.42, 129.27, 123.89, 123.71, 122.89, 122.10, 34.34; MS (ESI) $m/z = 364.02$ (M + H) $^+$

4.1.1.29. *N*-methyl-*N*-(5-(4-(pyridin-3-yl)thiophen-2-yl)pyridin-3-yl)cyclopropanecarboxamide (9**).** The compound was synthesized according to procedure **E** to give brown oil: yield 15.6%. The product was purified by CC (DCM/MeOH 100:2); mp 142–142.7 °C; ^1H NMR (500 MHz, DMSO) δ 9.07 (s, 1H), 8.93 (s, 1H), 8.57 (s, 1H), 8.53 (d, $J = 3.7$ Hz, 1H), 8.34 (s, 1H), 8.25 (s, 1H), 8.20–8.16 (m, 2H), 7.48 (dd, $J = 7.9, 4.8$ Hz, 1H), 3.31 (s, 3H), 1.22 (m, 1H), 0.89–0.84 (m, 2H), 0.70 (m, 2H); ^{13}C NMR (126 MHz, DMSO) δ 172.30, 149.12, 148.40, 147.76, 147.14, 140.71, 139.67, 139.28, 134.40, 133.18, 130.32, 124.67, 123.96, 123.89, 123.31, 36.97, 12.35, 8.20; MS (ESI) $m/z = 336.03$ (M + H) $^+$

4.1.1.30. *N*-ethyl-*N*-(5-(4-(pyridin-3-yl)thiophen-2-yl)pyridin-3-yl)cyclopropanecarboxamide (**10**). The compound was synthesized according to procedure **E** to give a beige solid: yield 21.2%. The product was purified by CC (DCM/MeOH 100:3); mp 140–142.2 °C; ¹H NMR (500 MHz, DMSO) δ 9.07 (d, *J* = 1.9 Hz, 1H), 8.94 (s, 1H), 8.58–8.44 (m, 2H), 8.36 (s, 1H), 8.24–8.19 (m, 2H), 8.18 (d, *J* = 1.3 Hz, 1H), 7.48 (dd, *J* = 7.8, 4.8 Hz, 1H), 3.78 (q, *J* = 6.3 Hz, 2H), 1.30 (m, 1H), 1.07 (t, *J* = 6.6 Hz, 3H), 0.88–0.81 (m, 2H), 0.67 (m, 2H); ¹³C NMR (126 MHz, DMSO) δ 171.81, 148.40, 148.17, 147.16, 144.66, 144.45, 139.55, 139.29, 139.02, 133.18, 131.82, 130.30, 124.79, 123.87, 123.32, 43.57, 12.99, 12.63, 8.15; MS (ESI) *m/z* = 350.05 (M + H)⁺

4.1.1.31. *N*-(5-(4-(pyridin-3-yl)thiophen-2-yl)pyridin-3-yl)pyrrolidine-3-carboxamide (**11**). The title compound was prepared by adding **compound 7b** to a mixture of TFA and DCM. The reaction mixture was stirred overnight at room temperature and then the solvent was removed *in vacuo* and purified by crystallization from ethanol to give yellow oil: yield 23.6%. ¹H NMR (500 MHz, MeOD) δ 8.97 (s, 1H), 8.66 (dd, *J* = 7.3, 1.8 Hz, 2H), 8.52 (d, *J* = 4.4 Hz, 1H), 8.47 (t, *J* = 2.2 Hz, 1H), 8.36–8.26 (m, 1H), 8.05 (s, 1H), 7.97 (dd, *J* = 3.7, 1.5 Hz, 2H), 7.61 (dd, *J* = 7.9, 5.1 Hz, 1H), 3.66 (dd, *J* = 11.7, 5.0 Hz, 1H), 3.49 (dd, *J* = 11.7, 7.7 Hz, 1H), 3.45–3.35 (m, 3H), 2.50–2.35 (m, 1H), 2.29 (m, *J* = 13.2, 5.9 Hz, 1H), 1.27 (dd, *J* = 14.8, 7.8 Hz, 1H); ¹³C NMR (126 MHz, MeOD) δ 173.24, 147.11, 146.14, 142.42, 142.07, 140.58, 140.04, 137.55, 137.47, 133.83, 132.00, 126.28, 125.31, 124.99, 124.79, 48.76, 46.56, 44.80, 30.38; MS (ESI) *m/z* = 350.93 (M + H)⁺

4.1.1.32. 2-(Piperidin-1-yl)-*N*-(5-(4-(pyridin-3-yl)thiophen-2-yl)pyridin-3-yl)acetamide (**12**). The compound was synthesized according to procedure **E** to give brick red oil: yield 17.5%. The product was purified by CC (DCM/MeOH 100:3); ¹H NMR (500 MHz, DMSO) δ 11.10 (s, 1H), 9.18 (s, 1H), 8.87 (s, 1H), 8.72 (s, 1H), 8.44 (d, *J* = 7.8 Hz, 1H), 8.37 (s, 1H), 8.27 (d, *J* = 8.0 Hz, 2H), 7.70 (s, 1H), 7.54 (d, *J* = 8.1 Hz, 1H), 4.20 (s, 2H), 3.51 (s, 2H), 3.09 (s, 2H), 1.80 (s, 4H), 1.70 (s, 1H), 1.40 (s, 1H); ¹³C NMR (126 MHz, DMSO) δ 163.87, 145.98, 144.77, 141.54, 140.51, 139.80, 138.44, 135.76, 130.95, 130.87, 128.49, 124.99, 124.05, 123.93, 122.75, 56.86, 53.09, 22.13, 20.97; MS (ESI) *m/z* = 379.09 (M + H)⁺

4.1.1.33. 2-Morpholino-*N*-(5-(4-(pyridin-3-yl)thiophen-2-yl)pyridin-3-yl)acetamide (**13**). The compound was synthesized according to procedure **E** to give a buff yellow solid: yield 7.7%. The product was purified by CC (DCM/MeOH 100:5); mp 174.3–175.8 °C; ¹H NMR (500 MHz, DMSO) δ 11.47 (s, 1H), 9.09 (d, *J* = 1.8 Hz, 1H), 8.81 (dd, *J* = 29.4, 2.0 Hz, 2H), 8.56 (dd, *J* = 4.8, 1.3 Hz, 1H), 8.42 (t, *J* = 2.0 Hz, 1H), 8.28 (d, *J* = 8.2 Hz, 1H), 8.22 (dd, *J* = 17.6, 1.3 Hz, 2H), 7.54 (dd, *J* = 7.9, 4.8 Hz, 1H), 4.21 (s, 2H), 3.89 (s, 4H), 3.33 (s, 4H); ¹³C NMR (126 MHz, DMSO) δ 174.82, 146.42, 141.55, 140.47, 139.97, 139.13, 135.13, 134.09, 130.65, 129.39, 124.22, 123.91, 123.41, 122.76, 122.71, 51.99, 45.30, 8.39; MS (ESI) *m/z* = 381.07 (M + H)⁺

4.1.1.34. *N*-(5-(Thiophen-2-yl)pyridin-3-yl)cyclopropanecarboxamide (**14**). The compound was synthesized according to procedure **B** using cyclopropanecarboxylic acid to give a brown solid: yield 45.4%. The product was purified by CC (DCM/MeOH 100:4); mp 149.8–151.1 °C; ¹H NMR (500 MHz, DMSO) δ 10.50 (s, 1H), 8.64 (d, *J* = 2.3 Hz, 1H), 8.60 (d, *J* = 2.1 Hz, 1H), 8.32 (t, *J* = 2.2 Hz, 1H), 7.65 (dd, *J* = 5.1, 1.1 Hz, 1H), 7.58 (dd, *J* = 3.6, 1.2 Hz, 1H), 7.19 (dd, *J* = 5.1, 3.6 Hz, 1H), 1.88–1.76 (m, 1H), 0.90–0.78 (m, 4H); ¹³C NMR (126 MHz, DMSO) δ 172.46, 140.42, 139.55, 139.26, 136.12, 129.50, 128.70, 126.91, 124.88, 121.99, 14.55, 7.51; MS (ESI) *m/z* = 244.99 (M + H)⁺

4.1.1.35. *N*-(5-(4-(1H-pyrazol-4-yl)thiophen-2-yl)pyridin-3-yl)cyclopropanecarboxamide (**15**). The compound was synthesized according to procedure **E** using 4-Pyrazoleboronic acid pinacol ester to give a white solid: yield 18.1%. The product was purified by CC (DCM/MeOH 100:4); mp 250–253.2; ¹H NMR (500 MHz, DMSO) δ 12.91 (s, 1H), 10.55 (s, 1H), 8.64 (t, *J* = 2.2 Hz, 2H), 8.36 (t, *J* = 2.0 Hz, 1H), 8.16 (s, 1H), 7.89 (d, *J* = 1.0 Hz, 2H), 7.64 (d, *J* = 0.9 Hz, 1H), 1.82 (dd, *J* = 6.8, 3.9 Hz, 1H), 0.95–0.79 (m, 4H); ¹³C NMR (126 MHz, DMSO) δ 172.50, 140.33, 139.68, 139.33, 136.58, 136.14, 135.16, 129.53, 125.61, 124.01, 121.84, 118.48, 116.62, 14.56, 7.54; MS (ESI) *m/z* = 311.02 (M + H)⁺

4.1.1.36. *N*-(5-(4-(1-methyl-1H-pyrazol-4-yl)thiophen-2-yl)pyridin-3-yl)cyclopropanecarboxamide (**16**). The compound was synthesized according to procedure **E** using 1-methyl-1H-pyrazole-4-boronic acid to give a buff yellow solid: yield 17.3%. The product was purified by CC (DCM/MeOH 100:3); mp 254.2–255.3; ¹H NMR (500 MHz, DMSO) δ 10.52 (s, 1H), 8.63 (s, 2H), 8.36 (s, 1H), 8.08 (s, 1H), 7.86–7.80 (m, 2H), 7.61 (d, *J* = 1.0 Hz, 1H), 3.86 (s, 3H), 1.87–1.74 (m, 1H), 0.92–0.78 (m, 4H); ¹³C NMR (126 MHz, DMSO) δ 172.48, 140.30, 139.77, 139.36, 136.38, 136.14, 134.79, 129.47, 127.91, 123.78, 121.85, 118.52, 117.38, 38.56, 14.54, 7.51; MS (ESI) *m/z* = 325.10 (M + H)⁺

4.1.1.37. *N*-(5-(4-(1-ethyl-1H-pyrazol-4-yl)thiophen-2-yl)pyridine-3-yl)cyclopropanecarboxamide (**17**). The compound was synthesized according to procedure **E** using **compound I** to give a light brown solid: yield 17.3%. The product was purified by CC (DCM/MeOH 100:4); mp 240.3–242; ¹H NMR (500 MHz, DMSO) δ 10.55 (s, 1H), 8.64 (s, 2H), 8.37 (s, 1H), 8.15 (s, 1H), 7.89–7.81 (m, 2H), 7.61 (d, *J* = 1.0 Hz, 1H), 4.14 (q, *J* = 7.3 Hz, 2H), 1.88–1.72 (m, 1H), 1.40 (t, *J* = 7.3 Hz, 3H), 0.93–0.82 (m, 4H); ¹³C NMR (126 MHz, DMSO) δ 172.53, 140.31, 139.76, 139.35, 136.25, 134.94, 130.70, 129.54, 126.47, 123.84, 121.83, 118.48, 117.18, 46.31, 15.39, 14.58, 7.56; MS (ESI) *m/z* = 339.07 (M + H)⁺

4.1.1.38. *N*-(5-(4-(1-propyl-1H-pyrazol-4-yl)thiophen-2-yl)pyridin-3-yl)cyclopropanecarboxamide (**18**). The compound was synthesized according to procedure **E** using **compound J** to give a white solid: yield 28.9%. The product was purified by CC (DCM/MeOH 100:3); mp 225.5–228.3; ¹H NMR (500 MHz, DMSO) δ 10.57 (s, 1H), 8.65 (s, 2H), 8.37 (s, 1H), 8.14 (s, 1H), 7.86 (d, *J* = 1.2 Hz, 1H), 7.85 (s, 1H), 7.62 (d, *J* = 1.2 Hz, 1H), 4.07 (t, *J* = 6.9 Hz, 2H), 1.84–1.78 (m, 3H), 0.86 (dd, *J* = 5.9, 2.9 Hz, 6H), 0.83 (s, 1H); ¹³C NMR (126 MHz, DMSO) δ 172.52, 140.22, 139.74, 139.28, 139.25, 136.31, 134.91, 129.61, 127.13, 123.85, 121.85, 118.48, 117.05, 52.95, 23.14, 14.56, 10.93, 7.55; MS (ESI) *m/z* = 353.04 (M + H)⁺

4.1.1.39. *N*-(5-(4-(1-isopropyl-1H-pyrazol-4-yl)thiophen-2-yl)pyridin-3-yl)cyclopropanecarboxamide (**19**). The compound was synthesized according to procedure **E** using **compound K** to give a beige solid: yield 24.2%. The product was purified by CC (DCM/MeOH 100:3); mp 198.1–200.6; ¹H NMR (500 MHz, DMSO) δ 10.57 (s, 1H), 8.66 (s, 2H), 8.38 (s, 1H), 8.20 (s, 1H), 7.86 (d, *J* = 18.6 Hz, 2H), 7.61 (s, 1H), 4.59–4.31 (m, 1H), 1.91–1.79 (m, 1H), 1.44 (d, *J* = 6.6 Hz, 6H), 0.86 (d, *J* = 4.6 Hz, 4H); ¹³C NMR (126 MHz, DMSO) δ 172.49, 140.25, 139.69, 139.30, 136.21, 135.86, 135.04, 129.52, 124.78, 123.85, 121.77, 118.33, 116.89, 53.00, 22.64, 14.54, 7.52; MS (ESI) *m/z* = 353.26 (M + H)⁺

4.2. Biological assays

4.2.1. Protein kinases and inhibition assays

Human Dyrk1A was expressed and purified as described earlier [43]. Dyrk1B and Clk1 were purchased from Life Technologies (lot

no. 877059G, Catalog no. PV4649 and lot no.1095729A, catalog no. PV3315). Woodtide substrate peptide for Dyrk1A and Dyrk1B (KKISGRSLPIMTEQ) and RS repeat substrate peptide for Clk1 (GRSRSRSRSRSRSRSR) were custom synthesized at the Department of Medical Biochemistry and Molecular Biology, Saarland University, Homburg, Germany. Kinase inhibition assays for Dyrk1A, Dyrk1B and Clk1 were performed as described previously, in the presence of 15 μ M ATP [43]. The calculated IC₅₀ values are representative of at least two independent determinations. The larger panel of kinases shown in Table 3 was screened by the SelectScreen Kinase Profiling Service, Thermo Fisher Scientific, Paisley, U.K.

4.2.2. Cell-based assays

Stock solutions of the inhibitors were prepared in dimethylsulfoxide (DMSO). All effects were compared to vehicle controls which contained DMSO at the respective final concentration in growth medium. Protein kinase activity of endogenous Dyrk1A in HeLa cells was assayed by measuring the phosphorylation of T434 in overexpressed GFP-SF3b1-NT as described previously [52]. Briefly, HeLa cells were transiently transfected in 6-well plates and treated with test compounds for 18 h. Total cellular lysates were subjected to Western blot analysis with the help of a custom-made rabbit antibody for phosphorylated T434 in SF3b1 and a commercial goat antibody for GFP (no. 600-101-215, Rockland Immunochemicals, Gilbertsville, PA, USA). Blots were developed using horseradish peroxidase (HRP)-conjugated secondary antibodies and enhanced chemiluminescent substrates. Signals were quantified using the AIDA Image Analyzer 5.0 program (Raytest, Straubenhardt, Germany). pT434 signals were normalised to total protein levels as determined from GFP immunoreactivity. GraphPad Prism 5.0 (GraphPad Software, La Jolla, CA, USA) was used for non-linear curve fitting (Hill slope –1).

Viability assays were performed using a 96-well plate format (20,000–30,000 cells per well). Cells were cultivated for 3 days before cell viability was assessed with the help of a tetrazolium dye assay (XTT assay, AppliChem GmbH, Darmstadt, Germany).

4.3. Physicochemical properties calculation

Calculation of key physicochemical properties was performed using ACD/Labs software (ACD/Percepta, 2012, Advanced Chemistry Development, Inc) as described previously [43].

4.4. Molecular docking studies

Molecular docking was performed as previously described using MOE [53]. To model the ATP binding site of Dyrk1B, which has not been crystallized, Met240 in the Dyrk1A crystal structure (PDB entry: 3ANR) was mutated *in silico* to leucine, followed by an energy minimization of the side chain using the rotamer explorer routine embedded in MOE.

4.5. Metabolic stability in a cell free assay

Evaluation of metabolic stability and determination of half-lives were carried out using human S9 fraction as described previously [44].

Notes

The authors declare no competing financial interest.

Acknowledgements

The excellent technical assistance by Simone Bamberg-Lember

is gratefully acknowledged. The authors would like to thank Prof. Dr. R. W. Hartmann and Prof. Dr. Christian Ducho for generously providing lab facilities to the M.E. group. S.S.D. and M.A.-H. acknowledge The Science & Technology Development Fund in Egypt (STDF) for funding through the GE-SEED, Project 17391. We are also grateful to the DAAD for the travelling support to S.S.D through GradUS Global and GERSS funds. The support by the DAAD in the framework "PPP Ägypten 15" (Project-ID 57190395) to M.E. is highly appreciated. Also, the support by the Deutsche Forschungsgemeinschaft (DFG) (Grant EN381/2-3) to M.E. is greatly acknowledged. We are also thankful for Dr. Mostafa M. Hamed and Mariam G. Tahoun (Helmholtz Institute for Pharmaceutical Research Saarland) for carrying out the metabolic stability studies.

Appendix A. Supplementary data

Supplementary data related to this article can be found at <https://doi.org/10.1016/j.ejmech.2018.08.097>.

Abbreviations

| | |
|-------------------------|--|
| AChE | Acetylcholine esterase |
| AD | Alzheimer's disease |
| APP | Amyloid precursor protein |
| ASF | Alternative splicing factor |
| BBB | Blood brain barrier |
| CC | Column chromatography |
| CDK | Cyclin dependant kinases |
| CID | collision induced dissociation |
| CK | Casein kinase |
| Clk | cdc like kinase |
| DS | Down's syndrome |
| Dyrk | Dual specificity tyrosine regulated kinase |
| GFP | Green fluorescent protein |
| HATU | 1-[Bis(dimethylamino)methylene]-1H-1,2,3-triazolo [4,5-b]pyridinium 3-oxid hexafluorophosphate |
| HBA | Hydrogen bond acceptor |
| HBD | Hydrogen bond donor |
| HBTU | N,N,N',N'-tetramethyl-O-(1H-benzotriazol-1-yl)uronium hexafluorophosphate |
| HIPK1 | Homeodomain-interacting protein kinase 1 |
| IC ₅₀ | Half maximal inhibitory concentration, MLCK2, Myosin light chain kinase 2 |
| NFAT | Nuclear factor of activated T cells |
| NFT | Neurofibrillary tangles |
| Pd(dppf)Cl ₂ | [1, 1'- Bis(diphenylphosphino)ferrocene] dichloropalladium(II) |
| PD | Parkinson's disease |
| PIM1 | Proviral integration site for Moloney murine leukemia virus-1 |
| TPSA | Topological polar surface area |
| TRKB | Tropomyosin receptor kinase B |
| SF3b1 | Splicing factor 3b1 |
| SRPK1 | Serine/arginine-rich protein kinase 1 |
| STK17A | Serine/threonine kinase 17A |

References

- [1] B. Smith, F. Medda, V. Gokhale, T. Duncley, C. Hulme, Recent advances in the design, synthesis, and biological evaluation of selective DYRK1A inhibitors: a new avenue for a disease modifying treatment of Alzheimer's? ACS Chem. Neurosci. 3 (2012) 857–872.
- [2] A. Ionescu, F. Dufrasne, M. Gelbcke, I. Jabin, R. Kiss, D. Lamoral-Theys, DYRK1A kinase inhibitors with emphasis on cancer, Mini Rev. Med. Chem. 12 (2012) 1315–1329.
- [3] W. Becker, Y. Weber, K. Wetzel, K. Eirnbter, F.J. Tejedor, H.G. Joost, Sequence characteristics, subcellular localization, and substrate specificity of DYRK-

- related kinases, a novel family of dual specificity protein kinases, *J. Biol. Chem.* 273 (1998) 25893–25902.
- [4] H. Kentrup, W. Becker, J. Heukelbach, A. Wilmes, A. Schurmann, C. Huppertz, H. Kainulainen, H.G. Joost, DyRK, a dual specificity protein kinase with unique structural features whose activity is dependent on tyrosine residues between subdomains VII and VIII, *J. Biol. Chem.* 271 (1996) 3488–3495.
 - [5] S. Himpel, P. Panzer, C. Eirmbter, H. Czajkowska, M. Sayed, L.C. Packman, T. Blundell, H. Kentrup, J. Grotzinger, H.G. Joost, W. Becker, Identification of the autophosphorylation sites and characterization of their effects in the protein kinase DYRK1A, *Biochem. J.* 359 (2001) 497–505.
 - [6] J. Guimera, C. Casas, C. Pucharcos, A. Solans, A. Domenech, A.M. Planas, J. Ashley, M. Lovett, X. Estivill, M.A. Pritchard, A human homologue of *Drosophila* minibrain (MNB) is expressed in the neuronal regions affected in Down syndrome and maps to the critical region, *Hum. Mol. Genet.* 5 (1996) 1305–1310.
 - [7] F.J. Tejedor, B. Hammerle, MNB/DYRK1A as a multiple regulator of neuronal development, *FEBS J.* 278 (2011) 223–235.
 - [8] J. Wegiel, W. Kaczmarek, M. Barua, I. Kuchna, K. Nowicki, K.C. Wang, S.M. Yang, J. Frackowiak, B. Mazur-Kolecka, W.P. Silverman, B. Reisberg, I. Monteiro, M. de Leon, T. Wisniewski, A. Dalton, F. Lai, Y.W. Hwang, T. Adayev, F. Liu, K. Iqbal, I.G. Iqbal, C.X. Gong, Link between DYRK1A overexpression and several-fold enhancement of neurofibrillary degeneration with 3-repeat tau protein in Down syndrome, *J. Neuropathol. Exp. Neurol.* 70 (2011) 36–50.
 - [9] W. Becker, U. Soppa, F.J. Tejedor, DYRK1A: a potential drug target for multiple Down syndrome neuropathologies, *CNS Neurol. Disord. - Drug Targets* 13 (2014) 26–33.
 - [10] F. Liu, B. Li, E.J. Tung, I. Grundke-Iqbal, K. Iqbal, C.X. Gong, Site-specific effects of tau phosphorylation on its microtubule assembly activity and self-aggregation, *Eur. J. Neurosci.* 26 (2007) 3429–3436.
 - [11] F. Liu, Z. Liang, J. Wegiel, Y.W. Hwang, K. Iqbal, I. Grundke-Iqbal, N. Ramakrishna, C.X. Gong, Overexpression of DyRK1A contributes to neurofibrillary degeneration in Down syndrome, *FASEB J.* 22 (2008) 3224–3233.
 - [12] Y.L. Woods, P. Cohen, W. Becker, R. Jakes, M. Goedert, X. Wang, C.G. Proud, The kinase DYRK phosphorylates protein-synthesis initiation factor eIF2B ϵ at Ser539 and the microtubule-associated protein tau at Thr212: potential role for DYRK as a glycogen synthase kinase 3-priming kinase, *Biochem. J.* 355 (2001) 609–615.
 - [13] J. Wegiel, C.X. Gong, Y.W. Hwang, The role of DYRK1A in neurodegenerative diseases, *FEBS J.* 278 (2011) 236–245.
 - [14] S.R. Ryoo, H.J. Cho, H.W. Lee, H.K. Jeong, C. Radnaabazar, Y.S. Kim, M.J. Kim, M.Y. Son, H. Seo, S.H. Chung, W.J. Song, Dual-specificity tyrosine(Y)-phosphorylation regulated kinase 1A-mediated phosphorylation of amyloid precursor protein: evidence for a functional link between Down syndrome and Alzheimer's disease, *J. Neurochem.* 104 (2008) 1333–1344.
 - [15] E.J. Kim, J.Y. Sung, H.J. Lee, H. Rhim, M. Hasegawa, T. Iwatsubo, S. Min do, J. Kim, S.R. Paik, K.C. Chung, DyRK1A phosphorylates alpha-synuclein and enhances intracellular inclusion formation, *J. Biol. Chem.* 281 (2006) 33250–33257.
 - [16] J.H. Sitz, K. Baumgartel, B. Hammerle, C. Papadopoulos, P. Hekerman, F.J. Tejedor, W. Becker, B. Lutz, The Down syndrome candidate dual-specificity tyrosine phosphorylation-regulated kinase 1A phosphorylates the neurodegeneration-related septin 4, *Neuroscience* 157 (2008) 596–605.
 - [17] M. Ihara, H. Tomimoto, H. Kitayama, Y. Morioka, I. Akiuchi, H. Shibasaki, M. Noda, M. Kinoshita, Association of the cytoskeletal GTP-binding protein Sept4/H5 with cytoplasmic inclusions found in Parkinson's disease and other synucleinopathies, *J. Biol. Chem.* 278 (2003) 24095–24102.
 - [18] M. Ihara, N. Yamasaki, A. Hagiwara, A. Tanigaki, A. Kitano, R. Hikawa, H. Tomimoto, M. Noda, M. Takamashi, H. Mori, H. Hattori, T. Miyakawa, M. Kinoshita, Sept4, a component of presynaptic scaffold and Lewy bodies, is required for the suppression of alpha-synuclein neurotoxicity, *Neuron* 53 (2007) 519–533.
 - [19] E. Im, K.C. Chung, DyRK1A phosphorylates parkin at Ser-131 and negatively regulates its ubiquitin E3 ligase activity, *J. Neurochem.* 134 (2015) 756–768.
 - [20] J. Shi, T. Zhang, C. Zhou, M.O. Chohan, X. Gu, J. Wegiel, J. Zhou, Y.W. Hwang, K. Iqbal, I. Grundke-Iqbal, C.X. Gong, F. Liu, Increased dosage of DyRK1A alters alternative splicing factor (ASF)-regulated alternative splicing of tau in Down syndrome, *J. Biol. Chem.* 283 (2008) 28660–28669.
 - [21] X. Yin, N. Jin, J. Gu, J. Shi, J. Zhou, C.X. Gong, K. Iqbal, I. Grundke-Iqbal, F. Liu, Dual-specificity tyrosine phosphorylation-regulated kinase 1A (DYRK1A) modulates serine/arginine-rich protein 55 (SRp55)-promoted Tau exon 10 inclusion, *J. Biol. Chem.* 287 (2012) 30497–30506.
 - [22] W. Qian, H. Liang, J. Shi, N. Jin, I. Grundke-Iqbal, K. Iqbal, C.X. Gong, F. Liu, Regulation of the alternative splicing of tau exon 10 by SC35 and DyRK1A, *Nucleic Acids Res.* 39 (2011) 6161–6171.
 - [23] V. La Cognata, V. D'Agata, F. Cavalcanti, S. Cavallaro, Splicing: is there an alternative contribution to Parkinson's disease?, *Neurogenetics*, 16 245–263.
 - [24] Z. Zhou, X.D. Fu, Regulation of splicing by SR proteins and SR protein-specific kinases, *Chromosoma* 122 (2013) 191–207.
 - [25] K. de Graaf, H. Czajkowska, S. Rottmann, L.C. Packman, R. Liliachis, B. Luscher, W. Becker, The protein kinase DYRK1A phosphorylates the splicing factor SF3b1/SAP155 at Thr434, a novel in vivo phosphorylation site, *BMC Biochem.* 7 (2006) 7.
 - [26] X. Yin, N. Jin, J. Shi, Y. Zhang, Y. Wu, C.X. Gong, K. Iqbal, F. Liu, DyRK1A overexpression leads to increase of 3R-tau expression and cognitive deficits in Ts65Dn Down syndrome mice, *Sci. Rep.* 7 (2017) 12.
 - [27] D. Toiber, G. Azkona, S. Ben-Ari, N. Toran, H. Soreq, M. Dierssen, Engineering DYRK1A overexpression yields Down syndrome-characteristic cortical splicing aberrations, *Neurobiol. Dis.* 40 (2010) 348–359.
 - [28] J. Bain, L. Plater, M. Elliott, N. Shpiro, C.J. Hastie, H. McLauchlan, I. Klevernic, J.S. Arthur, D.R. Alessi, P. Cohen, The selectivity of protein kinase inhibitors: a further update, *Biochem. J.* 408 (2007) 297–315.
 - [29] Y. Ogawa, Y. Nonaka, T. Goto, E. Ohnishi, T. Hiramatsu, I. Kii, M. Yoshida, T. Ikura, H. Onogi, H. Shibuya, T. Hosoya, N. Ito, M. Hagiwara, Development of a novel selective inhibitor of the Down syndrome-related kinase DyRK1A, *Nat. Commun.* 1 (2010) 86.
 - [30] T. Tahtouh, J.M. Elkins, P. Filippakopoulos, M. Soundararajan, G. Burgoyne, E. Durieu, C. Cochet, R.S. Schmid, D.C. Lo, F. Delhomme, A.E. Oberholzer, L.H. Pearl, F. Carreaux, J.P. Bazureau, S. Knapp, L. Meijer, Selectivity, cocrystal structures, and neuroprotective properties of leucettines, a family of protein kinase inhibitors derived from the marine sponge alkaloid leucettamine B, *J. Med. Chem.* 55 (2012) 9312–9330.
 - [31] S. Coutadeur, H. Benyamine, L. Delalonde, C. de Oliveira, B. Leblond, A. Foucourt, T. Besson, A.S. Casagrande, T. Taverne, A. Girard, M.P. Pando, L. Desire, A novel DYRK1A (dual specificity tyrosine phosphorylation-regulated kinase 1A) inhibitor for the treatment of Alzheimer's disease: effect on Tau and amyloid pathologies in vitro, *J. Neurochem.* 133 (2015) 440–451.
 - [32] R. Meinel, W. Becker, H. Falke, L. Preu, N. Loac, L. Meijer, C. Kunick, Indole-3-Carbonitriles as DYRK1A inhibitors by fragment-based drug design, *Molecules* 23 (2018).
 - [33] E. Friedman, Mirk/Dyrk1B in cancer, *J. Cell. Biochem.* 102 (2007) 274–279.
 - [34] K. Jin, S. Park, D.Z. Ewton, E. Friedman, The survival kinase Mirk/Dyrk1B is a downstream effector of oncogenic K-ras in pancreatic cancer, *Canc. Res.* 67 (2007) 7247–7255.
 - [35] E. Friedman, The kinase mirk/dyrk1B: a possible therapeutic target in pancreatic cancer, *Cancers* 2 (2010) 1492–1512.
 - [36] M. He, J. Gu, J. Zhu, X. Wang, C. Wang, C. Duan, Y. Ni, X. Lu, J. Li, Up-regulation of DyRK1b promote astrocyte activation following lipopolysaccharide-induced neuroinflammation, *Neuropeptides* 69 (2018) 7.
 - [37] R. Medeiros, F.M. LaFerla, Astrocytes: conductors of the Alzheimer disease neuroinflammatory symphony, *Exp. Neurol.* 239 (2013) 133–138.
 - [38] M. Belanger, P.J. Magistretti, The role of astroglia in neuroprotection, *Dialogues Clin. Neurosci.* 11 (2009) 281–295.
 - [39] R. Mathur, P.G. Ince, T. Minett, C.J. Garwood, P.J. Shaw, F.E. Matthews, C. Brayne, J.E. Simpson, S.B. Wharton, A reduced astrocyte response to beta-amyloid plaques in the ageing brain associated with cognitive impairment, *PLoS One* 10 (2015) e0118463.
 - [40] S. Abu Jhaisha, E.W. Widawati, I. Kii, R. Sonamoto, S. Knapp, C. Papadopoulos, W. Becker, DYRK1B mutations associated with metabolic syndrome impair the chaperone-dependent maturation of the kinase domain, *Sci. Rep.* 7 (2017) 6432.
 - [41] P.J. Duncan, D.F. Stojdl, R.M. Marius, K.H. Scheit, J.C. Bell, The Clk2 and Clk3 dual-specificity protein kinases regulate the intranuclear distribution of SR proteins and influence pre-mRNA splicing, *Exp. Cell Res.* 241 (1998) 300–308.
 - [42] J.M. Higgins, Haspin: a newly discovered regulator of mitotic chromosome behavior, *Chromosoma* 119 (2010) 137–147.
 - [43] C. Schmitt, D. Kail, M. Mariano, M. Empting, N. Weber, T. Paul, R.W. Hartmann, M. Engel, Design and synthesis of a library of lead-like 2,4-bis(heterocyclic) substituted thiophenes as selective DyRK/CLK inhibitors, *PLoS One* 9 (2014), e87851.
 - [44] S.S. Darwish, M. Abdel-Halim, M. Salah, A.H. Abadi, W. Becker, M. Engel, Development of novel 2,4-bispyridyl thiophenes as highly potent and selective DyRK1A inhibitors. Part I: benzamide and benzylamide derivatives, *Eur. J. Med. Chem.* 157 (2018) 1031–1050.
 - [45] T.T. Wager, R.Y. Chandrasekaran, X. Hou, M.D. Troutman, P.R. Verhoest, A. Villalobos, Y. Will, Defining desirable central nervous system drug space through the alignment of molecular properties, in vitro ADME, and safety attributes, *ACS Chem. Neurosci.* 1 (2010) 420–434.
 - [46] B. Baum, L. Muley, M. Smolinski, A. Heine, D. Hangauer, G. Klebe, Non-additivity of functional group contributions in protein-ligand binding: a comprehensive study by crystallography and isothermal titration calorimetry, *J. Mol. Biol.* 397 (2010) 1042–1054.
 - [47] B.R. Beno, K.S. Yeung, M.D. Bartberger, L.D. Pennington, N.A. Meanwell, A survey of the role of noncovalent sulfur interactions in drug design, *J. Med. Chem.* 58 (2015) 4383–4438.
 - [48] A.K. Ghose, T. Herbertz, R.L. Hudkins, B.D. Dorsey, J.P. Mallamo, Knowledge-based, central nervous system (CNS) lead selection and lead optimization for CNS drug discovery, *ACS Chem. Neurosci.* 3 (2012) 50–68.
 - [49] D. Huang, S.F. Poon, D.F. Chapman, J. Chung, M. Cramer, T.S. Reger, J.R. Roppe, L. Tehrani, N.D. Cosford, N.D. Smith, 2-(2-[3-(pyridin-3-yloxy)phenyl]-2H-tetrazol-5-yl) pyridine: a highly potent, orally active, metabotropic glutamate subtype 5 (mGlu5) receptor antagonist, *Bioorg. Med. Chem. Lett.* 14 (2004) 5473–5476.
 - [50] O. Fedorov, K. Huber, A. Eisenreich, P. Filippakopoulos, O. King, A.N. Bullock, D. Szklarczyk, L.J. Jensen, D. Fabbro, J. Trappe, U. Rauch, F. Bracher, S. Knapp, Specific CLK inhibitors from a novel chemotype for regulation of alternative splicing, *Chem. Biol.* 18 (2011) 67–76.
 - [51] G.D. Cuny, N.P. Ulyanova, D. Patnaik, J.F. Liu, X. Lin, K. Auerbach, S.S. Ray, J. Xian, M.A. Glicksman, R.L. Stein, J.M. Higgins, Structure-activity relationship

- study of beta-carboline derivatives as haspin kinase inhibitors, *Bioorg. Med. Chem. Lett* 22 (2012) 2015–2019.
- [52] N. Gockler, G. Jofre, C. Papadopoulos, U. Soppa, F.J. Tejedor, W. Becker, Har-mine specifically inhibits protein kinase DYRK1A and interferes with neurite formation, *FEBS J.* 276 (2009) 6324–6337.
- [53] A.K. ElHady, M. Abdel-Halim, A.H. Abadi, M. Engel, Development of selective Clk1 and -4 inhibitors for cellular depletion of cancer-relevant proteins, *J. Med. Chem.* 60 (2017) 5377–5391.
- [54] J. Bain, H. McLauchlan, M. Elliott, P. Cohen, The specificities of protein kinase inhibitors: an update, *Biochem. J.* 371 (2003) 199–204.
- [55] T. Anastassiadis, S.W. Deacon, K. Devarajan, H. Ma, J.R. Peterson, Comprehensive assay of kinase catalytic activity reveals features of kinase inhibitor selectivity, *Nat. Biotechnol.* 29 (2011) 1039–1045.
- [56] M.A. Pagano, J. Bain, Z. Kazimierzczuk, S. Sarno, M. Ruzzene, G. Di Maira, M. Elliott, A. Orzeszko, G. Cozza, F. Meggio, L.A. Pinna, The selectivity of inhibitors of protein kinase CK2: an update, *Biochem. J.* 415 (2008) 353–365.
- [57] C. Schmitt, P. Miralinaghi, M. Mariano, R.W. Hartmann, M. Engel, Hydroxybenzothiophene ketones are efficient pre-mRNA splicing modulators due to dual inhibition of Dyrk1A and Clk1/4, *ACS Med. Chem. Lett.* 5 (2014) 963–967.
- [58] G.D. Cuny, M. Robin, N.P. Ulyanova, D. Patnaik, V. Pique, G. Casano, J.F. Liu, X. Lin, J. Xian, M.A. Glicksman, R.L. Stein, J.M. Higgins, Structure-activity relationship study of acridine analogs as haspin and DYRK2 kinase inhibitors, *Bioorg. Med. Chem. Lett* 20 (2010) 3491–3494.

8. Appendix

8.1 Curriculum Vitae

Personal Information

| | |
|----------------|-------------------------------|
| Name | Mohamed Salah Rezk Abdelrahim |
| Birth data | 13 May 1987 in Cairo |
| Marital status | Married |
| Nationality | Egyptian |

Education and Research Experience

- **Post Graduate Studies** 2014-till now

Doctoral research, Pharmaceutical and Medicinal Chemistry department, Saarland University in Germany, Prof. Dr. R.W. Hartmann group under the supervision of PD Dr. Martin Frotscher

- **Post Graduate Studies** 2010-2011

Master of Science in Pharmaceutical Analytical Chemistry, German University in Cairo (GUC) Thesis entitled: "Potentiometric Determination of Famciclovir under Batch and FIA Conditions"

(Excellent with the highest honor)

- **Research Associate**, Leiden university, Netherlands August 2010- January 2011, Drug Delivery Technology department Prof. Wim Jiskoot

- **Undergraduate Study** 2004 – 2009

Bachelor of Science in Pharmacy and Biotechnology, German university in Cairo (GUC)

(Excellent with the highest honor)

- **Elementary, Middle and High School** 1992 - 2004

Abitur (English), Modern Nanner language school (MNLS)

Secondary school percentage: 99.3%

Honors and Scholarships

- LEXUS (Leiden Excellence Scholarship) granted by Leiden University in Netherlands, Winter 2010.
- Drug Design Summer School in Tübingen University, (granted by federal ministry of education and research BMBF in cooperation with DAAD and GUC), summer 2008
- Full scholarship for university study, (granted by German University in Cairo)
- The 4th place nationally in the Abitur, (honored by minister of education), summer 2004

8.2 Publications

- (1) Abdelsamie, A. S.; Herath, S.; Biskupek, Y.; Börger, C.; Siebenbürger, L.; **Salah, M.**; Scheuer, C.; Marchais-Oberwinkler, S.; Frotscher, M.; Pohlemann, T.; Menger, M. D.; Hartmann, R. W.; Laschke, M. W.; van Koppen, C. J. Targeted Endocrine Therapy: Design, Synthesis, and Proof-of-Principle of 17 β -Hydroxysteroid Dehydrogenase Type 2 Inhibitors in Bone Fracture Healing. *J. Med. Chem.* **2019**, 62 (3), 1362–1372.
- (2) **Salah, M.**; Abdelsamie, A. S.; Frotscher, M. Inhibitors of 17 β -Hydroxysteroid Dehydrogenase Type 1, 2 and 14: Structures, Biological Activities and Future Challenges. *Mol. Cell. Endocrinol.* **2018**.
- (3) **Salah, M.**; Abdel-Halim, M.; Engel, M. Design and Synthesis of Conformationally Constraint Dyrk1A Inhibitors by Creating an Intramolecular H-Bond Involving a Benzothiazole Core. *Medchemcomm* **2018**, 9 (6), 1045–1053.
- (4) Darwish, S. S.; Abdel-Halim, M.; **Salah, M.**; Abadi, A. H.; Becker, W.; Engel, M. Development of Novel 2,4-Bispyridyl Thiophene-based Compounds as Highly Potent and Selective Dyrk1A Inhibitors. Part I: Benzamide and Benzylamide Derivatives. *Eur. J. Med. Chem.* **2018**, 157, 1031–1050.
- (5) Darwish, S. S.; Abdel-Halim, M.; ElHady, A. K.; **Salah, M.**; Abadi, A. H.; Becker, W.; Engel, M. Development of Novel Amide-derivatized 2,4-Bispyridyl Thiophenes as Highly Potent and Selective Dyrk1A Inhibitors. Part II: Identification of the Cyclopropylamide Moiety as a Key Modification. *Eur. J. Med. Chem.* **2018**, 158, 270–285.
- (6) **Salah, M.**; Abdelsamie, A. S.; Frotscher, M. First Dual Inhibitors of Steroid Sulfatase (STS) and 17 β -Hydroxysteroid Dehydrogenase Type 1 (17 β -HSD1): Designed Multiple Ligands as Novel Potential Therapeutics for Estrogen-Dependent Diseases. *J. Med. Chem.* **2017**, 60 (9), 4086–4092.
- (7) Abdelsamie, A. S.; van Koppen, C. J.; Bey, E.; **Salah, M.**; Börger, C.; Siebenbürger, L.; Laschke, M. W.; Menger, M. D.; Frotscher, M. Treatment of Estrogen-Dependent Diseases: Design, Synthesis and Profiling of a Selective 17 β -HSD1 Inhibitor with Sub-Nanomolar IC 50 for a Proof-of-Principle Study. *Eur. J. Med. Chem.* **2017**, 127, 944–957.
- (8) Braun, F.; Bertoletti, N.; Möller, G.; Adamski, J.; Steinmetzer, T.; **Salah, M.**; Abdelsamie, A. S.; van Koppen, C. J.; Heine, A.; Klebe, G.; Marchais-Oberwinkler, S. First Structure–Activity Relationship of 17 β -Hydroxysteroid Dehydrogenase Type 14 Nonsteroidal Inhibitors and Crystal Structures in Complex with the Enzyme. *J. Med. Chem.* **2016**, 59 (23), 10719–10737.
- (9) **Salah, M.**; Abdel-Halim, M.; Keeton, A.; Franklin, D.; Bauer, M.; Boeckler, F. M.; Engel, M.; Hartmann, R. W.; Zhang, Y.; Piazza, G. A.; Abadi, A. H. Synthesis and Optimization of New 3,6-Disubstitutedindole Derivatives and Their Evaluation as Anticancer Agents Targeting the MDM2/MDMx Complex. *Chem. Pharm. Bull.* **2016**, 64 (1), 34–41.
- (10) **Salah, M.**; El Nashar, R. M. Dissolution Testing and Potentiometric Determination of Famciclovir in Pure, Dosage Forms and Biological Fluids. *Bioelectrochemistry* **2013**, 89, 26–33.

8.3 Conference Contributions

Topic: “First Dual Inhibitors of Steroid Sulfatase and 17 β -Hydroxysteroid Dehydrogenase Type 1: Designed Multiple Ligands as Novel Potential Therapeutics for Estrogen-Dependent Diseases”

Poster presentations:

Mohamed Salah, Ahmed S. Abdelsamie, Martin Frotscher. DPhG Jahrestagung, September 2017, Saarbrücken, Germany

Mohamed Salah, Ahmed S. Abdelsamie, Martin Frotscher. Doktorandentag der Naturwissenschaftlich-Technischen Fakultät der Universität des Saarlandes, November 2017, Saarbrücken, Germany

Oral presentations:

Mohamed Salah, Ahmed S. Abdelsamie, Martin Frotscher. DPhG Doktorandentagung, March 2018, Bad Dürkheim, Germany

Poster Prize:

American Chemical Society (ACS) best poster prize in Medicinal Chemistry, DPhG Jahrestagung, September 2017, Saarbrücken, Germany